PERFORMANCE-BASED SEISMIC DESIGN OF CONCRETE BRIDGES FOR DEFORMATION CONTROL THROUGH ADVANCED ANALYSIS TOOLS AND CONTROL DEVICES

Konstantinos I. Gkatzogias

A thesis submitted in partial fulfilment for the degree of

Doctor of Philosophy

City, University of London

School of Mathematics, Computer Science & Engineering
Civil Engineering Department

Research Centre for Civil Engineering Structures

London, December 2017

City, University of London

School of Mathematics, Computer Science & Engineering
Civil Engineering Department

Research Centre for Civil Engineering Structures

Doctoral Dissertation:

Performance-based seismic design of concrete bridges for deformation control through advanced analysis tools and control devices

Doctoral Candidate:

Konstantinos I. Gkatzogias, DiplEng, MSc
(Konstantinos.Gkatzogias.1@city.ac.uk)

1st Supervisor:

Professor Andreas J. Kappos
(Andreas.Kappos.1@city.ac.uk)

2nd Supervisor:

Dr. Agathoklis Giaralis

Examiners:

Professor Ashraf Ayoub, City, University of London
Professor Brian Broderick, Trinity College, Dublin

London, December 2017

To Ilia, Aristea, and Thalia

Contents

Chapter 3 Deformation-Based Seismic Design of Bridges with Energy Dissipation in the Piers

Chapter 4 Direct Estimation of Peak Seismic Response in Reduced-DOF Isolation and Energy Dissipation Systems

Chapter 6 Comparison of Def-BD with Alternative Design Procedures

Chapter 7 Conclusions and Recommendations for Future Research

Annex A Supplement to Chapter 3

List of Figures

List of Tables

Acknowledgements

A small note, hopefully expressing though, my deep gratitude to those who contributed to this work:

My supervisor *Prof. Andreas Kappos*, a tireless lecturer and researcher, for his continuous support and confidence in my expertise, infusing me his passion for earthquake structural engineering. His valuable guidance being constantly available during my doctoral studies, and his encouragement towards my involvement in various research and teaching activities can reflect only a small portion of his contribution to my academic and professional development through our collaboration dating back to 2008;

City, University of London, the *School of Mathematics Computer Science & Engineering*, and the *Research Centre for Civil Engineering Structures*, for funding my research efforts through a 3-year Doctoral Studentship along with travel and conference attendance funds;

Prof. Brian Broderick, *Prof. Ashraf Ayoub*, and *Dr. Agathoklis Giaralis*, for providing constructive feedback and valuable comments on my doctoral dissertation and transfer report;

Prof. Anastasios Sextos and *Dr. Evangelos Katsanos*, for their immediate response and upgrade of ISSARS software, facilitating the selection and scaling of natural records at the early stages of this work;

Dr. Panagiotis Mergos for sharing ideas on MATLAB code development;

Emeritus Prof. Christos Ignatakis for his inspiration and continual encouragement;

My 'fellow travellers' *KeyKey*, *Angelina*, and *Kiki*, for their unique contribution;

My *family* to whom this work is dedicated.

Konstantinos Gkatzogias
London, December 2017

Declaration

I grant powers of discretion to the University Librarian to allow this dissertation to be copied in whole or in part without further reference to me (the Author). This permission covers only single copies made for study purposes, subject to normal conditions of acknowledgement.

Abstract

The relatively few available practice-oriented proposals for *performance-based seismic design* of conventional and isolated bridges, aim primarily at a more consistent description of seismic demand and capacity of structures on the basis of simplified analysis, and to a lesser extent at the direct consideration of multi-level performance criteria using advanced analysis tools. In view of the type/device-specific existing methods, the present study presents a broad-scope methodology for the seismic design of bridges emphasising on (*i*) *displacement-based principles*, (*ii*) *use of nonlinear dynamic analysis*, and (*iii*) *explicit consideration of multiple performance levels* (PLs) and *objectives (POs)* in a *practical design context*, suitable for inclusion in design codes.

The *deformation-based design* (Def-BD) procedure, initially developed for seismic design of conventional (non-isolated) buildings, is first tailored to concrete bridges with energy dissipation in the piers. The key issues in this respect are the proper consideration of the intended plastic mechanism under the considered PLs, and the design of the bearings. The efficiency of the proposed design methodology is demonstrated by applying it to an actual bridge selected with a view to enabling comparisons among Def-BD, the *modal direct displacement-based design* (MDDBD), and a force-based code-type (Code-BD) method. Refined analysis along with the consistent performance-based design format within Def-BD, result in superior seismic performance. Significant cost reductions are achieved compared to MDDBD, whereas potential cost reductions may generally be obtained compared to 'standard' code design.

Considering the diversity of passive devices and their inherent weakness to optimise the bridge response under multiple PLs, a methodology is developed to enable the identification of the critical performance requirements and the comparative evaluation of different passive schemes at the early stages of design. Originating from an earlier study focusing on bilinear isolators, the method is extended with a view to developing generalised design equations (GDEs) capable of providing reliable estimates of peak response in linear/bilinear isolation systems with/without supplemental linear/nonlinear viscous damping under different PLs associated with code-based target spectra of different intensity. The Def-BD method is finally extended to address passive (isolation and energy dissipation) systems. Novel features are introduced, including (*i*) the use of GDEs for the preliminary 'near-optimal' selection of the basic system properties and the consideration of nonlinearity of viscous dampers, (*ii*) the enhancement of POs in line with the higher performance expected in the case of isolated bridges, (*iii*) specific conditions ensuring the effectiveness of the isolation system, and (*iv*) the proper consideration of the orthogonal component of seismic action under bidirectional excitation. The validity of the procedure is demonstrated by applying it to the bridge previously used to develop the Def-BD method for bridges with 'ductile-pier' behaviour. Alternative isolation schemes are investigated and compared with the design resulting from Eurocode 8 (Part 2), offering a useful insight into some pitfalls of modern code-based approaches. Assessment of the Def-BD designs reveals enhanced and controlled performance under multiple PLs, and significant cost reductions in the substructure design compared to the design for 'ductile-pier' response. On the other hand, further cost reduction observed in the case of the code-based design, results in reduced efficiency of the isolation system and improper performance of the piers.

In view of the previous remarks, Def-BD emerges as a rigorous methodology, applicable to most of the common concrete bridge configurations, albeit at the expense of additional computational effort associated with the use of nonlinear dynamic analysis and the design for multiple PLs. Nevertheless, minimum iterative effort is ensured by providing design 'routines' that facilitate the implementation and address implications resulting from the use of nonlinear dynamic analysis. Considering the suitable formulation of Def-BD, a framework of performance-based control principles for the future extension towards the integration of advanced structural control techniques, is finally set forth.

List of Symbols

Upper Case Latin

A	area / intensity measure
C	damping matrix
CL	confidence level (statistics)
D	diameter
E	modulus of elasticity / energy
EBE	energy balance error
EQ	earthquake action
F	damper force
G	shear modulus / permanent and quasi-permanent actions
GM	geometric mean
H	horizontal component of seismic action
I	moment of inertia / principal (component, axis)
K	stiffness matrix
L	length
M	bending moment / earthquake magnitude
MSE	mean-square error
N	axial force
P	probability / prestressing force
Q	variable (traffic) action
R	source-to-site distance
RMSE	root-mean-square error
RMSEn	normalised root-mean-square error
S	spectral (e.g. acceleration) / shape factor / site amplification factor
SEGM	standard error of the geometric mean
SEM	standard error of the arithmetic mean
SF	scaling factor
T	vibration period / time period (years) / thermal action
U	total displacement
V	shear force
W	elastic section modulus
Z	seismic hazard zone

Lower Case Latin

a	damper velocity coefficient / unloading parameter (hysteresis rule) / proportional damping constant / significance level (statistics)
b	reloading parameter (hysteresis rule)
c	damping coefficient
df	degrees of freedom (statistics)
e	eccentricity
f	force matrix / material strength / modification factor
g	acceleration of gravity
h	height
k	stiffness / slope of hazard curve
m	mass
n	axial load ratio / counter
q	behaviour or response modification factor
r	radius of gyration / residual (statistics) / correlation coefficient (statistics)
s	sample standard deviation of normally distributed data / smoothness parameter (hysteresis rule)
t	time / thickness / *t*-value in Student's t-distribution
u	relative displacement
w	weight
y	response variable
z	hysteretic dimensionless parameter

Indices

0	amplitude (peak value)
a	acceleration
acc	accumulation
b	bulk modulus
C	capacity
c	concrete / compression
cc	confined concrete
cr	cracked / critical
D	damping (force, energy) / deck
d	design / damper / displacement
dyn	dynamic
e	elastic / elastomer
eff	effective

epi	epicentral (distance)
eq	equivalent
g	gross / ground
h	hysteretic
I	isolator / inertia forces
inh	inherent
k	characteristic
L	lead core / design life
l	longitudinal (steel ratio)
lap	overlapping
m	mean
NL	nonlinear
nom	nominal
opt	optimal
p	post-elastic / pier
pl	plastic hinge
R	return (period) / rubber (elastomer) / resistance
r	rotational (bending) / residual (maximum)
ref	reference
res	residual (actual)
rup	rupture (distance)
S	elastic and inelastic resisting forces
s	shear (area, wave) / steel
sol	solid
sup	supplemental
T	tangent
t	tensile
tot	total
u	ultimate
v	velocity / vertical
w	transverse (steel ratio)
y	yield

Greek

β	fraction of seismic action
γ	shear strain
δ	standard deviation of lognormally distributed data
ε	shear strain

η	strength normalised to *PGV* / damping modification factor
θ	chord rotation / incidence angle / angle of peak response estimates
λ	device property modification factor / residual displacement accumulation factor
μ	ductility factor
ξ	damping ratio
ρ	reinforcing steel ratio
σ	stress
φ	curvature
ω	vibration frequency / reinforcing steel mechanical volumetric ratio

Operations, Other

$'$	bonded (area of elastomer)
$''$	effective (area of elastomer)
Γ	gamma function
Div	percentage divergence (error)
sgn	signum function
$\dot{x}$, $\ddot{x}$	first, second derivative of x
$\overline{x}$	normalised x
$\hat{x}$	sample arithmetic mean
$\mathbf{X}$	X matrix
$\sum$	sum
$\prod$	product
$\int$	integral

List of Abbreviations

1D	Unidirectional
2D	Bidirectional
2DOF	Two-Degree-Of Freedom
AASHTO	American Association of State Highway and Transportation Officials
Abt	Abutment
ACI	American Concrete Institute
ADRS	pseudo-Acceleration Displacement Response Spectrum
AMD	Active Mass Damper
Art	Artificial record (or suite of records)
ASCE	American Society of Civil Engineers
ATC	Applied Technology Council
Caltrans	California Department of Transportation
CEN	Comité Européen de Normalisation
CM	Centre of Mass
COMPDYN	Computational Methods in Structural Dynamics and Earthquake Engineering
CG	Centre of Gravity
CS	Centre of Stiffness
CSI	Computers and Structures Inc.
DBD	Displacement-Based Design
DDBD	Direct Displacement-Based Design
Def-BD	Deformation-Based Design
DI	Damage Index
DP	Design Property
EC	Eurocode
Ed	Editor / Edition
EERC	Earthquake Engineering Research Center
EMSh	Effective Mode Shape
EMSp	Effective Modal Superposition
EPPO	Earthquake Planning & Protection Organisation (Greece)
EQ	Level of Earthquake actions
FEMA	Federal Emergency Management Agency
FHWA	Federal Highway Administration
fib	féderation internationale du béton

FMS	Fundamental Mode Spectrum
FPB	Friction Pendulum Bearing
FSB	Flat Sliding Bearing
GDE	Generalised Design Equation
HDRB	High Damping Elastomeric Bearing
IDEC	Isolation Design Equations Code
IMP	Implicit Calculation
IRSA	Incremental Response Spectrum Analysis
JCSS	Joint Committee on Structural Safety
LB	Lower Bound
LDRB	Low Damping Elastomeric Bearing
LRB	Lead-Rubber Bearing
LVD	Linear Viscous fluid Damper
MANSP	Modal Adaptive Nonlinear Static Procedure
MC2010	Model Code 2010
MCEER	Multidisciplinary Center for Earthquake Engineering Research
MDDBD	Modal Direct Displacement-Based Design
MDOF	Multi-Degree-Of-Freedom
MMS	Modified Modal Superposition
MPA	Modal Pushover Analysis
MYD	Metallic Yield Damper
Nat	Natural record (or suite of records)
NEHRP	National Earthquake Hazards Reduction Program
NIST	National Institute of Standards and Technology
NL	Nonlinear
NLRHA	Non-Linear Response History Analysis
NLVD	Non-Linear Viscous Damper
NTC	Norme Tecniche per le Costruzioni
NZTA	New Zealand Transport Agency
PBD	Performance-Based Design
PBEE	Performance-Based Earthquake Engineering
PEER	Pacific Earthquake Engineering Research Center
PESDES	PErformance-based DEsign of Structures
PGA	Peak Ground Acceleration
PGD	Peak Ground Displacement
PGV	Peak Ground Velocity
PIM	Partially Inelastic Model
PL	Performance Level
PO	Performance Objective

PSV	Pseudo Spectral Velocity
RDOF	Reduced Degree-Of-Freedom
RHA	Response History Analysis
RM	Regression Model
RSA	Response Spectrum Analysis
RSN	Record Sequence Number (PEER)
SA	Semi-Active
SD	Section Designer
SDOF	Single-Degree-Of-Freedom
SEAOC	Seismology Committee of Structural Engineers Association of California
SP	Structural Performance
SRSS	Square Root of the Sum of Square
TMD	Tuned Mass Damper
UB	Upper Bound
VD	Viscous Damper
Ver	Version
Vol	Volume
WCEE	World Conference on Earthquake Engineering

Chapter 1
Introduction

"In simple terms, with confidence the designer should 'tell' the structure to be constructed, what it should do, rather than ask, by way of analysis, what it might do"

T. Paulay (2002)

1.1 Problem Statement

Performance-based earthquake engineering (PBEE) constitutes a quest of engineers to better understand the response of structures subjected to the seismic hazard, and reliably and economically implement scientific results in practice, with a view to protecting life while constraining within acceptable limits economic losses associated with damage (i.e. repair, replacement) and service interruption. The challenge raised by PBEE can be to a certain extent confronted (at least with the current state-of-the-art) within a pure probabilistic framework incorporating uncertainties and advanced analysis and modelling techniques (JCSS 2001). Probabilistic procedures in this direction aiming in addition at the development of a PBEE framework that can effectively communicate seismic performance to stakeholders in terms of casualties, direct costs, and loss of function, were recently the focus of concerted research efforts with regard to the seismic performance of buildings, known as the ATC-58 Project (ATC 2012). Focused so far primarily on 'life-safety' and 'direct-loss' considerations, current research efforts attempt to relate the residual post-earthquake operationality (i.e. *robustness*) of structures and systems (e.g. communities, networks) to the rate of recovery (i.e. *rapidity*) including its dependence on available resources (i.e. *redundancy*) and disaster management (i.e. *resourcefulness*), extending the concept of performance-based engineered structures to resilient systems (Krawinkler & Deierlein 2014, Cimellaro 2016). Despite their attractiveness, these probabilistic approaches cannot be justified (at least not yet) in a practical engineering context due to implications deriving from the 'economic implementation' requirement in the PBEE definition. The introductory statement in ATC-58-1, that the proposed procedure will be best utilised for critical facilities or other structures where increased performance can be justified, points to the previous remark. Considering the 'iterative nature' of design problems due to the introduction of additional variables, such as sizing, location, and connectivity of structural members, required at both ends (i.e. input, output) of the design procedure, the probabilistic approach is more suited for assessment purposes associated with the evaluation of the performance of existing structures or the safety format adopted in design codes (e.g. partial safety factor format in CEN 2002), rather than the design of new structures. This is reflected in the state of development of probabilistic design methods being less mature than relevant assessment procedures, and commonly involving

optimisation techniques (*fib* 2012c) as a means to isolate potential design solutions from a vast number of possible variable combinations, inevitably adding to further complexity.

'Virtuous circle' implications in design are by no means restricted to the probabilistic framework, and the requirement for iterations introduces complexity in deterministic approaches too. In this context, documents relevant to the evaluation of seismic performance and retrofitting currently pave the way in adopting performance-based approaches (Fardis 2013), contrary to the 'early work' of code drafting committees when standards for existing structures commonly followed the publication of those referring to the design of new structures. From a deterministic seismic design point of view, the PBEE objective may translate into an attempt to generate 'uniform-risk' structures (Priestley *et al*. 2007); i.e. designing structures with a predefined structural response (quantified with structural performance measures) and hence a known level of safety, damage, and loss under a specific, or preferably, multiple and discrete, levels of seismic action associated with preselected probabilities of exceedance within the design life of the structure under investigation. In principle, the performance-based objective can be sought by both force-based and displacement-based design procedures that should be seen as the means to address the PBEE concepts. Nevertheless, following the introduction of capacity design (Park & Paulay 1975), which can be seen as an early formulation of the performance-based seismic design concept, and the subsequent systematic identification of deficiencies in force-based approaches regarding the estimation of seismic response and ensuing damage in structures (Priestley 1993), the research community invested heavily since the 1990s (e.g. *fib* 2003) in the development of performance-based design (PBD) procedures involving displacement-based design concepts. PBD procedures aimed primarily at a more rational and consistent description of seismic demand and capacity of structures by promoting displacements, deformations and strains over forces, and to a lesser extent at the direct consideration of multi-level performance criteria dealt in most cases with the independent application of the method under different performance levels, or limit states according to the European terminology. In fact, a significant method classification criterion at the time was the explicit (or implicit) consideration of displacements implying the 'direct' design route from the definition of target displacements to the estimation of the required stiffness and strength of structural members without the need for performing iterations under a single performance level. Despite the evident and improved rationality compared to force-based approaches, these procedures have been merely incorporated in design codes which retained to the present day their force-based nature involving explicit verifications for a single performance level. A notable exception, in this respect, was the *direct displacement-based design* method (Priestley 1993) a version of which was included in Appendix I of the SEAOC (1999) Blue Book that provided guidance with regard to building applications; interestingly though, unlike Priestley's initial proposal, the SEAOC procedure explicitly required verification of the design through nonlinear static (pushover) analysis, as part of the 'design' procedure.

The key reason why displacement-based design methods were not formally adopted (at least on a stand-alone basis) by design codes can be traced within the definition of PBEE provided

previously. Design in its most general but not necessarily 'economic' form, can be perceived as an iterative assessment process where the performance of a preliminary designed system is assessed and the design methodology is repeated in its entirety until the target performance under a single or multiple performance level is met (Krawinkler *et al*. 2006). During this generalised and at the same time least attractive formulation, there is no specific restriction in the degree of sophistication and virtually all types of analysis from linear static to incremental nonlinear dynamic analysis (Vamvatsikos & Cornell 2002) may be used potentially involving probabilistic concepts (ATC 2012). Displacement-based design procedures developed during the last two decades with a view to upgrading existing design codes, although departing from force-based principles, were bounded at the same time by their 'driving force' (i.e. inclusion in codes and design practice). In their attempt to reconcile requirements emanating from the design principles of 'simplicity' and 'enhanced seismic performance', they involved deterministic approaches based mainly on linear equivalent static and/or dynamic analysis (e.g. Priestley 1993) of simplified models of the structure (e.g. Shibata & Sozen 1976), rather than rigorous procedures such as nonlinear dynamic analysis of multi-degree of freedom systems (e.g. Kappos 1997). This resulted initially in methodologies that were applicable to a class of structures only. Further sophistication, adopted subsequently to broaden their range of applicability, increased their complexity and may have been interpreted as inconsistent with the requirement for 'simplicity', thus preventing their adoption in design codes. A characteristic example refers to the case of the 'simplified' inelastic methods (i.e. those based on static analysis used primarily, but not exclusively, for evaluation purposes), which were recently made quite sophisticated in order to handle complex problems, but inevitably they also became quite cumbersome, increasing the associated computational effort to an extent that makes questionable the benefits gained by their implementation (Kappos *et al*. 2012b). On the other hand, the advantages of using nonlinear dynamic analysis for design purposes have been recognised since the early seventies (Blume 1973). Nevertheless, code drafting committees have been reluctant to adopt this type of analysis in the following years. Even after the adoption of inelastic dynamic analysis by codes such as *Eurocode 8* (CEN 2004b, 2005a), guidance was usually provided with regard to the selection and scaling of input accelerograms or the application for evaluation purposes (i.e. to provide an insight into the post-elastic response) instead of the provision of an integrated performance-based methodology applicable to the final design of a fairly broad class of structures.

The smooth, efficient and reliable operation of road and rail transport systems is vital to the sustainable and resilient economic growth and development of communities. Bridges lie at the core of these systems, which further act as lifelines for emergency relief after catastrophic events such as earthquakes and other natural hazards. The increased associated seismic risk derived from the higher vulnerability of bridges compared to other components of ground transport systems, and their critical role in the operationality of these networks was shown in past and recent earthquakes, e.g. Wenchuan, China 2008 (Kawashima *et al*. 2009), Maule, Chile 2010 (Kawashima *et al*. 2011). In this context, it seems logical to consider utilising advanced performance and resilience-based procedures (e.g. Karamlou & Bocchini 2015) also accounting for sustainability (e.g. Mackie *et al*.

2016) along with modern technologies (Domaneschi & Martinelli 2016, Sarkis & Palermo 2018) to protect bridge structures. Nevertheless, in a practice-oriented deterministic context, application of performance/displacement-based concepts in bridges has been in general limited compared to buildings (Kappos 2015a). Quite surprisingly considering the widespread use of seismic isolation in bridge engineering, the adoption of structural control techniques (passive, active, semi-active, hybrid) for enhancing the seismic performance of bridges and thus meeting more efficiently and reliably the objectives of PBEE within integrated methods has been even more limited, essentially restricted to passive systems (e.g. Priestley *et al*. 2007). Yet, implementation of structural control principles to mitigate undesirable vibrations of dynamically excited civil engineering structures in seismically-prone areas has attracted the attention of the research community for more than three decades (e.g. Housner *et al*. 1997) and numerous passive devices were successfully deployed worldwide to control the seismic response of bridges and other structures (Basu *et al*. 2014). Although a relatively limited number of active control solutions have been applied in full-scale bridge applications (Spencer & Nagarajaiah 2003) to mitigate the effect of non-seismic loads due to their extensive external power supply requirements and reduced reliability during major earthquake events (e.g. possible power supply failure), semi-active control emerges nowadays as a promising design alternative in bridge seismic engineering (Gkatzogias & Kappos 2016b) combining increased adaptability and reliability features as opposed to passive and active control schemes, respectively, while it was recently implemented mainly as a retrofit measure to control cable and/or deck vibrations in bridge structures across Asia, Europe and the USA.

The scarcity of design methodologies integrating structural control in a (deterministic) performance-based context is possibly associated with the early realisation of the criticality of displacements in systems incorporating base isolation and energy dissipations devices resulting in relatively advanced codes of practice (e.g. AASHTO 2010) compared to those addressing conventional (non-isolated) bridges. The advancements refer first to the adoption of displacement-based simplified approaches and second to the upgrade of nonlinear dynamic analysis to the preferred method of analysis especially when supplemental damping devices are involved. Notwithstanding the necessity of adopting advanced analysis approaches in these cases due to certain deficiencies of spectral approaches (Fardis *et al*. 2012), the previous improved characteristics provide also an indication of the current trend in bridge code standards that holds both for conventional and non-conventional structural systems. Given the currently available bridge design practice that involves challenging loading conditions and complex structural configurations, there is little doubt that an increasing number of practitioners utilise advanced analysis tools and sophisticated programs to estimate the response of bridges. In this context, development of performance-based methods aiming at 'simplicity' and/or based on equivalent static analysis may be deemed as inconsistent with current practice; rather one would seek a method that is comprehensive, applicable to a very broad class of bridges, and capable of incorporating the current state-of-the-art in bridge seismic engineering such as structural control techniques. Two recently released documents are in support of this trend, namely the US *Guide Specifications for*

LRFD Seismic Bridge Design (AASHTO 2011) providing a design alternative to the force-based *LRFD Bridge Design Specifications* (AASHTO 2012), and the *fib Model Code 2010* (*fib* 2012a, b) covering the design and the assessment of new and existing structures, respectively. Both documents reflect the long-expected recourse to pure displacement-based design principles, that interestingly is sought by means of advanced inelastic analysis tools rather that 'simplified' procedures and models of the structure aiming at 'direct' estimates of stiffness and strength. In fact, the more advanced (but also general and not bridge-specific) *fib Model Code 2010* (*fib* 2012a, b) sets nonlinear dynamic analysis as the reference analysis method and embraces a pure performance-based philosophy explicitly considering multiple performance levels, nevertheless, lacking, in virtue of its broad scope, a detailed design framework.

1.2 Scope and Research Objectives

In the light of the previous considerations (§1.1), the present study focuses on *how engineers can efficiently and economically design bridges for deformation control against the seismic hazard within a performance-based framework that reflects the current state-of-the-art in bridge engineering*. In response to this solution-based research question, a *performance-based seismic design* methodology for bridges is established, taking due account of multi-level performance requirements described in terms of post-earthquake operationality, damage, and feasibility of repair, and different performance objectives accounting for the adopted structural configuration and the importance of the studied bridge. *Efficient design* is sought by employing *displacement-based* principles and *advanced analysis* tools (i.e. nonlinear dynamic analysis, section analysis), allowing also the incorporation of *control hardware* (i.e. control devices). Advanced analysis, explicitly used in the design process rather than implicitly as an assessment tool, ensures enhanced and reliable structural performance of the bridge serving the *broad-scope* applicability of the proposed method while exploring *cost-effective* design solutions disengaged from conservative (i.e. on the side of safety) assumptions included in current force-based design/analysis procedures. The term 'cost-effective' characterises here economy of design in terms of capital/maintenance cost, and direct or indirect costs due to repair/replacement or service interruption, respectively, following seismic events associated with specific levels of seismic action. Acknowledging the inherent iterative nature of the design process when realistic structural systems are considered, particular attention is drawn to the thorough consideration and/or development of the required tools with a view to avoiding computationally intensive iterative analysis, i.e. economy of design in terms of computational cost, characterising available design schemes (§1.1). The above characteristics aim to deliver a rigorous design method that constraints the increased computational effort characterising complex design frameworks (§1.1) while treating identified deficiencies of alternative displacement-based methods or traditional design approaches included in current design codes, thus assigning an exploratory/comparative component to the primary solution-focused character of the research study.

In line with the current state-of-the-art of design standards as reflected in the recently released *fib Model Code 2010* (*fib* 2012a, b), the formulation of the method is explored in a deterministic design framework. It is envisaged that adoption of probabilistic and resilience-based procedures within the suggested method will constitute a future research objective; however, this falls beyond the scope of the present study. In a similar context, the suggested methodology for isolated bridges refers explicitly to the integration of passive structural control techniques. Nevertheless, performance-based research objectives for future integration of semi-active control devices are identified and an effort is made towards the adoption of a proper format that should serve as the point of reference for extending the suggested procedure to semi-actively controlled bridges. Several aspects of the methodology presented herein are specific to reinforced and/or prestressed concrete bridges which constitute the focus of this study; nevertheless, the basic 'philosophy' of design is also applicable to steel and composite bridges while general implementation guidelines are also provided for alternative and more complex structural configurations than those explicitly stated in the following objectives.

Overall, a framework for the seismic design of bridges suitable for inclusion in future performance-based design codes of practice is sought, without limitations related to the irregularity of the structural system considered or the intended degree of sophistication with regard to analysis and modelling techniques. Being capable of incorporating the current state-of-the-art in bridge seismic engineering within short-term upgrades of current design codes of practice, the proposed methodology may also serve as a link towards the adoption of more sophisticated design frameworks incorporating probabilistic and 'smart' (e.g. semi-active) technology.

In support to the above scope of the present research study, the following specific research objectives are identified with regard to the considered bridge configurations:

- Review of available practice-oriented design methodologies for bridges involving displacement-based design principles, and identification of current trends in bridge seismic engineering.

- Development of a rigorous design methodology addressing bridges having one or more piers rigidly connected to the deck, thus rendering pier ductility the main energy dissipation mechanism. The suggested method makes recourse to inelastic analysis tools (i.e. nonlinear dynamic analysis, nonlinear section analysis) and develops procedures to address and control a broad range of seismic design parameters (i.e. strains, deformations, ductility factors) under multiple performance levels, that are directly estimated during an ideally non-iterative application of the method. To this end, a fully-fledged performance-based context is introduced providing a logical design route that consists of distinct steps, each corresponding to a different performance level depending on the selected performance objective and associated with design of specific bridge members and type of verifications.

- Further development of the previous methodology, with regard to modifications required for the comprehensive treatment of seismically isolated bridges with or without supplemental

energy dissipation devices. The extended methodology, serving as a design alternative to the 'conventional' design approach of the previous objective, aims at a rational implementation of passive structural control devices in line with the current state of practice in the use of structural control in bridge engineering. Considering the diversity of passive control devices, reduction of the associated computational effort is explicitly addressed by developing design tools required for the direct comparative evaluation at the early design stages of the various alternative isolation schemes (that may be realised by the proper combination of passive devices), and the identification of 'near-optimal' design solutions accounting for different levels of seismic action.

- Comparative evaluation of the proposed methodology and alternative displacement/force-based design procedures in terms of efficiency in providing reliable estimates of response while satisfying diverse performance requirements, and economy of design.

1.3 Layout of the Dissertation

The present thesis is divided in seven chapters and six annexes, and is structured in line with the research objectives outlined in §1.2. Following the introductory considerations of the present chapter on the problem statement and the scope of the study, a review of the current state-of-the-art on available practice-oriented performance and displacement-based methodologies for the seismic design of bridges is presented in Chapter 2. The second research objective is sought in Chapter 3 and the third in Chapters 4 and 5, followed by a comparison of the suggested method with alternative design approaches in Chapter 6, while overall conclusions and future steps towards the further development of the proposed framework are discussed in Chapter 7. Supplementary information related mostly, though not exclusively, to numerical investigations and example applications included in Chapters 3, 4, 5, 6, is provided in Annexes A, B, C, D, respectively, followed by a list of references in Annex E. Annex F includes a record of articles published so far in peer-reviewed journals and conference proceedings, on issues dealt within the objectives of the present study. A more detailed description of the core chapters of the dissertation is provided in the following.

Chapter 3 provides a detailed description of the suggested design methodology, hereafter called *deformation-based design* (Def-BD) method, targeting bridges with energy dissipation in the piers. The proposed methodology originating from work by Kappos and his associates focused on the seismic design of buildings (e.g. Kappos & Manafpour 2001, Kappos & Panagopoulos 2004) is thoroughly presented; detailed steps of the proposed Def-BD methodology and required modifications with regard to previous versions are first put forward. Following a description of the adopted analysis and design framework, the efficiency of the proposed design methodology is subsequently demonstrated by applying it to an actual bridge designed according to 'standard' European practice and selected with a view to enabling comparison between Def-BD and

alternative design procedures. The suggested procedure and the resulting designs for two different seismic zones are evaluated in the light of nonlinear dynamic analysis using a number of spectrum-compatible motions, whereas certain deficiencies of current code-based design approaches derived from associating critical performance requirements with specific performance levels are also discussed.

A methodology for the development of design tools and aids capable of providing direct estimates of peak inelastic response in reduced degree-of-freedom isolation and energy dissipation systems is presented in Chapter 4. The dynamic equation of motion is first normalised to reduce the number of design parameters that significantly affect the response, and the sensitivity of normalised response quantities to the seismic intensity is investigated through extensive parametric nonlinear dynamic analysis of isolated single-degree-of-freedom systems with linear viscous damping; regression analysis is subsequently employed to develop generalised design equations suitable for design purposes. The procedure is further extended to address nonlinear viscous damping, and the effect of the transverse component of seismic action in two-degree-of freedom systems under bidirectional excitation.

The deformation-based design method, proposed in Chapter 3 for the seismic design of bridges relying on hysteretic energy dissipation through ductile behaviour of the piers, is extended in Chapter 5 to address seismically isolated bridges with or without supplemental energy dissipation devices, integrating the design tools developed in Chapter 4 (i.e. the third research objective). Following the general format of Chapter 3, a detailed description of the proposed analysis and design framework is first provided. The efficiency of the method under unidirectional and bidirectional excitation is subsequently explored by applying it to an actual concrete bridge previously used for the evaluation of bridges with energy dissipation in the piers. The suggested procedure and the resulting designs for three different isolation schemes are evaluated in the light of nonlinear dynamic analysis, offering a useful insight into some additional pitfalls of modern code-based approaches; a comparison among the different designs, with emphasis on both economy and structural performance, is also presented.

A comparison of the designs resulting from the application of the Def-BD method for ‘ductile-pier’ and seismically isolated bridges, with ‘standard’ code-type design procedures and the direct displacement-based design method (Priestley *et al.* 2007) (as extended by Kappos *et al.* 2013 to explicitly account for higher mode effects) is sought in Chapter 6, with a view to assessing both the structural performance and the economy of design. In addition, inherent deficiencies of code-type methods identified during the application of Def-BD in Chapters 3, 5, are further discussed. Overall conclusions and recommendations for future research are presented in Chapter 7, along with an attempt to introduce a framework of performance-based structural control principles required for the extension of the Def-BD method to deal with bridges integrating semi-active structural control techniques.

Chapter 2
Review of the State-of-the-Art

2.1 Introduction

In the quest for a 'new generation' of performance-based codes that will minimise direct and indirect losses due to earthquakes, several design procedures were developed (*fib* 2003), attempting to reconcile the requirements for *simplicity* (important in practical design) and *enhanced control of the performance* of both structural and non-structural members, while research efforts are underway towards probabilistic (*fib* 2012c) and resilience-based design (Cimellaro 2016) frameworks. Following the introductory statement in §1.1, performance-based seismic design, hereafter denoted as PBD, is set in a deterministic context wherein structures are designed with the aim to satisfy a specific performance objective depending on the importance of the structure under consideration. In line with the definitions provided in one of the pioneering documents in PBD (SEAOC 1995), the performance objective consists of multiple structural performance levels or limit states in European terminology (hereafter the term performance level is adopted due to its frequent use worldwide), each one describing the expected (target) or the desirable structural performance under a level of seismic action associated with a preselected probability of exceedance within the design life of the structure. Since resilience of bridge structures and network systems has been introduced so far in probabilistic (Decò *et al*. 2013) and optimisation-based (Bocchini & Frangopol 2012) frameworks, robustness and rapidity properties (§1.1) are only implicitly considered in the following, through the definition of specific structural performance levels at the start of the design process that can be qualitatively associated with the anticipated residual operationality of the bridge (e.g. AASHTO 2011) following a seismic event.

The inherent difficulties in developing PBD methods that strike a balance between 'simplicity' and 'controlled performance' along with the preference of each research group for focussing on specific design parameters (typically at the expense of others), resulted in marked differences among the suggested design approaches (Kappos 2015a). Identifying the suitability of displacements (§1.1) in describing damage, previous attempts to classify the different methods (Sullivan *et al*. 2003, *fib* 2003, Priestley *et al*. 2007) emphasised the role of displacement within the proposed design procedures differentiating among (*i*) traditional *force-based* design, (*ii*) *deformation-calculation-based* design, and (*iii*) *deformation-specification-based* design methods. In the second class, typically involving analysis of detailed multi-degree-of-freedom (MDOF) structural models, detailing was provided to ensure that the displacement capacity of the structural system and its members exceeds the demand, as opposed to the descriptive detailing rules commonly provided in force-based design procedures. Importantly, no attempt was made to control

the seismic action effects (i.e. displacement demand) through properly modifying the structural system (e.g. geometry, detailing). On the contrary, the third class of methods aimed at a specific structural performance typically employing simple single-degree-of-freedom (SDOF) representations of the structure (at least at first stages of design); included methods were further subdivided to '*indirect*' (i.e. those requiring iterations) and '*direct*' (with little or no iterations). The above classification is deemed rather feeble as it will become apparent later, and the above terms are only used in a loose context in the present chapter mainly for historic purposes.

Among the reasons behind this decision is that nowadays most of the displacement-based design (DBD) methods aim at specific performances to serve the multi-performance level objectives of PBD, and to this end, they introduce design aids and procedures to facilitate their implementation. Furthermore, it is identified that the design of realistic structures is an inherently iterative process irrespective of the previous characterisation of methods. The number of iterations is also an issue, since a deformation-calculation-based method applied in an iterative mode using advanced analysis and well-calibrated design criteria may involve less iterations than a deformation-specification-based one, relying on simplified models to describe the response of a complex structure. In this context, the term 'direct' is used in the following simply to refer to the method pioneered by Priestley (1993) that follows an inverse design route (§2.2.1, 2.3.2) compared to the conventional approach of design, rather than to indicate the need and/or the number of required iterations. On the contrary, the preferred classification herein involves the type of analysis adopted among standard linear static/dynamic analysis, and more advanced nonlinear static/dynamic, incremental dynamic analysis (in line with the common format of codes) (Fragiadakis *et al.* 2015), since this indicates the involved assumptions (e.g. representation of seismic actions, stiffness, damping etc.) and implies relevant limitations with regard to the field of application of each method.

Until recently, implementation of DBD concepts to bridges has been quite limited, despite their critical role in the roadway and railway networks and the fact that their vulnerability to earthquakes has long been established, particularly with regard to their post-earthquake operationality. Development of integrated design approaches addressing bridges equipped with structural control devices while aiming at a predefined structural response under a specific or, preferably, under multiple levels of seismic action within a practical design context, has been even more limited, essentially based on linear equivalent-static/dynamic analysis of passively controlled systems. In the following sections performance-based methodologies encompassing displacement-based principles and specifically addressing the seismic design of bridges are reviewed. The focus in on 'practice-oriented' methods by means of presenting methods that reflect and serve the current state-of-the-art of modern codes and standards (which is also discussed) having the potential to be included in future 'short-term' revisions, rather than design methods based on complex optimisation and/or probabilistic approaches (described in *fib* 2012c). Methods addressing bridges with energy dissipation in the piers (commonly termed 'ductile' in the literature) are first presented and reviewed in §2.2. Methods for bridges with structural control systems are presented in §2.3

targeting sensibly 'broad-scope' rather than 'device-specific' procedures. Identified current trends are summarised in §2.4.

2.2 Seismic Design of Bridges with Energy Dissipation in the Piers

In its present form (as included in current bridge design codes), the force-based approach for the seismic design of bridges with energy dissipation in the piers reduces elastic seismic forces by a factor (i.e. the behaviour or response modification factor in European and US terminology, respectively) to account for the intended ductile response of the bridge. Once the yielding piers are designed, the remaining components of the bridge are designed using capacity design principles. The member and bridge displacement capacities are presumed to be provided by prescriptive detailing. The procedure considers explicitly (i.e. through analysis) a single performance level associated with the 'design' seismic actions. Operationality requirements are assumed to be satisfied, while capacity design principles are introduced to implicitly ensure the formation of the intended plastic mechanism and the avoidance of brittle modes of failure up to a level of seismic action associated with the ultimate flexural strength of energy dissipation zones. The following DBD methods are presented as a design alternative to the 'standard' force-based approach, due to their efficiency and suitability in describing the structural performance, and thus serving the objectives of PBD when extended to multiple performance levels.

2.2.1 Available practice-oriented DBD methodologies

In contrast with most of the available performance-based design (PBD) procedures (encompassing displacement-based principles) oriented to the design of buildings (*fib* 2003), the first applications of the so-called '*direct displacement-based design*' (DDBD) method (Priestley 1993, 2003) were on bridges piers (e.g. Kowalsky *et al*. 1995). Contrary to force-based and deformation-calculation-based procedures where displacements commonly represent the end-result of the analysis-design process, DDBD introduces an inverse 'design route'; strength is specified with a view to obtaining a preselected target displacement response under a specific level of seismic action, rather than simply constraining the response below limit values of displacements. To this end, the 'substitute structure' approach is invoked (Shibata & Sozen 1976) that approximates the peak inelastic response of an MDOF system by the peak elastic response of an equivalent ('substitute') single-degree-of freedom (SDOF) system characterised by its secant stiffness at the peak displacement and an equivalent viscous damping ratio, representative of the combined inherent and hysteretic damping of the structure.

The procedure in its simplest form (i.e. considering an SDOF system) starts from a target displacement consistent with the damage allowed in terms of material strains and/or member drifts (Kowalsky 2000, Goodnight *et al*. 2016) under the considered performance level, and ensured by

an appropriate detailing of the structure. Estimating a reasonable value for the yield displacement from empirical relationships (Priestley *et al*. 2007), the target displacement translates into a displacement ductility demand and a corresponding equivalent damping ratio, calculated on the basis of an equivalent linearisation approach. Simple geometric considerations of energy equality per cycle of response to harmonic loading between a hysteretic and an equivalent linear oscillator (Rosenblueth & Herrera 1964, Kowalsky *et al*. 1995) were adopted in the early versions of the method (e.g. Kowalsky *et al*. 1995, Kowalsky 2002). The equivalent damping ratio expressions were empirically modified later (Grant *et al*. 2005, Priestley & Grant 2005, Dwairi *et al*. 2007, Khan *et al*. 2016) to minimise the error from the peak inelastic displacement derived from nonlinear dynamic analysis under earthquake excitation. The equivalent damping ratio is in turn used to reduce the selected displacement spectra, and thus account (indirectly) for nonlinear hysteretic behaviour. Entering the 'reduced' response spectrum with the adopted target displacement, provides the effective period and stiffness (secant values at target displacement) of the system; subsequently, the design base shear corresponding to the previously defined peak displacement and secant stiffness, is calculated and used to apply a 'traditional' equivalent lateral force design of the system. A notable alternative to the above equivalent linearisation approach was proposed by Chopra & Goel (2001) that promoted instead, the explicit use of constant-ductility inelastic spectra.

The early work by Kowalsky *et al*. (1995) dealing with individual bridge piers with monolithic pier-to-deck connection modelled as SDOFs, was first extended by Calvi & Kingsley (1995) to MDOF bridge systems. Using an assumed deformed configuration of the structure and an SDOF representation of the continuous-deck bridge based on work equivalence, the design process was essentially reduced to that of an SDOF system characterised by a target displacement, an effective mass, and an equivalent viscous damping ratio; the latter was calculated from the damping ratios of individual pier members weighted on the basis of flexural strain energy (Shibata & Sozen 1976). The estimation of the design base shear was followed by its distribution as inertia forces to the discretised masses of the MDOF structure in accordance with the target displacement profile, and structural analysis was performed to determine member design forces and displacements under the statically applied inertia forces considering member secant stiffness at the peak member displacements. The methodology was further extended by Kowalsky (2002) and Dwairi & Kowalsky (2006) differentiating the 'design route' as a function of the expected displacement patterns scenario (i.e. the 'shape' or 'mode' of deformation) of the bridge deck, namely, 'rigid body translation', 'rigid body translation with rotation', and 'flexible' pattern (Fig. 2.1). Classification of displacement patterns for continuous bridge structures subjected to transverse seismic excitation was performed at the beginning of the design process using a relative stiffness index (i.e. a function of the superstructure and substructure stiffness) calibrated through parametric nonlinear response history analyses (NLRHAs) of regular/irregular bridge systems. The effective mode shape (EMSh) procedure was introduced to estimate the displacement pattern and hence the displacement profile (i.e. pattern scaled to the target displacement of the critical pier) in the most evolved case of the 'flexible pattern' design route. The EMSh procedure consisted essentially of a modal analysis of

the MDOF system using the secant stiffness of the substructure members in an attempt to capture more realistic displacement profiles accounting to some extent for the effect of the higher modes in the inelastically deformed configuration of the bridge. Additional features of the method involved the definition of the SDOF equivalent viscous damping ratio from the damping ratios of both piers and abutments weighted on the basis of the work done (rather than flexural strain energy) in each member, and the introduction of capacity design principles to ensure that the desired failure mechanism can be achieved. The definition of the system equivalent viscous damping ratio was further refined by Priestley *et al*. (2007) to include the contribution of the deck.

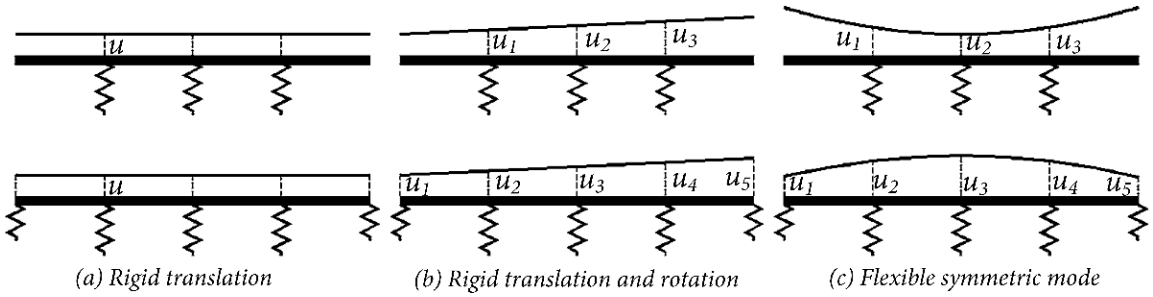

Fig. 2.1 Deck inelastic displacement pattern scenarios considered in Dwairi & Kowalsky (2006): Free (top) and integral (bottom) deck-to-abutment connection

The book by Priestley *et al*. (2007) presented a detailed treatment of the DDBD procedure and its application to different structural types, mainly focusing on buildings, but also addressing bridges. Specifically, regarding the design of bridges, a version of the method similar to, albeit simpler than, that of Dwairi & Kowalsky (2006) was presented, due to the substitution of the EMSh approach with the cruder adoption of a sine or parabolic-based displacement pattern at the start of the design process in the case of the flexible deck scenario that was subsequently revised using iterative static analysis. An approach similar to EMSh was maintained as an optional feature focusing on the estimation of forces and moments in capacity protected members. Further issues addressed in Priestley *et al*. (2007), involved the detailed presentation of the bridge design in the longitudinal direction (which often governs the seismic design of the bridge), the treatment of issues like the degree of fixity of columns indicating different pier-to-deck type of connections (monolithic, hinged, moveable bearings), and the effect of the substructure support conditions (footings, piles, etc.) and movement joints in the superstructure. Additional issues, such as soil-structure interaction of drilled shaft bents, skewed configurations of piers and/or abutments, conditions under which DDBD can be applied using predefined displacement patterns (including the case of expansion/contraction joints), and definition of stability-based target displacements that account for *P-Δ* effects at the start of the design process were studied by Suarez & Kowalsky (2007, 2010, 2011). Khan *et al*. (2014) extended the DDBD method to control the chord rotation of piers in the special case of reinforced concrete arch bridges.

The aforementioned studies performed on DDBD did not consider directly higher mode effects by virtue of the procedure's inherent limitation to structures wherein the fundamental mode dominates the response. Emerging from the adoption of the equivalent SDOF approach, this

limitation was partially addressed by the EMSh procedure (Kowalsky 2002, Dwairi & Kowalsky 2006) in defining the target displacement profile, but as anticipated, the procedure fell short in reproducing a fictitious displacement profile (consisting from nonsynchronous displacements due to the modal combination), and eventually reflecting the peak (and nonsynchronous) structural member response in systems with significant contribution of higher modes via static analysis (Kappos *et al*. 2013). Priestley and co-workers (Alvarez Botero 2004, Ortiz Restrepo 2006, Priestley *et al*. 2007) proposed as an alternative to nonlinear dynamic analysis, the 'Effective Modal Superposition' (EMSp) method, an approximate response spectrum analysis approach (as opposed to the EMSh which is a modal analysis method) analogous to what has been called 'Modified Modal Superposition' (MMS) by Priestley (2003) for cantilever wall design. In both approaches (i.e. EMSp, MMS) the inelastic first-mode design forces from the DDBD process were combined with the elastic forces from the higher modes using statistical combination rules. The only difference was the type of stiffness adopted in the modal analysis; EMSp adopted the secant stiffness at the peak displacement for yielding elements (as in the EMSh approach) contrary to the secant stiffness at yield used in MMS. It is worth noting that in EMSp, higher mode effects were considered only for determining the peak elastic responses of non-yielding members (e.g. deck transverse moment, abutment shear force). Inelastic responses, such as flexural strengths at plastic hinge locations, were computed directly from the first inelastic mode considering that the relevant mass participation factor was always more than 80%. In a subsequent study, Adhikari *et al*. (2010) introduced some additional considerations to account for higher mode effects on the flexural strength of plastic hinges in the case of long-span concrete bridges with limited ductile tall piers. Following the suggestion of Priestley *et al*. (2007), Adhikari *et al*. used a response spectrum analysis, after completion of the DDBD procedure, with two different design spectra (a 5%-damped design spectrum and a design spectrum with damping value obtained from the DDBD procedure) to determine the design responses (elastic and inelastic, respectively) at critical locations of the bridge as a combination of several modes. The previous recommendations were also adopted in the presentation of the method by Calvi *et al*. (2013).

In view of the previous constraints and the fact that bridges are structures wherein higher modes usually play a more critical role than in buildings (e.g. Liang *et al*. 2016), Kappos *et al*. (2012a, 2013) extended the DDBD procedure (building on the EMSh approach) to explicitly include higher mode effects in a more refined and broad-scope procedure, introducing additional design criteria to facilitate the implementation of the method in realistic bridges. The key issue in the extended procedure (Fig. 2.2), called '*modal direct displacement-based design*' (MDDBD), was the proper definition of $N + 1$ target-displacement profiles (where N represents the number of significant modes) and equal in number equivalent SDOF systems for applying the EMSh method and estimating the peak 'modal' earthquake forces. Each of the N SDOF structures was related to a corresponding modal target displacement profile, whereas the additional SDOF (used for iteration-control purposes) was associated with the combined modal profiles. The peak 'modal' response was then obtained by conducting N structural analyses (as many as the significant modes) of the

MDOF under the modal load patterns. The response quantities of design interest (displacements, plastic hinge rotations, internal member forces) were determined by combining the peak 'modal' responses (i.e. the *N* structural analyses) using an appropriate modal combination rule, and superimposing the pertinent combinations of permanent and transient actions. Additional issues addressed, included the proper consideration of the pier columns' degree of fixity to the deck by explicitly accounting for the equivalent cantilever pier heights (i.e. the span ratios), and the significance of a rational consideration of the superstructure torsional stiffness throughout the design procedure. MDDBD was found capable to properly predict the displacement response, and at the same time, define the corresponding peak structural response in terms of internal member forces accounting in both cases for the effect of higher modes.

Several developments in the DDBD method regarding geotechnical aspects of seismic design were recently summarised by Calvi *et al*. (2014), including an approach for the approximate consideration of nonlinear dynamic soil-structure interaction effects in the case of shallow foundations (Paolucci *et al*. 2013) while a similar procedure was proposed by Deng et al. (2014) to address rocking-dominated soil-foundation effects in the seismic response of bridge piers rigidly connected to the deck. Although in their current state of development the latter approaches attempt to consider the beneficial effect of rocking response in individual piers (rather than in MDOF systems), an exploration of rocking foundations as an isolation mechanism is clearly sought.

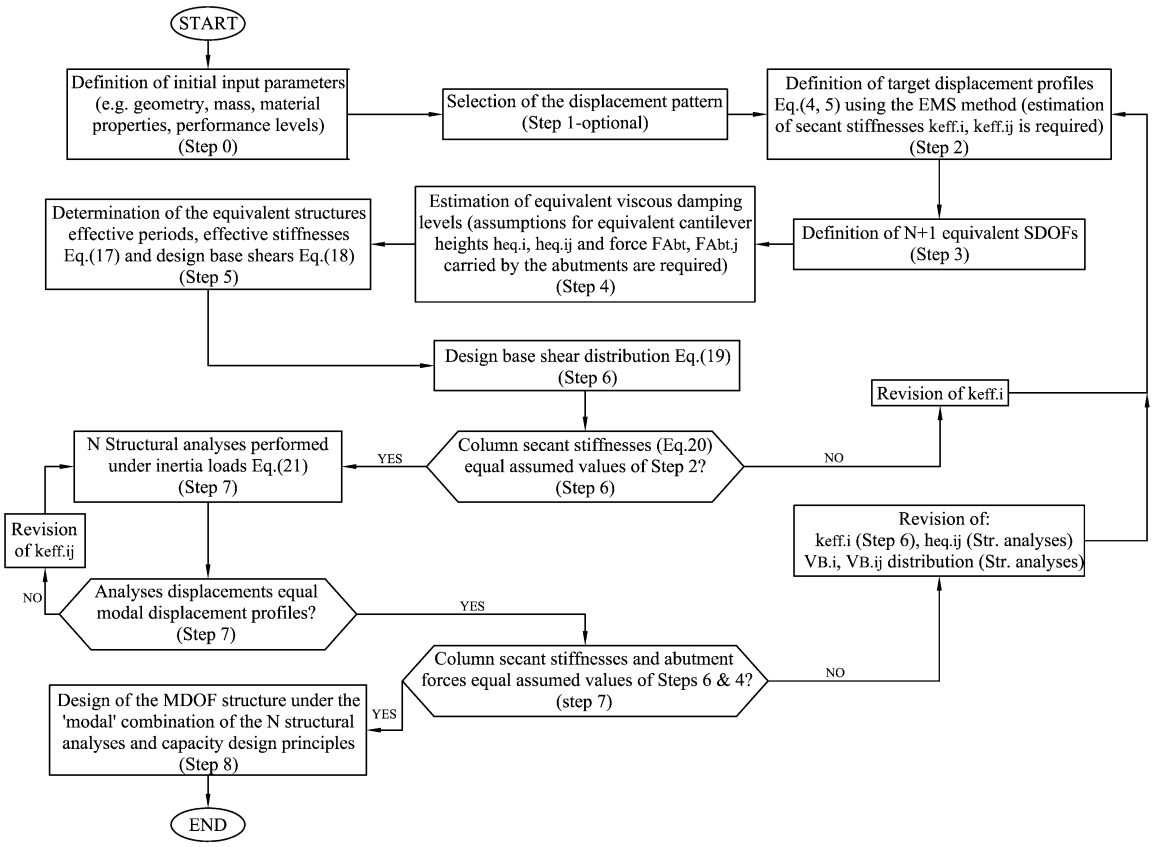

Fig. 2.2 Modal direct displacement-based design of bridges (Kappos *et al*. 2013)

In an alternative approach, that could qualify as *'indirect' displacement-based design* of bridges (§2.1), the concept of calculating inelastic deformation demands from elastic analysis, previously used by Fardis and co-workers for buildings (Panagiotakos & Fardis 1999, 2001), was extended to concrete bridges (Fardis 2007, Bardakis & Fardis 2011a). The structural systems considered, involved bridges with yielding piers, monolithic pier-to-deck connections, and superstructure restrained at the abutments in the transverse direction of the bridge (but free to move in the longitudinal direction). The methodology in its latest version (Bardakis & Fardis 2011a), initiates with the design of the structural system for non-seismic loads and proceeds to the estimation of the effective stiffness of members. In the case of in-plane bending of the deck, the adopted effective stiffness corresponds to the slope of the line connecting two characteristic points in moment-curvature (M-φ) curves, derived from section analysis of deck sections, to approximately account for the non-symmetric section and detailing of the deck. The first point corresponds to tendon-decompression under bending moments applying tensile stresses to the mean tendon, and the second point corresponds to yielding of common (non-prestressed) reinforcement for bending moments applying tensile stresses in the area of the deck section opposite to the mean tendon. Secant to yield stiffness is assumed for out-of-plane bending of the deck (i.e. about the vertical axis of the bridge) and bending of the piers. In the latter case (i.e. piers) secant to yield stiffness is provided from state-of-the-art equations accounting for the geometry and detailing of the section, while empirical equations are also provided to facilitate the implementation of the procedure at the first stage of design/iterations (Biskinis & Fardis 2010a). Inelastic deformation demands (i.e. chord rotations at pier ends, curvatures at deck sections) are then estimated for the two horizontal components of the 'design earthquake' through 5%-damped modal response spectrum analyses based on the effective stiffness of bridge members, and the 'equal displacement' approximation for member deformations. Modification factors derived from parametric NLRHA of different types of bridges (with respect to their structural regularity) are employed to account for differences in deformation demand quantities calculated from nonlinear dynamic and linear response spectrum analysis (Bardakis & Fardis 2011b). Pier flexural strength is estimated based on the peak inelastic deformation demands and assuming a uniform rotational ductility factor across the piers, while their transverse reinforcement is designed on the basis of providing a capacity larger than the required deformation demand (Biskinis & Fardis 2010b). Non-yielding of the deck under the peak deck curvatures is ensured by increasing prestress and/or the reinforcing steel over those quantities derived from the initial design under non-seismic loads. Finally, verification of bridge members in shear follows capacity design principles. The procedure is repeated so long as the effective stiffness of members calculated on the basis of the final geometry and detailing of members differs from the values used in response spectrum analysis of the bridge. Interestingly, the use of elastic response history (in lieu of response spectrum) analysis is suggested by the authors as a means to capture more effectively the dynamic characteristic of the studied bridge, and NLRHA is set as the final verification step when piers have significantly different height.

Unlike the previous design procedures based on *linear* equivalent static or dynamic analysis, there is no complete PBD method for bridges adopting *nonlinear* static (pushover), dynamic (response history), and incremental dynamic analysis. Since modelling of the nonlinear response of pier members requires prior definition of both their geometry and strength, which in reinforced concrete members is a function of detailing, nonlinear analysis has been so far integrated mainly within assessment rather than design methods. Among them, nonlinear static analysis methods have attracted the interest of practitioners, due to their appealing 'static' interpretation of dynamic excitation and response. Conceived as easier-to understand/implement compared to the more evolved NLRHA in terms of computational complexity (modelling of seismic input and hysteretic response), and analysis effort (sophisticated tools, post-processing), several alternative approaches were evolved.

According to the concepts first introduced by Freeman *et al*. (1975), and Fajfar & Fischinger (1987), laying the basis for the *capacity spectrum*, and the *N2* method, respectively, nonlinear static analysis based methods consist of a two-stage approach. During the first stage, the deformation capacity of an initially designed structural system is assessed via nonlinear static analysis resulting in a force-displacement response function, which in turn is used for the equivalent SDOF representation of the MDOF structure. The second stage focuses on the estimation of the inelastic displacement demand of the SDOF system under a specific level of seismic action. Alternative approaches (also adopted by several guidelines and code standards) estimate the inelastic demand on the basis of elastic spectra and correction coefficients (e.g. Nassar & Krawinkler 1991, FEMA 1997), over-damped spectra implicitly accounting for inelastic response similarly to DDBD (Freeman *et al*. 1975, ATC 1996), and inelastic spectra (Fajfar 1999, CEN 2004b, Chopra & Goel 1999). The static nonlinear analysis of the MDOF system is subsequently repeated (considering the SDOF displacement demand) to determine the inelastic response of individual members under the considered level of seismic actions. In an attempt to broaden the field of application of this concept to irregular structural systems with significant contribution of higher modes, different research groups extended the single-mode pushover approach with invariant (e.g. the N2 method; Fajfar & Fischinger 1987, Fajfar 2000, 2007) or adaptive (Aydınoğlu & Önem 2010) load/displacement patterns, to multi-mode procedures based on independent modal pushover analysis with invariant modal load patters (i.e. the modal pushover analysis - MPA – method; Chopra & Goel 2002), simultaneous multi-mode analysis with modal adaptive displacement patterns (i.e. the incremental response spectrum analysis - IRSA – method; Aydınoğlu 2004), and single-run pushover analysis with modal combined adaptive load/displacement patterns (e.g. the modal adaptive nonlinear static procedure - MANSP – method; Bracci *et al*. 1997). The adaptation of these methods to bridge structures has been also under scrutiny; e.g. the N2 by Isaković & Fischinger (2006, 2014), Isaković *et al*. (2008b), the MPA by Paraskeva *et al*. (2006), Paraskeva & Kappos (2010), Isaković & Fischinger (2011), the IRSA by Aydınoğlu & Önem (2009), Isaković & Fischinger (2011), and the MANSP by De Rue (1998). In the book by Kappos *et al*. (2012b) the above bridge-specific methods are reviewed, highlighting the problems encountered while

providing useful guidance with respect to the field of application and the proper implementation of each approach.

In a similar context, nonlinear dynamic analysis (Clough & Penzien 2003, Chopra 2012) and its pushover-type counterpart, i.e. incremental dynamic analysis (Vamvatsikos & Cornell 2002, 2004), have been extensively used over the last years as the most general, advanced, and rigorous assessment tools for virtually all types of structural systems including bridges (e.g. Falamarz-Sheikhabadi & Zerva 2016). The current state of development in the history representation of seismic action (Douglas & Aochi 2008, NEHRP 2011), the modelling of geometric and material nonlinearities with specific applications to bridge elements (Priestley *et al*. 1996, Chen & Duan 2003, Aviram *et al*. 2008, Kappos 2015b), soil-structure interaction and spatial variability of ground motion phenomena (Sextos 2013), along with the development of sophisticated software and the increase in computational power, paved the way towards the adoption of nonlinear dynamic analysis within evolved probabilistic/resilience-based design/assessment (Mackie & Stojadinović 2003, Karamlou & Bocchini 2015) and optimisation-based design frameworks (Fragiadakis *et al*. 2015). Despite being at the forefront of research efforts, these procedures can hardly be justified in a practical design context, particularly within design codes, leaving a considerable gap in practical design methodologies integrating nonlinear dynamic analysis in a deterministic context. The most notable exception in this respect, besides some earlier relevant attempts (e.g. Stone & Taylor 1994), is the *deformation-based design* (Def-BD) method proposed for the seismic design of buildings (Kappos 1997, Kappos & Manafpour 2001, Kappos & Panagopoulos 2004). The methodology proposed a deformation-calculation-based deterministic framework adopting both displacement and performance-based principles by means of explicitly addressing multiple performance levels in a single-run, contrary to the previously described elastic and nonlinear static approaches. However, it has not been tailored to bridges, and therefore falls beyond the scope of this section. Nevertheless, a brief description of its historic development along with its potential capabilities are presented in §2.4, since it represents the starting point of the present study.

In principle, nonlinear (static or dynamic) analysis can be applied for DBD adopting a deformation-calculation-based approach, i.e. calculation of the expected maximum displacement for an already designed structural system. Detailing can then be provided such that the displacement capacity of the bridge and its components exceeds the calculated maximum displacement. If a specific target performance is sought, subsequent iteration in proportioning of members may upgrade the previous concept to a deformation-specification-based approach in line with §2.1. Immediately perceived in such a design approach, is the associated computational effort especially when specific guidelines and rules towards convergence are missing, rendering as potential candidates for implementation only the relatively simple nonlinear-based approaches, such as the N2 method. Nevertheless, the above framework represents the current state-of-the-art in design codes and standards reflecting the long-expected recourse of codes to pure displacement-based design principles, as opposed to the force-based approaches that still remain the norm in seismic codes worldwide (e.g. CEN 2004b, 2005a, AASHTO 2012, ASCE 2016). The US *Guide*

Specifications for LRFD Seismic Bridge Design (AASHTO 2009, 2011) is in support of this trend, providing a design alternative to the force-based standard design practice in the USA prescribed in the *LRFD Bridge Design Specifications* (AASHTO 2012). Instead of prescribing a unique design route to the determination of pier design forces, AASHTO (2011) aims to ensure that the pier displacement demand is less than the displacement capacity, provided that non-seismic action effects and minimum detailing requirements are satisfied (which provide initial estimates of stiffness and strength). The displacement demand is calculated on the basis of elastic analysis properly adjusted through coefficients to approximate inelastic displacements. The displacement capacity, controlled by the longitudinal and transverse reinforcement of the piers, is assessed either through empirical equations or nonlinear static analysis, depending on the seismicity of the area. The pier design process is concluded when adequate displacement capacity is provided, followed by capacity design, and in this respect, AASHTO (2011) retains the single-performance level design of traditional codes. In the recent ACI-341 report (ACI 2016) an explicit definition of bridge performance levels is made, as a function of pier drift accounting for the equivalent cantilever pier height and the axial load ratio. Providing a simple means for constraining the drift demand below predefined limits associated with specific structural performance levels, the ACI approach may be interpreted as a first attempt to extend the AASHTO (2011) method to a multi-level performance-based design procedure.

Although in Europe the departure from force-based principles has not yet been realised within the EN1998-2 bridge design code (CEN 2005a), the previous trends toward deformation-calculation and deformation-specification-based approaches are confirmed in the recently released *Model Code 2010* (MC2010) (*fib* 2012a, b). Serving as a point of reference for future codes and standards, and covering the design and the assessment of new and existing structures, MC2010 builds upon previous developments included in EN1998-3 (CEN 2006), i.e. the European standard for the seismic assessment and retrofitting of buildings. Contrary to the displacement-based single-level verifications of the US standards, MC2010 requires explicit deformation-based verifications (i.e. member chord rotations) under at least two out of the four provided performance levels (Table 2.1) (Fardis 2013), i.e. operational or immediate use, and life-safety or near-collapse. Nonlinear dynamic analysis is set as the reference analysis method for deformation demand estimation as opposed to modal response spectrum analysis in EN1998-1, -2 (CEN 2004b, 2005a) and nonlinear static analysis (i.e. the N2 method) in EN1998-3 (CEN 2006). Notably, simple, yet efficient, nonlinear finite element models accounting for significant variations in the axial force of members and stiffness degradation are deemed adequate for the estimation of peak inelastic response in the design of new structures. The deformation capacity of members is estimated by a proposed physical model or by purely empirical expressions largely based on previous work by Fardis and co-workers (e.g. Biskinis & Fardis 2010b, 2013).

2.2.2 Problems associated with 'practice-oriented' DBD methods

Despite the fact that elastic analysis is currently adopted as the reference method in most codes for the seismic design of both buildings and bridges (e.g. CEN 2004b, 2005a), indicating procedures, such as DDBD, as excellent candidates for a smooth upgrade of codes towards more sophisticated methods of design (i.e. nonlinear analysis, explicit multi-performance objectives, probabilistic frameworks), the expected transition has not occurred yet, i.e. more than 20 years after they first appeared. Although the advantages of DBD procedures over traditional force-based approaches (*fib* 2003) are recognised, the fact remains that DBD procedures based on standard linear static and even dynamic analysis are applicable to a class of bridges only, involving regular configurations where the structural response can be reasonably approximated either by a 'substitute' SDOF structure (e.g. Priestley *et al*. 2007) or by 'equal displacement/deformation' rules applied to MDOF systems in combination with adjustment factors and calibration studies (e.g. Bardakis & Fardis 2011a).

Table 2.1 MC2010: Performance levels and associated levels of seismic action for ordinary facilities (Fardis 2013)

Performance limit state	**Facility operation**	**Structural condition**	**Deformation limit in *fib* MC2010**	**Seismic action per *fib* MC2010**
Operational (OP)	Continued use; any non-structural damage is repaired later	No structural damage	Mean value of yield deformation	Frequent: ~ 70% probability of being exceeded in service life
Immediate use (IU)	Safe; temporary interruption of normal use	Light structural damage (localized bar yielding, concrete cracking / spalling)	Mean value of yield deformation may be exceeded by a factor of 2.0	Occasional: ~ 40% probability of being exceeded in service life
Life safety (LS)	Only emergency or temporary use; unsafe for normal use; no threat to life during earthquake; repair feasible but possibly uneconomic	Significant structural damage, no imminent collapse; capacity for quasi-permanent loads and sufficient seismic strength / stiffness for life protection until repair	Safety factor γ^*_R of 1.35 against lower 5% fractile of plastic rotation capacity	Rare: 10% probability of being exceeded in service life
Near collapse (NC)	Unsafe for emergency use; life safety during earthquake mostly ensured but not fully guaranteed (hazard from falling debris)	Heavy structural damage, on the verge of collapse; strength barely sufficient for quasi-permanent loads, but not for aftershocks	Lower 5% fractile of plastic rotation capacity may be reached (γ^*_R = 1.0)	Very rare: 2–5% probability of being exceeded in service life

Key sources of the narrow scope of these methods are the reliability of equivalent linearisation approaches, and the important role that higher modes play in the inelastic response of bridges, even in some relatively short ones (Kappos *et al*. 2013). The first issue has attracted the interest of various research groups resulting in relevant comparative studies evaluating different linearisation approaches, such as those by Jennings (1968), Iwan & Gates (1979), Miranda & Ruiz-Garcia (2002), Makris & Kampas (2013a), to mention only a few. Besides the critique of equivalent

linearisation approaches included in the previous studies with regard to their ability to accurately predict the inelastic response or describe the modal properties of inelastic SDOFs, a persisting complication lies in the problematic transition from global SDOF response demand to local inelastic deformation demand of members. The issue was partially tackled with nonlinear static procedures since an MDOF nonlinear model of the bridge is 'pushed' to the target displacement providing a detailed representation of inelastic demand distribution, however the definition of seismic demand (as reflected on the target displacement) employs once more approximate linearisation approaches (Chopra & Goel 2000). Nevertheless, this partial treatment favoured their adoption in codes of practice for the assessment and/or design of bridges (§2.2.1). The extension of DBD methods to explicitly consider the effect of higher modes in bridge seismic design by employing eigenvalue analysis considerations has been presented for both linear (e.g. MDDBD) and nonlinear static-based (e.g. MPA, IRSA) methods resulting in both cases in encouraging results (Kappos *et al*. 2012b, Kappos *et al*. 2013). However, these methods may be conceived as too complex especially when juxtaposed with their initial objective, i.e. to avoid complex nonlinear dynamic analysis. In this regard, methods that intrinsically incorporate modal analysis may be more appealing (e.g. Bardakis & Fardis 2011a), albeit at the expense of increased uncertainty in estimating the response of irregular systems.

Further implications limiting the field of application may derive from limitations inherent in each method. A typical example refers to the case of 'direct' methods, such as DDBD, where a strict 'design route' is defined, starting from target displacements/deformations and heading towards the specification of the member properties required to achieve the target performance under a specific level of seismic action. A general limitation in this respect is the fact that not all bridges are, or should be made, displacement-controlled. There are two typical 'scenarios' wherein DDBD may not be meaningful (Kappos *et al*. 2012a). The first is associated with regions of low, moderate, and even moderate-to-high seismicity, where the maximum displacement associated with the corner period defining the beginning of the constant displacement branch of the spectrum (T_D) is lower than the yield displacement of the piers, even when no additional viscous damping (accounting for inelastic response) is introduced. It should be noted here that the long period range of displacement spectra (beyond about 2 s), which is quite important for displacement-based bridge design methods involving secant stiffnesses at maximum displacement, is not reliably represented in EN1998-1 (CEN 2004b) due to the paucity of digital records of ground motion with frequency content rich in this long-period range; however, significant work in this direction was recently carried out within the SHARE project (e.g. Weatherill *et al*. 2013). The second case refers to configurations of bridges where substantial displacements, accompanied by inelastic action, are not permitted, such as, the case of bridges with tall piers, or the case of short bridges with their deck restrained at the abutments (via seismic links, or monolithic pier-to-deck connection).

Returning to the issue of the computational effort involved in practice-oriented analysis methods, it should be underlined that iterations are an integral part of the design process when realistic (i.e. MDOF) structural systems are involved, irrespective of the earlier 'deformation-

specification' or 'deformation-calculation' characterisation of methods. With no exception, the DBD procedures presented in §2.2.1 involve iterations due to various reasons. The fundamental one, is that bridge structures (as most structural systems) are designed to withstand diverse actions that may include dead loads, prestressing, traffic, environmental actions and natural hazards. In cases wherein the dominant action cannot be clearly foreseen or simply does not exist (e.g. cases of low to moderate seismicity), iterations will be required to specify cost-effective design solutions that entail the specification of structural member topology and geometry (frequently considered 'given' in DBD procedures), while satisfying the requirements deriving from different combinations of actions. Additional complexity may arise by minimum requirements applied for dimensioning and detailing of reinforced concrete members resulting in further iterations or even loss of the advantages of a DBD design with regard to achieving specific (target) performances.

In the case of the 'direct' procedures, iteration will be introduced for several reasons typically associated with the assumptions of the adopted equivalent linearisation approach including among others the definition of the 'substitute' SDOF system (e.g. equivalent damping ratio, assumed displacement profile), the consideration of the degree of fixity of piers to the deck, soil-structure interaction phenomena and higher mode effects (Fig. 2.2). 'Indirect' deformation-calculation/ specification based approaches typically involve more detailed representations of the structure inherently integrating most of the previous issues. Herein, iterations will be introduced as a means to optimise the cost of the selected design solution employing in most cases of practical design an iterative mode, unless the bridge is overdesigned, rather than designed to meet reasonably closely the selected performance criteria, which would result in an economic design.

Irrespective of the adopted method, the required computational effort will also be a function of the number of directly controlled design parameters (Kappos 2015a). Satisfaction of limitations associated with the preferred performance measure adopted in each method, e.g. displacements in Priestley *et al*. (2007), drifts in ACI (2016), member deformations and stains of materials in Bardakis & Fardis (2011a), does not necessarily result in the overall satisfaction of the performance of the structural member or the entire system. Even when the correlation of different performance measures is assessed in detail in each iteration (e.g. by employing M-φ analysis when detailing is revised etc.), additional performance measures may be required to evaluate different design requirements. For example, control of pier displacements to avoid impact may be required in addition to target chord rotations based on allowable strains and pier span ratios, or in the case of elastomeric bearings, both stability and peak elastomer strain criteria may need to be fulfilled under a single performance level. An issue that deserves some consideration in the above discussion is that the increase of the number of iterations (and the associated computational time and effort) does not ensure either the accuracy of the results or the convergence of the iterative analysis, as shown in various studies (e.g. Chopra & Goel 2000, Kappos *et al*. 2013). On the contrary, both convergence and accuracy are functions of the approximations adopted in each methodology, e.g. efficiency of the secant stiffness and the equivalent viscous damping in predicting the inelastic response. An exception to the above rule is the case of nonlinear dynamic analysis where

refinement of the input data (e.g. consideration of a large number of representative records) is expected to yield more accurate results.

A final remark concerns the explicit consideration of multiple performance levels, i.e. a prerequisite for a method to be classified as a performance-based one, according to §2.1. Apart from the case of the Def-BD method (Kappos & Manafpour 2001) (based on NLRHA and referring to seismic design of buildings, §2.4), the DBD methods described in §2.2.1 based on linear static/dynamic and nonlinear static analysis, do not provide specific guidelines with regard to a multi-performance level application. Even when explicit consideration of various performance levels is required, e.g. in the ACI-341 (ACI 2016) and MC2010 (*fib* 2012a, b) approaches, guidelines are provided with respect to limit values of the adopted performance measure (e.g. drift, chord rotation), implying that an independent application of the entire procedure is required whenever a different performance level is checked.

2.3 Seismic Design of Bridges Integrating Structural Control Devices

2.3.1 Structural control approaches

Structural control systems aiming at the favourable response of structures that enable cost-effective construction and control of damage under different types of actions, can be classified according to the following four categories based on their operational mechanisms (Housner *et al*. 1997, Symans & Constantinou 1999):

- *Active control systems*: These are systems wherein an external (typically large) power source controls electrohydraulic or electromechanical actuator(s) that apply forces to the structure in a prescribed manner, based on feedback from sensors (optical, mechanical, electrical, chemical, etc.) that monitor either the excitation (feedforward/open loop control) or the structural response (feedback/closed loop control) or both (feedback-feedforward/closed-open loop control); the controlled forces can be used both to add and to dissipate energy in the structure. Active control systems are characterised by increased adaptability to a broad range of excitations.

- *Semi-active control systems*: External energy requirements in these systems are orders of magnitude lower than typical active control schemes. Typically, semi-active control devices do not add mechanical energy to the structural system. Control forces are developed as a result of the structural response (i.e. reactions) while their intensity is adjusted from the external power source based on closed/open/closed-open control. Semi-active control devices are often viewed as controllable passive devices, combining the adaptability of active systems and the reliability (due to the low energy requirements) of passive systems.

- *Passive control systems*: External power source is not required for operation in this type of control scheme; passive control devices impart forces in response to the motion of the structure. The energy in a passively controlled structural system cannot be increased by the passive control

devices; hence, these systems are inherently stable and relatively simple to design and construct. However, passive control systems are unable to adapt to structural changes and/or to excitations of different frequency content and intensity from that used for their design. In view of the previous remarks, systems were developed that can passively adapt their characteristics (i.e. *adaptive passive*) based on their internal construction (e.g. displacement-dependent behaviour of spherical sliding isolation bearings, Fenz & Constantinou 2008) instead of sensors and controllers; they aim at a system with improved characteristics compared to a purely passive one.

- *Hybrid control systems*: In this case, passive and semi-active or active control devices are combined in order to enhance the structural performance and alleviate the limitations of a purely active, semi-active or passive system, albeit at the expense of increased complexity and cost (especially of maintenance).

Implementation of the aforementioned control principles to mitigate undesirable vibrations of dynamically excited civil engineering structures in seismically-prone areas has attracted the attention of the research community in the last four decades resulting in diverse types of control devices (Table 2.2, Table 2.3, based on Soong *et al*. 1991, Housner *et al*. 1997, Spencer & Nagarajaiah 2003, Basu *et al*. 2014). Indeed, numerous devices have been successfully deployed world-wide to mitigate vibrations induced in civil structures by earthquake, wind, and human activities (Martelli *et al*. 2014). Passive base isolation (elastomer-based, sliding-based), supplementary energy dissipation (hysteretic, viscoelastic) devices, and combinations thereof, represent currently the norm in structural control seismic applications to bridges, involving primarily (but not exclusively) the use of low or high damping elastomeric bearings (LDRB/HDRBs), lead-rubber bearings (LRBs), flat sliding bearings (FSB), friction pendulum bearings (FPBs)), linear (LVDs) or nonlinear viscous fluid dampers (NLVDs), and less frequently metallic yield dampers (MYD) (Buckle *et al*. 2006, *fib* 2007, Constantinou *et al*. 2007b, 2011). On the other hand, only a relatively limited number of active, semi-active, and hybrid control solutions have been deployed in full-scale bridge applications to mitigate the effects of mainly non-seismic actions (Gkatzogias & Kappos 2016b), a fact that can be predominantly attributed to the reluctance of designers and the construction industry to adopt new technologies which, in many cases, are associated with high capital and maintenance cost.

Introduction of structural control techniques in seismic bridge applications aims at the reduction and redistribution of inertia forces (accelerations) in the superstructure and substructure elements (i.e. pier, abutments). This is achieved by introducing a continuous isolation interface between the deck and the substructure with low shear stiffness resulting in the elongation of the fundamental period of the bridge, while energy dissipation devices are optionally employed to control the subsequent increase of relative displacements at the isolation interface. The fundamental design principles of passive structural control systems, explicitly stated in modern bridge and building design codes (e.g. CEN 2005a, AASHTO 2010, ASCE 2016), may be summarised as follows;

Table 2.2 Classification of passive control devices

System	Typical control devices			Full-scale applications	Advantages	Disadvantages
Passive & adaptive passive	Base isolation:	Elastomeric bearings		Buildings & Bridges	Simple	Large displacements
		Lead-rubber bearings		Buildings & Bridges	Low cost	"Fixed" behaviour in general (adaptive passive devices 'adapt' their characteristics based on displacement aplitude)
		Sliding bearings		Buildings & Bridges	Easy to install	
		Sliding friction pendulum		Buildings & Bridges	Easy to maintain	
		Combination of bearings		Buildings & Bridges	No external energy	
		Other:	Spring-type systems	Buildings	Inherently stable	
			Rocking systems	Bridges		
			Sleeved-pile isolation system	Buildings		
			Roll-n-cage isolator	-		
	Energy dissipation:	Hysteretic devices:	Metallic yield dampers	Buildings & Bridges		
			Friction dampers	Buildings		
		Viscoelastic devices:	Viscoelastic solid damper	Buildings		
			Viscous fluid dampers	Buildings & Bridges		
		Re-centring devices:	Pressurized fluid damper	Buildings & Bridges		
			Preloaded spring-friction damper	Buildings & Bridges		
		Phase transformation devices	Shape memory alloy dampers	-		
		Dynamic vibration absorbers:	Tuned mass dampers (TMD)	Buildings & Bridges		
			Adaptive tuned mass dampers	-		
			Tuned liquid dampers	Buildings & Bridges		
			Tuned liquid column dampers	Buildings & Bridges		
		Other:	Coupling adjacent structures devices	Buildings		
			High damping rubber bearings	Buildings & Bridges		
			Rubber composite damper	Bridges		
			Cables surface profiling	Bridges		
			Negative stiffness devices	-		
			Impact damper	Bridges		

Table 2.3 Classification of semi-active, active, and hybrid control devices

System	Typical control devices		Full-scale applications	Advantages	Disadvantages
Semi-active (SA)	Variable orifice dampers:	SA viscous fluid damper	-	Easy to install Low external energy requirements Inherently stable Reliable	Increased cost (compared to passive systems) Limited control capacity
		SA vibration absorber	-		
		SA hydraulic damper	Buildings		
		Accumulated SA hydraulic damper	-		
	Stiffness control devices:	SA variable stiffness device	Buildings		
	Friction control devices:	Electromechanical actuator device	-		
		Piezoelctric friction dampers	-		
	Controllable fluid dampers:	Electrorheological dampers	-		
		Magnetorheological dampers	Buildings & Bridges		
	Adjustable tuned mass dampers		Buildings		
	Adjustable tuned liquid dampers		-		
	SA impact damper		-		
	Electro-inductive devices		-		
	SA negative stiffness devices		-		
Active	Active tendon system		-	"Smart" systems High adaptability	Increased cost Complicated systems External energy requirements Not inherently stable
	Active bracing system		-		
	Active mass damper (AMD)		Buildings & Bridges		
	Pulse generation system		-		
	Piezoelectric actuators		-		
	Active gyroscopic stabilizer		Buildings		
	Active damping bridge		Buildings		
	Negative stiffness devices		-		
Hybrid	Hybrid base isolation system (e.g. base isolation + SA dampers/active tendon)		Buildings	"Smart" and reliable systems	Lower cost (compared to active systems) Complicated systems
	Hybrid mass damper (e.g. TMD + actuator, AMD+TMD)		Buildings & Bridges		
	Hybrid damper-actuator bracing control (passive systems + hydraulic actuators)		-		

(*i*) support the superstructure and relevant vertical actions (i.e. high axial stiffness), (*ii*) provide lateral flexibility (i.e. beneficial effect of period shift) while being able to sustain non-seismic actions (e.g. brake, wind actions), (*iii*) provide energy dissipation to control relative displacements, and (*iv*) possess sufficient recentring (or restoring) capability to prevent substantial residual displacements. Investigation of the structural response of the considered bridge should address three critical states, namely, the state of peak deformation (critical for the deformation capacity of passive devices), peak total acceleration (critical for the design of substructure elements), and peak velocity (critical for the resistance of velocity-dependent energy dissipation devices). The fundamental design requirement in the above investigations is the elastic or limited inelastic response of the substructure considering the potential range of mechanical properties of devices due to external factors (e.g. corrosion, temperature, etc.). Among the different types of 'advanced' structural control techniques (Table 2.3), semi-active control emerges as a rational combination of efficiency and cost, since, in addition to the above principles, it makes it feasible to modify the characteristics of a structural system, for it to respond favourably to different types of excitation (i.e. increased adaptability compared to passive control systems), while having the potential of achieving the performance of pure active control systems without requiring large external power supply (a portable battery can be sufficient in most cases), and thus, resulting in enhanced reliability.

Overall, the socioeconomic consequences of earthquake damage to bridges can be grave (human casualties, emergency response operation interruption, long-term economic cost due to the need for alternative transportation routes during repair, retrofit, or replacement), while the performance of bridges during recent strong earthquakes was found to be not fully satisfactory (e.g. Maule, Chile 2010, Kawashima *et al*. 2011), and the size of the bridge stock exposed to seismic risk is ever increasing. Hence, it is anticipated that passive technology for mitigating seismic risk to bridges will continue to increasingly attract the interest of the engineering community in the years to come, potentially resorting to 'non-conventional' structural control techniques, inasmuch as the latter furnish low-cost, reliable, and robust control systems with minimal energy requirements.

2.3.2 Available practice-oriented DBD methodologies

The diversity of the available structural control devices (Table 2.2, Table 2.3) in terms of mechanical properties and induced modification of structural response, introduces an additional challenge in the formulation of performance-based methodologies encompassing displacement-based principles; i.e. to propose a method that is applicable to a broad class of devices in addition to that of structural systems. Among the methodologies presented in §2.2.1, DDBD is among the few that has been extended to seismically isolated structures, specifically bridges, owing to its convenient deformation-specification-based format.

An early direct displacement-based approach for the design of bridges with seismic isolation was presented by Priestley *et al*. (1996) and Calvi & Pavese (1997). The method followed the

general equivalent linearisation approach described in §2.2.1. In isolated bridges, a 'rigid body translation' pattern is assumed in both the longitudinal and the transverse direction of the bridge, i.e. a reasonable assumption in straight isolated bridges due to the low shear stiffness of the isolation interface (resulting in negligible flexural deformations of the deck) and the governing effect it has in suppressing deck torsional modes of vibration triggered by 'non-symmetric' substructures (e.g. piers of different height). Starting from a target displacement of the deck, the isolation system's target displacement at each pier/abutment location is defined by subtracting from the deck displacement a fraction of the pier yield displacement (e.g. 0.85) with a view to ensuring elastic pier response. Following a ductility-based philosophy originating from the yielding response of conventional concrete structures, the method assigns target displacement ductility factors to hysteretic isolators to define their yield displacement; i.e. an approach currently not preferred for isolation systems due to the uncertainty with regard to the definition of the yield displacement in common hysteretic isolators and its marginal significance for the peak response (Makris & Kampas 2013b). Equivalent viscous damping ratios are first calculated at each pier-isolation subsystem (i.e. consisting of the pier column members and the isolators on top of the pier) based on stiffness proportionality and accounting for both viscous (e.g. LVDs) and hysteretic (e.g. LRBs) sources of damping. The bridge system equivalent viscous damping ratio is then calculated as a weighted average of the different pier damping ratios based on the deck tributary mass of each pier/abutment. The design base shear, calculated following the procedure of §2.2.1, is distributed to the pier-isolation subsystems in proportion to the supported weight without requiring static analysis, and capacity design principles are used for the design of piers. Priestley *et al*. (2007) maintained the basic principles of the above procedure, substituting the 'target ductility' design strategy of hysteretic isolators with device-specific target equivalent damping ratios, defined nevertheless as a function of displacement ductility. The provided equations were largely based on the semi-empirical equivalent linearisation approach proposed by Grant *et al*. (2005) and Dwairi *et al*. (2007). Some further guidance for the design of isolators and dampers at the last step of the procedure was also provided, while the alternative of calculating the system global equivalent damping on the basis of the work done in each pier-isolation subsystem was also mentioned (Priestley *et al*. 2007, Calvi *et al*. 2013).

A more detailed displacement-based procedure with specific application to bridge decks isolated through bilinear isolators was presented by Jara & Casas (2006), providing specific guidelines for LRBs. A key issue in this proposal was the definition of the deck target displacement as the sum of independently defined pier and isolator target displacements based on allowable material strains. Inelastic response of pier members was allowed under seismic actions associated with a low probability of exceedance, a design approach not supported by earlier and more recent research studies (§2.3.3). The mechanical properties of LRBs and the pier geometry-detailing were iteratively specified until convergence to the target deck displacement was achieved, using the standard DDBD equivalent linearisation approach; i.e. secant stiffness at maximum response, combined with an empirical equivalent damping ratio proposed for the specific case of typical LRB

isolators. The derivation of the equivalent damping ratio followed the equivalent linearisation approach of Iwan & Gates (1979) based on the minimisation of the root mean square of the difference between the spectral displacements of a bilinear system and a family of potentially equivalent linear systems; the proposed model was later updated by Jara *et al*. (2012). Equivalent viscous damping ratios at the pier-isolation subsystem were calculated using a refined approach presented by Franchin *et al*. (2001) for the extension of equivalent linearisation approaches to MDOF bridge systems as described later.

The most complete DDBD approach for the design of isolated bridges addressing a wide range of isolation and energy dissipation devices was proposed by Cardone *et al*. (2009). The most interesting aspect of this approach is the provision of a specific design tool at the start of the design process that provides some useful guidance to the designer during the initial selection of the type of devices and the basic properties of the isolation system, an issue that is superficially addressed in earlier versions (e.g. Priestley *et al*. 2007). According to the proposed graphical procedure (Fig. 2.3) using high-damping elastic spectra in the pseudo-acceleration (S_a) vs. displacement (S_d) response spectra (ADRS) format, each type of passive device is characterised by a different range of equivalent viscous damping level (ξ) and hence associated to a different group of response spectra. Some broad limits of effective isolation periods represented by radial lines are first identified corresponding to $3T_{fixed}$ (i.e. three times the fundamental period of vibration of the bridge with fixed pier-to-deck connection) and T_D. The first limit is considered as the minimum effective isolation period having a marked beneficial effect in the reduction of seismic forces due to the period shift, i.e. a controversial criterion in the case of long bridges. The intersections of radial lines with the response spectra provide a preliminary range of possible design displacements, e.g. $u_{01} \sim u_0(T_D)$. This can be further constrained by associating the S_a with the yielding shear force V_y of the piers (i.e. divided with the tributary deck mass m to reflect S_a values in the left-hand side of Fig. 2.3) obtained by allowable longitudinal reinforcing steel ratios (ρ_l).

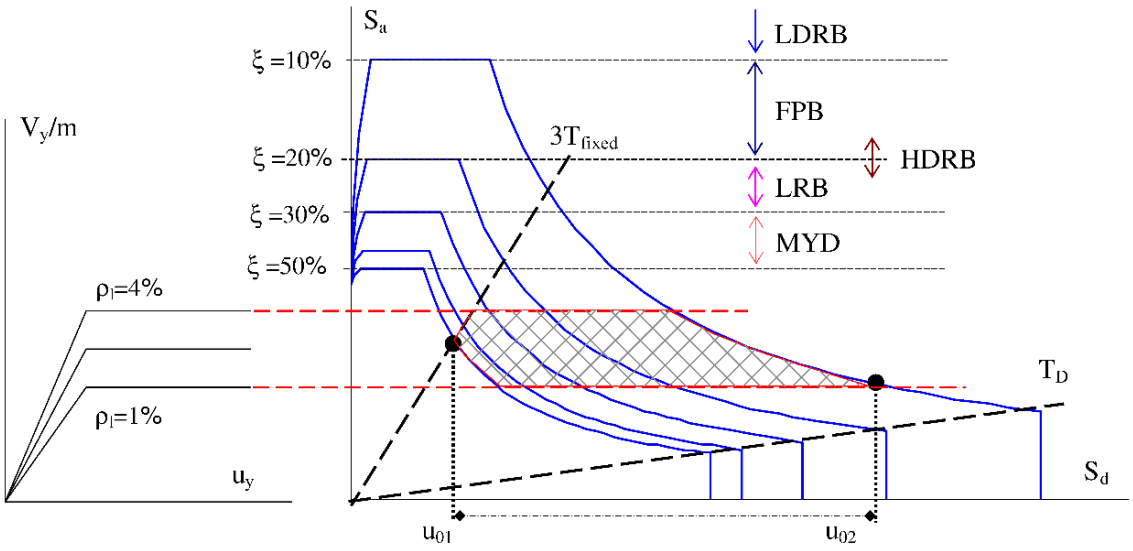

Fig. 2.3 Preliminary selection of isolation system type, design displacement and pier reinforcement ratio (Cardone *et al*. 2009)

Despite its crudeness in the classification of different isolation system devices and the disregard of the actual (i.e. increased) inertia forces transmitted to the substructure at the state of peak total acceleration when viscous dampers are involved, the procedure offers a starting point for the subsequent iterations that in general follow the DDBD procedure proposed by Priestley *et al*. (2007). An additional refinement of the method involves the stiffness distribution of isolators in proportion to the deck tributary masses at the pier/abutment locations, as a means to suppress the deck torsional modes of vibration. It should be noted though that despite the attractiveness of such a design strategy, this approach can hardly be justified in small to moderate bridges since the different isolator properties result in high cost of testing of devices typically required by codes (e.g. CEN 2005a, AASHTO 2010). Furthermore, in an attempt to depart from the purely static approach of analysis and design embraced in the previous methods, modal analysis of the pier-isolation subsystems is introduced to approximate in a more realistic way dynamic response parameters such as the distribution of the deck displacement to the piers/abutment and isolators, and the tributary mass of each subsystem (set equal to its first-mode participating mass) required for the calculation of the equivalent viscous damping ratio at the bridge level (Calvi & Pavese 1997).

A general conceptual design framework integrating passive viscous damper control schemes was presented by Calvi *et al*. (2010) for the special case of cable-stayed bridges. The framework included design considerations for the preliminary sizing of bridge structural members (i.e. deck, pylon, cables) and a DDBD approach for the identification of suitable characteristics for the deck-to-pylon connections in the longitudinal direction of the bridge. According to the latter, a target displacement (i.e. deck displacement relative to the pylon) and system equivalent damping ratio are first selected and the DDBD approach is subsequently followed to estimate the required system effective stiffness and base shear. The stiffness of isolation devices (e.g. LDRBs mounted between the deck and the pylon) is selected as the ratio of the shear force fraction that is not transferred by the cables to the target displacement (reduced to account for the pylon deformation). Dampers are designed at the last step to obtain the target system equivalent damping ratio assessed similarly to Calvi & Pavese (1997).

As in the case of bridges with energy dissipation in the piers, the displacement-based procedures presented so far for isolated systems cannot explicitly account for higher mode effects which can have a significant contribution to the response of highly non-symmetric systems (e.g. long-span and/or curved-in-plan bridges) or deep-valley bridges with massive tall piers. The extension of displacement-based design methods integrating equivalent linearisation approaches to MDOF systems was described in detail by Franchin *et al*. (2001) investigating also the non-proportional (or non-classical) form of the system damping matrix (Chopra 2012) due to the introduced equivalent damping ratios. The suggested procedure facilitates the linear dynamic (response spectrum) analysis of MDOF systems without the requirement to define a ‘substitute’ SDOF system, and it is applicable irrespective of the type of equivalent linearisation approach considered; e.g. based on geometric considerations of energy equivalence (Kowalsky 2002), statistical considerations or error minimisation (Iwan & Gates 1979), etc. Nevertheless, the degree of

accuracy of the method was found conditional on the efficiency of the linearisation approach in predicting the inelastic response of SDOF systems, hence linearisation equations addressing ductility and post-elastic stiffness slope values typical of bilinear isolation systems (e.g. Hwang & Sheng 1993, 1994, Jara *et al*. 2012) rather than yielding concrete members (Kowalsky 2002), are expected to yield better results. According to the method, the equivalent elastic properties of passive devices (i.e. effective stiffness $k_{eff,i}$, equivalent damping ratio $\xi_{eq,i}$) are first assumed and the system damping matrix is assembled considering the damping ratios as hysteretic, thus resulting in damping coefficients in the form of $c_i = 2\xi_{eq,i}k_{eff,i}$ (i.e. instead of viscous $2\xi_{eq,i}\sqrt{m_i k_{eff,i}}$) to avoid the definition of associated masses m_i. The hysteretic damping matrix is subsequently expressed in modal co-ordinates using common transformation rules. By neglecting modal coupling induced by non-proportionality, the hysteretic modal damping factor for each mode is determined from the corresponding term on the main diagonal and the modal equations can be solved. It should be noted that modal coupling is ignored based on previous investigations on a limited number of typical isolated bridge configurations yielding a minor effect of the damping matrix non-proportionality on the response as evaluated through complex modal analysis (Chopra 2012). The procedure requires iterations (due to the integrated equivalent linearisation approach) each one involving a modal and a response spectrum analysis using a response spectrum with modal damping-adjusted ordinates to specify the updated equivalent parameters of passive devices. It should be noted that alternative approaches enforcing the validity of proportionality of the damping matrix by maintaining classical normal modes are also available (Christopoulos & Filiatrault 2006), but such strategies are expected to assign different damping coefficients to viscous dampers raising once more cost issues due to the use of different devices.

Simplified versions of the above displacement-based design procedures represent in general the current state of development in bridge design standards. Typically, for single-mode dominated isolated bridges, European and US codes (e.g. CEN 2005a, AASHTO 2010) introduce an equivalent linearisation approach based on the secant stiffness at the peak displacement, and an equivalent viscous damping ratio derived from geometric considerations of energy equivalence. Contrary to the previous DDBD methodologies, a strict 'design route' aiming at the specification of bridge member properties (e.g. pier, isolators, etc.) resulting in a predefined (target) displacement or damping ratio under a specific level of seismic action is not required, and a more traditional analysis format is prescribed. Device properties are preselected based on engineering judgement and analysis iterations are employed with a view to approximating the inelastic response corresponding to the preselected devices rather than optimising the design solution. In this context, design aids such as equations that provide the damping coefficients of LVDs or NLVD required to obtain a target equivalent damping ratio for the pier-isolation subsystem (Hwang & Tseng 2005) can significantly reduce the required iterations. A simplified version of the method described by Franchin *et al*. (2001) is also typically included in codes to capture the potential contribution of higher modes. The analysis method, disregarding the damping non-proportionality effect, superposes via standard combination rules the isolated and the higher modes with prefixed modal

damping ratios without the need for a detailed calculation of modal damping ratios through proper transformation of the system damping matrix. The system equivalent damping ratio (as derived from the substitute SDOF system) is adopted for the isolated modes, defined as those having periods longer than a fraction (i.e. 0.8) of the fundamental mode (effective) period corresponding to k_{eff}, whereas a default modal damping value (e.g. 0.05) is assigned to all modes with shorter periods.

Irrespective of the accuracy of the above approximations included in both static and dynamic-based linearisation procedures, none of the above methods is able to capture the peak total inertia forces at the critical state of peak total acceleration (representing the peak seismic forces transferred from the deck to the substructure members) and the peak damping forces at the state of peak relative velocity (representing peak viscous damper forces) (§2.3.1), unless the main dissipative source of the isolation system has a purely hysteretic response behaviour. The issue emerges from the deviation of peak total acceleration and relative displacement from their associated pseudo-counterparts when viscous damping energy dissipation mechanisms with high values of damping coefficients are included in long-period structural systems (Chopra 2012), and it has been addressed by various research groups resulting in empirical measures of treatment (e.g. Pekcan *et al*. 1999, Ramirez *et al*. 2002, Palermo *et al*. 2016). In the most advanced code formulation (i.e. as included in ASCE 2016), the peak velocity is first estimated as the product of the pseudo-velocity and a correction factor, the latter being a function of the system equivalent damping ratio and the effective period. The peak seismic forces at the instant of peak total acceleration are subsequently estimated by properly combining the peak forces at the critical states of peak relative displacement and velocity accounting for the nonlinearity of viscous dampers.

The involved assumptions and approximations of the displacement-based equivalent linearisation procedure briefly discussed above, grant nonlinear dynamic analysis a more decisive role in the analysis of isolated bridges more so in the case when viscous damper mechanisms are included. Indeed, most of the described methodologies prompt the implementation of nonlinear dynamic analysis (Priestley *et al*. 2007) as a safeguard-verification tool or even include it as the final step of the design process (Cardone *et al*. 2009). In a similar context, modern codes (e.g. CEN 2005a, AASHTO 2010, ASCE 2016) enforce the use of nonlinear dynamic analysis in the design of isolated bridges when specific conditions apply; these typically are associated with site conditions (reduction of the efficiency of isolators when soil-structure-interaction phenomena are substantial), proximity to active faults (detrimental effects of excessive structural velocities), and upper values of effective period and equivalent viscous damping apply (potentially associated with analysis reliability due to non-proportionality effects). Nevertheless, even when the previous conditions dictate the use of nonlinear dynamic analysis, guidelines are typically provided for the assessment of a previously designed system

An interesting approach towards the adoption of nonlinear dynamic analysis within the design stage of isolated structures, thus providing a design alternative to the equivalent linearisation approaches, was presented by Ryan and co-workers initially for SDOF systems isolated through

hysteretic (bilinear) isolators (Ryan & Chopra 2004a, b, Sayani & Ryan 2009) and later extended to MDOF buildings (Ryan & Chopra 2006). With regard to the studies addressing isolated SDOF systems (having the potential for direct implementation in isolated bridges) the procedure reduces the dynamic equation of motion to a form such that the normalised relative displacement of the isolation system depends only on the isolation period T_p defined from the post-yield stiffness (in line with recent research findings by Makris & Kampas 2013b) and the normalised strength (i.e. system strength relative to the peak ground velocity), as opposed to the parameters of isolation period, non-normalised strength, and seismic intensity (expressed by *PGV*) in the non-normalised case. The yield displacement is treated as a constant parameter having a minor effect on the peak response; i.e. an assumption supported by earlier and recent studies (Makris & Chang 2000, Makris & Black 2004, Makris & Vassiliou 2011). The adopted normalisation allows the uncoupling of the (normalised) response from the level of seismic intensity while minimising the dispersion in peak normalised relative displacements for an ensemble of ground motions representing a specific seismic scenario. In addition, it facilitates the development of design equations for peak inelastic response estimation by statistically processing NLRHA results derived from the previous step. The proposed design equations can address explicitly the effect of bidirectional excitation which is approximately considered in all previous methodologies (typically by statistical directional combination rules); however, in its current form the method is presented independently for LRBs and FPBs isolators disregarding any source of viscous damping.

Guo & Christopoulos (2013) presented more recently, a similar performance-based design procedure for SDOF systems using supplemental dampers. The methodology focuses primarily on the retrofit design of nonlinear frame structures using a 'substitute structure' approach, which is beyond the scope of this section, nevertheless, it is addressed herein primarily because it attempts to provide the designer with graphical tools at the start of the design process with a view to directly assessing the performance of different damping solutions that satisfy a given set of performance targets and system constraints. The graphic design tool (called P-Spectra) relates nonlinear response quantities of SDOF systems to various damping parameters and dynamic system properties. Although P-Spectra construction requires an initial parametric nonlinear dynamic analysis of inelastic SDOF systems for different periods and strengths, the performance of various damping solution can be checked and modified for different performance levels with reduced computation effort at subsequent stages of design.

Despite the suitable adaptive nature of adaptive passive and semi-active devices in meeting efficiently and reliably multiple performance requirements (deriving from different performance levels) while contributing to resilience by reducing damage and repair/replacement time (Domaneschi & Martinelli 2016), there are no integrated broad-scope performance-based seismic design methodologies incorporating such devices. At the current state of their development, relevant 'adaptive-passive' studies focus on device-specific principals of operation, and analytical-experimental validations (Fenz & Constantinou 2008, Attary *et al*. 2015). In addition, in the case of semi-active devices some available general design guidelines are essentially restricted to

buildings (Kurata *et al*. 2002) while using complex structural control algorithms and optimisation techniques to investigate the structural response (e.g. Cha *et al*. 2014).

2.3.3 Problems associated with 'practice-oriented' DBD methods

The remarks associated with the need for iterations, the explicit consideration of a single performance level, and the narrow field of application due to the reduced efficiency of equivalent linearisation methods in estimating the peak response and considering higher mode effects, described in §2.2.2 for bridges with energy dissipation in the piers, generally apply to seismically isolated bridges, too.

Regarding the issue of iterations in bridges integrating passive control devices, attention is drawn to the ability of the methodology to provide design guidelines with a view to facilitating at the early stages of design the selection and comparative evaluation of the alternative isolation and energy dissipation schemes that may be realised by the combination of numerous available devices (Table 2.2). The DDBD approach as proposed by Priestley *et al*. (2007) provides some partial guidance in this respect by setting a target displacement and/or equivalent damping ratio at the start of the procedure. Yet, criteria for selecting these values are not addressed and in any case, are not clearly defined or appropriate, since neither deck displacement nor the system equivalent damping ratios are satisfactory indicators for damage in the isolators and the substructure elements of seismically isolated bridges. Deck displacements may directly indicate the cost of expansion/contraction joints but their distribution in the piers and isolators is rather simplistic based on static considerations that disregard the dynamic interaction of the substructure-isolation-deck system. Similarly, the equivalent damping ratio, expressed as a function of the displacement ductility of isolators (i.e. a design parameter of marginal interest to the designer as pointed by Makris & Kampas 2013a) is an indicator of the energy dissipation capacity, but does not provide information regarding potential damage in the piers. Ideally, preliminary selection criteria should address the displacement and energy dissipation capacity of the isolation system as a function of the shear transmitted to the substructure, thus indicating the cost of the substructure design. Some additional guidance in selecting devices while addressing the design of the substructure is provided in the approach by Cardone *et al*. (2009), while the more refined approaches by Ryan & Chopra (2004a, b) and Guo & Christopoulos (2013) that facilitate preliminary selections considering design requirements from different performance levels, are restricted to specific types of devices. These refined approaches are not suitable at the time for the design of seismically isolated bridges wherein both base isolation and energy dissipation devices are typically combined indicating the need for broad-scope rather than device-specific methods. Apart from the fact that codes do not provide specific recommendations regarding the above issue, the integration of equivalent linearisation approaches in the format described in §2.3.2 (i.e. introducing iterations as a means to evaluate the response of a selected passive system) leaves the designer with the task of conducting

numerous analyses when the performance of different isolation schemes and/or multiple design constraints are investigated.

As pointed in §2.2.2, the accuracy of results derived from equivalent linearisation approaches is not ensured by the introduction of iterations. Inherent limitations associated with the consideration of higher mode effects, the non-proportionality of the system damping matrix, and the unreliable estimation of peak relative velocities and total accelerations required for the design of viscous dampers and the substructure elements, respectively, were briefly discussed in §2.3.2 along with some approximate measures of treatment. Research studies on the efficiency of equivalent linearisation addressing specifically isolators (i.e. accounting for values of displacement ductility larger than 25) led in the past in contradictory results and suggestions (e.g. Hwang & Cheng 1994, Hwang & Chiou 1996), while recent studies (Makris & Kampas 2013a) questioned the rationality of using the 'non-physical' effective period to describe the period of vibration (i.e. the time needed for an oscillator to complete one cycle) that appears in the horizontal axis of the response spectrum. Instead, Makris & Kampas (2013a) proposed the use of the isolation period T_p defined from the post-yield stiffness of the isolation system as a simpler (i.e. iterations are not required for the isolation period definition) and more accurate indicator of maximum response, a strategy already adopted in codes for isolation systems consisting of sliding-based isolators (e.g. CEN 2005a, ASCE 2016). Similar studies on the accuracy of the effective period and equivalent damping ratio concepts to predict the inelastic response (peak displacement and forces) in SDOF systems subjected in near/far-fault ground motions (Dicleli & Budaram 2007a, b) and MDOF bridge systems (e.g. Franchin *et al*. 2001) reflect an emerging scepticism on the efficiency of equivalent linearisation approaches. Two remarks are worth to be noted here regarding the non-proportional formulation of the damping matrix and the suggestion by Franchin *et al*. (2001) that classical modal analysis (using real modes and the diagonal terms of the modal damping matrices) can provide a 'good' approximation of results. The first is that such a conclusion is valid for the considered bridge configurations that included irregular (but not non-symmetric) substructure properties and uniform distribution of viscous damping properties. The second remark to bear in mind is that the evaluated linearisation procedure was more refined than that typically allowed by codes (§2.3.2). Furthermore, the reliability of the peak displacement response is further reduced by the directional combination of response quantities derived from independent linear static/dynamic analysis in each principal direction of the bridge. In general, isolators should be designed to sustain the peak relative displacement that may occur in any random direction of the bridge under bidirectional excitation. In this regard, adoption of the common '100%+30%' combination rule (e.g. CEN 2005a) was found (Ryan & Chopra 2004b) to underestimate the peak displacement response determined by nonlinear dynamic analysis.

Further implications in the analysis and design of seismically isolated bridges emerge from the fundamental principles of passive systems presented in §2.3.1; i.e. the provision of an adequate restoring capability, and the consideration of a range of the design properties of passive devices. The restoring capability, associated with operationality requirements, is a design strategy common

in most codes (e.g. CEN 2005a, ASCE 2016), that dictates the presence of devices that can inherently apply recentring forces to the superstructure, thus preventing substantial residual displacements (u_{res}) after the seismic event and accumulation of displacements during a sequence of seismic events or under ground motion containing pulses, while allowing the prediction of displacement demand with less uncertainty (Constantinou *et al*. 2011). Recent investigations (Katsaras *et al*. 2008, Cardone *et al*. 2015) associating the restoring capability with the peak relative displacement (u_0) and the mechanical properties of isolators, emphasised the need to assess the restoring capability by statistically evaluating a large number of nonlinear dynamic analyses. Although, the previous efforts resulted in design charts (e.g. Fig. 2.4) facilitating its specification at the initial stages of design, such an approach has not been incorporated so far in the DBD procedures of §2.3.2. Regarding the second design principle, consideration of the variability of design properties of devices due to external factors (e.g. ageing, temperature, contamination, and wear), and verification of their nominal properties through 'prototype' testing (Constantinou *et al*. 2011) are measures employed in codes (e.g. CEN 2005a, ASCE 2016) to increase the reliability of the analysis. Since their effect on the structural response of critical members cannot be always easily foreseen, codes require two different sets of analysis considering upper and lower bound design properties of devices which increase further the required computational effort. As in the previous case, explicit reference to this issue is typically neglected in DBD procedures of §2.3.2.

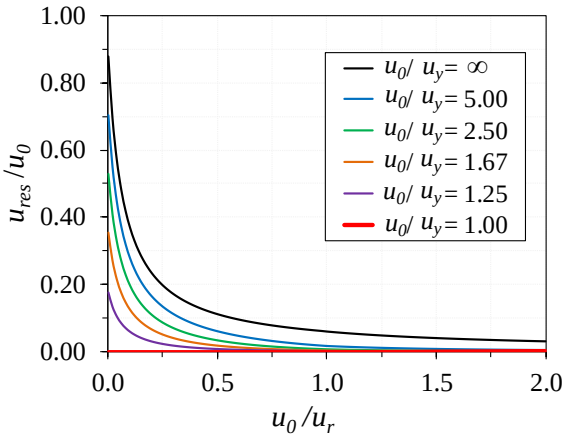

Fig. 2.4 Design value of the restoring capability (expressed as u_{res}/u_0) as a function of u_0/u_r and u_0/u_y, where u_y represent the yield displacement, and u_r the maximum residual displacement under which static equilibrium can be reached (depending on mechanical properties of isolators) (Katsaras *et al*. 2008)

An issue that remains to a certain degree obscured in DBD methods (in codes or otherwise) is the fundamental requirement for the elastic or limited inelastic response of the piers. An earlier version of the US Code (i.e. AASHTO 1991) specified behaviour factors for isolated bridges to be the same as those for non-isolated bridges, implying that this would result in comparable seismic performance of the substructure of isolated and non-isolated bridges, and relevant substructure cost reductions. The importance of adopting lower factors in the case of isolated bridges was soon stressed by Constantinou & Quarshie (1998) as a means to ensure the proper performance of the isolation system and control the sensitivity of isolated bridges in the substructure inelastic response.

In this context, a later version of the code introduced lower behaviour factors (i.e. in the range of 1.5 to 2.5) for substructures of isolated bridges that were retained in the last revision (i.e. AASHTO 2010), interestingly stating that even these values may not ensure proper behaviour of the isolation system or acceptable substructure performance under a very rare earthquake event. Similarly, EN1998-2 (CEN 2005a) specifies a maximum value equal to 1.5 implying essentially elastic response of the substructure under the 'design' earthquake since the ductility-based component of the behaviour factor is close to unity. Furthermore, recent studies (e.g. Vassiliou *et al*. 2013, Tsiavos *et al*. 2017) for the case of building structures demonstrated by dimensional analysis the validity of the previous concerns and showed that when inelastic action commences in a relatively stiff superstructure, the effectiveness of the isolation system diminishes and larger displacement demands are imposed on the yielding structure (compared to the case of a non-isolated one). In view of the previous considerations, a potential source of inconsistency lies in the design strategy of modern codes (e.g. CEN 2005a) according to which the components of the isolation system are designed under a higher level of seismic action than that corresponding to the 'design earthquake', without specifically addressing the effect of these actions on the substructure response.

2.4 Closing Remarks

In the light of the review presented in this chapter, it can be claimed that the current trend in performance-based seismic design of bridges is to make the attractive concept of DBD more suitable for the final design of a sufficiently broad class of bridges, so that it can be deemed suitable for practical application to real structures. The broad-scope requirement refers to different types of bridge designs (e.g. 'ductile-pier', isolated) and structural control devices, along with performance requirements deriving from multiple performance levels. To this end, state-of-the-art documents (*fib* 2012a, b, ACI 2016) seem to favour at the moment the use of advanced analysis and detailed modelling of structures rather than simplistic structural representations aiming at 'direct' estimates of structural properties. In a way, the above format is inclined towards deformation-calculation-based approaches applied in an iterative mode to obtain target performances, and hence may be deemed as an attempt to favour 'accuracy' at the expense of 'computational effort'.

Notwithstanding the importance of maintaining a balance among the design principles of 'simplicity' and 'enhanced seismic performance' and the practical value of simplified procedures in the preliminary stages of design, it is now recognised that an increasing number of engineers (researchers and practitioners alike) rely upon advanced analysis tools to estimate the response of bridge structures (especially when the bridge considered is of high importance) under challenging conditions (i.e. complex structural configuration and increasing size of bridges, site-effects, diversity of actions). The development of a good number of software packages for the inelastic analysis of bridges and other structures is the natural consequence of this trend.

Among the available candidates, nonlinear dynamic analysis represents the most suitable tool in obtaining broad-scope methods for the seismic design of bridges, dealing with most (if not all)

the pitfalls associated with the use of standard analysis and equivalent linearisation approaches (§2.2.2, 2.3.3). Additionally, it provides realistic representations of structural response, disengaged from statistical modal and directional combinations that may reduce the 'engineering perception'. Inevitably this comes at a cost, and implications arising from the adoption of nonlinear dynamic analysis should not be downplayed. Selection/generation and scaling (in time/frequency domain) of input accelerograms, analysis sensitivity, modelling of (material, geometric) nonlinearity (§2.2.2), represent continuously evolving fields, whereas in other, and perhaps more fundamental issues of nonlinear dynamic analysis, such as proper modelling techniques of structural damping, consensus has yet to be reached (Chopra & McKenna 2016, Hall 2016). Nevertheless, there is little doubt that design is heading towards frameworks that are even more complex, and nonlinear dynamic analysis introduced on the basis of simple and comprehensive nonlinear models, as proposed e.g. in MC2010 (*fib* 2012a, b) (§2.2.1), is expected to provide more reliable estimates and distribution of inelastic response while serving as a link to future generation of codes involving probabilistic and resilience-based considerations along with 'smart' structural control techniques (e.g. adaptive passive, semi-active).

In view of the previous remarks the present study attempts to develop a methodology for the seismic design of bridges with emphasis on (*i*) DBD principles of design, (*ii*) use of nonlinear (response history) dynamic analysis, and (*iii*) explicit consideration of multiple performance levels, in a practical design context suitable for inclusion in seismic bridge design codes. Acknowledging the iterative nature of the design process, particular attention is drawn on providing design 'routines' and guidelines that facilitate the implementation, reduce the computational effort, and address implications resulting from the use of nonlinear dynamic analysis. The point of reference in the following investigations is a method for the seismic design of conventional (non-isolated) buildings, originally proposed by Kappos (1997) and Kappos & Manafpour (2001), and further developed by Kappos and co-workers (Kappos & Panagopoulos 2004, Kappos *et al*. 2007, Kappos & Stefanidou 2010). The methodology in its most recent form requires, as a first step, the use of standard elastic (response spectrum) analysis to obtain a basic level of strength while ensuring that inelastic deformations of yielding elements are kept below certain limits corresponding to allowable damage. A set of spectrum compatible records is then selected and a detailed partially inelastic model is developed, wherein members are permitted to exhibit inelastic behaviour only at predetermined locations. The procedure employs inelastic dynamic analysis at different performance levels to verify inelastic deformations, design members that are not expected to yield, and provide detailing of critical sections using local deformation demand derived from analysis. In extending this procedure to bridge structures, levels of seismic actions are defined in line with the general requirements of MC2010 (Table 2.1) and specific performance/damage measures (strains, deformations, relative displacements) are used; nevertheless, as previously discussed, attempt is made to develop a method applicable irrespective of alternative definitions of levels of seismic actions in codes (e.g. Weatherill 2010) and structural performance of bridge members (e.g. Biskinis & Fardis 2010a, b, Goodnight *et al*. 2016) provided in the literature.

Chapter 3
Deformation-Based Seismic Design of Bridges with Energy Dissipation in the Piers

3.1 Introduction

The *deformation-based design* (Def-BD) method, initially proposed for the seismic design of buildings (Kappos 1997, Kappos & Manafpour 2001, Kappos & Panagopoulos 2004, Kappos *et al*. 2007, Kappos & Stefanidou 2010), is tailored herein to common bridge structural configurations having one or more piers rigidly connected to the deck either monolithically or through fixed bearings and/or seismic links. Aiming at the efficient design of bridges in a performance-based context, i.e. explicitly considering multiple performance levels (PLs) and different performance objectives (POs), the procedure initiates with a 'preliminary design' step establishing the basic characteristics of the structural system in terms of both economy and performance. Standard linear analysis and empirical relationships are used to estimate the required pier strength and bearing properties at this stage. A special type of nonlinear response history analysis (NLRHA) of the structural system is subsequently introduced in a number of successive design steps, each corresponding to a different performance level depending on the selected performance objective and associated with design of specific bridge members and type of verifications. During the successive design steps, a gradual refinement of the initial design solution is achieved by controlling essentially in a non-iterative way a fairly broad range of design parameters (i.e. strains, deformations, ductility factors).

The suggested procedure is presented with emphasis on the required modifications and/or extensions compared to the latest version of the methodology (i.e. Kappos & Stefanidou 2010) addressing seismic design of buildings; these are summarised as follows:

- Proper consideration of the different structural configuration of bridges (i.e. regarding the intended plastic mechanism) relying on hysteretic energy dissipation through ductile behaviour of the piers, as opposed to the case of buildings designed for ductile behaviour of the beam elements.

- Incorporation of 'design principles' and approaches to account for the peculiarities of 'ductile-pier' bridges associated with the limited number of the intended energy dissipation zones at the pier ends (i.e. refined estimation of allowed damage ensuring bridge operationality on a pier-by-pier basis, and proper definition of required pier strength), the expected elastic response of the deck, and the possibility to use bearings at the abutments and/or short piers.

- Identification of different performance objectives based on the importance of the bridge and adaptation of relevant performance requirements specifying the expected structural performance of specific bridge members under different levels of seismic action.

Detailed steps of the proposed Def-BD methodology and required modifications with regard to the 2010 version, are first put forward in §3.2. Following a description of the adopted analysis and design framework (§3.3.1-3.3.4), the efficiency of the proposed design methodology is subsequently demonstrated in §3.3.5 by applying it to an actual bridge designed according to 'standard' European practice and selected with a view to enabling comparison (§6.2) between Def-BD and the *direct displacement-based design* method (Priestley *et al*. 2007), as extended by Kappos *et al*. (2013) to explicitly account for higher mode effects. The suggested procedure and the resulting designs for two different seismic zones are evaluated in the light of nonlinear dynamic analysis using a number of spectrum-compatible motions, whereas certain deficiencies of current code-based design approaches derived from associating critical performance requirements with specific performance levels are also discussed (§3.3.6).

In view of the structural configuration of the considered bridges (i.e. 'ductile-pier' bridges), the proposed approach is developed with ductility of piers being (among others) the key design parameter; alternative design solutions involving special seismic isolation and energy dissipation devices are dealt with in Chapter 5.

3.2 Methodology

3.2.1 Performance-based design framework

The suggested procedure consists of four distinct steps (Fig. 3.1a) including a preliminary design and subsequent verifications involving nonlinear dynamic analysis at a number of performance levels (i.e. maximum three) depending on the performance objective sought in terms of bridge importance, i.e. consequences of failure on human life, short- and long-term (economic) effects from disruption of service, cost of repair and replacement, etc., similarly to code requirements (e.g. CEN 2005a). Five different importance classes (and the corresponding performance objectives) are defined, namely, *Non-essential* (bridges of minor importance), *Ordinary* (average importance), *Essential* (high importance), *Critical I* and *Critical II* (major importance). Classification in the last two depends on the target performance set by the bridge owner regarding the post-earthquake operationality following an extreme event. The performance objective is described with reference to the member (abutment, pier, deck, bearing, etc.) performance levels, each assessed on the basis of relevant structural performance (SP) criteria under an associated level of earthquake action (EQ). Four different SPs and EQs are introduced to formulate the 'performance matrix' depicted in Fig. 3.2. SPs are qualitatively described in terms of post-earthquake operationality, damage, and feasibility of repair, ranging from full service, negligible (or no) damage, and no need for repair in SP1, to disrupted service, severe damage, and unfeasible (in terms of economy) repair in SP4.

Representative structural performance criteria associated with each SP, defining member (upper) performance states within a '*design*' framework, are provided in Table 3.1 for piers (e.g. *fib* 2012b, Goodnight *et al*. 2016), bearings (e.g. Mori *et al*. 1997, CEN 2005a), abutments and foundation (CEN 2005a, Nielson 2005). A detailed description of relevant criteria is provided in §3.2.2-3.2.5.

EQs correspond to a 'frequent' event (EQI) having a high probability of exceedance (e.g. 70%) during the design life of the bridge, an 'occasional' event (EQII) with a lower probability (e.g. 40%), a 'rare' event (EQIII) with a low probability (e.g. 10%), and a 'very rare' (EQIV) seismic event with very low probability (e.g. 2~5%) of being exceeded in the design life of the structure (*fib* 2012a). The considered range of return periods T_R coupled with each SP is in line with the widely varying requirements prescribed in different bridge design codes and guidelines. For example, the return period T_R of a 'rare' event commonly associated with SP3 performance requirements in ordinary bridges (i.e. 'life-safety' verifications under the 'design' earthquake in code terminology) is defined as 475yrs in EN1998-2 (CEN 2005a), approximately 1000yrs in New Zealand (NZTA 2013) and US (AASHTO 2011, Caltrans 2013, FHWA 2006) design codes and guidelines, while even higher values have been proposed in the past (e.g. T_R = 2475yrs in ATC/MCEER 2004, but not adopted in a code). Although a review of the performance criteria adopted by current codes is beyond the scope of this study, adopting an increased useful life (e.g. 100yrs) and the same probability of exceedance as in buildings (i.e. 10%/100yrs instead of 10%/50yrs), yields a return period in the order of 1000yrs which is in line with the current trend in NZ and US codes (but not in EN1998-2). Similarly, the previous documents provide a return period within the range of 40 to 110yrs for the 'occasional' event commonly associated with SP2 (i.e. operationality) requirements in ordinary bridges, modifying either T_R or the severity of the performance requirements in the case of bridges of higher or lower importance. The 'frequent' event is rarely defined in bridge design codes, while the effects of the 'very rare' event are normally implicitly considered through capacity design approaches. The analysis type prescribed by the proposed method for each PL is reported in Fig. 3.2 and discussed in detail in the following sections.

Considering once more the example of an ordinary bridge, then the target performance of a single pier within the aforementioned framework (Fig. 3.3) is associated with pier yielding corresponding to undisrupted service of the bridge under EQI ($T_R \leq$ 50yrs), with limited inelastic pier response without significant disruption of service under EQII (T_R = 50~100yrs), with feasible repair of the pier and limited service of the bridge under EQIII (T_R = 500~1000yrs), and with 'ultimate' pier response along with no access of the bridge following an EQIV ($T_R \approx$ 2500yrs) event. It is worth noting that the definitions of 'expected performance' are generally in agreement with relevant requirements introduced in EN1998-2 (CEN 2005a) through the concept of 'importance classes' (i.e. I, II, III for less than average, average, and critical bridges) and 'importance factors' (i.e. 0.85, 1, 1.3, noting the 'very important' and/or 'special' bridges are not within the scope of EN1998-2).

Detailed steps of the procedure, including (for the sake of completeness) those that are essentially the same as in the 2010 version, are provided in Fig. 3.1b and thoroughly described in in §3.2.2-3.2.5.

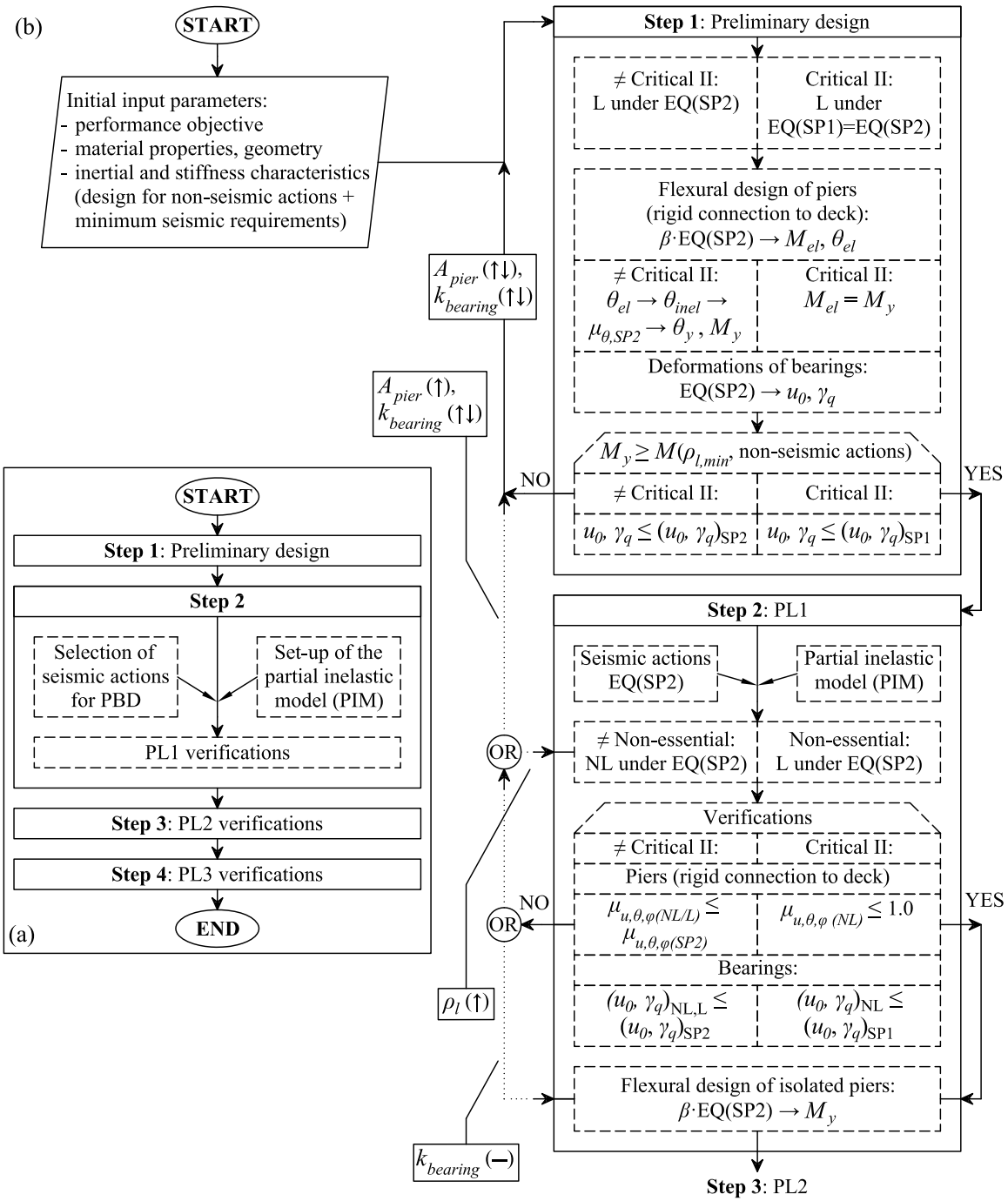

Fig. 3.1 Def-BD methodology: (a) General overview, (b) detailed steps

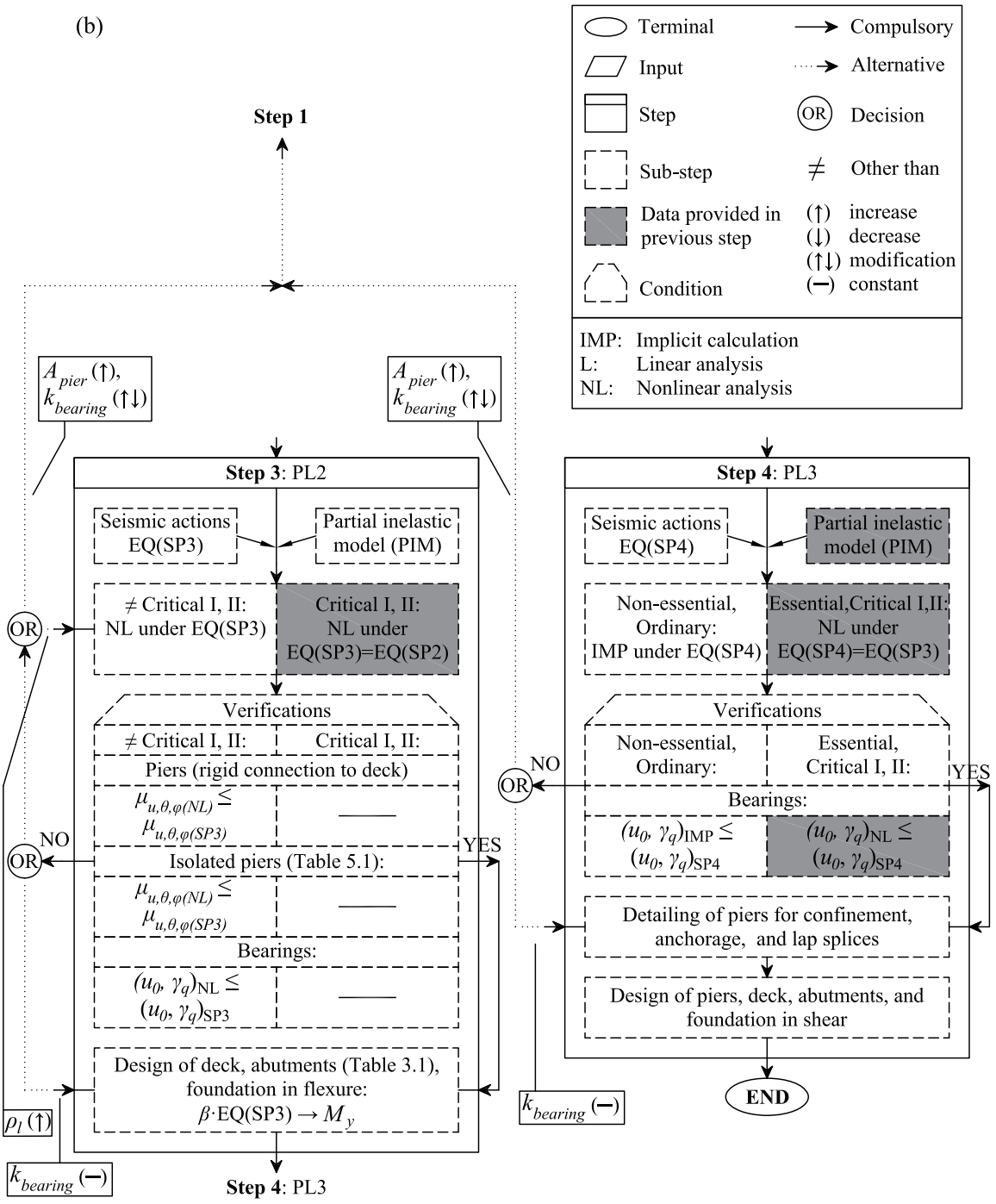

Contnd. Def-BD methodology: (a) General overview, (b) detailed steps

Seismic hazard		Structural performance level			
EQ	**T_R (yrs)**	**SP1**	**SP2**	**SP3**	**SP4**
EQI	<50	Ordinary	Non-essential	-	-
EQII	50-100	Essential	Ordinary	Non-essential	-
EQIII	500-1000	Critical I	Essential	Ordinary	Non-essential
EQIV	~2500	Critical II	Critical I	Essential	Ordinary
Service		Full	Operational	Limited	Disrupted
Damage		Negligible	Limited	Significant	Severe
Repair		No/Economic	Economic	Feasible	Non-feasible
Seismic hazard		**Analysis type per PL**			
EQI	<50	IMP	L	-	-
EQII	50-100	IMP	L+NL	NL	-
EQIII	500-1000	IMP	L+NL	NL	IMP
EQIV	~2500	L+NL	L+NL	NL	IMP

Analysis: Implicit calculation (IMP), Linear (L), Nonlinear (NL)

Importance: Non-essential, Ordinary, Essential, Critical I, Critical II

Fig. 3.2 Typical 'performance matrix' adopted in Def-BD method

Table 3.1 Suggested structural performance criteria for bridges with energy dissipation in the piers[1, 2]

Ductile bridges				
Member	SP1	SP2	SP3	SP4
Ductile pier	Yield	Conc. spalling	Impaired feasibility of repair	Ultimate response
	$\varphi \leq \varphi_y$	$\varphi \leq \varphi$ (ε_c=3.5-4‰)	$\varphi \leq \varphi$ (hoop yielding)	$\varphi \leq \min\varphi$ (ε_{ccu}, hoop fracture, long. bar buckling/fracture)
Elastomeric bearing	No damage	Yielding of anchor bolts, cracking of pedestals, lower limit for yielding of shims	Upper limit for yielding ~ severe bending of shims	Ultimate response
	$\gamma_q \leq 1/SF_{\gamma q}$	$\gamma_q \leq 1$	$\gamma_q \leq 1.5$~2	uplift, tension, stability
Seat-type abutment (non-activated)	-	-	Yield $M_{Abt} \leq M_{y,Abt}$	Ultimate response $u_0 \leq u_{clearance}$
Seat-type abutment (activated via sacrificial backwall or seismic link)	-	Activation $u_0 \leq u_{clearance}$	Yield $M_{Abt} \leq M_{y,Abt}$ $\mu_{\varphi,backwall} \leq 1.5$ $u_0 \leq 0.01h_{backwall}$	Backfill yield $u_0 \leq$ ~$0.1h_{backwall}$
Abutment rigidly connected to deck (integral or via seismic link)	-	-	Yield $M_{Abt} \leq M_{y,Abt}$ $u_0 \leq 0.01h_{abutment}$	Ultimate response $u_0 \leq$ ~$0.1h_{abutment}$
Foundation	-	-	Yield	Ultimate response

[1]Definition of symbols and terms included in this table is provided in §3.2.2-3.2.5

[2]Criteria for additional members (e.g. deck) and other type of bearings are described in §3.2.2-3.2.5

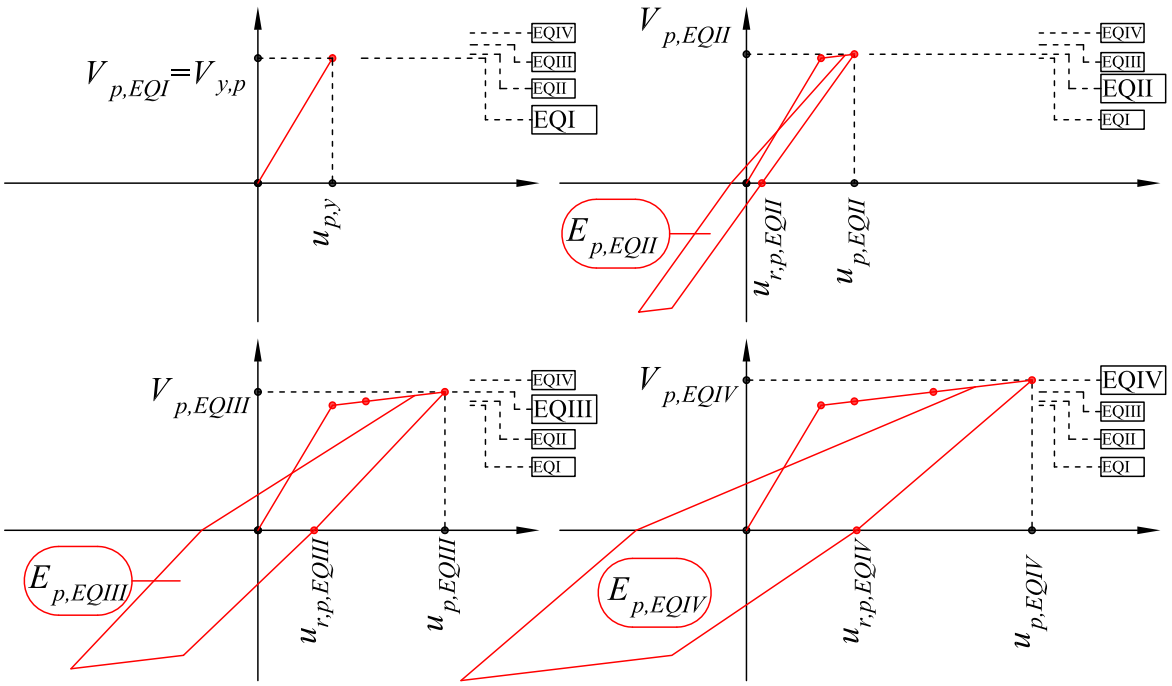

Fig. 3.3 Performance objective (i.e. approximations of actual shear V - displacement u curves) for an ordinary 'ductile-pier' bridge: Pier column under EQI, II, III, IV

3.2.2 Preliminary design (Step 1)

The purpose of this step is to establish a basic level of strength under the minimum considered level of seismic action, typically EQI (associated with SP1), with a view to ensuring that the bridge remains operational during and after an earthquake having a lower probability of exceedance, i.e. EQ(SP2). The 'operationality' SP2 verifications adopted herein include specific limits for strains, curvature and rotational ductility factors (Step 2 in §3.2.3) and the corresponding demands are estimated from inelastic analysis of a partially inelastic model of the structure in the next step. Since for inelastic analysis to be carried out the strength of the yielding zones has to be an input parameter, an initial elastic analysis is required, which would provide the strength of the members (selected energy dissipation zones) that will respond inelastically during the 'operationality' verifications of the next step; this analysis constitutes Step 1 and is a vital part of the procedure.

The design of the selected dissipating zones, like the pier end regions, is carried out using conventional elastic analysis (modal response spectrum, or equivalent static, analysis, depending on the importance of higher modes). The required strength of these zones is estimated taking into consideration the range within which the inelastic deformations should fall, which corresponds to the degree of damage allowed under EQ(SP2) (specifically the allowable rotational ductility factor). The procedure described in the following provides an initial estimate of the allowable rotational ductility factor on a pier-by-pier basis, while aiming at the development of permissible values of inelastic deformations under the EQ(SP2) event, since the latter are directly related to the reduction of element forces corresponding to elastic behaviour. This is an additional feature, not included in earlier versions of the method (tailored to buildings) that either included a serviceability

check, the result of which typically was that most members remained elastic (or were well below the allowable deformation limits) (Kappos & Panagopoulos 2004), or estimated the strength of the dissipating zones by adopting a fixed value for the allowable rotational ductility factor dictated by the extended number of intended energy dissipation zones (i.e. the beam ends) in a multi-storey building (Kappos & Stefanidou 2010).

To meet the aforementioned objective, pier bending moments (M_{el}) and chord rotations (θ_{el}) are first obtained from the results of a standard response spectrum (elastic) analysis (RSA). The pier stiffness considered at this stage is the secant value at yield, accounting for the effects of axial load ratio; in a practical context, the diagrams proposed by Priestley *et al.* (1996) and adopted by Caltrans (2013) can be used (e.g. Fig. 3.4), considering the axial load for the seismic combination, and assuming either a minimum reinforcement or that resulting from design for non-seismic loading (if higher than the minimum).

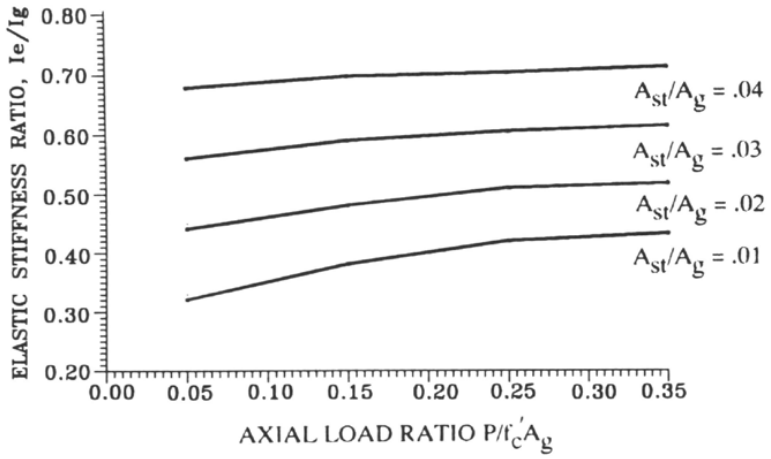

Fig. 3.4 Secant stiffness at yield of cracked RC circular sections (Priestley *et al.* 1996, Caltrans 2013)

Design for flexure is carried out in terms of design values of material strength (in reinforced concrete piers f_{cd} and f_{yd} for concrete and steel, respectively, according to Eurocode notation) using commonly available design aids. On the other hand, SP2 verifications (Step 2 in §3.2.3) are based on the results of inelastic analysis, for which mean values are commonly adopted (f_{cm} and f_{ym}). Furthermore, some members are expected to possess overstrength with respect to the design moments used in their dimensioning, due to detailing requirements, i.e. rounding (upwards) of required reinforcement areas and use of minimum reinforcement ratios specified by codes. For these reasons, the initial elastic analysis should be carried out for an appropriate fraction (β) of the seismic action associated with EQ(SP2). Due to the expected overstrength, the recommended β-factor is lower than the ratio f_{yd} / f_{ym} (equal to 0.79 if the mean yield strength of steel f_{ym} is taken as 10% higher than the characteristic strength f_{yk}). In addition, the β-factor should account for the differences in the bending moments derived from an RSA and those from a series of response history analyses (RHAs) for selected accelerograms (Step 2). Note that if β = 1 is selected, piers will not yield for EQ(SP2) deviating from the target performance set in §3.2.1. It is perhaps worth

noting that the problem of mixing design and mean values of material strength is by no means specific to the performance-based design method presented here; modern codes like Eurocode 8 (CEN 2004b, 2005a) and (even more so) their new versions currently being drafted, adopt both elastic and inelastic analysis methods and recommend using design values for strength verifications and mean values for displacement or deformation verifications.

Subsequently, elastic chord rotations θ_{el} are related to the corresponding inelastic ones θ_{inel}, using an empirical procedure proposed by Bardakis & Fardis (2011a); use of empirical factors to estimate θ_{inel} is an inherent limitation of the proposed procedure, since otherwise ductility factors cannot be estimated at this stage. The allowable chord rotation ductility factor $\mu_{\theta,SP}$ for SP2 in each pier is estimated based on allowable material strains (e.g. Biskinis & Fardis 2010a, b, Goodnight *et al*. 2016). Considering for example the simple Eq. (3.1), the allowable curvature (φ_{SP}), the yield curvature (φ_y) and the plastic hinge length are estimated using empirical relationships and diagrams (e.g. Kowalsky 2000, Priestley *et al*. 2007, Biskinis & Fardis 2010a, b, Cardone 2014) based on SP2 concrete and reinforcing steel strains corresponding to concrete spalling and/or maximum crack width (§3.2.3), whereas the equivalent cantilever height h_{eq} (i.e. the length from the critical section to the point of contraflexure, or the shear span) can be approximated from the results of the elastic analysis.

$$\mu_{\theta,SP} = 1 + \frac{\theta_{p,SP}}{\theta_y} = 1 + \frac{3 \cdot \left(\varphi_{SP} - \varphi_y\right) \cdot L_{pl}}{\varphi_y \cdot h_{eq}} \tag{3.1}$$

Referring to Fig. 3.5(left), having defined the target rotational ductility factor $\mu_{\theta,SP}$ and the maximum inelastic rotation θ_{inel} (this is the total chord rotation, not the plastic one) from the elastic chord rotation θ_{el} found in the elastic analysis, the yield rotation is calculated for every pier as $\theta_y = \theta_{inel} / \mu_{\theta,SP}$. For simplicity, one could assume first that the *M*-θ pier response is elastic-perfectly plastic and second that the initial slope of the elastoplastic and 'elastic' *M*-θ diagram are the same. Then the corresponding yield moment M_y can be easily computed, as the intersection of the elastic part of the diagram and the vertical line drawn at θ_y, as shown in Fig. 3.5(left); this is the moment to be used for the (flexural) design of the pier, implicitly related to a level of seismic actions (lower than those associated with EQ(SP2)) that correspond to the yield state of the bridge, i.e. EQ(SP1). A more accurate procedure for the definition of yield moments in the dissipating zones, accounting for the loading history of the structure (i.e. application of the pertinent combination of permanent and transient actions prior to the application of seismic loads), has been proposed by Kappos & Stefanidou (2010) for the case of buildings (Fig. 3.5(right)). However, in the case of bridges where the dissipating zones are expected to form in the piers (instead of the beams) this refinement is typically not necessary, since the bending moment induced in the piers by gravity loading is in most cases (at least those relevant to Def-BD) small compared to that from seismic loading.

Estimation of pier strength according to Fig. 3.5, implies that the effectiveness of the above empirical procedure in obtaining predefined (target) rotational ductility factors under a specific

level of seismic action, depends on whether the modelling assumptions adopted in the next step (involving NLRHA) are compatible with those used by Bardakis & Fardis (2011b). In the latter study, pier inelastic chord rotations were derived from NLRHA by employing lumped plasticity models coupled with the modified Takeda hysteresis rules (§3.3.2), and subsequently compared with elastic chord rotations to extract empirical correlation factors. This observation should not be perceived as a limitation of the Def-BD method with regard to modelling of the inelastic response of members. The designer may opt to adopt in Step 2 more refined modelling approaches, so long as the allowable (SP) deformation limits (refined in Step 2 using moment-curvature analysis) are consistently defined as a function of strains, deformations (curvatures, chord rotations), displacements or a combination thereof. For example, if fibre models are adopted, verifications in the next step may be performed directly on the basis of curvature ductilities μ_φ (analysis vs. SP criteria in the form of Table 3.1) or indirectly on the basis of chord rotation ductilities (analysis vs. SP criteria in the form of Eq. (3.1) considering the shear span and the spread of inelasticity directly from analysis). In this sense, Step 1 aims at a first estimation of the required strength; minor modifications required to diminish the divergence deriving from the incompatibility of modelling approaches can be performed in Step 2 (§3.2.3).

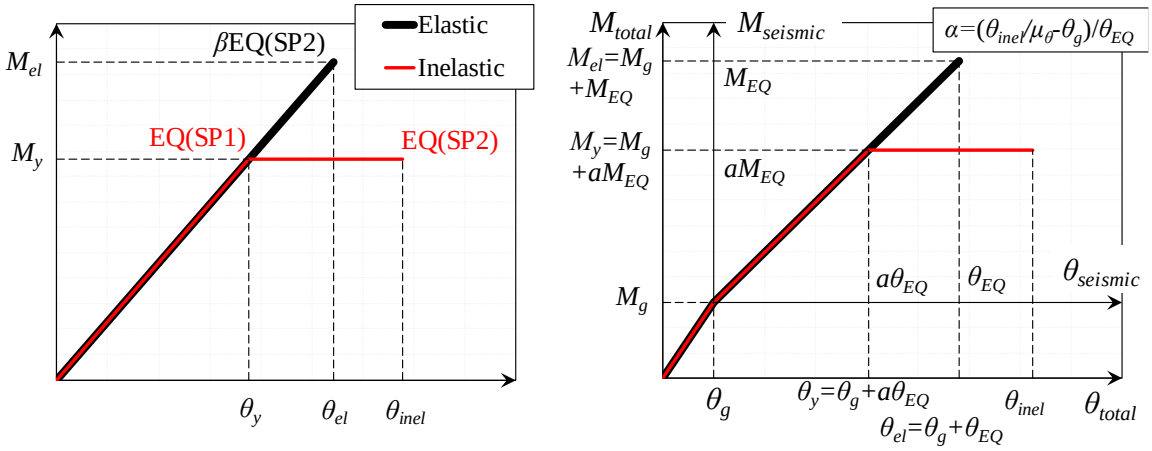

Fig. 3.5 Definition of pier yield moments: Bilinear (elastoplastic) (left) and trilinear (right) *M-θ* approximation

The reduced design moments, related directly to the target rotational ductility of Eq. (3.1) according to the previous procedure, are computed for the piers designated as ductile members, i.e. piers wherein energy dissipation zones are expected to form. Piers that are deliberately isolated from the intended plastic mechanism of the bridge through moveable bearings, such as short piers due to the ground topography along the longitudinal axis of the bridge or secondary piers serving the construction of the deck in balanced cantilever or incremental launching methods (Fardis *et al.* 2012), are designed in Step 2 to respond quasi-elastically under EQ(SP2) by adopting the SP criteria for piers in isolated bridges presented in detail in §5.2 (Table 5.1). The required longitudinal reinforcement ratio (ρ_l) in ductile piers is calculated using standard flexural design procedures and compared to the minimum requirements ($\rho_{l,min}$) according to code provisions. In case the

longitudinal reinforcement demands are found to be less than the minimum requirements, reduction of cross sections is in order (reduction of stiffness), otherwise deformations under EQ(SP2) will be lower than the allowable ones, which of course is an option, but does not optimise the cost of the bridge. An exception to the procedure described above for ductile piers, is the case of critical II bridges wherein pier member design moments are retrieved directly from linear analysis under βEQIV (Fig. 3.1b, Fig. 3.2) without reducing M_y (i.e. $\mu_{\theta,SP}$ = 1); verifications aiming to ensure elastic response of the piers under EQIV are performed with the aid of NLRHA in Step 2 (both EQ(SP1) and EQ(SP2) are associated with the same level of seismic action in critical II bridges).

In the case of bridges (and in contrast to buildings), deformation control in the piers does not fully guarantee that the bridge will remain operational; it is equally important to check that bearings (which are typically present unless a fully integral solution is adopted) also remain functional. Hence, peak relative displacements u_0 (or the corresponding strains γ_q) of bearings under the full 'operationality' actions EQ(SP2) (i.e. excluding the β-factor and adopting the 'equal-displacement' rule at this stage of design) should conform to the deformation criteria discussed in Step 2 (§3.2.3). In critical II bridges, the SP1 performance criteria are checked, similarly to the case of piers.

Clearly, this stage involves striking a balance between economy and performance. Depending on the initially selected input parameters of piers and bearings, some iterations (e.g. 2~3) may be required (Fig. 3.1b) to ensure economic design of the piers (i.e. strength close to the value estimated according to Fig. 3.5) and bearings (i.e. deformations close to the allowable values). The number of iterations will be minimised when minimum seismic code requirements, and requirements deriving from the design for non-seismic loads are adopted as input parameters. It is noted that this type of iterations is not inherent to Def-BD and is typically included in all design methods (§2.2.2); herein, it is based on linear analysis and performed at the start of the design process.

3.2.3 PL1 verifications (Step 2)

During this step a partially inelastic model (PIM) of the structure is set up, wherein the energy dissipation zones of the ductile members are modelled as yielding elements, with their strength based on the reinforcement calculated for the reduced column moments in Step 1. Energy dissipation zones may be assigned at both pier ends or just the bottom of the pier columns depending on the pier-to-deck connection (e.g. monolithic or through fixed bearings). In the same model, the remaining parts of the bridge, including isolated piers, are modelled as elastic members, apart from bearings exhibiting nonlinear behaviour under the considered PL. Since the dissipating zones have been designed for flexure at Step 1, the stiffness of the piers can now be calculated from moment-curvature (M-φ) analysis of sections using the longitudinal reinforcement ratio of the pier ends and mean values for strength of materials (f_{cm} and f_{ym} for concrete and steel, respectively), since deformations are to be checked at this stage.

NLRHA of the PIM also requires the definition of a suite of ground motions compatible with the selected design spectrum (for the considered EQ). Input motion may be represented by natural,

simulated, modified, and artificial accelerograms while selection/generation and scaling (in time/frequency domain) (Douglas & Aochi 2008, Katsanos *et al.* 2010) should be performed following, at a minimum, relevant code-based specifications; at least seven accelerograms are typically required according to codes (e.g. CEN 2004b, AASHTO 2011) if mean response quantities are to be used for design. The accelerogram set used for 3D analysis should include a pair or triplet of components for every seismic motion, depending on the importance of the vertical component for the design of the bridge. The ground motions should be selected/generated on the basis of the results of a seismic hazard analysis ('deaggregation' phase, wherein the 'design' magnitude M and source-to-site distance R are determined for the site in consideration). Hence the selected ground motions should conform to certain criteria concerning magnitude (e.g. M_w = 6.0~6.5), epicentral distance (e.g. R_{epi} = 10~25km), and peak ground acceleration (e.g. PGA > ~0.1g). Additional criteria, not specifically required by EN1998-1, but important all the same, are the similarity of spectra (of the selected motions to the target spectrum) and the reliable estimate of the mean structural response depending on the accepted variability of critical structural responses; software for such multi-criteria selection/generation of the design accelerograms is currently available, (e.g. Hancock *et al.* 2006, Iervolino *et al.* 2009, Katsanos & Sextos 2013).

The selected earthquake motions will be used for both this step and the following one, properly scaled to the level associated with the PL considered., i.e. EQ(SP2) and EQ(SP3) in Steps 2 and 3, respectively. It is noted here that the assumption that the shape of the design spectrum remains the same regardless of the intensity of the earthquake (e.g. the same for T_R = 100 and T_R = 500yrs) is strictly not valid, but is nevertheless commonly adopted, also herein, for simplifying the design procedure; of course, the procedure is applicable regardless of the degree of sophistication involved in selecting the ground motions, which is also related to the importance of the bridge. Depending on whether analysis is carried out separately in each direction of the bridge or simultaneously in both directions a different scaling procedure is in order. For instance, in the former case the procedure prescribed by EN1998-1 (CEN 2004b) can be used, while in the latter case the procedure of E1998-2 (CEN 2005a) is recommended; the issue is further discussed in the case study presented later in §3.3.4. In the case of bidirectional excitation, transformation of the pairs of horizontal components of seismic action to their principal axes and consecutive application along the principal axes of the bridge is deemed adequate during this and the following design steps of the procedure in the case of straight bridges, i.e. two sets of analyses per PL, the one assigning the major and minor components along the longitudinal and transverse axes of the bridge, respectively, and vice versa in the second set. In general, differences among the previous and the most critical angle of incidence are not expected to be significant (Moschonas & Kappos 2013); a more detailed investigation of the orthogonal component of seismic action involving application of components at a range of angles of incidence should be in order at the assessment stage or at the design stage of more complex bridge configurations (e.g. curved-in-plan bridges). In the case of non-essential bridges, NLRHA may be omitted (Fig. 3.1b) due to the reduced importance of the bridge and the

low associated seismic actions (Fig. 3.2), while the following verifications can be carried out by performing a standard elastic analysis (as in Step 1) with updated values of pier stiffness.

Verifications in this step are associated with 'operationality' (SP2) criteria (closure may be required mainly for inspection purposes) except for critical II bridges (no closure) wherein elastic member response is sought (i.e. SP1 requirements in Table 3.1 and Fig. 3.1b). Performance checks are carried out in terms of specific limits for maximum drifts and/or plastic deformations of critical members (i.e. the piers), which in turn are derived considering 'acceptable damage' indicators in the context of allowing the bridge to remain operational under the considered level of seismic action. Several criteria are discussed in *fib* (2007) and it is clear, that the proposals available in the literature vary substantially, from conservative ones (e.g. Choi *et al.* 2004) addressing columns not designed for seismic actions, to very daring ones (e.g. Priestley *et al*. 1996) intended for modern ductile bridge piers. A more appropriate way to define acceptable damage for R/C piers in line with the refined analysis tools used in the suggested procedure, is in terms of strains. For instance, it is clear that the functionality of the bridge will not be impaired if cover concrete does not spall, which typically occurs at compressive strains ε_c between 3.5 and 4‰ (Table 3.1). Likewise, steel tensile strains ε_s lower than 15‰, defined as the value of strain at which residual crack widths exceed 1 mm thus likely requiring repair through epoxy injection to prevent steel corrosion (Priestley *et al*. 1996), is also expected to ensure uninterrupted service of the bridge. Such strain values can then be used to derive limits for deformations (e.g. curvature and/or chord rotation ductility factors) and/or displacements (e.g. drifts), based on the results of the *M*-φ analysis of pier columns, and the equivalent cantilever height h_{eq} taken as the mean of the relevant response quantities observed during the NLRHAs. It is worth noting that there is no specific limitation in the adopted number and type of design criteria; displacement, chord rotation, and curvature limits derived from strains (e.g. relevant ductilities $\mu_{u,\theta,\varphi}$ in Fig. 3.1b) may be checked along with independent values proposed in the literature. Nevertheless, by duly exercising engineering judgment, a more limited number of deformations can be selected as controlled parameters, reducing the required computational effort and simplifying the procedure (Kappos 2015a).

Regarding the bearings, and considering the commonly adopted elastomeric bearings with bolted end plates, the SP2 deformation limit associated with functionality and expressed in terms of elastomer strain due to lateral deformation γ_q, could be set close to 1.0. This value is associated with potential cracking of pedestals and/or yielding of anchor bolts (Padgett 2007), or with the lower limit of yielding of steel shims (i.e. γ_q = 1~1.5, according to Mori *et al*. 1997). The same deformation limit combined with an appropriate safety factor $SF_{\gamma q}$ can be used to ensure 'no-damage' of the bearings (SP1 requirement) in critical II bridges (Fig. 3.1b). In the case of seat-type abutments designed to activate the backfill soil under higher seismic action levels through sacrificial backwalls or seismic links (Table 3.1), the width of joints defined by the relevant available clearance $u_{clearance}$ (in modern bridges normally located solely at the abutments, except for very long decks with intermediate joints) should be selected such that they remain open under EQ(SP2) to avoid damage to the backwalls.

If the adopted performance criteria are not satisfied (e.g. divergence from target deformations exceeding 10%), stiffening or softening of pier columns and bearings will be required. Modification of the longitudinal reinforcement ratio ρ_l is more appropriate for deformation control of the piers, and it can be evaluated on the basis of a limited number of NLRHAs within Step 2 without requiring recourse to Step 1 (Fig. 3.1b), since small variations of ρ_l are not expected to significantly affect the displacement demand. Analysis of the PIM for 2 or 3 different values of ρ_l under the same record (or pair of records), may provide adequate evidence for the required increase/decrease of the reinforcement ratio prior to re-performing the full set of analyses under the selected suite of records. On the other hand, the stiffness of bearings $k_{bearing}$ and the area of pier columns A_{pier} control effectively drifts and displacements. Adjusting the mechanical properties of bearings without altering their stiffness (e.g. increasing proportionally both the elastomer area and thickness in elastomeric bearings) will not require iterations. Modification of $k_{bearing}$ and/or A_{pier} represent the only cases wherein analyses should be repeated starting from Step 1. Nevertheless, according to the cases studied so far (i.e. §3.3, 5.3) no need for iterations has been identified, indicating the effectiveness of the previous step in defining the strength required to limit the inelastic deformations within allowable limits (at least when following a lumped plasticity modelling approach). In this context, this step is basically a verification of the target performance set in Step 1, and the above (iterative) options (dotted arrows in Fig. 3.1b) are included herein for the sake of generality.

Apart from checking the overall inelastic performance of the structural system and its consistency with the adopted SP criteria, moments retrieved from NLRHA in this step are used to design isolated (short, secondary) pier columns in flexure (Table 5.1). When design for flexure is carried out in terms of design values of material strength, pier moments derived from analysis (based on mean strength values) should be properly reduced using the β-factor, similarly to the previous step.

3.2.4 PL2 verifications (Step 3)

Analysis and verifications are not required for critical I and II bridges in this step, since both EQ(SP2) and EQ(SP3) are associated with EQIV (Fig. 3.1b, Fig. 3.2); verifications evaluating more stringent criteria (i.e. SP2) are performed under the same level of seismic action in Step 2. Analysis in the above cases will be meaningful only if a more refined model is introduced in Step 4 for verification purposes. Irrespective of the adopted PO, members considered elastic in setting up the PIM, i.e. the deck, the abutments, and the foundation, are designed in flexure in Step 3 (e.g. $M_{Abt} \leq M_y$ in Table 3.1) using analysis results derived from NLRHA under the selected set of input motions properly scaled to the level of seismic action associated with EQ(SP3) (i.e. EQIV for essential and critical bridges, Fig. 3.2). Pier members, both ductile and isolated, are modelled as yielding elements with their strength and stiffness characteristics derived from M-φ analysis considering the reinforcement ratios calculated in the previous step. Depending on the deck-to-

abutment connection (Table 3.1) and the importance of the bridge (e.g. essential, critical POs), additional nonlinear elements may be required to model the clearance provided between the deck and the abutments (e.g. 'gap' elements), the inelastic response of sacrificial backwalls (if any), and the hysteretic response of the backfill soil (e.g. nonlinear springs), while simpler modelling approaches are recommended in the case of non-essential bridges (e.g. §5.2.6). It should be noted that an abutment can exhibit different behaviour along the principal axes of the bridge; e.g. long-span decks supported on moveable bearings at the abutments in the longitudinal direction but restrained in the transverse direction through seismic links invoke different SP criteria in each direction according to Table 3.1.

In terms of structural performance, the selected SP criteria should ensure that the extent of damage is such that first it can be repaired after the earthquake (closure of the bridge will be required for a certain period) and second that there is no noticeable risk to life. This is an important step for buildings (Kappos & Stefanidou 2010) since several critical elements, in particular the columns (except at the base of the ground storey), are designed at this stage. In the case of bridges, it is very likely that the deck and the abutments will have (from 'non-seismic' load combinations) a higher strength than that required on the basis of this analysis. Nevertheless, consistency of the target performance set for the deck with the adopted modelling assumptions should be explicitly checked (especially in bridges of high importance), otherwise the validity of analysis results may be questionable. For example, adoption of deck flexural stiffness based on gross sections (i.e. a common assumption in bridge design codes) implies a design of the superstructure aiming at the uncracked, rather than the yielding state of deck sections in this PL (i.e. ductility close to cracking state $\varphi \approx \varphi_{cr}$). Although modern bridge design codes (e.g. CEN 2005a, AASHTO 2011, Caltrans 2013) require an explicit verification that the deck does not yield under capacity design actions developed when the components of the bridge energy dissipation system (e.g. i.e. the pier ends) reach their overstrength, this cannot ensure that prestressed concrete deck sections remain uncracked or close to the cracking state (when cracking bending moments are exceeded) under EQ(SP3) (i.e. 'design seismic actions' in code terminology) (Gkatzogias & Kappos 2016a). In fact, deck bending moments are expected to be closer to the yield moment, if piers yield under EQ(SP3). The adoption of the 'uncracked' state of the deck under EQ(SP3) facilitates in addition the bridge modelling, since the ratio of secant stiffness at yield to gross flexural stiffness varies significantly for different signs of the in-plane bending moments of the deck due to the highly unsymmetrical detailing of deck sections about the transverse axis of the bridge, and can be properly captured only by the introduction of nonlinearity in the members modelling the deck, increasing the complexity and relevant uncertainties of analysis. A notable exception regarding the target performance of the deck, is continuity slabs in decks consisting of precast-prestressed beams with cast in situ top slab, a configuration quite different from the box girder bridges that are the subject of the case study presented in §3.3. Such slabs will certainly yield under the considered level of seismic action, but this is perfectly within the design philosophy of such bridges and is also allowed by current codes. There is no need for verification of the plastic rotation either, since the shallow sections of R/C

slabs can develop very high rotations without rupture. Deck slab hinging can readily be addressed within the proposed procedure (by introducing inelasticity in the pertinent members of the PIM).

Deformation/displacement limits for the yielding elements of the ductile piers can be computed as in the previous step by adopting material strains that render feasible the repair of damaged piers. Bar buckling and significant damage to the core represent the states of the concrete members beyond which significant repair costs may hinder the feasibility of repair (Priestley *et al*. 1996). In view of the previous consideration, the above objective can be associated with the ultimate concrete strain deriving from the energy balance approach developed by Mander *et al*. (1988), as this value was found according to experimental results, to provide conservative estimates (by 50% or more) of the ultimate concrete strain associated with failure (Kowalsky 2000). A more appropriate criterion (Table 3.1) to serve the set objective within a *design* framework is the adoption of a concrete strain associated with yielding of confinement steel (Goodnight *et al*. 2016) prompting a change in the intervention strategy from epoxy injection of cracks and patching of cover concrete to higher cost retrofitting measures (e.g. steel jacketing, FRP, etc.). In general, the deformation demand in ductile piers is not expected to be critical at this PL apart from the cases wherein a seismic action higher than the one corresponding to bridges of average importance is adopted, while deformations in isolated piers should be constrained to values associated with ε_c = 3.5~4‰ according to Table 5.1. On the contrary, it is essential that bearing deformations be checked at this stage (Table 3.1); allowable strain γ_q values for typical elastomeric bearings can be set to 1.5~2.0 representing yielding and severe nonlinear flexural deformation of steel shims (Mori 1993, Padgett 2007). The upper value of the previous range is also adopted by EN1998-2 (CEN 2005a). If the adopted performance criteria are not satisfied, minor modifications of pier and bearing characteristics will be required typically without involving iterations; however, all available options are provided in Fig. 3.1b for the sake of generality (similarly to Step 2).

When movement of the deck is constrained at the location of the abutments due to a sacrificial abutment backwall (i.e. in the longitudinal direction of the bridge) or a rigid deck-to-abutment connection (e.g. deck integral with abutments, seismic links constraining the transverse movement of the deck), SP3 design criteria for the abutments can be defined on the basis of allowable deformations of the backwall (i.e. curvature ductility $\mu_{\varphi,backwall}$ in Table 3.1) and/or the backfill soil, respectively. In the latter case, soil deformations below the theoretical point of yield are expected to keep repair costs within tolerable limits. Yield deformations of the soil are given as $0.01h_{backwall}$ or $0.01h_{Abt}$ in Table 3.1 according to Nielson (2005), depending on the deck-to-abutment connection ($h_{backwall}$ and h_{Abt} represent the height of the sacrificial backwall/abutment).

3.2.5 PL3 verifications (Step 4)

To account for the less ductile nature of shear (or flexure-shear) failure, shear forces should be calculated for seismic actions corresponding to a higher level than EQ(SP3), except for essential and critical bridges where EQ(SP3) and EQ(SP4) coincide with EQIV (commonly associated with

a T_R of 2500 yrs and 'collapse-prevention' performance requirements) and hence required analysis results are provided from the previous step (Fig. 3.1b). To simplify the design procedure in non-essential and ordinary bridges, design and detailing for shear can be carried out using shear forces calculated from Step 3, implicitly related to EQ(SP4) through appropriately selected magnification factors SF_v. The adopted SF_v should account for the strain-hardening effect corresponding to higher plastic rotations at the level of seismic actions associated with EQ(SP4). Considering pier moment-chord rotation M-θ (or preferably shear-displacement V-u) response diagrams under EQ(SP3), SF_v can be easily defined by the expected increase of the pier chord rotation ductility μ_θ assumed equal to the increase of the displacement ductility μ_u (e.g. CEN 2005a). The latter can be reasonably estimated as a function of the return periods associated with EQ(SP3), EQ(SP4), and the linear approximation of the seismic hazard curve at the bridge site (Weatherill *et al.* 2010, 2013). An example of relevant calculations is provided in §3.3.3, 3.3.5; as an indication, SF_v is expected between 1.15 and 1.35 assuming that EQ(SP4) is characterised by twice the spectrum of EQ(SP3).

Detailing of R/C piers for confinement, anchorages and lap splices, with a view to providing the required curvature ductility capacity (associated with the ultimate confined concrete strain ε_{ccu}, bar buckling, etc., Table 3.1) is carried out with due consideration of the expected level of inelasticity following the provisions of EN1998-2 (CEN 2005a) for ductile members (i.e. piers in non-essential, ordinary, and essential bridges) and limited-ductile members (i.e. piers in critical I, II bridges, and isolated piers in all classes of bridge importance). However, instead of basing the detailing on the default curvature ductilities specified in the code (e.g. μ_φ = 13 for bridges with ductile behaviour), the actual μ_φ is used in this method, calculated from analysis under EQ(SP3), and implicitly associated with EQ(SP4) through magnification factors in the case of non-essential and ordinary bridges. This results in both more rational and, as a rule, more economic, detailing of the piers. Similarly to the estimation of shear forces, the increase of μ_φ under EQ(SP4) can be calculated from the relevant increase of μ_u using well known equations correlating global and local ductility measures (e.g. CEN 2005a). It is noted that this approach will yield conservative values of μ_φ under EQ(SP4) when natural records are scaled following the procedure prescribed in EN1998-2, and lower magnification factors can be adopted in this case (§3.3.5, 3.3.6).

Likewise, the deformation capacity of bearings that allow horizontal displacements should be checked for ultimate deformations (non-essential and ordinary bridges), uplift or maximum tensile stresses and stability (all classes of bridge importance); in the case of common elastomeric bearings, although under lateral deformations the shear strain at failure can exceed 400% (Konstantinidis *et al.* 2008), toppling considerations are more likely to yield the critical (i.e. allowable) γ_q strain limit under EQ(SP4) in non-essential and ordinary bridges. Forces on fixed bearings (such as pot bearings that constrain displacements), derived directly from NLRHA or implicitly estimated using SF_v, define their shear force resistance. With regard to the superstructure, non-significant yielding of the deck sections should be ensured under EQ(SP4) in non-essential and ordinary bridges in line with code requirements (e.g. CEN 2005a); flexural deformation of the deck in essential and critical I, II bridges are restrained in the previous step under the same level

of seismic action. In a similar context, when the structural configuration of the deck-to-abutment connection in non-essential and ordinary bridges results in the activation of the abutment-backfill system (through links or otherwise) followed by potential damage in the foundation (e.g. in piles), the ultimate deformations in the embankment should be checked (e.g. according to Nielson 2005 in Table 3.1).

3.3 Case Study

Design examples of the Def-BD methodology (described in §3.2) are presented in this section with a view to demonstrating the application of the required individual steps. The case study aims in addition to validate the efficiency of the proposed methodology in providing reliable estimates of response while satisfying diverse performance requirements in line with the second research objective in §1.2. In this context, the application of Def-BD is presented in §3.3.5, following the description of the adopted analysis/design framework including the input parameters of the studied bridge (§3.3.1), modelling issues (§3.3.2), target spectra associated with different PLs (§3.3.3), and the representation of seismic actions (§3.3.4); a validation study is subsequently performed in §3.3.6 employing nonlinear dynamic analysis under a suite of spectrum compatible records different than the one adopted at the design stage. Design examples in this section also serve as a benchmark, enabling comparisons in terms of structural performance and economy of design among the proposed Def-BD method for bridges with energy dissipation in the piers (Chapter 3), the Def-BD method for seismically isolated bridges (i.e. the third research objective presented in Chapter 5), and alternative design methodologies (i.e. the fourth objective presented in Chapter 6) including the *modal direct displacement-based design method* (MDDBD) (Kappos *et al*. 2013) and a code '*force-based*' design approach.

The studied structure is a variant (§3.3.1) of an actual bridge, i.e. Overpass T7 in Egnatia Motorway, N. Greece (Fig. 3.6(top)), of a type common in modern motorway construction in Europe. The decision to investigate an actual bridge, rather than idealised structures where typically simplified assumptions apply (e.g. adopting as a structural model an elastic beam-deck supported on inelastic springs-piers), is primarily associated with the intention to evaluate the efficiency of the proposed methodology for the final (as opposed to preliminary) design of bridges. Apart from providing the appropriate 'test-bed' for a realistic assessment of structural performance and (monetary and computational) cost, the above decision facilitates the identification of certain deficiencies of current code-based design approaches (§3.3.6, Chapter 6) by comparing the Def-BD design output with the 'as-build' state of the bridge as derived from the application of a 'code-based' design approach (Egnatia Motorway 2002). A key consideration in the selection of the specific bridge is associated with its structural configuration (§3.3.1) that results in an increased contribution of the second mode, rendering the specific bridge an interesting benchmark employed so far in the evaluation of both design (e.g. MDDBD in Kappos *et al*. 2013) and assessment (e.g. *modal pushover analysis* in Paraskeva *et al*. 2006) methodologies (thus further allowing self-

assessment and validation of numerical modelling and analysis results). In fact, the selection of Overpass T7 enabled the direct comparison of design results derived from the application of the Def-BD procedure proposed herein and the application of the MDDBD method in the same bridge presented in Kappos *et al*. (2013) (Chapter 6).

3.3.1 Description of studied bridge

The 3-span structure of total length equal to 99 m is characterised by a significant longitudinal slope (i.e. approximately 7% along the longitudinal *x*-*x* axis) of the 10-m wide prestressed concrete box girder deck that results in two single-column piers (cylindrical cross section with diameter D_p = 2.0 m in the actual bridge) of unequal height (i.e. clear heights of h_{Pier1} = 5.9 and h_{Pier2} = 7.9 m) (Fig. 3.6(bottom)). The deck is monolithically connected to the piers (Annex A, Fig. A.1(top), Fig. A.2) while it rests on its abutments through elastomeric bearings (Fig. A.1(bottom)). Movement in both directions is initially allowed at the abutments, while longitudinal and transverse displacements are restrained whenever a 100 mm (Fig. 3.6) and a 150-mm gap (Fig. A.1(top)) between the deck and the abutment is closed, respectively. The bridge rests on firm soil and both piers and abutments are supported on surface foundations (footings) of similar configuration (Fig. 3.6, Fig. A.1). The above geometrical characteristics (i.e. different pier heights and unrestrained response of the deck at the abutments) result in an increased contribution of the second mode. With a view to enabling meaningful and consistent comparisons between the Def-BD and the MDDBD procedures, certain design parameters associated with modelling issues and the definition of seismic actions are defined in the following sections in line with the study of Kappos *et al*. (2013).

In the analyses presented in the following, the focus is on the transverse response of the bridge (i.e. along the *y*-*y* axis). Although this was done for the sake of consistency with the MDDBD study (Kappos *et al*. 2013), it should be understood that the Def-BD methodology presented herein can inherently account for the response in both principal directions of the structure (§3.2), and in fact for seismic actions applied simultaneously in both directions (e.g. Kappos & Stefanidou 2010). In applying the Def-BD procedure to this bridge, the gap size and the characteristics of the bearings are treated as design parameters, i.e. adopting the non-activated seat-type abutment in Table 3.1 that triggers the second mode of vibration. The outcome of the MDDBD methodology regarding the geometry of the piers (i.e. D_p = 1.5 m) and the mechanical characteristics of the bearings was used as a starting point in the following applications (§3.3.5); elastomeric bearings are of rectangular shape (350 mm × 450 mm) with elastomer total thickness t_R of 88 mm, horizontal stiffness of k_e = 2506 kN/m and equivalent viscous damping ratio equal to ξ_e = 5%, while two bearings are placed at each abutment as in the actual bridge (Fig. A.1(top)). Concrete and steel properties were based on a characteristic concrete compressive strength of f_{ck} = 27.5 MPa and a steel yield strength of f_{yk} = 500 MPa, respectively, using EN1992-1-1 (CEN 2004a) equations to obtain correlated material mechanical properties. The bridge was designed adopting the 'ordinary bridge' PO implying ductile behaviour of the piers (Fig. 3.2, Table 3.1).

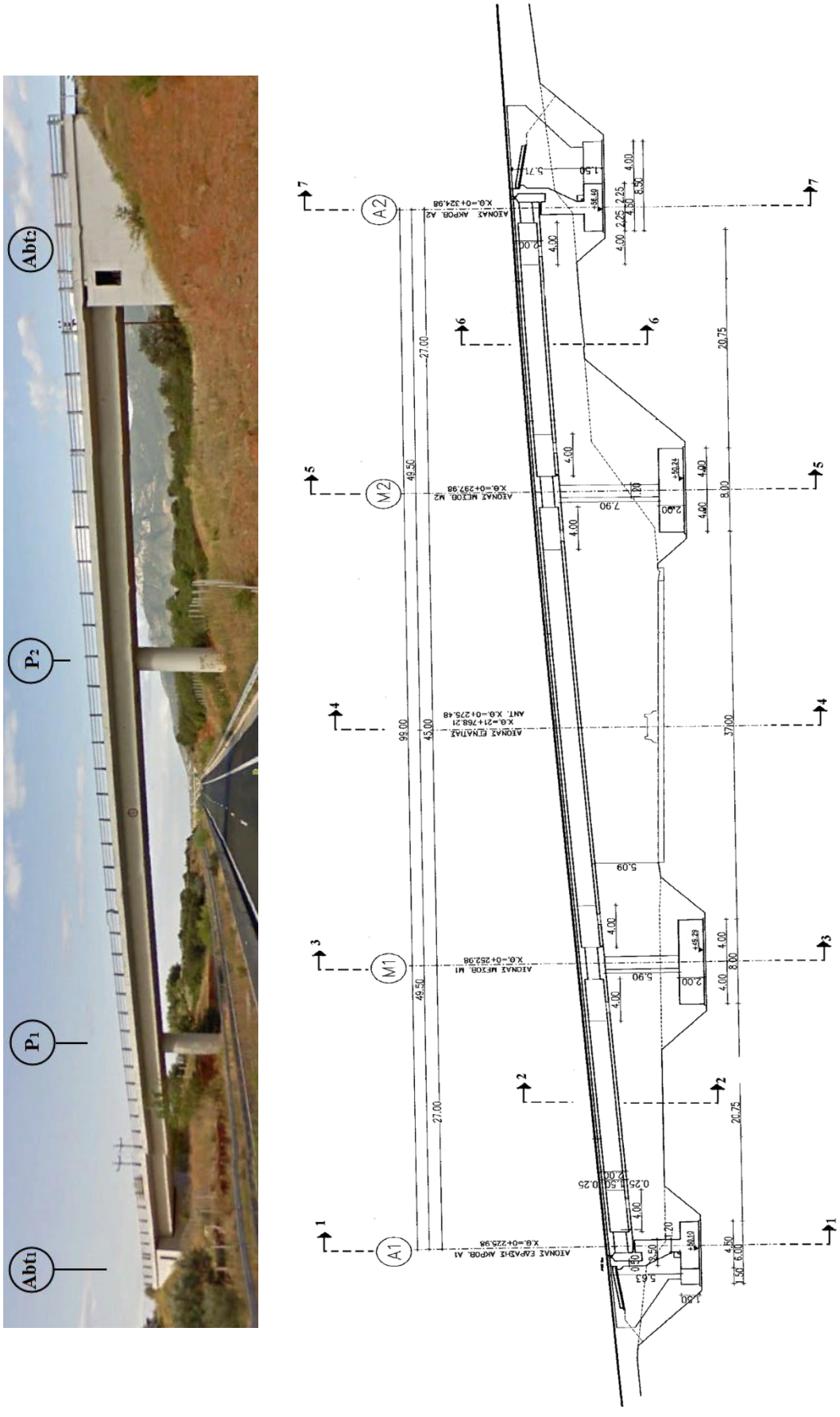

Fig. 3.6 Overpass T7, Egnatia Motorway, N. Greece: Google Earth (2011) view (top), longitudinal cross-section (Egnatia Motorway 2002) (bottom)

3.3.2 Modelling issues and numerical evaluation of dynamic response

Nonlinear dynamic analysis required in the case of Def-BD for both design (§3.3.5) and assessment (§3.3.6) purposes was carried out applying the unconditionally stable implicit Newmark constant average acceleration method (Carr 2004a) within the RUAUMOKO suite, i.e. RUAUMOKO 3D (Carr 2004b) and DYNAPLOT (for post-processing of analysis results, Carr 2004c), while SAP2000 (CSI 2009) was also used for additional verification. Analyses were performed using an integration time step equal to 0.005 or 0.01s after trial analysis, and accounting for the effect of geometric nonlinearities (*P-Δ* analysis). The system damping matrix was constructed by adopting (after some pilot analyses) the *Rayleigh* proportional damping model based on tangent stiffness to avoid overestimation of damping following the yielding of piers (Carr 2004b).

Appropriate nonlinear three-dimensional beam-column (i.e. 'frame type') members that in general follow the concept of the *Giberson* one-component (lumped plasticity) model, were introduced in the finite element model to simulate the inelastic response of the piers (Fig. 3.8). The modified Takeda degrading-stiffness hysteresis rules (Carr 2004b) with unloading and reloading parameters of a = 0.5 and b = 0, respectively, were adopted as also assumed in MDDBD (Kappos *et al*. 2013) for the estimation of the member equivalent viscous damping (Dwairi & Kowalsky 2006), disregarding strength degradation (a common assumption in seismic design of new bridges, Chapter 1) and axial force vs flexural yield moment interaction (i.e. N-M_y) since there are no changes in axial force that affect the yield moments related to the transverse response of this straight bridge (Fig. 3.7).

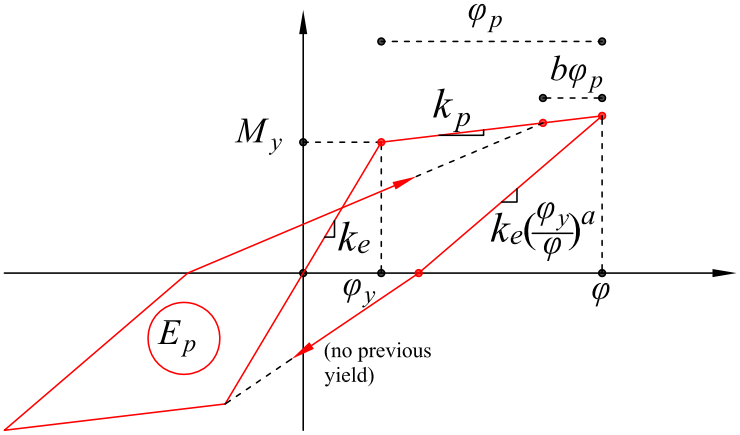

Fig. 3.7 Modified Takeda degrading-stiffness hysteresis model

Pier strength and stiffness characteristics, required to describe the strength envelope of the pier plastic hinges and the SP limit values for member deformations (§3.3.5), were obtained through M-φ analysis with the aid of the computer program RCCOLA.NET (Kappos & Panagopoulos 2011) adopting the model of Kappos (1991) for confined concrete, the model of Park & Sampson (1972) for reinforcing steel, and accounting for the performance criteria presented in Table 3.1, i.e. yield characterised by $\varphi = \varphi_y$, concrete spalling by $\varphi = \varphi(\varepsilon_c$ = 3.5-4‰), (the $\varphi = \varphi(\varepsilon_s$ = 15‰) operationality criterion was also considered but never found critical), hoop yielding by $\varphi = \varphi(\varepsilon_{c,wy})$ where $\varepsilon_{c,wy}$

corresponds to the concrete strain at the yielding of the transverse reinforcement (Goodnight *et al*. 2016), and 'ultimate' response characterised by the minimum of the curvatures associated with hoop fracture (Paulay & Priestley 1992), drop of concrete strength to $0.85f_c$, fracture of the longitudinal reinforcement (at a steel strain of ε_{su} = 90‰), and buckling of compression bars (Papia & Russo 1989, Paulay & Priestley 1992). Bilinear approximations of the moment-curvature curves were based on the equality of areas under the 'exact' and the bilinear *M*-*φ* curves. Shear deformations were approximately considered by adopting a reduction factor of the shear stiffness GA_s (*G*: shear modulus of concrete, A_s: shear area of concrete section) equal to the ratio of the flexural stiffness at yield (*y*) to the initial stiffness of the gross (*g*) section EI_y/EI_g (*E*: concrete modulus of elasticity, I: moment of inertia) (Priestley *et al*. 1996, Kappos 2015b).

The elastomeric bearings present at the abutments were modelled using linear 2-joint springs ('spring type' members' in RUAUMOKO, 'link' elements in SAP2000) with six independent deformations (i.e. 1 axial, 2 shear, 2 flexural and 1 torsional internal springs); a detailed presentation of the modelling assumptions along with the definition of mechanical properties of bearings is provided later in §5.3.2 for the general case of bilinear hysteretic isolators, noting that the variability of design properties (§5.3.3) is disregarded herein in line with code prescriptions for using low damping rubber bearings (LDRB) in non-isolated bridges (e.g. CEN 2005a).

The bending moments of the deck under the maximum considered seismic action (§3.3.5) were found in general lower than the deck cracking moments derived from *M*-*φ* analysis (§6.2.5), hence the deck was modelled using linear three-dimensional beam elements with flexural stiffness corresponding to the gross sections (§3.2.4). The different sections of the deck (i.e. D1, D2, D3, D4) (Fig. 3.6, Fig. 3.8, Fig. A.2) were initially modelled in the 'built-in' SECTION DESIGNER utility of SAP2000 (CSI 2009) to obtain stiffness properties, which were in turn assigned to the relevant linear beam elements. In deck elements where the relevant properties varied along the element length (due to the variable deck geometry, Fig. 3.6, Fig. 3.8), mean properties of the 'end-sections' were adopted in RUAUMOKO 3D and 'non-prismatic' elements with linear variability of properties in SAP2000. The torsional stiffness of the deck was set equal to 20% of the uncracked section torsional stiffness to approximately account for cracking due to torsion (Katsaras *et al*. 2009). In accordance with the adopted PO of ordinary bridges and type of deck-to-abutment connection (Fig. 3.2, Table 3.1), abutments were not included in the analysis model and the required clearance (i.e. the width of the gap in Fig. 3.8) between the deck and the seismic links of piers and abutments was treated as a design parameter (i.e. non-activated abutment-backfill system). Connectivity of the deck to the abutments (through the LDRB) and the piers was modelled according to Fig. 3.8, using rigid constrains and considering the height of the bearings (h_l) and the eccentricity of the deck mass centre. During the mass discretisation (deck translational mass *m* lumped at end-joints of deck elements), one third of the pier column mass was included in relevant deck joints (Fig. 3.8) according to Priestley *et al*. (1996). Soil-structure interaction phenomena were ignored (similarly to Kappos *et al*. 2013) as they were deemed to be minor in this bridge. The reference finite element model (Fig. 3.8) involved in total 32 three-dimensional frame and spring elements.

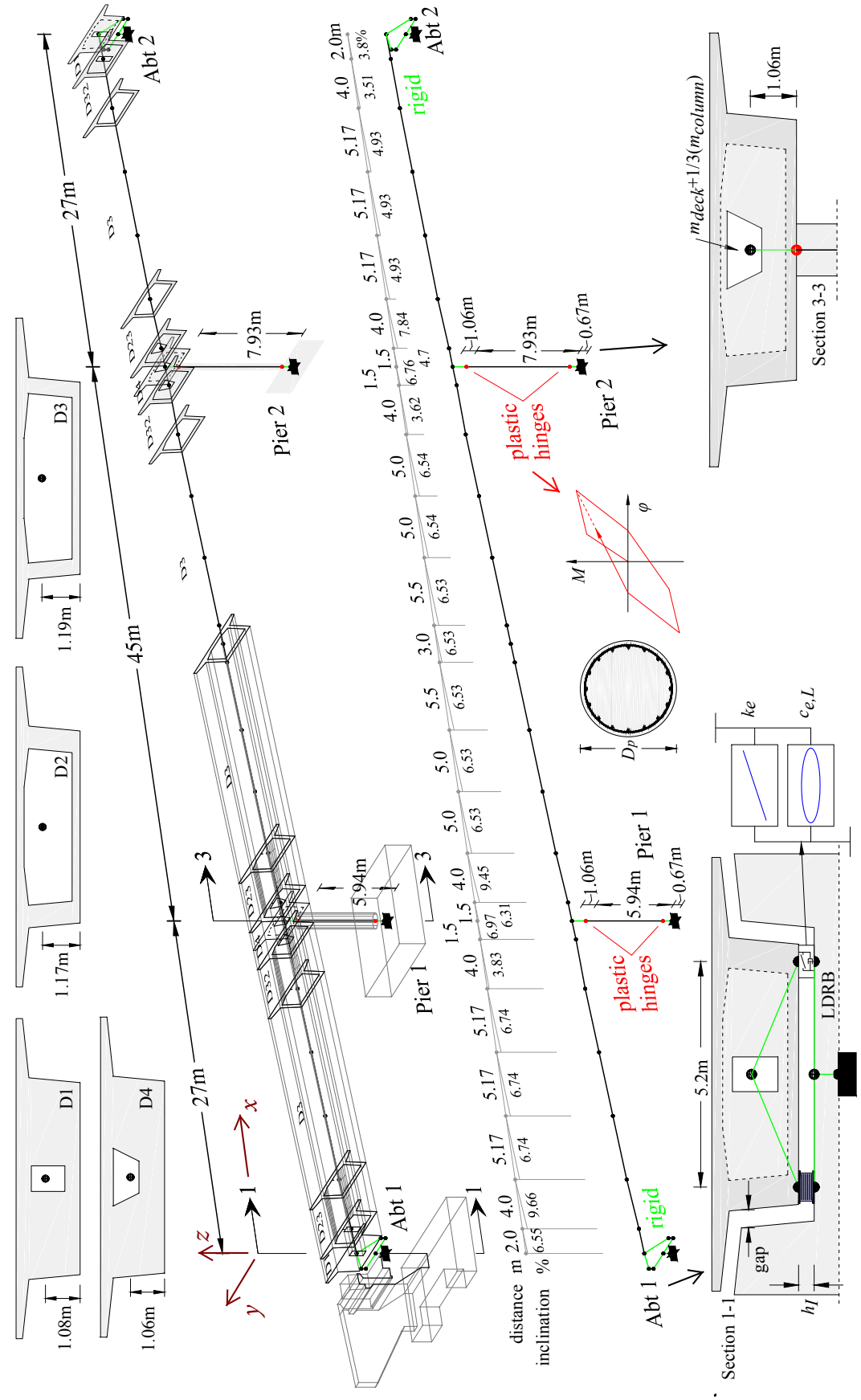

Fig. 3.8 Layout of the bridge configuration and finite element modelling

3.3.3 Target spectra

The EN1998-1 ‘Type 1’ (CEN 2004b) 5%-damped elastic spectrum was selected as the basis for seismic design corresponding to site conditions ‘C’ (Fig. 3.9). However, a significant modification compared to the Eurocode elastic response spectrum was made in line with recent research findings (e.g. Weatherill *et al*. 2013); the corner period defining the beginning of the constant displacement response range of the spectrum was set equal to T_D = 4.0 s as a more representative value of high seismicity regions compared to T_D = 2.0 s, the recommended value in EN1998-1. The adopted period is also in line with the early SEAOC (1999) recommendations, and equals the minimum value in ASCE/SEI 7-16 (ASCE 2016) that specifies values up to 16s. This modification, apart from being in line with recent research findings, was adopted in Kappos *et al*. (2013) as necessary for the MDDBD to be meaningful in the sense that short corner periods lead to small displacement values in the period range that is common in the *direct displacement-based design* method (which involves secant stiffness values at maximum displacement) and hence leads to conservative design (§2.2.2, Kappos *et al*. 2012a).

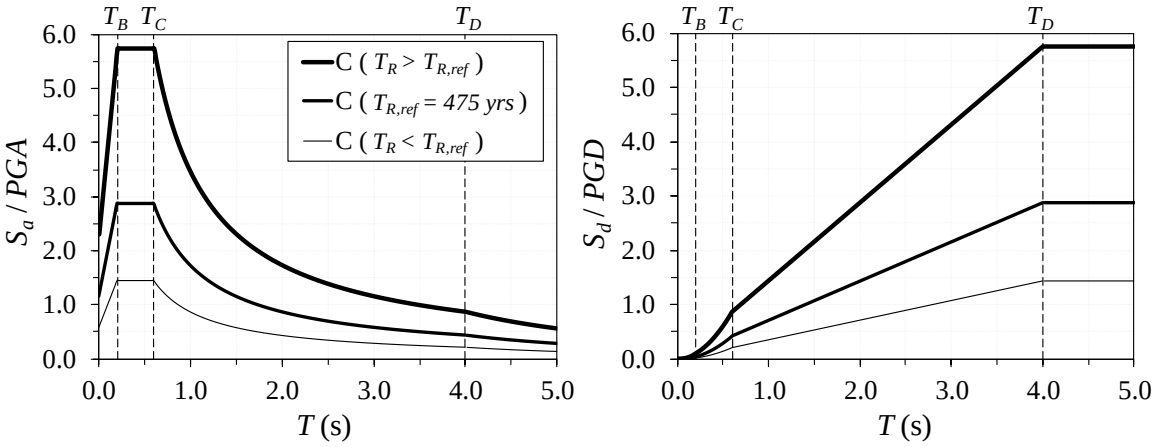

Fig. 3.9 1D target design horizontal acceleration S_a/PGA (left) and displacement S_d/PGD (right) response spectra for site conditions ‘C’ and different return periods T_R

The value of the probability of exceedance P_L in T_L years of a specific level of the seismic action is related to the mean return period T_R of the same action in accordance with the expression of Eq. (3.2);

$$T_R = -\frac{T_L}{\ln\left(1-P_L\right)} \tag{3.2}$$

Assuming that the seismic action is defined in terms of the reference peak ground acceleration (PGA) $\ddot{u}_{g0,ref}$ (CEN 2004b), the value of the modification factor SF_{EQ} (the importance factor according to EN1998 terminology) multiplying the reference seismic action to achieve the same probability of exceedance in T_L as in $T_{L,ref}$ years for which the reference seismic action is defined, can be estimated as;

$$SF_{EQ} = \frac{\ddot{u}_{g0}}{\ddot{u}_{g0,ref}} \approx \left(\frac{T_{L,ref}}{T_L} \right)^{-1/k} ; \quad P_L = P_{L,ref} \tag{3.3}$$

Substituting T_L and $T_{L,ref}$ from Eq. (3.2) in Eq. (3.3), provides an analogous expression of SF_{EQ} with respect to the mean return periods T_R and $T_{R,ref}$;

$$SF_{EQ} = \frac{\ddot{u}_{g0}}{\ddot{u}_{g0,ref}} \approx \left(\frac{T_{R,ref}}{T_R} \right)^{-1/k} \tag{3.4}$$

The value of the k exponent in Eqs. (3.3), (3.4) expresses the slope of a linear (in logarithmic space) approximation of the hazard curve at the site ranging between 1.5 and 4.5; its exact value depends on both the seismicity of the region (values increasing as the seismicity increases) and the spectral ordinate considered (decreasing values at longer periods) (Weatherill *et al*. 2013); herein a constant value of 2.4 was adopted while the corresponding SF_{EQ} (Eq. (3.4)) was uniformly applied to the reference target spectrum (Fig. 3.9) whenever a seismic action of different probability level was sought, assuming a constant shape of the target spectrum regardless of the intensity of the earthquake (§3.2.3).

A reference return period of $T_{R,ref}$ = 475yrs was selected along with two different seismic hazard zones (Z) associated with *PGA*s of 0.21g (ZII) and 0.31g (ZIII) roughly corresponding to seismic zonation in Greece (Kappos *et al*. 2013). It is noted that the zone associated with low seismicity areas (ZI) was not investigated due to complications relevant to the application of MDDBD (§2.2.2). Three different seismic action levels (EQ) were subsequently defined for T_R = 90 (EQII), 475 (EQIII), 2500 yrs (EQIV), resulting in the following *PGA*s ($\ddot{u}_{g0}$) for each seismic zone according to Eq. (3.4);

$$T_{R,EQII} = 90yrs, \quad SF_{EQII} \sim 0.5, \quad \ddot{u}_{g0,EQII} = 0.10g \text{ (ZII)}, \quad = 0.16g \text{ (ZIII)} \tag{3.5}$$

$$T_{R,EQIII} = T_{R,ref} = 475yrs, \quad SF_{EQIII} = 1, \quad \ddot{u}_{g0,EQIII} = 0.21g \text{ (ZII)}, \quad = 0.31g \text{ (ZIII)} \tag{3.6}$$

$$T_{R,EQIV} = 2500yrs, \quad SF_{EQIV} \sim 2, \quad \ddot{u}_{g0,EQIV} = 0.42g \text{ (ZII)}, \quad = 0.63g \text{ (ZIII)} \tag{3.7}$$

3.3.4 Representation of seismic action

In the examples presented in §3.3.5 (i.e. at the design stage) ground motion was represented by natural records, following the Eurocode (EC) 8 preferred (and common) approach of seismic action representation when recorded accelerograms satisfying relevant selection criteria are available. Selection and scaling of natural records (used in Steps 2, 3 of the Def-BD method, §3.2) followed

the EN1998-1 (CEN 2004b) and EN1998-2 (CEN 2005a) requirements along with a 'structure-specific' selection criterion (described in the following), and was performed with aid of the ISSARS software (Katsanos & Sextos 2013) that utilises the Next Generation Attenuation Strong-Motion database, PEER-NGA (Chiou *et al*. 2008). In the case of Zone II, 18 eligible pairs of seismic events were initially selected by adopting as preliminary search criteria a moment magnitude M_w = 6.5-7.0, epicentral distance R = 10-25 km, site conditions 'D' according to the NEHRP provisions (FEMA 2009) (roughly equivalent to subsoil class 'C' in CEN 2004b), and a *PGA* of 0.21-0.42g. It is noted that values of *PGA* were set in the previous range as a means to select ground motions with acceleration ordinates that would yield scaling factors close to 1.0 for EQIII.

The selected accelerograms were used as seed motions to form 31824 eligible suites of seven records scaled according to EN1998-1 by a single (i.e. global) scaling factor SF_{EC} so that the mean spectrum of each suite of records was not lower than 0.9 times the target spectrum within the period range $0.2T_1$~$1.5T_1$ (T_1: fundamental period along the transverse direction of the bridge) as prescribed for bridges (in EN1998-2), using either the H1 or the H2 set of horizontal components (i.e. notation used in the database of Chiou *et al*. 2008 to identify components). Suites of records were subsequently ranked according to the similarity of spectra (those of the selected motions to the EQIII target spectrum), as quantified by the normalised root-mean-square-error *RMSEn* (Katsanos & Sextos 2013). The number of records per suite was selected equal to seven, to reflect the minimum computational effort commonly required by codes worldwide in order to allow design of members using the mean estimate of the response. Yet, the selection of the suite of records adopted in the design was additionally based on a maximum accepted variability in the pier displacement response introducing a 'structure-specific' selection criterion with a view to improving the reliability of the mean response prediction (i.e. by suppressing the variability in the response) since the uncertainty of the input motion is already incorporated in the definition of the target spectrum (Katsanos & Sextos 2013). A limit value of the standard error of the mean (*SEM*) equal to 15% was adopted assuming a two-sided *Student-t* probability density function and 90% confidence level. Calculated *SEM* values were based on the results obtained from linear response history analysis of the bridge under the 18 eligible events. Although this procedure is automated in ISSARS, the software does not provide the option to assess *SEM*s on the basis of NLRHA that is expected to result in increased standard error values (§3.3.6). The issue of whether a limited number of natural records is deemed adequate to provide reliable estimates of mean response is discussed in more detail in the next chapter addressing isolated systems (i.e. Chapter 4) where a slightly different scaling procedure was adopted in an attempt to constraint efficiently the variability of NLRHA displacements (i.e. the critical response quantity for the isolation system) following a simpler approach (§4.2.2). Herein (i.e. §3.3), the mean response derived at the design stage from NLRHA using the previously described selection criteria and scaling procedure was compared during the assessment stage (§3.3.6) with the mean response derived from nonlinear dynamic analysis under a number of artificial records that were able to suppress the standard error within 15%.

Regarding the case of Zone III, although a more refined approach would require a ground motion selection based on different criteria (e.g. higher values of magnitude and *PGA*), the suite of records adopted in the design was selected from the bin of the 18 eligible pairs of seismic events used in Zone II for the sake of simplicity, and with a view to investigating how the final design is affected by a higher level of seismic action, disengaged from parameters associated with the differentiation of preliminary selection criteria; this inevitably led to a higher scaling factor compared to Zone II.

Since only the transverse response of the bridge is considered, implementation of the EN1998-2 scaling procedure within the same period range (i.e. $0.2T_1$~$1.5T_1$), wherein the ensemble 5%-damped elastic spectrum calculated from the SRSS spectra of all time histories is compared with 1.3 times the target spectrum, results in practically the same values of scaling factors. The above selection and scaling procedure resulted in the suites presented in Table 3.2 and Table 3.3 (addressing also the PEER-NGA unique record sequence number *RSN* identification code) that

Table 3.2 Peak ground acceleration *(PGA*), velocity (*PGV*), displacement (*PGD*), and Arias intensity (I_A) of selected suite of natural records (Zone II); unrotated (as-recorded) SF_{EC}-scaled H2 components

								SF_{EC} × H2 Component			
Earthquake			Region	Year	M_w	R_{epi}	SF_{EC}	*PGA*	*PGV*	*PGD*	I_A
No.	RSN	Name				(km)	(-)	(*g*)	(m/s)	(m)	(m/s)
1	6	Imperial Valley-02	USA	1940	6.95	12.99		0.254	0.352	0.258	1.674
2	165	Imperial Valley-06	USA	1979	6.53	18.88		0.301	0.356	0.153	1.663
3	185	Imperial Valley-06	USA	1979	6.53	19.81		0.261	0.589	0.378	1.179
4	189	Imperial Valley-06	USA	1979	6.53	12.43	1.18	0.599	0.366	0.065	3.834
5	995	Northridge-01	USA	1994	6.69	23.61		0.424	0.324	0.036	2.809
6	996	Northridge-01	USA	1994	6.69	16.99		0.287	0.353	0.056	1.183
7	1107	Kobe	JP	1995	6.90	24.20		0.408	0.327	0.114	2.364
			Minimum Value		6.53	12.43		0.254	0.324	0.036	1.179
			Maximum Value		6.95	24.20		0.599	0.589	0.378	3.834
			Mean					0.362	0.381	0.151	2.101

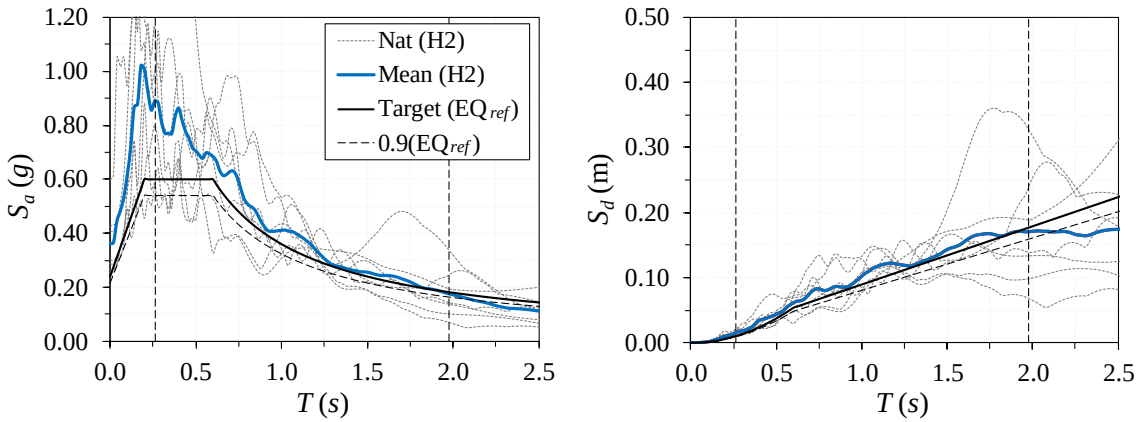

Fig. 3.10 Spectral matching of response acceleration (left) and displacement (right) EN1998-2-scaled mean spectra to the target spectrum (*PGA* of 0.21*g*, site 'C', $T_{R,EQIII}$) for the adopted suite of SF_{EC}-scaled natural (Nat) records considering H2 components (SEM_{Pier1}=13.2%, SEM_{Pier2}=13.5%)

exhibit the spectral matching depicted in Fig. 3.10 and Fig. 3.11 for Zones II and III, respectively, considering the H2 set of horizontal components; although *RMSEn* was found lower in the case of the H1 components, H2 was finally adopted, due to the superiority of this particular set with regard to the established confidence level of structural response (i.e. lower *SEM* values in pier displacement response). Ground motion intensity and energy characteristics of the SF_{EC}-scaled records presented in the tables incorporate the site ('C') amplification effect (i.e. intensity parameters are comparable to S_C = 1.15 times the peak ground characteristics of the target spectra) and apply higher spectral accelerations in the short periods of the considered $0.2T_1$~$1.5T_1$ range compared to the target spectrum.

As previously mentioned, the primary objective during the assessment stage (§3.3.6) was the evaluation of the mean response of the bridge under a seismic excitation that matches as closely as feasible the 'design excitation' (i.e. the target spectra) rather than the accurate estimation of the variability in seismic response around this mean. Considering also that the overestimation of the

Table 3.3 Characteristics of selected suite of natural records (Zone III); unrotated (as-recorded) SF_{EC} -scaled H2 components

								SF_{EC} × H2 Component			
Earthquake			Region	Year	M_w	R_{epi}	SF_{EC}	*PGA*	*PGV*	*PGD*	I_A
No.	RSN	Name				(km)	(-)	(*g*)	(m/s)	(m)	(m/s)
1	6	Imperial Valley-02	USA	1940	6.95	12.99		0.388	0.537	0.393	3.894
3	185	Imperial Valley-06	USA	1979	6.53	19.81		0.399	0.899	0.577	2.743
4	189	Imperial Valley-06	USA	1979	6.53	12.43		0.914	0.559	0.099	8.921
2	313	Corinth	GR	1981	6.60	19.92	1.81	0.534	0.457	0.128	2.774
5	949	Northridge-01	USA	1994	6.69	11.10		0.556	0.418	0.191	3.820
6	996	Northridge-01	USA	1994	6.69	16.99		0.438	0.538	0.086	2.753
7	1107	Kobe	JP	1995	6.90	24.20		0.622	0.499	0.173	5.501
			Minimum Value		6.53	11.10		0.388	0.418	0.086	2.743
			Maximum Value		6.95	24.20		0.914	0.899	0.577	8.921
			Mean					0.550	0.558	0.235	4.344

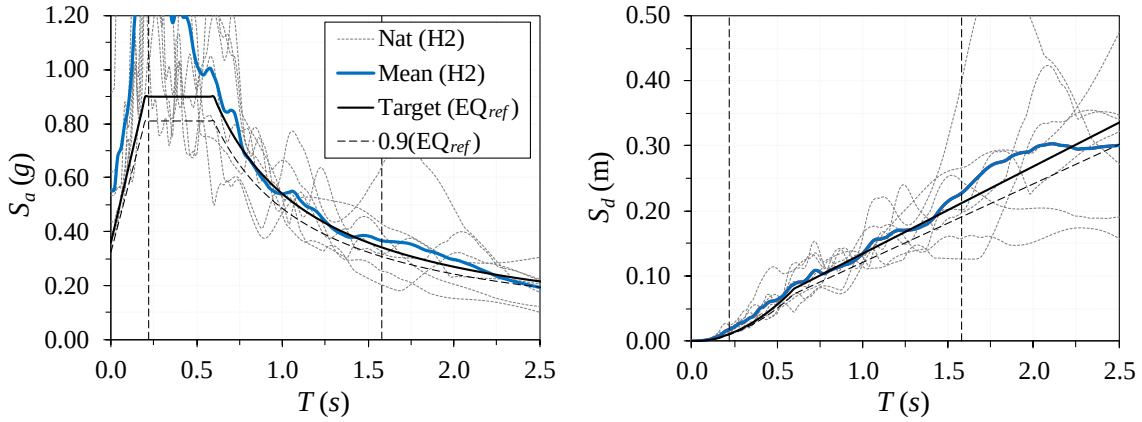

Fig. 3.11 Spectral matching of response acceleration (left) and displacement (right) EN1998-2-scaled mean spectra to the target spectrum (*PGA* of 0.31*g*, site 'C', $T_{R,EQIII}$) for the adopted suite of SF_{EC}-scaled natural (Nat) records considering H2 components (SEM_{Pier1}=12.3%, SEM_{Pier1}=14.7%)

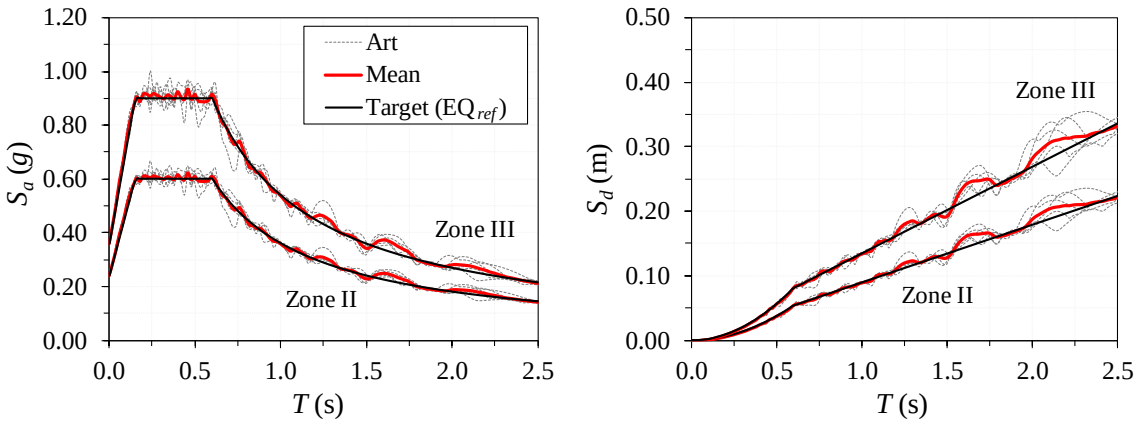

Fig. 3.12 Spectral matching of response acceleration (left) and displacement (right) mean spectra to the target spectrum ($T_{R,EQIII}$) for the suite of artificial records and two different seismic zones

equivalent number of cycles at the peak displacement, commonly associated with the use of artificial records, was not found to have a significant effect on the peak response (Iervolino *et al.* 2010) when degradation of strength in energy dissipating zones is disregarded (§3.3.2), NLRHAs were performed for each design case (Zone II, III) using five artificial records (identical to those used to assess the MDDBD approach in Kappos *et al.* 2013). The accelerograms were selected from a set of 10 records generated with the computer program ASING (Sextos *et al.* 2003) to fit the elastic design acceleration spectra associated with EQIII (Zone II), and scaled appropriately when a different PL or seismic zone was considered. The spectral matching of the suite of artificial records to the target spectrum is presented in Fig. 3.12. It should be noted that the adopted analysis format (i.e. adoption of natural records at the design stage and artificial records at the assessment stage) serves the objectives set in this investigation and does not represent by any means a restriction specific to the suggested methodology, which can be applied irrespective of the type of record selection and scaling procedures (§3.2.3).

3.3.5 Application of the Def-BD procedure

Step 1: A standard RSA was performed to provide the strength of the members (energy dissipation zones) that are expected to respond inelastically under EQII having a relatively high probability of exceedance (approximately 40% in 50yrs) according to the 'ordinary bridge' performance objective adopted herein (Fig. 3.2). The β-factor related to the required performance of the structure under the selected earthquake level (§3.2.2) was taken equal to 0.75. Pier stiffness was estimated on the basis of yield condition in the pier by taking into account the effects of axial load ratio as per Fig. 3.4, considering axial load from service loading (quasi-permanent combination), and assuming a minimum longitudinal reinforcement ratio ρ_l of 10‰. An effective flexural stiffness equal to 43% and 39% of the gross section was obtained for piers in Zones II and III, respectively (different diameter is used in each zone, see next steps).

The strength of the selected dissipation zones (i.e. the base and top of piers) was estimated taking into consideration the range within which the inelastic deformations should fall, which corresponds to the degree of damage allowed according to the SP2 'operationality' criteria (associated with EQII in ordinary bridges). The allowable rotational ductility factors $\mu_{\theta,SP}$ were estimated according to Eq. (3.1), where the index 'SP' indicates a deformation or ductility factor limit value associated with SP2 at this stage. Assuming an 'operationality'-related concrete strain between 3.5 and 4.0‰, φ_{SP2} was derived from relevant charts, proposed by Kowalsky (2000), φ_y and L_{pl} were obtained from Eqs. (3.8) and (3.9) respectively (Priestley *et al*. 2007), whereas h_{eq} was estimated from the results of RSA; the same equations were used in Kappos *et al*. (2013). Updated and more accurate values of strains, curvatures, chord rotations and ductility factors corresponding to specific PLs were computed in Step 2. $\mu_{\theta,SP}$ was found equal to 1.65 and 1.55 for Pier 1 and Pier 2, respectively, for Zone II design, and 1.58 and 1.48 for Zone III. Finally, the allowable strain of the bearings in the specific PL was assumed equal to 1.0 (Table 3.1).

$$\varphi_y = 2.25 \cdot \varepsilon_y / D_p \tag{3.8}$$

$$L_{pl} = k \cdot h_{eq} + 0.022 \cdot f_y \cdot \varnothing_L, \quad k = 0.2 \cdot \left(\frac{f_u}{f_y} - 1 \right) \leq 0.08 \tag{3.9}$$

Following the design process described in §3.2.2, elastic chord rotations θ_{el} were related to the corresponding inelastic ones (i.e. θ_{inel}), using an empirical magnification factor of 1.22 as recommended by Bardakis & Fardis (2011a). The reduced pier yield (design) moments, implicitly related to the flexural demand under EQI (Fig. 3.2, Table 3.1) that correspond to the yield state of the bridge, were calculated according to Fig. 3.5(left). The more accurate procedure for defining the pier design moments illustrated in Fig. 3.5(right) was not used since the pertinent combination of permanent and transient actions does not affect the transverse response of the bridge considered herein.

Using standard design aids for flexure with axial loading and design values for strength of materials, Step 1 yielded in the case of Zone II a longitudinal steel ratio of 10.4 ‰ for each pier column, with a diameter of 1.2m. It is worth noting that a 1.5m diameter was considered as a starting point for the case of Zone II, corresponding to the design outcome of the MDDBD method (§3.3.1); however, since the longitudinal reinforcement demand was found to be less than 10‰ (actually less than 5‰) and the shear strain of the elastomeric bearings was less than 1.0, the diameter was gradually reduced to 1.2m. As noted in §3.2.2, this type of iterations is not inherent to the methodology; in fact, it is associated with the decision to adopt as a starting point the outcome of the MDDBD methodology regarding the geometry of the piers (§3.3.1). The resulting design quantities are shown in Fig. 3.13, Fig. 3.14 (D-RSA case) and in Annex A (i.e. Table A.1, 'Design-RSA' column). $u_{0,y\text{-}y}$, $M_{x\text{-}x}$, $\theta_{x\text{-}x}$ in the figures represent relative displacements of the deck along the transverse axis of the bridge *y*-*y*, pier bending moments and chord rotations about the longitudinal

axis *x*-*x*, respectively (Fig. 3.8). Likewise, for Zone III (Table A.2), wherein a 1.7m diameter was selected, the design process yielded a longitudinal steel ratio of 12.5‰ and 9.5‰, accompanied by a minor exceedance (i.e. 7%) of the bearing strain limit at the right abutment (i.e. Abt 2 in Fig. 3.6), noting that a larger diameter of column would result in substantially lower ρ_l.

Step 2: A partially inelastic model of the structure was set up according to §3.2.3, 3.3.2. Assuming a code minimum transverse mechanical reinforcement ratio (i.e. $\omega_{w,min}$ = 0.18, according to EN1998-2), the strength and the effective stiffness of the dissipating zones, based on mean values for material properties and the ρ_l computed in Step 1, were defined through *M*-φ analysis (§3.3.2). Refined deformation limits (i.e. curvatures and curvatures ductility factors) based on the allowable strains associated with SP2 requirements (§3.3.2, Table 3.1) were subsequently calculated in this step. It should be noted that a strict approach requires the definition of different bilinear *M*-φ curves under different PLs for the same section and detailing, due to the adopted bilinearisation criterion (i.e. equality of areas under the 'exact' and the bilinear curve) and the relevant allowable strains, that result in different yield conditions and post-elastic slope of the bilinear curve. Nevertheless, for the sake of simplicity and to avoid the definition of different PIMs in cases wherein the pier longitudinal reinforcement ratio is not differentiated during Steps 2 and 3, the yield state (i.e. M_y, φ_y) and the post-elastic slope derived from a single approximation of the 'exact' curve based on the minimum transverse mechanical reinforcement ratio ρ_w, were assumed constant, adjusting only the relevant SP curvatures (associated with the allowable material strains). Apart from reducing the computational effort during analysis, the above simplification is not expected to yield significantly different results since a bilinear curve based on an allowable concrete strain of ε_c = 3.5‰ (i.e. SP2) would yield a lower M_y, but also a lower φ_y compared to the case when the minimum ρ_w is considered providing a larger allowable SP2 ductility limit under EQ(SP2). In a similar context, the adoption of a larger (than the minimum) ratio ρ_w at Step 4, that can be 2~3 times the minimum, further reduces the SP2 ductility limit but also provides some additional flexural strength, decreasing the deformation demand under EQ(SP2).

Inelastic dynamic analyses of the bridge were performed under the suite of records of Fig. 3.10 and Fig. 3.11 scaled to the level of seismic action associated with EQII. 'Operationality' verifications included specific limits for maximum curvature and chord rotation ductility factors in the case of piers, and specific strain limits in the case of the elastomeric bearings as per Table 3.1. Limits of chord rotation ductility factors were computed based on the refined yield and SP curvatures (resulting from the *M*-φ analysis), and the estimation of the pier equivalent cantilever heights according to the results of the NLRHA; the latter were calculated as the mean of the span ratio values observed in the piers during the seven RHAs at the time step each member enters the inelastic range (i.e. when the bending moment at the critical section first reaches the yield moment). Key results are discussed after the following step.

Step 3: Inelastic dynamic analyses were run for the same accelerograms, now scaled to EQIII. SP3 verifications also included limits for maximum curvature and chord rotation ductility factors for

columns, and strain limits for elastomeric bearings adopting a shear strain limit of 2.0. EN1998-2 (CEN 2005a) imposes the same deformation limit on the maximum total design strain under the 'design earthquake' (i.e. EQIII) which is associated with the combined effect of seismic design displacements u_{EQ} (including effects of torsional response around a vertical axis), long-term displacements due to the permanent and quasi-permanent actions u_G (e.g. prestressing after losses, shrinkage, creep), and displacements due to thermal actions u_T. Nevertheless, its adoption exclusively for the seismic design displacement should not be deemed incompatible since, in the transverse direction considered herein, u_G and u_T are equal to zero, while the value of u_{EQ} at the level of the deck soffit does not include a contribution from the rotation of the deck end section.

The displacement profiles obtained from the design Steps 2 and 3 (denoted with D in the figures) are also illustrated in Fig. 3.13, whereas in Fig. 3.14, Fig. 3.15 chord rotation demands resulting from the design procedure (D-NLRHA) are compared with the target deformations (SP). Further design quantities, i.e. effective stiffness, curvature and displacement ductility factors, column drifts, pier equivalent cantilever heights and elastomeric bearing strains, are presented in companion tables provided in Annex A (i.e. Table A.1, Table A.2). Displacements and deformations presented in the aforementioned figures and tables as the nonlinear case (NLRHA) are mean values calculated from pertinent quantities recorded in the structure during the seven RHAs, at the time step each member enters the inelastic range (yield state) and at the time step of maximum response.

It is evident that the performance requirements associated with the 'operationality' SP2 criteria control the design while excellent agreement is found between target deformations and design quantities resulting from NLRHA. This is mainly due to the consistent assumptions made for pier stiffness; simplifications in defining bilinear curves provided demand quantities that are on the side of safety. In the case of Zone II, further reduction of the column diameter aiming at bringing the demand closer to the deformation limit at the location of Abt 2 would render critical the design under the quasi-permanent combination of 'non-seismic' actions. A slight exceedance of the target deformations under EQII is observed at the base of Pier 1 (Fig. 3.14(left)); however, since the relevant curvature (or chord rotation) corresponds to a compressive concrete strain that is equal to 4‰ (i.e. within the range of accepted values in Table 3.1), it was deemed appropriate to proceed the design to the next step without increasing the pier longitudinal reinforcement. With regard to the performance of Pier 2 (for Zones II & III), a decrease of ρ_l (that would result in improved convergence) was omitted due to the adopted minimum ratio (i.e. 10‰). It is also worth noting that in the case of Zone II, the underestimation of the pier strength during the linear analysis (RSA) derives from the fact that the β-factor does not account for the increase in strength due to the effect of the increased axial load ratio n_k. Although this indicates the need for considering lower values of β (e.g. accounting for the ratio f_{cd} / f_{cm} in cases of high values of n_k), minimum reinforcement requirements preclude their adoption.

SP3 requirements were not found critical in any of the cases studied herein, although the bearing strains of the Abt 2 were close to the deformation limits (Table A.1, Table A.2: Row No. 20)

especially in the case of Zone III. In fact, pier deformation demands resulting from this PL were somewhat lower than the deformation limits corresponding to the minimum transverse reinforcement ratio ρ_w considered in Step 2 (Table A.1, Table A.2, Step 3, '$\rho_{w,min}$' column). In the tables provided in Annex A, design quantities at the top of the piers are also presented; however, as expected, these are not critical to the design since the base reinforcement is continued up to the pier top, according to common practice for low to medium height bridge columns.

Step 4: Design and detailing for shear in Step 4 was carried out using shear forces obtained from NLRHA under EQIII, implicitly related to those corresponding to the EQIV seismic action through appropriately selected magnification factors. In the case of Zone II, pier shear forces are not expected to increase under EQIV, due to the elastic-perfectly plastic bilinear approximation of the M-φ curves (Fig. 3.14, Fig. 3.15) derived from moment-curvature analysis, and the fact that piers exhibit inelastic behaviour at both ends (i.e. base and top) under EQIII. Nevertheless, a magnification factor SF_v of 1.10 was applied to account for the increase in flexural strength due to the expected increase of the transverse reinforcement ratio ρ_w associated with the shear and confining requirements of Step 4 (recall that a minimum ratio of transverse reinforcement was considered so far, assumed in Step 2). Regarding Zone III, a factor of 1.20 was used to account for the strain-hardening effect (Fig. 3.14, Fig. 3.15) considering an increase of μ_u in V-u diagrams equal to SF_{EQIV} (Eq. (3.7)). Pier shear design for the two seismic zones was performed according to the EN1998-2 (CEN 2005a) provisions using design values for material properties and assuming γ_{bd} = 1.0 (i.e. the safety factor against brittle failure) as a means to avoid over-conservatism introduced mainly from neglecting the shear 'carried by concrete' (Isaković *et al*. 2008a); the transverse reinforcement was found to be governed by the confinement requirements apart from the case of Pier 1 in Zone III.

Detailing of piers for confinement was carried out with due consideration of the expected level of inelasticity (quantified by μ_φ) under EQ(SP4) (Fig. 3.2). A magnification factor SF_φ equal to 2.0 was used to implicitly relate the curvature ductility demands derived from Step 3 to those expected under EQIV. The magnification factor was set equal to the expected increase of μ_u (i.e. SF_{EQIV}) (rather than that of μ_φ) as the latter was found to provide more reasonable approximations of inelastic demand as discussed in the following. Using the yield curvatures calculated in Step 2, the expected curvatures associated with EQIV were defined as $\varphi_{u,EQIV} = \mu_{\varphi,EQIV} \cdot \varphi_y$ and subsequently associated with anticipated ultimate concrete strains ε_{ccu} according to the moment-curvature analysis results of Step 2. The required transverse reinforcement ratios were then easily obtained as a function of the ultimate concrete strains in accordance with the stress-strain model adopted in Step 2 (i.e. Kappos 1991, §3.3.2). The above procedures (i.e. shear, confinement requirements) yielded transverse reinforcement ratios of $\rho_{w,Pier\ 1}$ = 12.4‰, $\rho_{w,Pier\ 2}$ = 10.6‰, and $\rho_{w,Pier\ 1}$ = 13.2‰, $\rho_{w,Pier\ 2}$ = 10.4‰ for Zones II and III, respectively.

The same magnification factor (i.e. $SF_{\gamma q}$ = 2) was also used to check that the bearings do not exceed their ultimate deformability based on stability criteria according to Eq. (3.10) (Constantinou *et al*. 2011);

$$N_{cr}' = \frac{\pi\sqrt{\lambda}G_R S r'}{t_R} A_{lap} \tag{3.10}$$

In the empirical Eq. (3.10), N_{cr}' is the buckling load of a bearing with bolted plates subjected to combined compression and lateral deformation, λ depends on the assumption for the value of the rotational modulus of the elastomeric bearing (λ = 2.25 for rectangular or square bearings), G_R is the nominal shear modulus of the elastomer, S is the shape factor of the bearing, r' is the radius of gyration of the bonded area of the elastomer ($r'^2 = I'/A'$, where I' is the moment of inertia and A' the bonded area of the bearing, i.e. the area of the steel reinforcing plates), A_{lap} is the reduced bonded area defined as the overlap between the top and bottom bonded elastomer areas of the laterally deformed bearing (hence a function of the bearing strain), and t_R is the total thickness of the elastomer. A more detailed presentation of elastomeric bearing verifications is provided in §5.3.5.1 for the general case of seismic isolators.

Considering the transverse response of the rectangular bearing (details of the bearings can be found in §3.3.1) mounted with the longer side parallel to the transverse direction of the bridge (to minimise the rotational restraint in the longitudinal direction) and equating the buckling load with the axial load of the bearing under EQIII implicitly related to EQIV by a magnification factor of 1.30 (the expected increase in the axial load of bearings can be approximated from the results of the RSA performed in Step 1), the previous relationship was re-ordered to derive the ultimate bearing strain (Table A.1, Table A.2: Row No. 30, 'SP4' column), that was in turn compared with the bearing strains recorded under EQIII and multiplied by $SF_{\gamma q}$ = 2.0. Similarly, EN1337-3 (CEN 2005b) adopts Eq. (3.10) to check the buckling stability of bearings under the 'design earthquake' (corresponding to EQIII) incorporating a safety factor of about 2 (for rectangular bearings). It is

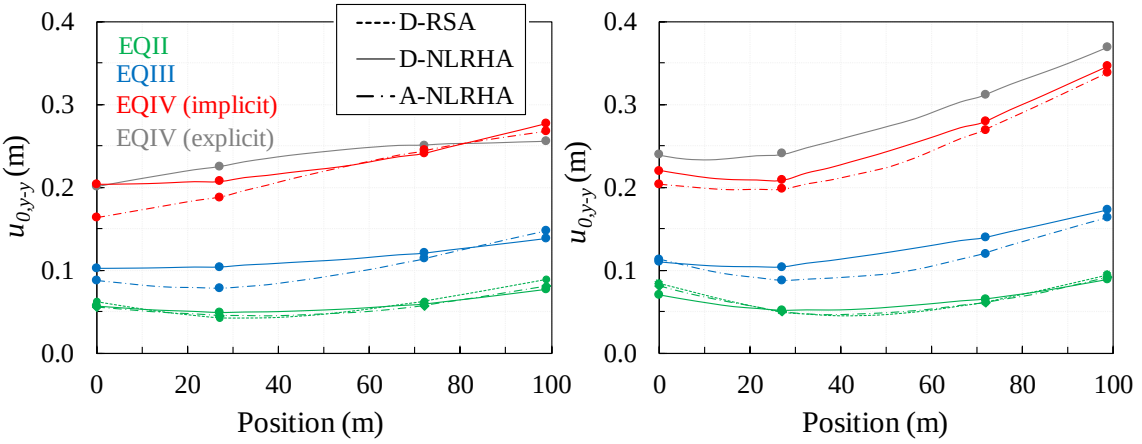

Fig. 3.13 Response spectrum (RSA) and nonlinear response history (NLRHA) peak displacement demands $u_{0,y\text{-}y}$, derived from design (D) and assessment (A) under EQII, EQIII, EQIV for Zone II (left) and III (right)

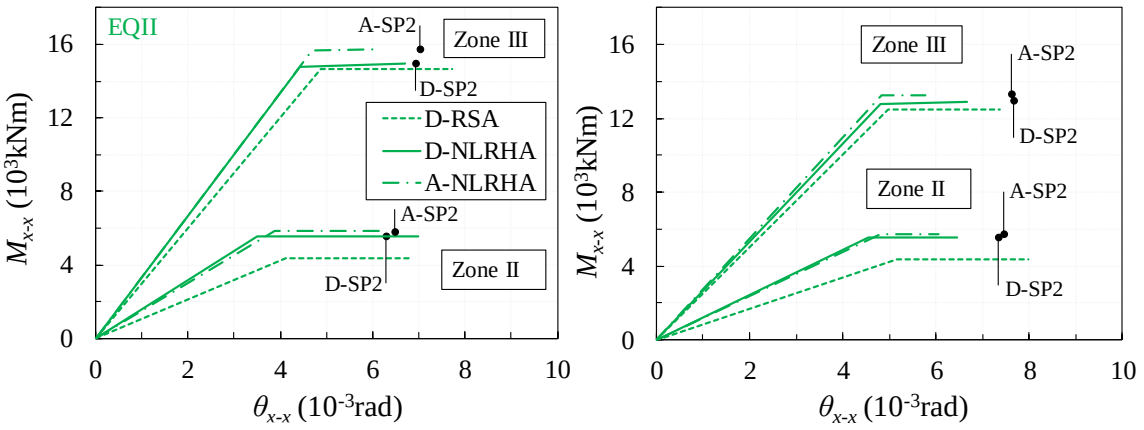

Fig. 3.14 Moment ($M_{x\text{-}x}$) vs. chord rotation ($\theta_{x\text{-}x}$) demand curves (RSA, NLRHA) derived from design (D) and assessment (A) in the case of Zones II and III, under EQII at the base of Pier 1 (left) and Pier 2 (right), compared with allowable SP2 deformation limits (solid dots)

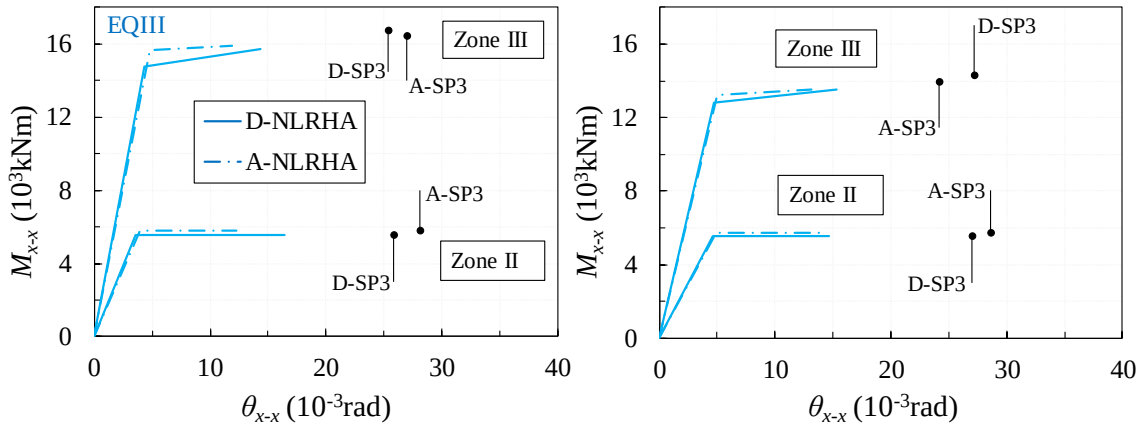

Fig. 3.15 Moment ($M_{x\text{-}x}$) vs. chord rotation ($\theta_{x\text{-}x}$) demand curves (NLRHA) derived from design (D) and assessment (A) in the case of Zones II and III under EQIII at the base of Pier 1 (left) and Pier 2 (right), compared with allowable SP3 deformation limits (solid dots)

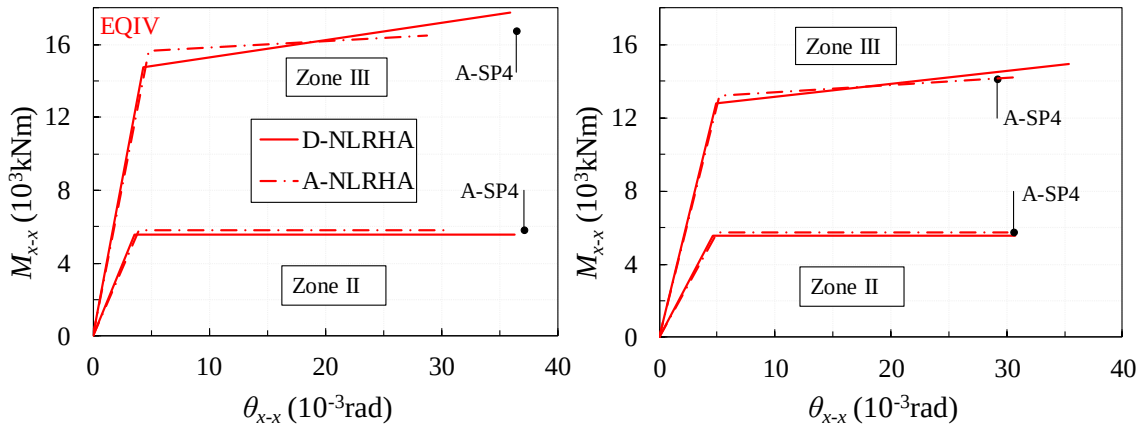

Fig. 3.16 Moment ($M_{x\text{-}x}$) vs. chord rotation ($\theta_{x\text{-}x}$) demand curves (NLRHA) derived from design (D) (explicitly calculated) and assessment (A) in the case of Zones II and III under EQIV at the base of Pier 1 (left) and Pier 2 (right), compared with allowable SP4 deformation limits (solid dots)

clear that in the case of Zone III (Table A.2), SP4 are the critical performance requirements given the exceedance of the deformation limit observed at the location of the right abutment under EQIV ($\gamma_{q,EQIV}$ = 3.9 > $\gamma_{q,SP4}$ = 3.0). In principle, a designer should opt for an upgrade of the displacement capacity of the (low-cost) elastomeric bearings (while maintaining their horizontal stiffness); on the other hand, an increase of the column diameter would penalise (in terms of cost) the flexural and shear design of piers under EQII, IV (i.e. adoption of minimum reinforcement ratios, increase of shear forces) and distort NLRHA results derived from the previous step (hence requiring iterations, Fig. 3.1b). Herein, the above solution (i.e. upgrade of bearings) is not adopted for the sake of consistency in the design results of Def-BD and MDDBD; it is noted that the bearings of the right abutment are the critical elements (i.e. govern the design) in both approaches.

Although not required by the suggested procedure (§3.2.5), the seismic demand deriving from explicitly considering the effects of EQIV is presented in Fig. 3.13, Fig. 3.16 (and Table A.1, Table A.2: 'Design-NLRHA' column); these values were determined from NLRHA assuming that EQIV is characterised by twice the spectrum of EQIII (Eq. (3.7)). Attention is finally drawn to the fact that the EQIV deformation demand (D-NLRHA) in Fig. 3.16 (and Table A.1, Table A.2) is not followed by an SP4 limit deformation, since the demand calculated at this stage of design is used directly for detailing the piers for confinement in Step 4 (i.e. SP limits cannot be calculated prior to detailing).

From the design quantities presented in the figures and summarised in the Annex A tables, it is seen that the pier ductilities resulting from explicit analysis are higher than the demand estimated implicitly through magnification factors (i.e. '*SF*·Step 3' column in Annex A tables), or else, the increase of deformation ductilities is larger than the considered SF_{EQIV}. The above indicates that an explicit consideration of EQIV by magnifying the ground motions associated with EQIII may lead to a more conservative design compared to the implicit magnification of response resulting from analysis under EQIII. Given that implicit design procedures should yield more conservative results compared to explicit analysis, the previous remark may be seen as an inconsistency of the method. Nevertheless, it simply points to the fact that the calibration of magnifications factors was made to obtain the peak response derived from assessment procedures accounting for the final design configuration of the structural elements (i.e. modification of yield properties attributed to final detailing and increased transverse reinforcement), using artificial records closely matching the design spectrum, and resulting in general to a safe design as demonstrated in §3.3.6.

3.3.6 Assessment of design

Assessment of the designs presented in the previous section was carried out in order to evaluate the efficiency of the proposed design procedure for the three different PLs associated with SP2, SP3, and SP4 requirements under EQII, EQIII, and EQIV, respectively, using the artificial records presented in §3.3.4. Moment-curvature analyses based on mean values for material properties and the final detailing of reinforcement according to the results of §3.3.5 were performed for each pier

section (§3.3.2) updating the deformation and ductility factor SP limits. The assessment focused mainly on whether the critical response quantities recorded during the design stage were close to those estimated at the assessment stage and whether the design can be deemed as safe, i.e. if the values resulting from analysis at the assessment stage are below the 'refined' SP limits.

In Fig. 3.13-Fig. 3.16 (supplemented by Table A.1 and Table A.2) mean response quantities of interest derived from the assessment procedure (denoted with A in the figures) are compared with those computed during the design (D) in the cases of Zones II and III. An overall agreement of deformation demand can be observed between design and assessment, more so in the case of EQII, where the piers enter the inelastic range without developing large deformations (as dictated by the SP2 requirements). The largest difference between design and assessment quantities is noted under EQIV (explicit case) in the area of Abt 1 and Pier 1, wherein large inelastic deformations develop, with differences decreasing in the area of Pier 2 and Abt 2. These differences imply that some conservatism is introduced during design. The overestimation of deformation demand in the case of explicit analysis (compared to the assessment case) is associated with the adoption of code-type linear scaling procedures (e.g. EN1998-2) that do not set an upper limit of spectral deviation to the mean (or the individual record) spectrum (Sextos *et al*. 2011) resulting in higher spectral ordinates over a broad period range (Fig. 3.10, Fig. 3.11); recall that the limit of 0.9 in §3.3.4 represents a threshold value applied to the mean spectrum. The above conservatism can be mitigated or further amplified by the increased variability in seismic response (quantified by the standard error measure), which in turn results from significant deviations of the individual record spectra from the target spectrum (related to the application of a single scaling factor as per EN1998), and from large inelastic deformation demands. Apart from 'poor' estimates of mean response (i.e. of low reliability, Shome *et al*. 1998) further practical complications may be induced, e.g. the problematic definition of mean response when both elastic and inelastic quantities are involved (discussed later in §5.3.6.2), as opposed to the assessment stage wherein response quantities are expected to be less affected by the adopted scaling procedure and the increased variability.

To quantify the introduced conservatism and assess its significance, the mean displacement demand at the top of Pier 1 under EQIV, derived from each possible suite of n = 3, 5, and 7 artificial records formed out of the initial bin of 10 records, is plotted against the normalised root-mean-square-error *RMSEn* (representing the 'goodness-of-fit' of each suite) in Fig. 3.17. It is seen that the suite of 7 natural records used at the design stage (represented by a solid line since its *RMSEn* corresponds to a value in the order of 0.15 located beyond the *RMSEn* -axis limit) predicts reasonably well the mean displacement, providing an estimate located at the upper part of the sample-means obtained from the alternative suites of artificial records. In this regard, the 'structure-specific' selection criterion regarding the limitation of the response variability (assessed on the basis of linear RHA) was able to prevent unrealistic mean response values (Sextos *et al*. 2011). Yet, the increased associated standard error values due to the vibration of the bridge in the inelastic range (~30% in Fig. 3.18) indicate that the selected suite estimates the mean response with less confidence compared to artificial suites of 5 records. In the latter case values of *SEM* are

constrained below 15%, associated in most cases with lower sample-means as illustrated in Fig. 3.17 (more clearly in the case of n = 3 records). In any case, improved mean estimates can be attained from natural records by (*i*) setting upper spectral deviation limits, (*ii*) increasing the number of records, and/or (*iii*) selecting records based on 'structure-specific' criteria evaluated on the basis of NLRHA. Nevertheless, adopting the third approach in combination with the EN1998 scaling procedures is prohibitive due to the significantly increased computational effort involved; e.g. investigating the range of standard error values derived from all possible suites of 7 records formed out of a bin with 10 eligible events would require 840 nonlinear dynamic analyses (due to the 840 different scaling factors) in contrast to the 10 NLRHAs used to construct the relevant chart in Fig. 3.17.

Mean response quantities derived at the assessment stage under EQIV were found closer to the design quantities implicitly estimated from NLRHA results under EQIII through magnifications factors; although the implicit approach cannot capture significant modifications of the dynamic characteristics of the bridge due to the increased inelastic deformations, as indicated by the different shape of displacement profiles in Fig. 3.13(left), it resulted in better approximations of the peak response indicating the efficiency of the selected *SFs* (§3.3.5). Regarding the structural performance evaluation of the bridge at the assessment stage, the design was found to be safe, in that the bridge response satisfied the SP deformation limits associated with the relevant PLs (even in the case of EQII-Zone II where a slight exceedance of the deformation limit was observed during design at the base of Pier 1), since the deformation demand derived from the assessment procedure was in general lower that the one derived at the design stage. Only in the case of the SP4 assessment verifications (under EQIV and Zone III) a minor exceedance of the deformation capacity (~6%) was recorded at the base of Pier 2 (Fig. 3.18(right)). Similar conclusions are drawn with respect to the shear strength, the confinement requirements and the bearing strains (the exceedance of bearing strains at Abt 2 under EQIV-Zone III was discussed in §3.3.5).

Apart from the introduced conservatism during the design, the reduced deformation demand (compared to the relevant deformation capacity) in the EQII-Zone III assessment case (Fig. 3.14) is also ascribed to the bilinear approximation of the moment-curvature curves at the design stage (based on the equality of areas under the 'exact' and the bilinear M-φ curve) that included a post-elastic branch with a non-zero slope and thus entailed a lower (effective) yield moment (deriving from the consideration of a minimum ρ_w in Step 2). In this case, a zero post-elastic slope of the M-φ curve is expected to lead to smaller discrepancy between design and assessment quantities (as in the case of Zone II). Nevertheless, in the example studied herein, the adoption of elastic-perfectly plastic curves in Zone III would not result to a substantially different design output since an attempt to reduce ρ_l during design (aiming to match more closely the deformation limits) would be obstructed by the adopted minimum reinforcement requirements. Despite these minor differences in the verifications between design and assessment, both stages indicate the SP2 'operationality' criteria as the critical ones for the flexural design of the piers in both seismic zones. Highlighting a deficiency of code-type (force-based) design procedures to satisfy 'operationality' requirements

by defining 'strength' on the basis of 'life-safety' verifications (in general described by the SP3 requirements in Table 3.1), this outcome also implies that following an 'occasional' seismic event, significant repair costs may be required in bridges designed according to the minimum requirements set by codes.

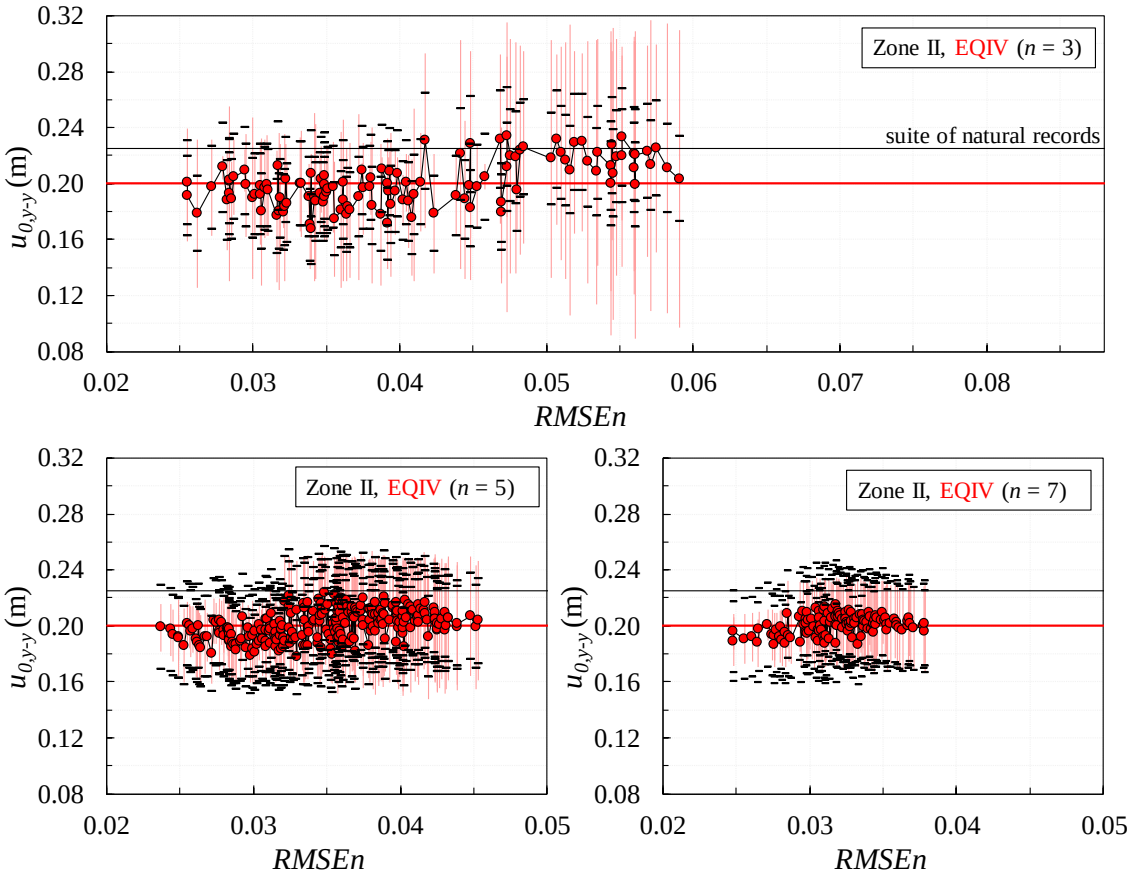

Fig. 3.17 Sample-mean estimates of Pier 1 displacements $u_{0,y\text{-}y}$ (dots), confidence intervals (error bars in red), target variability (i.e. ±15%, dashes) and mean of sample-means (red line) derived from NLRHA under EQIV considering suites of n=3, 5, 7 artificial records versus *RMSEn*, also compared with u_0 derived from RHA under the suite of 7 natural records (black line)

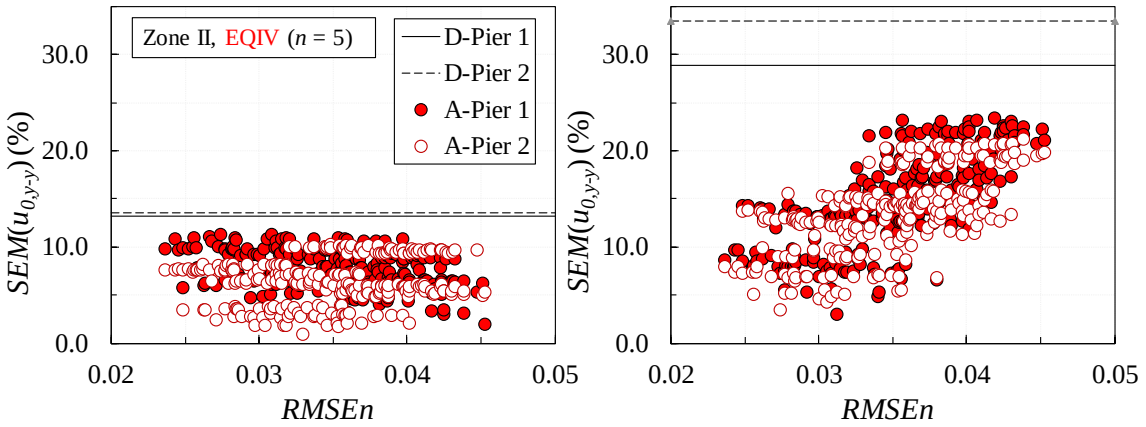

Fig. 3.18 *SEM* of peak pier displacements $u_{0,y\text{-}y}$ (dots) derived from linear (left) and nonlinear (right) RHA under EQIV versus *RMSEn*, considering alternative suites of 5 artificial records, also compared with *SEM*(u_0) values derived from RHA under the suite of 7 natural records used in design (D-Pier 1, 2)

3.4 Closing Remarks

A *deformation-based design* procedure initially developed for seismic design of buildings was tailored herein to bridge structures, aiming at efficient structural design for multiple performance levels through the control of a fairly broad range of design parameters and the aid of nonlinear dynamic analysis. To this purpose, required extensions and/or modifications to the version of the method developed for buildings (Kappos & Stefanidou 2010) were presented.

The key issues in this respect were the proper consideration of the intended plastic mechanism in the case of bridges under the relevant PLs, allowing yielding of the piers instead of the superstructure, and also the design of the bearings (which are typically not used in buildings, except in isolation schemes). Improvements including the preliminary estimation of pier stiffness, strength, and expected inelastic response on a member-by-member basis in Step 1, along with the inelastic modelling of dissipating zones, and the estimation of allowable deformation limits and confinements requirements on the basis of refined section analysis in subsequent steps (i.e. Step 2 to Step 4), represent novel features of the methodology that were feasible mainly due to the smaller number of dissipating elements compared to the generally large number of beam plastic hinges in buildings. Further modifications, addressed specific bridge engineering aspects such the proper (and simplified, compared to buildings) definition of required strength in dissipating zones, the expected elastic response of the deck, and the explicit treatment of elastomeric bearings (i.e. required verifications and consideration of appropriate deformation limits). Finally, an integrated performance-based design framework was set by introducing different performance objectives explicitly accounting for the importance of the bridge under investigation, and properly adapting the relevant performance requirements.

The validity of the suggested procedure was verified by applying it to an actual bridge previously used as a case study for a different performance based-design approach (Kappos *et al*. 2013). The following conclusions were drawn based on the application of the methodology and the evaluation of design for two different seismic zones adopting the ‘ordinary bridge’ performance objective:

- Regarding the application of the Def-BD method, SP2 ‘operationality’ criteria governed the flexural design of the piers in both seismic zones considered. Excellent agreement was found between target deformation quantities and seismic action effects resulting from NLRHA under EQII, due to the consistent assumptions made for pier stiffness, while adopted simplifications in defining bilinear curves provided demand quantities being on the side of safety. SP3 verifications were not found to be critical, resulting in deformation demands similar to deformation limits that corresponded to code requirements for minimum transverse reinforcement. On the other hand, EQ(SP4) (i.e. EQIV for ordinary bridges) imposed critical (with respect to stability) deformations at the elastomeric bearings.

- Assessment of the two designs by NLRHA using artificial records closely matching the design spectrum associated with each PL, revealed that the suggested design procedure predicted well

the structural response generally resulting in safe design, in the sense of respecting the relevant deformation limits with only occasional and marginal exceedances. Adopting a 'structure-specific' ground motion selection criterion by constraining the variability of elastic responses prevented a significant overestimation of peak inelastic response quantities, commonly introduced during design when code-type scaling procedures are applied to natural records over a large period range without setting an upper limit to the maximum deviation from the target spectrum.

- At both the design and assessment stages, the criticality of 'operationality' requirements was confirmed in defining the flexural strength of the piers, revealing at the same time an inherent weakness of code-type procedures commonly assuming that relevant requirements are met when strength is estimated on the basis of 'life-safety' verifications.
- Limited iterative effort using linear analysis was required during the first step of the procedure, wherein the initially selected diameter of the piers was gradually reduced to ensure that the required longitudinal reinforcement ratio ρ_l was higher than the adopted minimum ratio $\rho_{l,min}$. This is a standard iterative process aiming at cost effective design of the piers irrespective of the adopted design methodology.

Chapter 4
Direct Estimation of Peak Seismic Response in Reduced-DOF Isolation and Energy Dissipation Systems

4.1 Introduction

A methodology for the development of generalised design equations (GDEs) capable of providing direct estimates of peak inelastic response (i.e. without requiring iterations) in reduced degree-of-freedom (RDOF) isolation and energy dissipation systems is presented in this chapter. The starting point is a procedure previously proposed by Ryan & Chopra (2004a, b) for bilinear hysteretic isolation systems, disregarding any source of viscous damping; it involves first the normalisation of the dynamic equation of motion with a view to uncoupling the (normalised) response from the level of seismic intensity and minimising the dispersion in peak normalised relative displacements $\overline{u}_0$ and total accelerations $\ddot{\overline{U}}_0$, and second the development of design equations by statistically processing nonlinear response history analysis results derived from the previous step.

In contrast to the Ryan & Chopra (2004a, b) methodology where the key idea is to diminish the effect of the record-to-record intensity variability within an ensemble of motions characterising a specific seismic scenario (i.e. moment magnitude M_w, closest distance to the ruptured area R_{rup}), and hence estimate the peak response with higher confidence, uncoupling the normalised response from seismic intensity is seen herein from a different perspective, i.e. the reliable estimation of peak inelastic response under different performance levels (PLs) associated with hazard levels expressed as a single target spectrum (common frequency content) but scaled to different intensities. In this respect, the suggested methodology includes the following *modifications and advancements* compared to the Ryan & Chopra (2004a, b) approach:

- Extension of the field of application to a wider range of seismic isolation systems that may consist of linear and bilinear isolators (e.g. low or high damping elastomeric bearings (LDRB/HDRBs), lead-rubber bearings (LRBs), flat sliding bearings (FSB) and friction pendulum bearings (FPBs)), supplementary energy dissipation devices (i.e. linear (LVDs) and nonlinear viscous dampers (NLVDs)), as well as combinations thereof, hence covering most isolation schemes commonly used in modern bridges.

- Derivation of generalised design equations for the direct estimation of inelastic response under code-compatible spectra in terms of both peak relative displacements u_0 and total accelerations $\ddot{U}_0$, since the maximum force of the isolation and energy dissipation system ($m\ddot{U}_0$) is not directly associated with u_0 due to the introduction of viscous dampers (VDs).

- Derivation of GDEs for two-degree-of freedom (2DOF) systems accounting for linear viscous damping and bi-directional excitation.

- Use of GDEs to identify ‘near-optimal’ characteristics of the isolation and energy dissipation system.
- Integration of ‘design principles’ by means of using design (target) spectra (code-type or site-specific) and code-compatible scaling procedures; herein the EN1998-1 (CEN 2004b) design spectrum with some modifications is adopted.

In this context, an analysis framework is first presented in §4.2 including the definition of target spectra associated with different PLs, alternative representation of seismic actions, modelling issues and statistical processing procedures. The dynamic equation of motion is then normalised to reduce the number of design parameters that significantly affect the response. The sensitivity of normalised response quantities to the seismic intensity is investigated via extensive parametric nonlinear dynamic analysis of isolated single-degree-of-freedom (SDOF) systems with linear viscous damping (§4.3); regression analysis is finally employed to develop GDEs. The aforementioned procedure is further extended to address nonlinear viscous damping in §4.4, and the effect of the transverse component of seismic action in 2DOF systems under bidirectional excitation in §4.5.

The design equations provided in this chapter strictly refer to the EN1998-1 ‘Type 1’ spectrum, and isolation systems consisting of elastomer-based isolators; nevertheless, the procedure was fully automated within the MATLAB (Mathworks 2016) code IDEC (*Isolation Design Equations Code*) to facilitate the development of GDEs in different cases. Considering that GDEs can be extracted for prescribed target spectra and provided as ready-to-use design tools, the suggested procedure represents an alternative to equivalent linearisation approaches commonly adopted by codes, and as such, it can be implemented either on a ‘stand-alone’ basis in isolated bridges with stiff substructure and insignificant torsional effects, or for preliminary design purposes in more complex systems and design procedures. Herein, the methodology presented in this chapter is incorporated in the Def-BD methodology of seismically isolated bridges for the preliminary design of the isolation-energy dissipation system and the substructure (i.e. Step 1 in §5.2).

4.2 Analysis Framework

4.2.1 Target spectra

Any type of design spectrum (code-type or resulting from site-specific hazard analysis or zonation study) can be used as the target spectrum. Herein the EN1998-1 ‘Type 1’ (CEN 2004b) 5%-damped elastic spectrum was selected as the basis for seismic design under unidirectional excitation (denoted as 1D) (Fig. 4.1). The corner period defining the beginning of the constant displacement response range of the spectrum was set equal to T_D = 4.0 s as a more representative value of high seismicity regions compared to T_D = 2.0 s (the recommended value in EN1998-1) in line with §3.3.3. Identifying the importance of displacements in the design of isolated bridges, EN1998-2

(CEN 2005a) allows similarly the specification of a T_D value that is longer than the value prescribed in the National Annex to EN 1998-1 (CEN 2004b).

Assuming that the seismic action is defined in terms of the reference peak ground acceleration (*PGA*) $\ddot{u}_{g0,ref}$ (CEN 2004b), the value of the modification factor SF_{EQ} required to scale the reference seismic action with a return period $T_{R,ref}$ to a different period T_R was calculated according to §3.3.3 (Eq. (3.4)). Similarly to §3.2.3, the shape of the design spectrum was assumed the same regardless of the intensity of the earthquake. The previous assumption enables the use of the same design equations irrespective of the performance level (PL) under consideration, since, as it will be shown in §4.3-4.5, the formulation of GDEs depends on the frequency content rather than the intensity of the target spectrum.

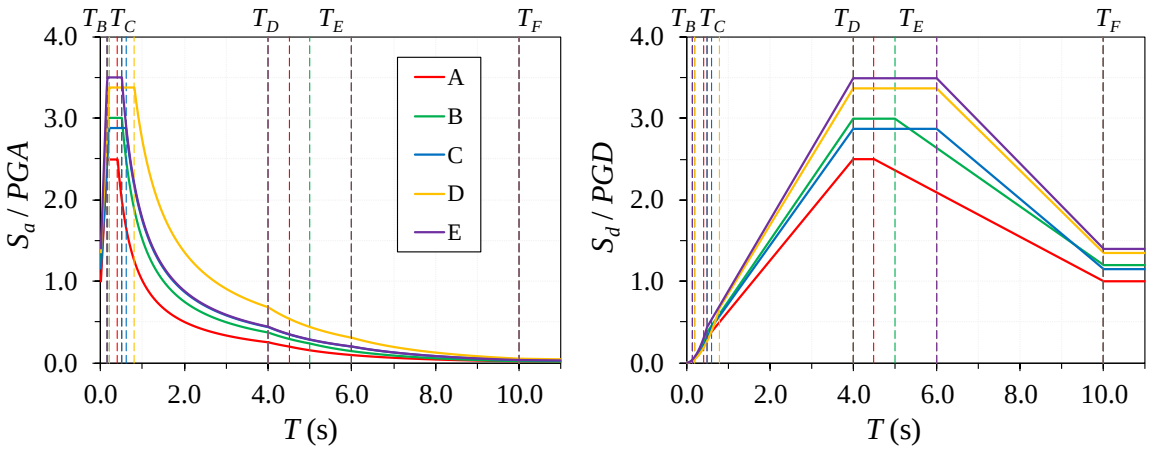

Fig. 4.1 Reference 1D target design horizontal acceleration S_a/PGA (left) and displacement S_d/PGD (right) response spectra for different site conditions (SF_{EQ}=1.0, $T_{R,ref}$=475yrs)

The target spectrum under bidirectional excitation (denoted as 2D) was represented by the square root of the sum of squares (SRSS) of the target spectra per horizontal direction assuming unidirectional excitation, resulting in $\sqrt{2}EQ_{ref}$ for the reference seismic action (Fig. 4.3) in line with EN1998-2 (CEN 2005a). Although this may be considered a rather conservative approach, it was selected herein with a view to assessing the expected increase in u_0, $\ddot{U}_0$ when records are scaled according to EN1998-2 (§4.5.3).

Generalised design equations presented in §4.3-4.5 strictly refer to a frequency content associated with site conditions 'C' (site amplification factor S_C = 1.15) (Fig. 4.1, Fig. 3.9) and a period range of 1.0~5.0 s, somewhat extended compared to the range of practical interest in the design of isolated bridges (1.5~4.0 s); however, the procedure was fully automated within a MATLAB (Mathworks 2016) code that can derive GDEs for 'user-defined' target spectra and period range, provided that a relatively small number of spectrum-compatible acceleration records is specified (§4.2.3).

4.2.2 Representation of seismic action

Nonlinear response history analyses (NLRHAs) presented in the following sections were performed under different ensembles of artificial and natural records. Artificial accelerogram generation was based on the Gasparini & Vanmarcke (1976) approach using the Saragoni & Hart (1974) envelope function with a total duration (t_n) of 25s and time step (dt) of 0.01s. Three alternative suites were generated (Seismosoft 2016) to fit the reference target spectrum (Fig. 3.9), namely, Art A (Annex B, §B.1.1), Art B (Fig. 4.2), and Art C (§B.1.1), consisting of 5, 10, and 20 artificial records, respectively (Table 4.1); the records were properly scaled using SF_{EQ} to represent seismic actions associated with different return periods.

Table 4.1 Peak ground acceleration (*PGA*), velocity (*PGV*), displacement (*PGD*), and Arias intensity (I_A) of artificial excitations; individual records (left), suites of records (right)

No.		*PGA* (*g*)	*PGV* (m/s)	*PGD* (m)	I_A (m/s)
1	1_H1	0.240	0.301	0.165	1.037
2	2_H1	0.240	0.320	0.142	1.355
3	3_H1	0.240	0.320	0.128	1.106
4	4_H1	0.240	0.355	0.139	0.948
5	5_H1	0.240	0.309	0.158	1.247
6	6_H1	0.240	0.290	0.126	0.927
7	7_H1	0.240	0.299	0.138	1.210
8	8_H1	0.240	0.266	0.142	1.283
9	9_H1	0.240	0.301	0.123	1.053
10	10_H1	0.240	0.270	0.127	1.290
11	1_H2	0.241	0.372	0.171	1.162
12	2_H2	0.240	0.279	0.108	1.297
13	3_H2	0.240	0.291	0.132	1.320
14	4_H2	0.240	0.261	0.139	1.088
15	5_H2	0.240	0.320	0.139	1.384
16	6_H2	0.240	0.323	0.130	1.545
17	7_H2	0.240	0.302	0.151	1.367
18	8_H2	0.241	0.330	0.136	1.125
19	9_H2	0.240	0.307	0.163	1.112
20	10_H2	0.240	0.342	0.104	1.578

Set	*PGA* (*g*)	*PGV* (m/s)	*PGD* (m)	I_A (m/s)
A		1, 2, 4, 5, 8_H1		
Min:	0.240	0.266	0.139	0.948
Max:	0.240	0.355	0.165	1.355
GM:	0.240	0.309	0.149	1.163
B		1 - 10_H1		
Min:	0.240	0.266	0.123	0.927
Max:	0.240	0.355	0.165	1.355
GM:	0.240	0.302	0.138	1.136
C		1 - 20		
Min:	0.240	0.261	0.104	0.927
Max:	0.241	0.372	0.171	1.578
GM:	0.240	0.307	0.137	1.209
D_H1		1 - 10_H1 (× 1.13)		
Min:	0.271	0.301	0.140	1.186
Max:	0.272	0.401	0.187	1.735
GM:	0.272	0.342	0.156	1.455
D_H2		1 - 10_H2 (× 0.85)		
Min:	0.204	0.221	0.088	0.783
Max:	0.204	0.315	0.145	1.136
GM:	0.204	0.264	0.115	0.927

To investigate the effect of the transverse component of seismic action in bidirectional excitation using artificial records, an additional suite (Art D) was formed by arranging the previously generated acceleration histories in 10 pairs of horizontal components (H1, H2). In line with the concept of principal axes (Penzien & Watabe 1974) described later in the section (for the case of natural records), each pair was characterised by a near-zero correlation coefficient (§B.1.1) and an intensity ratio of the horizontal component spectra equal to 0.75 according to López *et al.* (2006) for far-field ground motions and long vibration periods (i.e. >1.5s). Consistency to the target spectrum $\sqrt{2}EQ$ for bidirectional excitation (§4.2.1) was established by scaling H1 and H2 components with the scaling factors SF_{H1}=1.13SF_{EQ} and SF_{H2} = 085SF_{EQ} that maintain the adopted

intensity ratio (Fig. 4.3). In addition, it was ensured that the ensemble spectrum (i.e. the geometric mean *GM* of the SRSS spectra of the individual records) was not lower than 0.9 times the 2D target response spectrum (CEN 2005a), in the entire period range (i.e. 0~5.0 s). Ground motion intensity and energy parameters for individual records and suites of records are presented in Table 4.1.

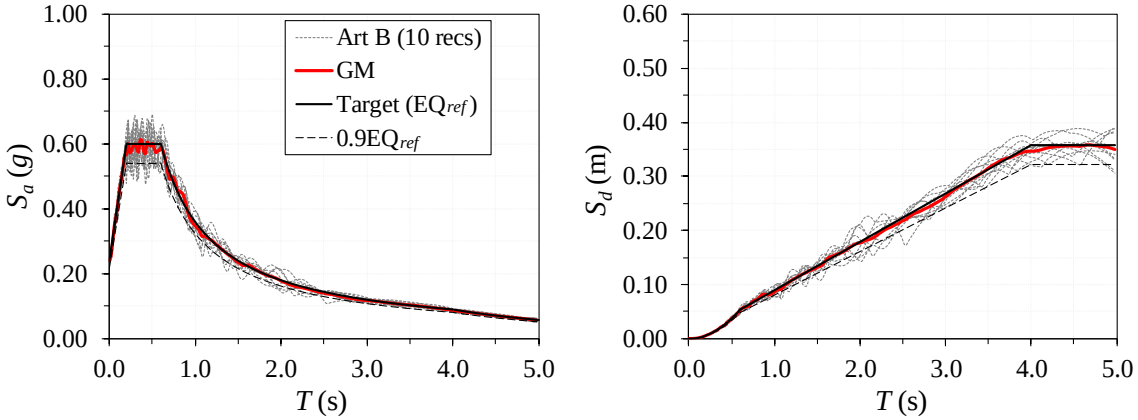

Fig. 4.2 Spectral matching of response acceleration (left) and displacement (right) geometric mean (*GM*) spectra to the 1D target spectrum (*PGA* of 0.21*g*, site 'C', $T_{R,ref}$) for Art B suite of artificial records

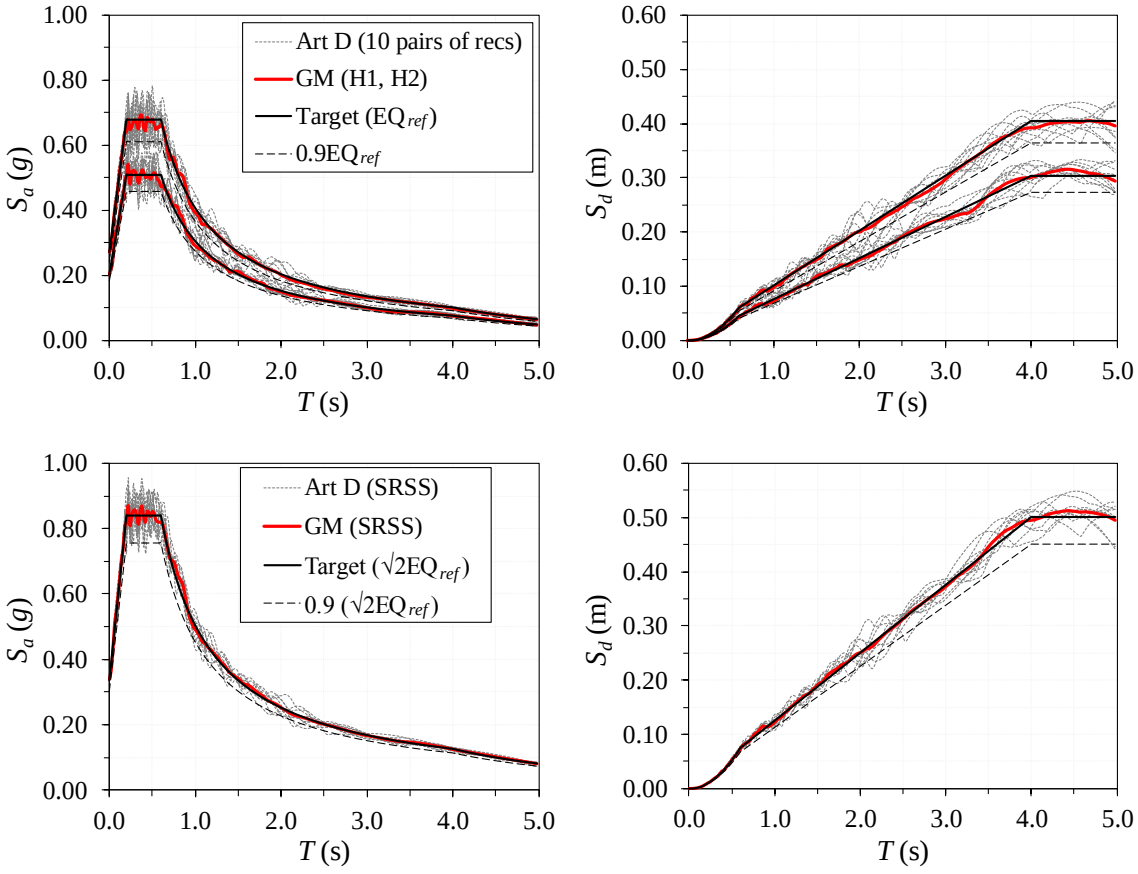

Fig. 4.3 Spectral matching of response acceleration (left) and displacement (right) geometric mean (*GM*) spectra to the 1D component (PGA_{H1} of 0.24*g*, PGA_{H2} of 0.18*g*, site 'C', $T_{R,ref}$) (top) and 2D (PGA_{2D} of 0.30*g*) (bottom) target spectra for the Art D suite of SF_H-scaled artificial records

Selection and scaling of natural records aimed at forming a suite for assessment purposes with a mean spectrum that matches as closely as feasible the target spectrum while suppressing the variability in structural response, since the uncertainty of the input motion is already incorporated in the definition of the target spectrum (Katsanos & Sextos 2013). Considering the target spectra described in §4.2.1, eligible pairs of seismic events were initially selected from the PEER NGA-West 2 (http://ngawest2.berkeley.edu/) database (Ancheta *et al*. 2013) excluding records containing long velocity pulses.

Adopted preliminary search criteria were moment magnitude M_w = 6.5~7.0, closest distance from the record site to the ruptured area R_{rup} = 20~40km, average shear wave velocity to a depth of 30 m $V_{s,30}$ = 180~360 m/s (corresponding to site conditions 'C' of EN1998-1, CEN 2004b), and lowest usable frequency 0.2 Hz (corresponding to a period of 5.0 s). The sample of eligible events was further constrained by assessing the similarity of spectra of the selected records to the target spectrum over the entire period range; the overall fit was quantified herein by the mean-square-error (*MSE*) of the differences (summed over the period range) between the spectral accelerations of the record S_a^H (or the SRSS spectrum of the pair of records S_a^{SRSS}) and the 1D (or 2D) target spectrum S_a^{targ}, computed using the natural logarithms of spectral accelerations as per Eq. (4.1). SF_{MSE} in the same equation represent the local (i.e. per record or pair of records) scaling factors that minimise *MSE* over the considered period range according to Eq. (4.2);

$$MSE = \sum_i \left\{ w(T_i) \left[\ln\left(S_a^{t\,\arg}(T_i)\right) - \ln\left(SF_{MSE} \cdot S_a^{H/SRSS}(T_i)\right) \right]^2 \right\} \Big/ \sum_i w(T_i) \tag{4.1}$$

$$\ln SF_{MSE} = \sum_i \left[w(T_i) \ln\left(S_a^{t\,\arg}(T_i) \Big/ S_a^{H/SRSS}(T_i)\right) \right] \Big/ \sum_i w(T_i) \tag{4.2}$$

In Eqs. (4.1) and (4.2), $w(T_i)$ is a function allowing consideration of weights to different parts of the target spectrum; equal weights (i.e. $w(T_i) = 1$) were applied in the corner periods within the selected range of 0~5.0 s. Adopting an allowable SF_{MSE} of 0.7~2.5 and employing the above procedure initially for the H1 components (Ancheta *et al*. 2013) and subsequently for the pairs of horizontal components of the NGA preliminary selected pairs, resulted in the suite of 16 eligible records presented in Table 4.2, Fig. 4.4, and Table 4.3, Fig. 4.5, for analysis under uni- and bidirectional excitation, respectively.

In the case of bidirectional excitation, the horizontal components of selected events shown in Table 4.3 were rotated into their principal axes defined as the axes along which the two horizontal components are uncorrelated (i.e. $r = 0$) and assumed statistically independent (Penzien & Watabe 1974). The major principal axis (I) is defined as the one parallel to the major principal component (HI), i.e. the component with the larger Arias intensity, as opposed to the minor principal axis (II) and component (HII) associated with the smaller I_A. The counter-clockwise rotation angle $0 \leq \theta_{r=0} \leq 90^o$ (Table 4.3) (for which the correlation coefficient between two (unrotated) acceleration

histories is zero) and the rotated acceleration histories, were calculated according to Rezaeian & Der Kiureghian (2012) (§B.1.1).

Ground motion intensity and energy characteristics of the SF_{MSE}-scaled records presented in Table 4.2 and Table 4.3 incorporate (similarly to the data of Table 4.1) the site ('C') amplification effect (i.e. intensity parameters are comparable to S_C = 1.15 times the peak ground characteristics of the target spectra) and present a good overall match to the relevant values derived in the case of

Table 4.2 Characteristics of natural records; unrotated (as-recorded) SF_{MSE}-scaled H1 components

							SF_{MSE} × H1 Component			
Earthquake			Region	Year	M_w	R_{rup}	SF_{MSE}	PGA	PGV	PGD	I_A
No.	RSN	Name				(km)	(-)	(g)	(m/s)	(m)	(m/s)
1	68	San Fernando	USA	1971	6.61	22.77	1.17	0.262	0.254	0.186	0.923
2	176	Imperial Valley-06	USA	1979	6.53	21.98	2.25	0.266	0.363	0.246	1.392
3	761	Loma Prieta	USA	1989	6.93	39.85	2.03	0.389	0.259	0.122	1.281
4	772	Loma Prieta	USA	1989	6.93	30.49	2.54	0.340	0.321	0.098	1.681
5	776	Loma Prieta	USA	1989	6.93	27.93	0.75	0.278	0.474	0.243	1.257
6	778	Loma Prieta	USA	1989	6.93	24.82	1.05	0.283	0.466	0.207	0.894
7	1008	Northridge-01	USA	1994	6.69	29.74	2.49	0.247	0.340	0.134	1.417
8	1057	Northridge-01	USA	1994	6.69	31.74	2.18	0.313	0.334	0.096	1.569
9	1100	Kobe	JP	1995	6.90	24.85	1.50	0.330	0.318	0.119	1.300
10	1110	Kobe	JP	1995	6.90	24.78	1.27	0.273	0.345	0.137	2.025
11	4840	Chuetsu-oki	JP	2007	6.80	29.45	2.51	0.228	0.326	0.202	2.203
12	4849	Chuetsu-oki	JP	2007	6.80	22.18	1.28	0.324	0.563	0.176	1.388
13	4853	Chuetsu-oki	JP	2007	6.80	27.90	1.38	0.290	0.480	0.134	1.558
14	4883	Chuetsu-oki	JP	2007	6.80	29.91	2.06	0.275	0.293	0.130	1.794
15	5784	Iwate	JP	2008	6.90	35.12	1.69	0.233	0.457	0.161	1.913
16	6953	Darfield	NZ	2010	7.00	24.55	1.24	0.246	0.365	0.249	1.597
			Minimum Value		6.53	21.98	0.75	0.228	0.254	0.096	0.894
			Maximum Value		7.00	39.85	2.54	0.389	0.563	0.249	2.203
			Geometric Mean					0.283	0.363	0.158	1.470

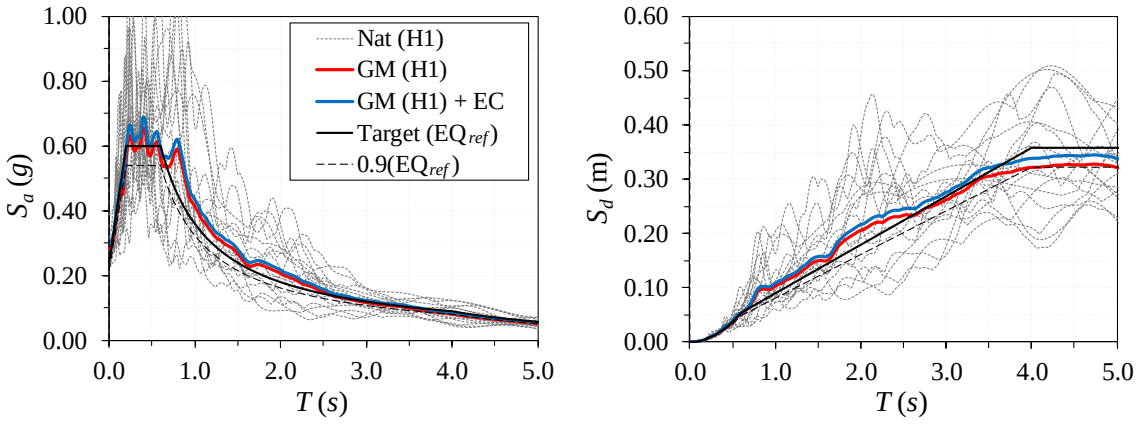

Fig. 4.4 Spectral matching of response acceleration (left) and displacement (right) geometric mean (*GM*) and EN1998-2-scaled geometric mean (*GM*+EC) (SF_{EC}=1.05) spectra to the 1D target spectrum (*PGA* of 0.21g, site 'C', $T_{R,ref}$) for the adopted suite of SF_{MSE}-scaled natural (Nat) records considering H1 components

artificial records, noting however, their superiority in terms of both intensity and energy (PGV, I_A). Finally, according to the Eurocode (EC) 8 requirement, the ensemble spectra depicted in Fig. 4.4 and Fig. 4.5 were scaled by a global (i.e. per suite) scaling factor SF_{EC} (equal to unity in the case of artificial records) to ensure that their spectral values are not lower than 0.9 times the target spectra (CEN 2005a) over the entire period range (i.e. 0~5.0 s); SF_{EC} was found equal to 1.05 in both cases of target spectra (1D, 2D) associated mainly with relevant exceedances in the short (i.e.

Table 4.3 Characteristics of natural records; rotated SF_{MSE}-scaled HI & HII components

					SF_{MSE} × HI Component				SF_{MSE} × HII Component			
Earthquake			$\theta_{r=0}$	SF_{MSE}	PGA	PGV	PGD	I_A	PGA	PGV	PGD	I_A
No.	RSN	Name	(deg)	(-)	(g)	(m/s)	(m)	(m/s)	(g)	(m/s)	(m)	(m/s)
1	68	San Fernando	21.3	1.61	0.356	0.328	0.239	1.850	0.282	0.326	0.158	1.102
2	176	Imp. Valley-06	42.3	2.47	0.295	0.466	0.241	1.854	0.258	0.414	0.186	1.458
3	761	Loma Prieta	48.4	2.37	0.435	0.430	0.232	2.115	0.305	0.272	0.169	1.473
4	772	Loma Prieta	30.4	2.47	0.275	0.308	0.099	1.624	0.274	0.416	0.117	1.500
5	776	Loma Prieta	89.1	0.72	0.267	0.454	0.231	1.152	0.128	0.224	0.143	0.408
6	778	Loma Prieta	2.7	0.87	0.238	0.307	0.123	0.788	0.231	0.383	0.176	0.609
7	1008	Northridge-01	20.6	2.49	0.443	0.309	0.086	1.816	0.248	0.268	0.141	1.358
8	1057	Northridge-01	13.4	2.09	0.305	0.323	0.106	1.481	0.156	0.343	0.159	0.869
9	1100	Kobe	41.0	1.62	0.259	0.234	0.201	1.530	0.310	0.369	0.171	1.508
10	1110	Kobe	7.6	1.25	0.275	0.341	0.140	1.957	0.159	0.259	0.129	0.858
11	4840	Chuetsu-oki	62.5	1.87	0.350	0.519	0.158	1.520	0.177	0.276	0.132	1.139
12	4849	Chuetsu-oki	43.9	1.10	0.325	0.556	0.172	1.171	0.209	0.276	0.078	0.874
13	4853	Chuetsu-oki	63.3	1.15	0.344	0.576	0.148	1.865	0.163	0.230	0.084	0.888
14	4883	Chuetsu-oki	47.6	1.86	0.267	0.263	0.117	1.742	0.231	0.241	0.084	1.128
15	5784	Iwate	67.1	1.40	0.178	0.377	0.102	1.348	0.157	0.243	0.147	1.106
16	6953	Darfield	0.3	0.96	0.213	0.539	0.467	1.200	0.190	0.280	0.189	0.947
		Minimum Value	0.3	0.72	0.178	0.234	0.086	0.788	0.128	0.224	0.078	0.408
		Maximum Value	89.1	2.49	0.443	0.576	0.467	2.115	0.310	0.416	0.189	1.508
		Geometric Mean			0.293	0.381	0.162	1.519	0.210	0.295	0.137	1.022

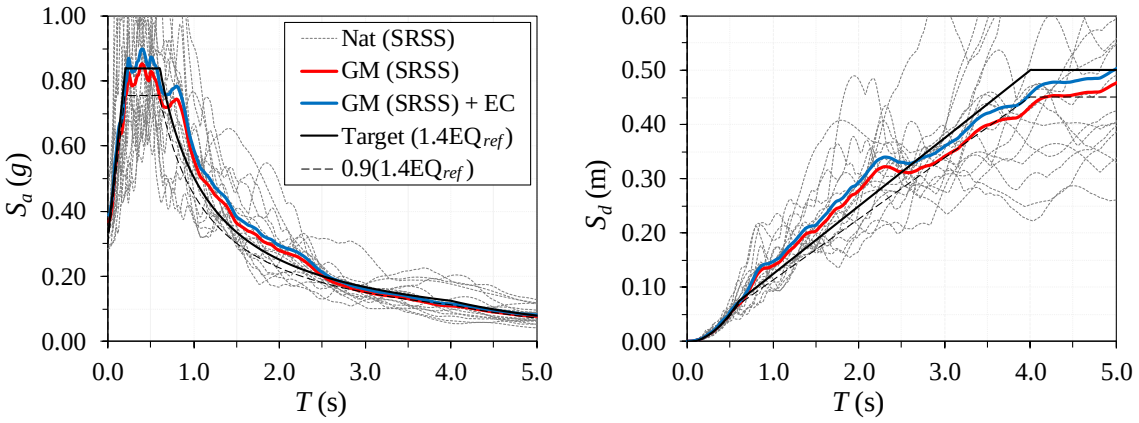

Fig. 4.5 Spectral matching of response acceleration (left) and displacement (right) geometric mean (GM) and EN1998-2-scaled geometric mean (GM+EC) (SF_{EC}=1.05) SRSS spectra to the 2D target spectrum (PGA_{2D} of 0.30g, site 'C', $T_{R,ref}$) for the adopted suite of rotated and SF_{MSE}-scaled natural (Nat) records

0.1-0.2s) and long (≥ 4.0 s) period range. In view of the previous considerations, the scaling factor *SF* per record and considered probability of exceedance is determined as per Eq. (4.3) attempting to reduce the variability of responses through SF_{MSE} as opposed to the 'structure-specific' selection criterion used in §3.3.4.

$$SF = SF_{MSE} SF_{EC} SF_{EQ} \tag{4.3}$$

The design (or target) value of peak ground velocity (*PGV*) $\dot{u}_{g0}$, required during the development of generalised design equations, was selected herein equal to the geometric mean of *PGVs* of the records included in Art B suite (i.e. 0.302m/s for T_R = 475yrs, SF_{EQ} = 1). The above decision was driven first from the fact that the selected value was close to the mean *PGV* derived from relationships proposed in recent research studies (varying from 0.244 to 0.345 with a mean of 0.301m/s, §B.1.1) compared to the rather unconservative estimate provided by EN1998-2 (CEN 2005a) and the Italian Code (NTC 2008) (i.e. 0.225m/s, §B.1.1), and second, from a prerequisite of the methodology presented in §4.3-4.5 to use records with an ensemble spectrum that closely matches the target spectrum in terms of shape and *PGV*, noting that further scaling of records aiming at a target *PGV* that is significantly different from the geometric mean of *PGVs* of the selected records would distort their 'goodness-of-fit' presented in Fig. 4.4; the issue is further discussed in §4.3.2.

4.2.3 Modelling issues and numerical evaluation of dynamic response

Response history analyses (RHAs) according to §4.3-4.5 were performed using the unconditionally stable implicit Newmark constant average acceleration method (Carr 2004a); the procedure was fully automated with the development of the MATLAB (Mathworks 2016) code IDEC that enables parametric nonlinear dynamic analysis of RDOFs using RUAUMOKO 3D (Carr 2004b) and DYNAPLOT (Carr 2004c) in batch mode, post-processing of results involving data collection, statistical processing (§4.2.4), regression analysis, development of generalised design equations (§4.3.3), and diagram plotting, with average time of less than 5s per analysis and post-processing of a single case, using an 8 GB RAM 2.20 GHz quad core processor.

A bilinear hysteretic and a dashpot element were used to model the inelastic force-displacement response of isolators and viscous dampers according to Fig. 4.6 and Fig. 4.7, respectively. The restoring shear force (*V*) of the bilinear isolator can be described by Eq. (4.4), where $u(t)$ represents the displacement history, k_p the post-elastic stiffness, and V_0 is the shear resistance of the isolator at zero displacement (i.e. the characteristic strength in US terminology). $z(t)$ is a hysteretic dimensionless parameter of the Bouc–Wen model (Wen 1975, 1976) governed by the evolution equation (4.5) (i.e. a function of u, $\dot{u}$, and the initial stiffness k_e); defining the fraction of the applied V_0 (maxima of ±1) or else the 'yielding history' (Ryan & Chopra 2004b), $|z(t)| = 1$ when the system enters the inelastic range and $|z(t)| < 1$ otherwise (i.e. elastic response). u_y in Eq. (4.5) represents

the yield displacement and s controls the smoothness of the transition from the elastic to the inelastic range in the force-deformation relationship; for $s = 8$ a sharp transition is obtained. For V_0 equal to zero the hysteretic response collapses to linear behaviour with stiffness equal to k_p (Fig. 4.6);

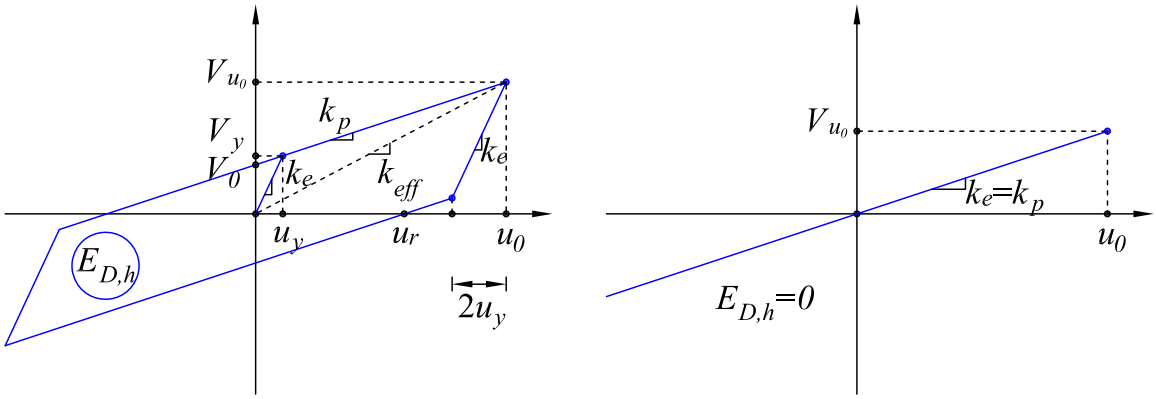

Fig. 4.6 Force-displacement response of bilinear hysteretic (left) and linear (right) isolator

$$V(t) = V_0 z(t) + k_p u(t) \tag{4.4}$$

$$\dot{z} = \frac{1}{u_y}\left(\dot{u}(t) - \frac{1}{2}\left|\dot{u}(t)\right| z(t)\left|z(t)\right|^{s-1} - \frac{1}{2}\dot{u}(t)\left|z(t)\right|^{s}\right) \tag{4.5}$$

The behaviour of the bilinear isolator is intrinsically determined by three parameters, which can be selected as V_0, u_y, and k_p. The yield displacement of the isolation system was reported in earlier studies (e.g. Makris & Chang 2000, Makris & Vassiliou 2011) to have a minor impact on the maximum inelastic response; herein a constant value associated with different groups of yielding isolators was introduced similarly to Ryan & Chopra (2004a, b) in order to capture more accurately the peak response, and at the same time limit the complexity of the proposed generalised design equations (§4.3-4.5). In addition, u_y was considered constant for different values of the post-yield stiffness k_p (i.e. instead of assuming a constant ratio of k_e / k_p) resulting to an initial stiffness that is directly proportional to the yield strength (V_y) according to the suggestion of Ryan & Chopra (2004b). Therefore, Eqs. (4.6), (4.7) were used to express k_e and V_y as functions of V_0, k_p, and u_y for modelling purposes;

$$k_e = \frac{V_0}{u_y} + k_p \tag{4.6}$$

$$V_y = k_e u_y \tag{4.7}$$

Finally, the hysteretic energy $E_{D,h}$ dissipated per cycle at the maximum displacement u_0 (represented by the area of the hysteresis loop in Fig. 4.6) is given as;

$$E_{D,h} = 4V_0\left(u_0 - u_y\right) = 4\left(V_y u_0 - V_{u_0} u_y\right) \tag{4.8}$$

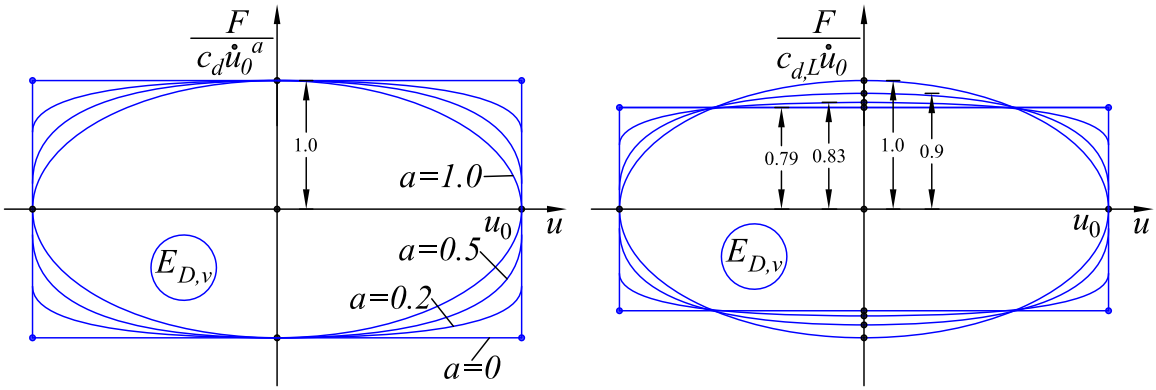

Fig. 4.7 Force-displacement response of linear (a=1) and nonlinear (a<1) viscous damper under a cycle of harmonic motion; dampers of equal c (force normalised to the peak damping force) (left), dampers of equal dissipated energy (force normalised to the peak linear damping force) (right)

The axial force (F) in the general case of nonlinear viscous dampers can be analytically expressed as a fractional velocity power law as per Eq. (4.9) where $c_{d,NL}$ is the damping coefficient (i.e. units of force per velocity raised to the power of a), a is a real positive velocity coefficient with typical values for seismic applications in the range of 0.1~1 (Christopoulos & Filiatrault 2006, Di Paola & Navarra 2009), and $sgn(\cdot)$ is the signum function.

$$F_{NL}(t) = c_{d,NL}\,\mathrm{sgn}\left(\dot{u}(t)\right)\left|\dot{u}(t)\right|^a \tag{4.9}$$

The energy dissipated by the nonlinear damper during a cycle of harmonic motion $u = u_0 \sin\omega t$ is determined by Eq. (4.10) where $\Gamma(\cdot)$ represents the gamma function;

$$E_{D,v,NL} = \int_0^T F\dot{u}\,dt = \pi c_{d,NL} {u_0}^{a+1} \omega^a \frac{2^{2+a}\Gamma^2\left(1+\alpha/2\right)}{\pi\Gamma\left(2+\alpha\right)} = \pi c_{d,NL} {u_0}^{a+1} \omega^a f\left(\Gamma,\alpha\right) \tag{4.10}$$

Introducing a = 0 and a = 1, Eqs. (4.9) and (4.10) collapse to the limit cases of pure friction (Eqs. (4.11) and (4.12)) and linear viscous dampers (Eqs. (4.13) and (4.14)), respectively.

$$F_{NL}(t) = c_{d,NL}\,\mathrm{sgn}\left(\dot{u}(t)\right) \tag{4.11}$$

$$E_{D,v,NL} = 4c_{d,NL}u_0 \tag{4.12}$$

$$F_L(t) = c_{d,L}\dot{u}(t) \tag{4.13}$$

$$E_{D,v,L} = \pi c_{d,L} {u_0}^2 \omega \tag{4.14}$$

The effect of the nonlinear parameter a on the response envelope is illustrated on the left-hand side of Fig. 4.7 where $F/c_d\dot{u}_0$ (i.e. F normalised to the peak damper force) is plotted against $u = u_0 \sin\omega t$.

The response of nonlinear viscous dampers was investigated in this study following the 'energy-equivalence' approach (Lin & Chopra 2002) according to which energy-equivalent dampers are characterised by two dimensionless and independent parameters; i.e. the parameter a and the equivalent damping ratio $\xi_{d,NL}$, associated with the degree of nonlinearity and the energy dissipation capacity, respectively. Equating the energy per cycle of harmonic motion of a linear damper (i.e. Eqs. (4.10)) to Eq. (4.14)) yields the damping coefficient c_{NL} of an energy-equivalent nonlinear damper (i.e. dissipating energy equal to the energy of the linear damper);

$$c_{d,NL} = \frac{(u_0\omega)^{1-a}}{f(\Gamma,\alpha)} c_{d,L} \tag{4.15}$$

Substituting Eq. (4.15) in Eq. (4.9) yields the damper force of the energy-equivalent nonlinear damper (Eq. (4.16)) and the associated ratio (i.e. nonlinear to linear) of peak damper forces (Eq. (4.17));

$$F_{NL}(t) = \frac{(u_0\omega)^{1-a}}{f(\Gamma,\alpha)} c_{d,L} \operatorname{sgn}\left(\dot{u}(t)\right)\left|\dot{u}(t)\right|^a \tag{4.16}$$

$$\frac{F_{0,NL}}{F_{0,L}} = \frac{1}{f(\Gamma,\alpha)}\left(\frac{u_0\omega}{\dot{u}_0}\right)^{1-a} \tag{4.17}$$

For energy-equivalent dampers of a = 0, 0.2, 0.5, 1, under harmonic motion ($\dot{u}_0 = \omega u_0$), Eq. (4.17) results in the peak force reductions depicted in Fig. 4.7. In the case of an SDOF system under non-harmonic excitation, the response should be assessed at $\omega = \omega_p$ (i.e. the system's isolated frequency) (Chopra 2012) and the ratio of forces depends additionally on the ratio of the pseudo-velocity PSV (= $u_0\omega_p$) to the peak relative velocity $\dot{u}_0$.

Considering again the SDOF system of mass m, isolation frequency ω_p, and a nonlinear viscous damper of $c_{d,NL}$, the equivalent damping ratio $\xi_{d,NL}$ can be expressed using Eq. (4.10) and $\omega = \omega_p$, by Eq. (4.18) which reduces in the form of Eqs. (4.19), (4.20) for a = 0 and a = 1;

$$\xi_{d,NL} = \frac{E_{D,v,NL}}{2\pi k_p {u_0}^2} = \frac{c_{d,NL}}{2m\omega_p} \frac{f(\Gamma,\alpha)}{\left(u_0\omega_p\right)^{1-a}} \tag{4.18}$$

$$\xi_{d,NL} = 2c_{d,NL} / \pi k_p u_0 \tag{4.19}$$

$$\xi_{d,L} = c_{d,L} / 2m\omega_p \tag{4.20}$$

In summary, the isolation schemes depicted in Fig. 4.8 can be realised by properly combining the modelling parameters describing the force-displacement response of the bilinear hysteretic and dashpot element, i.e. the strength at zero displacement V_0, the post-yield stiffness k_p (associated with the isolation period T_p), the yield displacement u_y, the damping ratio ξ of energy equivalent dampers, and the velocity exponent a.

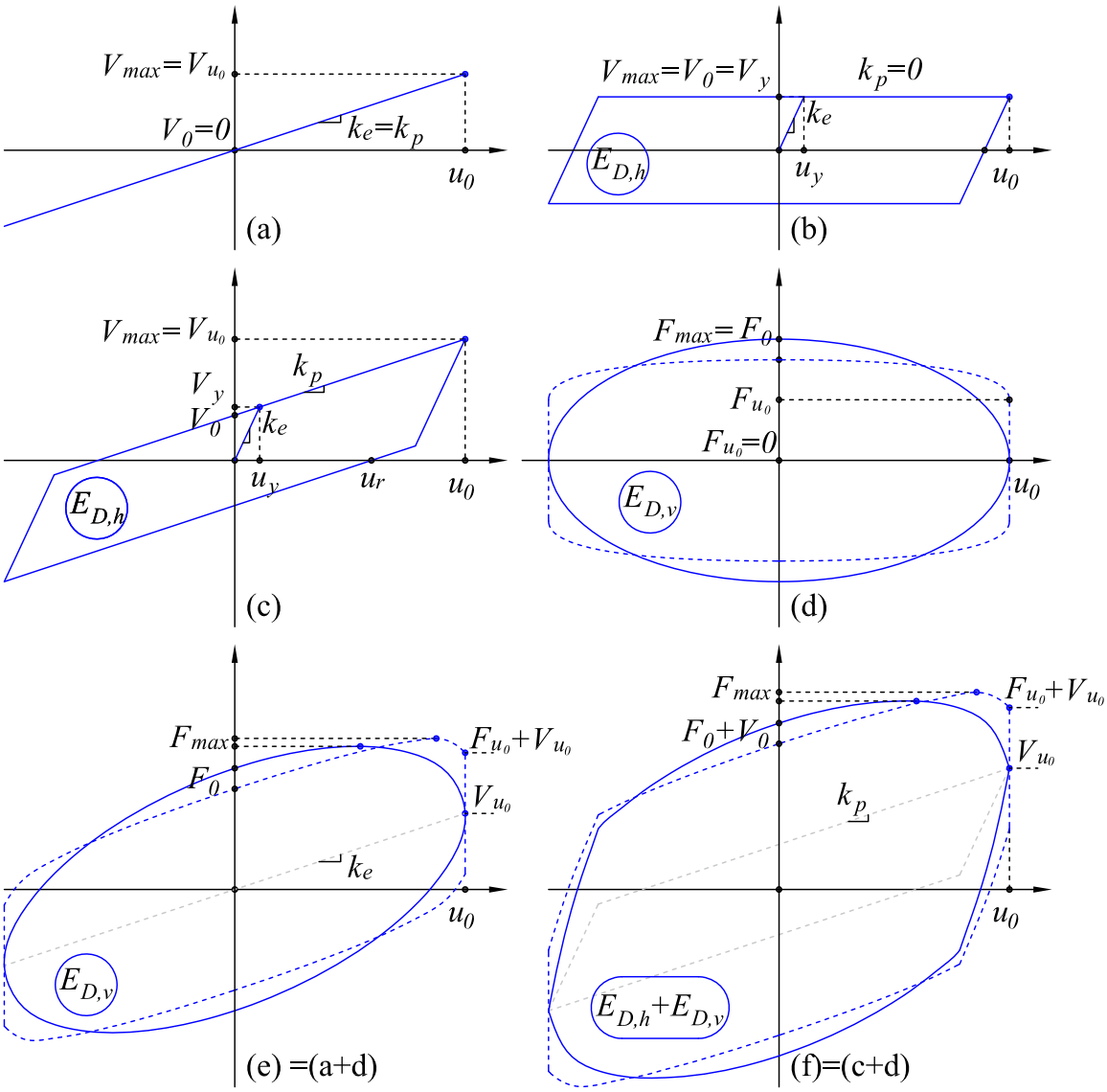

Fig. 4.8 Idealisation of force-displacement response of common isolation systems: (a) elastic, (b) elastoplastic (rigid-plastic if $u_y \to 0$), (c) elastoplastic with stiffening (rigid-plastic with stiffening if $u_y \to 0$), (d) equivalent energy linear (solid) and nonlinear (dashed) viscous, (e) equivalent energy linear (solid) and nonlinear (dashed) viscoelastic, (f) equivalent energy linear (solid) and nonlinear (dashed) elastoviscoplastic with stiffening (viscoplastic with stiffening if $u_y \to 0$)

4.2.4 Statistical processing of key response quantities

In the following sections, the dynamic response retrieved from analysis of isolation and energy dissipation systems under a suite of records was characterised by the *geometric mean* (*GM*) of responses under individual records (or pair of records in bidirectional analysis), and the *standard error of the geometric mean* (*SEGM*) estimate employed to assess the reliability of the geometric mean prediction according to §B.1.2. The central tendency measure of geometric mean is preferred over the more common arithmetic mean mainly due to its consistency with lognormally distributed data, i.e. an assumption which was found to be realistic for earthquake response quantities. It should be noted, nevertheless, that the above decision has a minor effect on results so long as a consistent definition of the central tendency is adopted both on scaling of accelerograms (§4.2.2) and analysis results processing (Hancock *et al*. 2008). The standard error of the sample geometric mean estimate is the standard deviation of the sampling distribution of the geometric mean and represents the dispersion of sample-means around the true (i.e. the population) geometric mean.

Assuming that the sample size is small (i.e. number of records $n < 30$), exact confidence intervals of the geometric mean estimate (GM_L, GM_U) and associated *SEGM* limits defined as percentages of the estimated geometric mean ($SEGM_L$, $SEGM_U$) can be calculated (§B.1.2) by considering a *CL* confidence level and *n-1* degrees of freedom *df* for the two-sided *Student-t* probability density function. In the analyses presented in §4.3-4.5, peak absolute seismic response quantities (i.e. peak relative displacement and total acceleration) are of interest, hence, reported *SEGM* (%) values correspond to the upper (and more conservative) confidence interval. For example, given a sample of *n* peak relative displacements resulted from dynamic analysis of an isolated system under a suite of *n* records ($df = n$-1), a confidence level of 90%, a sample geometric mean *GM*, and *SEGM* limits equal to $SEGM_L$ and $SEGM_U$, then if one were to construct many response samples of the same *n* drawn from the same population, and the standard deviation of the samples remained constant, approximately 90% of the ± $SEGM_U$ confidence intervals (which would differ for each sample) would encompass the true mean (Cox & Hinkley 1974), or in other words, the sample-mean peak relative displacement is estimated with a confidence band of approximately ± $SEGM_U$ (Katsanos & Sextos 2013). A limit value of $SEGM_U$ = 15% of GM with a 90% confidence level was generally adopted herein to assess the accuracy of the mean estimates rather than introduce an increase in values derived from analysis.

4.3 Isolated SDOF System with Linear Viscous Damping

4.3.1 Dynamic equation of motion

The dynamic equation of motion of an SDOF system is reformed herein with a view to uncoupling the response from the seismic intensity and thus linearising the structural dynamics problem. The key advancement in this procedure is the explicit consideration of linear viscous damping as opposed to earlier studies (Ryan & Chopra 2004a, b, Sayani & Ryan 2009) wherein viscous

damping was ignored. The considered SDOF system (Fig. 4.9) idealises an isolated straight bridge with a rigid deck of total mass *m* under unidirectional excitation. The deck is mounted on a single isolator of hysteretic force-displacement response and a single LVD representing the combined response of the bridge isolators and dampers, respectively, while the effect of the substructure's stiffness (elastic or inelastic), inertial, and damping characteristics is disregarded.

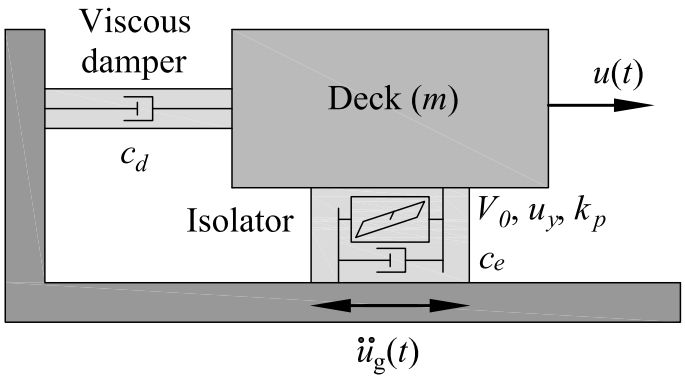

Fig. 4.9 Idealised SDOF system

Applying the dynamic equilibrium of inertia (f_I), elastic (or inelastic) (f_S) and damping (f_D) resisting forces at each time instant *t* according to *D'Alembert*'s principle, the differential equation governing the displacement of the idealised SDOF is written as:

$$\left[f_I(t)\right]+\left[f_D(t)\right]+\left[f_S(t)\right]=0 \tag{4.21}$$

Substituting in the previous equation the shear force of the bilinear isolator (Eq. (4.4)) and the axial force of the LVD (Eq. (4.13)) results in:

$$\left[m\left(\ddot{u}(t)+\ddot{u}_g(t)\right)\right]+\left[\left(c_{e,L}+c_{d,L}\right)\dot{u}(t)\right]+\left[V_0 z\left(t,k_e,u,\dot{u}\right)+k_p u(t)\right]=0 \tag{4.22}$$

$$\ddot{u}(t)+\left[\left(\left(c_{e,L}+c_{d,L}\right)/m\right)\dot{u}(t)\right]+\left[\bar{v}_0 g z\left(t,k_e,u,\dot{u}\right)+\omega_p^2 u(t)\right]=-\ddot{u}_g(t) \tag{4.23}$$

In Eqs. (4.22), (4.23), $u(t)$, $\dot{u}(t)$, $\ddot{u}(t)$ are the relative displacement, velocity and acceleration of *m*, respectively, $\ddot{u}_g$ is the ground acceleration, and ω_p is the isolation frequency associated with the post-elastic stiffness k_p and isolation period T_p. The damping coefficients $c_{e,L}$, $c_{d,L}$ (Eqs. (4.20), (4.24)) associated with viscous damping originating from the rubber of elastomer-based isolators (i.e. linear) and LVDs, respectively, represent 'quantifiable' sources of damping, hence, they are kept constant during NLRHA as opposed to 'unquantifiable' sources (e.g. inherent damping of deck and substructure) where the constant parameter should be the critical damping ratio (Ray *et al*. 2013).

$$c_{e,L}=2m\omega_p\xi_{e,L},\quad c_{d,L}=2m\omega_p\xi_{d,L} \tag{4.24}$$

It is noted that inherent structural damping is deliberately disregarded on the basis that neither the deck nor the pier deformations are associated with the *u* dynamic degree of freedom in the idealised SDOF (Fig. 4.9) which represents the horizontal relative displacement of the rigid (i.e. undeformed) deck or else the deformation of the isolation system, excluding the effect (i.e. deformations) of the substructure.

$\bar{v}_0$ represents the normalised strength of the hysteretic part of the isolator to the weight of the superstructure (i.e. the seismic coefficient) according to Eq. (4.25), where V_0 is defined in §4.2.3 and g is the acceleration of gravity, and it can be also seen as the acceleration at yield of a rigid-plastic system with strength V_0;

$$\bar{v}_0 = \frac{V_0}{mg} \tag{4.25}$$

z is the dimensionless parameter (Eq. (4.5)), and $\ddot{u}_g$ is the ground acceleration.

The maximum residual displacement u_r under which the system can be in static equilibrium (Fig. 4.6), corresponding to a shear force of $\pm 2V_0$ and representing a system property (i.e. independent of the excitation), is equal to;

$$u_r = \frac{V_0}{k_p} \tag{4.26}$$

Dividing Eq. (4.23) by u_r and substituting $c_{e,L}$, $c_{d,L}$, $\bar{v}_0$ from Eqs. (4.24), (4.25), reduce the equation of motion in the normalised form of Eqs. (4.27)-(4.29) (symbols with bars represent normalised quantities);

$$\ddot{\bar{u}}(t) + \left[2\omega_p\left(\xi_{e,L} + \xi_{d,L}\right)\dot{\bar{u}}(t)\right] + \left[\omega_p^2\left(z\left(t, k_e, u, \dot{u}\right) + \bar{u}(t)\right)\right] = -\left(\omega_p^2 / \eta\omega_D\right)\ddot{\bar{u}}_g(t) \tag{4.27}$$

$$\ddot{\bar{u}}(t) = \ddot{u}(t)/u_r\,,\ \dot{\bar{u}}(t) = \dot{u}(t)/u_r\,,\ \bar{u}(t) = u(t)/u_r \tag{4.28}$$

$$\ddot{\bar{u}}_g(t) = \ddot{u}_g(t)/\dot{u}_{g0} \tag{4.29}$$

The normalised strength η (Eq. (4.27)), which describes the system strength relative to the *PGV* ($\dot{u}_{g0}$), is defined according to Eq. (4.30) where the frequency ω_D, included to render η a dimensionless quantity, corresponds to the period T_D marking the transition from the velocity-sensitive to the displacement-sensitive region of the target spectrum (Fig. 4.1);

$$\eta = \frac{\bar{v}_0 g}{\omega_D \dot{u}_{g0}} = \frac{\omega_p^2 u_r}{\omega_D \dot{u}_{g0}} \tag{4.30}$$

The characterisation of the isolation system strength by η along with the consideration of a constant yield displacement (§4.2.3), reduce the governing parameters that influence the response to the natural period defined from the post-yield stiffness (i.e. the isolation period T_p), the normalised strength η, and the damping ratio ξ (= $\xi_{e,L}$ + $\xi_{d,L}$) of the isolation system, as opposed to the parameters T_p, V_0, c (= $c_{e,L}$ + $c_{d,L}$), u_y, $\dot{u}_{g0}$ in the non-normalised case of Eq. (4.22). More specifically, Eq. (4.27) indicates that the normalised response is independent of the seismic intensity rendering the non-normalised quantities linearly proportional to u_r according to Eq. (4.28). The numerical study in §4.3.2 investigates the validity of the previous statement in typical isolation schemes with linear viscous damping and explores its practical value in design with the aid of statistical analysis (§4.3.3).

4.3.2 Parametric analysis of SDOF system

The normalised relative displacement and total acceleration response histories $\bar{u}(t)$, $\ddot{\bar{u}}(t)$ can be found either directly by solving Eq. (4.27) for selected values of ξ, η, ω_p (or T_p), and u_y, or indirectly by first solving Eq. (4.22) with values of c, V_0, k_p corresponding to ξ, η, T_p, and u_y, and then by calculating the normalised response from Eq. (4.28). In the latter case, c and k_p are given by Eq. (4.24), (4.31), and V_0 is calculated from Eqs. (4.26), (4.30) rearranged as Eq. (4.32); Eqs. (4.6), (4.7) are finally required to define the bilinear hysteresis parameters in line with the considerations of §4.2.3. In all cases, $\dot{u}_{g0}$ represents the scaled *PGV* of the considered record (not the mean) according to §4.2.2; for a specific value of η this results in a variation of $\bar{v}_0$ with seismic intensity (i.e. per record) according to Eq. (4.30).

$$k_p = 4\pi^2 m / T_p^{\,2} \tag{4.31}$$

$$V_0 = \eta m \omega_D \dot{u}_{g0} \tag{4.32}$$

Geometric means of peak normalised relative displacements $\bar{u}_0$, total accelerations $\ddot{\bar{U}}_0$, logarithmically transformed response quantities $\ln\bar{u}_0$, $\ln\ddot{\bar{U}}_0$ (i.e. natural logarithms), and non-normalised relative displacements u_0 and total accelerations $\ddot{U}_0$ under Art B suite (Fig. 4.2) are presented in Fig. 4.10 for a range of design parameters (i.e. $\xi_{e,L}$ = 0.05, $\xi_{d,L}$ = 0~0.25, η = 0~1.5, T_p = 1~5 s). Considering T_D = 4.0 s, the mean *PGV* for Art B (i.e. $\dot{u}_{g0}$ = 0.604 m/s for $T_R \approx$ 2500yrs), and a range for $\bar{v}_0$ from 0.0 to 0.15, Eq. (4.30) leads to an approximate range of η from 0.0 to 1.50; larger η values are expected if lower seismic intensities are considered, noting however, that in the latter case low $\bar{v}_0$ values will be normally selected. The yield displacement u_y is considered equal to 1cm representing the yield displacement of elastomer-based hysteretic isolators (e.g. LRBs) (Ryan & Chopra 2004b) while the viscous damping ratio of the elastomer ξ_e and the supplemental dampers ξ_d were dealt as a single variable due to the inherent linearity of the system according to §4.3.1. An issue that requires some further consideration in the case of linear systems (η = 0), is

the computation of normalised response quantities (Eq. (4.28)); zero strength (η or $\bar{v}_0$) results in zero residual displacement u_r rendering impossible the derivation of normalised quantities according to the definitions provided in §4.3.1. The issue was treated numerically by adopting η = 0 when solving Eq. (4.22) and a relatively low value of η equal to 0.01 when calculating the normalised response as per Eq. (4.28) since the system response was found practically insensitive to such a small increase of strength. This approach deals also with a different problem associated with the logarithmic transformation of data with zero values required in §4.3.3.

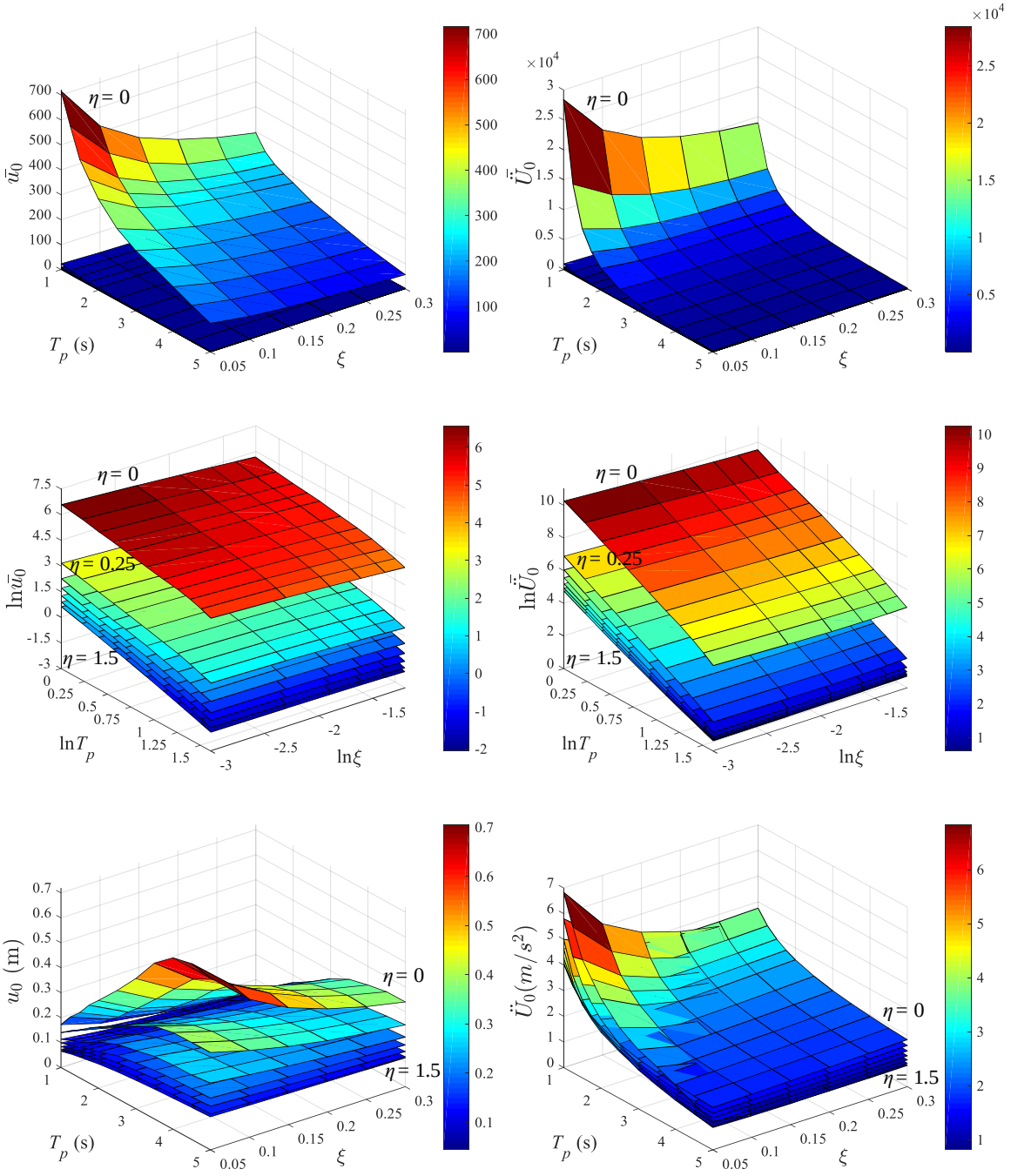

Fig. 4.10 NLRHA results under Art B suite: *GM* of peak normalised response ($\bar{u}_0$, $\ddot{\bar{U}}_0$), log-transformed peak normalised response (ln$\bar{u}_0$, ln$\ddot{\bar{U}}_0$), and non-normalised response (u_0, $\ddot{U}_0$) for PGA=0.42g (T_R≈2500yrs, SF_{EQ}=2)

Each surface in Fig. 4.10 represents a three-dimensional spectrum associated with a specific value of η. Top surfaces (η = 0) corresponding to normalised data are located at a greater distance compared to the cases of $\eta \neq 0.01$ due to the normalisation with respect to a relatively small value of u_r according to the previous considerations. Dispersion δ, and hence *SEGM*, of non-normalised response depends on the generation and/or scaling approach adopted for the considered suite of records, while in the case of normalised response the normalization procedure of §4.3.1 is equivalent, in terms of dispersion, to scaling of records to a common *PGV*; in other words, if records were scaled to the same *PGV*, dispersion and *SEGM* of u_0, $\bar{u}_0$ and $\ddot{U}_0$, $\bar{\ddot{U}}_0$ would be identical.

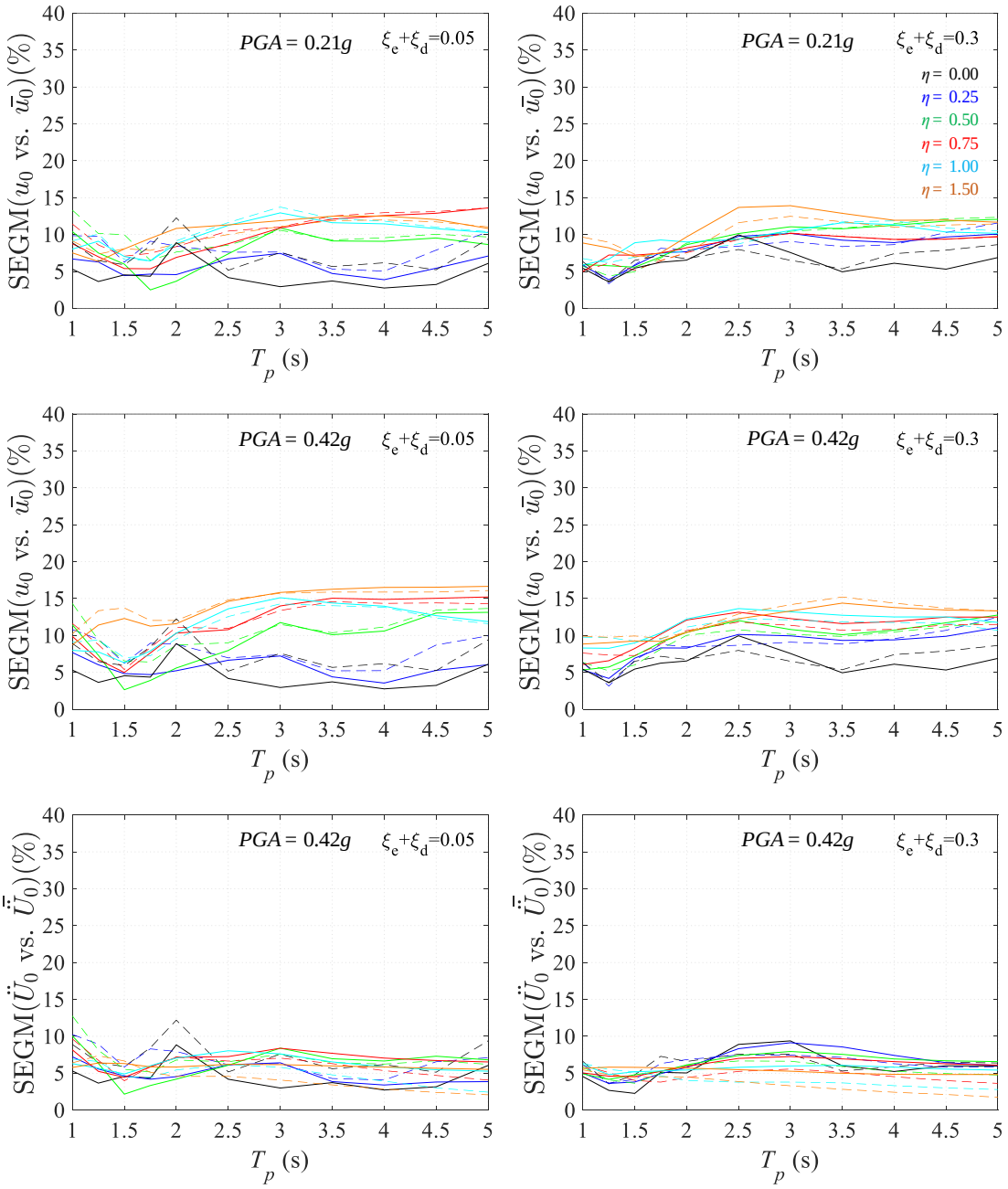

Fig. 4.11 NLRHA results under Art B suite: *SEGM* (%) of u_0, $\ddot{U}_0$ (solid) and $\bar{u}_0$, $\bar{\ddot{U}}_0$ (dashed) for PGA=0.21g (T_R=475yrs, SF_{EQ}=1), PGA=0.42g (T_R≈2500yrs, SF_{EQ}=2), ξ=5, 30%, and η=0~1.5

In Fig. 4.11, *SEGM* of normalised and non-normalised response estimates are plotted for different values of ξ, η, T_p. Upper values of *SEGM* are close to 15% with a 90% confidence level in the case of $\bar{u}_0$ and lower than 10% in the case of $\ddot{\bar{U}}_0$, corresponding to values of dispersion δ (Eq. (B.13)) lower than 0.25 and 0.20, respectively, which in turn are lower than δ values reported by Ryan & Chopra (2004b) for bilinear isolation systems disregarding viscous damping (i.e. 0.3~0.6 referring to normalised displacements). Although such low values of *SEGM* allow for reliable mean response estimation, it should be noted that statistical processing of non-normalised response results in

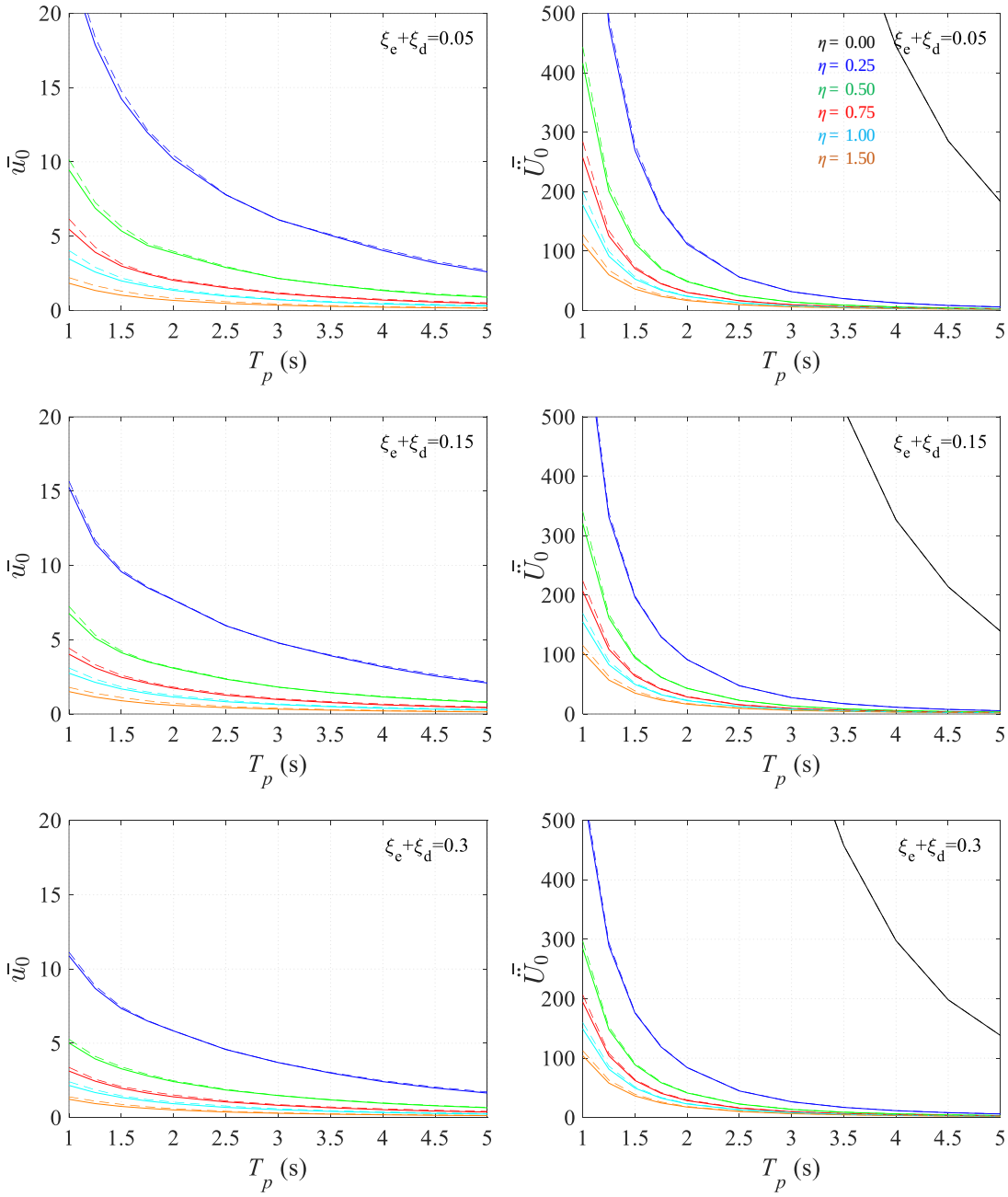

Fig. 4.12 NLRHA results under Art B suite: *GM* of $\bar{u}_0$ (left) and $\ddot{\bar{U}}_0$ (right) for *PGA*=0.21*g* (T_R=475yrs, SF_{EQ}=1) (dashed), *PGA*=0.42*g* (T_R≈2500yrs, SF_{EQ}=2) (solid), ξ=5, 15, 30%, and η=0~1.5

similar *SEGM* values (Fig. 4.11) due to the low scattering of artificial spectra around their mean (and target) values (Fig. 4.2), and the resulting low variability of response estimates (i.e. low δ values).

In view of the previous considerations, the main advantage of the normalisation approach described in §4.3.1 lies in the fact that the seismic intensity has indeed a negligible effect on the mean normalised peak response of linear/nonlinear isolation systems with or without supplemental linear viscous damping as illustrated in Fig. 4.12 and Fig. 4.13 for two different seismic intensities;

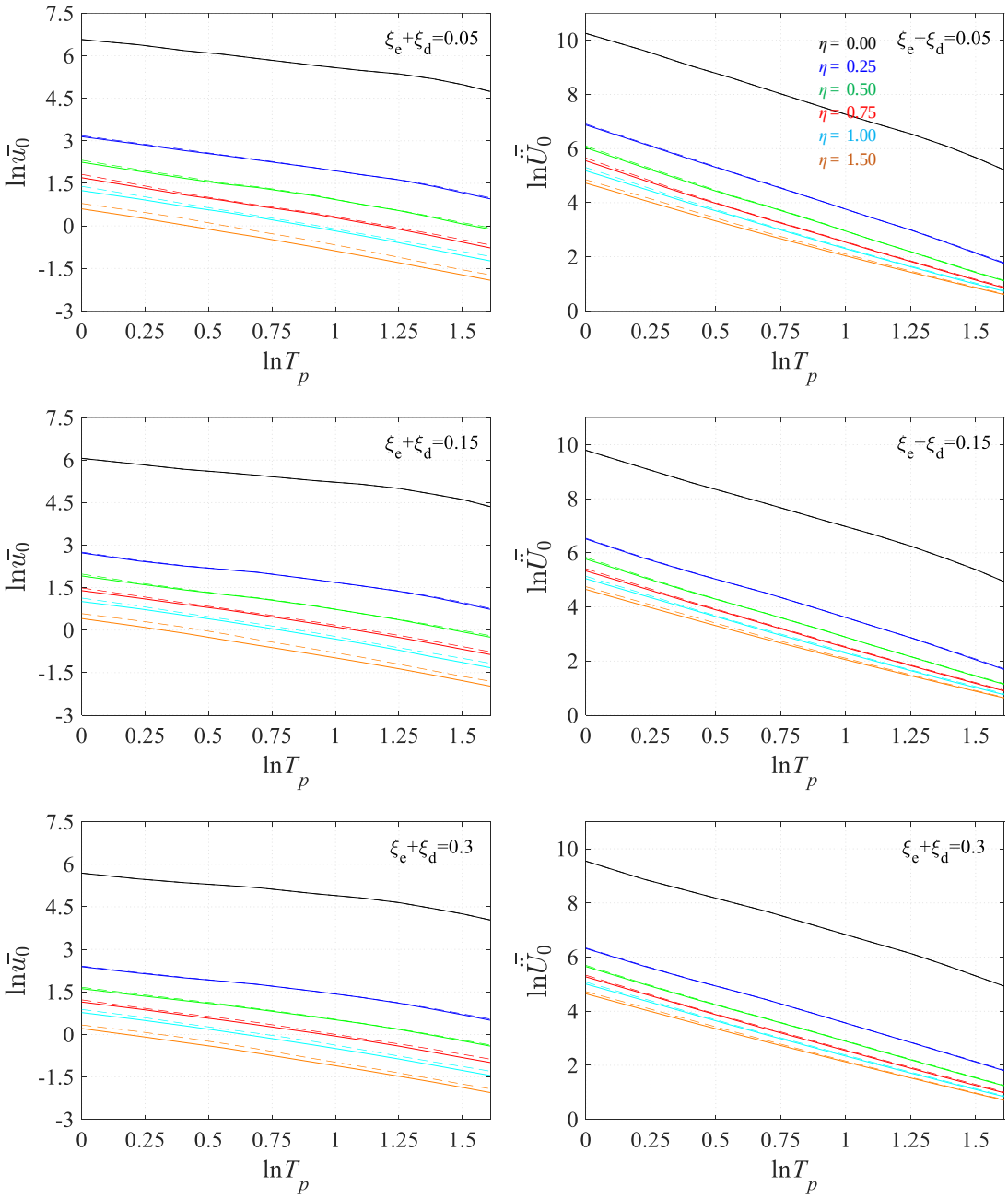

Fig. 4.13 NLRHA results under Art B suite: *GM* of $\ln\bar{u}_0$ (left) and $\ln\ddot{\bar{U}}_0$ (right) for PGA=0.21g (T_R=475yrs, SF_{EQ}=1) (dashed), PGA=0.42g (T_R≈2500yrs, SF_{EQ}=2) (solid), ξ=5, 15, 30%, and η=0~1.5

in fact, the minor influence of the increased intensity is evident only in the displacement response of systems with increased η and/or short isolation periods that are of little interest in seismic isolation of bridges. $SEGM(\bar{u}_0)$ values roughly indifferent to the increase of seismic intensity (Fig. 4.11) support the above statement. The combination of increased reliability in mean response estimation and the independence of the normalised response from the seismic intensity allows the development of generalised design equations (§4.3.3).

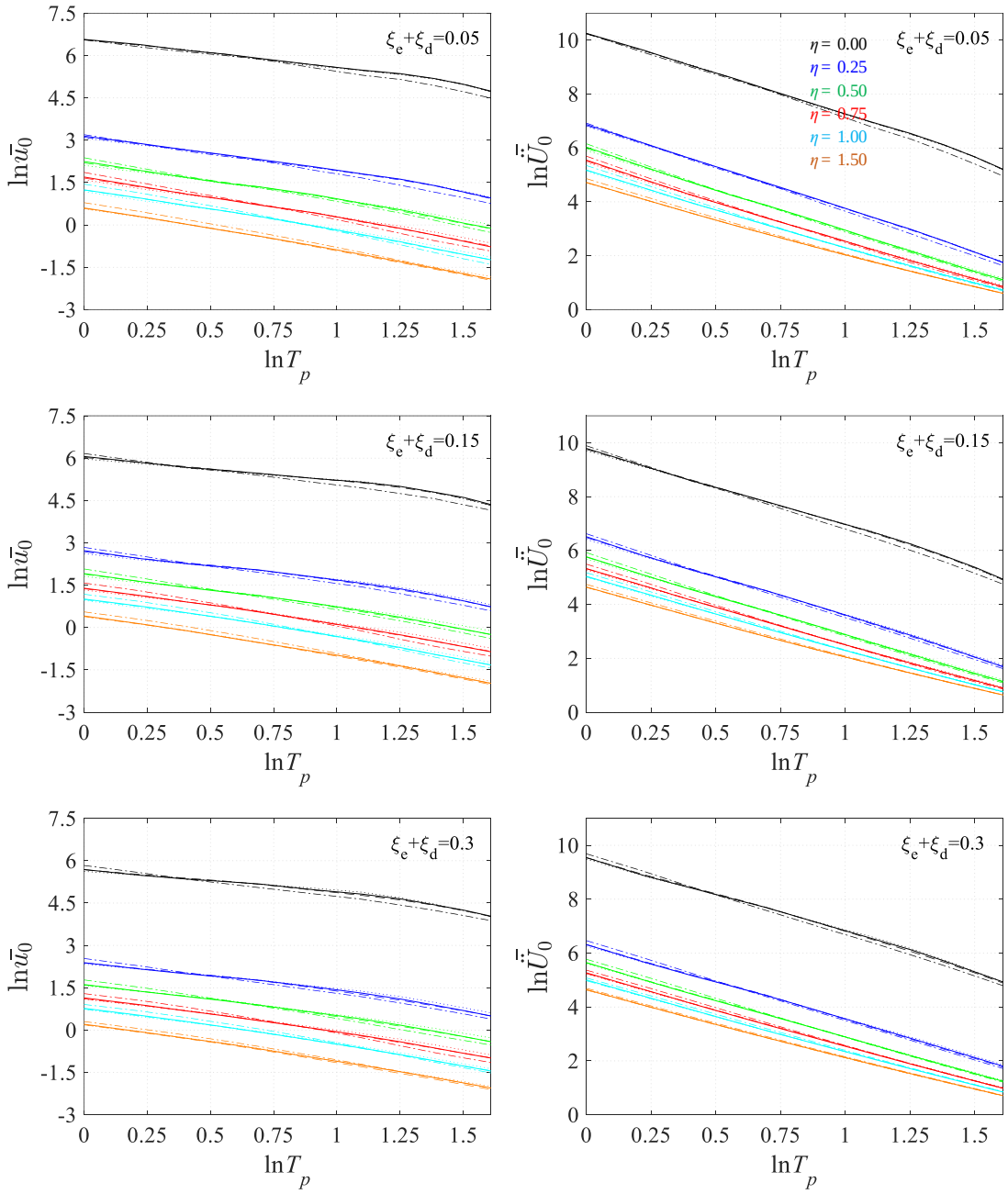

Fig. 4.14 NLRHA results under Art A (dotted), Art B (solid), Art C (dashed), Nat(H1) (SF_{EC}=1) (dashed-dotted): *GM* of $\ln\bar{u}_0$ (left) and $\ln\ddot{\bar{U}}_0$ (right) for PGA=0.42g (T_R≈2500yrs, SF_{EQ}=2), ζ=5, 15, 30%, and η=0~1.5

Prior to proceeding to the aforementioned task, the effect of the number and type of the adopted suite of accelerograms on the normalised/non-normalised relative displacement and total acceleration response is investigated. To this purpose, the procedure described earlier was re-applied using the Art A, C, and Nat(H1) (SF_{EC} = 1) suites of artificial and natural records (§4.2.2). Normalised response quantities $\bar{u}_0$, $\bar{\ddot{U}}_0$ are first plotted in Fig. 4.14 revealing some divergence from the Art B suite response, mainly in the case of displacements derived from analysis under Nat(H1). Deviation of curves in plots of normalised response are attributed primarily to the 'goodness-of-fit' of the *GM* spectrum of the selected records to the target spectrum (Fig. 4.2, Fig. 4.4) since the normalised inelastic spectra of Fig. 4.14 are disengaged from the effect of seismic intensity.

Shifting from the normalised response of Fig. 4.14 to non-normalised relative displacements and total accelerations, depicted in Fig. 4.15, requires the definition of a target (or design) value for *PGV* (i.e. $\dot{u}_{g0}$). In other words, having established the mean normalised peak response by solving Eq. (4.22) or Eq. (4.27) under different suites of records and statistically processing the results, the non-normalised response should be subsequently derived from Eqs. (4.28), (4.30) using a design *PGV* provided either by the code or a site-specific hazard analysis (or even the relationships cited in §B.1.1). Adopting, as discussed earlier in §4.2.2, a design value of *PGV* equal to 0.302m/s for T_R = 475yrs, SF_{EQ} = 1 (i.e. equal to the *GM* of *PGV*s of records included in Art B suite), results in the non-normalised response presented in Fig. 4.15 for $T_R \approx$ 2500yrs. In this case (i.e. non-normalised response), the accuracy in mean response estimation will now depend, in addition to 'goodness-of-fit' to the target spectrum, on the degree of matching of the design *PGV* to the *GM* of the *PGV*s of the individual records included in the considered suite. This is valid for the suites of artificial records and especially Art B resulting in response estimates that clearly follow the target spectra (Fig. 4.2) in the case of ξ = 5%, η = 0, and T_R = 475yrs (Fig. 4.18). It is also seen (Fig. 4.15) that the number of records in the case of artificial records does not have a significant effect on the estimated response; only the Art A (5 records) curves seem to slightly diverge from Art B results. On the other hand, the suite of 16 natural records underestimates significantly relative displacements, and total accelerations for low values of ξ and η, due to the adoption of a design *PGV* that is smaller than the *GM* of records *PGV*s (i.e. 0.363m/s for T_R = 475yrs, SF_{EQ} = 1, Table 4.2), further distorting the spectral matching depicted in Fig. 4.4 and implying that a larger number of natural records (i.e. >16) may be required to describe more efficiently the shape and the design *PGV* of the target spectra. These trends derive from a marked difference between the Ryan & Chopra (2004a, b) approach and the extended method presented herein; the former uses a number of records associated with a specific seismic scenario to determine a target spectrum and a design *PGV*, while the latter sets a (code/site-specific-based) target spectrum (and design *PGV*) as the starting point, and requires the selection of spectrum and intensity compatible records.

To further assess the reliability of mean response estimates, *SEGM* of normalised response is plotted in Fig. 4.16 for the considered suites and a representative value of ξ = 5%, considering that usually *SEGM* of responses marginally decreases with the increase of ξ (see for example Fig. 4.11 for Art B case). In general, *SEGM*($\bar{u}_0$) was found more difficult to be limited within a preselected

value, herein ±15% of *GM* with a 90% confidence level, compared to *SEGM*($\ddot{\bar{U}}_0$). Art A curves also imply that even when artificial records are used, more than 5 records may be required to constraint *SEGM*($\bar{u}_0$) due to the increased standard deviation of inelastic response (i.e. upper values of δ approximately equal to 0.3 and 0.25 for $\bar{u}_0$ and $\ddot{\bar{U}}_0$, respectively); nevertheless, in the latter case satisfactory results will still be obtained, according to Fig. 4.15, leading to some conservatism in displacement response estimation, as opposed to the unconservative estimates derived from the use of the Nat(H1) suite. In the latter case (i.e. natural records), resulting peak *SEGM*($\bar{u}_0$, $\ddot{\bar{U}}_0$) values are constrained approximately below 20% corresponding to δ values of 0.4 which remain at the

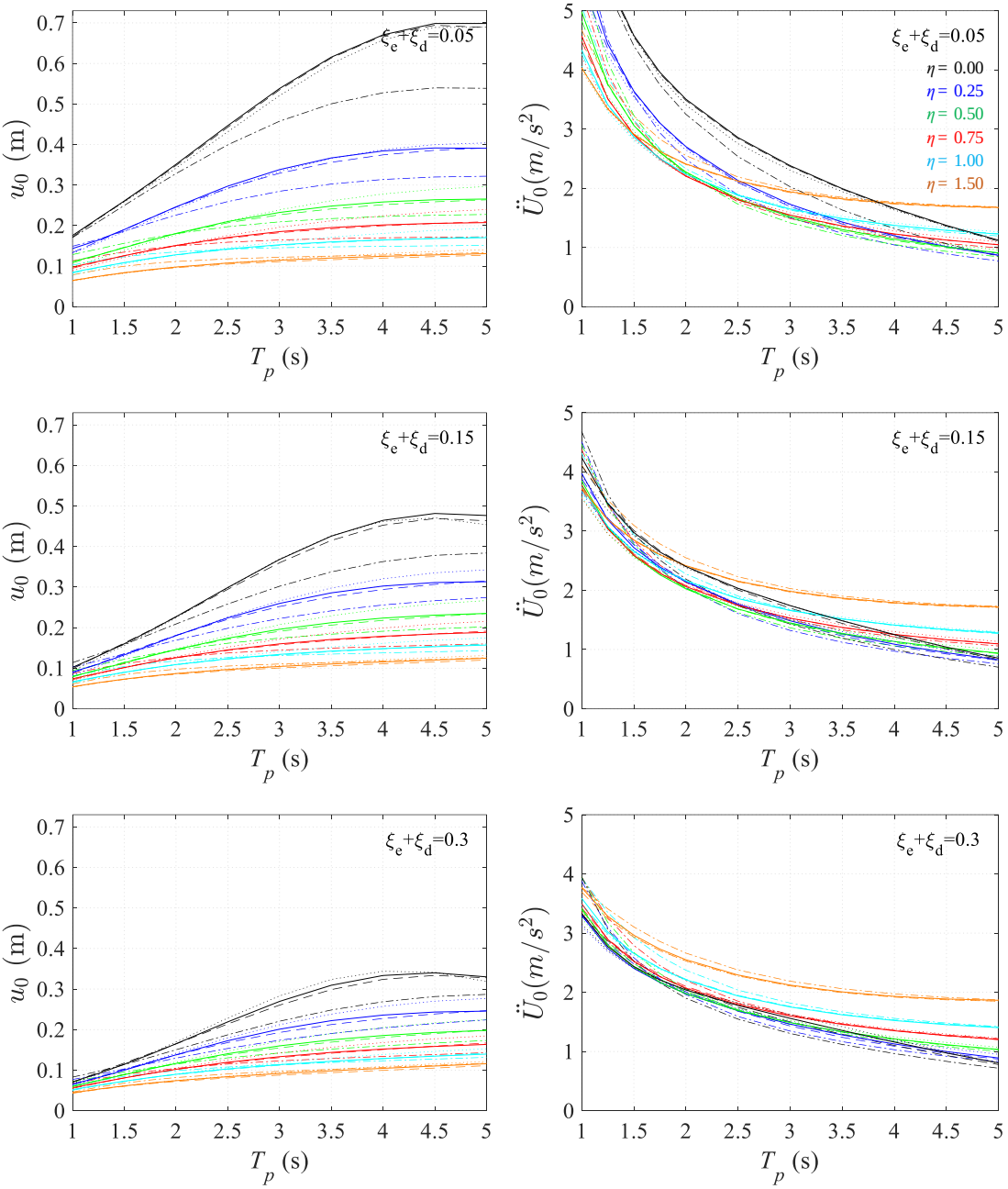

Fig. 4.15 NLRHA results under Art A (dotted), Art B (solid), Art C (dashed), Nat(H1) (SF_{EC}=1) (dashed-dotted) suites: *GM* of u_0 (left) and $\ddot{U}_0$ (right) for *PGA*=0.42*g* (T_R≈2500yrs, SF_{EQ}=2), ξ=5, 15, 30%, and η=0~1.5

lower limit of the values reported in Ryan & Chopra (2004b) indicating the effectiveness of the normalisation procedure of §4.3.1, but reveal once more that a larger number of records will be required to attain a predefined degree of reliability compared to artificial records. The effectiveness of the scaling approach introduced in §4.2.2 for natural records is evident in Fig. 4.17, since peak *SEGM* values of non-normalised response was found somewhat increased but in general of the same order as $SEGM(\bar{u}_0, \ddot{\bar{U}}_0)$ values.

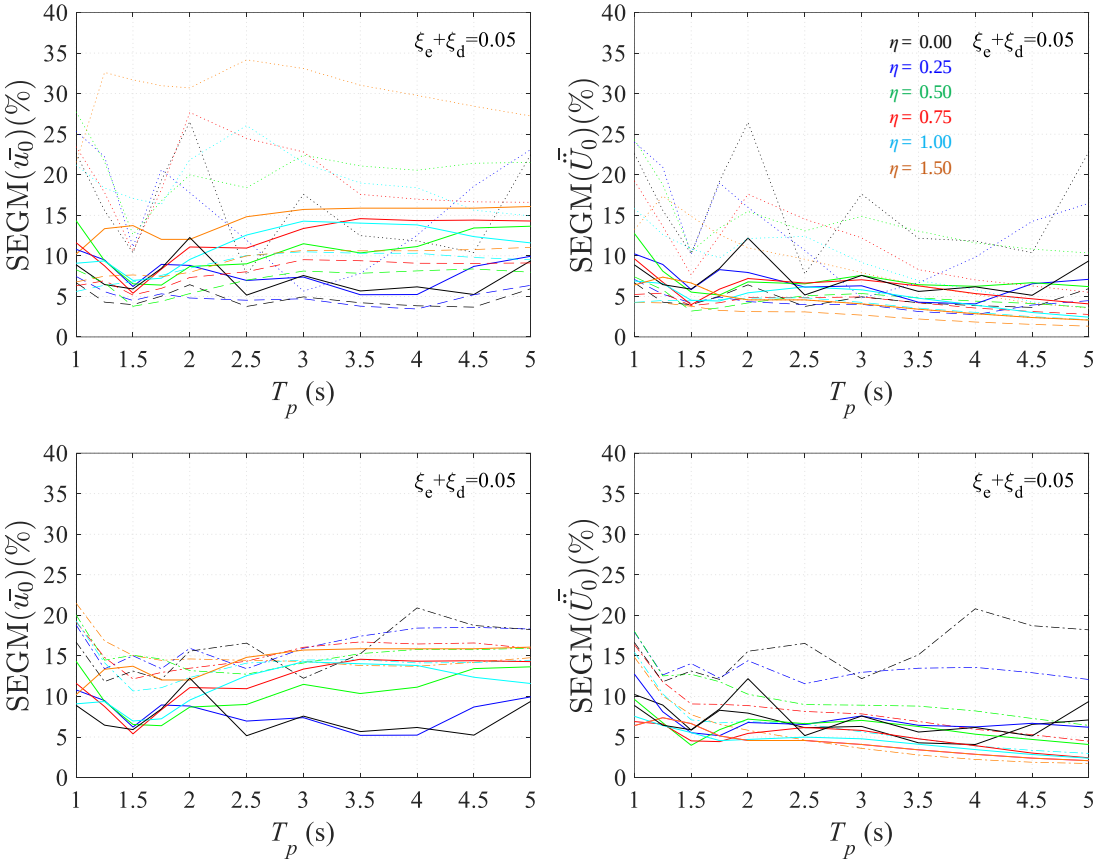

Fig. 4.16 NLRHA results under Art A (dotted), Art B (solid), Art C (dashed) (top), Art B (solid), Nat(H1) (SF_{EC}=1) (dashed-dotted) (bottom) suites: *SEGM* of $\bar{u}_0$ (left) and $\ddot{\bar{U}}_0$ (right) for PGA=0.42g (T_R≈2500yrs, SF_{EQ}=2), ζ=5%, and η=0~1.5

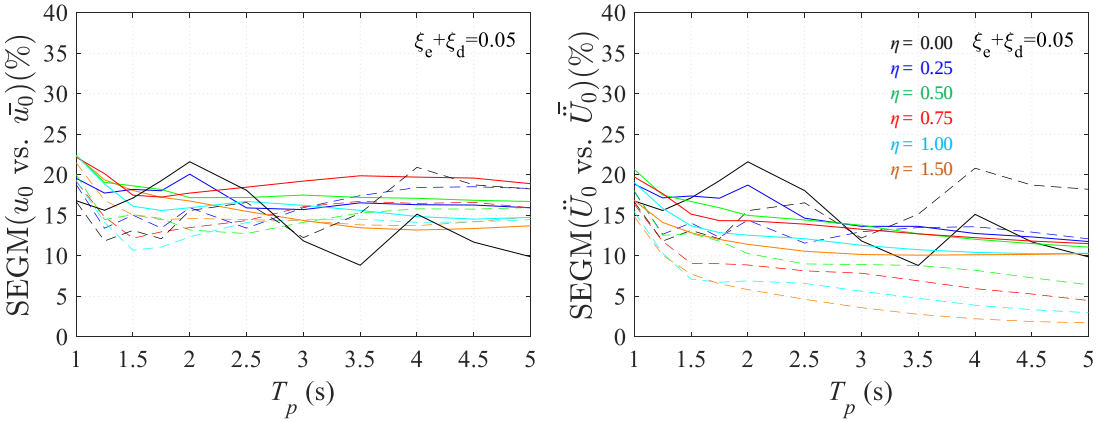

Fig. 4.17 NLRHA results under Nat(H1) (SF_{EC}=1) suite: *SEGM* (%) of u_0, $\ddot{U}_0$ (solid) and $\bar{u}_0$, $\ddot{\bar{U}}_0$ (dashed) for PGA=0.42g (T_R≈2500yrs, SF_{EQ}=2), ζ=5%, and η=0~1.5

Considering the degree of complexity and the computational effort involved when natural records are used to derive the normalised response (i.e. difficulties in selecting records compatible with the shape and *PGV* of code-based target spectra over a wide range of periods, use of additional selection criteria, scarcity of recorded accelerograms associated with selected criteria, increased number of records and analyses) in contrast with the simpler approach of artificial records that can easily satisfy the above requirements and provide robust estimates of mean response within a purely 'intensity-based' (ATC 2012) design framework disregarding member strength degradation (which is reasonable in seismically designed bridges), generalised design equations are hereafter developed for the Art B suite. The inherent variability of natural records can be considered at a later stage of design using a more refined type of analysis as in the design method proposed in Chapter 5. Nevertheless, if required, based on the objective of the analysis (§4.1), derivation of GDEs based ideally on a large number of natural records, is feasible using the IDEC code (§4.2.3).

4.3.3 Derivation of generalised design equations

Uncoupling the response from the seismic intensity allows the development of generalised design equations that can provide direct estimates of normalised relative displacements $\bar{u}_0$ and total accelerations $\bar{\ddot{U}}_0$ as a function of ξ, η, T_p, irrespective of the performance level and associated intensity under consideration. The problem of deriving GDEs can be tackled by developing regression models extending to a 3D-space (x-x axis: T_p, y-y axis: ξ, z-z axis: η). To this end, linear regression equations were fitted to the logarithmically transformed normalised response derived from NLRHAs (§4.3.2) since it was found that $\ln\bar{u}_0$ and $\ln\bar{\ddot{U}}_0$ vary almost linearly with $\ln\xi$ and $\ln T_p$ (Fig. 4.10). Different linear regression models using three independent predictors (i.e. ξ, η, T_p) were developed for $\bar{u}_0$ and $\bar{\ddot{U}}_0$ since peak total accelerations (and hence maximum forces) in the isolation and energy dissipation system cannot be directly associated with peak relative displacements due to the introduction of viscous damping (i.e. f_D term in Eq. (4.21)) with values of ξ in general larger than 5%, i.e. the maximisation of total accelerations and relative displacements occurs at different time intervals (Fig. 4.8). Although complex regression models can be derived using the IDEC code, an effort was made to simplify the relevant design equations with a view to increasing their usefulness in practical design, therefore different GDEs were extracted for linear (η = 0) and nonlinear systems ($\eta \neq 0$).

High-degree polynomials are first fitted to the normalised response variable $\bar{y}$ (i.e. $\bar{u}_0$ or $\bar{\ddot{U}}_0$) resulting in GDEs of the general form of Eq. (4.33) for a complete m-degree polynomial with q terms, where j, k, l indices are permuted accordingly, and b_i coefficients are estimated using the method of least squares. u_0 and $\ddot{U}_0$ response can be subsequently predicted by shifting GDEs of Eq. (4.33) to the non-normalised space using Eq. (4.34) (in analogy to Eq. (4.28)) that accounts for a specific seismic intensity in terms of *PGV* through Eq. (4.30). Equations in the form of Eq. (4.34) provide direct estimates of u_0 and $\ddot{U}_0$ under different PLs associated with target spectra of common frequency content but different intensity (§4.2.2).

$$\ln \bar{y}_m\left(\ln \xi, \ln \eta, \ln T_P\right) = \sum_{i=0}^{m} b_i \left(\ln \xi\right)^j \left(\ln \eta\right)^k \left(\ln T_P\right)^l, \quad j+k+l \le i \qquad \left[q=(m+1)(m+2)(m+3)/6\right] \tag{4.33}$$

$$y_m = u_r \exp\left(\ln \bar{y}_m\left(\ln \xi, \ln \eta, \ln T_P\right)\right) \tag{4.34}$$

Stepwise regression is finally employed to assess the statistical significance of terms using the *R*-squared criterion (Mathworks 2016) and reduce the total number of terms in the model.

The 'goodness-of-fit' of the regression models was assessed both in terms of limiting the divergence of the predicted response from analysis results (i.e. residuals), and in terms of identifying 'near-optimal' isolation systems under different seismic intensities; a 'near-optimal' isolation system is defined herein as the one that results in 'near-minimum' peak total acceleration $\ddot{U}_0$ similarly to Inaudi & Kelly (1993). Regarding the first assessment criterion, the predicted-to-observed deviation of responses was quantified by common statistical measures such as R-squared (R^2), and root mean square error (RMSE) (Mathworks 2016). r_{max} (Eq. (4.35)) represents in addition the maximum percentage residual of a regression model prediction $y_{i,GDE}$ with regard to the corresponding analysis value $y_{i,RHA}$ (i.e. the geometric mean of peak responses derived from statistical processing of response history analysis results as per §4.2.4), while r_{GM} (Eq. (4.36)) is the geometric mean of residuals in the data sample; n is the product of the different damping, strength, and period values $n_\xi \cdot n_\eta \cdot n_{Tp}$ (i.e. the number of observations-grid intersections in Fig. 4.10).

$$r_{\max}(\%) = 100 \cdot \max\left(\left|\frac{y_{i,GDE} - y_{i,RHA}}{y_{i,RHA}}\right|, \left|\frac{y_{i+1,GDE} - y_{i+1,RHA}}{y_{i+1,RHA}}\right|, \ldots, \left|\frac{y_{N,GDE} - y_{N,RHA}}{y_{N,RHA}}\right|\right) \tag{4.35}$$

$$r_{GM}(\%) = 100 \cdot \sqrt[n]{\prod_{i=1}^{n}\left(\left|\frac{y_{i,GDE} - y_{i,RHA}}{y_{i,RHA}}\right|\right)} \tag{4.36}$$

Representative results of different *m*-degree regression models (RM) with *q* terms ($m \times q$) are presented in Table 4.4 for two different seismic intensities associated with T_R = 2500yrs (Fig. 4.19) and T_R = 475yrs (Fig. 4.18); the first was used to develop the regression models and the second to assess the robustness of models in predicting estimates of non-normalised response under a different seismic intensity. As expected, models of $\eta = 0$ predict response quantities under different earthquake intensities with the same accuracy due to their inherent linearity; a minor decrease in accuracy is observed when models are used to predict the response under T_R = 475yrs.

In general, all models present excellent fit based on R^2, *RMSE* measures (Table 4.4), and the larger r_{max} values are mainly associated either with the upper limit of the considered period range (i.e. T_p = 5s) (which is not common even in isolated bridges) or with low values of u_0 and $\ddot{U}_0$. Nevertheless, a significant reduction of terms results in models that fail to predict the shape (or curvature) of displacement and acceleration curves.

Table 4.4 Evaluation of alternative linear regression models for 1D excitation based on 'goodness-of-fit'

	Model				u_0		Model			$\ddot{U}_0$	
η =0	T_R (yrs)	$m \times q$	R^2	*RMSE*	r_{max} (%)	r_{GM} (%)	$m \times q$	R^2	*RMSE*	r_{max} (%)	r_{GM} (%)
RM1	475	4 × 15			3.46	0.95	4 × 15			3.76	1.10
	2500		0.999	0.019	3.46	0.96		1.000	0.020	3.75	1.11
RM2,3	**475**	**3 × 5**			**10.87**	**1.81**	**2 × 5**			**12.87**	**3.17**
	2500		**0.996**	**0.039**	**10.87**	**1.81**		**0.999**	**0.052**	**12.84**	**3.17**
RM4	475	1 × 3			26.66	4.16	1 × 3			26.88	4.57
	2500		0.979	0.087	26.65	4.17		0.997	0.087	26.91	4.57
$\eta \neq 0$	T_R (yrs)	$m \times q$	R^2	*RMSE*	r_{max} (%)	r_{GM} (%)	$m \times q$	R^2	*RMSE*	r_{max} (%)	r_{GM} (%)
RM1	475	4 × 35			20.36	5.82	4 × 35			12.43	2.94
	2500		1.000	0.014	3.96	0.66		1.000	0.009	2.73	0.41
RM2	475	3 × 11			23.92	6.28	3 × 11			14.27	2.80
	2500		1.000	0.024	8.01	1.16		1.000	0.027	10.44	1.30
RM3	**475**	**2 × 8**			**22.32**	**6.79**	**2 × 8**			**20.58**	**2.94**
	2500		**0.999**	**0.045**	**16.76**	**2.36**		**0.999**	**0.044**	**17.41**	**2.48**
RM4	475	2 × 7			24.22	7.66	2 × 7			21.03	2.90
	2500		0.998	0.0541	21.21	3.13		0.999	0.0562	17.23	2.49

This is of particular importance when identification of 'near-optimal' isolation systems is additionally sought by the adopted regression model, and is more conveniently illustrated by plotting the inelastic spectra in a u_0-$\bar{v}_0$, $\ddot{U}_0$-$\bar{v}_0$ format (e.g. Fig. 4.20) that facilitates the identification of isolation schemes (ξ, $\bar{v}_0$, T_p) with a 'near-optimal' performance (i.e. min$\ddot{U}_0$). In Fig. 4.20, $\ddot{U}_0$(opt) curves represent a visualisation of the design criterion of min$\ddot{U}_0$ per T_p, and u_0(opt) indicates the corresponding relative displacements of the isolation system, both plotted for the case of ξ = 5% where relevant deviations from RHA are more significant and involve response quantities of higher magnitude.

It is seen that RM2 can accurately capture the location of 'near-optimal' isolation systems for the entire range of T_p = 1~5s, however, the simpler RM3 model was finally adopted since it is deemed adequate for practical applications in bridge engineering (i.e. T_p = 1.5~4s). GDEs (i.e. Eq. (4.34)) in the case of RM3 take the general form of Eqs. (4.37) and (4.38) wherein y represents either u_0 or $\ddot{U}_0$, and the seismic intensity is expressed for convenience in terms of *PGA* at bedrock, i.e. $\ddot{u}_{g0}$ in m/s^2. In the case of elastomer-based isolators and a target spectrum with a frequency content corresponding to site conditions 'C' of EN1998-1 (CEN 2004b) Eq. (4.37) is simplified according to the data of Table 4.5.

Since earlier studies (e.g. Makris & Chang 2000, Makris & Vassiliou 2011) have demonstrated that the response of isolated structures is not sensitive to the exact value of u_y, the regression coefficients of Table 4.5 may also be used to approximately predict the peak inelastic response of isolation systems consisting of friction-based devices (u_y<1mm); however, derivation of case-specific GDEs using IDEC is expected to yield finer response estimates both in terms of accuracy in peak response prediction and 'near-optimal' system identification.

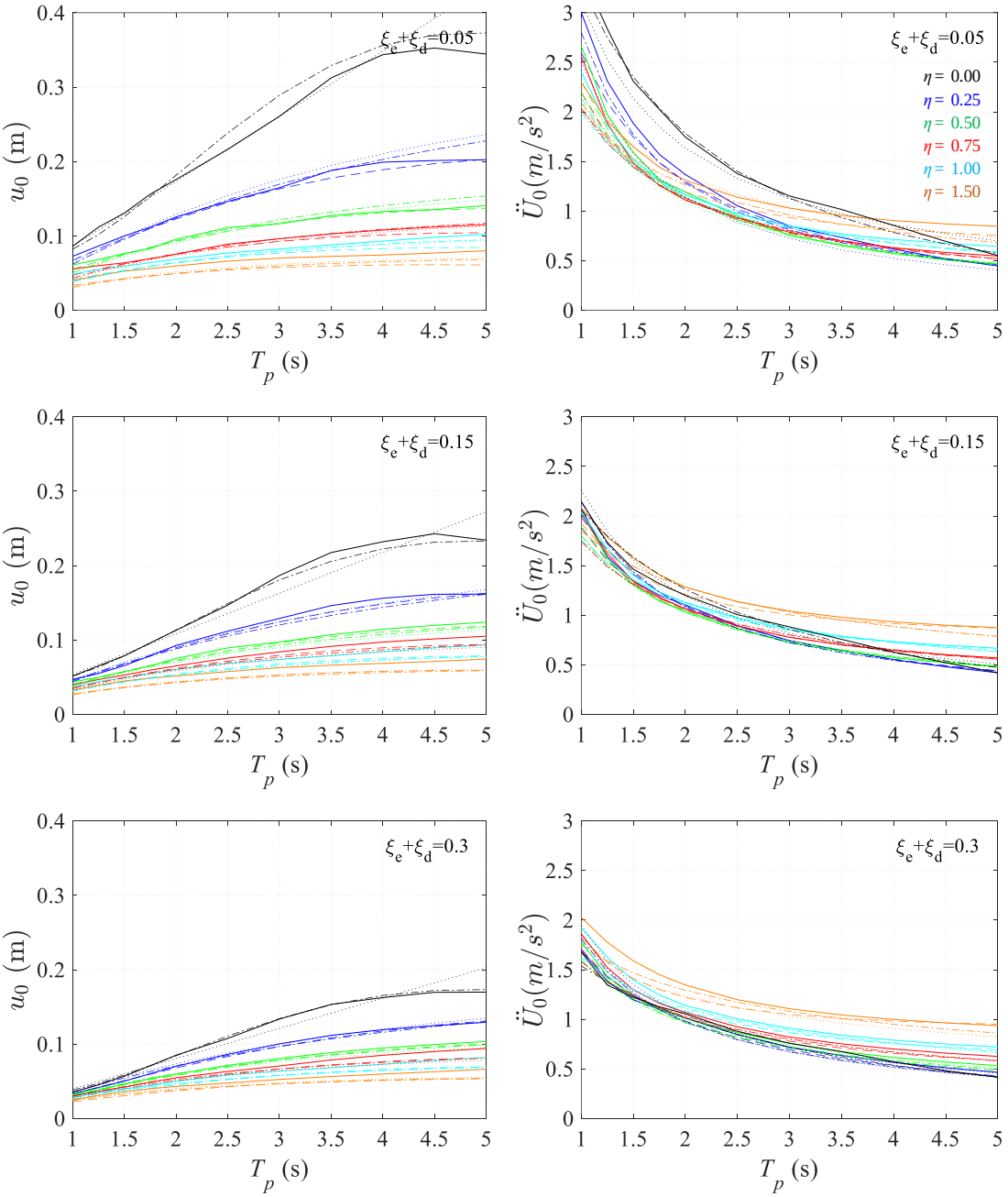

Fig. 4.18 NLRHA u_0 (left) and $\ddot{U}_0$ (right) under Art B (solid) compared to response predicted from RM2 (dashed), RM3 (dashed-dotted), and RM4 (dotted) for PGA=0.21g (T_R=475yrs, SF_{EQ}=1), ξ=5, 15, 30%, η=0~1.5

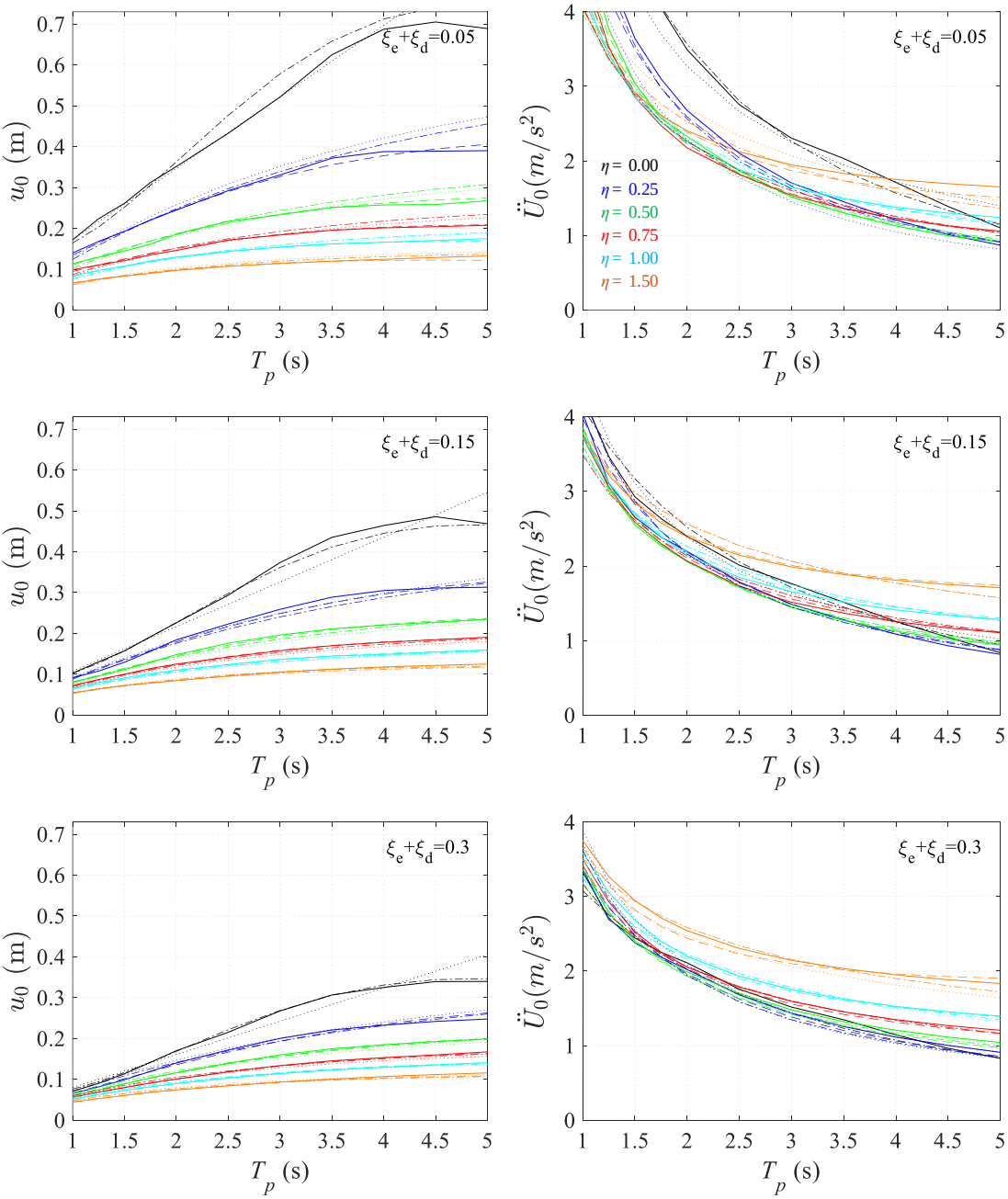

Fig. 4.19 NLRHA u_0 (left) and $\ddot{U}_0$ (right) under Art B (solid) compared to response predicted from RM2 (dashed), RM3 (dashed-dotted), and RM4 (dotted) for PGA=0.42g (T_R~2500yrs, SF_{EQ}=2), ξ=5, 15, 30%, η=0~1.5

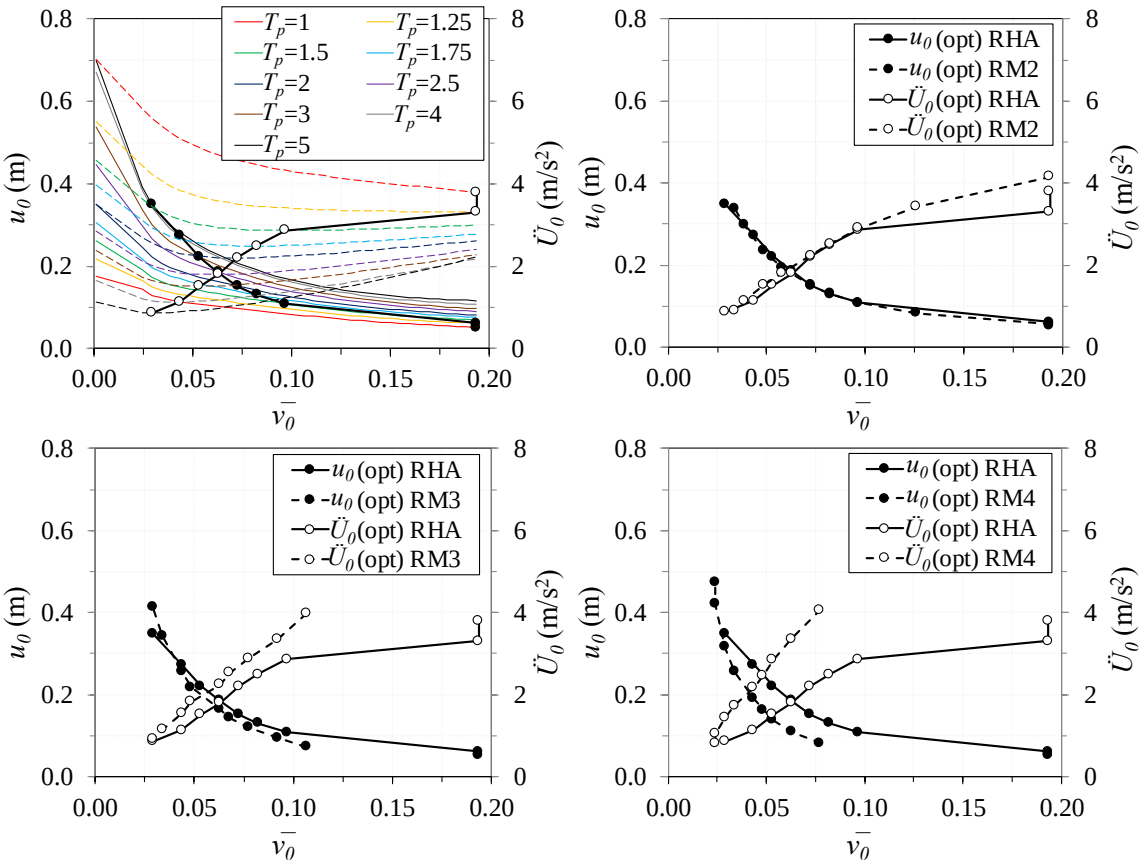

Fig. 4.20 NLRHA response u_0 (solid), $\ddot{U}_0$ (dashed), optimal peak total accelerations $\ddot{U}$opt (solid) and corresponding relative displacements $u$opt (solid) under Art B suite, compared to $u$opt, $\ddot{U}$opt (solid) derived from RM2, RM3, RM4 (dashed) for PGA=0.42g (T_R≈2500yrs, SF_{EQ}=2), ξ=5%, 1D excitation

$$y = \frac{0.362e^{\text{Int}}}{2\pi g}\xi^{(\beta+\gamma\ln\eta+\delta\ln T_p)}\eta^{(1+\varepsilon+\zeta\ln\eta+\kappa\ln T)}T_p^{(2+\lambda+\mu\ln T_p+\nu(\ln T_p)^2)}\ddot{u}_{g0} \tag{4.37}$$

$$\eta = 4.31\frac{\bar{v}_0 g}{a_g} \tag{4.38}$$

Table 4.5 RM3 regression coefficients: EN1998-1, site conditions 'C' (CEN 2004b), 1D excitation

Case	*y*	*Int*	*β*	*γ*	*δ*	*ε*	*ζ*	*κ*	*λ*	*μ*	*ν*
η =0	u_0	5.245	-0.428	-	-	-	-	-	-1.194	0.797	-0.443
	$\ddot{U}_0$	8.952	-0.419	-	0.150	-	-	-	-2.266	-0.226	-
η =0.25-1.5	u_0	0.623	-0.178	0.097	-	-1.192	-0.095	-0.175	-1.100	-0.209	-
	$\ddot{U}_0$	4.769	-0.114	0.094	0.128	-0.754	0.153	0.255	-2.393	-	-

4.4 Isolated SDOF System with Nonlinear Viscous Damping

4.4.1 Dynamic equation of motion

The procedure described in §4.3.1 is further extended in the following to investigate the effect of non-linear viscous dampers (NLVDs) on the peak response of isolated SDOF systems. In this context, the dynamic equation of motion of the idealised system of Fig. 4.9 is re-written substituting in Eq. (4.21) the shear force of the bilinear isolator (Eq. (4.4)) and the axial force of the LVD (Eq. (4.13)) and NLVD (Eq. (4.9));

$$\ddot{u}(t)+\left[\left(c_{e,L}\dot{u}(t)+c_{d,NL}\,\mathrm{sgn}\left(\dot{u}(t)\right)\left|\dot{u}(t)\right|^{a}\right)\Big/m\right]+\ldots \\ \ldots+\left[\bar{v}_0 gz\left(t,k_e,u,\dot{u}\right)+\omega_p^2 u(t)\right]=-\ddot{u}_g(t) \tag{4.39}$$

The constant damping coefficients $c_{e,L}$, $c_{d,NL}$ associated with viscous damping originating from elastomer-based isolators and NLVDs, respectively, are expressed by Eqs. (4.24) and (4.18) introducing the 'energy-equivalence' approach (Lin & Chopra 2002) described in §4.2.3; the unknown displacement amplitude u_0 required for the calculation of $c_{d,NL}$ (Eq. (4.15)) when $a \neq 1.0$ is defined herein as the peak displacement of the SDOF with an energy-equivalent LVD of $\xi = \xi_{e,L}+\xi_{d,NL}$ and $a = 1$.

$$\ddot{u}(t)+\left[2\omega_p\xi_{e,L}\dot{u}(t)+\frac{2\omega_p\xi_{d,NL}\left(u_0\omega_p\right)^{1-a}}{f(\Gamma,\alpha)}\mathrm{sgn}\left(\dot{u}(t)\right)\left|\dot{u}(t)\right|^{a}\right]+\ldots \\ \ldots+\left[\bar{v}_0 gz\left(t,k_e,u,\dot{u}\right)+\omega_p^2 u(t)\right]=-\ddot{u}_g(t) \tag{4.40}$$

The characterisation of NLVDs by the 'energy-equivalence' approach (i.e. dampers of the same damping ratio ξ but different a) is introduced as the first of the two conditions required to uncouple the response from the seismic intensity. The second condition involves the characterisation of the isolation system strength by η as described in §4.3.1. Dividing Eq. (4.40) by u_r (Eq. (4.26)), the equation of motion is reduced in the normalised form of Eqs. (4.41)-(4.43);

$$\ddot{\bar{u}}(t)+\left[2\omega_p\xi_{e,L}\dot{\bar{u}}(t)+\frac{2\omega_p\xi_{d,NL}\left(\bar{u}_0\omega_p\right)^{1-a}}{f(\Gamma,\alpha)}\mathrm{sgn}\left(\dot{\bar{u}}(t)\right)\left|\dot{\bar{u}}(t)\right|^{a}\right]+\ldots \\ \ldots+\left[\omega_p^2\left(z\left(t,k_e,u,\dot{u}\right)+\bar{u}(t)\right)\right]=-\left(\omega_p^2/\eta\omega_D\right)\ddot{\bar{u}}_g(t) \tag{4.41}$$

$$\ddot{\bar{u}}(t)=\ddot{u}(t)/u_r,\ \dot{\bar{u}}(t)=\dot{u}(t)/u_r,\ \bar{u}(t)=u(t)/u_r \tag{4.42}$$

$$\bar{\ddot{u}}_g(t) = \ddot{u}_g(t)/\dot{u}_{g0} \tag{4.43}$$

The normalised equation of motion along with the consideration of a constant yield displacement (§4.2.3), reduce the governing parameters that influence the response to the isolation period T_p (or frequency ω_p), the normalised strength η, the damping ratio ξ (= $\xi_{e,L}$ + $\xi_{d,NL}$), and the nonlinearity of dampers (i.e. parameter a) as opposed to the parameters T_p, V_0, $c_{e,L}$, $c_{d,NL}$, a, u_y, $\dot{u}_{g0}$ in the non-normalised case of Eq. (4.39). More specifically, Eq. (4.27) indicates that the normalised response is independent of the seismic intensity rendering the non-normalised quantities linearly proportional to u_r according to Eq. (4.28). The following numerical study (§4.3.2) investigates the validity of the previous statement by exploring the effect of nonlinearity of viscous dampers in Eq. (4.41).

4.4.2 Parametric analysis of SDOF system

The numerical study of §4.3.2 is repeated in this section by calculating the normalised response of representative isolation and energy dissipation systems for a range of design parameters (i.e. $\xi_{e,L}$ = 0.05, $\xi_{d,NL}$ = 0~0.25, η = 0~1.5, T_p = 1~5s, a = 0.2~1, u_y = 1cm) under the suite of artificial records Art B (Fig. 4.2). Similarly to §4.3.2, $\bar{u}(t)$, $\bar{\ddot{u}}(t)$ response histories can be found either directly by solving Eq. (4.41) for the selected values of ξ, a, η, T_p, u_y, or indirectly by first solving Eq. (4.39) with corresponding values of $c_{e,L}$, $c_{d,NL}$, V_0, k_p, (i.e. Eqs. (4.24), (4.18), (4.31), (4.32), respectively) and then by calculating the normalised response from Eq. (4.42). In case the nonlinearity parameter a equals unity, Eq. (4.41) is simplified to Eq. (4.27) (i.e. linear viscous damping) and §4.3.2 applies.

Statistical processing of parametric analysis results reveals that the range of $SEGM(\bar{u}_0, \bar{\ddot{U}}_0)$ is not significantly affected by the value of the nonlinearity parameter of viscous dampers, implying small differentiations of u_0 and $\ddot{U}_0$ response compared to the case of linear viscous damping (a = 1); Fig. 4.21 presents $SEGM$ values for ξ = 15 and 30% that are close to those resulting for linear damping (a = 1) with peak values below 15% and 10% for relative displacements and total accelerations, respectively, which allow meaningful statistical analysis of the results and reliable mean response estimation. Furthermore, it was found that the seismic intensity has a negligible effect on the mean normalised response irrespective of the degree of the nonlinearity of viscous dampers, or else, the reduction of the velocity exponent a in Eq. (4.41) reduces the maximum axial force developing in the dampers (Fig. 4.7(right)) without significantly affecting the system's overall response (i.e. $\bar{u}_0$, $\bar{\ddot{U}}_0$). In Fig. 4.22, where the log-transformed normalised mean peak response is plotted under two different earthquake intensities (i.e. T_R of 475 and 2500yrs), the minor influence of the increased intensity is mainly evident in the displacement response of systems with increased η and/or short isolation periods similarly to Fig. 4.13 (i.e. regardless of the a value).

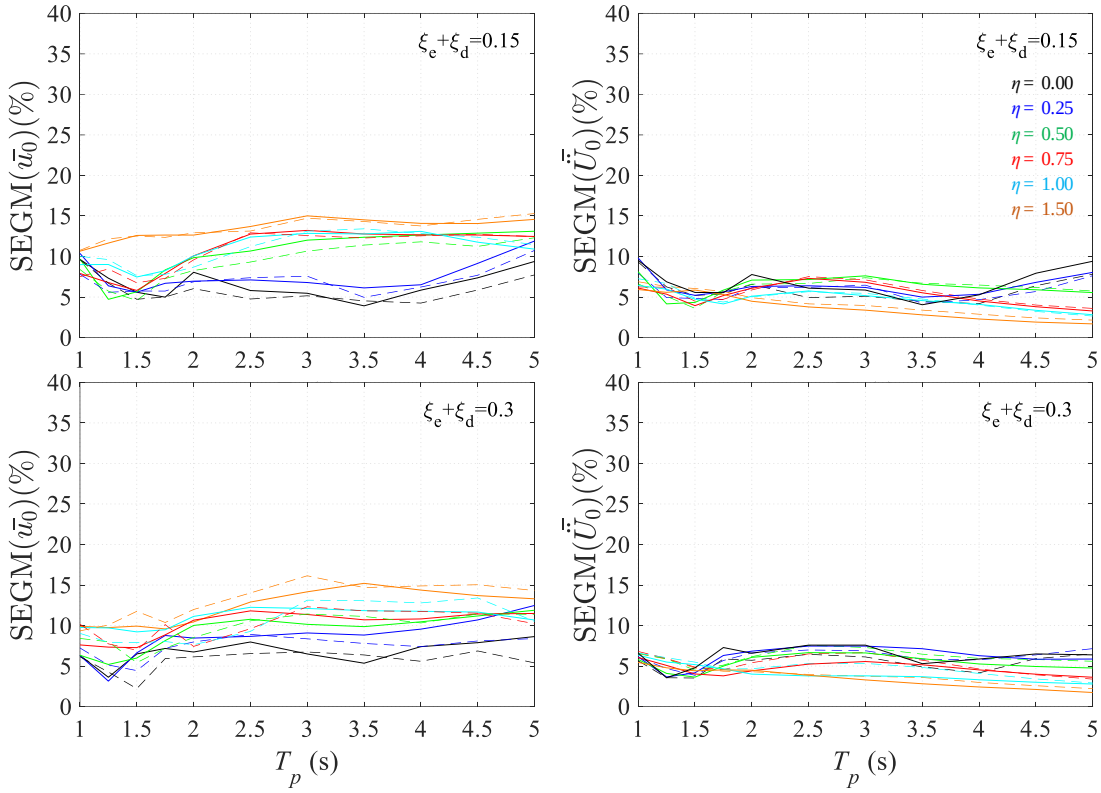

Fig. 4.21 NLRHA results under Art B suite: *SEGM* (%) of $\bar{u}_0$ (left) and $\ddot{\bar{U}}_0$ (right) considering energy-equivalent VDs of a=1 (solid) and a=0.2 (dashed) for PGA=0.42g (T_R≈2500yrs, SF_{EQ}=2), ξ=15%, 30%

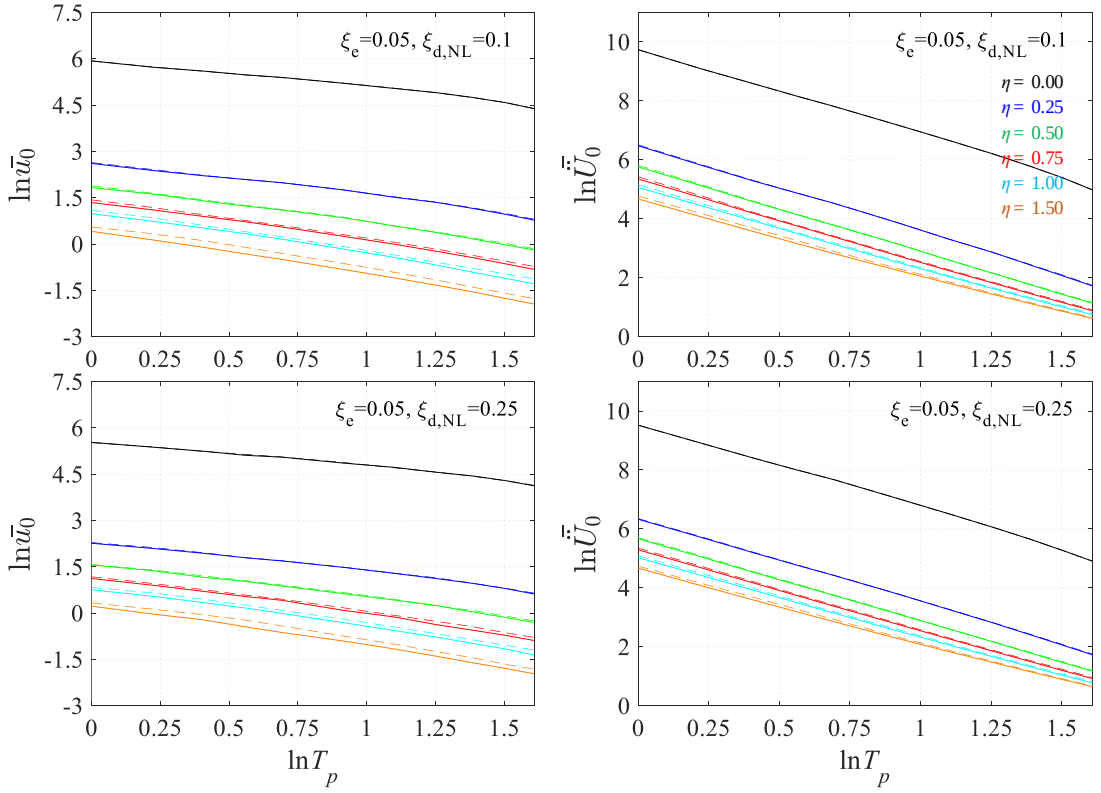

Fig. 4.22 NLRHA results under Art B suite: *GM* of ln$\bar{u}_0$ (left) and ln$\ddot{\bar{U}}_0$ (right) for PGA=0.21g (T_R=475yrs, SF_{EQ}=1) (dashed), PGA=0.42g (T_R≈2500yrs, SF_{EQ}=2) (solid), ξ=15, 30%, and a=0.2

The insignificant effect of α on the peak inelastic response is more clearly illustrated in Fig. 4.23 where the non-normalised u_0, $\ddot{U}_0$ response is evaluated for energy-equivalent damper systems of a = 0.2, 0.4, 0.6, 1.0 and different values of normalised strength (the case of ξ_e = 0.05, ξ_d = 0 is excluded from the figures of this section as this coincides with the ξ = 0.05 case of §4.3.2). It is seen that the influence of the nonlinearity of dampers in the displacement response becomes stronger as $\xi_{d,NL}$ increases and a reduces.

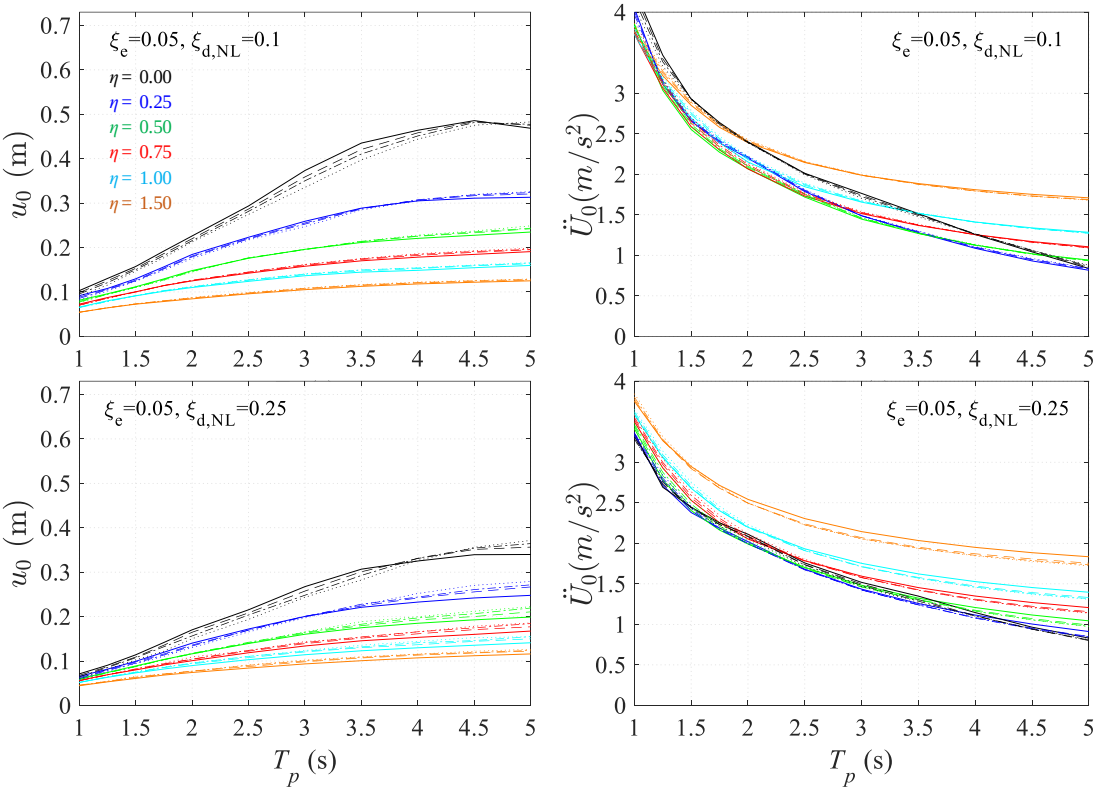

Fig. 4.23 NLRHA results under Art B suite: *GM* of u_0 (left) and $\ddot{U}_0$ (right) considering energy-equivalent VDs of a=1 (solid), a=0.6 (dashed), a=0.4 (dashed-dotted), a=0.2 (dotted) for PGA=0.42g (T_R≈2500yrs, SF_{EQ}=2)

More specifically, considering a total damping ratio of ξ = 0.30, divergences (Div) in the range of ±15% and ±10% are displayed between the a = 1, and a = 0.2 cases of displacement response (Fig. 4.24), depending on η and T_p but being relatively insensitive to the seismic intensity (not shown in Fig. 4.24), while Divu_0 further reduces to ±10% with the increase of a to 0.4. Total accelerations are even less affected, exhibiting values of Div$\ddot{U}_0$ within -7.5~5% in the case of a = 0.2, and -7.5~2.5% in the case of a = 0.4. Useful from a design point of view is the remark that as ξ increases, positive Div values indicating increase in seismic response due to the introduction of nonlinearity in viscous damping are mainly observed for (*i*) long periods in the case of u_0, (*ii*) short periods in the case of $\ddot{U}_0$, and (*iii*) increased values of normalised strength η in both u_0 and $\ddot{U}_0$ cases.

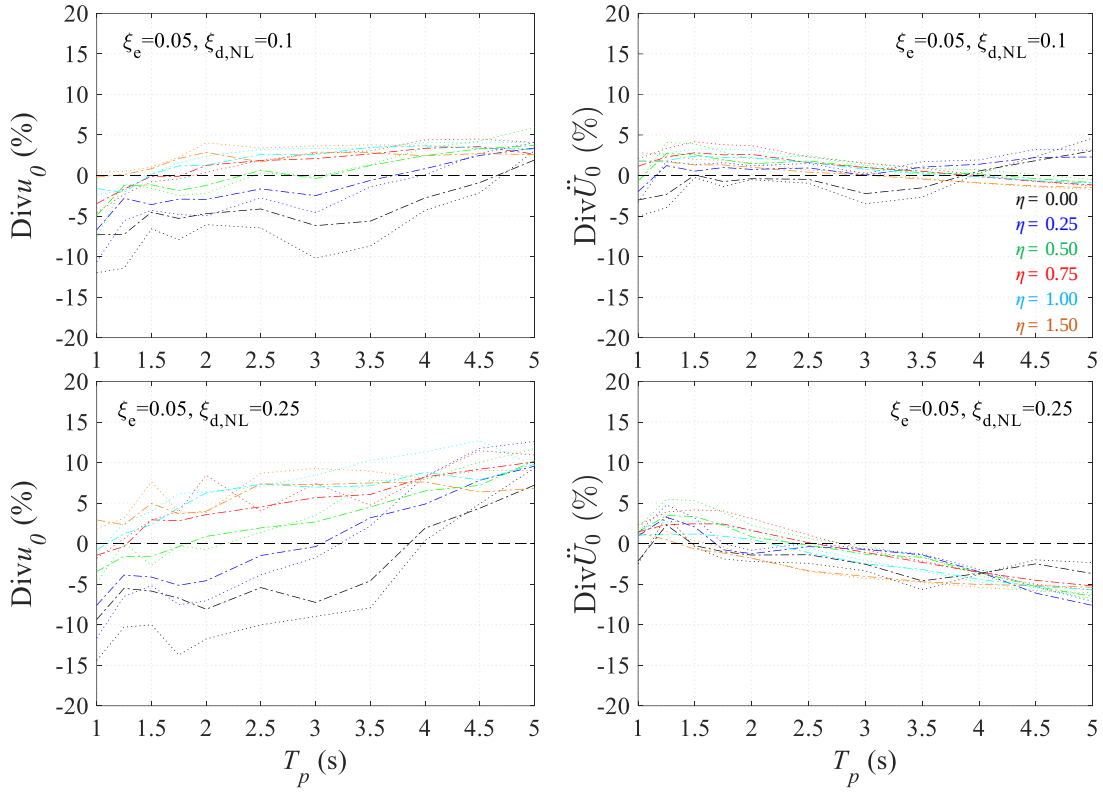

Fig. 4.24 NLRHA results under Art B suite: *GM* of u_0 (left) and $\ddot{U}_0$ (right) considering energy-equivalent VDs of a=0.4 (dashed-dotted), a=0.2 (dotted) for PGA=0.42g (T_R≈2500yrs, SF_{EQ}=2)

4.4.3 Derivation of generalised design equations

The independence of the normalised response from the seismic intensity combined with increased reliability in mean response estimation, allows the development of generalised design equations following the procedure described in §4.3.3. Nevertheless, since the introduction of nonlinearity in viscous dampers was found in §4.4.2 to have a minor effect on the overall response of different isolation and energy dissipation systems with maximum divergence response rates mainly associated with low displacement amplitudes at short periods (Fig. 4.23, Fig. 4.24), the parameters influencing the $\bar{u}_0$, $\bar{\ddot{U}}_0$ response can be further reduced (§4.4.1) to ξ (= $\xi_{e,L}$ + $\xi_{d,NL}$), η, and T_p, (i.e. excluding a), resulting in the regression model and GDEs that were developed in §4.3.3, and thus limiting the complexity of design equations (by limiting the number of considered independent variables during regression analysis).

The effectiveness of the RM3 model in predicting the inelastic response in the case of systems with nonlinear viscous damping is demonstrated in Fig. 4.25 and Fig. 4.26, where response quantities predicted by GDEs (Table 4.5) are compared with analysis results derived for the a = 1 and a = 0.2 cases under two different seismic intensities associated with T_R = 475 and 2500yrs.

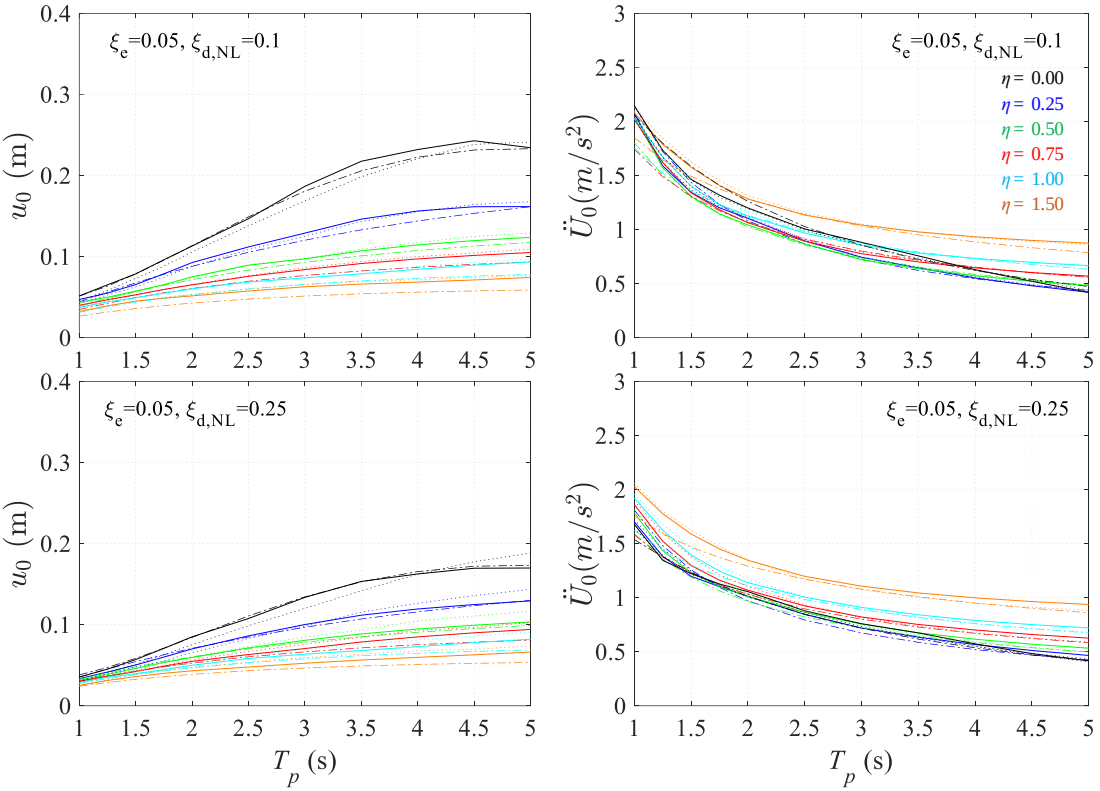

Fig. 4.25 NLRHA u_0 (left) and $\ddot{U}_0$ (right) under Art B considering energy-equivalent VDs of a=1 (solid), a=0.2 (dotted), compared to RM3 predicted response (dashed-dotted) for PGA=0.21g (T_R=475yrs, SF_{EQ}=1)

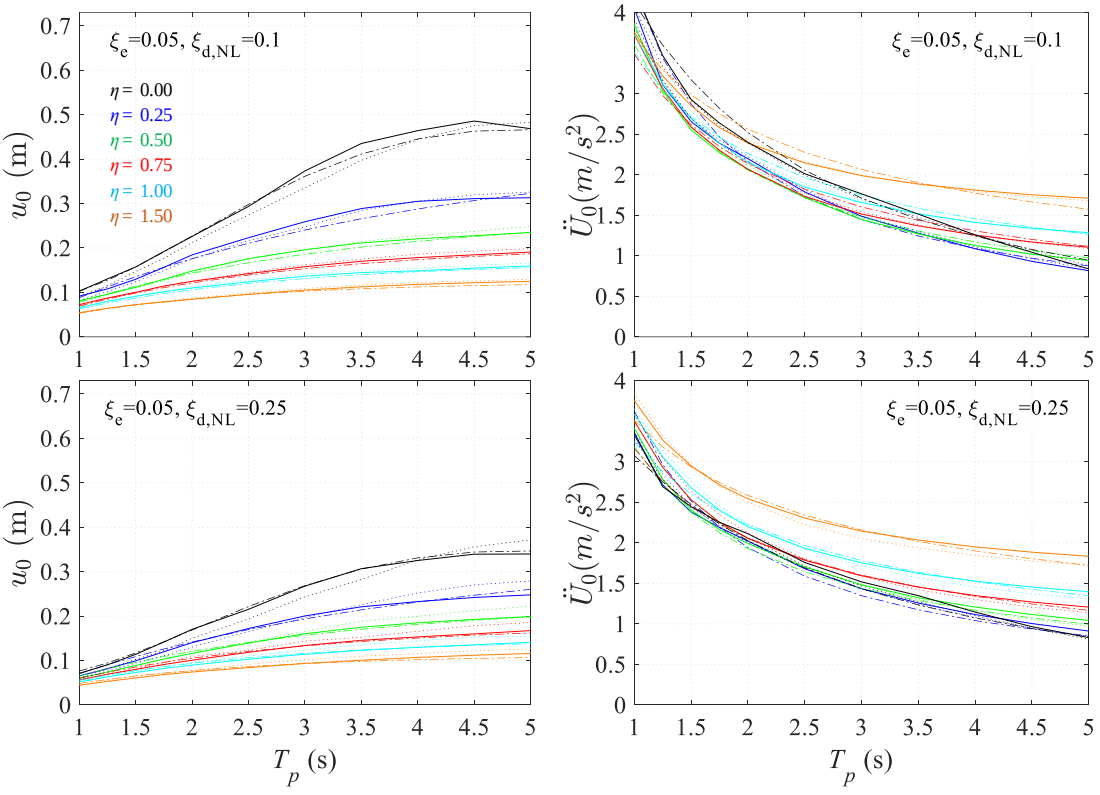

Fig. 4.26 NLRHA u_0 (left) and $\ddot{U}_0$ (right) under Art B considering energy-equivalent VDs of a=1 (solid), a=0.2 (dotted), compared to RM3 predicted response (dashed-dotted) for PGA=0.42g (T_R≈2500yrs, SF_{EQ}=2)

4.5 Isolated 2DOF System with Linear Viscous Damping

4.5.1 Dynamic equation of motion

The procedure described in §4.3.1 is further extended in the following to investigate the effect of bidirectional excitation on the peak response of isolated 2DOF systems with linear viscous damping. In this context, the dynamic equation of motion of the idealised system of Fig. 4.9 is re-written considering two dynamic degrees of freedom along *x*-*x* and *y*-*y* horizontal axes and identical mass (m) stiffness (k_p), strength (V_0) and damping ($c_{e,L}$, $c_{d,L}$) characteristics of the deck, hysteretic isolator and linear damper in both directions (symbols in bold represent quantities in vector form);

$$\left[\boldsymbol{f_I}(t)\right]+\left[\boldsymbol{f_D}(t)\right]+\left[\boldsymbol{f_S}(t)\right]=0 \tag{4.44}$$

$$\begin{bmatrix} f_{I,x}(t) \\ f_{I,y}(t) \end{bmatrix}+\begin{bmatrix} f_{D,x}(t) \\ f_{D,y}(t) \end{bmatrix}+\begin{bmatrix} f_{S,x}(t) \\ f_{S,y}(t) \end{bmatrix}=0 \tag{4.45}$$

Substituting in each horizontal direction the shear force of the bilinear isolator (Eq. (4.4)), the axial force of the LVD (Eq. (4.13)), and considering bidirectional interaction between the isolator yield forces with a circular yield surface (i.e. $|\boldsymbol{z}|\leq 1$) (Huang 2002), result in Eq. (4.46);

$$\ddot{\boldsymbol{u}}(t)+\left[\frac{\left(c_{e,L}+c_{d,L}\right)}{m}\dot{\boldsymbol{u}}(t)\right]+\left[\bar{v}_0 g\boldsymbol{z}\left(t,k_e,\boldsymbol{u},\dot{\boldsymbol{u}}\right)+\omega_p^2\boldsymbol{u}(t)\right]=-\ddot{\boldsymbol{u}}_{\boldsymbol{g}}(t) \tag{4.46}$$

Dividing Eq. (4.46) by u_r (Eq. (4.26)) and substituting $c_{e,L}$, $c_{d,L}$ by Eq. (4.24), reduce the equation of motion in the normalised form of Eqs. (4.47)-(4.49);

$$\begin{bmatrix} \bar{\ddot{u}}_x(t) \\ \bar{\ddot{u}}_y(t) \end{bmatrix}+2\omega_p\left(\xi_{e,L}+\xi_{d,L}\right)\begin{bmatrix} \bar{\dot{u}}_x(t) \\ \bar{\dot{u}}_y(t) \end{bmatrix}+\omega_p^2\left(\begin{bmatrix} z_x\left(t,k_e,\boldsymbol{u},\dot{\boldsymbol{u}}\right) \\ z_y\left(t,k_e,\boldsymbol{u},\dot{\boldsymbol{u}}\right) \end{bmatrix}+\begin{bmatrix} \bar{u}_x(t) \\ \bar{u}_y(t) \end{bmatrix}\right)=\ldots$$
$$\ldots=-\left(\omega_p^2/\eta\omega_D\right)\begin{bmatrix} \bar{\ddot{u}}_{gx}(t) \\ \bar{\ddot{u}}_{gy}(t) \end{bmatrix} \tag{4.47}$$

$$\bar{\ddot{\boldsymbol{u}}}(t)=\ddot{\boldsymbol{u}}(t)/u_r\,,\ \bar{\dot{\boldsymbol{u}}}(t)=\dot{\boldsymbol{u}}(t)/u_r\,,\ \bar{\boldsymbol{u}}(t)=\boldsymbol{u}(t)/u_r \tag{4.48}$$

$$\bar{\ddot{\boldsymbol{u}}}_{\boldsymbol{g}}(t)=\ddot{\boldsymbol{u}}_{\boldsymbol{g}}(t)/\dot{u}_{g0,2D} \tag{4.49}$$

The normalised strength η in Eq. (4.47), which describes the system strength relative to the *PGV*, is defined according to Eq. (4.50);

$$\eta = \frac{\bar{v}_0 g}{\omega_D \dot{u}_{g0,2D}} = \frac{\omega_p^2 u_r}{\omega_D \dot{u}_{g0,2D}} \tag{4.50}$$

Under bidirectional excitation, the peak ground velocity $\dot{u}_{g0,2D}$ characterising the seismic intensity of a pair of horizontal components is defined as the *PGV* of the SRSS spectrum of the pair of records scaled to the target spectrum under unidirectional excitation (i.e. the target spectrum of the single component, Fig. 4.1); $\dot{u}_{g0,2D}$ is approximated as follows;

$$\dot{u}_{g0,2D} = \frac{\sqrt{\dot{u}_{g0,x}{}^2 + \dot{u}_{g0,y}{}^2}}{\sqrt{2}} \tag{4.51}$$

The above definition is preferred over '*the PGV of the stronger component of ground motion*' adopted in Ryan & Chopra (2004a, b) for the sake of compatibility with the target spectra and the scaling approach adopted in §4.2, and hence, with relevant code-based requirements (e.g. EN1998-2, CEN 2005a). More specifically, Eq. (4.51) enables direct comparisons of relevant response quantities derived from analysis under unidirectional excitation (§4.3.1) associated with the target spectra of Fig. 4.1 and bidirectional excitation associated with the target spectra of Fig. 4.3, since in both cases a specific η value will correspond to (nearly) the same isolation system strength (i.e. $\bar{v}_0$).

The peak inelastic normalised ($\bar{u}_0$, $\ddot{\bar{U}}_0$) and non-normalised (u_0, $\ddot{U}_0$) response under bidirectional excitation is defined according to Eqs. (4.52), (4.53) as the peak values of response histories defined by adding the relevant response vectors in *x*-*x* and *y*-*y* axes. The angles at which relevant peak response quantities are developed, are identical in the cases of non-normalised and normalised response (i.e. independent of the normalisation procedure of §4.5.1) and are calculated from Eq. (4.54) (i.e. with respect to the *x*-*x* axis) where t_i and t_j represent the time instances at which $\bar{u}_{0,2D}$ and $\ddot{\bar{U}}_{0,2D}$ (or $\bar{u}_{0,2D}$ and $\ddot{\bar{U}}_{0,2D}$) are recorded;

$$\bar{u}_{0,2D} = \max_t \sqrt{\bar{u}_x(t)^2 + \bar{u}_y(t)^2}, \quad \ddot{\bar{U}}_{0,2D} = \max_t \sqrt{\ddot{\bar{U}}_x(t)^2 + \ddot{\bar{U}}_y(t)^2} \tag{4.52}$$

$$u_{0,2D} = \max_t \sqrt{u_x(t)^2 + u_y(t)^2}, \quad \ddot{U}_{0,2D} = \max_t \sqrt{\ddot{U}_x(t)^2 + \ddot{U}_y(t)^2} \tag{4.53}$$

$$\theta_{\bar{u}_0} = \tan^{-1}\left(\left|\frac{\bar{u}_y(t_i)}{\bar{u}_x(t_i)}\right|\right) = \theta_{u_0}, \ \theta_{\ddot{\bar{U}}_0} = \tan^{-1}\left(\left|\frac{\ddot{\bar{U}}_y(t_j)}{\ddot{\bar{U}}_x(t_j)}\right|\right) = \theta_{\ddot{U}_0} \quad \left(0 \le \theta \le 90^o\right) \tag{4.54}$$

The characterisation of the isolation system strength by η along with the consideration of a constant yield displacement (§4.2.3), reduce the governing parameters that influence the response to the natural period defined from the post-yield stiffness (i.e. the isolation period T_p), the

normalised strength η, and the damping ratio ξ (= $\xi_{e,L}$ + $\xi_{d,L}$) of the isolation system, as opposed to the parameters T_p, V_0, c (= $c_{e,L}$ + $c_{d,L}$), u_y, $\dot{u}_{g0}$ in the non-normalised case of Eq. (4.46). More specifically, Eq. (4.47) indicates that the normalised response is independent of the seismic intensity rendering the non-normalised quantities linearly proportional to u_r according to Eq. (4.48). The following numerical study (§4.5.2) investigates the efficiency of the above normalisation procedure in uncoupling $\bar{\boldsymbol{u}}(t)$, $\ddot{\bar{\boldsymbol{U}}}(t)$ from the seismic intensity, and thus developing GDEs, and presents some useful comparisons of peak inelastic response under uni- and bidirectional excitation.

4.5.2 Parametric analysis of 2DOF system

The numerical study of §4.3.2 is repeated in this section by calculating the normalised response of representative isolation and energy dissipation systems for a range of design parameters (i.e. $\xi_{e,L}$ = 0.05, ξ_d = 0~0.25, η = 0~1.5, T_p = 1~5s, u_y = 1cm) under Art D, and Nat(SRSS) (SF_{EC} = 1) suites of artificial and natural records (§4.2.2). Similarly to §4.3.2, $\bar{\boldsymbol{u}}(t)$, $\ddot{\bar{\boldsymbol{U}}}(t)$ response histories can be found either directly by solving Eq. (4.47) for the selected values of ξ, η, T_p, u_y, or indirectly by first solving Eq. (4.46) with corresponding values of $c_{e,L}$, $c_{d,NL}$, V_0, k_p, (i.e. Eqs. (4.24), (4.18), (4.31), (4.32), respectively, using $\dot{u}_{g0,2D}$) and then by calculating the normalised response from Eq. (4.48).

In Fig. 4.27, *SEGM* of normalised and non-normalised response estimates are plotted for different values of ξ, η, T_p. Upper values of *SEGM* in the case of the Art D suite are lower than 15% with a 90% confidence level in the case of $\bar{u}_0$ and lower than 10% in the case of $\ddot{\bar{U}}_0$ similarly to unidirectional excitation (§4.3.2), apart from η = 1.50 that exhibits peak values of *SEGM*($\bar{u}_0$) around 20% ($\delta \approx 0.3$); this is an indication that an increase in the number of artificial records may be required to attain the same degree of reliability with unidirectional excitation for increased η values. The seismic intensity has once more a negligible effect on the normalised peak response (Eq. (4.52)) as demonstrated in Fig. 4.28 for two different seismic intensities, indicating the effectiveness of the normalisation procedure proposed in §4.5.1. The combination of the above properties allows the development of generalised design equations in §4.5.3.

Relevant implications emerging from the use of natural records (§4.3.2) apply also in the case of bidirectional excitation using the Nat(SRSS) suite. Increased computational effort involving a larger number of records and analyses will be required to attain the same degree of reliability with the case of artificial records (e.g. increased *SEGM* values in Fig. 4.27 for Nat(SRSS)), and effectively control the shape and the *PGV* of the mean spectrum of the selected records to match the target spectra and design *PGV*. Fig. 4.29 and Fig. 4.30 reveal that adopting the Nat(SRSS) suite underestimates u_0 and $\ddot{U}_0$, in accordance with Fig. 4.14 and Fig. 4.15 for unidirectional excitation, due to the adoption of a design *PGV* that is smaller than the *GM* of records *PGV*s (i.e. 0.353m/s for T_R = 475yrs, SF_{EQ} = 1, derived from Table 4.3 and Eq. (4.51)), further distorting the spectral matching depicted in Fig. 4.5.

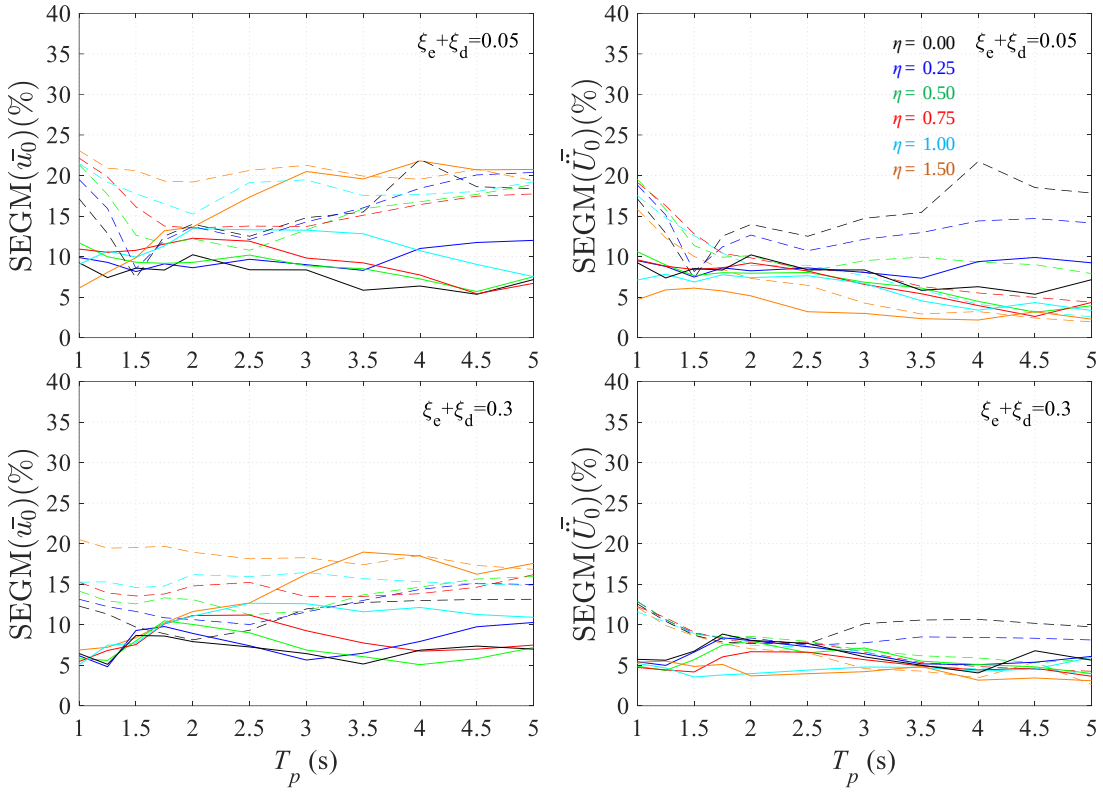

Fig. 4.27 NLRHA results under Art D (solid), Nat(SRSS) (SF_{EC}=1) (dashed) suites: *SEGM* of $\bar{u}_0$ (left) and $\ddot{\bar{U}}_0$ (right) for PGA=0.42g (T_R≈2500yrs, SF_{EQ}=2), ξ=5, 30%, and η=0~1.5

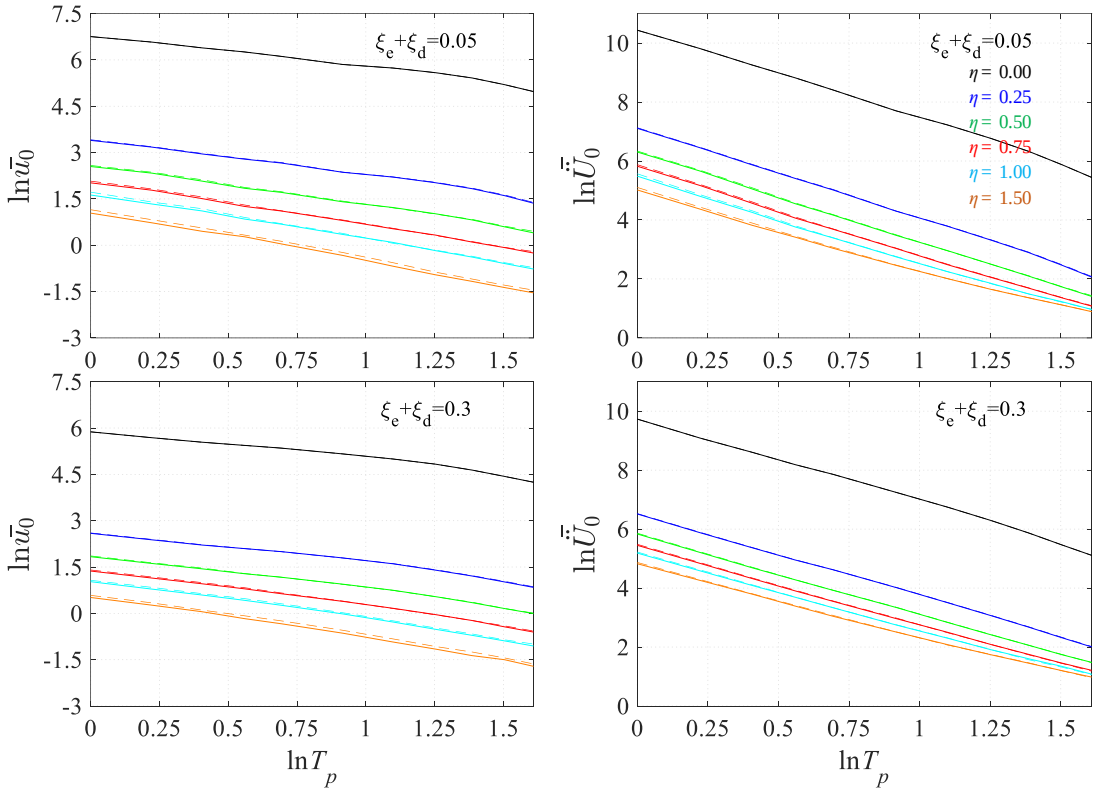

Fig. 4.28 NLRHA results under Art D suite: *GM* of ln$\bar{u}_0$ (left) and ln$\ddot{\bar{U}}_0$ (right) for PGA=0.21g (T_R=475yrs, SF_{EQ}=1) (dashed), PGA=0.42g (T_R≈2500yrs, SF_{EQ}=2) (solid), ξ=5, 30%, and η=0~1.5

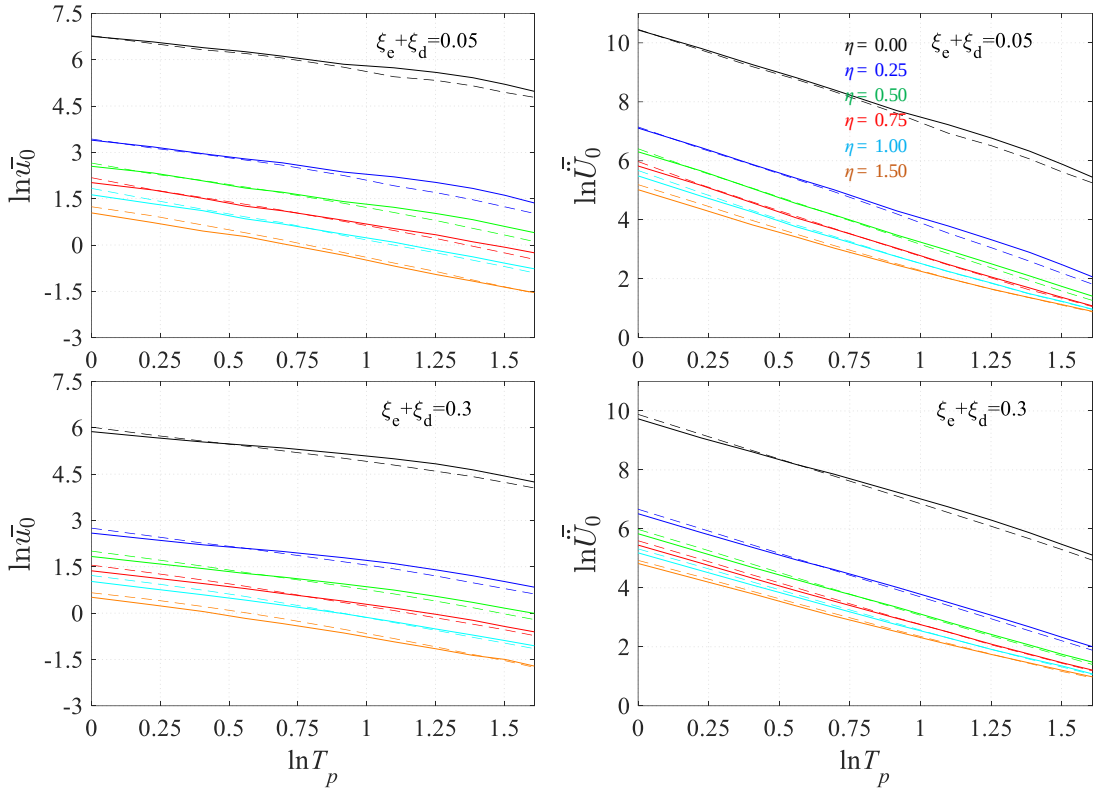

Fig. 4.29 NLRHA results under Art D (solid), Nat(SRSS) (SF_{EC}=1) (dashed) suites: *GM* of $\ln\bar{u}_0$ (left) and $\ln\ddot{\bar{U}}_0$ (right) for *PGA*=0.42*g* (T_R≈2500yrs, SF_{EQ}=2), ξ=5, 30%, and η=0~1.5

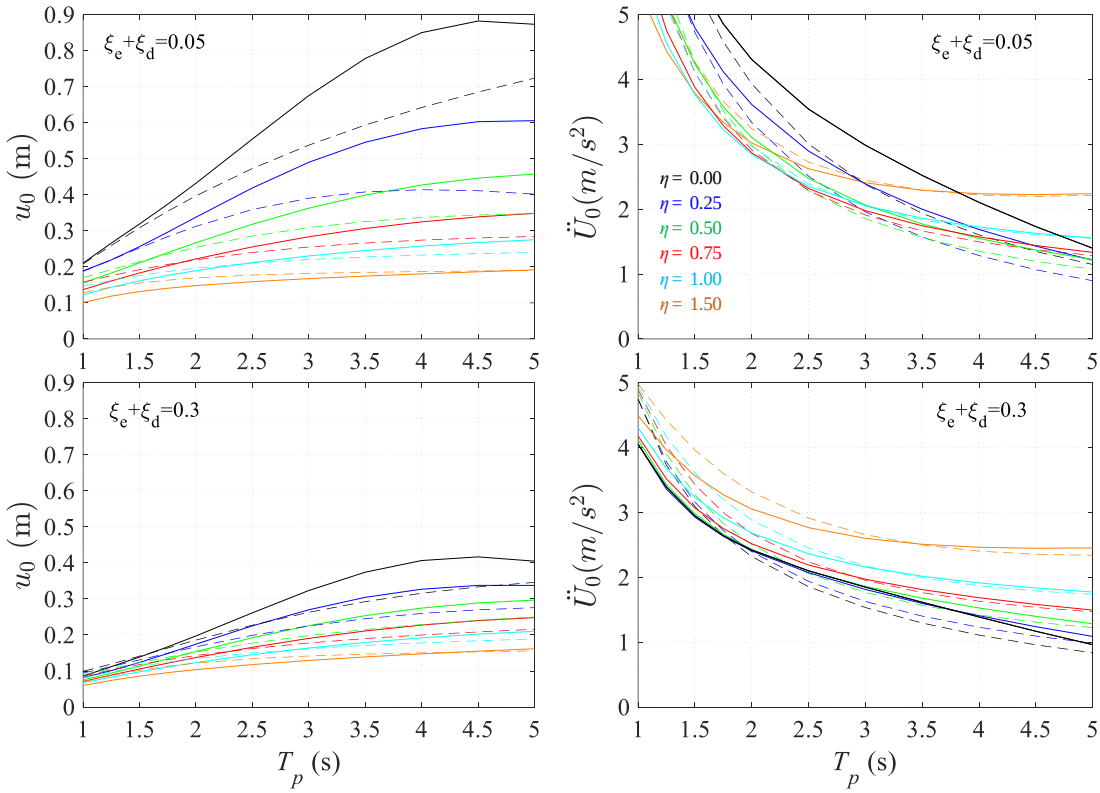

Fig. 4.30 NLRHA results under Art D (solid), Nat(SRSS) (SF_{EC}=1) (dashed) suites: *GM* of u_0 (left) and $\ddot{U}_0$ (right) for *PGA*=0.42*g* (T_R≈2500yrs, SF_{EQ}=2), ξ=5, 30%, and η=0~1.5

Fig. 4.31 presents a comparative evaluation of peak non-normalised response u_0 and $\ddot{U}_0$ resulting from NLRHA of the considered isolation and energy dissipation schemes under unidirectional and bidirectional excitation (§4.5.1) associated with T_R≈2500yrs. A significant increase in peak response estimates is observed in the case of bidirectional excitation wherein u_0 and $\ddot{U}_0$ incorporate the effect of the transverse component of seismic action according to the definitions of Eq. (4.53). More importantly, Fig. 4.31 displays the expected increase in relative displacements and total accelerations when the target spectrum under bidirectional excitation is defined according to EN1998-2 (CEN 2005a) requirements as √2 times the target spectrum of the single component (§4.2.2), noting that the adopted intensity ratio of the horizontal component spectra (i.e. 0.75, with SF_{H1} = 1.13SF_{EQ} and SF_{H2} = 085SF_{EQ}) was found to have a rather insignificant effect on the peak resultant response derived from Eq. (4.53) (compared to the case of SF_{H1} = SF_{H2} = SF_{EQ}, i.e. intensity ratio of components equal to unity, not shown herein); in fact, the 0.75 ratio was selected to evaluate in a more realistic context (López *et al*. 2006) the angle of peak response quantities. Furthermore, design codes (e.g. CEN 2005a, AASHTO 2010) usually constraint response spectrum and nonlinear dynamic analysis results by relevant response quantities calculated from the *fundamental mode method* (CEN 2005a), however, without providing specific guidelines on the proper consideration of the transverse component of seismic action in the latter method. Hence, the expected increase in u_0 and $\ddot{U}_0$ can serve as a means to

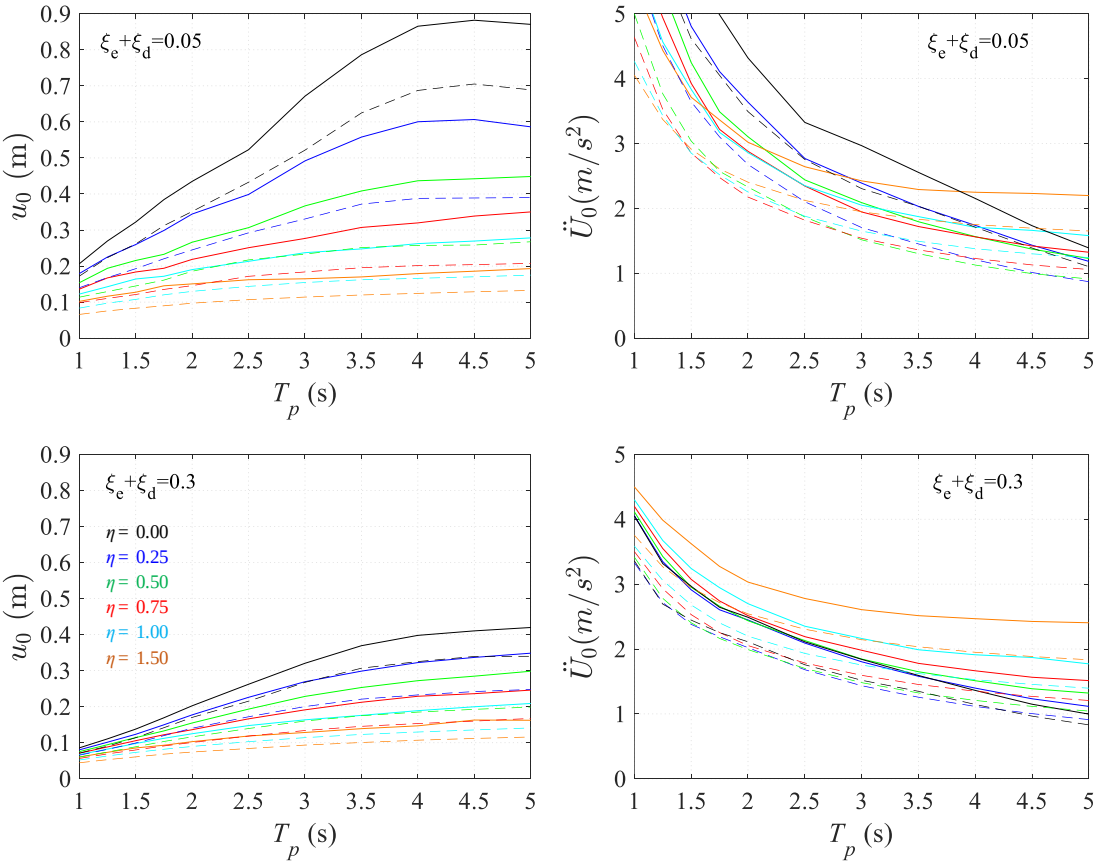

Fig. 4.31 NLRHA results under Art B (dashed), Art D (solid) suites: *GM* of u_0 (left) and $\ddot{U}_0$ (right) for *PGA*=0.42*g* (T_R≈2500yrs, SF_{EQ}=2), ξ=5, 30%, and η=0~1.5

evaluate the consistency of results among different analysis types (e.g. by appropriately scaling the response calculated from the *fundamental mode method*), and in this context, is quantified with the aid of regression analysis in §4.5.3.

Returning to the issue of the angle of peak responses, Fig. 4.32 reports θ_{u0} and $\theta_{\ddot{U}0}$ values derived from parametric analysis results using the Art D suite (strong component assigned to *y-y* axis) and Eq. (4.54); solid lines represent geometric means of observed values from analyses under the considered suite (i.e. 10 pair of records), while solid dots represent recorded values per individual analysis (i.e. observations). Interestingly, as ξ increases, mean angles stabilise close to the value associated with the seismic intensity ratio of horizontal components adopted in analysis (i.e. $\tan^{-1}(1 / 0.75) = 53^{o}$) representing approximately the incidence angle of the resultant of components. However, the reliability of the adopted measure of central tendency (i.e. *GM*) is significantly reduced with peak *SEGM*(u_0, $\ddot{U}_0$) values exceeding 100% due to the increased scattering of observations presented in Fig. 4.32. In fact, clear response patters cannot be identified and θ_{u0} and $\theta_{\ddot{U}0}$ may take any value within 0-90°; this justifies and encourages the common practice of designing isolators to sustain the maximum relative displacement in any random direction (but unfortunately not always required by codes, e.g. CEN 2005a) and indicates the need for applying

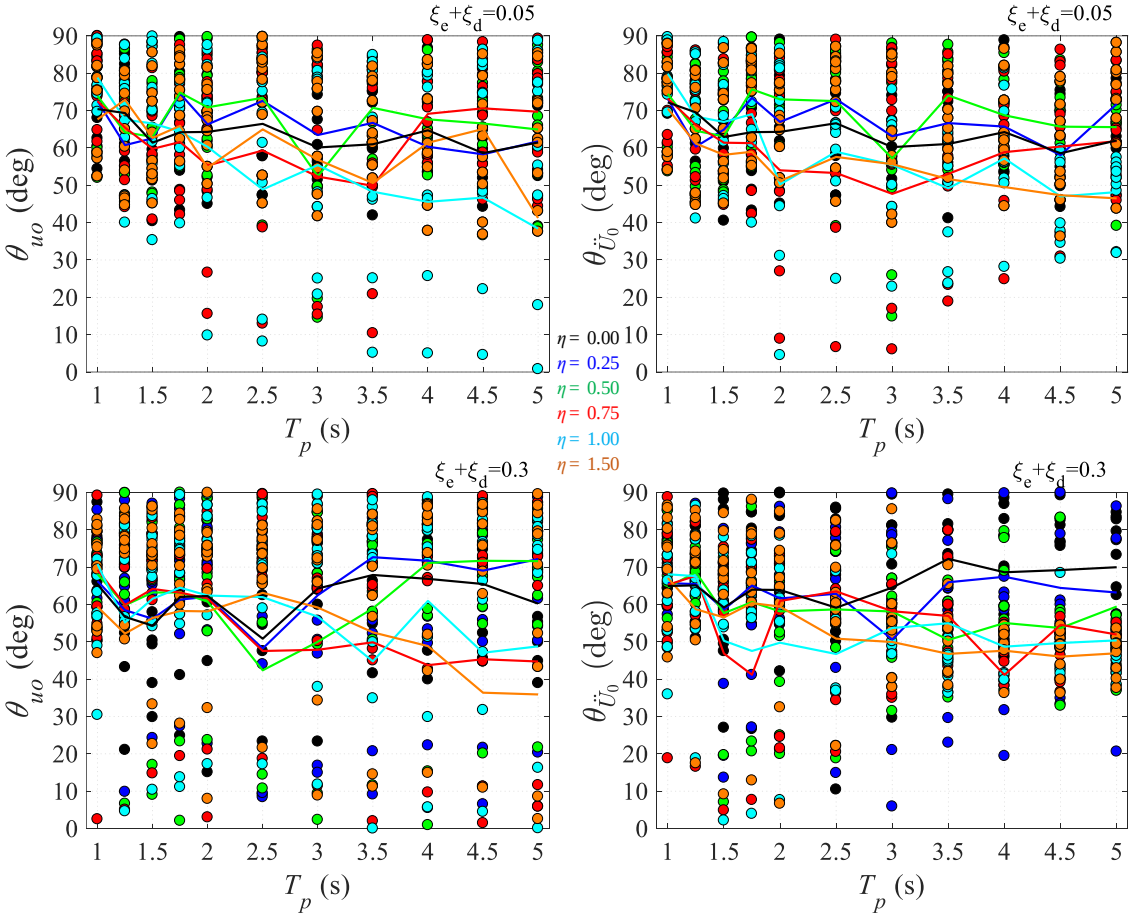

Fig. 4.32 NLRHA results under Art D suite (HI assigned to *y-y* axis): Angles θ with respect to *x-x* axis (discrete dots), *GM* of θ per η (solid) for u_0 (left) and $\ddot{U}_0$ (right), PGA=0.42g (T_R≈2500yrs, SF_{EQ}=2), ξ=5, 30%, and η=0~1.5

the selected records at different angles of incidence when designing the substructure of isolated bridges, unless a more conservative approach is adopted. Results from analysis using the suite of natural records (not presented herein) support the previous statements.

4.5.3 Derivation of generalised design equations

Following the procedure described in §4.3.3, regression models and associated GDEs (Eqs. (4.33), (4.34)) were first developed for the case of bidirectional excitation, and subsequently assessed in terms of accuracy in peak response prediction and effectiveness in 'near-optimal' system identification (§4.3.3). Table 4.6 and Fig. 4.33-Fig. 4.35 include representative results of different *m*-degree regression models (RM) with *q* terms ($m \times q$) presented for two different seismic intensities associated with T_R = 475yrs and T_R = 2500yrs (Fig. 4.19) as in Table 4.4 and Fig. 4.18-Fig. 4.20 for unidirectional excitation.

Table 4.6 Evaluation of different linear regression models for 2D excitation based on 'goodness-of-fit'

	Model				u_0		Model			$\ddot{U}_0$	
η =0	T_R (yrs)	$m \times q$	R^2	*RMSE*	r_{max} (%)	r_{GM} (%)	$m \times q$	R^2	*RMSE*	r_{max} (%)	r_{GM} (%)
RM1	475	4 × 15			6.09	0.90	4 × 15			6.52	0.93
	2500		0.999	0.018	6.09	0.90		1.000	0.019	6.53	0.93
RM2,3	**475**	**3 × 5**			**12.46**	**1.74**	**3 × 5**			**13.34**	**1.97**
	2500		**0.996**	**0.037**	**12.46**	**1.74**		**0.999**	**0.051**	**13.34**	**2.05**
RM4	475	1 × 3			25.35	4.25				25.40	4.19
	2500		0.981	0.082	25.35	4.25		0.997	0.080	25.40	4.20
RM5	475	3 × 5			11.49	2.16	2 × 5			11.43	3.13
	2500		0.996	0.037	11.49	2.16		0.999	0.051	11.43	3.13
$\eta \neq 0$	T_R (yrs)	$m \times q$	R^2	*RMSE*	r_{max} (%)	r_{GM} (%)	$m \times q$	R^2	*RMSE*	r_{max} (%)	r_{GM} (%)
RM1	475	4 × 35			11.31	2.43	4 × 35			8.98	1.23
	2500		1.000	0.015	5.66	0.72		1.000	0.012	4.54	0.57
RM2	475	3 × 11			12.27	3.18	3 × 11			10.73	2.03
	2500		0.999	0.029	10.57	1.54		1.000	0.028	10.28	1.45
RM3	**475**	**2 × 8**			**21.89**	**4.19**	**2 × 8**			**21.93**	**3.09**
	2500		**0.998**	**0.051**	**24.80**	**2.70**		**0.999**	**0.055**	**21.54**	**3.10**
RM4	475	2 × 7			23.20	5.05	2 × 7			21.11	3.40
	2500		0.997	0.064	22.76	3.26		0.998	0.070	20.27	3.38
RM5	475	2 × 8			25.73	5.77	2 × 8			22.12	3.12
	2500		0.995	0.078	27.32	4.14		0.998	0.061	21.72	3.10

The RM3 regression model was adopted herein since it exhibits similar behaviour to the case of unidirectional excitation, i.e. predicting accurate peak response quantities and adequately identifying the location of 'near-optimal' systems for practical applications. GDEs (i.e. Eq. (4.34)) in this case take the general form of Eqs. (4.37) and (4.38). In the case of elastomer-based isolators and the target spectra of §4.2.2, Eq. (4.37) is simplified according to the data of Table 4.7. The seismic intensity is expressed in terms of *PGA* at bedrock (i.e. $\ddot{u}_{g0}$ in m/s^2) of the target spectrum under unidirectional excitation (according to Eq. (4.51)).

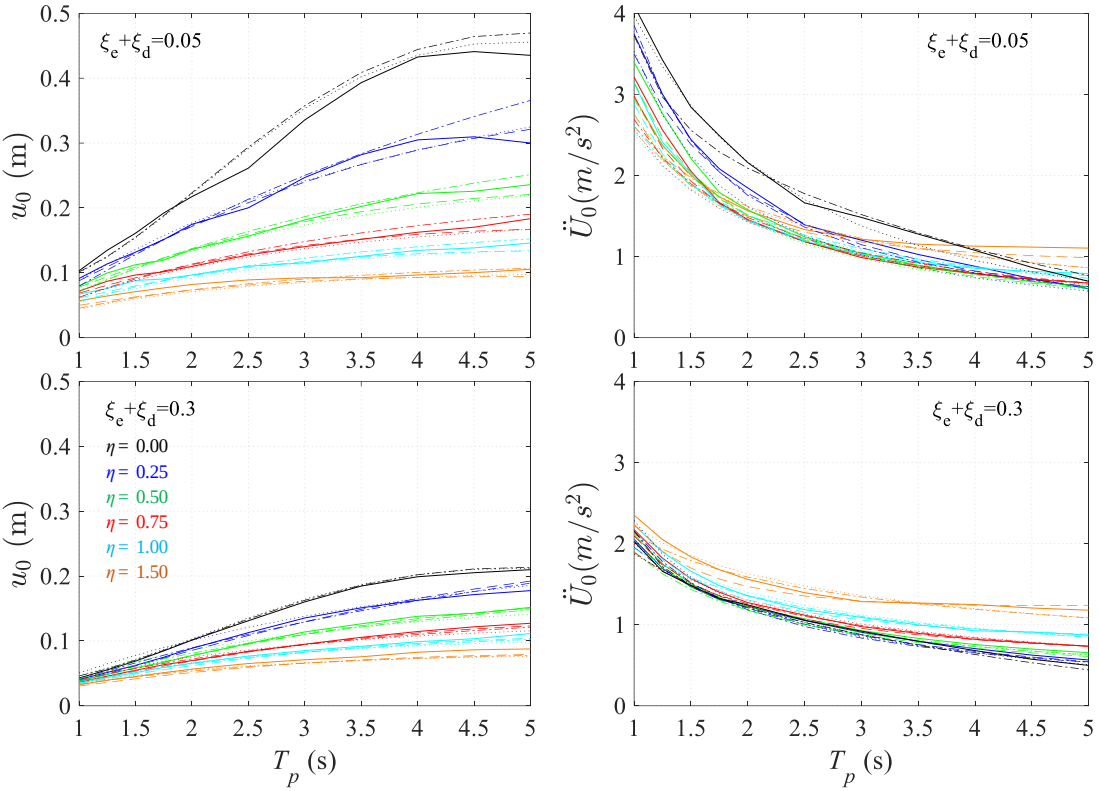

Fig. 4.33 NLRHA response u_0 (left) and $\ddot{U}_0$ (right) under Art D (solid) suite compared to response predicted from RM3 (dashed-dotted), and RM5 (dotted) for PGA=0.21g (T_R=475yrs, SF_{EQ}=1), ζ=5, 30%

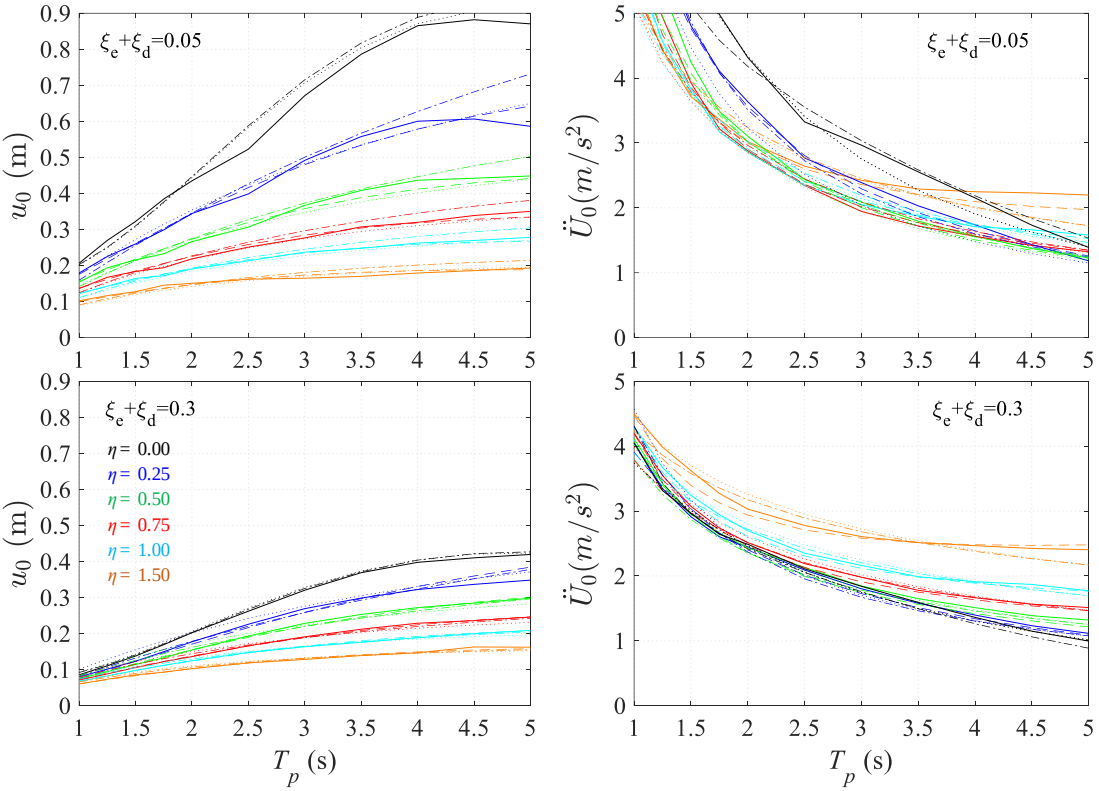

Fig. 4.34 NLRHA response u_0 (left) and $\ddot{U}_0$ (right) under Art D (solid) suite compared to response predicted from RM3 (dashed-dotted), and RM5 (dotted) for PGA=0.42g (T_R≈2500yrs, SF_{EQ}=2), ζ=5, 30%

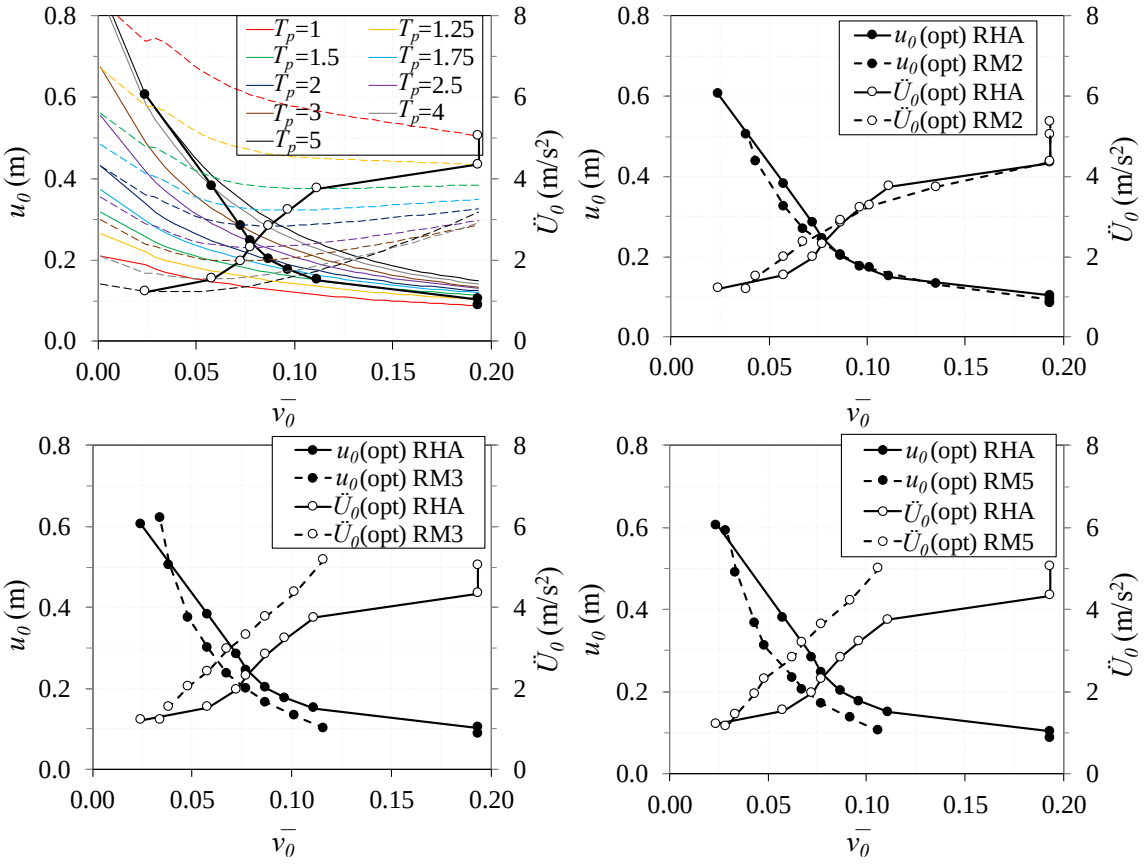

Fig. 4.35 NLRHA response u_0 (solid), $\ddot{U}_0$ (dashed), optimal peak total accelerations $\ddot{U}$opt (solid) and corresponding relative displacements $u$opt (solid) under Art D suite, compared to $u$opt, $\ddot{U}$opt (solid) derived from RM2, RM3, RM5 (dashed) for PGA=0.42g (T_R≈2500yrs, SF_{EQ}=2), ξ=5%, 2D excitation

Table 4.7 RM3 regression coefficients: EN1998-1, site conditions 'C' (CEN 2004b), 2D excitation

Case	*y*	*Int*	*β*	*γ*	*δ*	*ε*	*ζ*	*κ*	*λ*	*μ*	*ν*
η =0	u_0	5.418	-0.440	-	-	-	-	-	-1.206	0.803	-0.438
	$\ddot{U}_0$	9.425	-0.305	-	-	-	-	-	-3.165	0.756	-0.399
η =0.25-1.5	u_0	0.865	-0.222	0.106	-	-1.126	-0.131	-0.230	-1.074	-0.185	-
	$\ddot{U}_0$	4.890	-0.163	0.116	0.152	-0.715	0.157	0.249	-2.335	-	-

Table 4.8 RM5 regression coefficients: EN1998-1, site conditions 'C' (CEN 2004b), 2D excitation

Case	*y*	*Int*	*β*	*γ*	*δ*	*ε*	*ζ*	*κ*	*λ*	*μ*	*ν*
η =0	u_0	5.445	-0.428	-	-	-	-	-	-1.194	0.797	-0.443
	$\ddot{U}_0$	9.148	-0.419	-	0.150	-	-	-	-2.266	-0.226	-
η =0.25-1.5	u_0	0.978	-0.178	0.097	-	-1.192	-0.095	-0.175	-1.100	-0.209	-
	$\ddot{U}_0$	5.001	-0.114	0.094	0.128	-0.754	0.153	0.255	-2.393	-	-

Representing an alternative to RM3, RM5 model (Table 4.8) was developed by constraining the regression coefficients (except for the Intercept (*Int*) term) to the values obtained from RM3 under unidirectional excitation since the relevant coefficient values were found reasonably close (i.e. Table 4.7 vs. Table 4.5). This approach allows further simplification of the adopted models since

the peak response under bidirectional excitation can be calculated from GDEs of unidirectional excitation by simply scaling relevant response quantities according to Eqs. (4.55)-(4.58).

$$u_{0,2D} = \frac{e^{\text{Int,2D}}}{e^{\text{Int,1D}}} u_{0,1D} = 1.22 u_{0,1D} \quad (\eta = 0) \tag{4.55}$$

$$\ddot{U}_{0,2D} = \frac{e^{\text{Int,2D}}}{e^{\text{Int,1D}}} \ddot{U}_{0,1D} = 1.22 \ddot{U}_{0,1D} \quad (\eta = 0) \tag{4.56}$$

$$u_{0,2D} = \frac{e^{\text{Int,2D}}}{e^{\text{Int,1D}}} u_{0,1D} = 1.43 u_{0,1D} \quad (\eta \geq 0.25) \tag{4.57}$$

$$\ddot{U}_{0,2D} = \frac{e^{\text{Int,2D}}}{e^{\text{Int,1D}}} \ddot{U}_{0,1D} = 1.26 \ddot{U}_{0,1D} \quad (\eta \geq 0.25) \tag{4.58}$$

Eqs. (4.55)-(4.58) reflect in addition the 'mean increase' in relative displacements and total accelerations due to the introduction of the transverse component of seismic action when target spectra are defined according to EN1998-2 (CEN 2005a), thus, offering an effective means to evaluate results deriving from different types of analysis according to §4.5.2. It is also noted that the calculated magnification factors are in line with the upper limit of values proposed by Fardis *et al*. (2012) (i.e. 1.15~1.25), without however presenting background analysis in support of these suggestions.

Although the case of the 2DOF system with nonlinear viscous damping under bidirectional excitation was not explicitly checked, the minor effect of the nonlinearity of viscous damper in u_0, $\ddot{U}_0$ response under unidirectional excitation (§4.4) implies that GDEs presented in this section can provide reasonable estimates of peak response in the case of systems involving NLVDs too.

4.6 Closing Remarks

A methodology for the direct estimation of peak inelastic response in bilinear isolation systems was extended in this chapter with a view to developing generalised design equations capable of providing reliable estimates of peak inelastic response under different performance levels (PLs) associated with code-based target spectra of common frequency content but different intensity, while properly capturing the effect of linear/nonlinear viscous damping, and hence addressing a wide range of isolation and energy dissipation configurations. The procedure starts with the normalisation of the dynamic equation of motion of SDOF and 2DOF systems representing idealised isolated bridge decks under uni- and bidirectional excitation, respectively, aiming at uncoupling the normalised response from the seismic intensity and limiting the dispersion of peak normalised relative displacements $\bar{u}_0$ and total accelerations $\bar{\ddot{U}}_0$. Subsequently, it progresses to the

development of generalised design equations by statistically processing (with the aid of regression analysis) response quantities derived from parametrically solving the normalised equation of motion. The following conclusions were drawn from extensive parametric nonlinear dynamic analysis of the idealised RDOFs associated with three different cases, namely, (*i*) isolated SDOFs with linear viscous damping, (*ii*) isolated SDOFs with nonlinear viscous damping, and (*iii*) isolated 2DOFs with linear viscous damping:

- Two conditions were identified and introduced in order to uncouple the normalised response from the seismic intensity; the first involved the characterisation of the isolation system strength by η (i.e. strength at zero displacement V_0 normalised to the seismic intensity as expressed by the peak ground velocity (PGV) $\dot{u}_{g0}$); the second was associated with the characterisation of nonlinear viscous dampers by the 'energy-equivalence' approach (i.e. dampers of the same damping ratio ξ but different a). The above conditions along with the assumption of a constant value for the yield displacement u_y reduce the governing parameters that significantly affect the response to the isolation period T_p, the normalised strength η, and the damping ratio of energy-equivalent dampers ξ, as opposed to the parameters of isolation period T_p, strength V_0, linear/nonlinear damping coefficients $c_{e,L}$, $c_{d,NL}$, nonlinear parameter a, yield displacement u_y, and seismic intensity $\dot{u}_{g0}$ in the non-normalised case.

- The suggested normalisation procedure was found effective since the seismic intensity had a negligible effect on the mean normalised peak response (i.e. $\bar{u}_0$ and $\bar{\ddot{U}}_0$) of linear/bilinear isolation systems with or without supplemental linear/nonlinear viscous damping (i.e. in all three cases considered), and the standard error of the mean (*SEGM*) statistical measure characterising the degree of reliability in mean response estimation was constrained in low levels.

- Integration of 'design principles' in the suggested procedure, by means of using code-compatible scaling procedures and target spectra, require the selection and/or generation of records with mean characteristics (i.e. mean spectrum, mean *PGV*) that closely match the target properties (i.e. shape of target spectrum and design *PGV*). The above requirements have certain implications associated with increased computational effort when natural records are used. On the other hand, artificial (or synthetic) accelerograms may easily satisfy the above requirements (using a relatively small number of records) and provide robust estimates of mean response when member strength degradation is not considered (which is a reasonable assumption in *seismic design* of bridges).

- The combination of increased reliability in mean response estimation and the insensitivity of the normalised response to the seismic intensity allows the development of generalised design equations for the direct estimation of non-normalised relative displacements u_0 and total accelerations $\ddot{U}_0$ since the maximum force of the isolation and energy dissipation system ($m\ddot{U}_0$) cannot be directly associated with u_0 due to the introduction of viscous dampers (VDs).

Developed regression models were assessed both in terms of accuracy in peak response prediction and effectiveness in 'near-optimal' system identification.

- In the case of bidirectional excitation, the large dispersion in the angles at which peak response occurs, justifies and encourages the common practice of designing isolators to sustain the maximum relative displacement in any random direction; it also indicates the need for applying the selected records at different angles of incidence when designing the substructure.
- Development of regression models by constraining the regression coefficients of relevant models under unidirectional excitation revealed expected mean increases of 22% in u_0 and $\ddot{U}_0$ response of linear systems ($\eta = 0$), and 43% in u_0 and 26% in $\ddot{U}_0$ in the case of nonlinear systems ($\eta \neq 0$). Such magnification factors offer an effective means to evaluate results derived from different types of analysis according to code requirements.
- Results presented in this chapter address a target spectrum with a frequency content corresponding to site conditions 'C' of EN1998-1 (CEN 2004b) and focus on elastomer-based isolators. Nevertheless, the procedure was fully automated within the MATLAB (Mathworks 2016) code IDEC (*Isolation Design Equations Code*) to facilitate the development of GDEs in other cases.
- The suggested procedure represents an alternative to equivalent linearisation approaches commonly adopted by codes, and as such, it can be implemented either on a 'stand-alone' basis, or for preliminary design purposes in more refined design procedures. Herein, the methodology presented in this chapter is incorporated in Def-BD methodology of seismically isolated bridges for the preliminary design of the isolation-energy dissipation system and the substructure in Chapter 5.

Chapter 5
Deformation-Based Design of Seismically Isolated Bridges

5.1 Introduction

The *deformation-based design* (Def-BD) method, proposed in Chapter 3 for seismic design of bridges relying on hysteretic energy dissipation through ductile behaviour of the piers, is extended in this chapter to address seismically isolated bridges with (or without) supplemental energy dissipation devices, focusing on systems wherein a continuous 'isolation interface', formed between the superstructure and all the substructure elements, allows movement of the deck in both principal directions of the bridge. Accounting for multiple performance levels (PLs) and different performance objectives (POs), the proposed method initially identifies the critical hazard level and 'near-optimal' alternatives of the isolation system in terms of both economy and performance, based on the inelastic response of a reduced-degree-of-freedom (RDOF) system (Chapter 4). By incorporating nonlinear response history analysis (NLRHA) of the multi-degree-of-freedom (MDOF) system in a number of successive design steps that correspond to different performance levels, it subsequently leads (essentially in a non-iterative way) to a refinement of the initial design solution through the control of a broad range of material strains and deformations.

Sharing the same principal concepts and analysis tools (notably nonlinear dynamic analysis) with the procedure for bridges with energy dissipation in the piers (§3.2), by means of providing a logical design route wherein specific members design and type of verifications are associated with certain performance levels depending on the selected performance objective, the version of the methodology incorporating seismic isolation and energy dissipation systems entails some key modifications summarised as follows:

- Enhancement of performance objectives (i.e. expected structural performance under different seismic hazard levels) to properly reflect the higher performance expected in the case of seismically isolated bridges (when bridges of the same PO are compared) along with specific conditions ensuring the effectiveness of the isolation system under the considered PLs (e.g. the proper consideration of the intended plastic mechanism of the substructure under the relevant PLs).

- Use of generalised design equations (i.e. methodology developed in Chapter 4) for preliminary design purposes with a view to providing the required tools for a direct comparative evaluation, at the early stages of design, of the various alternative isolation schemes that may be realised by properly combining isolation and supplementary energy dissipation devices providing linear and/or nonlinear viscous damping, while avoiding computationally intensive iterative analysis.

- Proper consideration of the adverse effect of the orthogonal component of seismic action under bidirectional excitation.
- Incorporation of ‘design principles’ and approaches to account for the peculiarities of seismically isolated bridges that arise from the use of passive control devices, i.e. realisation and design of the selected scheme through base isolation and energy dissipation devices (interchangeably referred as ‘passive’ in the following), and the treatment of the variability of their design properties (DPs).

The above modifications along with the basic principles of Def-BD, aim to deliver a rigorous design method that constraints the increased computational effort characterising complex design frameworks (§1.1) while treating ‘well-documented’ deficiencies of traditional equivalent linearisation techniques, such as the requirement for iterative structural analysis, the inaccurate estimation of inelastic response due to the introduction of the ill-defined (i.e. non-physical) ‘effective’ isolation period (Makris & Kampas 2013b) and the ‘equivalent’ damping ratio (Franchin *et al*. 2001, Miranda & Ruiz-Garcia 2002), the approximate estimation of relative velocities required for the calculation of peak damper forces (Chopra 2012), and the inconsistent treatment of systems with non-classical (or non-proportional) damping matrices (Franchin *et al*. 2001, Chopra 2012).

Detailed steps of the proposed Def-BD methodology and required modifications with regard to §3.2, are first put forward in §5.2. Following a description of the adopted analysis and design framework (§5.3.1-5.3.4), the efficiency of the method under unidirectional excitation is subsequently explored in §5.3.5.1 by applying it to an actual concrete bridge previously used for the evaluation of Def-BD in the case of bridges with energy dissipation in the piers (referred also as ‘ductile-pier’ bridges in the following for the sake of brevity) (§3.3.1). The suggested procedure and the resulting designs for three different isolation schemes are evaluated in the light of NLRHA using a number of spectrum-compatible motions, offering a useful insight into some additional pitfalls of modern code-based approaches (§5.3.5.2); a comparison among the different designs, with emphasis on both economy and structural performance, is also presented. Following the same design and assessment format, the effect of bidirectional excitation in the design procedure is investigated in §5.3.6.

5.2 Methodology

5.2.1 Performance-based design framework

The suggested procedure consists of five distinct steps (Fig. 5.1a) including a preliminary design and subsequent verifications involving nonlinear response-history analysis (NLRHA) at a number of performance levels depending on the performance objective sought in terms of bridge importance as in §3.2.1. Herein, three different importance classes are defined, in contrast to the

five classes considered in the case of bridges designed for ductile behaviour of the piers (for reasons explained in the following), namely, *Non-essential* (bridges of minor importance), *Ordinary* (average importance), and *Essential* (high importance). Similarly to 'ductile-pier' bridges, the performance objective is described with reference to the member (abutment, pier, deck, isolator, etc.) structural performance level (SP) and the associated seismic action (EQ), whereas four different SPs and EQs are introduced to formulate the 'performance matrix' depicted in Fig. 5.2. SPs are qualitatively described in terms of post-earthquake operationality, damage, and feasibility of repair; representative structural performance criteria associated with each SP defining member (upper) performance states within a '*design*' framework, are provided in Table 5.1 and presented in detail in §5.2.2-5.2.6. EQs correspond to a 'frequent' (EQI), an 'occasional' (EQII), a 'rare' (EQIII) and a 'very rare' (EQIV) seismic event, while the considered range of return periods T_R coupled with each SP is in line with the widely varying requirements prescribed in different codes according to §3.2.1.

The 'performance matrix' in Fig. 5.2, combined with the structural performance criteria in Table 5.1, assigns higher POs to isolated bridges compared to the corresponding importance classes of 'ductile-pier' bridges (also included in the figure for the sake of comparison). This is in line with code specifications (e.g. CEN 2005a, AASHTO 2010) regarding the necessity of limiting the inelastic response of the substructure, aiming at the proper performance of the isolation system, since it has been demonstrated (Constantinou & Quarshie 1998, Vassiliou *et al*. 2013, Tsiavos *et al*. 2017) that when inelastic action develops, the effectiveness of the isolation system may be reduced, resulting in larger deformation demands in the isolated structure. In the light of the previous consideration, controlled inelastic response of the piers (e.g. associated with spalling of concrete cover) is allowed under the highest SP considered in ordinary bridges (i.e. SP3). In this context, the SP3 criterion in 'ductile-pier' bridges (Table 3.1), associated with the feasibility of repair in the piers, is omitted in seismically isolated bridges (Table 5.1) since the essential requirements in the latter case (i.e. seismic isolation) are the proper performance of the isolation system under EQ(SP3) (dictating a more stringent criterion compared to 'hoop yielding' in Table 3.1), and 'collapse-prevention' under EQ(SP4) (identical criteria in both 'ductile-pier' and isolated bridge piers). On the other hand, the SP3 requirements of seismic isolators (Table 5.1) are relaxed compared to common (non-seismic) bearings allowing for the development of their ultimate deformability under EQ(SP3) (i.e. EQIV for ordinary and essential bridges). This strategy emerges from the activation of seismic links and the abutment-backfill system under EQ(SP4) (explicitly checked only in non-essential bridges according to §5.2.6), indicating that inertia forces of the deck are transferred directly to substructure elements without the engagement of moveable bearings and dampers (i.e. a state described as 'locked' in Table 5.1). The 'critical' PO, associated with bridges of major importance in the case of energy dissipation in the piers, is not defined in isolated bridges. The reason behind this, is that such a design approach would result in a practically inactive isolation system (i.e. base shear V lower than, or close to, the shear resistance of the isolation system at zero displacement V_0) under the highest (and only considered) hazard level, i.e. EQIV.

Considering for example an ordinary seismically isolated bridge, then the target performance of a single pier and the isolators located on its top (Fig. 5.3) is associated with the 'operationality' performance state of isolators corresponding to undisrupted service of the bridge under EQII (T_R = 50~100yrs), with quasi-elastic response of piers and limited damage in the isolators without

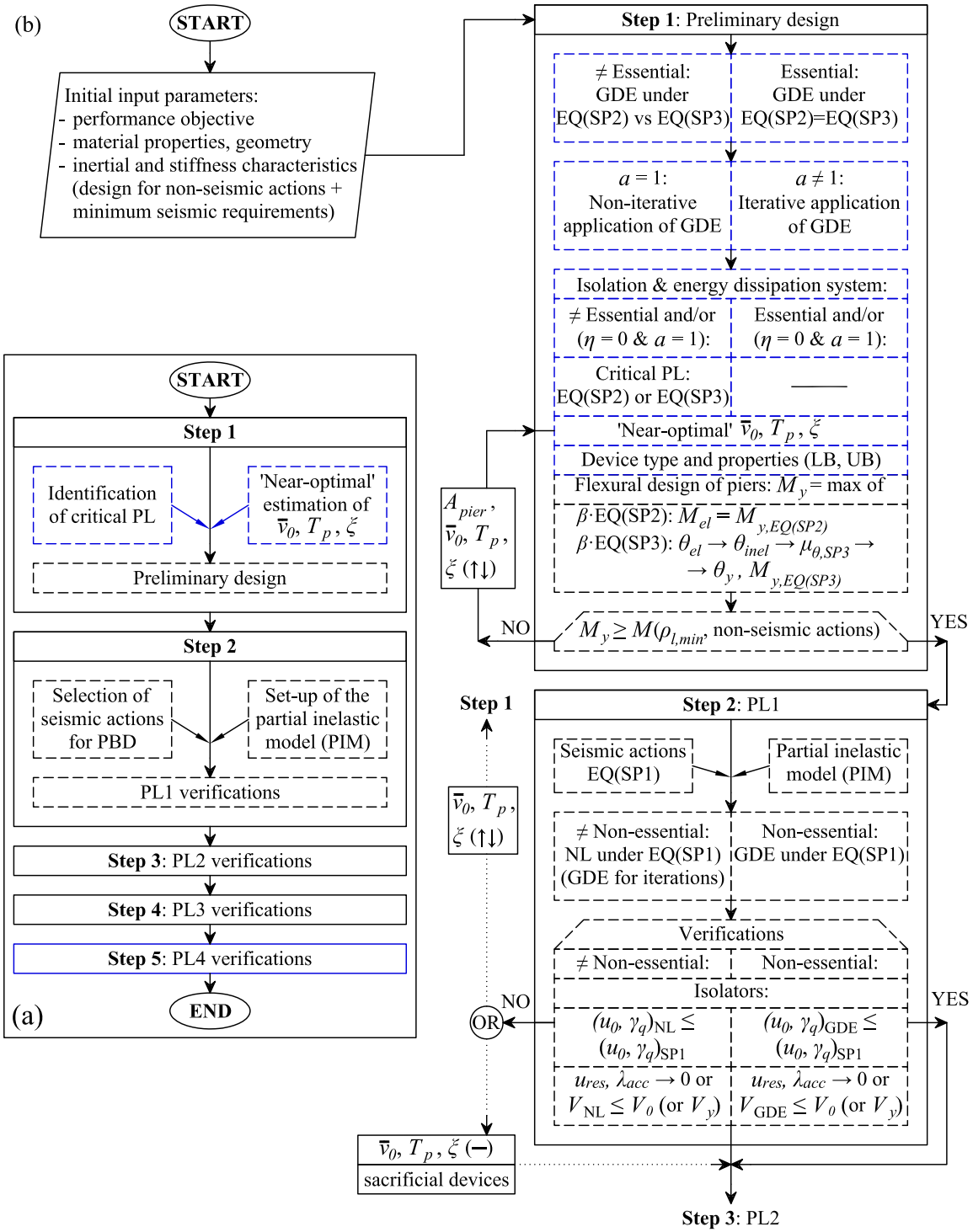

Fig. 5.1 Def-BD methodology for seismically isolated bridges: (a) General overview, (b) detailed steps (in blue: additional required steps compared to 'ductile-pier' bridges)

significant disruption of service under EQIII (T_R = 500~1000yrs), and with 'ultimate' response of isolators, limited inelastic response of piers, and limited service of the bridge under EQIV ($T_R \approx$ 2500yrs).

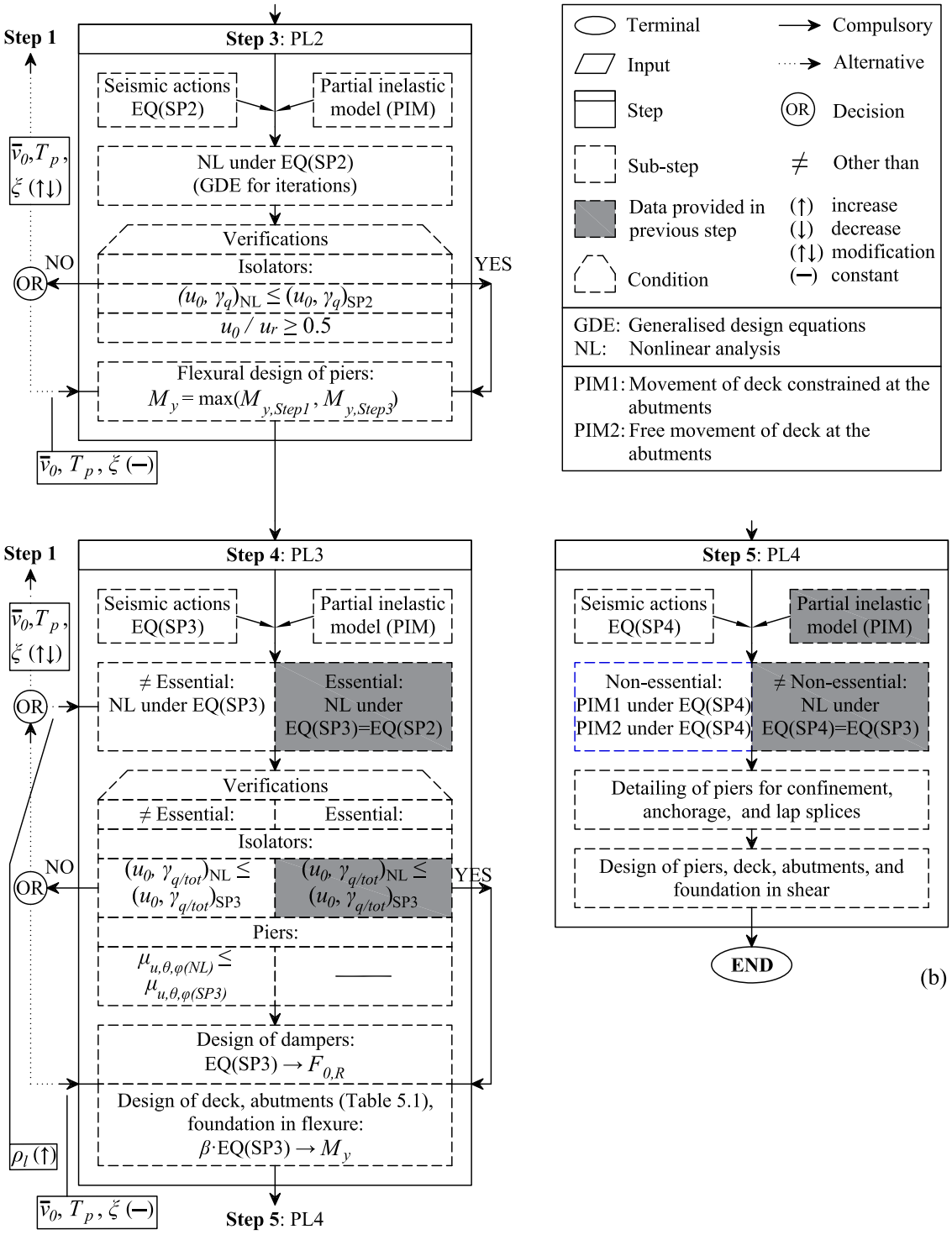

Contnd. Def-BD methodology for seismically isolated bridges: (a) General overview, (b) detailed steps (in blue: additional required steps compared to 'ductile-pier' bridges)

Seismic hazard		Structural performance			
EQ	**T_R (yrs)**	**SP1**	**SP2**	**SP3**	**SP4**
EQI	<50	Ductile		-	-
EQII	50-100	Isolated	Ductile		-
EQIII	500-1000		Isolated	Ductile	
EQIV	~2500			Isolated	Ductile

Service	Full	Operational	Limited	Disrupted
Damage	Negligible	Limited	Significant	Severe
Repair	No/Economic	Economic	Feasible	Non-feasible

Seismic hazard		'Ductile-pier' bridges: Analysis type per PL			
EQI	<50	IMP	L	-	-
EQII	50-100	IMP	L+NL	NL	-
EQIII	500-1000	IMP	L+NL	NL	IMP
EQIV	~2500	L+NL	L+NL	NL	IMP
Seismic hazard		**Isolated bridges: Analysis type per PL**			
EQI	<50	GDE	-	-	-
EQII	50-100	NL	GDE+NL	-	-
EQIII	500-1000	NL	GDE+NL	GDE+NL	-
EQIV	~2500	-	GDE+NL	GDE+NL	NL

Analysis: Generalised design equations (GDE), Implicit calculation (IMP), Linear (L), Nonlinear (NL)

Importance: Non-essential, Ordinary, Essential, Critical I, Critical II

Fig. 5.2 'Performance matrix' adopted in Def-BD method

Table 5.1 Suggested structural performance criteria for seismically isolated bridges[1, 2]

Isolated bridges				
Member	SP1	SP2	SP3	SP4
Isolated pier	-	Yield $\varphi \leq \varphi_y$	Conc. spalling $\varphi \leq \varphi(\varepsilon_c$=3.5-4‰)	Ultimate response $\varphi \leq \min\varphi(\varepsilon_{ccu}$, hoop fracture, long. bar buckling/fracture)
Elastomeric bearing	No damage $\gamma_q \leq 1/SF_{\gamma q}$	Yielding of anchor bolts, cracking of pedestals, lower limit for yielding of shims $\gamma_q \leq 1$	Ultimate response $\gamma_q \leq 2.5$, $\gamma_{tot} \leq 7$, tension, stability	Locked Link activation
Bilinear hysteretic isolator (restoring capability)	Full service $u_{res}, \lambda_{acc} \rightarrow 0$ $V \leq V_0$ (or V_y)	Operational $u_0/u_r \geq 0.5$	-	-
Viscous damper	-	-	Ultimate response $u_0 \leq u_{stroke}$ $F_0 \leq F_{0,R}$	Locked Link activation
Abutment	-	-	Activation $M_{Abt} \leq M_{y,Abt}$ $u_0 \leq u_{clearance}$	Ultimate response Backfill activation
Foundation	-	-	Yield	Ultimate response

[1]Definition of symbols and terms included in this table is provided in §5.2.2-5.2.6

[2]Criteria for additional members (e.g. deck) and other type of bearings are described in §5.2.2-5.2.6

The analysis type prescribed by the proposed method for each PL is reported in Fig. 5.2 and discussed in detail in the following sections. To meet current code requirements (e.g. CEN 2005a, AASHTO 2010, ASCE 2016), member verifications should be performed for both lower bound (LB) and upper bound (UB) design properties of isolators and dampers, i.e. two different sets of analysis per PL, each set, in the case of nonlinear dynamic analysis, consisting of seven (or more) pairs or triplets of accelerograms (since the vertical component of seismic action may have a critical effect on the in-plane deformation of the deck) applied using different incidence angles (§4.5.2). The scheme proposed in §5.2.2-5.2.6 reduces the required sets of analyses to two per each PL, noting however, that performing the 'full set' of analyses and designing members using their 'envelope' response will in any case minimise the associated cost of the adopted design solution.

For the sake of completeness detailed steps of the procedure, including those that are essentially the same with §3.2, are provided in Fig. 5.1b and thoroughly described in §5.2.2-5.2.6.

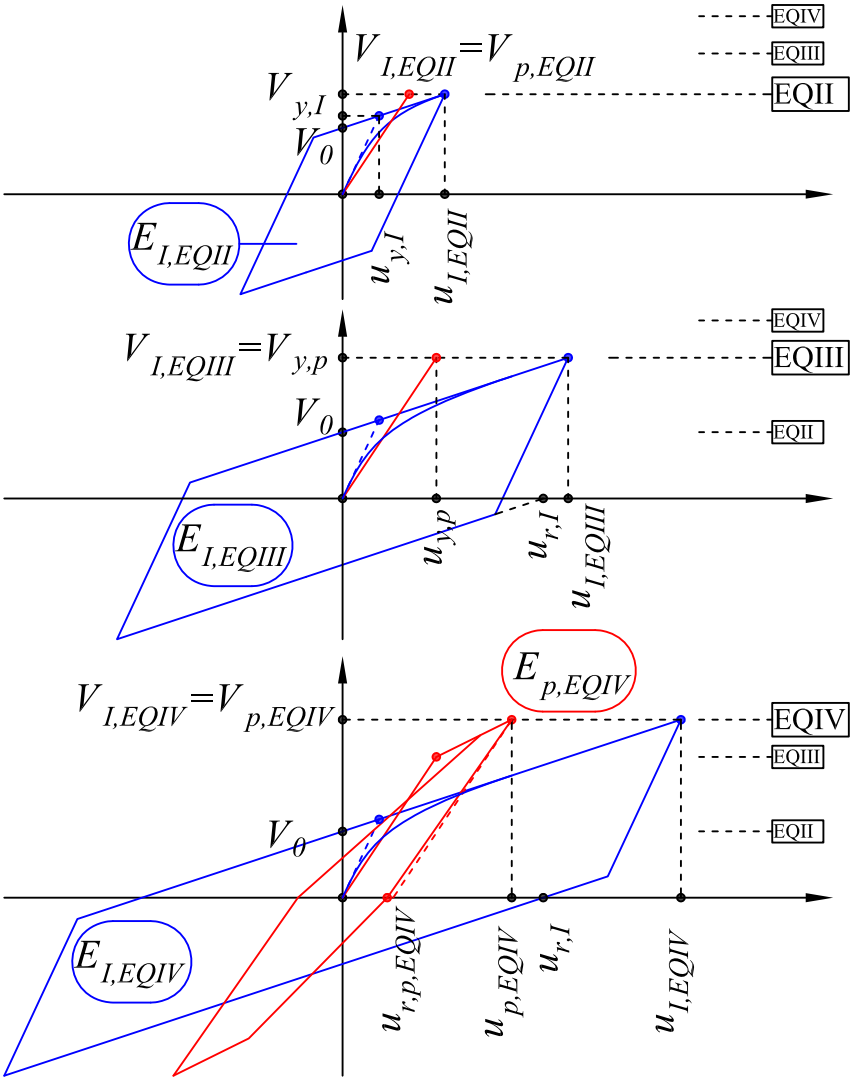

Fig. 5.3 Performance objective for an ordinary seismically isolated bridge: Pier column (p: in red) and bilinear isolators response (I: in blue) under EQII, III, IV

5.2.2 Preliminary design (Step 1)

In the case of isolated bridges, the first step aims at the identification of the critical (in terms of economy and performance) PL and at a first 'near-optimal' estimation of the basic parameters of the isolation system, namely, its (normalised) strength $\bar{v}_0$, post-elastic stiffness k_p (or isolation period T_p), and damping ratio ξ; according to the definitions provided in Chapter 4, $\bar{v}_0$ represents the ratio V_0 / (mg), where m the isolated mass. The 'near-optimal' isolation solution is defined herein as the one that results in 'near-minimum' peak total acceleration $\ddot{U}_0$ of the superstructure while keeping within allowable limits the peak relative displacements u_0 of the isolation system and the deformations of the substructure (piers) (Inaudi & Kelly 1993). Different approaches can be explored by duly exercising engineering judgement.

Both objectives of the preliminary design can be investigated either on the basis of an elastic (e.g. response spectrum) analysis by introducing an iterative equivalent linearisation technique, similar to code-based approaches (e.g. CEN 2005a), or on the basis of the approach developed in Chapter 4 using generalised design equations (GDEs) that provide direct estimates of u_0, $\ddot{U}_0$ for an RDOF as a function of ξ, η (i.e. strength normalised to seismic intensity, §4.3-4.5), and T_p, under different PLs associated with target spectra (e.g. code-based) with the same frequency content but different intensity. The latter approach, apart from being compatible with the framework of Def-BD (i.e. estimated response based on nonlinear dynamic analysis), has also the potential to remedy certain pitfalls of common equivalent linearisation procedures (§5.1). To this end, 'design equations' in the form of Eqs. (4.37) and (4.38) are used in this step to identify both the reference (or critical) PL and a 'near-optimal' isolation scheme, recalling that GDEs can be extracted for code-prescribed target spectra and be provided as ready-to-use tools; although development of regression models is required in cases wherein spectra of different frequency content are adopted, the procedure can be easily performed using the IDEC code as discussed in Chapter 4.

u_0 and $\ddot{U}_0$ inelastic spectra for the adopted seismic actions EQ(SP2) and EQ(SP3) are first established by plotting GDEs in a u_0-$\bar{v}_0$, $\ddot{U}_0$-$\bar{v}_0$ format (Fig. 5.4), facilitating the identification of isolation schemes (ξ, $\bar{v}_0$, T_p) with a 'near-optimal' performance under different earthquake intensities, and systems consisting of different passive devices. The above 'near-optimal' selections for a given ξ are characterised by a constant value of η (i.e. the 'near-optimal' η is independent of the seismic intensity) but in general correspond to different 'actual' isolation schemes due to either the variation of $\bar{v}_0$ (see Eq. (4.38) and optimal selections denoted with blue in Fig. 5.4) or the variation of $c_{d,NL}$ since the latter depends on u_0 when $a < 1$ according to Eq. (4.15). Fig. 5.4, in agreement with other studies (e.g. Ramallo *et al*. 2002), indicates that when an isolated structural system designed for optimal performance under a 'rare' event (e.g. optEQIII) is subjected to stronger ground motions (e.g. EQIV), it results in suboptimal u_0 response compared to the displacement response of a system optimised for the higher seismic action (i.e. optEQIV). On the other hand, increased $\ddot{U}_0$ (and hence base shear) are obtained in the case of the optEQIV system when the latter is subjected to shorter return period events (e.g. EQIII). In design terms, the previous observation may be translated into an increased cost of isolators in the first case and an

increased cost of reinforcing steel in the concrete piers in the second. In view of the previous remark, the decision on the reference PL to be used, or else, the level of earthquake under which the isolation and energy dissipation system is 'near-optimally' selected, i.e. EQ(SP2) or EQ(SP3), should be made cautiously apart from the case of inherently linear systems (as explained in the following), and in essential bridges wherein the isolation system is activated only under EQ(SP2) (Fig. 5.1b). In all other cases, the divergence from the optimal response when the selected system is subjected to a different PL and/or different DPs along with its relevant effect on economy and performance, should be considered. It is noted that the variability of mechanical properties can be easily assessed provided that the relevant input (i.e. ξ, $\bar{v}_0$, T_p corresponding to LB-DP or UB-DP) is used in Eqs. (4.37) and (4.38).

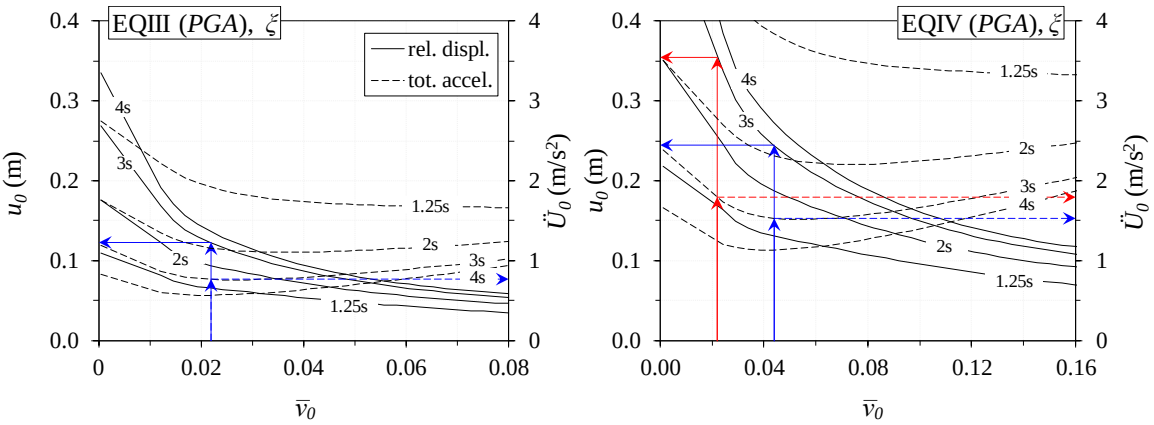

Fig. 5.4 Direct peak response estimation of RDOF systems (m, ξ, T_p=3.0 s, a=1.0) optimally designed (in blue) under EQIII (i.e. optEQIII) (left), EQIV (i.e. optEQIV) (right), and corresponding response of optEQIII under EQIV (in red)

Based on the 'energy-equivalence' approach presented in §4.4, Eq. (4.37) and the corresponding inelastic spectra (Fig. 5.4) can additionally predict with sufficient accuracy the response of systems equipped with nonlinear viscous dampers (NLVDs) since the nonlinear parameter a was found to have a minor impact on u_0 and $\ddot{U}_0$. By approximating the response of a NLVD with an energy-equivalent linear viscous damper LVD, Eq. (4.37) can provide direct estimates of response for systems with the same ξ but different a. However, since $c_{d,NL}$ depends on u_0, an iterative application of Eq. (4.37) (i.e. in contrast with design procedures based on effective properties that require iterative structural analysis) will be required whenever the response of a 'near-optimally' selected system is sought under a PL and/or DPs other than those used for its selection. The procedure can be summarised as follows:

i. u_0 and $\ddot{U}_0$ response estimates of a 'near-optimally' selected system (ξ, $\bar{v}_0$, T_p, and $a < 1$) under the reference seismic action are directly calculated from Eq. (4.37) assuming $a = 1$.

ii. Assuming $\xi_e = 0.05$ (in the case of elastomer-based isolators) and $\xi_d = \xi - \xi_e$, c_e and c_d are calculated under the reference seismic action using Eqs. (5.1) and (5.2) (i.e. Eqs. (4.24) and (4.18)), and u_0 from Step (*i*).

$$c_{e,L} = 2m\omega_p\xi_{e,L} \tag{5.1}$$

$$c_{d,NL} = \frac{2m\omega_p\xi_{d,NL}\left(u_0\omega_p\right)^{1-a}}{f(\Gamma,\alpha)} \tag{5.2}$$

iii. c_e, c_d, $\bar{v}_0$, T_p are subsequently modified to account (whenever required) for the variability of design properties of devices, otherwise they are kept constant (i.e. corresponding to specific devices).

iv. η and $\xi = \xi_e + \xi_d$ are calculated under the different PL and/or design properties by re-arranging Eqs. (5.1) and (5.2). Assuming that $a < 1.0$, calculation of $\xi_{d,NL}$ requires the definition of an energy-equivalent linear system which in turn will provide the unknown u_0 under the considered PL and/or DPs. An initial estimate of $\xi_{d,NL}$ can be derived from Eq. (5.2) by assuming $a = 1$, thus uncoupling the above calculation from the displacement response.

v. Substituting ξ, η (from Step *iv*) and T_p (from Step *iii*) in Eq. (4.37) provides initial estimates of u_0 and $\ddot{U}_0$ under the different PL and/or DPs.

vi. Once u_0 has been determined, Steps (*iii*) to (*v*) are repeated until all relevant design quantities (i.e. ξ, u_0 and $\ddot{U}_0$) have practically stabilised; normally, no more than 2~3 iterations will be required.

When $a = 1.0$ Step (*vi*) will be redundant (i.e. no iterations required), whereas the decision on the adopted reference level of seismic action will have no effect on the system's optimal response in the special case of $a = 1.0$ and $\eta = 0$, due to the system's inherent linearity (Fig. 5.1b). The selection of a system with a 'near-optimal' performance may also encompass various design constraints, such as, maximum deformations of the isolation system (i.e. u_0), adequate restoring capability (§5.2.3, 5.2.4), a base shear ($m\ddot{U}_0$) resulting in reinforcing steel demands close to the minimum requirements (e.g. in cases when non-seismic loads affect the pier dimensions), a maximum damper force F_0, or simply target values for T_p, ξ, $\bar{v}_0$, accounting for both economy and market availability of dampers, isolators, and expansion/contraction joints. Note also that the decision on the type of devices required to materialise the selected system will normally follow the selection of ξ, η, T_p, apart from the case when specific restrictions apply. Table 5.2 and Fig. 4.8 provide some useful guidance in support of this task by associating specific design parameters (ξ, η, T_p, u_y) with common passive schemes, and corresponding force-displacement responses. Examples of the above procedure are presented in §5.3.5, 5.3.6.

Selecting an isolation and energy dissipation system will result in a first estimation of the geometrical and mechanical (LB, UB) properties of devices to be used in subsequent steps, so long as ξ, η, and T_p of the selected system are properly distributed to a sufficient number of units located at the piers and abutments. The distribution of the basic properties of the isolation system should

account for the weight distribution of the deck to the substructure, and the (potential) minimisation of the eccentricity between the centre of stiffness of the substructure-isolation system and the centre of mass of the supported deck as a means to mitigate torsional effects. Uniformity of the stiffness of piers with different height can be achieved to some extent by tailoring the isolator properties so that the bearing stiffness counterbalances the difference in pier stiffness (Fardis *et al*. 2012, Jara *et al*. 2013). Notwithstanding the importance of the previous factors, reliability and cost issues will normally dictate the above distribution, e.g. selection of two isolators per pier/abutment is the most reliable and cost-effective design solution in the case of box girder section decks (Constantinou *et al*. 2011), while identical devices are preferable in small-to-moderate bridges since the cost for testing of devices is minimised. It is worth noting that the constraint of maintaining classical normal modes (i.e. distribution of damping coefficients proportional to the lateral stiffness of the substructure members) does not apply here due to the use of NLRHA, hence, optimal distributions of dampers can be explored (e.g. Christopoulos & Filiatrault 2006).

Distribution of properties of the selected isolation system and determination of LB/UB-DPs of devices will also provide an estimate of the pier strength required to ensure the target performance under the selected reference level of seismic action, i.e. quasi-elastic response of piers under EQ(SP2) or controlled inelastic response under EQ(SP3) (Fig. 5.3). Regarding the second case, the strength at the pier ends should be established to retain the effectiveness of the isolation system under an 'extreme' event through proper consideration of the range within which the inelastic deformations should fall, associated with the degree of damage allowed under EQ(SP3) (i.e. curvature φ corresponding at a concrete strain of ε_c = 3.5~4‰ in Table 5.1). To meet this objective, the procedure described in Step 1 of Def-BD for 'ductile pier' bridges (§3.2.2), used to ensure that the bridge remains operational during and after EQ(SP2), can be fully implemented herein for EQ(SP3) without requiring an elastic analysis; pier column forces and chord rotations can be estimated from the maximum inertia force transferred through the isolator to the pier top, and a proper estimation of pier equivalent cantilever heights h_{eq} (e.g. based on the distribution of bending moments along the pier height derived from statically applying a unit displacement to the deck). In case the longitudinal reinforcement demand ρ_l is found to be less than the minimum requirement, reduction of cross sections is in order. When non-seismic loads dictate the area of the piers (A_{pier}), ξ, $\bar{v}_0$, T_p can be modified instead, aiming at increased total accelerations as a means to exploit the available pier strength (provided due to the minimum ρ_l requirement), reduce the relative displacements of the isolation system, and thus minimise its cost. The procedure shown as a closed loop in Fig. 5.1b, simply involves the selection of appropriate values of ξ, $\bar{v}_0$, T_p from plotted diagrams (e.g. Fig. 5.4), rather than iterative analysis required in the case of equivalent linearisation approaches.

An issue deserving some further consideration relates to the case of bidirectional excitation; Eq. (4.37) in this case provides the peak relative displacement $u_{0,2D}$ and total acceleration $\ddot{U}_{0,2D}$ (i.e. the peak values of response histories defined by adding the relevant response vectors along the principal axes of the bridge, §4.5.1), but the angles at which these peak response estimates are

expected to develop remain unknown. This is of minor importance in the case of displacements so long as the passive devices are designed in such a way that they can sustain $u_{0,2D}$ in any random direction (§4.5.2), but it may result in conservative or unconservative design of the piers depending on the adopted $\theta_{\ddot{U}0}$ value. Given that extensive parametric NLRHA of different isolation systems has demonstrated that $\theta_{\ddot{U}0}$ may take any value within the 0~90° range when the two horizontal components of seismic action are applied along the longitudinal and transverse direction of the bridge (§4.5.2), design of substructure members should be performed for the most adverse of the effects derived by independently applying the maximum inertia force $m\ddot{U}_{0,2D}$ in the principal directions of the bridge.

Table 5.2 Isolation and energy dissipation schemes

	Design Parameters				
No.	ξ_e	ξ_d	η	k	u_y (m)
1	≥0.05	0	0	k_e (=k_p)	-
2	~0.05	≥0.05	0	k_e (=k_p)	-
3	~0.05	≥0.05	0	k_e (=k_p)	-
4	0	0	≥0.25	k_p	~0.001
5	0	≥0.05	≥0.25	k_p	~0.001
6	~0.05	0	≥0.25	k_p	~0.001
7	~0.05	≥0.05	≥0.25	k_p	~0.001
8	~0.05	0	≥0.25	k_p	~0.01
9	~0.05	≥0.05	≥0.25	k_p	~0.01

No.	V-u Response	Isolation hardware
1	Viscoelastic (apx. elastic in LDRB case)	HDRBs (LDRBs)
2	Viscoelastic	LDRBs + LVDs
3	Rigid viscoplastic with stiffening	LDRBs + NLVDs
4	Elastoplastic (apx. rigid plastic) with stiffening	FPBs
5	Elastoviscoplastic (apx. rigid viscoplastic) with stiffening	FPBs + L/NLVDs
6	Elastoviscoplastic (apx. rigid plastic) with stiffening	FPBs/FSBs + LDRBs
7	Elastoviscoplastic (apx. rigid viscoplastic) with stiffening	FPBs/FSBs + LDRBs + L/NLVDs
8	Elastoviscoplastic (apx. elastoplastic) with stiffening	LRBs, LRBs + LDRBs
9	Elastoviscoplastic with stiffening	LRBs + L/NLVDs, LRBs + LDRBs + L/NLVDs

HDRB:	High damping rubber bearing	FPB:	Friction pendulum bearing
LDRB:	Low damping rubber bearing	FSB:	Flat sliding bearing
(N)LVD:	(Nonlinear) Linear viscous fluid damper	LRB:	Lead rubber bearing

Finally, it is noted that convergence of response quantities derived from GDEs and the MDOF analysis in the following steps, depends on the substructure's stiffness (potentially involving limited inelastic response in the piers) and inertial characteristics that are ignored in Step 1. Consideration of the latter parameters is deemed superfluous at this stage since their effect on u_0 is not expected to be significant except for the case of very flexible and/or massive piers (Dicleli &

Buddaram 2006), and subsequent steps of the method involve NLRHA of a detailed model of the bridge.

5.2.3 PL1 verifications (Step 2)

During *Step 2*, a partially inelastic model (PIM) of the structure is set up and SP1 verifications are performed based on the results of NLRHA for appropriately defined ground motions. Hysteretic isolators and dampers are modelled as nonlinear spring and dashpot elements, respectively (§4.2.3), with mechanical properties as defined in Step 1 based either on LB-DPs or UB-DPs or both, as described in the following. In the same model, the remaining parts of the bridge are modelled as elastic members. The flexural stiffness of prestressed concrete deck elements is calculated assuming uncracked deck sections while reinforced concrete pier column stiffness should correspond either to yield (e.g. moment M vs. curvature φ analysis of sections based on ρ_l estimated in Step 1) or to the gross section; pier stiffness under EQ(SP1) is expected to have a minor effect on isolator deformations used in the following verifications. NLRHA of the PIM also requires the definition of a suite of ground motions, which should be compatible with the selected design spectrum. Selection and scaling of input motions can be performed according to the procedures described in §3.2.3. The selected earthquake motions will be used for both this step and the following ones, and they should be properly scaled to the level associated with the PL considered; alternatively, different suites of motions can be established for each PL based on different selection criteria and shape of target spectra in a more refined approach (e.g. Baker & Cornell 2006) that is expected to be more relevant in the case of bridges of higher importance. Based on the pier design approach adopted in Step 1, rotation of the pairs of horizontal components of seismic action into their principal axes (e.g. §4.2.2) and consecutive application along the principal axes of the bridge is deemed adequate during this and the following steps of the procedure in the case of straight bridges; a more detailed investigation involving application at a range of critical angles of incidence is in order in the case of more complex bridge configurations.

Verifications under EQ(SP1) seismic actions should be carried out in terms of both ‘operationality’ and ‘structural performance’ of the bridge, hence, design criteria in this PL (Table 5.1) should ensure both ‘full’ service of the bridge (i.e. no closure) and ‘negligible’ (or preferably no-) damage of the passive devices. The ‘operationality’ requirement can be satisfied by providing an adequate restoring capability, a design strategy common in most codes (e.g. CEN 2005a, ASCE 2016), by dictating the presence of devices that can inherently apply recentring forces to the superstructure, thus preventing substantial residual displacements (u_{res}) after the seismic event and accumulation of displacements during a sequence of seismic events or under ground motion containing pulses, while allowing the prediction of displacement demand with less uncertainty (Constantinou *et al*. 2011). The parameter mainly affecting the restoring capability of typical bilinear seismic isolation systems, defined as u_{res} / u_0, is the ratio u_0 / u_r (Fig. 2.4), where u_{res} is the residual displacement bounded by the maximum residual displacement u_r (Eq. (4.26)) under which

static equilibrium can be reached, i.e. $-u_r \leq u_{res} \leq u_r$. Due to the non-monotonic variation of u_{res} with respect to the ratio u_0 / u_r (Katsaras *et al*. 2008), the restoring capability and/or the accumulation of residual displacements during a sequence of seismic events expressed by the accumulation factor λ_{acc} (varying from zero for systems with no accumulation up to 1.0 for systems with full accumulation of residual displacements), should be assessed on the basis of design charts, like those proposed by Katsaras *et al*. (2008) and Cardone *et al*. (2015) for elastomer- and friction-based isolators, respectively. The relevant charts were derived from statistical analysis of responses from a large number of NLRHAs since the absence of u_{res} in NLRHA results under few (e.g. 3–10) horizontal pairs of spectrum-compatible records is not always indicative of sufficient restoring capability (Katsaras *et al*. 2008, Fardis *et al*. 2012).

In view of the previous remarks, the 'operationality' requirement can be satisfied by providing an adequate restoring capability with a view to limiting residual displacements u_{res} and the accumulation factor λ_{acc} to near-zero values (Table 5.1), and hence, ensuring 'full' service of the bridge. Efficiency of restoring capability can be addressed either by adopting a minimum value of u_0 / u_r, i.e. equal to 0.5 in EN1998-2 (CEN 2005a) (corresponding to u_{res} / $u_0 \leq 0.10$ according to Katsaras *et al*. 2008) or by directly assessing via relevant charts the expected value of u_{res} since the rule of u_0 / $u_r \geq 0.5$ may be too conservative considering the low values of u_0 involved in SP1. In the latter case (i.e. direct evaluation of u_{res}), engineering judgement will be required in defining allowable u_{res} values associated with the 'closure/non-closure' state of the bridge (e.g. horizontal offsets of approximately 20 and 30 mm were associated with 'non-' and 'brief-closure' in Porter 2004), noting that the capability of bilinear isolation systems is expected on average to be more critical for seismic motions involving small-to-moderate displacements (Katsaras *et al*. 2008) and UB-DPs; i.e. increase of u_0 / u_r (either by increase of u_0 or decrease of u_r) results in the reduction of u_{res} (Fig. 2.4). A more stringent ('force-based') 'operationality' criterion under EQ(SP1) can be the limitation of the isolation base shear below V_0 (or V_y) assuming UB-DPs; this will ensure zero u_{res} of the deck in the case of sliding bearings (both horizontal and vertical if friction pendulum bearings are considered), and thus, 'full' serviceability of the bridge, but is more difficult to apply in lead rubber bearings due to the actual gradual transition from the elastic to the inelastic range of response (i.e. uncertainty with regard to the definition of the yield displacement u_y, Fig. 5.3) requiring a conservative estimation of u_y. Considering the requirement for 'no- damage' of isolators, an upper limit on shear strains due to lateral deformation γ_q corresponding to first visible damage should be applied in the case of elastomer-based isolators and LB-DPs combined with an appropriate safety factor $SF_{\gamma q}$ (Table 5.1); a value of γ_q close to 1.0 can be adopted, associated with potential cracking of pedestals and/or yielding of anchor bolts (Padgett 2007) and with the lower limit of yielding of steel shims (i.e. 1~1.5) according to Mori *et al*. (1993, 1997), similarly to §3.2.3.

Use of UB- or LB-DPs of devices during the analysis in this step, is recommended for the verification of 'force-based' (including restoring capability) or 'deformation-based' operationality criteria, respectively. In the (common) case wherein both types of criteria are involved, analysis should be based either on UB- or LB-DPs depending on which is the most critical one (§5.3.5).

Verifications associated with mechanical properties not accounted for in the analysis should be conducted using conservative estimates of the demand implicitly related to analysis results through proper modification factors; the latter can be calculated as the ratio of the relevant UB/LB design quantities derived from GDEs. Alternatively, the designer may opt to apply consecutively UB- and LB-DPs, in this and the following PLs, to ensure a minimum cost of the adopted isolation solution. If the adopted performance criteria are not satisfied, mechanical properties of devices should be modified. Adjusting the mechanical properties of isolators without altering their stiffness (e.g. increasing proportionally both the elastomer area and thickness in elastomer-based isolators) will not require iterations, similarly to §3.2.3. In case ξ, $\bar{v}_0$, T_p are modified, conformity to the requirements of Step 1 (i.e. performance under the reference PL) can be evaluated using GDEs, without performing additional NLRHAs (Fig. 5.1b). When the required modifications in this step do not satisfy the target performance set in Step 1, alternative (probably less economical) design options can be explored, such as adding sacrificial devices that can restrain the relative movement of the deck to the piers for the shear forces under EQ(SP1). In any case, operationality verifications at this step are not expected to be critical for piers, as the latter are designed for responding quasi-elastically up to the next PL. A notable exception to the procedure described above, is the case of non-essential bridges, wherein NLRHA is omitted and response quantities required for the relevant verifications are approximately estimated by GDEs, due to the reduced importance and the low associated seismic actions.

5.2.4 PL2 verifications (Step 3)

During analysis in *Step 3*, the PIM should be used with pier stiffness corresponding to yield and UB-DPs of devices as modified in Step 2. SP2 verifications (Table 5.1) should ensure that the extent of damage is such that the bridge can be repaired after the earthquake without significant disruption of service. Regarding the isolation system, the previous requirement can be expressed as an adequate restoring capability allowing for u_{res} that can result in a 'brief' closure of the bridge (e.g. $u_0 / u_r \geq 0.5$), and 'limited' damage in the isolators (e.g. $\gamma_q \approx 1$) (Table 5.1), both evaluated according to the previous step. Required modifications of the mechanical properties of devices should be assessed based on the requirements of Steps 1 and 2, and are dealt in line with §5.2.3 (Fig. 5.1b). The performance sought for the substructure at this PL refers to essentially elastic response of piers (i.e. curvature φ lower than the yield curvature φ_y in Table 5.1), hence pier response retrieved from NLRHA in this step is used to design pier columns in flexure (i.e. definition of pier yield moments M_y in Fig. 5.1b). When design for flexure is carried out in terms of design values of member resistance (hence using commonly available design aids), pier moments derived from analysis (based on mean values of strength) should be properly reduced by the β-factor similarly to Def-BD of 'ductile-pier' bridges (§3.2.2). The final ρ_l ratio should be selected by adopting the highest demand derived from Steps 1 and 3.

5.2.5 PL3 verifications (Step 4)

Verification of the 'near-optimal' performance sought in Step 1 and subsequently modified in Steps 2, 3, constitutes the primary objective in this step involving the three critical states of the isolation system, namely, the states of peak deformation (critical for the deformation capacity of passive devices), peak total acceleration (critical for the design of substructure elements), and peak velocity (critical for the resistance of the dampers and their anchorage to the bridge members). Analysis is not required for essential bridges in this step, since both EQ(SP2) and EQ(SP3) are associated with EQIV (Fig. 5.1b, Fig. 5.2). Analysis in the above case will be meaningful only if a more refined model is introduced in Step 4 for verification purposes (i.e. aiming to assess in more detail potential changes of ξ, $\bar{v}_0$, T_p applied in the Step 3, or the LB response if the latter was omitted in §5.2.4).

In addition to the components of the isolation and energy dissipation system, piers are modelled in Step 4 as yielding elements, with strength and stiffness characteristics derived from M-φ analysis using ρ_l ratios determined in Step 3. Adoption of LB-DPs during analysis, followed by an explicit calculation of the deformation demand in the isolation system, or adoption of UB-DPs that will provide an accurate estimation of the deformations in the substructure, should be based on comparisons of the estimated response from GDEs with the available capacity of substructure members and devices, also accounting for the ensuing cost of overpredictions in response estimation. For example, if the estimated displacement demand of the isolators from Step 1 (i.e. from GDEs) is close to the capacity of the devices selected in subsequent steps, it is preferable to adopt LB-DPs during the analysis under EQ(SP3) with a view to assessing accurately, through analysis, the deformation demand in the isolation system normally associated with the increased cost of passive devices (except for isolation systems formed exclusively from LDRB), and implicitly, through modification factors, the pier deformation demand. The designer may also opt for analysing the isolated bridge under both LB- and UB-DPs, ensuring that neither the devices nor the substructure members (piers) are overdesigned.

The deformation capacity of passive devices should be checked for ultimate deformations (e.g. strain limits according to CEN 2005a, 2009 in Table 5.1) accounting for residual displacements (Cardone *et al*. 2015) so that the isolation system can sustain possible aftershocks. Uplift or maximum tensile stresses that may result in unseating of friction-based and cavitation of elastomer-based isolators, respectively, should be constrained, ensuring also their stability (e.g. SP3 performance criteria in §5.3). Required modifications of the mechanical properties of devices are assessed with the aid of GDEs in line with the previous steps. With regard to the piers, it should be verified that the deformation demand is consistent with accurately estimated limit values derived from M-φ analysis, allowing for controlled inelastic response of piers under EQ(SP3) (i.e. EQIV for ordinary and essential bridges in Fig. 5.2). Increase of the longitudinal reinforcement ratio ρ_l will be required if the demand exceeds the relevant deformation limit in Table 5.1, requiring iterative analysis within Step 4 (Fig. 5.1b). Nevertheless, it should be noted that neither device property modifications nor ρ_l adjustments were required in the examples studied so far (§5.3)

indicating the effectiveness of Step 1 in estimating the inelastic response; in this context, the above options are included in Fig. 5.1b for the sake of generality.

Damper forces and relative displacements derived from analysis in this step define their axial force resistance ($F_{0,R}$) and stroke ($u_{0,stroke}$), respectively. Furthermore, members considered elastic in setting up the PIM (i.e. capacity-protected members in Eurocode terminology) such as, the deck, abutments, and foundation, are designed in flexure for the action effects resulting from NLRHA. Design of the superstructure should aim at the non-cracked, rather than non-yielding, state of deck sections (similarly to SP3 requirements for 'ductile-pier' bridges in §3.2.4), whereas activation of the abutment-backfill system should be avoided under the seismic actions of this PL by providing a sufficient clearance ($u_{clearance}$ in Table 5.1) to accommodate the total design displacement (involving displacements due to seismic, permanent, quasi-permanent, and thermal actions, e.g. CEN 2005a) in both principal directions of the bridge. Seismic links (stoppers/shear keys) are introduced as a second line of defence against seismic actions exceeding EQ(SP3), and their inclusion in the PIM is not required (clearance between the link and the deck is treated as a design parameter) unless a non-essential bridge is under consideration (see next step).

5.2.6 PL4 verifications (Step 5)

The final step involves explicit analysis only in the case of non-essential bridges, wherein the target performance set in Table 5.1 and Fig. 5.2 is assessed through NLRHA under EQ(SP4). A realistic bridge response involves exhaustion of clearances followed by pounding effects between the deck and the substructure, activation of seismic links (i.e. 'locked' state in Table 5.1), activation of the abutment-backfill system resulting in damage in foundation members (e.g. in piles) and/or permanent deformations in the embankment, increased inelastic deformations in the piers, and reduction of the effectiveness of the isolation system. Given that analysis complexity required to properly capture the above modes of failure (e.g. modelling of pier-link-deck, backfill-abutment-deck interactions) along with relevant uncertainties in structural response are disproportionate to the associated low importance of the bridge, a simpler approach is recommended. This involves two sets of analyses under EQ(SP4) using the PIM of Step 4, the first assuming that deck displacements are constrained at the location of abutments while the second allowing free movement of the deck ends, with a view to estimating the ultimate response of abutments and piers, respectively, considering UB-DPs of passive devices in both cases. In all other POs, this step includes detailing of piers for confinement, anchorages and lap splices with due consideration of the expected level of inelasticity, and member shear design under EQ(SP4) (which coincides with EQIV in ordinary and essential bridges) and UB-DPs. Finally, in case the characteristics of the selected isolation devices deviate from those of typical devices provided by the manufacturer, checking of stresses in reinforcing shims (internal plates) and design of end plates should also be performed during this step (e.g. CEN 2005b, Constantinou *et al*. 2011).

5.3 Case Study

5.3.1 Description of studied bridge

The efficiency of the proposed design procedure is demonstrated by applying it to a 3-span bridge that has similar characteristics with the T7 Overpass, previously used in §3.3 as a case study of Def-BD for bridges designed for ductile behaviour of the piers. Specifically, the superstructure has identical geometrical and detailing characteristics on the basis that the deck design is governed by non-seismic actions (§6.2.5); the 10m wide prestressed concrete box girder deck with a total length of L = 99 m and a longitudinal slope of 7%, is supported by two single-column piers of cylindrical section and heights h_{Pier1} = 5.9 and h_{Pier2} = 7.9 m. The substructure lies on firm soil and both piers and abutments have surface foundations (footings). In contrast to T7, where the deck is monolithically connected to the piers, and rests on the abutments through elastomeric bearings, the isolated deck rests on all piers and abutments through isolators (described later) that allow its movement in any horizontal direction. Apart from the modification of the pier-to-deck connection, the clear height of the piers is reduced herein to accommodate the pier cap (height of 1.5 m) (Fig. 5.5). For the sake of consistency and with a view to enabling a meaningful comparison with T7, certain design parameters associated with modelling issues and the definition of seismic actions are defined in the following sections in line with §3.3, while in all subsequent designs the 'ordinary bridge' PO is adopted (Fig. 5.2). The isolated bridge is first designed under unidirectional excitation in §5.3.5 exploring the performance of different isolation and energy dissipation schemes, focusing on the transverse response of the bridge. The effect of bidirectional excitation in the design procedure is accounted for in §5.3.6.

5.3.2 Modelling issues and numerical evaluation of dynamic response

Response history analyses (RHAs) presented in §5.3.5, 5.3.6 for both design and assessment purposes were performed using the unconditionally stable implicit Newmark constant average acceleration method (Carr 2004a); the procedure was fully automated within a MATLAB script (Mathworks 2016) that enables parametric nonlinear dynamic analysis of MDOFs using RUAUMOKO 3D (Carr 2004b) and DYNAPLOT (Carr 2004c) in batch mode, post-processing of results involving data collection and statistical processing according to §4.2.4, and diagram plotting.

Bilinear hysteretic 2-joint springs (i.e. 'spring type') and dashpot (i.e. 'damping type') elements with six independent deformations (i.e. 1 axial, 2 shear, 2 flexural and 1 torsional internal springs/dampers) were used in RUAUMOKO 3D to model the elastic/inelastic force-displacement response of isolators and viscous dampers, realising through proper combination of their mechanical characteristics different passive systems according to Fig. 4.8 and Table 5.2 (Fig. 5.5). The effect of cavitation on the tensile axial stiffness of elastomer-based isolators was not explicitly considered during analysis, but a maximum tensile stress ensuring linear axial force-deformation

response with a tensile stiffness approximately equal to the compression stiffness was adopted and verified during design in line with experimental results (Warn 2006) and code requirements (e.g. CEN 2009). Likewise, the stability of elastomer-based isolators was verified at the design stage and the variation of the critical buckling load with lateral deformations (Weisman & Warn 2012) was not introduced in nonlinear dynamic analysis. In analyses involving two horizontal components of seismic action (§5.3.6), bidirectional interaction between the isolator yield forces was accounted for by considering a circular yield surface for shear forces (Huang 2002) as per §4.5.1.

The post-elastic shear stiffness of elastomer-based isolators (i.e. equal to the elastic horizontal stiffness of LDRBs) was calculated from Eq. (5.3) (Naeim & Kelly 1999), where G_R, and t_R are the shear modulus, and the total thickness of the elastomer, respectively.

$$k_p = k_R = \frac{G_R \cdot A_R''}{t_R} \tag{5.3}$$

In Eq. (5.3), the effective plan area A_R'' represents the bonded area of the isolator (i.e. corresponding to the area of the steel reinforcing plates A_R') increased by half the rubber cover area to account for the effect of the latter on the horizontal stiffness (Constantinou *et al*. 2011). For the case of circular LDRBs (Eq. (5.5)) and LRBs (Eq. (5.6)) that were adopted herein (§5.3.5, 5.3.6), the total (A_R), bonded (A_R') and effective (A_R'') areas are given as functions of the external, bonded, and effective diameters (i.e. D_I, D_I', D_I'') disregarding the area of the lead core A_L (associated with D_L), noting that according to EN15129 (CEN 2009), at least 4 mm of elastomer should cover laterally the edge of the steel plate;

$$D_I = D_I' + 20 = D_I'' + 10 \quad \text{(mm)} \tag{5.4}$$

$$A_{LDRB} = \frac{\pi D_i^2}{4}, \quad A_{LDRB}' = \frac{\pi D_i'^2}{4}, \quad A_{LDRB}'' = \frac{\pi D_i''^2}{4} \tag{5.5}$$

$$A_{LRB} = \frac{\pi\left(D_I^2 - D_L^2\right)^2}{4}, \quad A_{LRB}' = \frac{\pi\left(D_I'^2 - D_L^2\right)^2}{4}, \quad A_{LRB}'' = \frac{\pi\left(D_I''^2 - D_L^2\right)^2}{4} \tag{5.6}$$

In the case of LRBs, the shear resistance at zero displacement V_0 was associated with the yield force of the lead core V_{Ly} (and hence its plan area A_L) according to Eq. (5.7) where G_L and f_{Ly} represent the shear modulus and yield stress of the lead. Subsequently, the initial stiffness k_e of the isolator was calculated from Eq. (4.6) in line with the considerations of §4.2.3.

$$V_0 = G_L \frac{u_y}{t_R} A_L = f_{Ly} A_L = k_L u_y = V_{Ly} \tag{5.7}$$

To approximately account for the low confinement of lead in LRBs located at the abutments (due to the lower axial loads applied from the deck in this location compared to LRBs on top of the piers), the shear resistance V_0 of abutment bearings was reduced by assuming a 25% decrease in the yield stress of lead f_{Ly} (Ryan *et al*. 2005, Constantinou *et al*. 2011).

The torsional stiffness of the elastomer-based isolators was ignored, whereas the axial (k_v) and flexural (k_r) stiffnesses were calculated from Eqs. (5.8) and (5.9), respectively (Naeim & Kelly 1999), where I'' represents the moment of inertia of the effective section of the isolator as per Eq. (5.10) (LDRBs) and Eq. (5.11) (LRBs).

$$k_v = \frac{E_c \cdot A_R''}{t_R} \tag{5.8}$$

$$k_r = \frac{E_r \cdot I_R''}{t_R} \tag{5.9}$$

$$I_{LDRB}'' = \frac{\pi D_I''^4}{64} \tag{5.10}$$

$$I_{LRB}'' = \frac{\pi \left(D_I'' - D_L\right)^4}{64} \tag{5.11}$$

The compression (E_c) and bending (E_r) moduli in Eqs. (5.8), (5.9) were calculated following the suggestions of Van Engelen & Kelly (2015) that provide the following equations for circular solid pads;

$$\frac{1}{E_c} = \frac{1}{6G_R S^2} + \frac{4}{3E_b} \tag{5.12}$$

$$\frac{1}{E_r} = \frac{1}{2G_R S^2} + \frac{3}{2E_b} \tag{5.13}$$

E_b is the bulk modulus of the elastomer assumed equal to 2000 MPa (CEN 2005b, 2009). The same equations were also applied in the case of LRBs considering that the 'confined' lead core of modern isolators prevents the lateral expansion of the elastomer layers under axial loading as opposed to hollow elastomeric bearings. In the same context, the shape factor S, representing the ratio of the loaded (i.e. bonded) area to the area of the elastomer that is free to bulge in a single elastomer layer of t_i thickness, was derived from Eqs. (5.14), (5.15) in the case of circular solid LDRBs (S_{sol}), and circular LRBs (S_{LRB});

$$S_{sol} = \frac{D_I{}'}{4t_i} \tag{5.14}$$

$$S_{LRB} = \frac{D_I{}'^2 - D_L{}^2}{4D_I{}'t_i} \tag{5.15}$$

Viscous damping originating from the rubber of elastomer-based isolators was introduced in the form of uncoupled linear dashpot elements connected in parallel with the shear internal springs of the 'spring-type' elements (Fig. 5.5), with constant damping coefficients $c_{e,L}$ calculated from Eq. (5.1) assuming a damping ratio of $\xi_{e,L}$ = 5% at the corresponding translational isolated mode of vibration, i.e. mode derived from classical modal analysis of the isolated bridge assuming that isolators vibrate at their post-elastic stiffness k_p. Linear/nonlinear dashpot elements were introduced to model the response of supplemental linear/nonlinear viscous damping devices (i.e. LVDs/NLVDs) according to §4.2.3; in this case $c_{d,L}$, $c_{d,NL}$ along with the stroke and the maximum force of the fluid dampers represent design parameters and are unknown at the start of the design procedure.

The inelastic response of the piers was modelled in accordance with the assumptions provided in §3.3.2. Axial force and flexural yield moment interaction (i.e. N-M_y) was not considered in analysis since in isolated bridges the variation of pier axial forces affecting the yield moments at the pier ends is expected to be low (also verified through analysis). Nevertheless, the coupled yielding response of piers was captured by considering the bidirectional interaction of yielding moments (i.e. M_x-M_y) with a circular yielding surface resulting from the double symmetry (in terms of both geometry and detailing) of the cylindrical column sections. Likewise, pier strength and stiffness characteristics, required to describe the strength envelope of the pier plastic hinges and the SP limit values for member deformations, were obtained through M-φ analysis accounting for the performance criteria presented in Table 5.1 (described in §3.3.2). Elastic frame elements were used to model pier cap beams (Fig. 5.5).

The deck, having geometry identical to the case of the 'ductile-pier' bridge in §3.3.2, was modelled using linear three-dimensional beam elements with flexural stiffness corresponding to the gross sections, since the bending moments of the deck under the maximum considered seismic action (§5.3.4) were found in general lower than the deck cracking moments derived from M-φ analysis (§6.2.5). In accordance with the adopted PO of ordinary bridges (Table 5.1, Fig. 5.2), abutments were not included in the analysis model and the required clearance between the deck and the seismic links of piers and abutments was treated as a design parameter (§5.2.5). Connectivity of the deck to the abutments (through passive devices) and the piers was modelled according to Fig. 5.5 using rigid constrains and considering the height of the isolators (h_I) and the eccentricity of the deck mass centre. During the mass discretisation, one third of the pier column mass was included in relevant pier cap joints (Fig. 5.5). Soil-structure interaction phenomena were ignored in line with §3.3.2.

The system damping matrix [$\boldsymbol{C}$], in general of non-classical form, was assembled from the damping matrices of the different sub-systems (Chopra 2012) of the bridge, namely, the isolation and energy dissipation system representing 'quantifiable' sources of (supplemental) damping (i.e. [$\boldsymbol{C}_{D,sup}$]), and the structural members of the bridge representing 'unquantifiable' sources of (inherent) damping (i.e. [$\boldsymbol{C}_{D,inh}$]) (Ray *et al*. 2013). Several pilot analyses were performed with a view to assessing the performance of alternative damping model options available in RUAUMOKO 3D (Carr 2004a, b) in terms of minimising (*i*) the energy (*E*) balance error *EBE* of Eq. (5.16) (energy terms defined according to Christopoulos & Filiatrault 2006), (*ii*) the effect of 'spurious' damping forces that may result in unbalanced moments (Chopra & McKenna 2016), and (*iii*) the hysteretic 'inherent' damping force vs. relative velocity response emerging from the consideration of a tangent stiffness proportional damping matrix (Carr 2004a); energy terms in Eq. (5.16) and 'inherent' damping forces are provided directly as output response histories in RUAUMOKO suite (Carr 2004a, b, c).

$$EBE(\%) = 100\frac{E_{input} - \left(E_{kinetic} + E_{damping} + E_{strain} + E_{hysteretic}\right)}{E_{input}} \tag{5.16}$$

A tangent stiffness proportional damping matrix (Eq. (5.17)) was finally adopted for the structural members of the bridge properly assembled with the damping contributions of the dashpot members (modelling viscous damping resulting from the elastomer of isolators and VDs), in order to obtain the damping matrix for the complete system [$\boldsymbol{C}$] used as a secant damping matrix (Carr 2004a, b); this is a variation of the Rayleigh tangent stiffness damping model where the mass-proportional component is disregarded and the damping forces at each time-step are calculated assuming a secant formulation of the damping matrix, i.e. the product of the damping matrix (calculated using the tangent stiffness matrix [$\boldsymbol{K}_T$]) times the current vector of velocities of the structure (Eq. (5.18)) with a view to eliminating the unrealistic 'inherent' damping hysteretic effects (Carr 2004a, Chopra & McKenna 2016). In cases when NLVDs are included in the analysis model, the damping forces are calculated assuming a tangent formulation of the damping matrix [$\boldsymbol{C}$] (Eq. (5.19)) where the damping forces at the end of the time-step are the damping forces at the beginning of the time-step plus the tangent stiffness proportional damping matrix multiplied by the increment of the velocity vector; although this damping model inevitably exhibits damping hysteretic effects it is preferred due to potential numerical errors associated with the use of the secant formulation in systems involving NLVDs (Carr 2004b).

$$\left[\boldsymbol{C}_{D,inh}\right] = a_k\left[\boldsymbol{K}_T\right], \qquad a_k = \xi_i\frac{2}{\omega_i} \tag{5.17}$$

$$\left[\boldsymbol{f}_D\left(t+dt\right)\right] = \left[\boldsymbol{C}\right]\left[\dot{\boldsymbol{u}}\left(t+dt\right)\right] \tag{5.18}$$

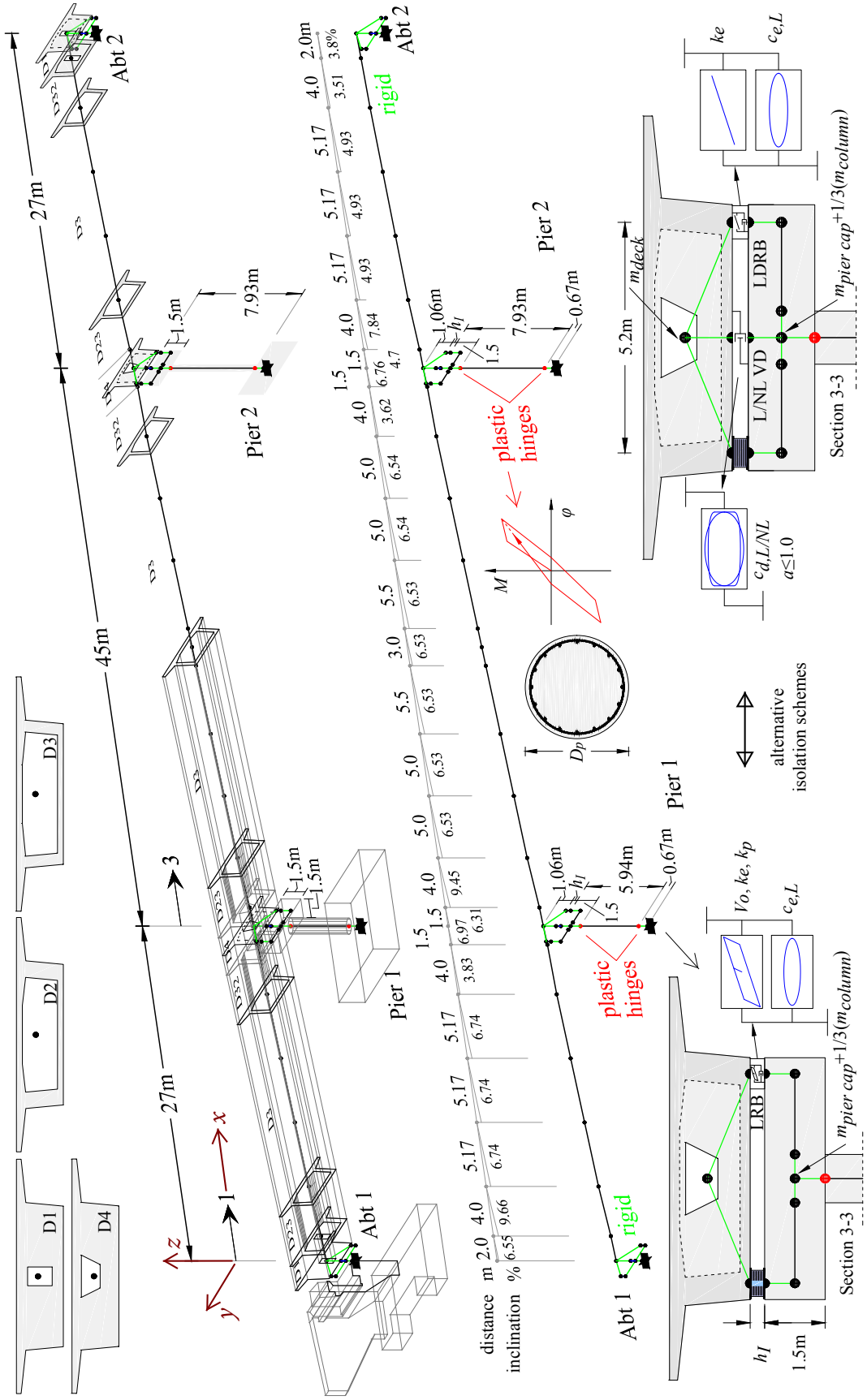

Fig. 5.5 Layout of the bridge configuration and finite element modelling

$$\left[\boldsymbol{f}_D(t+dt)\right]=\left[\boldsymbol{f}_D(t)\right]+[\boldsymbol{C}]\left[\boldsymbol{d\dot{u}}(t)\right] \tag{5.19}$$

In Eq. (5.17), the constant coefficient a_k was calculated using the first translational isolated modal frequency ($\omega_i = \omega_1$) derived from classical modal analysis of the bridge performed using the post-elastic stiffness of isolators (k_p) and setting ξ_i = 1% similarly to the suggestions of Ryan & Polanco (2008), Fardis *et al*. (2012), Pant *et al*. (2013) regarding modelling of 'inherent' damping in base-isolated structures.

The reference finite element model of the isolated bridge involving in total 68 three-dimensional frame, spring, and dashpot elements, is presented in Fig. 5.5 for different isolation and energy dissipation schemes (§5.3.5, 5.3.6).

5.3.3 Variability of design properties of isolation and energy dissipation devices

Based on code requirements, the nominal design properties of passive devices should be in general validated via special 'prototype' testing, while the variation of these properties due to external factors (e.g. Annex J in EN1998-2, CEN 2005a), such as ageing (including corrosion) (f_1), temperature (f_2), contamination (f_3), and wear (expressed as cumulative travel) (f_4), should be taken into account in the design, quantified either through special tests or, for common isolator types, estimated on the basis of simplified procedures. Herein, the variation of design properties was calculated adopting the simplified approach of the informative Annex JJ in EN1998-2, CEN (2005a) (or informative Annex J in EN15129 CEN 2009) that applies modification factors (i.e. λ-factors) to the nominal properties of isolators (DP_{nom}) as a means to estimate lower LB- and UB-design properties of isolators as per Eqs. (5.20)-(5.22) (ψ_{fi} = 0.7 for ordinary bridges). The variation of the nominal damping coefficient of viscous dampers was assumed equal to ±15% (Constantinou *et al*. 2007a).

In general, the design properties of cyclic response of elastomer-based isolators influenced by the above factors are the strength V_0 and post-elastic stiffness k_p. A conservative range of variation of the nominal properties of f_{Ly} (resulting in the variation of V_0) for use during the preliminary design of isolated bridges (i.e. before 'prototype' testing) is given by Constantinou *et al*. (2011) considering the yield stress of lead during the first cycle of seismic motion $f_{Ly,1}$ and the average yield stress during the first three cycles of seismic motion $f_{Ly,3}$. Minimum and maximum nominal values of G_R (resulting in the variation of k_p) were defined according to CEN (2009). The estimated bounds of design properties are presented in Table 5.3.

$$LBDP = \min DP_{nom} \tag{5.20}$$

$$UBDP = \max DP_{nom}\left(\lambda_{U,f1}\lambda_{U,f2}\lambda_{U,f3}\lambda_{U,f4}\right) \tag{5.21}$$

$$\lambda_{U,fi} = 1 + \left(\lambda_{\max,fi} - 1\right)\psi_{fi} \tag{5.22}$$

Table 5.3 Isolation and damper LB and UB design properties

Property	DP_{nom}		λ-factors								DP	
	Min	Max	$\lambda_{max,f1}$	$\lambda_{U,f1}$	$\lambda_{max,f2}$	$\lambda_{U,f2}$	$\lambda_{max,f3}$	$\lambda_{U,f3}$	$\lambda_{max,f4}$	$\lambda_{U,f4}$	*LB*	*UB*
$f_{Ly,3}$ (MPa)	10.00	12.07	1.00	1.00	1.30	1.21	1.00	1.00	1.20	1.14	10.00	22.48
$f_{Ly,1}$ (MPa)	13.50	16.29										
G_R (MPa)	1.1·0.7	1.4·0.7	1.10	1.07	1.10	1.07	1.00	1.00	1.00	1.00	0.77	1.12
c $(kN/(m/s)^a)$	$0.85c_{nom}$	$1.15c_{nom}$	-	-	-	-	-	-	-	-	$0.85c_{nom}$	$1.15c_{nom}$

5.3.4 Target spectra and representation of seismic action

The target spectra presented in §4.2.1 were adopted herein for unidirectional and bidirectional (2D) excitation, assuming site conditions 'C' (compatible with 'design equations' of Chapter 4). Selecting a reference return period of $T_{R,ref}$ = 475yrs, and a *PGA* of 0.21g (i.e. identical to the hazard zone ZII case in 'ductile-pier' bridges, §3.3.3), three different seismic action levels (EQ) were defined according to Eqs. (3.5)-(3.7) for unidirectional excitation. Using the definitions provided in §4.2.1 (i.e. definition of 2D target spectra), the following *PGA*s ($\ddot{u}_{g0}$) were calculated for the case of bidirectional excitation;

$$T_{R,EQII} = 90yrs, \quad SF_{EQII} \sim 0.5, \quad \ddot{u}_{g0,EQII,2D} = 0.15g \tag{5.23}$$

$$T_{R,EQIII} = T_{R,ref} = 475yrs, \quad SF_{EQIII} = 1, \quad \ddot{u}_{g0,EQIII,2D} = 0.30g \tag{5.24}$$

$$T_{R,EQIV} = 2500yrs, \quad SF_{EQIV} \sim 2, \quad \ddot{u}_{g0,EQIV,2D} = 0.59g \tag{5.25}$$

Selection and scaling of natural records used for design purposes (i.e. Steps 2-4 of the Def-BD methodology described in §5.2) followed in general the procedure described in §4.2.2 (i.e. different scaling factor per record). Eligible pairs of seismic events were initially selected from the PEER NGA-West 2 (http://ngawest2.berkeley.edu/) database (Ancheta *et al*. 2013) excluding records containing long velocity pulses. Adopted preliminary search criteria were moment magnitude M_w = 6.5~7.0, closest distance from the recording site to the ruptured area R_{rup} = 20~40km, average shear wave velocity to a depth of 30 m $V_{s,30}$ = 180~360 m/s (corresponding to site conditions 'C', CEN 2004b), and lowest usable frequency 0.2 Hz (corresponding to a period of 5.0 s). The sample of eligible events was further constrained by assessing the similarity of spectra of the selected records to the target spectrum over the period range of 0.3~5s using the *MSE* indicator (Eq. (4.1)). The site-to-source distance adopted herein is larger than the 10-25km range considered in §3.3.4 with a view to ensuring that the selected records are free of 'near source' effects that fall beyond

the scope of this study, noting that codes (e.g. CEN 2005a, AASHTO 2010, 2011) usually consider a threshold distance value of 10km below which explicit consideration of 'near-source' effects is required (by means of a site-specific characterisation of seismic ground motion). Nevertheless, design of the isolated bridge for R_{rup} = 10~25km yielded practically the same design requirements (Gkatzogias & Kappos 2017), thus, rendering results presented in §5.3.5 directly comparable with those of §3.3.

Adopting an allowable SF_{MSE} of 0.7~1.5, a suite of 7 eligible pairs of records was selected allowing design of members using the mean estimate of the response. The scaling procedure described in §4.2.2 (Eq. (4.3)) was preferred over the approach followed in the case of the 'ductile-pier' bridge as a simpler means to reduce uncertainty in mean response estimation arising from the increased variability in seismic response when a limited number of records is used in line with Shome *et al*. (1998). Recall that the same objective was sought in §3.3.4 by applying the EN1998-2 (CEN 2005a) scaling procedure (i.e. using a single 'global' scaling factor) along with a 'structure-specific' selection criterion that required the evaluation of a large number of alternative suites on

Table 5.4 Characteristics of natural records; unrotated (as-recorded) SF_{MSE}-scaled H2 components

							SF_{MSE} × H2 Component			
Earthquake			Region	Year	M_w	R_{rup}	SF_{MSE}	PGA	PGV	PGD	I_A
No.	RSN	Name				(km)	(-)	(g)	(m/s)	(m)	(m/s)
1	169	Imperial Valley-06	USA	1979	6.53	22.03	0.88	0.306	0.289	0.177	2.516
2	776	Loma Prieta	USA	1989	6.93	27.93	1.10	0.197	0.341	0.217	0.957
3	778	Loma Prieta	USA	1989	6.93	24.82	0.89	0.248	0.318	0.130	0.824
4	987	Northridge-01	USA	1994	6.69	28.30	1.29	0.412	0.347	0.086	1.689
5	4860	Chuetsu-oki	JP	2007	6.80	23.18	1.26	0.331	0.234	0.196	1.722
6	5781	Iwate	JP	2008	6.90	38.04	1.46	0.514	0.341	0.188	3.319
7	6923	Darfield	NZ	2010	7.00	30.53	1.06	0.319	0.346	0.129	1.785
			Minimum Value		6.53	22.03	0.88	0.197	0.234	0.086	0.824
			Maximum Value		7.00	38.04	1.46	0.514	0.347	0.217	3.319
			Geometric Mean					0.319	0.314	0.154	1.656

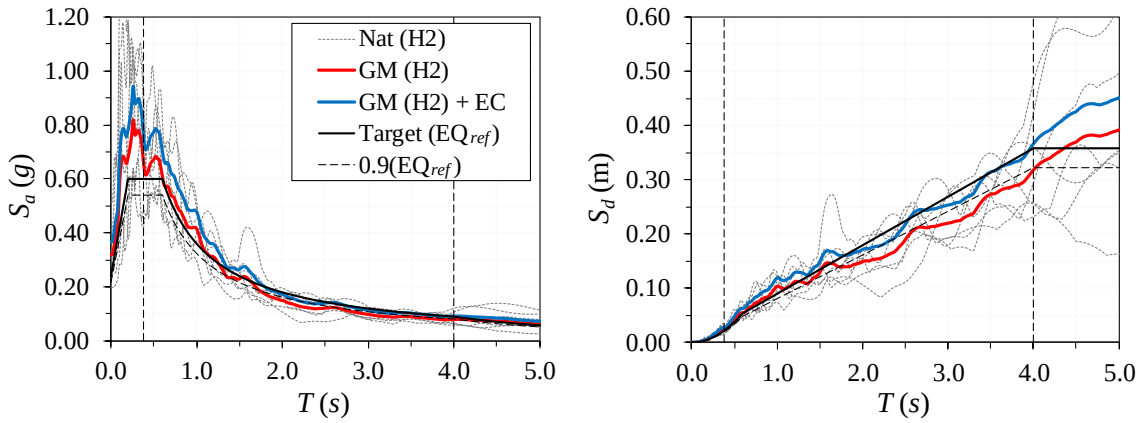

Fig. 5.6 Spectral matching of response acceleration (left) and displacement (right) geometric mean (*GM*) and EN1998-2-scaled geometric mean (*GM*+EC) (SF_{EC}=1.15) spectra to the 1D target spectrum (*PGA* of 0.21*g*, site 'C', $T_{R,EQIII}$) for the adopted suite of SF_{MSE}-scaled natural (Nat) records considering H2 components

the basis of an allowable standard error value, and hence increased computational effort. Employing the scaling procedure of §4.2.2 initially for the H2 components (H2 represents notation used in the PEER NGA-West 2 database to identify components), and subsequently for the pairs of horizontal components, resulted in the spectral matching presented in Table 5.4, Fig. 5.6, and Table 5.5, Fig. 5.7, for analysis under uni- and bidirectional excitation, respectively. In the case of bidirectional excitation, the horizontal components H1, H2 of the selected events shown in Table 5.5 were transformed into principal components (i.e. HI, HII) as per §4.2.2. Although the dispersion of spectral ordinates around the target spectrum is reduced within the period range of interest (especially in the case of accelerations) compared to Figs. 3.10, 3.11, deviation of the mean spectrum from the target still exists in the short period range introducing some conservatism in higher mode response. Elimination of this source of conservatism usually requires the use of a larger number of records (e.g. Fig. 4.5) than the seven adopted here in line with the minimum requirement commonly set by codes, while the adoption of an upper limit of spectral deviation in each record is a harsher selection criterion that requires a large number of available records.

Table 5.5 Characteristics of natural records; rotated SF_{MSE}-scaled HI & HII components

					SF_{MSE} × HI Component				SF_{MSE} × HII Component			
Earthquake			$\theta_{r=0}$	SF_{MSE}	PGA	PGV	PGD	I_A	PGA	PGV	PGD	I_A
No.	RSN	Name	(deg)	(-)	(g)	(m/s)	(m)	(m/s)	(g)	(m/s)	(m)	(m/s)
1	169	Imp. Valley-06	79.9	0.91	0.317	0.287	0.185	2.761	0.213	0.237	0.122	1.971
2	776	Loma Prieta	89.1	0.73	0.270	0.458	0.233	1.173	0.129	0.226	0.144	0.416
3	778	Loma Prieta	2.7	0.87	0.238	0.308	0.123	0.790	0.231	0.384	0.176	0.611
4	987	Northridge-01	38.1	1.53	0.494	0.383	0.095	2.527	0.572	0.306	0.075	2.081
5	4860	Chuetsu-oki	13.1	1.06	0.331	0.314	0.114	2.338	0.238	0.173	0.158	1.152
6	5781	Iwate	29.4	1.41	0.716	0.311	0.140	3.904	0.436	0.266	0.147	2.841
7	6923	Darfield	39.7	0.97	0.387	0.458	0.243	1.719	0.268	0.310	0.229	1.178
		Minimum Value	2.73	0.73	0.238	0.287	0.095	0.790	0.129	0.173	0.075	0.416
		Maximum Value	89.06	1.53	0.716	0.458	0.243	3.904	0.572	0.384	0.229	2.841
		Geometric Mean	27.31	1.04	0.368	0.354	0.153	1.935	0.269	0.264	0.143	1.220

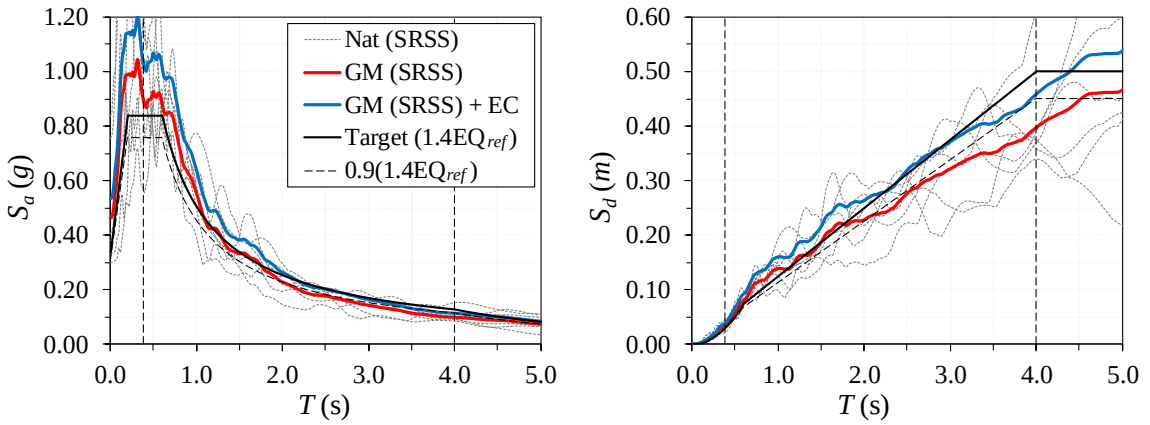

Fig. 5.7 Spectral matching of response acceleration (left) and displacement (right) geometric mean (*GM*) and EN1998-2-scaled geometric mean (*GM*+EC) (SF_{EC}=1.15) SRSS spectra to the 2D target spectrum (PGA_{2D} of 0.30g, site 'C', $T_{R,EQIII}$) for the adopted suite of rotated and SF_{MSE}-scaled natural (Nat) records

Ground motion intensity and energy characteristics of the SF_{MSE}-scaled records presented in Table 5.4, Table 5.5 (addressing also the PEER-NGA unique identification code *RSN*) incorporate the site (i.e. 'C') amplification effect (i.e. intensity parameters are comparable to S_C = 1.15 times the peak ground characteristics of the target spectra) and present a good overall match to the relevant values derived in the case of the Art B and D artificial suites (Table 4.1, Fig. 4.2, Fig. 4.3), noting however, their superiority (mainly) in terms of energy (i.e. I_A). Artificial records are used for assessment purposes adopting the analysis format of §3.3 with a view to assessing accurately the mean response under the 'design excitation' rather than its true dispersion. SF_{EC} global (i.e. per suite) scaling factors ensuring that ensemble spectral values are not lower than 0.9 times the target spectra over the period range of $(0.2\sim1.5)T_{eff}$ (CEN 2005a), where T_{eff} is associated with the secant stiffness at the maximum displacement, were calculated in §5.3.5.1, 5.3.6.1.

5.3.5 Unidirectional excitation

5.3.5.1 Application of the Def-BD procedure

The focus in the following is on the design and assessment of three common isolation schemes that are representative of some of the available options and design criteria that can be explored (Table 5.2). The efficiency of the adopted schemes within the design examples of this section was evaluated using both approaches with regard to the variability of the properties of devices during design (i.e. 'reduced' and 'full' set of analyses according to §5.2); at the assessment stage (§5.3.5.2), safety checks were performed for the element force and displacement demands resulting from each possible combination of design properties (LB, UB) and PL. Furthermore, the outcome of the Def-BD methodology in §3.3.5 regarding the geometry of the piers (i.e. diameter D_p = 1.2m) was used as a starting point, focusing on the transverse response of the bridge, specifically, the pier, deck, and isolation system response, i.e. design of the abutments and the foundations was not considered. A general description of the design steps is provided in the following while detailed results are presented in tabular form in Annex C.

Step 1: Within the first step, Eqs. (4.37), (4.38) and Table 4.5 were used to plot inelastic spectra in the form of Fig. 5.8 (i.e. in a u_0-$\bar{v}_0$, $\ddot{U}_0$-$\bar{v}_0$ format) corresponding to different levels of seismic action (i.e. EQIII, EQIV) and an isolated deck mass m of 2545tn; similar spectra can be plotted for different combinations of ξ, η, T_p, and *PGA*s representing different isolation schemes under various PLs. In Fig. 5.8, the $\ddot{U}(opt)$ curve represents a visualisation of the design criterion of minimum $\ddot{U}_0$ for each T_p, while $u(opt)$ indicates the corresponding relative displacements of the isolation system. It should be noted that the abrupt change in the slope of the u_0, $\ddot{U}_0$ curves is due to the regression model adopted during the formulation of the generalised design equations; further refinement of the estimates requires the use of higher-order models, which is deemed redundant since divergence from analysis results is evident only in the case of short isolation periods that are of little interest in bridge isolation applications.

In Table 5.6, the mechanical characteristics and the estimated peak response of three alternative isolation systems (denoted with the first number in the first column) are presented, namely, the strength $\bar{v}_0$ (Eq. (4.25)) expressed also as η (i.e. normalised to the seismic intensity according to Eq. (4.38)), isolation period T_p, damping ratio ξ, peak relative displacement u_0, and peak total acceleration $\ddot{U}_0$. Characteristics and response in blue correspond to 'near-optimally' selected isolation schemes (i.e. optimal curves in Fig. 5.8) under the reference seismic action associated herein with LB-DPs (i.e. EQIII in the upper part, and EQIV in the lower part of the table). 'Near-optimal' response estimates derive from the direct application of GDEs (Eq. (4.37)), i.e. sub-step (*i*) in §5.2.2. The corresponding response estimates of the same system under a different PL and/or UB design properties (denoted with black) are derived from Eqs. (4.37) and (4.38) according to the procedure described in §5.2.2, sub-steps (*ii*)-(*vi*). Response estimates provided for UB-DPs are expected to yield the critical response quantities for the substructure elements. Implementation of GDEs does not require iterations (i.e. sub-step *vi* in §5.2.2) when linear viscous damping with a = 1.0 is considered (i.e. No. 1.1, 2.1, 1.2, 2.2). On the contrary, introduction of nonlinearity in damping (a = 0.2 in No. 3.1, 3.2) involves the iterative application of GDEs (sub-steps *iii* to *v* in §5.2.2) to predict the system's response under PLs and/or DPs that are different from those used during its 'near-optimal' selection (in which case the response is assumed equal to that of a = 1.0).

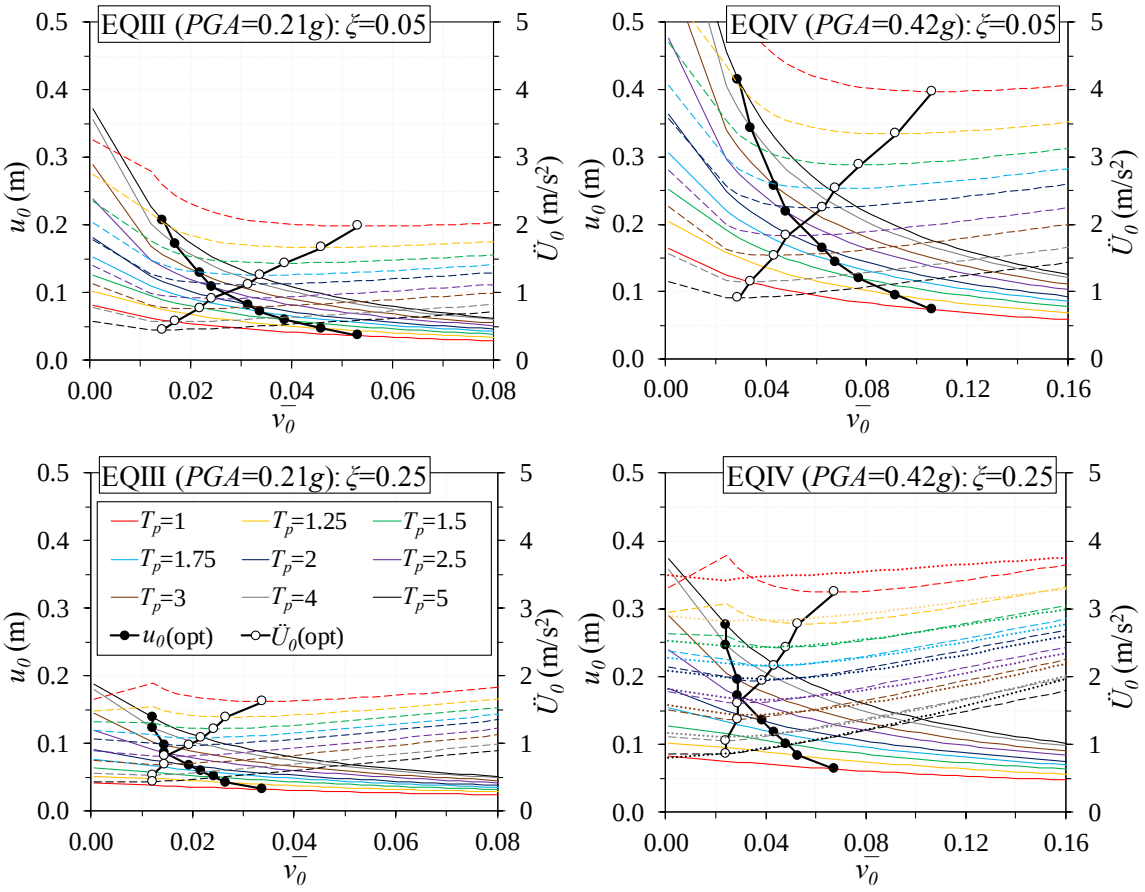

Fig. 5.8 Peak relative displacements u_0 (solid), total accelerations $\ddot{U}_0$ (dashed), optimal peak total accelerations $\ddot{U}_0$(opt) and optimal relative displacements u_0(opt) of the deck under EQIII (left) and EQIV (right) predicted from GDEs. Dotted acceleration curves (bottom-right) represent 'exact' (NLRHA) results

Table 5.6 Comparison of peak responses among SDOF systems optimised for different earthquake intensities

No.	DP	$\bar{v}_0$	T_p (s)	ξ	η	u_0 (m)	$\ddot{U}_0$ (m/s^2)	ξ	η	u_0 (m)	$\ddot{U}_0$ (m/s^2)	Δu_0 (%)	$\Delta \ddot{U}_0$ (%)
		opt EQIII		opt EQIII (1)				EQIV (2)				100·[(2) - (4)] / (4)	
						a =1.0							
1.1	LB	0.022	3.00	0.05	0.45	0.129	0.77	0.05	0.23	0.363	1.69	41	10
	UB	0.049	2.49	0.05	1.01	0.072	0.98	0.05	0.51	0.216	1.84	49	-6
						a =1.0							
2.1	LB	0.001	2.50	0.25	0.01	0.120	0.89	0.25	0.01	0.240	1.78	0	0
	UB	0.001	2.07	0.27	0.01	0.092	1.01	0.27	0.01	0.183	2.03	0	0
						a =0.2							
3.1	LB	0.001	2.50	0.25	0.01	0.120	0.89	0.15	0.01	0.302	2.07	26	17
	UB	0.001	2.07	0.29	0.01	0.089	0.99	0.17	0.01	0.227	2.37	27	20
		opt EQIV		EQIII (3)				opt EQIV (4)				100·[(3) - (1)] / (1)	
						a =1.0							
1.2	LB	0.044	3.00	0.05	0.90	0.086	0.83	0.05	0.45	0.258	1.54	-34	8
	UB	0.098	2.49	0.05	2.02	0.044	1.22	0.05	1.01	0.145	1.97	-39	24
						a =1.0							
2.2	LB	0.001	2.50	0.25	0.01	0.120	0.89	0.25	0.01	0.240	1.78	0.0	0.0
	UB	0.001	2.07	0.27	0.01	0.092	1.01	0.27	0.01	0.183	2.03	0.0	0.0
						a =0.2							
3.2	LB	0.001	2.50	0.49	0.01	0.090	0.74	0.25	0.01	0.240	1.78	-25	-17
	UB	0.001	2.07	0.59	0.01	0.066	0.80	0.29	0.01	0.178	1.98	-26	-19

In the last two columns of Table 5.6, non-optimal responses are compared with their optimal counterparts through the calculation of the relevant increase/decrease in peak relative displacement Δu_0 and total acceleration $\Delta \ddot{U}_0$ (according to the provided equation indicating the section of table used). It is seen that when an isolated system with T_p = 3.0 s, ξ = 0.05 (i.e. linear viscous damping with a = 1.0) and optimally selected $\bar{v}_0$ under EQIII (i.e. No. 1.1) is subjected to EQIV, it develops higher u_0 (~41% for LB-DPs) and lower $\ddot{U}_0$ (~6% for UB-DPs) demand compared to the response of a system designed with the same ξ and T_p, but with $\bar{v}_0$ aiming at the minimisation of $\ddot{U}_0$ under EQIV (No. 1.2). On the other hand, an optEQIV system subjected to EQIII and UB-DPs, develops ~39% smaller u_0 (expected to have an adverse effect on the restoring capability, §5.2.3) and ~24% larger $\ddot{U}_0$ demand compared to the optEQIII system. It is worth mentioning that the 6% decrease of $\ddot{U}_0$ for UB-DPs should be assessed on the basis of the SP2 performance criterion for quasi-elastic pier response under EQIII (Fig. 5.2, Table 5.1), while the 24% increase of $\ddot{U}_0$ for UB-DPs on the basis of the limited inelastic response requirement under EQIV, without knowing a priori which of the two criteria is the most critical for the design of the piers. In other words, optimising the selected system under EQIII will yield at best a 24% reduction in the pier shears (i.e. reduction in substructure cost), accompanied, nevertheless, by a 41% larger displacement capacity requirement for isolators (i.e. increase in the isolation system cost). The decision on the reference seismic action has no effect on systems with η = 0, ξ = 0.25 and a = 1.0 (e.g. No. 2.1, 2.2), due to their inherent linearity. Note that strictly speaking, No. 2.1, 2.2 are not optimally selected according to Fig. 5.8 since the minimisation of $\ddot{U}_0$ is achieved for $\eta \neq 0$, but the resulting total accelerations are fairly

similar. Finally, consideration of a = 0.2 yields both smaller u_0 (25~26%) and $\ddot{U}_0$ (17~19%) when EQIV is set as the reference seismic event (i.e. No. 3.2 compared to No. 3.1). Furthermore, the associated absolute quantities (i.e. u_0 and $\ddot{U}_0$ in No.3.2) are lower than those of a = 1.0 (i.e. No. 2.2), thus indicating an additional beneficial effect on the specific system's response (among others, as explained in the following) emerging from the introduction of nonlinearity in viscous dampers.

In general, the adopted approach should be based on the evaluation of data in the form of Table 5.6 for different isolation schemes accounting for both economy and market availability of materials and devices. Herein, EQIV was set as the reference level of seismic action and the three alternative isolation schemes presented in Table 5.6 were investigated; in line with Table 5.2, No. 1.2 was materialised by (circular) LRBs, No. 2.2 by the combined use of (circular solid) LDRBs and linear VDs, while No. 3.2 is differentiated (compared to No. 2.2) only with respect to the incorporation of nonlinear VDs. The first scheme was selected on the grounds that the distributed base shear ($m\ddot{U}_0$) to the piers results in pier longitudinal reinforcement ratio ρ_l larger than the minimum required while keeping u_0 of the deck below the maximum displacement obtained during the design of the bridge for ductile behaviour (i.e. ~0.27m in §3.3), the second as an alternative design solution resulting in similar u_0 under EQIV (considering LB-DPs) and $m\ddot{U}_0$ under EQIII, IV (and UBDPs), and the third, as an alternative to No. 2.2 aiming at a 25% reduction of the maximum force carried by the viscous dampers (by adopting a = 0.2 according to the following), and the investigation of the effect of the nonlinearity of VDs on the bridge overall response.

The required characteristics of isolation devices were defined by considering the properties of the isolation schemes in Table 5.6 under the reference seismic action associated with LB-DPs. Due to the relatively small length of the studied bridge it was deemed appropriate to use 8 identical isolators (i.e. two per abutment/pier) and four identical supplemental VDs (i.e. one per abutment/pier); it is recalled that only the transverse response is addressed at this stage, and normally, VDs will also be provided in the longitudinal direction of the bridge. In the LRB system, the required strength ($V_{0,LB}$ = 0.044mg = 1087kN) was distributed among pier ($V_{I0,LB(Pier)}$ = 155kN) (Eq. (5.26)) and abutment isolators ($V_{I0,LB(Abt)}$ = 117kN) (Eq. (5.27)), hence providing the required diameter of the lead core (D_L = 0.141m) (Eqs. (5.7), (5.28)), by considering that the yield stress of lead (f_{Ly}) in abutment bearings is 25% lower than the f_{Ly} of pier bearings to account for the low confinement of lead due to the smaller vertical loads (§5.3.2);

$$V_{I0,LB(Pier)} = \frac{V_{0,LB}}{0.75 \cdot n_{I(Abt)} \cdot 2 + n_{I(Pier)} n_{Pier}} \tag{5.26}$$

$$V_{I0,LB(Abt)} = 0.75 V_{I0,LB(Pier)} \tag{5.27}$$

$$D_{L(Pier)} = D_{L(Abt)} = 2\sqrt{\frac{V_{I0,LB(Pier)}}{\pi f_{Ly,LB(Pier)}}} \tag{5.28}$$

In Eq. (5.26), $n_{I(Abt)}$ and $n_{I(Pier)}$ represent the number or isolators per abutment and pier (i.e. 2), and n_{Pier} is the number of the piers. The diameter of the isolators was defined as D_I = 0.750m assuming an allowable vertical stress $\sigma_{v,max}$ = 12MPa, while the required $k_{p,LB} = 4\pi^2 m / T_{p,LB}^2$ of the isolation system was evenly distributed to all isolators ($k_{Ip,LB} = k_{p,LB} / 8$ = 1396 kN/m) providing the required height of the elastomer t_R = 0.235m from (Eq. (5.3));

$$t_R = \frac{\pi G_{R,LB}(D_I^2 - D_L^2)}{4k_{Ip,LB}} \tag{5.29}$$

An isolator with 25 layers of elastomer, each having thickness of t_i = 0.009 (i.e. t_R = 0.225m) was finally adopted, resulting in the revised properties presented in Table 5.7; revision of mechanical characteristics accounted also for the bonded and effective areas of the isolators (whenever required) using the equations provided in §5.3.2. Similar considerations yielded the required geometrical and mechanical characteristics of LDRBs (also included in Table 5.7), while UB-DPs of isolators were calculated based on the previous properties of devices and $G_{R,UB}$ = 1.12MPa, $f_{Ly,UB}$ = 22.5MPa, according to Table 5.3.

Assuming that $\xi_{e,L}$ = 5% is provided by the elastomer of LDRBs (corresponding to $c_{e,L} = 4\pi m\xi_{e,L} / T_p$ required for modelling purposes as per §5.3.2), the LB damping coefficient of LVDs ($c_{d,L,LB}$ = 640 kN/(m/s) per damper) was defined by considering $\xi_{d,L}$ = 20% (= 25-5%) and equating the energy/cycle of the 4 dampers to the energy/cycle of the single damper, i.e. following a 'uniform damping' distribution approach (Whittle *et al*. 2012);

$$c_{d,L,LB} = \frac{4\pi\xi_{d,L,LB}/T_{p,LB}}{4} \quad \text{(per damper)} \tag{5.30}$$

Considering $c_{d,L,UB} = 1.35c_{d,L,LB}$ (i.e. ±15% variability of the nominal c_d according to Table 5.3), the maximum force carried by a single damper $F_{0,L}$ was estimated equal to 558kN by Eq. (5.31), where f_v represents a velocity correction factor accounting for the differentiation of $\dot{u}_0$ from the pseudo-velocity PSV (= $\omega_p u_0$) (§4.2.3). f_v is provided by Ramirez *et al*. (2002) as a function of the damping ratio and isolation period (herein equal to 1.16 adopting the UB properties of Table 5.6; ξ_{UB} = 0.29, $T_{p,UB}$ = 2.07s).

$$F_{0,L} = 1.35c_{d,L,LB}\omega_{p,UB}u_{0,UB}f_v \tag{5.31}$$

In the case of NLVDs, substituting u_0 = 0.240m (Table 5.6) and a = 0.2 in Eq. (5.2) resulted in $c_{d,NL,LB}$ = 355 kN/(m/s)$^{0.2}$. The expected reduced peak damper force due to a = 0.2 was defined by Eq. (4.17) equal to $F_{0,NL} = 0.74F_{0,L}$ = 413 kN (i.e. a reduction of 26%); different reductions may be sought by regulating a, ξ, and T_p. Design properties of isolators and dampers are summarised in Table 5.7; although satisfying relevant code requirements (CEN 2005a, CEN 2009), the adopted properties do not correspond to specific commercial devices available on the market, with a view to assessing the structural response of alternative isolation schemes irrespective of specific features

introduced by different manufacturers. Plot of specific design solutions corresponding to commercial devices on the GDE charts can facilitate the design procedure in a design office environment.

Using the LB- and UB-DP of isolators and VDs (Table 5.7) in GDEs, the displacement and shear response was calculated (shown as Step 1 in Annex C, Table C.1); small deviations from the data of Table 5.6 are due to the implementation of GDEs with the final device properties of Table 5.7. Shear forces per abutment or pier ($V_{Abt/Pier,i}$) were computed according to Eq. (5.32), that assumes a rigid horizontal movement of the deck and accounts for the elastic and hysteretic part (if any) of the isolator (1st term), and the damping forces due to the elastomer of the isolators and the VDs (2nd term).

$$V_{Abt/Pier,i} = n_{I(Abt/Pier)}\left(V_{I0} + k_{Ip}u_0\right) + \frac{m\ddot{U}_0 - \sum_{i=1}^{4} n_{I(Abt/Pier)}\left(V_{I0} + k_{Ip}u_0\right)}{2 + n_{Pier}} \tag{5.32}$$

Table 5.7 Geometrical and mechanical properties per device

Device Property		LRB	LDRB	LVD (a =1.0)	NLVD (a =0.2)
D_I	(m)	0.75	0.75	-	-
D_L	(m)	0.14	-	-	-
n_i	(no. of layers)	25	15	-	-
$t_{R,i}$	(m)	0.009	0.011	-	-
t_R	(m)	0.225	0.165	-	-
h_I	(m) (device height)	0.35	0.26	-	-
k_v	(kN/m)	1426363	1701799	-	-
k_r	(kNm/rad)	24895	26670	-	-
$V_{I0,LB(Abt)}$	(kN)	117	-	-	-
$k_{Ip,LB(Abt)}$	(kN/m)	1418	2007	-	-
$c_{e,LB(Abt)}$	(kN/(m/s))	134	160	-	-
$c_{d,LB(Abt)}$	(kN/(m/s)^a)	-	-	639	355
$V_{I0,LB(Pier)}$	(kN)	156	-	-	-
$k_{Ip,LB(Pier)}$	(kN/m)	1418	2007	-	-
$c_{e,LB(Pier)}$	(kN/(m/s))	134	160	-	-
$c_{d,LB(Pier)}$	(kN/(m/s)^a)	-	-	639	355
$V_{I0,UB(Abt)}$	(kN)	263	-	-	-
$k_{Ip,UB(Abt)}$	(kN/m)	2067	2925	-	-
$c_{e,UB(Abt)}$	(kN/(m/s))	162	193	-	-
$c_{d,UB(Abt)}$	(kN/(m/s)^a)	-	-	865	480
$V_{I0,UB(Pier)}$	(kN)	351	-	-	-
$k_{Ip,UB(Pier)}$	(kN/m)	2067	2925	-	-
$c_{e,UB(Pier)}$	(kN/(m/s))	162	193	-	-
$c_{d,UB(Pier)}$	(kN/(m/s)^a)	-	-	865	480

Use of UB shear forces along with estimated values for the equivalent cantilever height of piers (based on preliminary analysis) within the procedure described in §3.2 provided an estimate for the required pier strength associated with the allowable 'serviceability'-related concrete strain of ε_c = 3.5~4.0‰ (i.e. SP3 requirement), resulting in provided reinforcement ratios of $\rho_{l,Pier1}$ = 6.1, $\rho_{l,Pier2}$ = 11.1‰ (LRB), $\rho_{l,Pier1}$ = 4.7, $\rho_{l,Pier2}$ = 10.1‰ (LVD), and $\rho_{l,Pier1}$ = 4.4, $\rho_{l,Pier2}$ = 9.4‰ (NLVD) in each scheme; a reduction of ρ_l demand in the piers of the bridge equipped with NLVDs consistent with the minor reduction of the base shear (~2%) was observed. Corresponding pier yield moments (M_y) defined through M-φ analysis (Kappos & Panagopoulos 2011) considering a minimum transverse mechanical reinforcement ratio (ρ_w) for limited ductile bridges (CEN 2005a) are provided in Table C.1 (Row No. 19), while the minimum ρ_l ratio was defined in accordance with the suggestions in Gkatzogias & Kappos (2016a) (§6.2.6, Eq. (6.1)).

Steps 2, 3: In Step 2, 7 ground motion records were selected and scaled according to §5.3.4 (Table 5.4, Fig. 5.6); the SF_{EC} global scaling factor ensuring that ensemble spectral values are not lower than 0.9 times the target spectra over the period range of (0.2~1.5)T_{eff} was found equal to 1.15 in all cases. The effective period T_{eff} associated with the secant stiffness at the maximum displacement was calculated using Eq. (5.33); this is the only stage wherein an effective property enters the procedure, maintained for the sake of compatibility with the scaling requirement of EN1998-2 (CEN 2005a).

$$T_{eff} = 2\pi \sqrt{\frac{m}{\frac{V_0}{u_0} + k_p}} \tag{5.33}$$

The PIM of the structure was subsequently set up (§5.3.2); the strength and stiffness of piers and isolators were modelled using the outcome of Step 1. NLRHAs were performed under the selected suite of records scaled to the level of seismic action associated with EQII (Step 2) and subsequently to EQIII (Step 3); results given in Table C.1 represent the mean response. SP1 (Step 2) and SP2 (Step 3) verifications included specific limits for residual displacements u_{res} of LRBs as per Eqs. (5.34)-(5.37) (Katsaras *et al*. 2008), and shear strains in the elastomer due to lateral deformation $\gamma_q = u_0 / t_R$, both assessed at the isolator level;

$$u_{res} = \frac{0.893 u_{rm,dyn}}{1 + 14.184 \min\left\{u_0/u_r, 1\right\}} \tag{5.34}$$

$$u_{rm,dyn} = u_r \frac{1 + u_y/u_r - \sqrt{\left(1 - \min\left\{1, u_0/u_r\right\}\right)^2 + 4u_y/u_r}}{1 + u_y/u_r} \geq 0 \tag{5.35}$$

$$\lambda_{acc} = \frac{1}{1+88.595\left(u_0/u_r\right)^{1.3}} \tag{5.36}$$

$$u_{res}^{n_{EQ}} = \lambda_{acc} u_{res}\left(n_{EQ}-1\right)+u_{res} \tag{5.37}$$

In Eqs. (5.34)-(5.37), $u_{rm,dyn}$ represents the dynamic residual displacement limit (Katsaras *et al*. 2008), and u_{res}^{nEQ} is the increased residual displacement accounting for the accumulation effect of n_{EQ} successive earthquakes; herein n_{EQIII} = 5 was considered. SP1 and SP2 limits to residual displacements were set equal to 15 and 30mm (Porter 2004), respectively, whereas the EN1998-2 limit of u_{res} / $u_0 \leq 0.1$ (Katsaras *et al*. 2008, CEN 2005a) was also checked under EQIII (i.e. SP2 limit in Step 3). Elastomer strain limits were set equal to 0.5 (SP1, Step 2) and 1.0 (SP2, Step 3) as per Table 5.1.

Analyses for the LRB scheme under EQII (Step 2) and EQIII (Step 3) were based on UB-DP since during the selection of bearings in Step 1, k_{Ip} and D_I (related to the adopted limit of $\sigma_{v,max}$), rather than limit strain values, were found to control t_R. UB-DP facilitated an explicit (i.e. UB-E in Table C.1) calculation of u_{res} but required an implicit calculation of LB deformations (i.e. LB-I in Table C.1) that are critical in checking γ_q. A modification factor equal to $u_{0,LB}$ / $u_{0,UB}$ = 0.086/0.044 (Table 5.6; No. 1.2, EQIII) was used to implicitly estimate LB deformations from UB analysis results. In the case of the VD schemes, the restoring capability was not checked, due to the linear response of isolators, and LB-DPs were adopted under EQII, allowing for an explicit (LB-E) calculation of deformations and strains of the isolation system. Analyses under EQIII were based on UB-DPs similarly to the LRB scheme; modification factors equal to $u_{0,LB}$ / $u_{0,UB}$ = 0.120/0.092 (LVD) and 0.090/0.066 (NLVD) (Table 5.6; No. 2.2, 3.2, EQIII) were used in the implicit calculation of LB deformations. For comparison purposes, design results (Table C.1) include also γ_q strains (in grey) calculated by explicitly considering LB-DP (LB-E) in each isolation scheme. None of the isolation system verifications was found to be violated in Steps 2 and 3, with the EN1998-2 SP2 limit of u_{res} / $u_0 \leq 0.1$ being the most critical one for the LRB scheme, whereas the implicit approach was found capable of conservatively estimating deformations without significant overestimations in most cases. Likewise, pier strength requirements under EQIII were lower than those of Step 1 (more so in the case of the LVD scheme), hence, it was deemed appropriate to proceed to Step 4 without further modifications.

Steps 4: Analysis under EQIV, required for Step 4 and 5 verifications, was carried out in all schemes for UB-DPs for the reason stated in the previous steps, thus enabling an explicit calculation and verification of the response in the substructure. The curvature ductility demand μ_φ in pier sections was found somewhat lower than the values corresponding to ε_{cu} = 3.5-4.0‰, thus verifying the target performance set in Step 1 for controlled inelastic response of the substructure. UB-DPs were also used to check tensile stresses (σ_t) in isolators adopting a limit of $2G_R$ in line

with EN15129 (CEN 2009). On the contrary, verifications of elastomer shear strains due to vertical compression γ_c and lateral deformations γ_q, along with bearing stability, required an implicit estimation of isolator deformations; modification factors equal to 0.256/0.144 (LRB scheme), 0.240/0.183 (LVD scheme), and 0.240/0.178 (NLVD scheme) were employed in this step (Table C.1; Step 1). γ_c strains due to the maximum compressive vertical isolator loads $N_{I,max}$ were calculated from Eqs. (5.38) and (5.39) (Constantinou *et al*. 2011), where the factor f_1 (fixed at 1.5 in CEN 2005b) accounts for the isolator shape (*S* factor), the effect of rubber compressibility (E_b), and the location of the point where the strain is calculated;

$$\gamma_c = \frac{N_{I,\max}}{A_{lap} G_R S} f_1 \tag{5.38}$$

$$f_1 \leq 1 + 2\frac{S^2 G_R}{E_b} \tag{5.39}$$

A_{lap} in Eq. (5.38) is the overlapping area between the top and bottom bonded elastomer areas of the laterally deformed isolator, calculated according to Constantinou *et al*. (2011), excluding the area of the lead core (CEN 2009) in the case of LRBs. Shear strains due to lateral deformation γ_q, and total strains in the elastomer of isolators $\gamma_{tot} = \gamma_c + \gamma_q$ were limited to 2.5 and 7.0, respectively, (CEN 2009), disregarding the insignificant shear strains due to angular rotation in γ_{tot}. In the LRB scheme, the maximum isolator deformations used in calculating γ_q were conservatively increased by ${u_{res}}^{nEQ}$ to account for the accumulation effect of past earthquake events.

Stability of isolators was assessed on the basis of Eq. (5.40) (Constantinou *et al*. 2011) that provides the critical buckling load in the laterally un-deformed configuration of hollow isolators, i.e. ignoring the lead core of LRBs and assuming $D_L = 0$ in the case of LDRBs;

$$N_{cr} = 0.218\frac{G_R D'^4}{t_{R,i} t_R} \cdot \frac{\left(1 - \frac{D_L}{D'}\right)\left(1 - \frac{{D_L}^2}{D'^2}\right)}{\left(1 + \frac{{D_L}^2}{D'^2}\right)} \tag{5.40}$$

The buckling load in the laterally deformed configuration N'_{cr} that accounts for the reduction of N_{cr} with the increase of lateral deformation was estimated adopting the overlapping area approach (Buckle and Liu 1994, Sanchez *et al*. 2013);

$$N_{cr}' = N_{cr}\frac{A_{lap}}{A'} \geq 0.15 N_{cr} \tag{5.41}$$

Stability of the isolator was deemed to be ensured when the design criterion of Eq. (5.42) was satisfied;

$$\frac{N_{cr}'}{N_{I,\max}} \geq 1.1 \tag{5.42}$$

Isolator strains and stability requirements lay within the adopted limits in all schemes; isolator deformations in the NLVD case were somewhat reduced in agreement with the parametric analysis results presented in §4.4.2, and the stability criterion was more critical in the case of LRBs. The uplift criterion was the most critical especially in LRB and NLVD schemes where the tensile stresses were found close to the stress corresponding to cavitation (i.e. $2G_R$), noting though, that the σ_t values used in verifications (and included in Table C.1: Row No. 28) represent the peak (rather than the mean) response recorded during NLRHAs. Attention should be also drawn to the fact that an attempt to reduce t_R aiming to match more closely the adopted SP strain limits is obstructed by $\sigma_{v,max}$ (i.e. a reduction of t_R requires the reduction of D_I to obtain a target k_{Ip}) which does not pose a strict limitation nor is it a code requirement (inasmuch as the total strains γ_{tot} lie within allowable limits) but it is considered good common practice and is typically recommended by manufacturers. The previous limitation applies also to the ratio $N_{cr}' / N_{I,max}$ governed by the plan dimensions of the isolator. The required axial force resistance of LVDs and NLVDs ($F_{0,R}$) was estimated in Step 4 as 652 and 455 kN, respectively, exhibiting a reduction of ~30% due to the introduction of a = 0.2; the previous correspond to a 17% (LVDs) and 10% (NLVDs) increase of the F_0 values estimated during preliminary design where the target reduction in axial forces (due to a) was set equal to 26%. The designer may choose to use more than one dampers per abutment/pier location (typically placed in pairs) in order to reduce the required axial force resistance (per damper) without significantly affecting analysis results.

Step 5: Shear forces in abutments and piers were found in good agreement with values estimated in Step 1 indicating the effectiveness of GDEs and Eq. (5.32) in predicting and properly distributing the base shear. Shear design performed according to CEN (2005b) for limited ductile bridges (assuming γ_{bd} = 1, §3.3.5) yielded pier transverse reinforcement ratios of $\rho_{w,Pier1} = \rho_{w,Pier2}$ = 7.1‰ (LRB), $\rho_{w,Pier1}$ = 6.7, $\rho_{w,Pier2}$ = 6.3‰ (LVD, NLVD); transverse reinforcement requirements were essentially the same in both VD schemes resulting in identical steel ratios that were slightly lower that those required in the LRB scheme. Finally, flexural design of the deck was not critical, since analysis moments were found in general lower than the deck cracking moments derived from *M*-φ analysis in §6.2.5, and therefore was not investigated further.

5.3.5.2 Assessment of design

Assessment of the alternative designs was carried out to evaluate the efficiency of the proposed procedure for the three different PLs and the considered range of DP of devices (i.e. LB, UB), accounting for all possible combinations of isolator properties and PLs. Since the primary objective of the assessment was the study of the transverse response of the bridge under a seismic excitation

that matches as closely as feasible the 'design excitation' (i.e. the design spectra), NLRHAs were performed for the Art B suite of artificial records (Table 4.1, Fig. 4.2) used to develop the generalised design equations, scaled appropriately (through SF_{EQ}, §5.3.4) to correspond to the level of seismic action associated with the considered PL. The strength and stiffness of piers was also updated based on *M-φ* analyses accounting for the final detailing of column critical sections. Fig. 5.9 compares mean estimates of deck and pier peak relative displacements derived from the design and assessment stages, while selected mean values of response quantities for the most critical checks are provided for the three alternative isolation schemes in Table C.2.

Regarding the structural performance evaluation of the bridge at the assessment stage, all designs were found safe, in that they satisfied the design criteria associated with each PL. In general, the demand estimated from assessment was very close to that calculated at the design stage despite the adoption of different type of records; deviations are ascribed either to the implicit (and conservative) estimation of response, or to the higher energy content of records adopted in design (§5.3.4) when explicitly calculated response quantities are compared. The first source of conservatism can be eliminated with an explicit calculation of deformations during Step 4; peak isolator/damper deformations, member shears, and damper axial forces (corresponding to the three critical states of maximum deformation, total acceleration, and velocity, respectively) presented excellent agreement between the two stages (Table 5.8) with noticeable differences only in the case of UB deformations under EQIII (i.e. Step 3) commented later. The introduced conservatism due to implicit analysis is in accordance with the expectation that an implicit procedure should yield results on the safe side (but not overconservative) compared to explicit analysis; based on the relevant discussion in §3.3.5, 3.3.6 this indicates the efficiency of the scaling procedure in controlling significant record and mean spectral deviations from the target spectra, but also the effect of base isolation on filtering out the contribution of higher modes associated with the region of high spectral deviations in Fig. 5.6. It is worth noting though that the implicit approach, although more conservative (as it ought to be), did not result in overdesigning members and devices in the specific example studied herein. Elimination of the second source of conservatism requires the adoption of a suite with a larger number of natural records with a view to describing more effectively the 'design seismic action' (both in terms of shape and intensity/energy characteristics), and increasing the reliability of response estimates by reducing *SEGM* values as discussed in §3.3.6, 4.3.2. Representative *SEGM* values of deck and pier responses derived from design and assessment are presented in Fig. 5.10, where it is seen that the Art B suite was able to keep *SEGM* values of responses below the limit of 15% adopted in §4.3.2 apart from the case of pier curvatures due to the high sensitivity of this design parameter to moment variations. Furthermore, the standard error values of displacements under the natural suite are of the same order with those reported in §3.3.6, demonstrating a relevant equivalence of the scaling approaches adopted in §3.3.4, 5.3.4, with that of Chapter 5 involving less computational effort.

Discrepancies among design Step 1 and the assessment stage may also be attributed to minor deck torsional effects, the elimination of which would require devices of different properties at

each pier and abutment location, an approach not justified in small-to-moderate bridges. In general, the fairly close match of isolator/damper deformations and shear/axial member forces derived from design/assessment with those of Step 1 (Table 5.8), indicates the minor effect of the substructure on the peak response of devices under EQIV and the efficiency of GDEs in predicting the response of a system equipped with linear/nonlinear viscous dampers and/or $\eta \neq 0$. In a similar context, peak deck displacements (Fig. 5.9) were found to be close to the peak isolator/damper deformations (Table C.1, Table C.2).

As mentioned previously some noticeable differences among design and assessment stages were observed in the case of UB deformations under EQIII in the LRB and NLVD schemes (Table 5.8); in fact, the increased isolator deformations at the design stage overestimated their restoring capability, representing a case wherein overestimation of seismic action effects may not be on the safe side. Nevertheless, only a marginal violation of the relevant criterion (i.e. $u_{res} / u_0 = 0.11 > 0.10$) was spotted out at the assessment stage (Table C.2: Row No. 6). This type of deviation is normally associated with the selected suite of ground motions since the estimated displacement from GDEs under UB-DPs and EQIII (i.e. 0.044 and 0.066 for LRBs and NLVDs, respectively) are closer to those of the assessment. With regard to the remaining verifications at the assessment stage, stability and uplift verifications were more favourable compared to the design stage, and inelastic response of piers (e.g. Fig. 5.11) was found to be within the adopted limit values.

In summary, all systems exhibited similar performance satisfying all adopted design criteria under the studied PLs; Fig. 5.12 demonstrates total shear force (including damper axial forces) vs. average relative displacement of the alternative isolation systems under a natural record (from those used for design) and an artificial record (used for assessment only). The slightly increased stiffness of the LVD and NLVD schemes is due to the increased area of the elastomer compared to the hollow section of LRBs. In terms of mean response, the LVD scheme resulted in relatively lower pier demand compared to the LRB option; reductions of 13% and 9% were recorded with regard to pier longitudinal and transverse reinforcing steel (i.e. reductions in terms of steel weight w_{sl}, w_{sw}, respectively) assuming that base reinforcement ratios are also adopted at the pier top (for the sake of compatibility with §3.3), but these minor differences are mainly attributed to the reduced value of f_{Ly} adopted in the case of abutment LRBs that in turn resulted in an increase of the shear force carried by the piers in the LRB scheme. Besides providing a safeguard mechanism against excessive structural velocities through the introduction of nonlinearity in the damper force-velocity relationship (Fig. 5.13), NLVDs further reduced pier w_{sl} by 7%, while during assessment the peak damper axial force was found reduced by 26% (i.e. equal to the value estimated in Step 1) without significantly affecting the overall bridge response in terms of isolation system deformations and deck displacements (Table C.1, Table C.2, Fig. 5.12); in fact, reductions in u_0 and $\ddot{U}_0$ were in line with the expected performance (e.g. Fig. 4.24). The final decision on the scheme to be adopted should account for the cost and availability of relevant materials and devices (and the associated availability of skills and cost of labour). In addition, all isolation schemes resulted in reductions in pier w_{sl} (i.e. 22% in the LRB, 32% in the LVD, 37% in the NLVD scheme), and w_{sw} (i.e. 38% in

the LRB, 43% in the VD schemes) within critical regions compared to the design of the T7 Overpass (i.e. 'ductile' pier response in §3.3), indicating that higher performance objectives adopted in isolated bridges do not necessarily result in higher initial cost of sub-structure design (§2.3.3) when the isolation system is quasi-optimally selected. Although the previous reductions are able to compensate for the initial cost of the isolation system only in the case when common isolators (e.g. low damping rubber bearings) are used to form a continuous isolation interface, or potentially in the case of very tall piers where pier reinforcement reductions of the same order can result in more significant savings, seismic isolation may emerge as an appealing design alternative if reduction in the life-cycle cost of the bridge is taken into account.

Table 5.8 Percentage response differences between design (D) and assessment (A) stages

Property			LRBs				LDRBs + LVDs (a=1.0)				LDRBs + NLVDs (a=0.2)			
Response	DP	EQ	Abt 1	Pier 1	Pier 2	Abt 2	Abt 1	Pier 1	Pier 2	Abt 2	Abt 1	Pier 1	Pier 2	Abt 2
$\frac{u_{0,A}-u_{0,D}}{u_{0,D}}$ (%)	LB	IV (Step 1)	-3	-6	-10	0	1	-3	-7	4	-8	-12	-17	-6
	UB-E	III (Step 3)	-31	-36	-40	-27	3	3	3	4	-20	-19	-22	-20
	LB-E	IV (Step 4)	-3	-3	-3	-3	6	5	5	6	0	3	2	0
$\frac{V_A-V_D}{V_D}$ (%)	UB-E	IV (Step 1)	-4	-11	-12	2	8	-5	-9	12	5	-7	-11	11
		IV (Step 4)	-11	-7	-7	-8	-1	0	0	0	-8	-5	-4	-3
$\frac{F_{0,A}-F_{0,D}}{F_{0,D}}$ (%)	UB-E	IV (Step 1)	-	-	-	-	2	1	-5	6	6	5	5	7
		IV (Step 4)	-	-	-	-	-10	-8	-7	-9	-3	-3	-3	-3

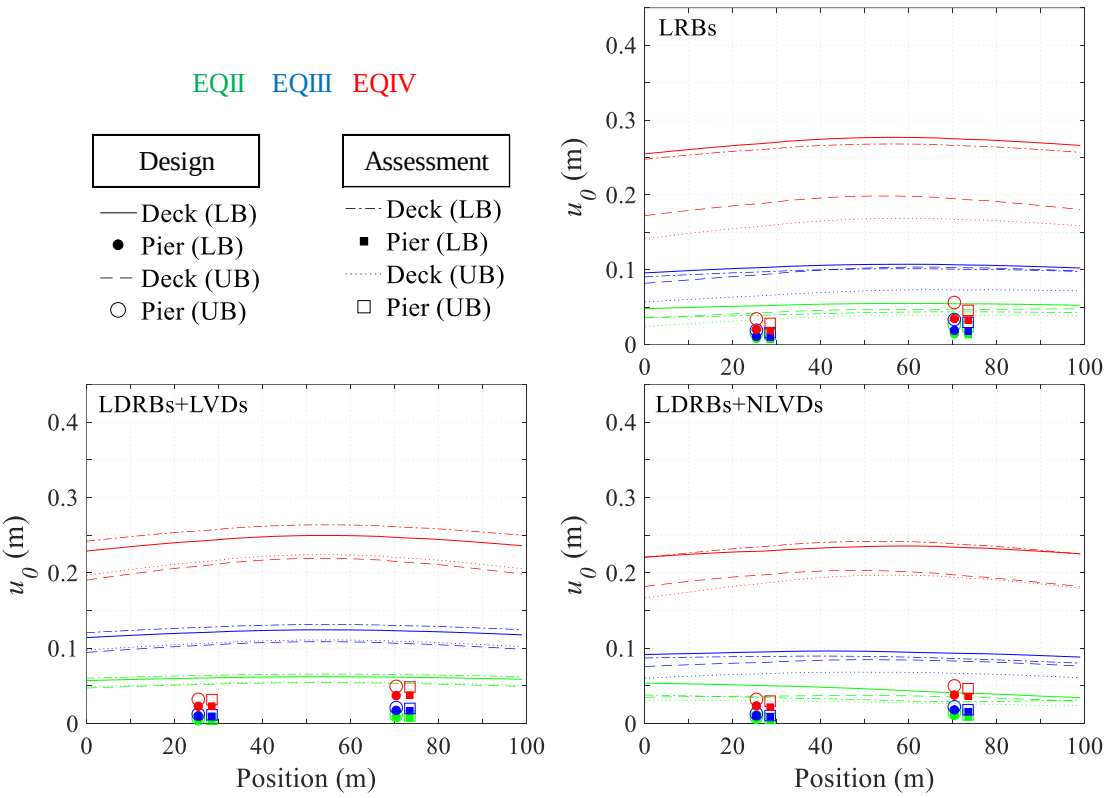

Fig. 5.9 *GM* of deck and pier peak relative (to the ground) displacements u_0 derived from design and assessment

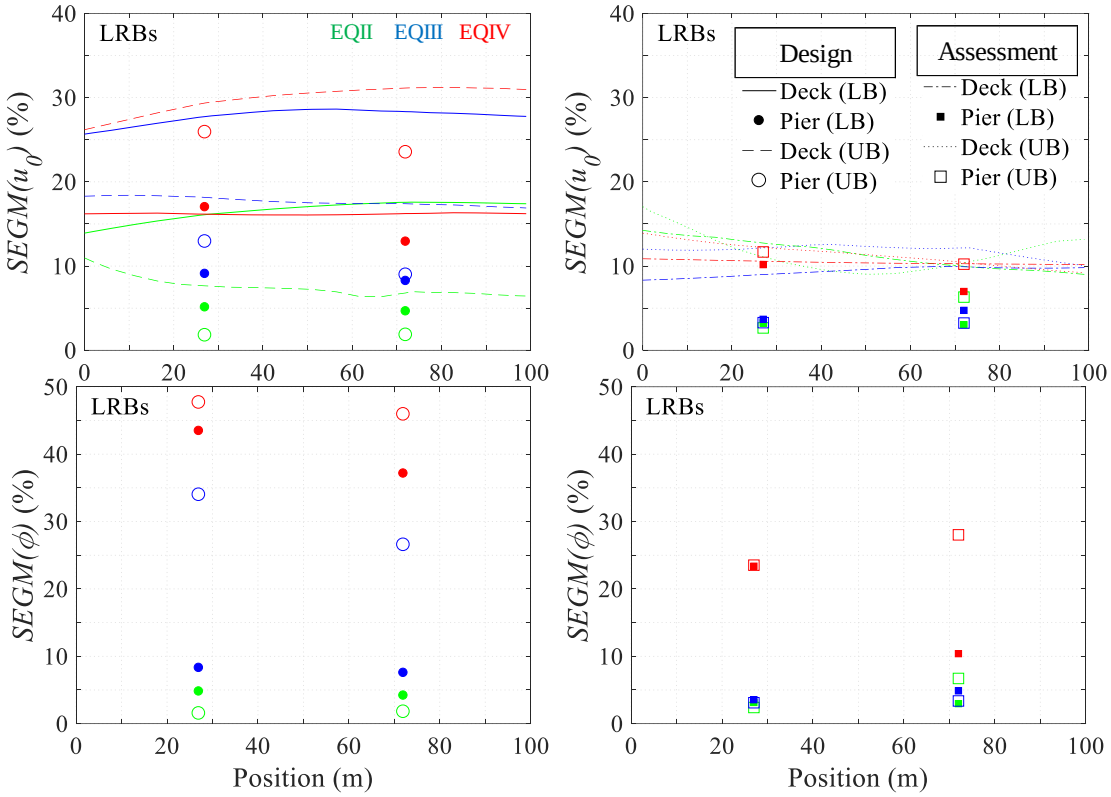

Fig. 5.10 *SEGM* (%) of peak relative (to the ground) deck and pier displacements u_0, and curvatures φ at the pier base derived from design (left) and assessment (right) stages in the case of the LRB scheme

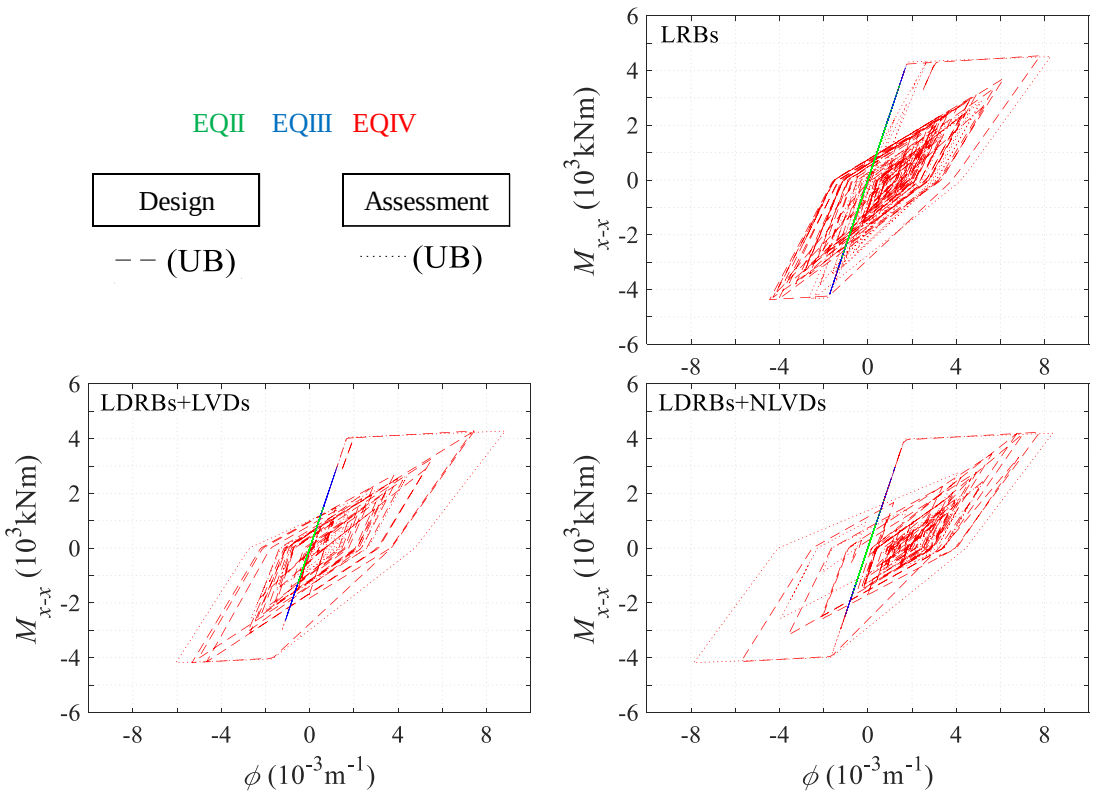

Fig. 5.11 *M-φ* response histories at the base of Pier 1 under *RSN*=776 (design), Art 1 (assessment), and UB-DPs

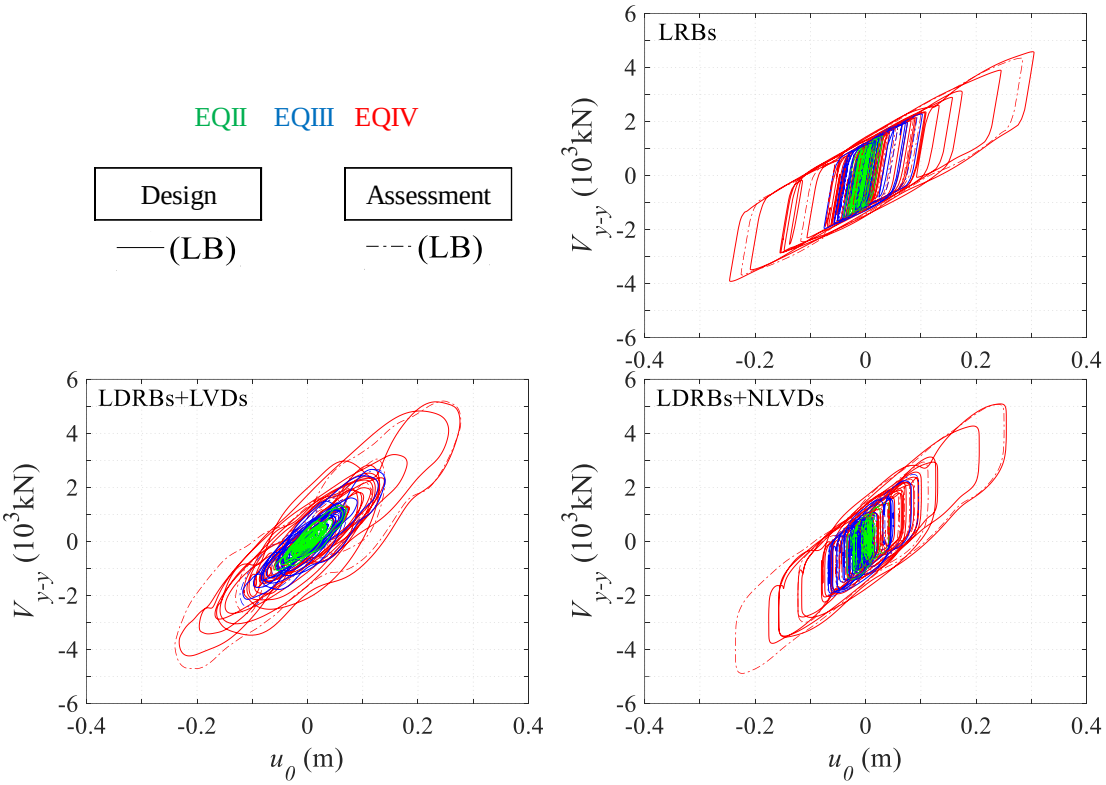

Fig. 5.12 Total shear force V vs. average relative displacement histories u_0 of alternative isolation systems under *RSN*=776 (design), Art 1 (assessment), and LB-DPs

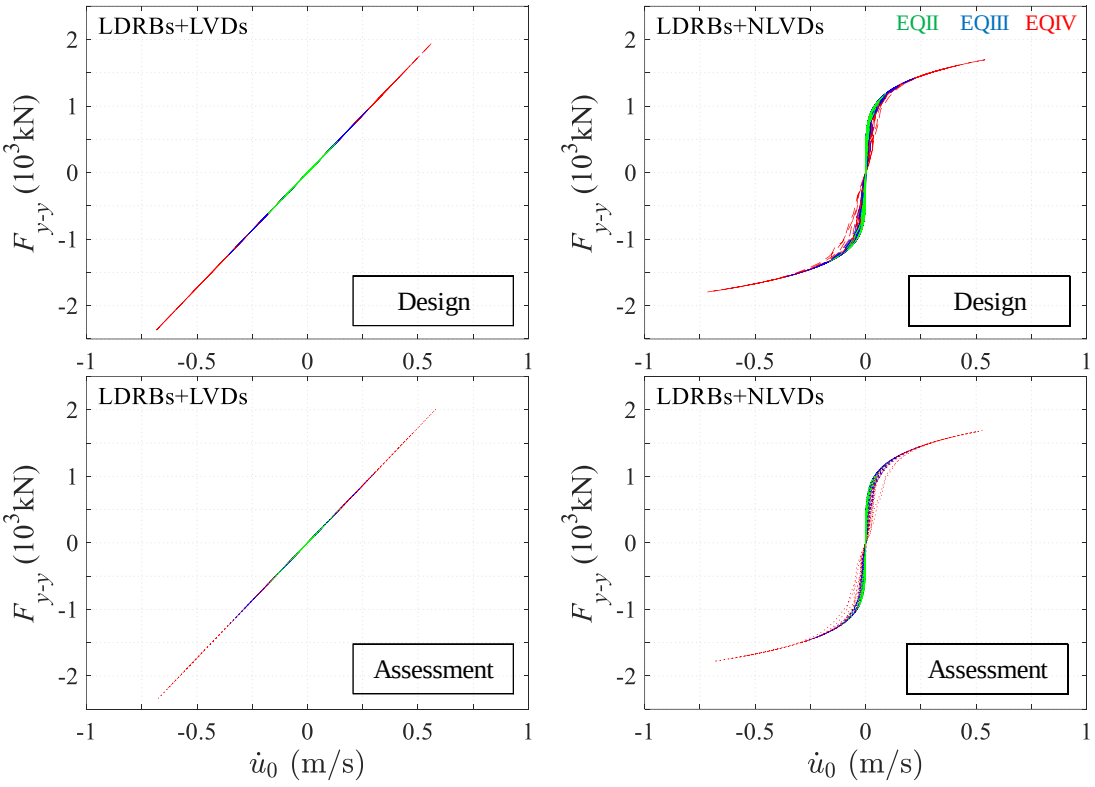

Fig. 5.13 Total damper axial force F vs. average relative velocity $\dot{u}_0$ histories of VD isolation systems under *RSN*=776 (design), Art 1 (assessment), and UB-DPs

PL3 (i.e. SP3 verifications under EQIV in Fig. 5.2) governed in general the design of the bridge in all considered isolation schemes. Specifically, allowable vertical stresses, stability and uplift considerations were found to control the characteristics of the isolators, while the requirement for limited inelastic response controlled the longitudinal reinforcement demand in the piers. The above results deriving from the implementation of Def-BD raise concerns with regard to the EN1998-2 (CEN 2005a) approach of limiting the inelastic response of piers under the 'design' rather than the 'maximum considered' seismic actions. Apart from the relevant safety issues associated with the potentially significant reduction of the effectiveness of the isolation system under a 'very rare' seismic event (i.e. exceeding the 'design actions'), the approach seems inconsistent with the increased reliability required from the isolation system by the same code, i.e. designing isolators under 1.5 times the 'design action' displacements when increased pier ductility demands are expected to distort the proper performance of isolators by reducing their relative displacement. The issue is further discussed in Chapter 6.

5.3.6 Bidirectional Excitation

5.3.6.1 Application of the Def-BD procedure

The isolated bridge described in §5.3 is designed in this section considering the effect of the orthogonal component of seismic action. Due to the fairly similar performance of the alternative isolation systems investigated in §5.3.5 under unidirectional excitation, the LRB scheme was selected herein to demonstrate the implementation of the Def-BD method in the general case when both horizontal components of seismic action are considered. In this respect, the efficiency of the adopted scheme was evaluated using the 'explicit' approach with regard to the variability of the properties of devices during design and assessment (i.e. 'full' set of analyses) aiming at the accurate evaluation of the relevant effects in seismic response among the different designs. In the same context, the basic characteristics (ξ, $\bar{v}_0$, T_p) of the isolation system, and hence the mechanical properties of isolators, were selected to be identical to those adopted during design under unidirectional excitation (Table 5.7), also ignoring long-term isolator deformations due to the permanent and quasi-permanent actions (e.g. prestressing, shrinkage, creep), and thermal actions, to enable direct comparisons. The adopted isolation solution (i.e. $\xi = 0.05$, $\bar{v}_{0,LB} = 0.044$, $T_p = 3.0$ s) is also in good agreement with the 'near-optimal' isolation scheme (i.e. $\xi = 0.05$, $\bar{v}_{0,LB} = 0.048$, $T_p = 3.0$ s) resulting in the minimization of total accelerations defined by plotting Eqs. (4.37), (4.38), and Table 4.7 (i.e. GDEs for bidirectional excitation) in the form of Fig. 5.14. Note that deformations, forces etc. reported in the following for bidirectional excitation represent peak response quantities having an unknown angle (Eq. (4.54)) with respect to the longitudinal axis (x-x) of the bridge, unless otherwise noted (e.g. shear force $V_{x\text{-}x}$ represents shear force recorded along axis x-x). GDEs for bidirectional excitation provide directly peak response estimates (§4.5), while in the case of NLRHA response histories of relevant design quantities along the x-x and y-y axes

were first combined (through vector addition at each time-step, similarly to §4.5.1) prior to obtaining their peak (absolute) values that were subsequently statistically processed (§4.2.4).

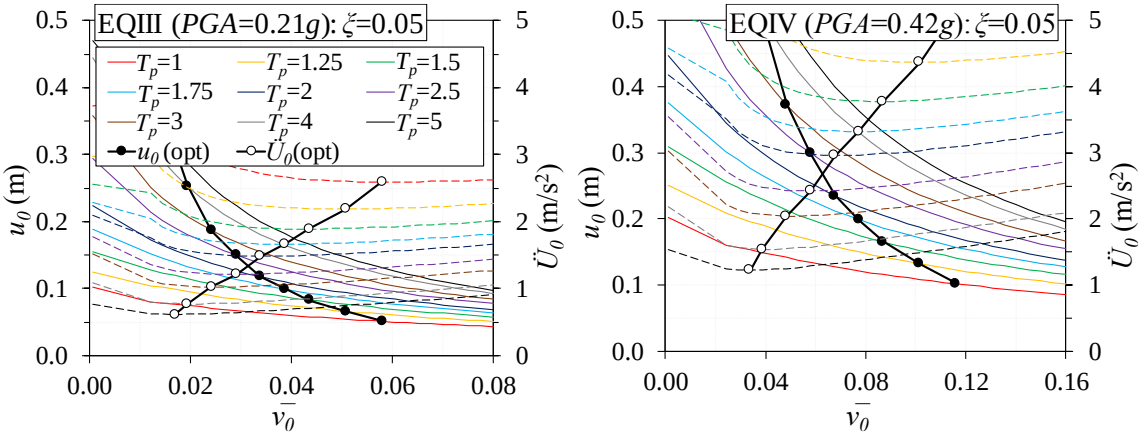

Fig. 5.14 Peak relative displacements u_0 (solid), total accelerations $\ddot{U}_0$ (dashed), optimal peak total accelerations $\ddot{U}_0$(opt) and corresponding relative displacements u_0(opt) of deck under EQIII (left) and EQIV (right) predicted from GDEs under bidirectional excitation

Table 5.9 Comparison of peak responses among RDOF systems optimised for different levels of seismic action

No.	DP	$\bar{v}_0$	T_p (s)	ξ	η	u_0 (m)	$\ddot{U}_0$ (m/s^2)	ξ	η	u_0 (m)	$\ddot{U}_0$ (m/s^2)	Δu_0 (%)	$\Delta\ddot{U}_0$ (%)
		opt EQIII		opt EQIII (1)				EQIV (2)				100·[(2) - (4)] / (4)	
LRBs													
1.1	LB	0.022	3.00	0.05	0.45	0.129	0.77	0.05	0.23	0.363	1.69	41	10
	UB	0.049	2.49	0.05	1.01	0.072	0.98	0.05	0.51	0.216	1.84	49	-6
LRBs (2D)													
4.1	LB	0.022	3.00	0.05	0.45	0.197	1.02	0.05	0.23	0.522	2.30	33	12
	UB	0.049	2.49	0.05	1.01	0.110	1.27	0.05	0.51	0.325	2.45	48	-4
		opt EQIV		EQIII (3)				opt EQIV (4)				100·[(3) - (1)] / (1)	
LRBs													
1.2	LB	0.044	3.00	0.05	0.90	0.086	0.83	0.05	0.45	0.258	1.54	-34	8
	UB	0.098	2.49	0.05	2.02	0.044	1.22	0.05	1.01	0.145	1.97	-39	24
LRBs (2D)													
4.2	LB	0.044	3.00	0.05	0.90	0.132	1.07	0.05	0.45	0.393	2.05	-33	5
	UB	0.098	2.49	0.05	2.02	0.065	1.54	0.05	1.01	0.219	2.55	-40	21

Step 1: In Table 5.9, the estimated peak response of the adopted scheme is presented (i.e. No. 4.2) and compared with the estimated response under unidirectional excitation (i.e. No. 1.2, adopted in §5.3.5), denoting with blue the response that corresponds to the reference seismic action associated with LB-DPs; it is seen that similarly to No. 1.2, the adopted scheme (optimised under EQIV) is expected to develop ~40% smaller u_0 and ~21% larger $\ddot{U}_0$ demand when subjected to EQIII and UB-DPs compared to the optEQIII system (i.e. No. 4.2), and results in ~33% smaller u_0 under EQIV (again compared to No. 4.2). Note also that the ratios of peak response under bidirectional excitation to the response estimates under unidirectional excitation are in the range of 1.48~1.53 for u_0 and 1.26~1.33 for $\ddot{U}_0$, i.e. close to the ratios provided by Eqs. (4.57) and (4.58), indicating

their efficiency for an approximate estimation of seismic action effects under two horizontal components of seismic action.

Using the LB- and UB-DP of isolators and VDs (Table 5.7) in GDEs, the displacement and shear response (Eq. (5.32)) was calculated (shown as Step 1 in Table C.3). Given that the angle of $\ddot{U}_0$ is unknown, the calculated UB shear forces were applied independently to the transverse (denoted as $\ddot{U}_0$ // y-y in Table C.3) and longitudinal direction of the bridge ($\ddot{U}_0$ // x-x) resulting in $\rho_{l,Pier1}$ = 6.9‰, $\rho_{l,Pier2}$ = 9.7‰ in the first case assuming elastic response (i.e. $\mu_{\theta,SP3}$ = 1.0 during the yield moment definition procedure as per §3.2.2), and in $\rho_{l,Pier1}$ = 8.3‰, $\rho_{l,Pier2}$ = 15.0‰ in the second (i.e. adopting $\mu_{\theta,SP3}$ = 1.2), for a pier column diameter equal to D_p = 1.5m. It is noted that the outcome of the Def-BD methodology in §5.3.5 regarding the geometry of the piers (i.e. D_p = 1.2m) was first used, resulting in impractically high reinforcement ratios (i.e. >3.5‰ in Pier 2), hence the diameter was gradually increased to 1.5m. The criticality of the longitudinal direction of the bridge regarding the flexural design of the piers is attributed to the (common) configuration of this straight isolated deck seated on single-column piers, and more specifically to the increase of the equivalent cantilever height h_{eq} of piers in the longitudinal direction approaching the value of the total pier height (i.e. clear column height plus pier cap), as opposed to the transverse direction where the pier cap and the torsional stiffness of the deck partially restrain the rotation of the top end of the piers, reducing h_{eq} and thus the bending moments at the pier base.

Step 2-5: NLRHAs were performed as per §5.2 under the selected suite of pair of records (i.e. HI, HII) scaled using $SF_{EQ}SF_{EC}$ to the level of seismic actions associated with EQII, III, IV (i.e. Steps 2-4) for two incidence angles, θ_{EQ} = 0° and θ_{EQ} = 90° (i.e. 2 DPs × 3 PLs × 2 θ_{EQ} × 7 records = 84 NLRHAs) according to Fig. 5.15 (mean results for each PL are provided in Table C.3, denoting in bold the verifications that were critical for the bridge design).

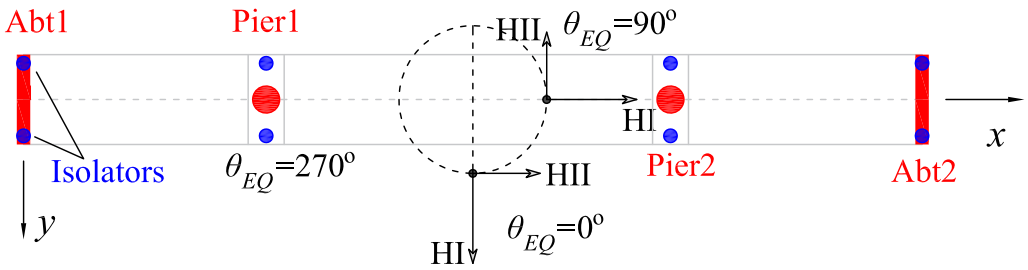

Fig. 5.15 Definition of angle of incidence θ_{EQ} of HI, HII components with regard to the longitudinal (x-x) and transverse (y-y) axes of the bridge: cases considered during the design stage

SP1-SP4 verifications (i.e. Steps 2-5) were in general more demanding compared to the 1D design of the bridge apart from the restoring capability requirements under EQIII (i.e. u_{res} / u_0 criterion) due to the beneficial effect of the increased isolator deformations (§5.2.3). The 'non-yielding' requirement of the piers under EQIII was once more not critical, and the requirement for 'limited inelastic response' under EQIV governed the flexural design of the piers with curvature ductility demand close to the SP3 deformation limits (Table C.3: Row No. 24, 25). The case of θ_{EQ} = 90° was more critical for isolator strains due to lateral deformations (except for bearings located

on top of Pier 2), curvature ductility requirements in the piers, and shear forces in the abutments, as opposed to elastomer strains due to vertical compression, stability of isolators (being in general the most critical verification), and pier shear design, that were critical for θ_{EQ} = 0°. The above can be justified to a certain extent on the basis of the pier response in each direction of the bridge as discussed earlier; in the longitudinal direction piers behave as cantilevers with reduced lateral stiffness compared to the transverse direction (due to the increased h_{eq}), more so in the case of Pier 2 ($h_{Pier2} \geq h_{Pier1}$), resulting along with the inelastic response under EQIV in the reduction of the effectiveness (i.e. the deformations) of isolators, the amplification of bending moments and curvature ductility demands μ_{φ} at the base of the piers, and the increase of the shear forces carried by the abutments. On the other hand, the lever arm of axial forces between isolators of the same pier in the transverse direction of the bridge, increases the applied axial compressive loads rendering critical the stability verification along this direction. In contrast to the expectation that maximum tensile forces would also develop under θ_{EQ} = 0°, the maximum σ_t was recorded for θ_{EQ} = 90° at the location of Abutment 2; this type of apparent inconsistencies, derives from the fact that the angle at which peak response occurs, may vary significantly from the incidence angle of the resultant of seismic components, as shown in §4.5.2 and discussed in more detail in the following.

5.3.6.2 Assessment of design

Assessment of the design presented in §5.3.6.1 was carried out to evaluate the efficiency of the proposed procedure for the three different PLs and the considered range of DPs of devices. The primary objective of the assessment was the detailed investigation of the bidirectional excitation effects on the bridge response under the 'design excitation' similarly to §5.3.5.2; NLRHAs were performed for the Art D suite of artificial records (Table 4.1, Fig. 4.3) used to develop the generalised design equations, scaled appropriately (through SF_{EQ}, §5.3.4) to correspond to different earthquake levels and applied at angles within the range of 0~180° (at an increment of 22.5°) according to Fig. 5.16 (i.e. 2 DPs × 3 PLs × 9 θ_{EQ} × 10 pairs of records = 540 NLRHAs). Fig. 5.17 compares mean estimates of deck and pier peak relative (to the ground) displacements derived from the design and assessment stages, whereas selected mean values of response quantities for the most critical checks are provided in Table C.4 (providing also the critical incidence angle of seismic components θ_{EQ} for each member verification).

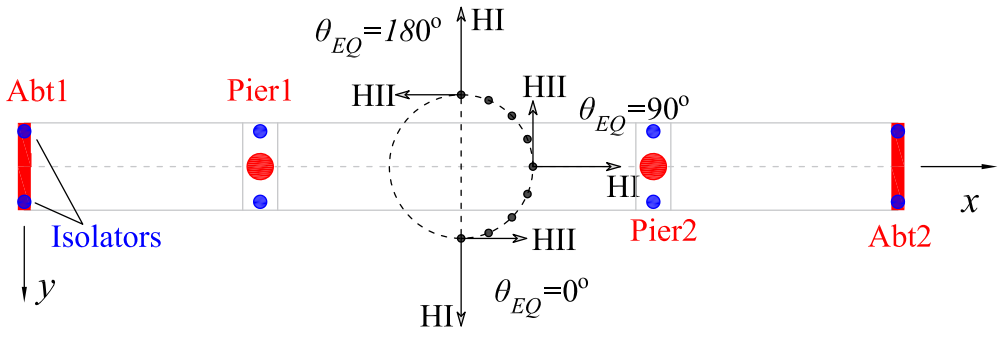

Fig. 5.16 Incidence angles θ_{EQ} investigated at the assessment stage

The design was found safe, in that it satisfied the design criteria associated with each PL. The demand derived from assessment was in general close to that derived at the design stage; relative displacements of the deck presented excellent agreement for LB-DPs (Fig. 5.17) Although displacements along the longitudinal (i.e. $u_{0,x\text{-}x}$) and transverse direction of the bridge (i.e. $u_{0,y\text{-}y}$) are significantly affected by the incidence angle θ_{EQ}, resulting in a wide range of responses, the peak displacements u_o derived from the vector addition of the response histories $u_{0,x\text{-}x}$, $u_{0,y\text{-}y}$ are practically constant. The variation of the angle at which u_0 is developed is evident in Fig. 5.18 where the total shear force of isolators is plotted against the average relative displacement history of devices along the longitudinal and transverse direction of the bridge for a natural (design stage) and an artificial record (assessment stage), and $\theta_{EQ} = 90^o$; despite the relatively close values of u_0 in the resultant response history plot (i.e. vector sum), $u_{0,x\text{-}x}$ and $u_{0,y\text{-}y}$ are differentiated indicating a different angle of peak responses.

An overview of the isolator deformation demand derived from the 540 NLRHAs is presented in the polar charts of Fig. 5.19 where mean values of u_0 are plotted against θ_{EQ} (for each PL) and compared with relevant SP design criteria. Clearly, the SP3 requirement for stability governs the design of the isolators while u_0 exhibits small variations with θ_{EQ} similar to those of deck displacements (Fig. 5.17). The small variation of u_0 with θ_{EQ} is particularly important since it implies that consideration of two (or even one) incidence angles are adequate to assess the deformation demand of the isolation system, even though the critical angle (per isolator and type of verification) generally deviates from the 0^o and 90^o values considered herein during the design stage (Table C.4). The validity of the previous remark covers in general straight bridges irrespective of the structural configuration of the piers so long as their inelastic response is constrained (e.g. different column section, single/multi-column pier), due to the governing effect of the (typically) 'symmetric' isolation interface (i.e. identical mechanical properties along the principal directions of the bridge) over 'non-symmetric' substructures (recall that even the circular single-column piers of the studied bridge exhibit different behaviour along the two axes of the bridge). In cases of 'non-symmetric' passive systems, e.g. dampers with different damping coefficients along the principal axes of an isolated straight bridge, or in general curved-in-plan isolated bridges, a more detailed investigation involving application of the records at a range of critical angles is required.

Isolator u_0 values derived from assessment and LB-DPs were in excellent agreement with relative displacements derived from Step 1 (i.e. GDEs) and subsequent steps of design as shown in Fig. 5.20 and Table C.3 respectively. In this context, verifications critical for LB-DPs (i.e. elastomer strains, stability) yielded similar results, slightly more favourable during the assessment stage. As in the case of unidirectional excitation, noticeable differences in the isolation system response were identified only for UB-DPs (Fig. 5.17) resulting in an overestimation of the restoring capability during design (Table C.3: Row No. 14), however, without violating the u_{res} / u_0 criterion in assessment, due to the beneficial effect of the second component of seismic action in increasing u_0 (Table C.4: Row No. 6). Finally, maximum tensile stresses were found to be reduced during the assessment stage.

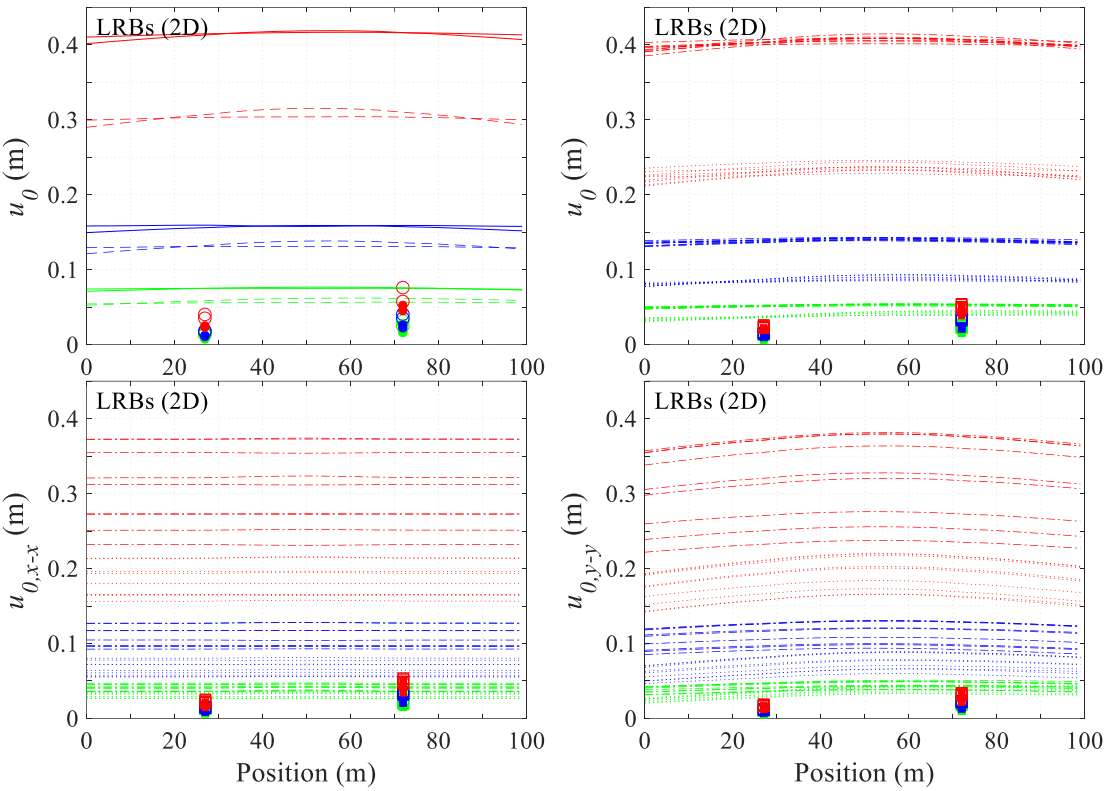

Fig. 5.17 GM of peak relative deck and pier displacements derived from design for θ_{EQ}=0, 90º (top-left), and from assessment for θ_{EQ}=0-180º (top-right, bottom) (legend is provided in Fig. 5.21)

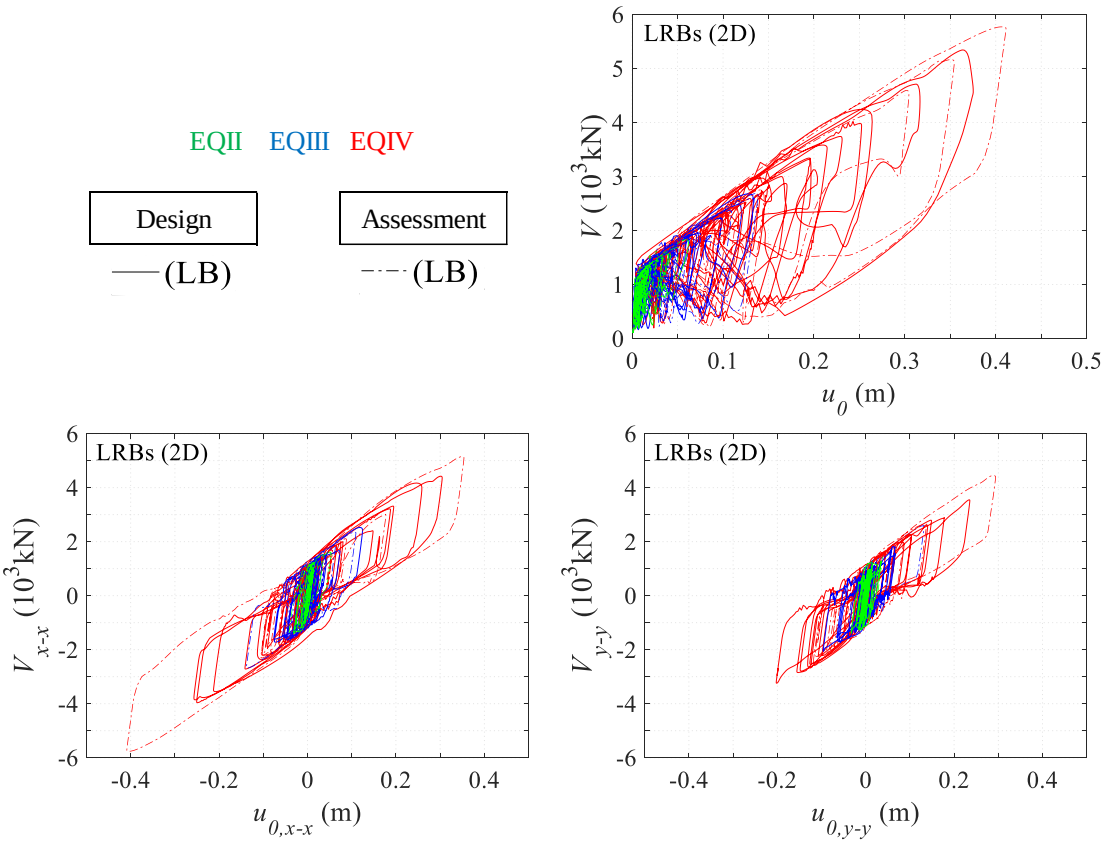

Fig. 5.18 Total shear force V vs. average relative displacement histories u_0 under *RSN*=776 (design), Art 1 (assessment), LB-DPs, and θ_{EQ}=90º

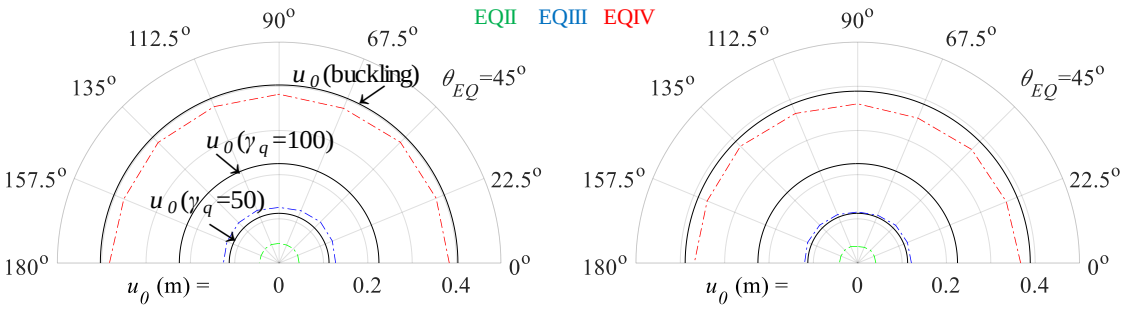

Fig. 5.19 *GM* of peak relative displacements u_0 of isolator located on top of Pier 1 (left) and Pier 2 (right) derived from assessment for θ_{EQ}=0-180° and LB-DPs, compared with SP requirements per PL

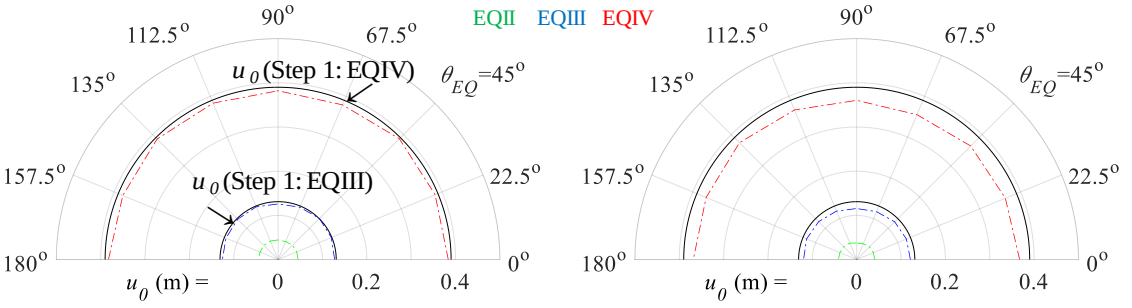

Fig. 5.20 *GM* of peak relative displacements u_0 of isolator located on top of Pier 1 (left) and Pier 2(right) derived from assessment for θ_{EQ}=0-180° and LB-DPs, compared with Step 1 (preliminary design) values

The deviations in UB response indicate that a larger number of records may be required to describe more effectively the 'design seismic action' and increase the reliability of response estimates by reducing *SEGM* values. In Fig. 5.21, it is seen that the Art D suite adopted in assessment was able in most cases to constrain *SEGM* values below 15% apart from the curvature demand at the base of the piers (maximum values near 35%); on the contrary, the suite of natural records used in design resulted in larger *SEGM* values of displacements and pier ductility (the latter, not shown in Fig. 5.21, being close to 100%) and in general larger curvature ductility and shear demand in the piers. A representative example is provided in Fig. 5.22 where *M*-φ response histories about *y*-*y* and *x*-*x* axes are provided for a natural (design) and an artificial record (assessment) at the base of Pier 1 under UB-DPs and θ_{EQ} = 90°. Although the resultant response history mostly displays a seemingly distorted pattern, it provides in a clear and concise manner the maximum ductility requirement along the bilinear envelope *M*-φ curve (derived from section analysis and introduced in the finite element model), as opposed to relevant plots along *x*-*x* and *y*-*y* axes wherein peak inelastic responses cannot be easily identified due to the interaction of yield moments. Considering the polar diagrams of Fig. 5.23 and Fig. 5.24 to summarise analysis results derived from assessment and UB-DPs, it is clear that the SP2 criterion regarding the quasi-elastic response of piers under EQIII is not critical in any of the θ_{EQ} cases.

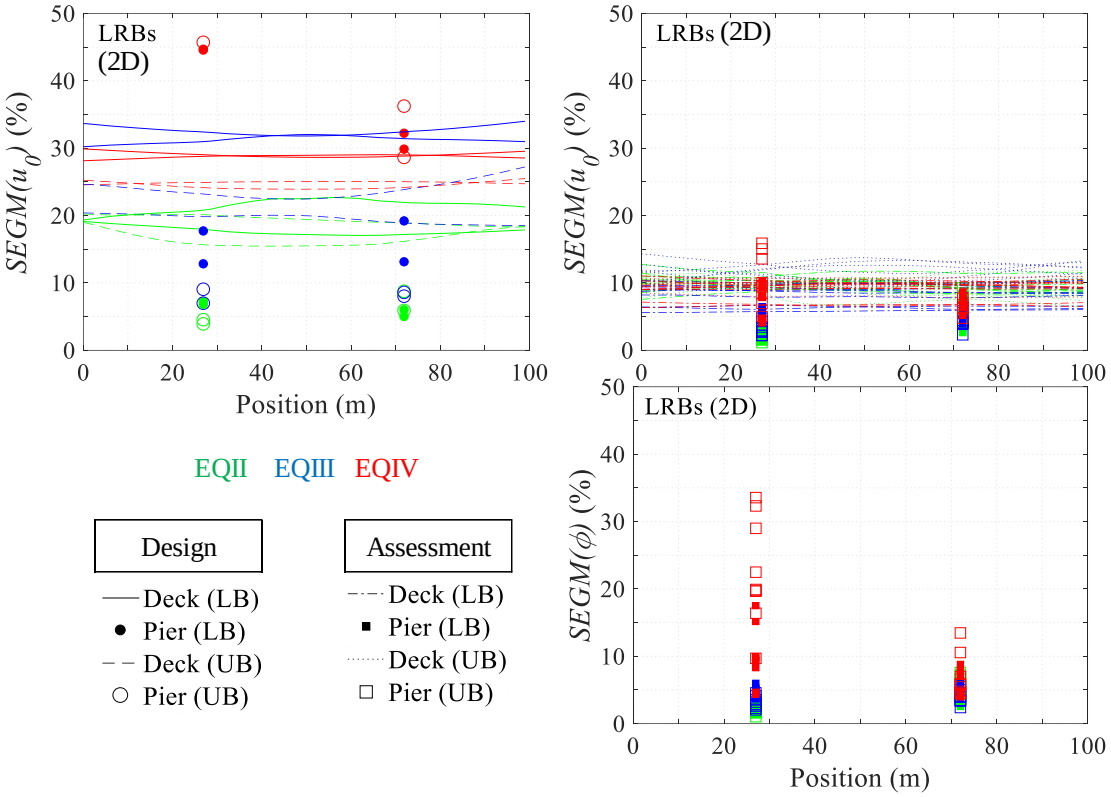

Fig. 5.21 *SEGM* (%) of peak relative deck and pier displacements u_0, and ductilities φ at the pier base derived from design (θ_{EQ}=0°, 90°) (left) and assessment (θ_{EQ}=0-180°) (right) stages

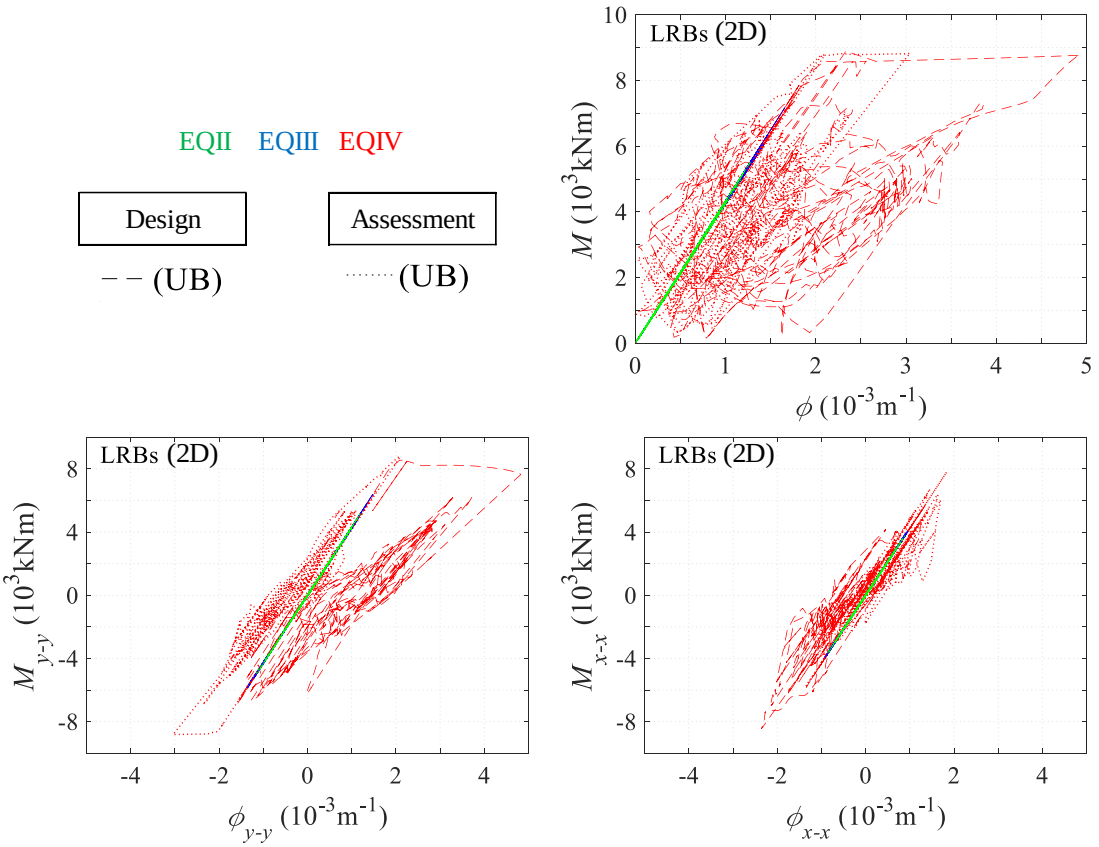

Fig. 5.22 *M-φ* response histories at the base of Pier 1 under *RSN*=987 (design), Art 1 (assessment), θ_{EQ}=90°, and UB-DPs

In fact, bending moments imply elastic response of the piers under EQIV (with adequately restrained *SEGM*(*M*) values, Fig. 5.23), while mean curvatures at the base of piers (Fig. 5.24) indicate limited inelastic response in Pier 1 for θ_{EQ} = 0~135°. It is worth noting here that differentiations in response (elastic according to moments and inelastic based on curvatures) emerge from the problematic definition of mean response when both elastic and inelastic quantities are involved, resulting in mean values of moments and curvatures that do not correspond to the same point in the adopted envelope *M*-φ curve derived from section analysis and subsequently used in NLRHAs. It can be argued that the linear response indicated by moments should be adopted due to their high reliability, or that the critical response quantity should be the mean curvature requirement increased by the associated *SEGM* in a more conservative approach (i.e. the upper confidence interval 1.35φ, obtaining the peak *SEGM*(φ)=35% from Fig. 5.24(left)), but in any case pier curvature demands remain lower than the SP3 limit (ε_c = 3.5-4‰) indicating a potential source of conservatism in the design procedure of §5.2 under bidirectional excitation. Given that the longitudinal reinforcement ratio was defined in Step 1 (§5.3.6.1) without further modifications in the next steps, this is clearly due to differentiations in the base shear estimation-distribution, and the design approach of applying the maximum total acceleration $\ddot{U}_0$ independently to the transverse and longitudinal direction of the bridge. The shears carried by the piers in Step 1 were indeed higher than those of the assessment stage approximately by 10% (Table C.3, Table C.4) which is similar to the case of unidirectional excitation, and hence is not expected to introduce significant conservatism. Furthermore, the maximum pier moment mean values under EQIV and UB-DPs were derived from θ_{EQ} = 90° in both piers (as assumed during preliminary design) but the associated analysis moment (i.e. sample) values developed at angles of θ_M within the range of 0~35° as illustrated in Fig. 5.25, in contrast to the zero θ_M value adopted in design. Similar comments apply for the case of the mean peak curvature derived from a different incidence angle (θ_{EQ} = 67.5°, again due to the problematic mean definition) but with sample peak values developed once more at θ_φ = 0~35° (Fig. 5.26). Note that the application of the base shear calculated in Step 1 (i.e. GDEs) at an angle of 35°, reduced to account for the limited inelastic response of the piers (§3.2.2), would result to a 17% reduction of the required pier longitudinal reinforcing steel.

This type of conservatism cannot be easily eliminated unless a detailed investigation of the effect of the incidence angle is performed, aiming at the identification of the range of θ_M (or θ_φ). Inevitably this will require a significantly increased computational effort; 540 NLRHAs were required to investigate the effect of bidirectional excitation using 10 pairs of artificial records applied at an increment of 22.5° within the range of 0~180°. A large number of analyses will be normally required to suppress standard error values of responses using natural records at the design stage; recall that the suite of 7 records was not able to restrain *SEGM* (φ) values, generally resulting in overestimated ductility demands that were close to the adopted SP3 criteria (Table C.3), and therefore reduction of reinforcement ratios was not allowed. In addition, knowing the range of θ_M does not decisively resolve the issue of selecting a proper angle value, since mean values of moments used in design do not correspond to a specific θ_M while means values of angles are not

statistically meaningful quantities (§4.5.2). In view of the previous considerations the approach of applying $\ddot{U}_0$ independently along the principal axes of the bridge is recommended at the design stage.

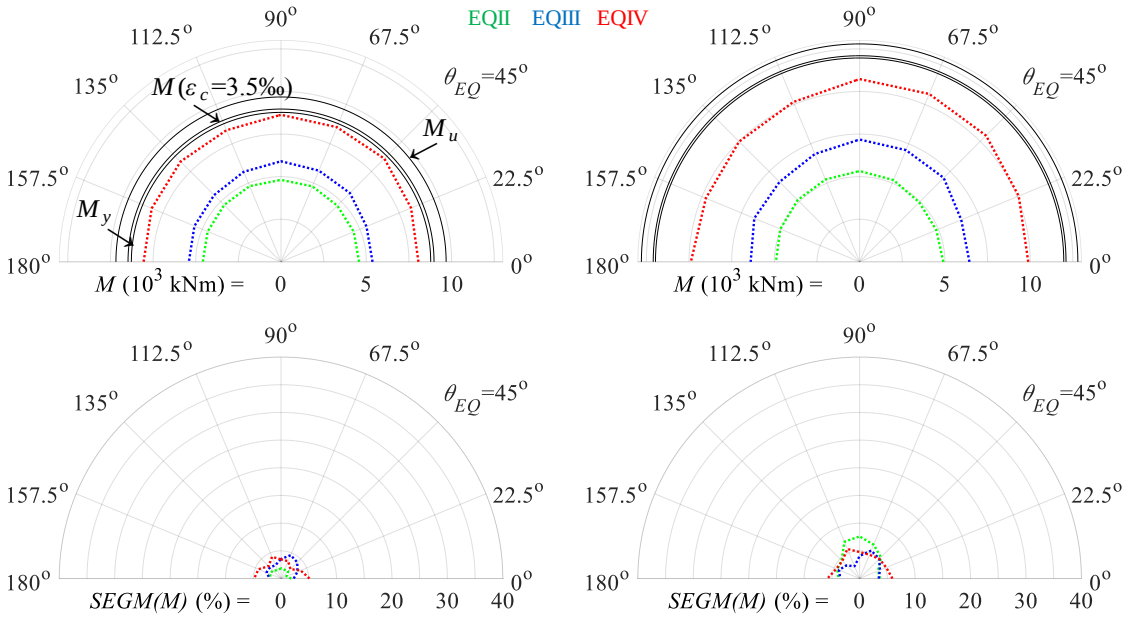

Fig. 5.23 *GM* (top) and *SEGM* (bottom) of moments M at the base of Pier 1 (left) and Pier 2 (right) derived from assessment for θ_{EQ}=0-180° and UB-DPs

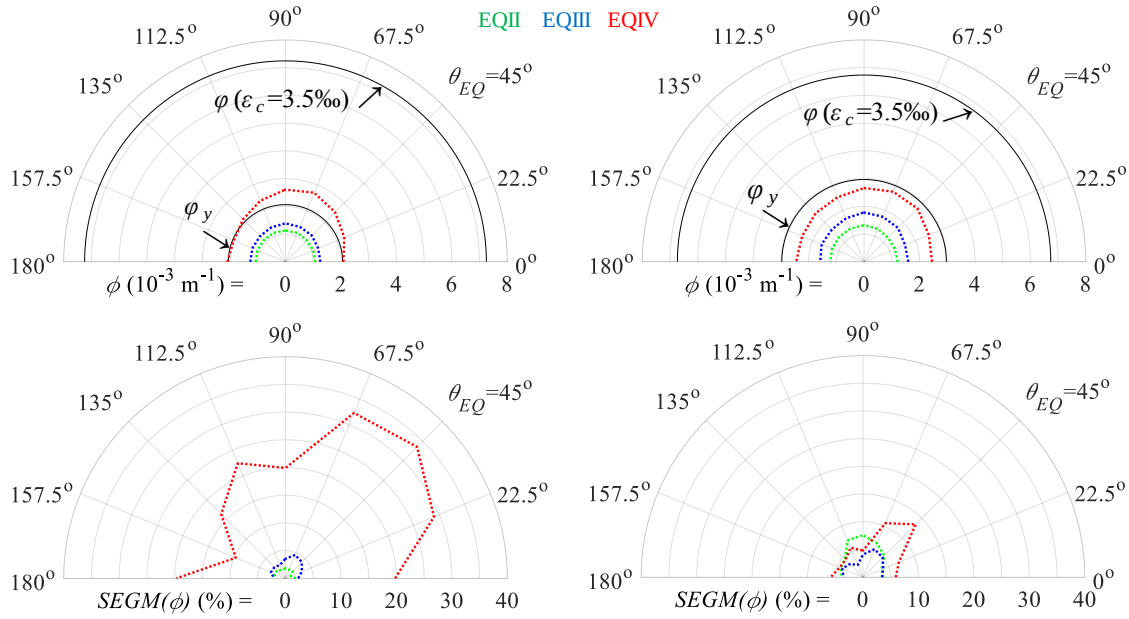

Fig. 5.24 *GM* (top) and *SEGM* (bottom) of curvatures φ at the base of Pier 1 (left) and Pier 2 (right) derived from assessment for θ_{EQ}=0-180° and UB-DPs

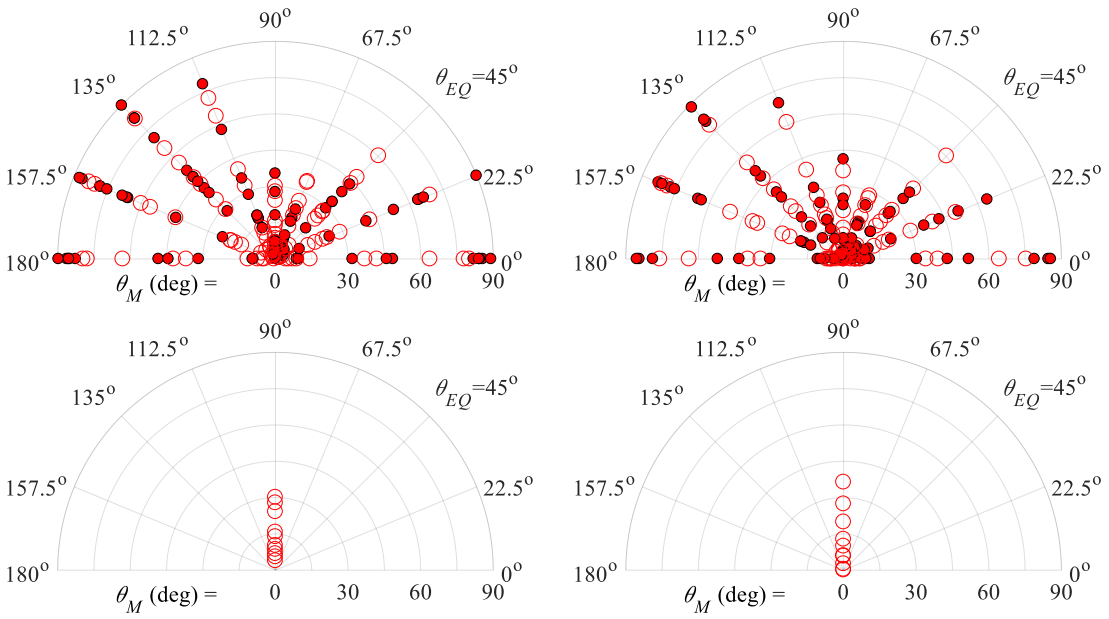

Fig. 5.25 Angles of peak bending moments θ_M at the base of Pier 1 (left) and Pier 2 (right) derived from NLRHA under EQIV (assessment) for θ_{EQ}=0-180°, LB-DPs (solid dots), and UB-DPs (hollow dots)

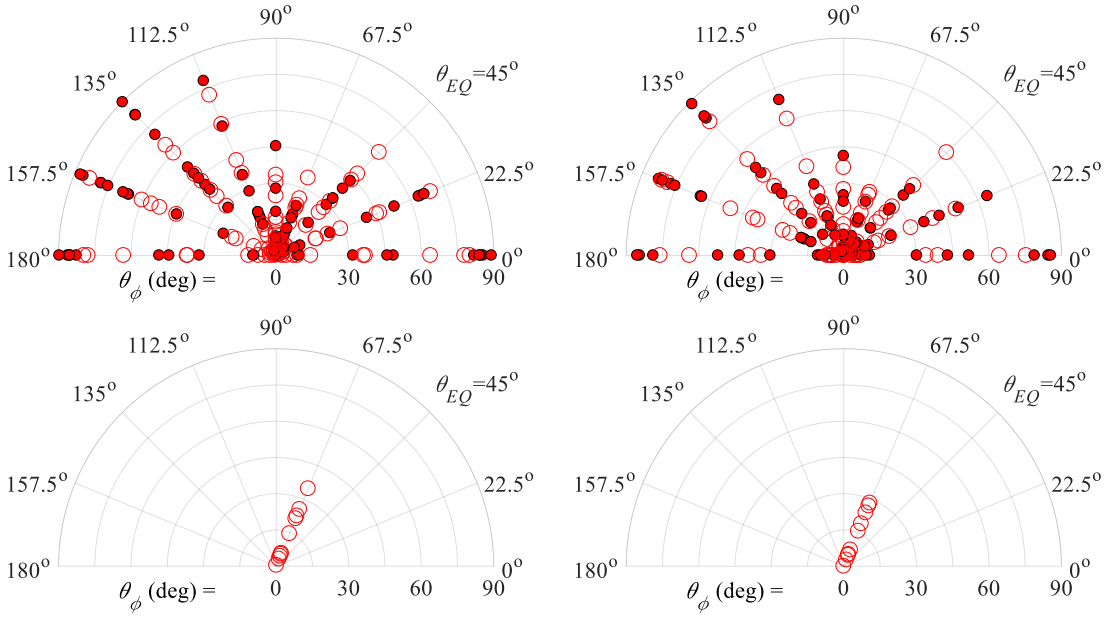

Fig. 5.26 Angles of peak bending moments θ_M at the base of Pier 1 (left) and Pier 2 (right) derived from NLRHA under EQIV (assessment) for θ_{EQ}=0-180°, LB-DPs (solid dots), and UB-DPs (hollow dots)

5.4 Closing Remarks

A *deformation-based design* procedure previously proposed for bridges with energy dissipation in the piers was extended herein to seismically isolated bridges. Aiming at efficient structural design for multiple performance levels, through the control of a broad range of design parameters and the aid of nonlinear dynamic analysis, the suggested procedure initially identifies the basic characteristics of the structural system and subsequently associates design of specific bridge

members and type of verifications with certain performance levels depending on the selected performance objective. Key features of the deformation-based design method for seismically isolated bridges are summarised as follows:

- Considering the inherent weakness of passive devices to optimise the bridge response (i.e. seismic actions effects close to target structural performance resulting in minimum cost) under multiple performance levels due to their fixed mechanical properties, the use of generalised design equations enables the identification of the critical performance level and the comparative evaluation of different isolation schemes at the early stages of design. This provides the designer with the quantitative tools required to select a 'near-optimal' design solution in terms of both economy (e.g. total cost of alternative solutions) and structural performance; it also accounts for additional design constraints associated with the critical states of the isolated system (i.e. states of peak relative displacement, total acceleration, and relative velocity).

- An iterative application of GDEs is introduced during preliminary design to properly capture the effect of nonlinearity of viscous dampers at that stage, as opposed to the case of linear viscous damping devices wherein no iterations are required. In either case, no iterative structural analysis is needed while nonlinear dynamic analysis at subsequent steps deals with certain pitfalls of equivalent linearisation approaches that are based on 'non-physical' effective properties, e.g. non-classical damping systems, estimation of peak velocity.

- Design of substructure members in the general case of bidirectional excitation is performed in preliminary design for the most adverse of the effects derived by independently applying the maximum inertia force $m\ddot{U}_0$ in the principal directions of the bridge. Transformation of the pairs of horizontal components of seismic action into principal components and consecutive application along both directions of the bridge is deemed adequate during the following steps in the case of straight bridges and passive systems with 'symmetric' mechanical properties along the principal directions of the bridge; a more detailed investigation involving application of the records at a range of critical angles of incidence is needed in the case of more complex bridge configurations.

- Enhanced performance objectives reflect the higher performance expected in the case of seismically isolated bridges ensuring the effectiveness of the isolation system under the considered PLs by restraining deformations, providing an adequate restoring capability, and properly considering the intended plastic mechanism of the substructure.

- Further features involve the realisation of the selected scheme through base isolation and energy dissipation devices accounting for the variability of their design properties. An implicit approach for considering variability of DPs reduces the required sets of nonlinear dynamic analyses, noting however, that performing the 'full set' of NLRHAs and designing members using their 'envelope' response ensures in all cases that neither devices nor substructure members are overdesigned.

The validity of the procedure was first investigated by applying it to the transverse direction of the bridge previously used to develop the Def-BD method for 'ductile-pier' bridges. Implementation of the suggested procedure was demonstrated adopting the 'ordinary bridge' performance objective in the cases of three alternative isolation schemes, namely, (*i*) deck isolated with lead rubber bearings (LRBs), (*ii*) low damping rubber bearings (LDRBs) and linear viscous dampers (LVDs), (*iii*) LDRBs and non-linear viscous dampers (NLVDs). The effect of the orthogonal component of seismic action was subsequently explored in the case of the LRB scheme. The following conclusions were drawn from the above investigations:

- Preliminary design displayed significant variations in member response depending on the selected critical performance level, highlighting the significance of the relevant decision along with specific cost implications. EQIV and the associated performance requirements governed in general the bridge design in all considered isolation schemes under both unidirectional and bidirectional excitation. More specifically, allowable vertical stresses, stability, and uplift considerations were found to control the characteristics of the isolators, while the requirement for limited inelastic response and shear design controlled the longitudinal and transverse reinforcement ratios in the piers, respectively. Assessment of designs by NLRHA using suites of artificial records closely matching the design spectrum associated with each PL, revealed that the suggested procedure predicted well the structural response in terms of displacement and shear force demand both at the stages of preliminary design (indicating the effectiveness of GDEs) and the subsequent steps. In addition, Def-BD generally resulted in safe design, in the sense of respecting the adopted design criteria.

- Deviations in response estimations between design and assessment may be introduced due to the implicit approach in considering the variability of design properties, the adopted scaling approach and minimum number of considered records, and due to torsional effects in the deck. In the specific example studied herein, the implicit approach, although more conservative, did not result in overdesigning members and devices. Although the adopted scaling approach resulted in displacement estimates close to those derived from the assessment using artificial records (involving less computational effort compared to the approach used in the 'ductile-pier' bridge), the suite of 7 natural records (as commonly required by codes) was not in general able to restraint standard error values of mean responses below the adopted limit of 15%, resulting in overestimations of local ductility demands. The substructure had a minor effect on the peak response of the isolation system.

- Among the isolation schemes investigated under unidirectional excitation, i.e. LRBs, LDRB+LVDs, and LDRB+NLVDs, the second resulted in slightly lower seismic demand in the piers compared to the LRB option due to the adopted reduced yielding stress of the lead core in the abutment isolators. Besides providing a safeguard mechanism against excessive structural velocities, introduction of nonlinearity in viscous dampers effectively constrained peak damper forces according to the set target performance without significantly affecting the

overall bridge response. A relatively lower seismic demand was found for the bridge type and seismic scenario considered herein, resulting in further reduction of the pier longitudinal reinforcement compared to the LVD case. In addition, all isolation schemes resulted in lower pier reinforcement demand compared to the design for ductile response, indicating that optimally selected isolation systems can provide significant cost reductions in substructure design while satisfying a higher performance objective. In this context, seismic isolation may emerge as an appealing design alternative, if reduction in the life-cycle cost of the bridge is taken into account.

- Implementation of the method in the case of the LRB scheme under *bidirectional* excitation revealed the efficiency of the procedure in predicting the deformation response of the isolation system. In particular, small variations of peak deformations with the incidence angle indicate that consideration of the horizontal seismic components of pairs of records along the two axes of the bridge can adequately assess the deformation demand in isolation systems with symmetric distribution of mechanical properties, despite the fact that the exact value of the critical incidence angle (per isolator and type of verification) was found in general different from the values considered in design (i.e. 0^o and 90^o). Although the design methodology predicted well the shear forces developed in the piers, flexural design for the most adverse of the effects derived by independently applying the maximum inertia force in the two directions of the bridge, resulted in conservative design with regard to pier longitudinal reinforcement assessed in the order of 1-17%. Nevertheless, this design approach is recommended unless a detailed investigation of the effect of the incidence angle is performed involving a large number of analysis sets.

- Apart from achieving robust designs satisfying multi-objective structural performance criteria under different levels of seismic action, implementation of the suggested procedure further revealed some inherent weakness of the 'force-based' provisions in EN1998-2 (CEN 2005a) and other codes. These refer to the adequacy of seven records in predicting the mean response when upper limit spectral deviations and excessive variability are not addressed (discussed in a previous comment), and the limitation of the inelastic pier response in isolated bridges under the 'design' rather that the 'maximum considered' seismic actions. The latter, apart from raising safety issues, seems inconsistent with the increased reliability required from the isolation system by the same code.

- Although movement of the deck was allowed in both directions of the bridges that have been investigated so far using passive systems with identical properties along the principal axes of the bridge, the extension of the procedure to different configurations is deemed quite straightforward. Such cases may involve decks supported on moveable bearings in the longitudinal direction, but restrained in the transverse direction via seismic links (i.e. common configuration in railway bridges), or placement of dampers with different properties along the longitudinal and transverse axes of the bridge. In the former case, preliminary design of the

isolation system and the piers in the longitudinal direction of the bridge should be performed according to the first step of the procedure for isolated bridges (§5.2.2). The strength in the piers should be defined from the most adverse of the effects derived by applying a response spectrum analysis similarly to the preliminary design of 'ductile-pier' bridges (§3.2.2), and the maximum inertia force $m\ddot{U}_0$ transferred to the substructure through the isolation system in the longitudinal direction, allowing for some limited inelastic response depending on the adopted performance objective. Non-symmetric damping properties should be dealt by calculating peak inertia forces per direction of the bridge using GDEs for bidirectional excitation (along with the relevant damping ratios), prior to applying them independently in the relevant direction. A detailed investigation of the effect of bidirectional excitation (using a range of incidence angles) will be required in both previous cases.

Chapter 6
Comparison of Def-BD with Alternative Design Procedures

6.1 Introduction

A comparison of the designs resulting from the application of the *deformation-based design* (Def-BD) method for 'ductile-pier' and seismically isolated bridges, with 'standard' code-type design procedures, is sought in this chapter with a view to assessing both the structural performance and the economy of design focusing mainly on the piers, the deck, and the base isolation/energy dissipation devices. Specifically, in the case of bridges with ductile behaviour, the seismic performance of the bridge designed in §3.3 for the seismic hazard zone ZII is compared in §6.2 with the performance of the actual bridge (Egnatia Motorway 2002) designed according to a code (EPPO 2000) that is similar to EN1998-2 (CEN 2005a) with regard to the engineering aspects that are under investigation herein, thus representing 'standard' design according to European practice, denoted hereafter as *code-based design* (Code-BD). Def-B designs for ZII, III (§3.3) are also compared in §6.2 with the design outcome derived from the application of a different performance-based design procedure, namely the *modal direct displacement-based design* (MDDBD) method, in the same bridge (Kappos *et al*. 2013). Considering the case of the bridge isolated with lead rubber bearings (LRBs) and accounting for the effect of bidirectional excitation, comparisons between Def-BD (§5.3.6) and EN1998-2 (CEN 2005a) are made, following the design (and assessment) of the studied bridge according to Eurocode 8 in §6.3. In addition, inherent deficiencies of code-type methods identified during the application of Def-BD in Chapters 3, 5, are further discussed in §6.2, 6.3, respectively.

6.2 Bridge Designed for Ductile Behaviour of the Piers

6.2.1 Description of studied bridge

The selected structure (i.e. Overpass T7 in Egnatia Motorway, N. Greece) (Fig. 3.6) is described in §3.3.1 along with relevant assumptions adopted to ensure consistency among Def-BD, Code-BD, and MDDBD. In summary, the transverse response of the bridge was investigated adopting the 'ordinary bridge' performance objective (PO) (Fig. 3.2), while the gap between the deck and the abutments was treated as a design parameter in all three design cases; i.e. in the case of Code-BD (corresponding to the 'as-built' state of the bridge) the relevant gaps of the actual bridge provided in §3.3.1 were ignored during assessment (§6.2.5) adopting the non-activated seat-type abutment (Table 3.1). The design of the deck under 'non-seismic' load combinations was obtained from Egnatia Motorway (2002), and adopted as the starting point in all design cases, i.e.

considering identical geometry and detailing. Seismic action effects on the deck are discussed in the following sections.

6.2.2 Modelling issues and numerical evaluation of dynamic response

Nonlinear response history analyses (NLRHAs) required only for assessment purposes in the case of MDDBD (Kappos *et al*. 2013) and Code-BD (§6.2.5) were performed according to §3.3.2. Likewise, member limit deformations associated with each structural performance (SP) level were defined during assessment in accordance with the same section (§3.3.2) and Table 3.1.

Moment-curvature (M-φ) analysis of the *A*-*A* deck section (Fig. 6.7), i.e. next to the pier, was performed in order to evaluate the seismic performance of the superstructure with the aid of the 'built-in' SECTION DESIGNER (SD) utility of SAP2000 (CSI 2015) adopting the material stress-strain laws provided in §3.3.2. The detailing of section *A*-*A* and the section modelled in SD (CSI 2015) are presented in Fig. 6.1; it is noted that tendons were not modelled since the prestressing effect was considered as part of the external actions, whereas confinement of the concrete within the web of the box girder section was ignored. The latter assumption was adopted for the sake of simplicity (evaluation of the ductility capacity was not an issue in this investigation) as it is expected to have a minor effect on the flexural strength and initial stiffness of the deck section required to assess the relevant SP design criteria, i.e. cracking and yielding under EQ(SP3) and EQ(SP4), respectively (§3.2).

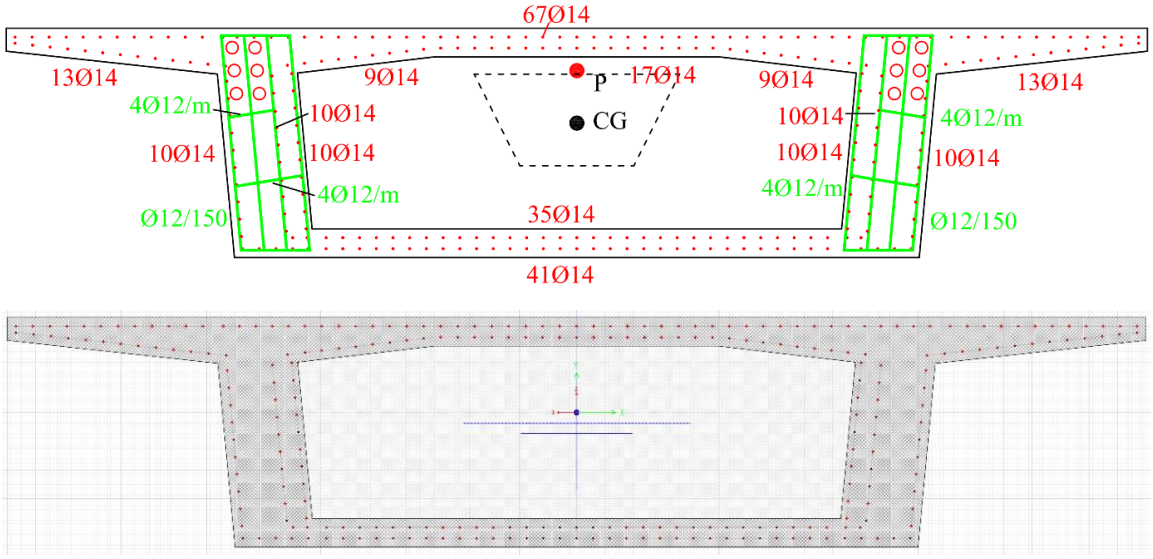

Fig. 6.1 Detailing of Overpass T7 deck section *A*-*A* (top) and section modelling in SD (bottom)

6.2.3 Target spectra and representation of seismic action

As opposed to Def-BD cases that included explicit verifications under multiple performance levels (PLs) and associated seismic actions (defined according to §3.2.1, 3.3.3, 3.3.4), Code-BD and

MDDBD designs involved response spectrum analysis (RSA) under a single target spectrum associated with T_R = 475yrs in Fig. 3.9 (i.e. EQIII). Code-BD was performed for a seismic hazard zone associated with a *PGA* of 0.14*g* (denoted as ZI), whereas zones ZII (*PGA* of 0.21*g*) and ZIII (*PGA* of 0.31*g*) were considered in MDDBD, similarly to Def-BD (§3.3.3). During the assessment stage, the inconsistency in the level of the design seismic actions was treated according to §6.2.5, while different levels of seismic actions, represented by the artificial records described in §3.3.4 (Fig. 3.12), were defined by Eqs. (3.5)-(3.7).

6.2.4 Application of design procedures

Following the philosophy of code-type approaches, explicit verifications during design in Code-BD and MDDBD approaches involved the evaluation of 'life-safety' verifications (e.g. SP3 requirements in Table 3.1) under the design seismic actions (i.e. EQIII for ordinary bridges); 'operationality verifications were considered to be met when 'life-safety' verifications were satisfied while capacity design principles were introduced to ensure the formation of the intended plastic mechanism and the avoidance of brittle modes of failure up to a level of seismic action associated with the ultimate flexural strength of plastic hinge zones.

Code-BD represents a 'force-based' approach typically included in design codes worldwide. Following the definition of member stiffness (flexural stiffness of the deck corresponding to gross sections and reduced pier stiffness accounting for cracking in line with CEN 2005a), a response spectrum analysis is first performed under the 'design spectrum' properly reduced by the 'behaviour factor' q to implicitly consider the reduction of seismic action effects due to inelastic action as a function of the selected structural configuration of the bridge, the axial load ratio and the shear span ratio of the piers, and the accessibility of the intended plastic hinge zones. Analysis results are subsequently used for the flexural design of the dissipating zones in the piers along with transverse reinforcement detailing rules aiming at predefined curvature ductility levels (i.e. confinement requirements according to CEN 2005a), while flexural design of members (or member zones) expected to remain elastic, and shear design are performed on the basis of capacity design (CEN 2005a). Seismic displacements required in dimensioning of bearings, clearances etc. are obtained from RSA under the elastic (i.e. q = 1) spectrum so long as a reasonable convergence between member stiffness assumed prior to analysis and stiffness based on the provided strength is achieved, otherwise iterative application of the method (analysis and design) is required (i.e. when the required strength is significantly higher than the assumed value used to estimate the stiffness of piers, according to EN1998-2). As noted earlier, Code-BD corresponds to the 'as-built' state of the bridge, hence, the design was not preformed within this study; rather, the outcome of the 'actual' design of the bridge was adopted herein for assessment purposes.

The MDDBD method, briefly described in §2.2.1, represents an extension to the standard '*direct displacement-based design'* method (Priestley *et al*. 2007) required to properly capture the effect of higher modes, a feature of significant importance in the studied bridge due to the increased

contribution of the second mode in the seismic response. Details on the MDDBD methodology regarding the involved design assumptions, steps, identified limitations, and a detailed presentation of its implementation in the same bridge considering a single PL (i.e. 'life-safety' verification under EQIII) can be found elsewhere (Kappos *et al*. 2012a, 2013, Kappos 2015a). Although a different SP3 requirement was assumed for the flexural design of the piers in Kappos *et al*. (2013) (i.e. a target column drift equal to 3%) as opposed to strain-based criteria adopted in Def-BD (SP3 requirements in Table 3.1), results from the two procedures are directly comparable due to the fact that the allowable shear strains (i.e. γ_q = 2.0) in the elastomer of the low damping rubber bearings located at the abutments (identical in Def-BD, MDDBD, Table 6.1) governed the bridge design in both approaches. Shear design and detailing for confinement in MDDBD were performed on the basis of capacity design principles and prescriptive detailing rules, respectively, as in Code-BD.

Design results obtained from the application of the Def-BD (§3.3.5), the Code-BD (Egnatia Motorway 2002), and the MDDBD (Kappos *et al*. 2013) procedures are summarised in Table 6.1, noting that the deck geometry and detailing are identical in all considered cases. Immediately perceived from the results presented in Table 6.1, is the significant conservatism adopted in the case of Code-BD (ZI) resulting in pier dimensions and detailing similar to the MDDBD outcome

Table 6.1 Design outcome derived from different methodologies

Method	Zone	Member	Section (m)	h or t_R [1] (m)	$\rho_{l,req}$ [2] (‰)	A_l [3] (cm^2)	ρ_l [3] (‰)	$Vol.,_l$ [4] (m^3)	Bars	ρ_w [3] (‰)	$Vol.,_w$ [5] (m^3/m)	Hoops (per mm)
Def-BD	ZII	Pier 1	D_p = 1.2	5.94	9.7	118	10.4	0.229	24Ø25	12.4	0.021	Ø16/60
		Pier 2	D_p = 1.2	7.93	10.2	118	10.4		24Ø25	10.6		Ø16/70
		LDRB [6]	0.35×0.45	0.088	-	-	-	-	-	-	-	-
	ZIII	Pier 1	D_p = 1.7	5.94	12.5	285	12.5	0.481	58Ø25	13.2	0.047	2Ø16/75
		Pier 2	D_p = 1.7	7.93	9.2	216	9.5		44Ø25	10.4		2Ø16/95
		LDRB	0.35×0.45	0.088	-	-	-	-	-	-	-	-
Code-BD	ZI	Pier 1	D_p = 2.0	5.94	-	471	15.0	0.918	96Ø25	9.8	0.055	(Ø16+14) /75
		Pier 2	D_p = 2.0	7.93	-	471	15.0		96Ø25	9.8		(Ø16+14) /75
		LDRB	0.35×0.45	0.044	-	-	-	-	-	-	-	-
MDDBD	ZII	Pier 1	D_p = 1.5	5.94	9.8	177	10.0	0.391	36Ø25	9.1	0.026	2Ø14/95
		Pier 2	D_p = 1.5	7.93	12.4	221	12.5		45Ø25	7.9		2Ø14/110
		LDRB	0.35×0.45	0.088	-	-	-	-	-	-	-	-
	ZIII	Pier 1	D_p = 2.0	5.94	11.5	363	11.6	0.960	74Ø25	10.4	0.058	2Ø16/80
		Pier 2	D_p = 2.0	7.93	19.0	599	19.1		122Ø25	10.4		2Ø16/80
		LDRB	0.35×0.45	0.088	-	-	-	-	-	-	-	-

[1] h : clear height of pier, t_R : total rubber thickness

[2] Required reinforcement at the base of the pier

[3] Provided reinforcement at the base & top of the pier

[4] Provided volume of reinforcing steel

[5] Provided volume of reinforcing steel per metre of column length

[6] Low damping rubber bearing

under a significantly higher level of seismic action (i.e. ZIII). This level of conservatism is by no means specific to the 'code-type' approach followed in Code-BD; potential sources such as the control of pier longitudinal reinforcement ratios ρ_l by 'non-seismic' load combinations or minimum code requirements, and the directional combination of responses along the principal axes of the bridge (in the actual design as opposed to Def- BD and MDDBD cases focusing on the transverse response only) can hardly justify the overestimation of steel and concrete area demand depicted in Table 6.1. On the contrary, in the studied case the above conservatism should be attributed to the common (and on the safety side) approach adopted by several designers of overdesigning members (e.g. by adopting conservative assumptions regarding the directional combination, higher minimum steel requirements and/or lower behaviour factors than the values prescribed in the code), and to the multilevel reviewing process of the design required by the owner/state (as in this case), usually resulting in the adoption of the envelope 'requirements' derived from different reviewers/designers, perhaps more so in the case of 'small' bridges where the above approaches do not normally result in onerous cost increase with regard to the overall construction cost. Although the above obstruct (if not render impossible) a comparison between Code-BD and the other approaches in terms of economy, it offers the ability to assess the attained seismic performance of a bridge designed according to European practice (§6.2.5). Considering the design cases that can be directly compared in terms of both economy and structural performance, Def-BD yielded notable reductions in pier longitudinal reinforcing steel (w_{sl}), transverse steel (w_{sw}), and concrete (w_c) weight (or volume) compared to MDDBD, equal to Δw_{sl} = 41%, Δw_{sw} = 17%, Δw_c = 36% in the case of ZII, and Δw_{sl} = 50%, Δw_{sw} = 20%, Δw_c = 28% in the case of ZIII, noting that in MDDBD the transverse reinforcement was governed by shear design performed in accordance with capacity design principles (as adopted in current codes).

6.2.5 Assessment of Code-BD and comparison with Def-BD

Assessment of the structures resulting from Def-BD (under EQII-IV) and MDDBD (under EQIII) are presented in detail in §3.3.6 and Kappos *et al*. (2013), respectively. Herein, with a view to enabling meaningful and consistent comparison between the cases of Def-BD (ZII) and Code-BD (ZI) (i.e. designed for different levels of seismic actions (§6.2.3), assessment of Code-BD was performed in terms of a normalised intensity measure A / A_d, where A corresponds to the intensity measure considered (i.e. *PGA* of $\ddot{u}_{g0}$), and A_d is the design intensity (corresponding to EQI, Fig. 3.2), i.e. the *PGA* that causes the first yielding in the bridge which in design terms means that the pier with the lowest ρ_l reaches its flexural design strength M_{Rd}. Another important issue dealt with the previous approach is the conservatism adopted during design in the Code-BD case as described in §6.2.4. Considering the cases studied herein, A_d corresponds to a *PGA* of 0.05g in Def-BD (ZII), and 0.12g in Code-BD implying an adopted behaviour factor of 1.2 (instead of the value 3.1 allowed by the code) and indicating the significant overdesign of the piers in the actual bridge, given that Code-BD was performed for a lower seismic zone than Def-BD. The efficiency of each

design was examined under three different levels of seismic actions defined with respect to the normalised intensity measure A / A_d and the assumptions adopted in the Def-BD case (§6.2.3), i.e. EQII (A / A_d = 2.3), EQIII (A / A_d = 4.5), and EQIV (A / A_d = 9.1). Def-BD (ZII) and Code-BD results derived from the above assessment procedure, are discussed in the following with regard to the 'ordinary bridge' seismic performance objective (§3.2.1), i.e. SP2 verifications under EQII, SP3 verifications under EQIII, and SP4 verifications under EQIV. In this context, violated performance requirements reported for the actual bridge refer to the bridge assessed for the normalised seismic actions, hereafter referred as Code-BDn to differentiate it from the response of the bridge under non-normalised seismic actions (Code-BD, Egnatia Motorway 2002) (not presented herein) where all code requirements under the 'design' seismic action were satisfied.

In Fig. 6.2, the displacement envelopes derived from design and assessment of Code-BDn are compared with those computed during the implementation of Def-BD (ZII) (reproduced here for ease of reference). Likewise, Fig. 6.3-Fig. 6.5 provide chord rotation demands in the piers under the normalised levels of seismic actions along with allowable deformation limits (SP requirements); additional design quantities for the case of Code-BDn are provided in Annex D (i.e. Table D.1). Increased drifts (Table D.1 vs. Table A.1) and displacements (Fig. 6.2) were recorded in the case of Code-BDn for all three considered PLs. Pier chord rotation limits were satisfied in the case of Pier 2 under EQII, in both piers under EQIII, and violated in all other cases, while shear resistance was found inadequate under EQIV. The above remarks (regarding the pier flexural response) are also illustrated in Fig. 6.6 where flexural damage in the piers, quantified by a damage index (DI) equal to the ratio of the required rotational ductility factor μ_θ over the maximum allowed rotational ductility factor $\mu_{\theta,SP4}$, is plotted against the normalised intensity measure A / A_d, and compared with 'allowable damage' corresponding to SP deformation limits; i.e. DI(EQi) > DI(SPi) and DI(EQIV) > 1 suggest a violation of the relevant SP requirement and member failure, respectively. Bearing strain deformation limits were generally violated under the normalised seismic actions (Table D.1), indicating that the design of the actual bridge (Egnatia Motorway 2002) was conservative with regard to the design of piers but not the design of bearings.

Similarly to SP4 requirements in Def-BD (§3.2.4, 3.2.5), modern codes (e.g. CEN 2005a, AASHTO 2011, Caltrans 2013) require an explicit verification that the 'capacity protected' deck remains elastic when the adjacent components of the bridge energy dissipation system (e.g. the pier ends) reach their overstrength. EN1998-2 (CEN 2005a) in particular, requires that no significant yielding occurs in the deck under the capacity design effects determined from equilibrium conditions at the intended plastic mechanism, when all intended flexural hinges develop an upper fractile of their flexural resistance (i.e. their overstrength). A general procedure for the estimation of the capacity design effects in each principal direction of the bridge considering both signs of the seismic action is provided in Annex G of EN1998-2 (CEN 2005a). With a view to evaluating the requirement of no significant yielding in the case of Code-BD, the EN1998-2 (Annex G) (CEN 2005a) procedure was applied in the bridge considered herein, and its efficiency was subsequently explored by NLRHA in Gkatzogias & Kappos (2016a). Some interesting remarks derived from the

previous study, relevant to implications emerging from the application of code-type procedure compared to Def-BD, are summarised in the following in order to facilitate discussion in §6.2.6.

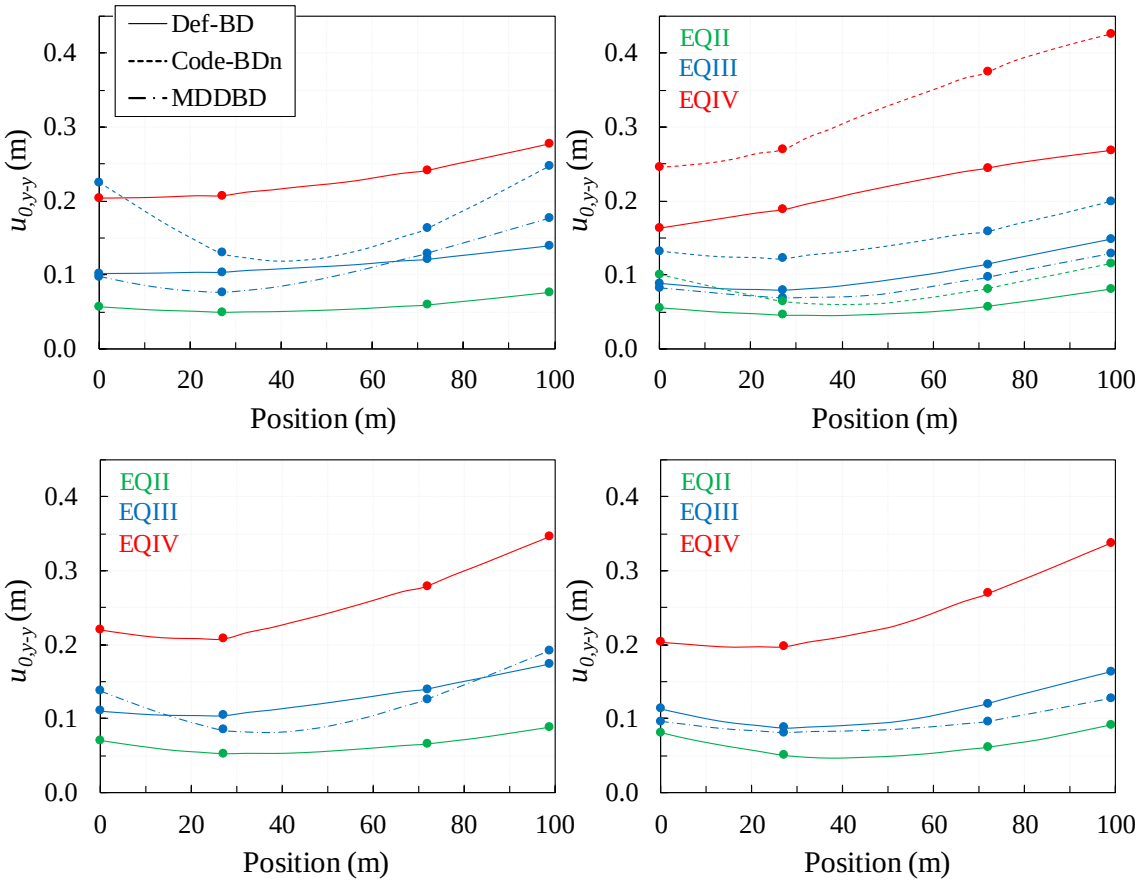

Fig. 6.2 Peak displacement demand $u_{0,y\text{-}y}$, derived from design (left) and assessment (right) of Def-BD (ZII), Code-BDn, MDDBD (ZII) (top), and Def-BD (ZIII), MDDBD (ZIII) (bottom) under EQII, EQIII, EQIV

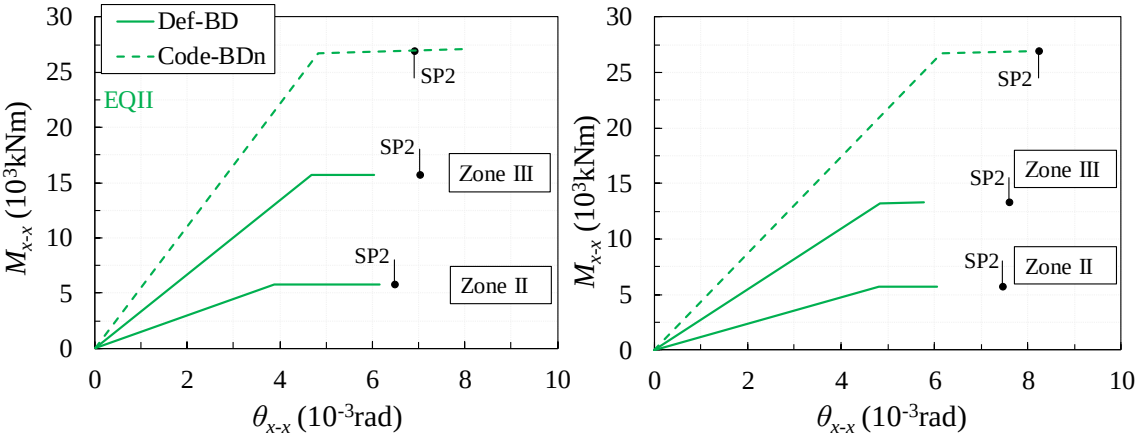

Fig. 6.3 Moment ($M_{x\text{-}x}$) vs. chord rotation ($\theta_{x\text{-}x}$) demand curves derived from assessment of Def-BD (ZII, ZIII), Code-BDn under EQII at the base of Pier 1 (left) and Pier 2 (right), compared with allowable SP2 deformation limits (solid dots)

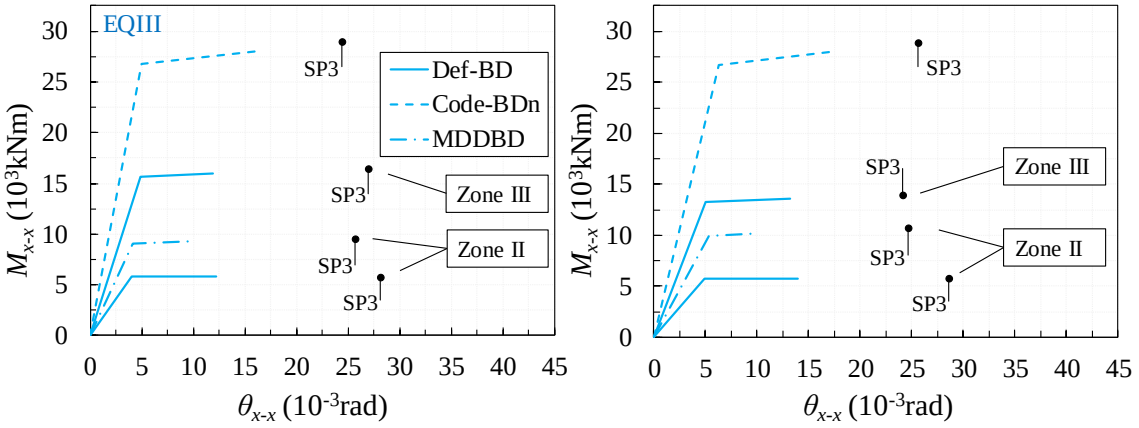

Fig. 6.4 Moment ($M_{x\text{-}x}$) vs. chord rotation ($\theta_{x\text{-}x}$) demand curves derived from assessment of Def-BD (ZII, ZIII), Code-BDn, MDDBD (ZII) under EQIII at the base of Pier 1 (left) and Pier 2 (right), compared with allowable SP3 deformation limits (solid dots)

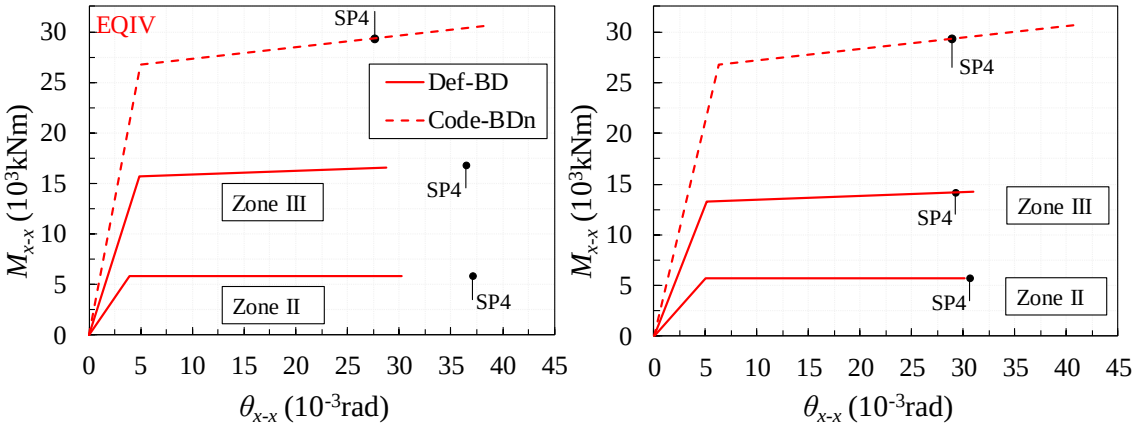

Fig. 6.5 Moment ($M_{x\text{-}x}$) vs. chord rotation ($\theta_{x\text{-}x}$) demand curves derived from assessment of Def-BD (ZII, ZIII), Code-BDn, under EQIV at the base of Pier 1 (left) and Pier 2 (right), compared with allowable SP4 deformation limits (solid dots)

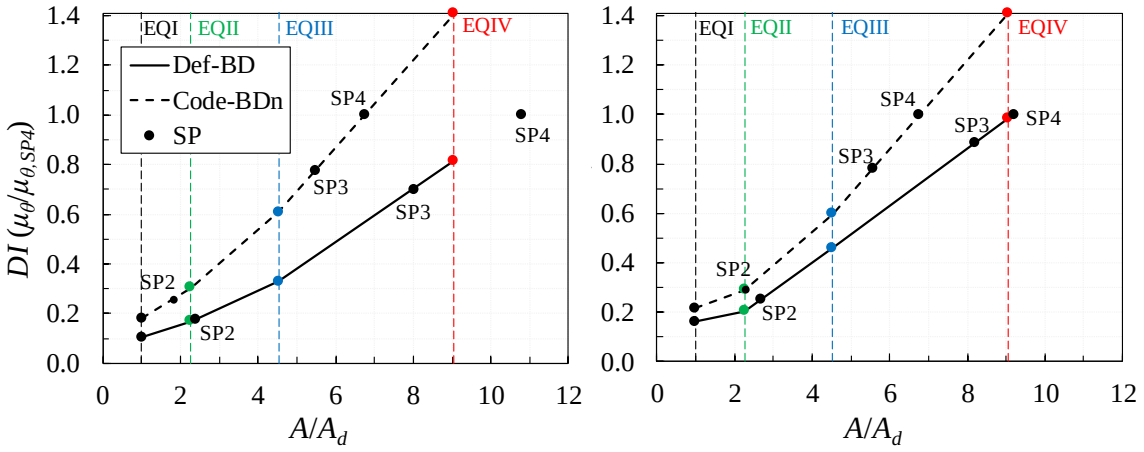

Fig. 6.6 Pier damage indices (*DI*) derived from assessment of Def-BD (ZII), Code-BDn, under EQII, EQIII, EQIV at the base of Pier 1 (left) and Pier 2 (right), compared with allowable *DI* limits (SP)

Implementation of the EN1998-2 (Annex G) (CEN 2005a) procedure appears to be less straightforward when the transverse direction of a bridge is considered given that the definition of the intended plastic mechanism may not be as obvious as in the case of the longitudinal direction involving yielding at both pier ends. Specifically, as the complexity of the system increases, e.g. the number of piers, significance of higher mode effects, non-simultaneous yielding among pier columns of different geometry/detailing or between column ends, the EN1998-2 assumption that all intended pier column plastic hinges reach their overstrength at the same time can result in a significant overestimation of the capacity design effect on the deck. In the case of T7, if yielding of piers is assumed at both ends (i.e. top and base), the application of the code procedure will result in deck capacity design moments (i.e. $M_{D,C}$) in the order of $200 \cdot 10^3$ kNm, significantly overestimating the relevant values found (later) through nonlinear dynamic analysis of the bridge (i.e. in the order of $35 \cdot 10^3$ kNm). In view of the previous consideration, the plastic mechanism presented in Fig. 6.7 was assumed, involving yielding only at the base of the piers. In Fig. 6.8(left) $M_{D,C}$ moments (about *z-z* axis) derived from the 'EN1998-2' procedure are compared with deck moments derived from NLRHA under the considered suite of artificial records (§6.2.3) scaled up to a level of seismic actions that entailed a seismic demand at the base of the short (critical) pier (i.e. Pier 1) approximately equal to its flexural capacity; i.e. A / $A_d \approx 6.7$ in Fig. 6.6(left). M-φ curves are provided for a range of prestressing force (Egnatia Motorway 2002), i.e. P_{min}, P_{max} considered as part of the external actions.

Although the EN1998-2 (CEN 2005a) approach cannot always predict the location of the critical moment (Gkatzogias & Kappos 2016a), Fig. 6.8(left) reveals that it can provide reasonably conservative estimates of the critical deck moment magnitude, on condition that the selected plastic mechanism describes realistically the structural performance of the bridge up to a level of seismic action corresponding to the flexural resistance of piers; the peak EN1998-2 capacity design moment (among all *A-A* deck sections) was found to be ~23% higher than the relevant value derived from NLRHA. In any case (EN1998-2 or NLRHA), capacity design moments remained below the deck yield moments and close to the deck cracking moments (i.e. moments at the instant of the first crack due to flexure, corresponding to a secant stiffness of EI_{cr} = (0.90~0.98)EI_g depending on the value of P) (Fig. 6.8(left)). Hence, the 'no significant yielding' requirement of EN1998-2 (CEN 2005a) was respected ensuring the validity of analysis results since gross flexural stiffness EI_g of the deck was assumed during design. In the case of Def-BD, deck moments (not shown in Fig. 6.8) were found significantly lower under EQIV (in the order of $13 \cdot 10^3$ kNm) due the lower pier strength, noting also that in this case both the plastic mechanism and the deck stiffness can be explicitly evaluated through NLRHA.

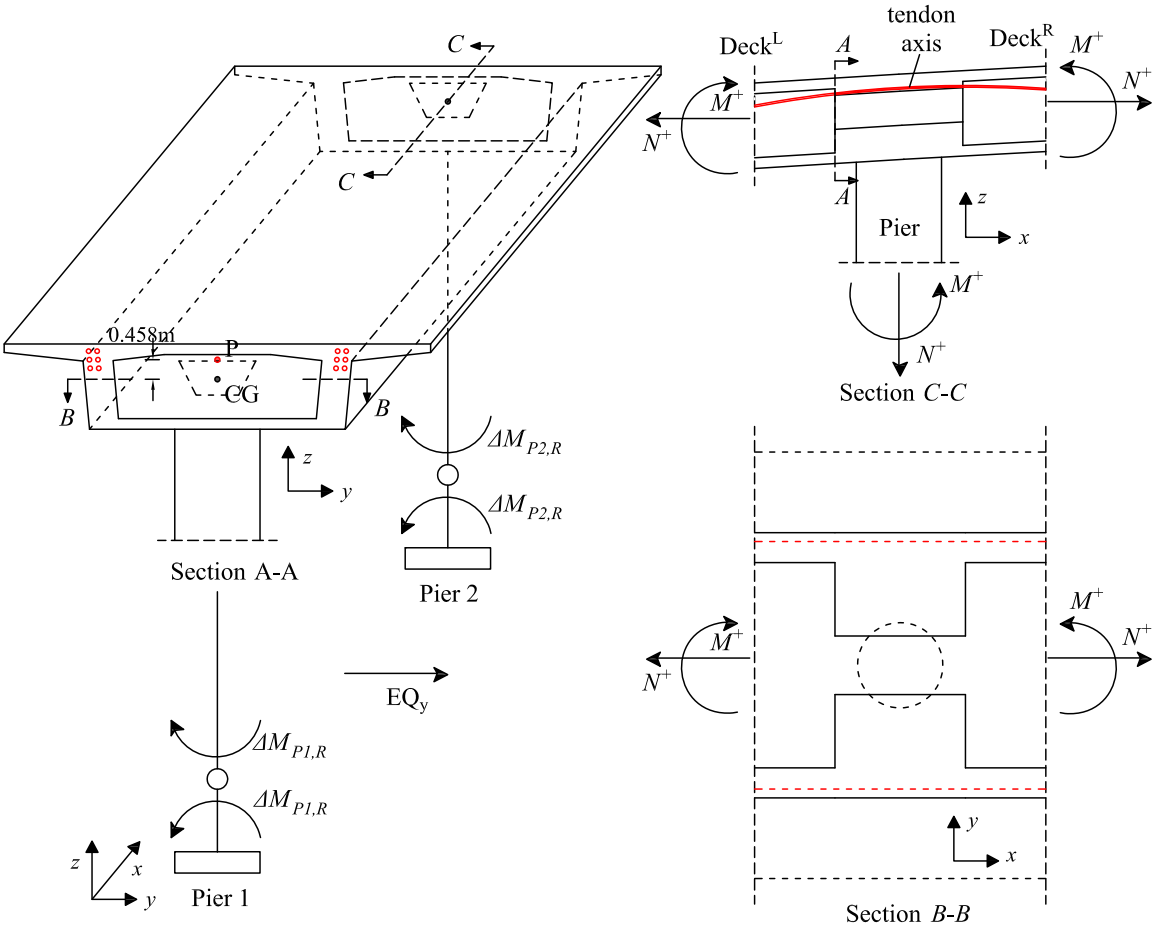

Fig. 6.7 Intended plastic mechanism under the transverse component of seismic action and vertical eccentricity of the prestressing force (P) with regard to the centre of gravity (CG) of section A-A, transverse (B-B) and longitudinal (C-C) section at pier-to-deck connections and sign convention (right)

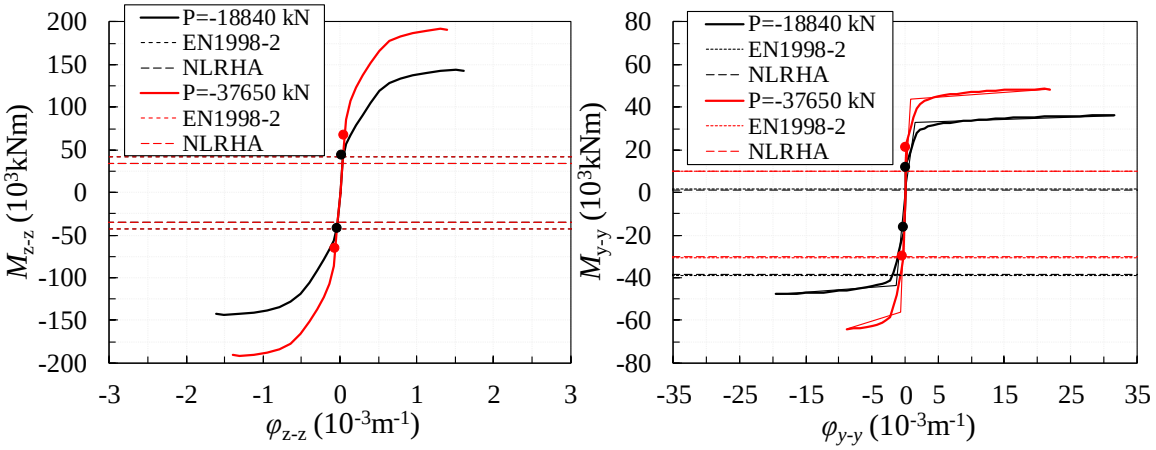

Fig. 6.8 'Exact' and bilinear M-φ curves of deck section A-A under P_{min}, P_{max}, compared with deck cracking moments (solid dots) and 'capacity design' moments (dashed lines) obtained from the EN1998-2 and NLRHA-based approaches applied in the transverse (left) and longitudinal (right) direction of the bridge

6.2.6 Evaluation of different designs

Despite the notable differences (summarised in Table 6.2) among the design principles adopted by the methodologies discussed herein with regard to the type of analysis, the definition of the seismic input, the type of stiffness and damping used to control design quantities, the range of directly controlled parameters and the number of iterations required (Kappos 2015a), both performance-based approaches (i.e. Def-BD, MDDBD) aim at a specific structural performance (defined on the basis of deformations) under single or multiple levels of seismic actions, and not surprisingly yield in general similar drifts and displacements, at least for the PL for which explicit verifications were carried out in both procedures, i.e. SP3 verifications under EQIII. This is evident in Fig. 6.2(right) where the deck displacement profiles derived from the assessment of Def-BD and MDDBD designs are compared. MDDBD yields 15 and 20% lower displacements (or drifts) at Pier 2 in the case of ZII and ZIII, respectively. The relevant reductions in bearing deformations located at Abutment 2 are 13 and 22%, whereas smaller differences are observed for Abutment 1 and Pier 1 (Fig. 6.2(right)). Resulting deviations in the assessed response should be evaluated duly considering the underlying design assumptions; the ability of each methodology to accurately capture the structural response during the design stage, under a specific level of seismic action entailing inelastic response, depends primarily on the type of analysis used (along with the associated seismic input and the definition of stiffness-damping properties) and the complexity (or irregularity) of the studied structure.

In this regard, Def-BD represents the most refined approach (Table 6.2) resulting in the best match between design and assessment displacement profiles; deviations are attributed to the sensitivity of analysis results to the seismic input and specifically to ground motion selection and/or scaling procedures, while improved mean predictions (i.e. smaller discrepancies between design and assessment quantities) can be attained as discussed in §3.3 at the expense of increased computational effort. On the other hand, modal analysis, forming part of MDDBD, attempts to capture the maximum probable response to a given seismic action based on equivalent properties (i.e. secant pier stiffness at the maximum displacement, equivalent viscous damping) and the statistical combination (e.g. SRSS) of peak ‘modal’ responses at the instant of maximum response (i.e. after the formation of plastic hinges). In addition to certain concerns (§2.2.2) regarding the efficiency of equivalent linearisation approaches in predicting inelastic seismic action effects in single-degree-of-freedom systems vibrating mostly at lower than peak displacement amplitudes, the aforementioned type of analysis cannot account for the modification of the dynamic characteristics of the structure during the successive formation of plastic hinges in multi-degree-of freedom systems, and thus its efficiency is expected to decrease as the degree of structural irregularity and the level of seismic action increase. It should be stressed that displacement profiles presented in Fig. 6.2 consist of non-simultaneous peak deformations corresponding to mean values derived from a series of NLRHAs or to statistically combined peak modal values; in either case, the displacement profile curvature in the specific bridge configuration indicates the contribution of higher modes in the seismic response rather than an ‘actual’ deformed shape of the bridge deck

which mainly exhibits a 'rigid body' translational response due to the unrestrained conditions at the abutments (Kappos *et al*. 2013). In this context, the increased curvature in the MDDBD displacement profile (i.e. increased contribution of second mode) derived at the design stage, resulted in an overestimation of displacements at the critical elements of the studied bridge, i.e. the elastomeric bearings in Abutment 2 (Fig. 6.2(left)). The described phenomenon, prevalent in bridges rather than buildings (Ayala & Escamilla 2013), is similar in nature to the reduced efficiency of the Def-BD method in accurately describing the shape of the displacement profile (or else the dynamic properties) under EQIV when the implicit approach is used (Fig 3.13), and is even more intense in the case of force-based code approaches, like Code-BDn (Fig. 6.2). In the latter case (i.e. Code-BDn), modal analysis is performed using the elastic stiffness of the structure (or more accurately the secant stiffness at yield in the case of piers) disregarding altogether the effects of nonlinearity on the dynamic characteristics of the studied system, resulting in significant shape deviations between the 'design' and 'assessment' Code-BDn profiles. It is worth noting that the significant contribution of the second ('elastic') mode in the case of Code-BDn (design stage) is also triggered by the reduced ratio of deck-to-pier stiffness (Isaković *et al*. 2012) (i.e. increased pier dimensions and strength, Table 6.1) compared to the other design cases.

Table 6.2 Key characteristics of different design methodologies

Method features	Def-BD	MDDBD	Code-BD
Seismic input	Acceleration spectrum, suite of accelerograms	Displacement spectrum	Acceleration spectrum
Analysis	Linear static/dynamic, nonlinear dynamic	Linear static, modal	Linear static/dynamic
Pier stiffness	Secant stiffness at yield, M-φ analysis	Secant stiffness at maximum response	Secant stiffness at yield
Damping	Fully populated damping matrix	Equivalent viscous damping	Modal damping ratios and behaviour factor
Controlled deformation parameters	No restriction (strains, deformations, displacements)	Strains (implicitly), displacements (explicitly)	Displacements (implicitly)
Explicitly controlled PLs per application	Multiple	Single	Single
Required iterations per application	Limited number	Significant number	Iterative application based on assumed-calculated strength

Proceeding to the ability of different approaches to satisfy the adopted performance requirements without being over-conservative (indicating their ultimate efficiency), Def-BD and MDDBD approaches were found to be safe in the sense of satisfying the relevant performance requirements (i.e. SP2 to SP4 in the case of Def-BD, and SP3 in the case of MDDBD). Nevertheless, anchoring a displacement profile of increased curvature at the target displacement (i.e. $\gamma_q \cdot t_R$ = 0.176m) of the critical member (i.e. LDRBs in Abutment 2, Fig. 6.2(left)) and

following the iterative equivalent linearisation approach of MDDBD (Kappos *et al*. 2013), resulted in higher reinforcing steel and concrete area demand in the piers. On the contrary, the rigorous evaluation of inelastic deformations by incorporating refined analysis procedures (e.g. NLRHA, *M-φ* analysis) in the case of Def-BD brought the deformation demand closer to the pertinent deformation limits, leading to cost reduction (reported in §6.2.4) without jeopardizing the desired performance under multiple PLs. Bearing displacements at Abutment 2 are lower compared to the MDDBD case under EQIII (Fig. 6.2(left)) because the design of piers and bearings is governed by SP2 and SP4 requirements that are implicitly considered in MDDBD (and Code-BD) but not necessarily satisfied, as demonstrated in the case of Code-BDn (Fig. 6.3-Fig. 6.6, Table D.1) which can be deemed equivalent to a code-type design of the bridge under a higher level of seismic action than that corresponding to Zone I (disengaged from the effects of introduced conservatism). Considering the actual bridge design under the non-normalised seismic action (Code-BD, Egnatia Motorway 2002), it is evident that due to the conservatism adopted with regard to the design of the piers and the lower level of seismic action considered, the structural performance will be superior to that of Def-BD in terms of recorded damage in the piers under the 'design' seismic actions (i.e. non-normalised EQIII); yet, this is achieved at an increased cost, while it does not ensure an overall satisfactory performance of the bridge under a higher level of seismic action unless all bridge members are consistently overdesigned.

In line with the principal concepts of Def-BD (§3.2.1), design of the deck is based on distinct performance requirements sought under different levels of seismic action and properly incorporated within the design procedure to ensure efficient performance under multiple PLs, and consistency between design requirements and modelling assumptions (regarding the stiffness of deck elements) (§3.2.4, 3.2.5). Based on the assessment of the structural performance of the deck, presented in detail only for the critical case of Code-BD (§6.2.5) where the fairly 'strong' piers (Table 6.1) could have compromised the set structural performance requirements, it was found that capacity design principles involved in Code-BD and MDDBD resulted in the 'no significant yielding' criterion being satisfied under the capacity design effects while the magnitude of deck moments justified the adoption of 'uncracked' gross deck sections during analysis. Nevertheless, this is not always the case; implementation of the investigation presented in §6.2.5 in the longitudinal direction of the bridge (presented in detail in Gkatzogias & Kappos 2016a, but not herein) results in the deck performance illustrated in Fig. 6.8(right), i.e. flexure about *y-y* axis using the sign convention of Fig. 6.7 (Section *C-C*) and accounting for the eccentricity of the tendons (and the prestressing force *P*) with regard to the centre of gravity (CG) of the deck section in *z-z* direction. Deck yield moments were found in general higher than the capacity design moments under both levels of prestressing force, however, only a minor exceedance of the capacity design moment is observed in the case of P_{max} and negative flexure of the deck, lying well within the cracked state of the deck section.

Results presented in Fig. 6.8(right) indicate that the target performance for no significant yielding in the deck is generally achieved. However, the proximity of flexural demand to the yield

moment of the deck (corresponding to a secant stiffness at yield $EI_y = 0.31EI_g$ for P_{max} and negative flexure) raises concerns with regard to the common assumption adopted in EN1998-2 (and the US codes) that prestressed concrete deck sections remain uncracked under the design seismic actions. In fact, no significant yielding of the deck under the 'capacity design effects' cannot ensure that cracking in deck sections will be avoided under the seismic design situation (involving EQIII) since the magnitude of deck moments under EQIII is expected to be close to that of capacity design moments if piers yield under this level of seismic action, reducing the validity of analysis results (e.g. non-conservative estimation of displacement demand) especially in cases of increased seismic intensity and relatively low level of prestressing. The issue discussed is by no means specific to the longitudinal response of straight bridges as implied by the case studied herein; the out-of-plane flexural demand of the deck is expected to be significantly higher in the common case of straight/curved-in-plan bridges wherein the displacement response of the deck is restrained at the abutments.

As a general remark, the outcome of Def-BD (§3.3.5) and MDDBD (Kappos *et al*. 2013) was affected to a certain degree by the adopted minimum longitudinal reinforcement ratio $\rho_{l,min}$ considered equal to 10‰. Strictly following the Eurocode provisions, since $\rho_{l,min}$ is not specified in EN1998-2 (CEN 2005a) for bridge concrete pier columns, the EN1992-1-1 (CEN 2004a) limit regarding all types of concrete columns applies, described by the upper part of Eq. (6.1) where N represents the column axial force in the seismic design situation (positive when compressive), f_{yd} is the design yield strength of reinforcing steel, and A_{Pier} is the area of the pier column section. In practice, however, the EN1992-1-1 limit is often perceived by practitioners as too low, thus usually replaced with the 10‰ limit prescribed for buildings in EN1998-1 (CEN 2004b) which is rather high for bridge pier columns. Given that the fundamental requirement for providing a minimum ratio is to ensure a minimum local ductility in bridge piers, $\rho_{l,min}$ can be defined according to Eq. (6.1) as the maximum of the values specified in EN1992-1-1 and the EN1998-2 Handbook (HB) (Fardis *et al*. 2012) which provides a sufficient amount of steel reinforcement ($\rho_{l,min,HB}$), and hence a design value of flexural strength of the pier section M_{Rd}, not less than the cracking moment represented by the right-hand part of the inequality; W_{Pier} is the elastic section modulus, and f_{ctm} is the mean value of the concrete tensile strength (N positive if compressive).

$$\rho_{l,\min} = \max\left\{\begin{array}{c}\rho_{l,\min,\mathrm{EN1992}} = \max\left(0.10N/\left(f_{yd}A_{Pier}\right), 0.002\right) \\ \rho_{l,\min,\mathrm{HB}} : M_{Rd} \geq W_{Pier}\left(f_{ctm} + N/A_{Pier}\right)\end{array}\right\} \tag{6.1}$$

Adopting Eq. (6.1) is expected to reduce material cost in low-to-moderate seismicity regions in all methodologies, especially those involving capacity design principles (i.e. MDDBD, Code-BD). Furthermore, high $\rho_{l,min}$ ratios were found in Gkatzogias & Kappos (2016a) to amplify 'irregular' seismic response in the piers (in terms of inelastic deformation demand), thus penalising critical piers with lower behaviour factors according to EN1998-2 (CEN 2005a) requirements, reducing the reliability and cost-effectiveness of the design.

Overall, what essentially differentiates Def-BD from other methods is its ability to control a broader range of design parameters (i.e. from strains up to flexural deformations and drifts) and PLs (i.e. two explicitly and two implicitly considered) within a single application of the method; clearly, one can run MDDBD and Code-BD for different PLs (i.e. multiple applications of the method) but this would require at least double the computational effort, if at all feasible in the case of MDDBD due to limitations related to low and moderate seismic levels of seismic actions (§2.2.2).

6.3 Seismically Isolated Bridge

6.3.1 Description of studied bridge

The bridge under investigation is described in §5.3.1 along with relevant design assumptions introduced to ensure consistency between the bridge designed for ductile behaviour of the piers (§3.3) and the seismically isolated bridge (§5.3). Herein, the case of the bridge isolated with lead rubber bearings (LRBs) is considered, adopting the 'ordinary bridge' performance objective, and accounting for the effect of bidirectional excitation. Design of the bridge according to EN1998-2 (CEN 2005a) and assessment of the bridge's seismic performance is presented in §6.3.2-6.3.5; a comparative evaluation of EN1998-2 and Def-BD (§5.3.6) designs is also provided in §6.3.5.

6.3.2 Modelling issues and numerical evaluation of dynamic response

An elastic finite element model of the bridge was used in response spectrum analyses of the multi-degree-of-freedom (MDOF) system as required by EN1998-2 (CEN 2005a) design. Pier flexural stiffness used in RSAs was the secant value at yield, while isolator shear stiffness was modelled using the secant value at maximum relative displacement of the isolator, resulting in the effective stiffness k_{eff} and isolation period T_{eff} along each principal direction of the bridge. The rest of the bridge stiffness properties were defined according to §5.3.2 considering also the variability of design properties of isolators as per §5.3.3. An effective (i.e. equivalent) viscous damping ratio ξ_{eff} accounting for the energy dissipated in the isolators and defined according to CEN (2005a) (§6.3.4), was used to model damping in modes having periods longer than $0.8T_{eff}$; in all other modes, a damping ratio equal to 5% was adopted. Nonlinear response history analyses (NLRHAs) required for assessment purposes in the case of EN1998-2 design, were performed according to §5.3.2, 5.3.3. Likewise, member limit deformations associated with each structural performance (SP) level were defined during assessment in accordance with §5.3.2, 5.3.3 and Table 5.1.

6.3.3 Target spectra and representation of seismic action

The target spectra presented in §5.3.4 for unidirectional (1D) and bidirectional (2D) excitation were adopted herein. 1D target acceleration spectra associated with T_R = 475yrs (i.e. EQIII) were used during the EN1998-2 design performed separately in each principal direction of the bridge (involving explicit analysis only under EQIII) prior to the directional combination of response quantities (§6.3.4) according to CEN (2005a). The 'design' acceleration spectrum used in RSA was derived by multiplication of the target (i.e. elastic, ξ = 5%) acceleration spectrum by the damping modification factor η_{eff} implicitly considering the reduction of seismic accelerations due to the introduction of additional damping at the isolation interface (i.e. ξ_{eff}, in general different along each principal direction of the bridge) for periods longer than $0.8T_{eff}$ (§6.3.2, Fig. 6.9). During the assessment stage, 2D target spectra, artificial records used to represent the seismic action, and scaling of records to different levels of seismic action were defined according to §5.3.4.

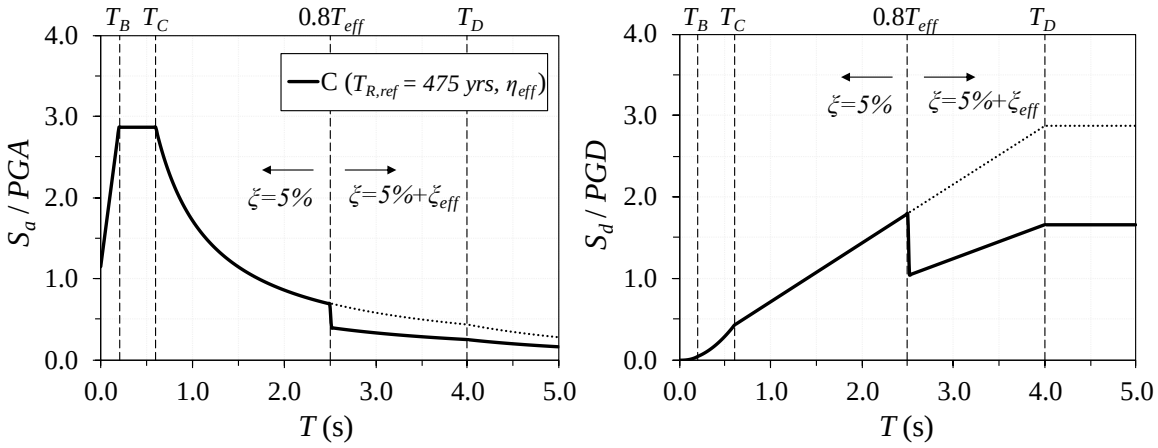

Fig. 6.9 1D design horizontal acceleration S_a /*PGA* (left) and displacement S_d /*PGD* (right) response spectra for site conditions 'C' ($T_{R,EQIII}$=475yrs) used in EN1998-2 design

6.3.4 Application of the EN1998-2 design procedure

Among the EN1998-2 (CEN 2005a) prescribed analysis methods for seismically isolated bridges, namely, (a) *fundamental mode spectrum* (FMS) analysis, (b) *multi-mode spectrum* analysis, and (c) *time-history nonlinear* analysis, corresponding to RSA of an equivalent single-degree-of-freedom (SDOF) system, RSA of an equivalent MDOF system, and NLRHA of the MDOF system, respectively, the following iterative analysis scheme was adopted applying sequentially the first two spectral approaches (i.e. (a) in Steps *i-iii*, and (b) in Steps *iv-vi*) independently along the longitudinal and transverse direction of the bridge also accounting for the lower bound (LB) and upper bound (UB) design properties (DPs) of isolators; nonlinear dynamic analysis was used to assess the bridge seismic performance in §6.3.5.

i. Considering the shear resistance at zero displacement V_0 and the post-elastic stiffness k_p of the isolation system, and assuming an initial value for the peak deformation u_0, the effective

stiffness k_{eff} of the isolation system (Fig. 4.6) was calculated according to Eq. (6.2), ignoring the effect of the substructure in the seismic response;

$$k_{eff} = V_0 / u_0 + k_p \tag{6.2}$$

ii. The effective period T_{eff} and damping ξ_{eff} corresponding to k_{eff} and u_0 were calculated according to Eqs. (6.3), (6.4) adopting an effective mass m_{eff} equal to the mass of the deck;

$$T_{eff} = 2\pi\sqrt{m_{eff} / k_{eff}} \tag{6.3}$$

$$\xi_{eff} = \frac{1}{2\pi}\left(\sum_i E_{D,i} \Big/ k_{eff} u_0^2\right) \tag{6.4}$$

$\Sigma E_{D,i}$ in Eq. (6.4) represents the sum of dissipated energies of all isolators in a full deformation cycle at the displacement u_0 calculated according to Eq. (4.8).

iii. The peak relative displacement u_0 and total acceleration $\ddot{U}_0$ of the equivalent SDOF, characterised by T_{eff}, ξ_{eff} and located at the stiffness centre (CS) of the composite substructure-isolation system (Fig. 6.10), were derived from the design response spectra (Fig. 6.9) defined according to §6.3.3 using the damping modification factor η_{eff};

$$\eta_{eff} = \sqrt{\frac{0.10}{0.05 + \xi_{eff}}} \geq 0.4 \tag{6.5}$$

Once u_0, $\ddot{U}_0$ were determined, Steps (*i*)-(*iii*) were repeated until all relevant design quantities were practically stabilised prior to proceeding to Step (*iv*). It is worth noting that the pseudo-acceleration retrieved from Fig. 6.9 was directly associated with $\ddot{U}_0$ and the peak shear force $V = m_{eff}\ddot{U}_0$ due to the absence of viscous dampers in the considered isolation scheme (i.e. LRBs).

iv. Considering the shear resistance at zero displacement $V_{I0(Abt/Pierj)}$ and the post-elastic stiffness $k_{Ip(Abt/Pierj)}$ of isolators located on the abutment seat or on pier j (i.e. sum of properties of individual isolators at substructure element j), and assuming an initial value for the isolator relative deformation $u_{I0,j}$ at the same location (Fig. 6.10), the effective stiffness k_{Ieff} of the isolation system at j was calculated according to Eq. (6.6);

$$k_{Ieff,j} = V_{I0,j} / u_{I0,j} + k_{Ip,j} \tag{6.6}$$

During the first application of Step (*iv*), $u_{I0,j}$ was assumed equal to the value of u_0 derived from Step (*iii*). In a similar context, providing reasonable estimates for the equivalent cantilever pier height $h_{eq,Pier\,j}$, and the secant stiffness at yield of the column section $EI_{y,Pierj}$ (e.g. Fig. 3.4), the pier lateral stiffness $k_{Pier\,j}$ was approximated using Eq. (6.7) (Kappos *et al*. 2013), and the

composite pier-isolator flexural stiffness $k_{eff,j}$ from Eq. (6.8); at the abutments $k_{eff,j}$ was considered equal to $k_{Ieff,j}$.

$$k_{Pier\ j} = \frac{h_{eq,Pier\ j}}{h_{Pier\ j}} \cdot \frac{3EI_y}{h_{eq,Pier\ j}^3} \tag{6.7}$$

$$k_{eff,j} = \frac{1}{\left(1/k_{Ieff,j}\right) + \left(1/k_{Pier\ j}\right)} \tag{6.8}$$

v. The effective period T_{eff} and damping ξ_{eff} of the bridge were recalculated to account for the substructure flexibility according to Eqs. (6.3), (6.4), using the effective stiffness defined by Eq. (6.9) and setting u_0 equal to $u_{I0,CS}$ (Eq. (6.10), Fig. 6.10).

$$k_{eff} = \sum_j k_{eff,j} \tag{6.9}$$

$$u_{I0,CS} = u_{D0,CS} k_{eff} \Big/ \sum_j k_{Ieff,j} \tag{6.10}$$

In the case of unidirectional excitation along the longitudinal direction of the bridge, CS coincides with the mass centre of the deck (CM) due to the bridge symmetry across the *x*-*x* axis (i.e. $e_{y\text{-}y} = 0$). Considering the transverse response of the bridge the eccentricity of CS with respect to CM was calculated from Eq. (6.11), where x_j is the distance of the substructure member *j* from Abutment 1, and *L* is the total length of the deck. During the first application of Step (*v*), $u_{0,CS}$ was assumed equal to the u_0 value derived from Step (*iii*).

$$e_{x-x} = \frac{\sum_j x_j k_{eff,j,y-y}}{\sum_j k_{eff,j,y-y}} - \frac{L}{2} \tag{6.11}$$

vi. Having defined the design acceleration response spectrum using ξ_{eff} from Step (*v*) in Eq. (6.5), RSA was performed according to §6.3.2 adopting k_{Ieff} and EI_y for isolator and pier stiffness, respectively. Steps (*iv*)-(*vi*) were repeated, until all relevant design quantities (i.e. displacements, member forces) were practically stabilised; during iterations $u_{0,j}$, $k_{Pier\ j}$, T_{eff}, u_{CS} were obtained directly from structural analysis results.

vii. Response estimates derived from the independent application of Steps (*iv*)-(*vii*) along the principal axes of the bridge, and the application of permanent (*G*) and traffic action (Q), were combined according to the following expressions;

$$1.35G + 1.50Q \tag{6.12}$$

$$G + 0.2Q \pm EQIII_{x-x} \pm 0.3EQIII_{y-y} \tag{6.13}$$

$$G + 0.2Q \pm 0.3EQIII_{x-x} \pm EQIII_{y-y} \tag{6.14}$$

Expressions (6.13), (6.14) were used to evaluate the seismic response of the isolation system under bidirectional excitation. In the case of the substructure, seismic action effects derived from RSA were divided by q = 1.5 (CEN 2005a) prior to their combination with 'non-seismic' actions and the subsequent design of piers in flexure; shear design and detailing for confinement, buckling, etc. followed EN1998-2 (CEN 2005a) requirements for 'limited ductile' bridges, and the assumed value of EI_y was additionally verified by M-φ analysis. Verification of the deck was not performed, since analysis moments were found in general lower than the deck cracking moments presented in §6.2.5.

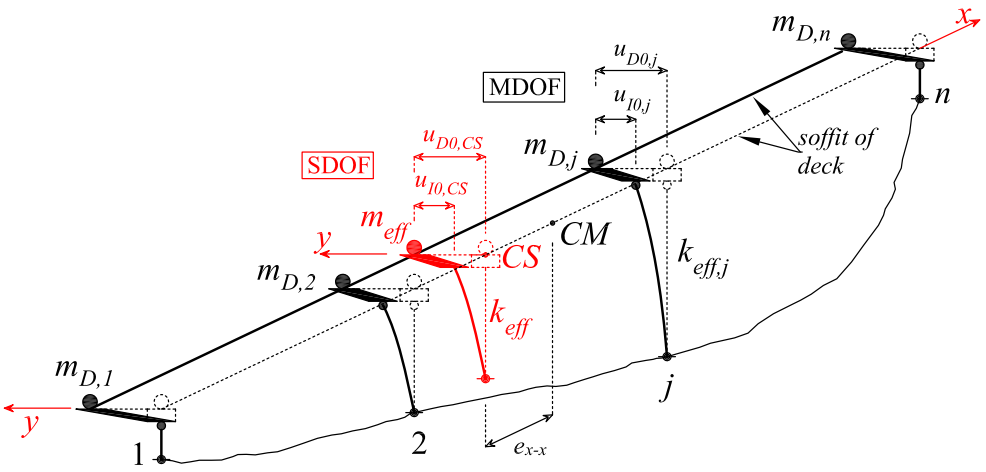

Fig. 6.10 Definition of equivalent SDOF system according to EN1998-2 design

Clearly, application of the above procedure involves a number of iterations which is expected to increase significantly (without ensuring accuracy in analysis results as shown in the following) when the characteristics of the passive devices required as an input in Step (*i*) are not known (as is typically the case in the design of a new bridge), and additional design criteria, such as those included in Def-BD, are sought, e.g. 'near-optimal' selection of isolation system properties based on multi-level performance requirements using charts in the form of Fig. 5.4. In addition, due to the different analysis principles in EN1998-2 and Def-BD, design is expected to yield different properties of isolators even if a common target performance is sought in both methods, thus complicating direct comparisons. In view of the previous consideration, the design outcome of the bridge designed to the Def-BD approach in §5.3.6 (regarding the isolator properties and the diameter of the piers) was used herein, focusing mainly on the predicted response and the design of the piers rather than the appropriate selection of device properties according to the EN1998-2 approach. The previous approach enables direct comparisons among the two methods while

indicating potential pitfalls that would have been encountered if isolators were selected according to the EN1998-2 method.

Iterative application of Steps (*i*)-(*iii*) under EQIII, yielded the results of Table 6.3, which are independent of the considered direction of the bridge due the symmetric mechanical properties of LRBs; three iterations were required in each case of DPs of isolators using the mechanical properties of Table 5.7 and adopting as initial values of u_0 (Step *i*) those resulting from the generalised design equations (GDEs) for unidirectional excitation (§4.3.3). Design quantities are also compared with relevant values derived from GDEs and mean values derived from NLRHA of the SDOF system under the Art B suite of artificial records (Fig. 4.2), indicating that EN1998-2 overestimates displacements and forces approximately by 30% (LB-DPs) and 10% (UB-DPs), respectively, compared to NLRHA results (corresponding deviations of GDEs from NLRHA results are 4% and 1%). EN1998-2 (CEN 2005a), similarly to US codes (e.g. AASHTO 2010, ASCE 2016) sets the analysis results derived from the FMS method as lower bounds to the RSA and NLRHA results adopting a maximum ratio of NLRHA (or RSA) to FMS displacement and force response equal to 0.80. Although the above limitation is promoted as a means of evaluating the soundness of results deriving from more complex analysis procedures (Fardis *et al*. 2012), data provided in Table 6.3 are indicative of the larger deviations that can be expected when FMS is compared with NLRHA of the MDOF system, thus penalising the nonlinear dynamic approach with no specific evidence of erroneous application of the method.

Table 6.3 Peak response quantities derived from alternative methods

Response quantity	EQ	DP	EN1998-2 (Steps *i*-*iii*) (1)	Def-BD (GDEs) (2)	NLRHA (3)	(3) / (1)	(3) / (2)
u_0 (m)	III	LB	0.106	0.085	0.082	0.77	0.96
	III	UB	0.055	0.044	0.045	0.82	1.02
	IV	LB	0.212	0.256	0.243	1.15	0.95
	IV	UB	0.109	0.144	0.140	1.28	0.97
$\ddot{U}_0$ (m/s^2)	III	LB	0.91	0.83	0.81	0.89	0.97
	III	UB	1.34	1.23	1.22	0.91	0.99
$V = m\ddot{U}_0$ (kN)	III	LB	2320	2125	2056	0.89	0.97
	III	UB	3412	3122	3095	0.91	0.99

EN1998-2 (CEN 2005a) sets also a requirement for 'increased reliability' of the isolation system identifying the critical role of its displacement capacity to the safety of the isolated bridge; this requirement is deemed to be satisfied by verifying the passive devices for a higher level of seismic action (than that corresponding to EQIII) considered implicitly through the amplification of relative displacements derived from analysis under EQIII. Herein, an amplification factor of 2.0 was adopted which is larger than the recommended value of 1.5 (i.e. a nationally determined parameter) for the sake of consistency with the definition of target spectra in §6.2.3 (i.e. adoption of SF_{EQIV}=2.0 in Def-BD). It is seen (Table 6.3) that despite the overestimation of displacements under EQIII and the higher amplification factor, the EN1998-2 spectral approach underestimates u_0 by 13% (LB-

DPs). It should be noted that neither of the above deviations, i.e. overestimation and underestimation of u_0 under EQIII and EQIV respectively is on the safety side, since the first results in overestimating the restoring capability of the isolation system (§5.2.3) and the second in under-designed isolators.

Consideration of the MDOF system (accounting for the pier flexibility, §6.3.2) during application of Steps (*iv*)-(*vi*) under LB-DPs required two iterations per principal direction of the bridge, while in the case of UB-DPs, three and four iterative applications were required in the transverse and longitudinal direction, respectively, to keep deviations of relevant response quantities (from one iteration to another) below 10%. Subsequent implementation of Step (*vii*) resulted in the detailing provided in Table 6.4, also compared with the design outcome of the Def-BD approach (§5.3.6). Significant reductions in longitudinal (i.e. 58%) and transverse (i.e. 28%) reinforcing steel volume were observed in the case of EN1998-2; ρ_l was governed by minimum requirements defined in accordance with Eq. (6.1), and ρ_w by confinement requirements.

Table 6.4 Outcome of Def-BD and EN1998-2 methodologies

Method	Member		Section (m)	h or t_R [1] (m)	$\rho_{l,req}$ [2] (‰)	A_l [3] (cm^2)	ρ_l [3] (‰)	$Vol.,_l$ [4] (m^3)	Bars	ρ_w [3] (‰)	$Vol.,_w$ [5] (m^3/m)	Hoops (per mm)
Def-BD	Pier 1	(top)	D_p = 1.5	4.44	-	74	4.2	0.304	15Ø25	5.9	0.019	Ø14/75
		(base)	D_p = 1.5	4.44	8.2	147	8.3		30Ø25			
	Pier 2	(top)	D_p = 1.5	6.43	-	133	7.5		27Ø25	6.3		Ø14/70
		(base)	D_p = 1.5	6.43	14.7	265	15.0		54Ø25			
	LRB[6]	-	D_I = 0.75	0.225	-	-	-	-	-	-	-	-
EN1998-2	Pier 1	(top)	D_p = 1.5	4.44	-	72	4.1	0.129	19Ø22	4.4	0.013	Ø14/110
		(base)	D_p = 1.5	4.44	-	72	4.1		19Ø22	4.4		
	Pier 2	(top)	D_p = 1.5	6.43	-	72	4.1		19Ø22	4.4		Ø14/110
		(base)	D_p = 1.5	6.43	-	72	4.1		19Ø22	4.4		
	LRB[6]	-	D_I = 0.75	0.225	-	-	-	-	-	-	-	-

[1] h : clear height of pier, t_R : total rubber thickness

[2] Required reinforcement at the base/top of the pier

[3] Provided reinforcement at the base/top of the pier

[4] Provided volume of reinforcing steel

[5] Provided volume of reinforcing steel per metre of column length

[6] Lead rubber bearing

In Table 6.4 discrepancies in steel demand between EN1998-2 and Def-BD approaches can be easily explained on the basis of the design assumptions made in each method. The peak 'design' shear carried by each pier in Def-BD was calculated considering the peak deck total acceleration under EQIV and bidirectional excitation (i.e. $\ddot{U}_0 \approx 2.55$ m/s^2, Table 5.9, No. 4.2 UB-DPs), a β-factor of 0.75 (mainly accounting for the difference in mean and design values of material strength, §3.2.2), and a target rotational ductility factor under EQIV equal to $\mu_{\theta,SP3} = 1.2$ (§5.3.6.1), resulting simplistically in $0.75 \cdot 2.55 / 1.2 = 1.59$ m/s^2. On the other hand, the peak pier shear in the EN1998-2 approach was derived from the peak deck total acceleration under EQIII and unidirectional

excitation (i.e. $\ddot{U}_0 \approx 1.34$ m/s^2, Table 6.3, UB-DPs), a behaviour factor of $q = 1.5$, and the consideration of the effect of the orthogonal component of seismic action through the directional combination of response quantities according to expressions (6.13), (6.14), i.e. $((1.34 / 1.5)^2 + (0.3 \cdot 1.34 / 1.5)^2)^{0.5} = 0.93$ m/s^2. The previous simplistic calculations reveal as the main sources of steel reduction in the case of EN1998-2, the inconsistent safety format adopted by Eurocode 8 in 'response spectrum' and 'response history' analysis methods regarding the effect of bidirectional excitation, the limitation of the inelastic pier response in isolated bridges under the 'design' (i.e. EQIII) rather than the 'maximum considered' seismic actions (i.e. EQIV), and the differences in response quantities resulting from 'spectral' and rigorous 'direct integration' methods. The effect of the previous design assumptions on the inelastic response of the studied bridge is discussed in the following section.

6.3.5 Assessment of EN1998-2 design and comparison with Def-BD

Considering the different features of the EN1998-2 and Def-BD methodologies for seismically isolated bridges summarised in Table 6.5, a comparative evaluation of the bridge seismic performance attained from each approach is presented in this section. An immediate observation derived from the description of the EN1998-2 'spectral' approach (similar to that of other modern codes, e.g. ASCE 2016), in §6.3.4 is the identification of the criticality of displacements in seismically isolated structures and their explicit consideration within the design procedure, as opposed to 'pure' force-based approaches commonly adopted by codes for bridges with energy dissipation in the piers that address displacements at the final stage of design (§6.2.4). In this sense, the key features of the EN1998-2 approach in Table 6.5 are closer to those of the MDDBD rather than the Code-BD approach in Table 6.2; although EN1998-2 does not include a strict 'design route' aiming at the specification of strength that results in a predefined (target) displacement under a specific level of seismic action (the cornerstone of the *direct displacement-based design* philosophy), the equivalent linearisation approaches involved in the two procedures share the same basic principles.

To facilitate a detailed comparison of the EN1998-2 and Def-BD methods, the EN1998-2 design (§6.3.4) was first assessed following in general the format described in §5.3.6.2; i.e. the bridge structural performance was evaluated under three different PLs considering the range of DPs of devices (§6.3.2, 6.3.3) and different angles of incidence according to Fig. 5.16 (i.e. identical to the Def-BD case). As per §5.3.6, and unless specifically noted (e.g. $V_{x\text{-}x}$), deformations, forces etc. reported in the following figures represent peak response quantities calculated from the directional combination of responses according to expressions (6.13), (6.14) (i.e. vector addition of peak response quantities derived from the application of the method in each principal direction of the bridge) at the design stage, and the combination of response histories of relevant quantities along the *x*-*x* and *y*-*y* axes (i.e. vector addition at each time-step, §4.5.1) prior to obtaining their peak (absolute) values, at the assessment stage where NLRHA was involved.

Table 6.5 Key characteristics of Def-BD and EN1998-2 design methodologies

Method features	Def-BD	EN1998-2 ('spectral' approach)
Seismic input	Acceleration spectrum, suite of accelerograms	Acceleration/ displacement spectrum
Analysis	generalised design eqs., nonlinear dynamic	Linear static/dynamic
Pier stiffness	'Gross' section stiffness/secant stiffness at yield, M-φ analysis	'Gross' section stiffness/ secant stiffness at yield
Isolator stiffness	Stiffness degradation models	Secant stiffness at maximum response
Damping	Fully populated damping matrix	Equivalent viscous damping in fundamental mode, behavior factor in substructure design
Controlled deformation parameters	No restriction (strains, deformations, displacements)	Displacements (explicitly)
Explicitly controlled PLs per application	Multiple	Single
Required iterations per application	Limited number	Significant number

Fig. 6.11(right) compares estimates of peak relative (to the ground) displacements of the deck and piers derived from the design and assessment stages in the case of EN1998-2. Different 'design' displacement profiles under the same level of seismic actions and DPs correspond to different cases of combination of actions in line with expressions (6.13), (6.14) ('design' case) or to different angle of incidence ('assessment' case). Isolator peak relative deformations are presented in tabular form in Annex D, Table D.2 along with additional response quantities derived from the design and assessment stages.

Due to the typically symmetric properties of the isolation interface, directional combination of responses according to expressions (6.13), (6.14) prescribed in EN1998-2 for the case of RSA (used herein at the design stage), is expected to result in peak response quantities approximately equal to $\sqrt{(1^2+0.3^2)} = 1.04$ times the values derived under unidirectional excitation. In other words, due to the symmetry of the isolated structure, there is no significant differentiation of peak responses along a principal direction of the bridge deriving from the orthogonal component of seismic action, even in the case of non-symmetric substructures (of straight bridges). On the other hand, extensive parametric NLRHA of nonlinear isolation systems under bidirectional excitation in §4.5.3, using records scaled to a target spectrum that is defined as $\sqrt{2}$ times the target spectra under unidirectional excitation in line with CEN (2005a) requirements for nonlinear dynamic analysis (i.e. the 2D target spectrum also adopted in the Def-BD case study for the sake of consistency), showed that peak displacements under unidirectional excitation are expected to increase approximately by a factor of 1.43 according to Eq. (4.57).

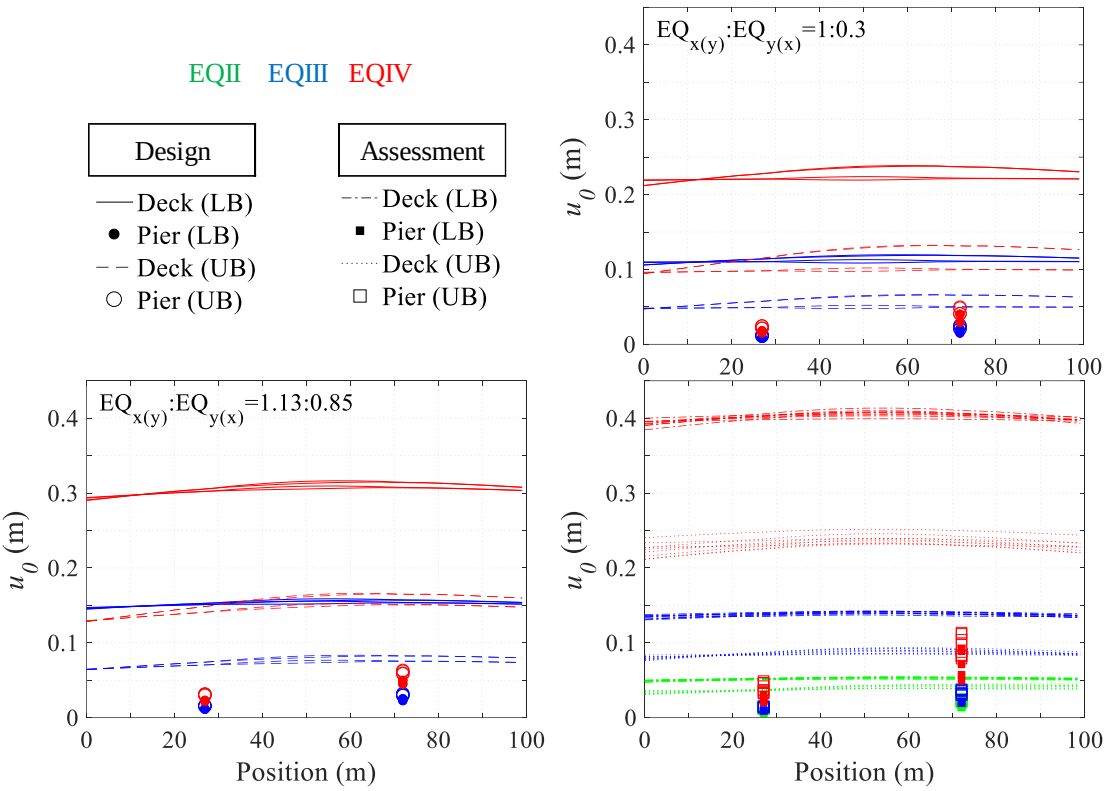

Fig. 6.11 Deck and pier peak relative displacements u_0 derived from EN1998-2 design (top-right, bottom-left) and assessment for θ_{EQ}=0-180° (Fig. 5.16) (bottom-right)

In the bridge studied herein, the above different approaches in considering the effect of bidirectional excitation during the design and assessment stages resulted in differences of 22% (LB-DPs) and 67% (UB-DPs) in deck displacements under EQIII (Fig. 6.11(right)). Improved convergence can be achieved when the effect of bidirectional excitation is considered at both stages using the same approach. For example, adopting during the design stage the target spectra of horizontal components used at the assessment stage (Fig. 6.11(left)) constraints relevant displacement deviations under EQIII within a range of 10-20% attributed to the approximate nature of the equivalent linearisation approach (Table 6.3) and the assumption that peak responses along the principal axes of the bridge occur simultaneously (as opposed to the case of uncorrelated components of seismic action, §4.2.2). This is practically equivalent to the SRSS directional combination of peak responses derived from independent RSA under the 1D target spectrum, an approach dictated in Model Code (*fib* 2012) and available in CEN (2005a) only for bridges with energy dissipation in the piers (i.e. not for isolated systems). The SRSS directional combination will also increase the reinforcing steel demand bringing the 'design' total acceleration (i.e. $\approx \sqrt{2} \cdot 1.34 / 1.5 = 1.26$ m/s^2) closer to the value derived from Def-BD, thus mitigating the effect of the uncontrolled inelastic response in the piers described in the following. In any case, Fig. 6.11 and Table D.2 demonstrate a significant underestimation of relative displacements under EQIV indicating the risk of under-designing isolators, and the inadequacy of the EN1998-2 design approach in estimating the peak displacement response through the implicit amplification of EQIII

displacements by SF_{EQIV}, since the increase in peak displacement response is disproportionate to the increase of seismic actions (e.g. NLRHA case in Table 6.3). The fact that the relevant SP requirements of the isolation system are met at the assessment stage (see Table D.2), is attributed to the adoption of the isolator properties derived from the Def-BD method which is capable of reliably estimating the peak response under multiple PLs irrespective of the definition of the target spectrum under bidirectional excitation.

Comparison of the peak deck displacements derived during assessment of the EN1998-2 and Def-BD designs, i.e. Fig. 6.11(bottom-right) vs. Fig. 5.17(top-right), reveals nearly identical displacement profiles despite the significant reduction in pier strength in the EN1998-2 case, i.e. the substructure response has a negligible effect on the deck relative displacement demand, similarly to the case of buildings (e.g. Vassiliou *et al*. 2013). Nevertheless, the distribution of the deck displacements to the isolators and the piers is differentiated among the considered design cases as implied by the increased pier displacements in Fig. 6.11, more so in the case of Pier 2. Transferring part of the displacement demand from the isolation interface to the substructure reduces the efficiency of the isolation system, or else, the amount of energy dissipated by the isolators, as indicated by the reduced area of the EN1998-2 hysteretic loops in Fig. 6.12 providing the total shear force of isolators plotted against the average relative displacement history of devices for the EN1998-2 and Def-BD designs under an artificial record (assessment stage) and θ_{EQ} = 90°.

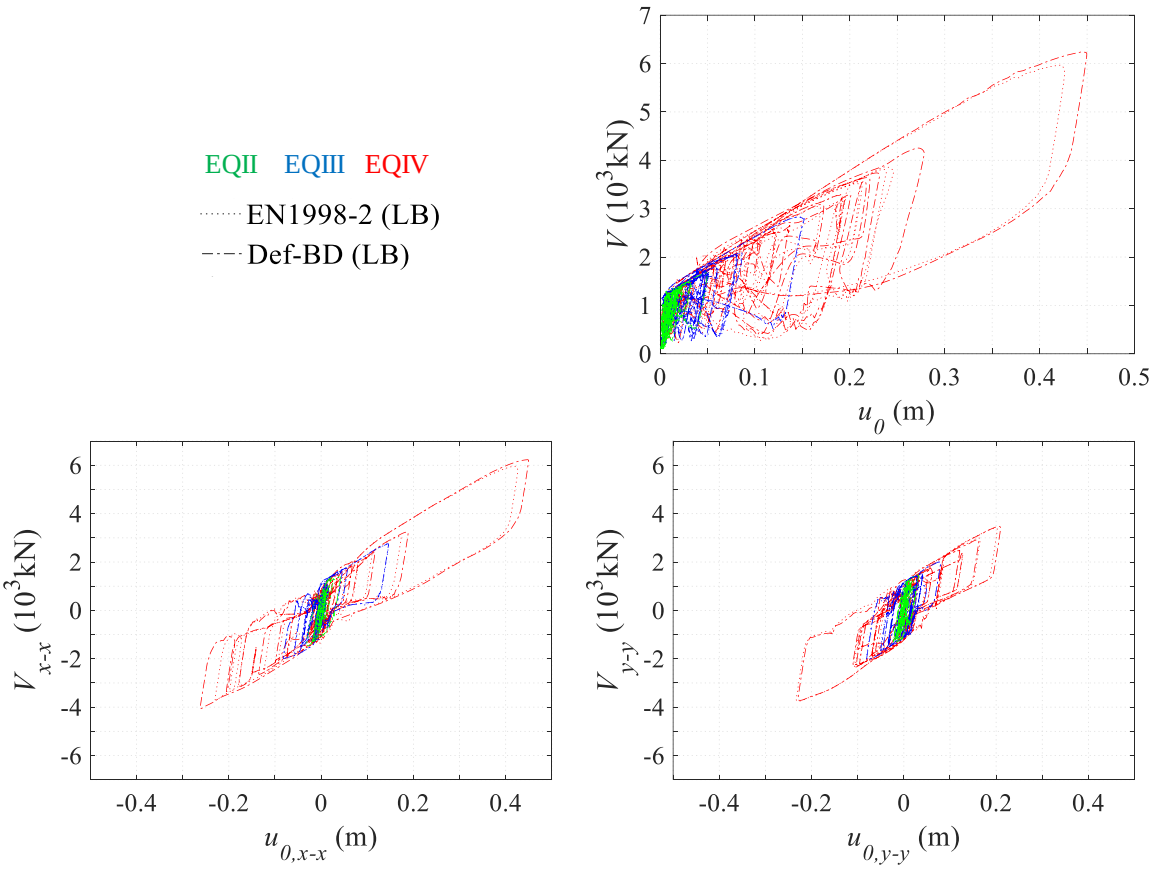

Fig. 6.12 Total shear force V vs. average relative displacement histories u_0 derived from EN1998-2 and Def-BD under Art 4 (assessment), LB-DPs, and θ_{EQ}=90°

An overview of the isolator deformation demand derived from the entire set of NLRHAs performed during assessment is presented in the polar charts of Fig. 6.13 where mean values of u_0 are plotted against θ_{EQ} (for each PL) and compared with relevant SP design criteria; the figure highlights the reduction in the displacement response of isolators located on top of Pier 2 mainly in the range of θ_{EQ} = 0~135°, as opposed to the Def-BD case (Fig. 5.19) where the relevant demand under EQIV follows the target SP3 requirements (Table 5.1) regardless of the considered incidence angle.

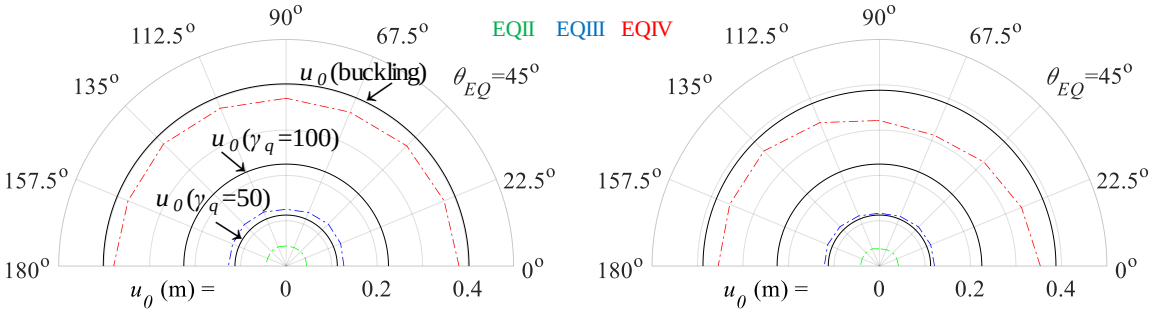

Fig. 6.13 *GM* of peak relative displacements u_0 of isolator located on top of Pier 1 (left) and Pier 2 (right) derived from assessment for θ_{EQ}=0-180° and LB-DPs, compared with SP requirements per PL

The reduction in the energy dissipated in the isolation system is counterbalanced in the case of EN1998-2 by a significant increase in the inelastic deformation of the piers compared to Def-BD as shown in the representative moment vs. curvature plots of Fig. 6.14 under the Art 4 artificial record, θ_{EQ} = 90°, and UB-DPs; in this case the lower provided pier reinforcing steel ratios reported in Table 6.1 yielded six times larger curvature demand at the base of Pier 2 under EQIV. Considering the polar diagrams of Fig. 6.15 to summarise analysis results derived from assessment and UB-DPs, it is clear that the SP3 criterion aiming at the controlled inelastic response of the piers is violated in most cases contrary to the Def-BD method wherein the ductility demand was constrained below the value corresponding to ε_c = 3.5‰ (Fig. 5.24). Specifically, the lower pier strength in the case of EN1998-2 design reduces the efficiency of isolators bringing the deformation demand in Pier 2 close to its flexural capacity for θ_{EQ} = 45~90°. It is worth noting that exceedance of SP4 deformation limits (Table 5.1, Table D.2) was avoided by the decision to apply the minimum reinforcing steel requirements during the EN1998-2 design in §6.3.4, thus providing some overstrength, instead of reducing the pier dimensions, in which case the inelastic ductility demand would have further increased. Furthermore, the shear capacity of piers assessed according to CEN (2005a) was also found inadequate in the case of the EN1998-2 design under EQIV and UB-DPs (Table D.2).

The structural performance of piers, considered undesirable by modern design codes for the reasons presented in §2.3.3, further highlights the inconsistent approach of the code in designing the components of the isolation system under a higher level of seismic action than that corresponding to EQIII, as a means to ensure the 'increased reliability' requirement, without specifically addressing the effect of these actions on the substructure response. On the grounds that the pier response will control the proper performance of the isolation system and the bridge overall

response, design of the isolation system under higher seismic actions is expected to be meaningful when followed by relevant verifications on the piers, implying the necessity in the case of EN1998-2 to limit the inelastic pier response under higher actions than those associated with the 'design' earthquake.

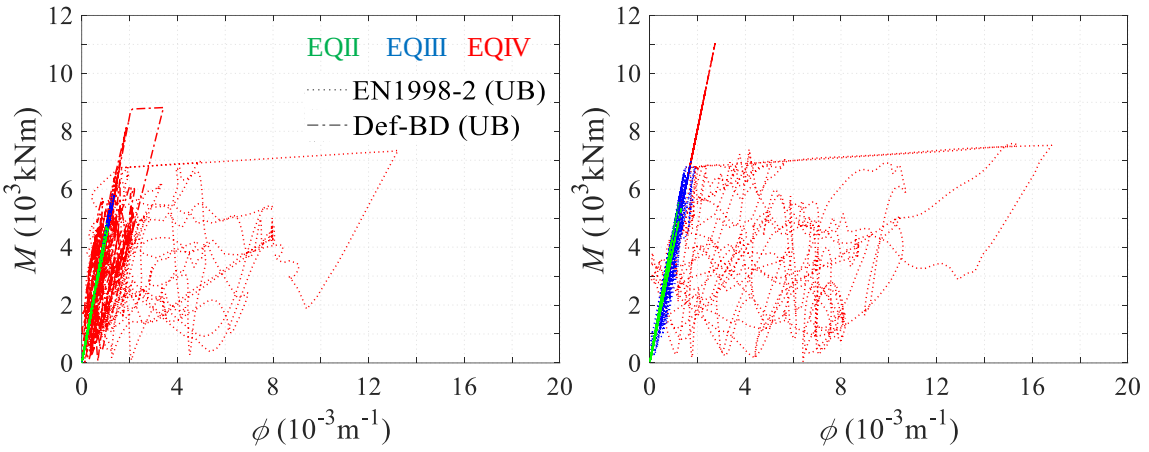

Fig. 6.14 *M-φ* response histories at the base of Pier 1 (left) and Pier 2 (right) derived from EN1998-2 and Def-BD under Art 4 (assessment), θ_{EQ}=90º, and UB-DPs

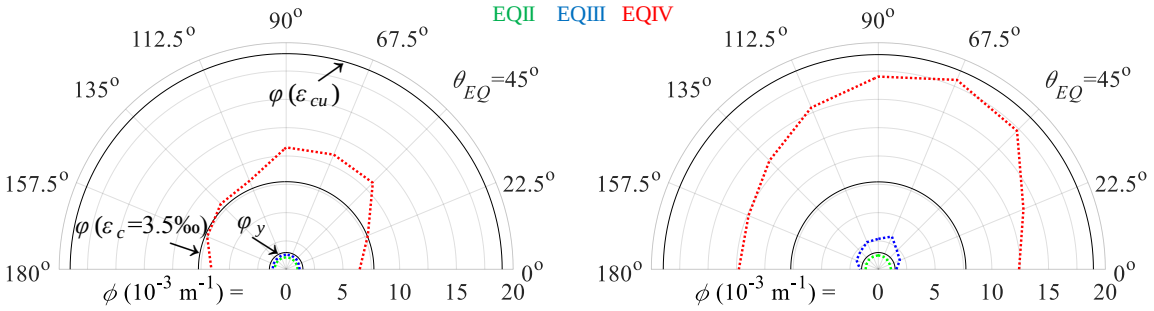

Fig. 6.15 *GM* of curvatures *φ* at the base of Pier 1 (left) and Pier 2 (right) derived from EN1998-2 assessment for θ_{EQ}=0-180º and UB-DPs

6.4 Closing Remarks

A comparative evaluation of designs resulting from the application of alternative design procedures to the same bridge, was presented in this chapter with a view to assessing both the structural performance and the economy of design attained from the proposed *deformation-based design* method.

Considering the case of the bridge with monolithic pier-to-deck connections, the following conclusions were drawn based on the assessment of designs resulting from the deformation-based design (Def-BD) method, the modal direct displacement-based design (MDDBD) method, and a force-based code-type (Code-BD) method (corresponding to the actual bridge design):

- Adopting refined analysis and modelling approaches, and providing a consistent performance-based design format within the Def-BD framework (i.e. explicit consideration of multiple PLs), resulted in superior seismic performance in the case of Def-BD. This was demonstrated by the control of various design parameters and structural performance requirements over multiple performance levels within a single application of the method. Significant cost reductions were achieved compared to the MDDBD procedure, whereas potential cost reductions may also be obtained when compared to force-based code-type procedures due to the adoption of more rational design approaches accounting for the seismicity of the site in lieu of 'standard' capacity design considerations.

- The above render Def-BD a rigorous methodology, applicable to most of the common concrete bridge configurations without practical limitations related to the irregularity of the structural system considered. Inevitably, this comes at the expense of additional computational time and effort associated with the use of nonlinear dynamic analysis and the explicit consideration of multiple PLs. Nevertheless, minimum iterative effort is ensured by estimating pier strength on the basis of allowable deformations, and by providing a logical analysis-design route wherein each step corresponds to a different performance level.

- MDDBD resulted in similar structural performance to Def-BD for the explicitly verified common PL (i.e. SP3 requirements); nevertheless, the inherent inability of the former method to account for the modification of the dynamic characteristics of the structure during the successive formation of plastic hinges, along with the introduction of an equivalent linearisation approach, resulted in an increase in pier dimensions and reinforcing steel requirements. Disregarding altogether the effect of the pier inelastic response on the estimation of the dynamic characteristics of the bridges in the case of Code-BD, resulted in the highest deviation among the displacement response assumed during the design and the response assessed through rigorous nonlinear dynamic analysis.

- Assessment of Code-BD under normalised levels of seismic action (i.e. Code-BDn), introduced to enable meaningful comparisons with Def-BD, revealed multiple violations of the adopted performance requirements for the PLs that are commonly implicitly considered in code-type procedures (SP2, SP4). This confirmed that definition of strength on the basis of 'life-safety' design criteria does not necessarily ensure controlled structural performance under different PLs associated with 'operationality' and 'collapse-prevention' requirements. On the other hand, if the performance of the actual bridge under the non-normalised seismic action is considered, all relevant verifications are satisfied due to the adopted over-conservatism in design.

- Capacity design verification of the bridge deck, required in the cases of MDDBD and Code-BD, in line with the EN1998-2 (Annex G) provisions (CEN 2005a) and a more refined approach involving NLRHA and M-φ analysis of pier and deck sections indicated that the 'no significant yielding' requirement of the deck was satisfied. However, certain pitfalls were also identified.

Specifically, the definition of the intended plastic mechanism in the transverse direction of the bridge may not be obvious, especially as the complexity of the system increases, while the de facto adoption of 'uncracked' gross section in modelling the flexural stiffness of the deck, may render questionable the validity of analysis results.

Considering the case of the seismically isolated bridge, the following conclusions were drawn based on the assessment of designs resulting from the deformation-based design (Def-BD) method, and the method prescribed in EN1998-2 (CEN 2005a) as applied herein:

- Although the EN1998-2 design method for seismically isolated bridges aims at the explicit verification of displacements, the adopted equivalent linearisation approach may involve a significant number of iterative applications when the characteristics of the passive devices are not known at the beginning of the design procedure, as is common in the design of a new bridge. Further iterations will be required if additional design criteria, such as those included in the proposed Def-BD, are sought, e.g. by setting a target performance under multiple performance levels with respect to peak deformations, energy dissipation, minimisation of the substructure design cost, etc. On the contrary, preliminary selections in Def-BD are facilitated by using GDEs.

- The introduced iterations in EN1998-2 do not necessarily ensure an accurate estimation of peak response due to the approximate nature of the equivalent linearisation approach. In the bridge studied herein, i.e. deck isolated through hysteretic isolators, the EN1998-2 approach, initially applied to an equivalent SDOF system of the bridge and subsequently to the MDOF system accounting also for the substructure, resulted in deviations of displacement response within a range of 10-30% compared to rigorous nonlinear dynamic analysis results. Furthermore, the implicit estimation of deformations under EQIV was found inadequate to capture the peak inelastic response of isolators indicating the risk of underestimating their required deformation capacity.

- Application of the EN1998-2 design procedure resulted in significant reductions in reinforcing steel demands. Nevertheless, subsequent assessment of the design in line with the (CEN 2005a) requirements indicated that the main sources of this reduction, namely, (*i*) the inconsistent consideration of the effect of bidirectional excitation in different analysis methods, (*ii*) the limitation of the inelastic pier response in isolated bridges under the 'design' (i.e. EQIII) rather than the 'maximum considered' seismic actions (i.e. EQIV), and (*iii*) the deviation of response quantities resulting from 'spectral' equivalent linearisation approaches, may compromise the safety of the isolated structure under EQIV by imposing large inelastic deformations in substructure elements, in contrast to the reliable and stable performance exhibited in the case of Def-BD.

- The above deficiencies of equivalent linearisation approaches may be more pronounced in isolation systems incorporating velocity dependent energy dissipation devices (e.g. fluid

viscous dampers, not investigated in this chapter), since their inherent inability to estimate the peak inertia forces transferred to the substructure will require recourse to more complex approximate procedures (e.g. Constantinou *et al*. 2011) unless nonlinear dynamic analysis is adopted (i.e. a strategy typically preferred by designers when viscous dampers are involved).

Chapter 7
Conclusions and Recommendations for Future Research

7.1 Conclusions

Considering the current trends in performance-based seismic design of bridges, a *performance-based seismic design* methodology was developed within a *deterministic* framework. The method involves *displacement-based design* principles and aims at the efficient design of a *broad class* of common bridge configurations using *advanced analysis* tools. The suggested procedure considers explicitly (through analysis under different levels of seismic action) multiple performance levels, and different performance objectives accounting for the adopted structural configuration and the importance of the studied bridge. This is in contrast with 'standard' code-type or other displacement-based design procedures that require explicit consideration of a single performance level, assuming that design requirements associated with different performance-levels are implicitly satisfied (Chapters 2, 6). In the proposed method, multi-level performance requirements are clearly stated and described in terms of post-earthquake operationality, damage, and feasibility of repair. Acknowledging the inherent iterative nature of the design process when realistic structural systems are considered, particular attention was drawn to the thorough consideration and/or development of the required tools with a view to avoiding computationally intensive iterative analysis. Main findings of the study are summarised in subsequent sections in a bullet-point format followed by additional discussion and comments in plain text, while detailed conclusions can be found in closing sections of relevant chapters (i.e. §3.4, 5.4, 6.4). Conclusions in the following sections are presented with regard to the different bridge structural configurations considered in this study, namely, bridges with energy dissipations in the piers (§7.1.1), and seismically isolated bridges (§7.1.2). Recommendations for future research are provided in §7.2 following the same format. In addition, a framework of performance-based control principles for the future extension of the procedure towards the integration of advanced structural control techniques, is briefly set forth in §7.2.3.

7.1.1 Bridges with energy dissipation in the piers

A deformation-based design (Def-BD) procedure initially developed for seismic design of conventional (i.e. non-isolated) buildings (Kappos & Stefanidou 2010) was tailored to bridge structures, aiming at efficient structural design for multiple performance levels through the control of a fairly broad range of design parameters and the aid of nonlinear dynamic analysis.

The key issues in this respect were the following:

- Proper consideration of the intended plastic mechanism in the case of bridges under the considered performance levels, allowing yielding of the piers instead of the superstructure, and also the design of the bearings (typically not used in buildings, except in isolation schemes).
- Preliminary estimation of pier stiffness, strength, and expected inelastic response on a member-by-member basis, and inelastic modelling of dissipating zones, estimation of allowable deformations limits and confinement requirements on the basis of refined section analysis in subsequent steps. The above characteristics represent novel features of the methodology that were feasible mainly due to the smaller number of dissipating elements compared to the generally large number of beam plastic hinges in buildings.
- Modifications addressing specific bridge engineering aspects such as the proper (and simplified, compared to buildings) definition of required strength in dissipating zones, the expected elastic response of the deck, and the explicit treatment of elastomeric bearings (i.e. required verifications and consideration of appropriate deformation limits).
- Introduction of different performance objectives explicitly accounting for the importance of the bridge under investigation, and proper adjustment of relevant performance requirements, within an integrated performance-based design framework.

The validity of the suggested procedure was demonstrated by adopting a specific design – assessment format serving the purposes of the included investigations. Specifically, the proposed method was first applied to an actual bridge adopting the '*ordinary bridge*' performance objective, and considering different seismic zones. Ground motion was represented by natural records, following the EN1998-2 (CEN 2005a) prescriptions for seismic action representation, selection, and scaling (common in other codes too), along with a 'structure-specific' ground motion selection criterion (quantified by the statistical measure of the standard error of the mean) used to limit the variability of response estimates and hence increase the reliability of their mean. Resulted designs were then assessed using artificial records closely matching the design spectrum associated with each performance level. Comparisons in terms of both economy and performance were made among designs resulting from the deformation-based design (Def-BD) method, the modal direct displacement-based design (MDDBD) method, and a force-based code-type (Code-BD) method (corresponding to the actual bridge design).

The following conclusions apply with respect to the efficiency of the previous methods in providing reliable estimates of response, satisfying diverse performance requirements, and leading to cost-effective design solutions by applying a reasonable computational effort.

- Refined analysis and modelling approaches, along with the consistent performance-based design format within the Def-BD framework (i.e. explicit consideration of multiple performance levels), resulted in superior seismic performance compared to the MDDBD and the code-type design methods.

- Significant cost reductions were achieved in the case of Def-BD compared to the MDDBD procedure, whereas potential cost reductions may generally be obtained compared to force-based code-type procedures due to the adoption of more rational design approaches accounting for the seismicity of the site in lieu of 'standard' capacity design considerations.

- Minimum iterative effort was ensured in Def-BD due to the integrated logical analysis-design route that consists of distinct design steps. Each step corresponds to a different performance level (depending on the selected performance objective) and is associated with inelastic modelling and design of specific bridge members and/or type of verifications. On the contrary, MDDBD and code-type procedures involve iterations within a single application of the method (accounting for a single performance level), and iterative application of the method or implicit/capacity design considerations to account for different performance levels.

The seismic performance superiority of the Def-BD framework was demonstrated by accurate predictions of peak inelastic demand and the control of various design parameters and structural performance requirements over multiple performance levels, with only occasional and marginal exceedances. Adopting a 'structure-specific' ground motion selection criterion by constraining the variability of elastic responses, prevented a significant overestimation of peak inelastic response quantities, commonly introduced during design when code-type scaling procedures are applied using a small number of natural records. MDDBD resulted in similar structural performance to Def-BD for the explicitly verified common performance level (i.e. SP3 requirements); nevertheless, the inherent inability of the former method to account for the modification of the dynamic characteristics of the structure during the successive formation of plastic hinges, along with the introduction of an equivalent linearisation approach, resulted in an increase in pier dimensions and reinforcing steel requirements. Disregarding altogether the effect of the pier inelastic response on the estimation of the dynamic characteristics of the bridges in the case of Code-BD, resulted in the highest deviation among the displacement response assumed during the design and the response assessed through rigorous nonlinear dynamic analysis (direct cost evaluations were skipped due to the over-conservatism adopted in the design of the actual bridge).

'Operationality' (SP2) criteria were found to govern the flexural design of the piers in all cases of Def-BD. Verifications associated with 'feasible repair' and 'limited service' (SP3) criteria were not found to be critical, resulting in pier deformation demands similar to deformation limits that corresponded to code requirements for minimum transverse reinforcement. Verifications associated with the 'severe damage' and 'disrupted service' of the bridge (i.e. SP4) imposed critical (with respect to stability) deformations at the bearings and defined the required transverse reinforcement of members. Assessment of Code-BD under levels of seismic action consistent with those used in Def-BD (i.e. Code-BDn), introduced to enable meaningful comparisons with Def-BD, confirmed that definition of strength on the basis of 'life-safety' (SP3) design criteria does not necessarily ensure controlled structural performance under different performance levels associated with 'operationality' (SP2) and 'collapse-prevention' (SP4) requirements, indicating an inherent

weakness of code-type single-performance level procedures where SP2 and SP4 criteria are implicitly considered. In a similar context, verifications of the deck for seismic actions were not found critical in any of the considered methods. However, certain drawbacks of deck capacity design considerations required in the cases of MDDBD and Code-BD, were identified; i.e. the problematic definition of the intended plastic mechanism in the transverse direction of the bridge, and the potentially inappropriate adoption of 'uncracked' gross section in modelling the flexural stiffness of the deck. Both issues are effectively considered within the Def-BD framework.

Based on the aforementioned findings, Def-BD emerges as a rigorous methodology, applicable to most of the common concrete bridge configurations without practical limitations related to the irregularity of the structural system considered. Inevitably this comes at the expense of additional computational time and effort associated with the use of nonlinear dynamic analysis (i.e. in modelling nonlinearity and properly defining the seismic input), and the design of different members at different steps of the procedure involving various levels of seismic action. Apart from the integrated logical design route, additional measures in reducing the computational effort involve the estimation of pier strength using design 'routines' accounting for the adopted target performance, and the investigation (in the case of seismically isolated bridges) of an alternative, and as a rule, simpler scaling approach.

Overall, what essentially differentiates Def-BD from other methods is its ability to effectively control a broader range of design parameters (i.e. from strains up to flexural deformations and drifts) under different earthquake levels (two explicitly and two implicitly considered) within a non-iterative application of the method.

7.1.2 Bridges with passive control systems

7.1.2.1 Development of generalised design equations

Considering the diversity of passive devices along with their inherent weakness to optimise the bridge response under multiple performance levels, a methodology was developed to enable the identification of the critical performance requirements and the comparative evaluation of different isolation schemes at the early stages of design. This provides the designer with the quantitative tools required to select a 'near-optimal' design solution in terms of both economy (e.g. total cost of alternative solutions) and structural performance; it also accounts for additional design constraints associated with the critical states of the isolated system, i.e. states of peak relative displacement, total acceleration, and relative velocity. Originating from an earlier study focusing on bilinear isolators (Ryan & Chopra 2004b), the method was extended here with a view to developing generalised design equations (GDEs) capable of providing reliable estimates of peak inelastic response in linear/bilinear isolation systems with or without supplemental linear/nonlinear viscous damping under different performance levels associated with code-based target spectra of common frequency content but different intensity. Three different cases, were explicitly considered,

namely, (*i*) isolated single-degree-of-freedom (SDOF) systems with linear viscous damping, (*ii*) isolated SDOFs with nonlinear viscous damping, and (*iii*) isolated two-degree-of-freedom (2DOF) systems with linear viscous damping.

The following conclusions, regarding the development of the methodology and its usefulness in practical applications, were drawn from extensive parametric nonlinear dynamic analysis of the idealised RDOFs:

- The dynamic equation of motion of SDOF and 2DOF systems representing idealised isolated bridge decks under unidirectional and bidirectional excitation, respectively, was normalised, aiming at uncoupling the normalised response from the seismic intensity and limiting the dispersion of peak normalised relative displacements $\bar{u}_0$ and total accelerations $\ddot{\bar{U}}_0$. Two conditions were identified in this respect; the first involved the characterisation of the isolation system strength by η (i.e. strength at zero displacement V_0 normalised to the seismic intensity as expressed by the peak ground velocity *PGV*); the second was associated with the characterisation of nonlinear viscous dampers by the 'energy-equivalence' approach (i.e. dampers of the same damping ratio ξ but different velocity exponent *a*). The above conditions along with the assumption of a constant value for the yield displacement u_y (associated with the type of isolators) reduced the governing parameters that significantly affect the response, to the isolation period T_p, the normalised strength η, and the damping ratio of energy-equivalent dampers ξ. Furthermore, they allowed the development of GDEs (with the aid of regression analysis) for the direct estimation of non-normalised relative displacements u_0 and total accelerations $\ddot{U}_0$.

- Integration of 'design principles', by means of using code-compatible scaling procedures and target spectra, required the selection and/or generation of records with mean characteristics (i.e. mean spectrum, mean *PGV*) that closely match the target properties (i.e. shape of target spectrum and design *PGV*). The above requirements were associated with increased computational effort when natural records were used. On the other hand, artificial accelerograms satisfied easily the above requirements (using a relatively small number of records) and provided robust estimates of mean response so long as member strength degradation was not considered.

- In the case of bidirectional excitation, further investigations on the dispersion in the angles at which peak response occurs, justified the common practice of designing isolators to sustain the maximum relative displacement in any random direction; it also indicated the need for applying the selected records at different angles of incidence when designing the substructure. Moreover, development of simplified bidirectional models by constraining the regression coefficients of relevant models under unidirectional excitation, revealed the expected mean increase in peak responses due to the effect of the second component of seismic actions, when the EN1998-2

(CEN 2005a) scaling procedure is employed, providing an effective means to evaluate results derived from different types of analysis.

- The developed regression models were assessed both in terms of accuracy in peak response prediction and effectiveness in 'near-optimal' system identification while the procedure was fully automated within the developed code IDEC (*Isolation Design Equations Code*) to facilitate the development of GDEs in cases different from those considered herein (i.e. target spectrum with a frequency content corresponding to site conditions 'C' of EN1998-1 (CEN 2004b) and elastomer-based isolators).

The suggested procedure represents an alternative to equivalent linearisation approaches commonly adopted by codes, and as such, it can be implemented either on a 'stand-alone' basis, or for preliminary design purposes in more refined design procedures, such as the Def-BD method.

7.1.2.2 Deformation-based design of seismically isolated bridges

The Def-BD method previously proposed for bridges with energy dissipation in the ductile piers was subsequently extended to seismically isolated bridges. Sharing the same principles, the suggested procedure initially identifies the basic characteristics of the structural system and subsequently associates design of specific bridge members and type of verifications with certain performance levels depending on the selected performance objective.

Key features of the deformation-based design method for seismically isolated bridges are the following:

- Use of GDEs for the preliminary 'near-optimal' selection of the basic properties of the isolation and energy dissipation system according to §7.1.2.1.
- Iterative application of GDEs during preliminary design to properly capture the effect of nonlinearity of viscous dampers at that stage, as opposed to the case of linear viscous damping devices wherein no iterations are required. In either case no iterative structural analysis is needed.
- Preliminary design of substructure members in the general case of bidirectional excitation for the most adverse of the effects derived by independently applying the maximum inertia force $m\ddot{U}_0$ in the principal directions of the bridge. Transformation of the pairs of horizontal components of seismic action into principal components and consecutive application along both directions of the bridge in subsequent steps.
- Enhanced performance objectives reflecting the higher performance expected in the case of seismically isolated bridges and ensuring the effectiveness of the isolation system under the considered performance levels.

- Realisation of the selected scheme through base isolation and energy dissipation devices accounting for the variability of their design properties.

The above features along with the use of nonlinear dynamic analysis that remedies certain pitfalls of equivalent linearisation approaches (§2.3.3) results in informed preliminary selections without the requirement of iterative analysis. The isolation system is characterised by meaningful properties having a significant effect on the response (as opposed to the 'non-physical' effective properties), while higher mode effects, non-proportionality of the system damping matrix, and the actual peak velocities are explicitly considered. The intended plastic mechanism of the substructure in the state of peak total accelerations, and an adequate restoring capability are ensured. Furthermore, the variability of design properties of devices is addressed both at the preliminary selection of the isolation system and at subsequent verifications using nonlinear dynamic analysis results disengaged from statistical modal and directional combination approximations. An implicit approach for considering the above variability can reduce the required sets of nonlinear dynamic analyses.

The validity of the procedure was demonstrated by applying it to the transverse direction of the bridge previously used to develop the Def-BD method for bridges with energy dissipation in the piers following the same design – assessment format. Three alternative isolation schemes were investigated, namely, (*i*) deck isolated with lead rubber bearings (LRBs), (*ii*) low damping rubber bearings (LDRBs) and linear viscous dampers (LVDs), (*iii*) LDRBs and non-linear viscous dampers (NLVDs). The effect of the orthogonal component of seismic action was subsequently explored in the case of the LRB scheme; the latter case (i.e. LRB scheme under bidirectional excitation) was also compared with the design resulting from the 'spectral' method prescribed in EN1998-2 (CEN 2005a).

The following conclusions apply with respect to the efficiency of the previous methods in providing reliable estimates of response, satisfying diverse performance requirements, and leading to cost-effective design solutions by applying reasonable computational effort.

- Assessment of designs revealed that the Def-BD procedure predicted well the structural response in terms of displacement and shear force demand both at the stages of preliminary design (indicating the effectiveness of GDEs) and the subsequent steps, while generally resulting in safe design, in the sense of respecting the adopted multi-level performance requirements. On the other hand, the EN1998-2 method did not ensure an accurate estimation of peak response due to the approximate nature of the equivalent linearisation approach and the implicit estimation of deformations under the maximum level of seismic actions.

- Application of the EN1998-2 design procedure resulted in significant reductions in reinforcing steel demands (for the piers). However, subsequent assessment of the design, indicated that the main sources of this reduction, namely, (*i*) the inconsistent consideration of the effect of bidirectional excitation in different analysis methods, (*ii*) the limitation of the inelastic pier

response in isolated bridges under the ‘design’ rather than the ‘maximum considered’ seismic actions, and (*iii*) the deviation of response quantities resulting from the ‘spectral’ equivalent linearisation approach, may compromise the safety of the isolated bridge by imposing large inelastic deformations in substructure elements.

- Preliminary selections and subsequent verifications in Def-BD are facilitated with the use of GDEs, displaying in a simple and concise manner significant variations in peak response deriving from different performance levels, isolation schemes, and the variability of design properties of devices. On the contrary, the EN1998-2 design method may involve a significant number of iterative applications especially when the characteristics of the passive devices are not known at the beginning of the design procedure, as is common in the design of a new bridge.

Verifications associated with the deformation (and stability) capacity of isolators and the controlled inelastic response of piers (SP3 requirements) under the maximum level of the considered seismic actions, governed in general the Def-BD designs in all considered isolation schemes under both unidirectional and bidirectional excitation, highlighting the necessity for a detailed evaluation of this specific performance level in isolated bridges. Deviations in response estimations between design and assessment may be introduced due to the implicit approach in considering the variability of design properties, the adopted scaling approach and minimum number of considered records, and due to torsional effects in the deck. In the examples studied herein, the implicit approach, although more conservative, did not result in overdesigning members and devices. Although the adopted scaling approach applying different scaling factors in each record (or pair of records) resulted in displacement estimates close to those derived from the assessment using artificial records (involving less computational effort compared to the EN1998-2 approach), the suite of 7 natural records (as commonly required by codes) was not in general able to limit standard error values of mean responses, resulting in overestimations of local ductility demands. The piers had a minor effect on the peak response of the isolation system.

Among the isolation schemes investigated under unidirectional excitation in the case of Def-BD, LRBs and LDRB+LVDs resulted in similar bridge performance. Besides providing a safeguard mechanism against excessive structural velocities, introduction of nonlinearity in viscous dampers in the LDRB+NLVD scheme effectively constrained peak damper forces according to the set target performance without significantly affecting the overall bridge response. A relatively lower seismic demand in the piers was found for the bridge type and seismic scenario considered herein. In addition, all isolation schemes resulted in lower pier reinforcement demand compared to the design for ductile pier response, indicating that optimally selected isolation systems can provide significant cost reductions in substructure design while satisfying a higher performance objective.

Implementation of the Def-BD method under bidirectional excitation revealed the efficiency of the procedure in predicting the deformation response of the isolation system. Small variations of peak deformations with the incidence angle indicated that consideration of the horizontal seismic

components of pairs of records along the two axes of the bridge can adequately assess the deformation demand in isolation systems with symmetric distribution of mechanical properties. Although the design methodology predicted well the shear forces developed in the piers, flexural design for the most adverse of the effects derived by independently applying the maximum inertia force in the two directions of the bridge resulted in conservative design with regard to pier longitudinal reinforcement (increase of 1-17%). Nevertheless, the design approach of applying $m\ddot{U}_0$ in each principal direction of the bridge is recommended unless a detailed investigation of the effect of the incidence angle is performed involving a large number of analysis sets.

Considering the EN1998-2 'spectral' approach, the approximate nature of the equivalent linearisation approach resulted in deviations of displacement response within a range of 10-30% compared to rigorous nonlinear dynamic analysis results, despite the introduction of iterations. The implicit estimation of deformations under the maximum level of seismic actions was found inadequate to capture the peak inelastic response of isolators indicating the risk of underestimating their required deformation capacity. Apart from the iterations introduced due to the secant-stiffness-based formulation of the equivalent linearisation approach, and the unknown device properties at the start of the design process, the number of iterations will further increase if additional design criteria, such as those included in the proposed Def-BD, are sought (e.g. by setting a target performance under multiple performance levels with respect to peak deformations, energy dissipation, minimisation of the substructure design cost, etc.). Although such design constraints are not required by EN1998-2, they might be employed by designers to identify cost effective design solution so long as the relevant code requirements are satisfied.

The proposed Def-BD methodology for isolated bridges refers explicitly to the integration of passive structural control techniques. Nevertheless, an effort was made towards the adoption of a proper format that should serve as the point of reference for extending the suggested procedure to bridges incorporating advanced structural control techniques (e.g. adaptive passive, semi-active). The suitable formulation of Def-BD and steps towards the 'advanced control' objective, are discussed in more detail in a following section (§7.2.3).

7.2 Recommendations for Future Research

Recommendations for future research are listed herein as '*short-term*' and '*long-term*' objectives, depending on the complexity they introduce. Subsequent sections focus mainly on the first class consisting of further investigations required to assess the effectiveness of the proposed design framework using in principle the formulation of the Def-BD method as presented in this study. Among them, the effectiveness of the Def-BD method in bridges adopting a higher performance objective than the '*ordinary*' (i.e. bridge of average importance) considered herein, and the investigation of the effect of the vertical component of seismic action (not addressed in this study for the sake of simplicity during this first formulation of the method), represent common research objectives, irrespective of the considered bridge configuration. Similarly, the effect of spatial

variability of ground motion in long bridges and/or bridges founded on diverse site conditions (not addressed herein) need to be explored in both conventional and isolated bridge configurations. Research recommendations that are expected to revise and/or extend basic principles of the method are characterised as 'long-term' objectives. In this context, the explicit consideration of uncertainties in more complex probabilistic and resilience-based design frameworks potentially involving optimisation approaches, and the incorporation of advanced structural control techniques (e.g. semi-active control), are expected to require significant changes in the formulation of the method (as in relevant design codes of practice) and hence these serve as long-term research objectives.

7.2.1 Bridges with energy dissipation in the piers

Future short-term research objectives should focus on evaluating the effectiveness of the suggested procedure regarding the treatment of design issues that were partially (or not) addressed here, and the implementation in bridge systems wherein Def-BD is expected to be more valuable for the proper estimation of the actual inelastic response and hence their efficient design. Although §3.2 provides specific guidelines for the explicit consideration of the effect of bidirectional excitation, design examples in the case of bridges with energy dissipation in the piers were restricted to the study of the transverse response, as a means to facilitate and enable comparisons with designs resulting from different methodologies. In a similar context, application of Def-BD to complex bridge configurations, is also in order. The case study in §3.3 addressed a relatively short bridge wherein piers of different height and unrestrained response of the deck at the abutments triggered an increased contribution of the second mode. Additional structural configurations with strong influence of higher mode are long bridges with non-symmetric substructures and/or curved-in-plan superstructures. Furthermore, soil-foundation-structure interaction and alternative configurations of abutment-to-deck connections, need to be explored. The latter, were dealt in the design framework (Table 3.1) of the suggested procedure but were not supported so far through integrated case studies. To this end, design examples focusing on connections that activate the abutment-backfill system in both (integral, through links) or in a single direction of the bridge, characterised by complex member interactions (e.g. backfill soil-abutment-deck), should be investigated.

Due to the suitable formulation of the method, investigation of the above issues is deemed straightforward and their consideration should be addressed with a view to maintaining the required computational effort within reasonable limits; i.e. providing simple rules for integration within the proposed multi-performance level procedure, assessing the efficiency of Step 2 in obtaining target performances with little or no iterations, and the efficiency of Step 4 in implicitly estimating the peak inelastic demand under EQ(SP4) using properly selected magnification factors.

7.2.2 Bridges with passive control systems

As in the case of §7.2.1, short term research objectives entail the investigation of the efficiency of the proposed methods (i.e. GDEs, Def-BD) in structural systems that are currently not supported by detailed case studies. The development of GDEs was based to some extent on the adoption of constant yield displacement u_y values associated with specific types of (herein elastomer-based) isolators. This assumption was largely based on previous studies (e.g. Makris & Black 2004) demonstrating by dimensional analysis that for a given value of the dimensionless strength, the solution for the dimensionless peak displacement is nearly independent of the dimensionless yield displacement, even when u_y is varied by two orders of magnitude (e.g. 0.0001~0.01), further concluding that under earthquake shaking, an isolated bridge exhibits the same peak displacement regardless of the type of isolators (so long as they possess the same V_0 and T_p). The effect of the previous assumptions on GDEs providing non-normalised peak response estimates in linear/bilinear isolation systems with linear/nonlinear viscous damping has not yet been explored in detail (e.g. the case of friction-based isolators with/without viscous dampers). In a similar context, a worth to pursue investigation is the case of isolators combined with nonlinear viscous dampers under bidirectional excitation (§4.5.3), where due to the minor effect of the nonlinearity of viscous damper in the peak inelastic response, the developed GDEs are expected to yield reasonable results. In all previous cases, the developed IDEC code can greatly facilitate the investigation, targeting also less common damping systems that were not addressed herein, such as, metallic yield dampers.

Considering the Def-BD procedure, an attempt was made to identify and quantify conservatism introduced in design due to representations of seismic action adopted or recommended by codes. To this end, natural records were used at the design stage that typically introduce conservatism in design when combined with common code-type scaling procedure for reasons described in detail in the relevant chapters. Additional measures to constrain the variability of responses with a view to obtaining more reliable estimates of response were explored. Even so, the variability of local inelastic deformation measures (e.g. ductility factors) cannot be easily constrained and additional measures of treatment such as the increase of the minimum number of records (e.g. to 11 in the recent ASCE 2016), or the use of artificial/synthetic records should be further explored, noting that the latter option may provide an efficient means towards the previous objectives when issues such as the degradation of strength are disregarded (e.g. nonlinear analysis framework within *fib* 2012a, b). A different source of potential conservatism deserving some consideration, i.e. the flexural design of the piers for the most adverse of the effects derived by independently applying the maximum inertia force (obtained by GDEs under bidirectional excitation) in the two directions of the bridge, is difficult to constrain; this is due to the unknown angle at which peak responses develop, noting though, that the expected increase in cost of reinforcement is insignificant compared to the cost of isolators in the case of small to moderate bridges.

Regarding the issue of complex bridge configurations, simple rules such as those provided herein for the verification of straight bridges with passive systems having ‘symmetric’ mechanical

properties along the principal directions of the bridge, should be sought to avoid exhaustive sets of dynamic analysis under various angles of incidence. Although movement of the deck was allowed in both directions of the bridges that have been investigated so far using passive systems with identical properties along the principal axes of the bridge, the extension of the procedure to different configurations, such as decks supported on moveable bearings in the longitudinal direction, but restrained in the transverse direction via seismic links (i.e. common configuration in railway bridges), or placement of dampers with different properties along the longitudinal and transverse axes, were explicitly addressed. Nevertheless, comprehensive case studies are required in support of the guidelines provided for the proper implementation of the method in §5.4.

Additional work is clearly required to assess the effect of site conditions (reduction of the efficiency of isolators when soil-structure-interaction phenomena are substantial), proximity to active faults (detrimental effects of excessive structural velocities), and the potential cost benefits in isolation solutions derived from Def-BD (presented in this study with respect to the design of the substructure), when life-cycle cost considerations of the bridge are taken into account.

7.2.3 Bridges with advanced structural control techniques

Implementation of advanced structural control techniques has not yet been well addressed in a comprehensive way as a (performance-based) design option that can result in the same (or superior) performance compared to other design alternatives (e.g. adoption of passive control schemes) but at a lower cost (in a life-cycle context). In this respect, further development of current performance-based design procedures to account for the improvement in structural performance due to a rational implementation of structural control devices, in line with the current trends in the use of structural control in bridge engineering (Gkatzogias & Kappos 2016b), constitutes a decisive step for the wider acceptance of ‘smart’ technology (i.e. adaptive passive and semi-active) and should be sought within the following framework of objectives, specifically referring to seismic loading but which can (and often should) also be adapted to other dynamic loadings:

- Design bridge structures that can respond favourably to earthquakes with different frequency content (e.g. proximity to active seismic faults, local site conditions, site affected by different seismic sources) and various intensity levels, associated with multiple performance levels such as serviceability-operationality, damage limitation, and life safety.
- Enhance the effectiveness of standard passive control systems by introducing novel control devices and hybrid control (e.g. increase the effectiveness of a base isolation system on relatively soft ground).
- Address and reconcile the widely varying requirements emerging from the application of different types of actions (e.g. braking loads from vehicles, wind in long cable-stayed bridges, earthquake actions).

- Reduce the bridge response by establishing a non-resonant state under earthquake excitations.
- Increase the bridge design working life using life-cycle cost considerations.

In view of the previous performance-based structural control framework, an effort was made towards the adoption of a proper format in the Def-BD method that may facilitate the extension of the suggested procedure towards the first design objective, and specifically the favourable response under multi-level performance requirements. In this respect, incorporation of adaptive passive devices is deemed straightforward according to the following, and hence could be considered a short-term objective. The design of adaptive passive devices, e.g. spherical sliding isolation bearings with various concave surfaces (Fenz & Constantinou 2008) or a single concave surface with variable friction coefficients (Calvi *et al*. 2016) which modify their stiffness (and hence the isolation period T_p) and damping ratio as a function of the displacement amplitude, can be dealt with in Def-BD in the context of 'optimisation'. Design of a seismically isolated bridge with adaptive passive devices should aim at 'near-optimal' structural performances under multiple performance levels instead of a single critical one, e.g. under EQ(SP2) and EQ(SP3), or under EQ(SP1), EQ(SP2) and EQ(SP3) (Table 5.1), thus, outperforming passive schemes wherein 'near-optimal' performance under a selected performance level is normally associated with sub-optimal (hence non-economic) response under a different one (§5.2.2). To this effect, Step 1 of the Def-BD method (§5.2.2) can be applied for the performance levels associated with EQ(SP2) and EQ(SP3) (i.e. for two reference levels of seismic action) with a view to estimating the required mechanical properties of the adaptive passive device (ξ, V_0, T_p) for each performance level, and hence, minimising the cost of both the substructure (e.g. reinforcing steel in piers) and the isolation system (displacement capacity of isolators). Subsequent steps should aim at the verification of the pier and isolator response with the aid of nonlinear dynamic analysis in line with §5.2, requiring though, the introduction of 'device-specific' hysteresis rules characterising the more complex behaviour of these devices.

The Def-BD in its current form, may be used for the design of semi-active devices operating in a passive mode (e.g. magnetorheological dampers under a constant voltage) with a view to introducing different damping coefficients in different parts of structures using the same device (e.g. in a highly non-symmetric bridge). Furthermore, the Def-BD scheme may be employed for the preliminary selection of 'near-optimal' semi-active device properties as in the case of adaptive passive devices. Nevertheless, introduction of control algorithms will be required to modify the mechanical properties of semi-active devices in real-time (i.e. during the earthquake) and this, hence, represents a long-term objective.

Annex A
Supplement to Chapter 3

A.1 Case Study [§3.3]

A.1.1 Description of studied bridge [§3.3.1]

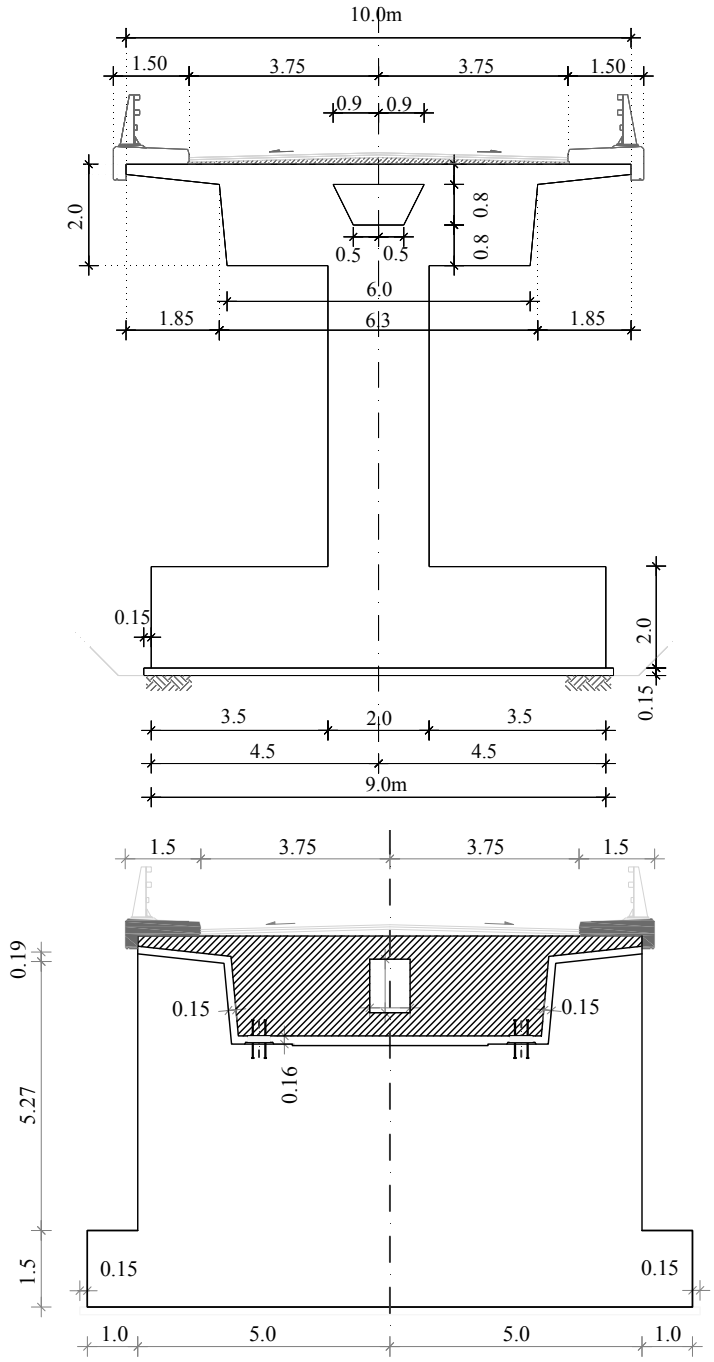

Fig. A.1 Lateral cross-sections of Overpass T7 (Egnatia Motorway 2002, Paraskeva 2013): Pier 1 (Section 3-3 in Fig. 3.6) (top), Abutment 1 (Section 1-1 in Fig. 3.6) (bottom)

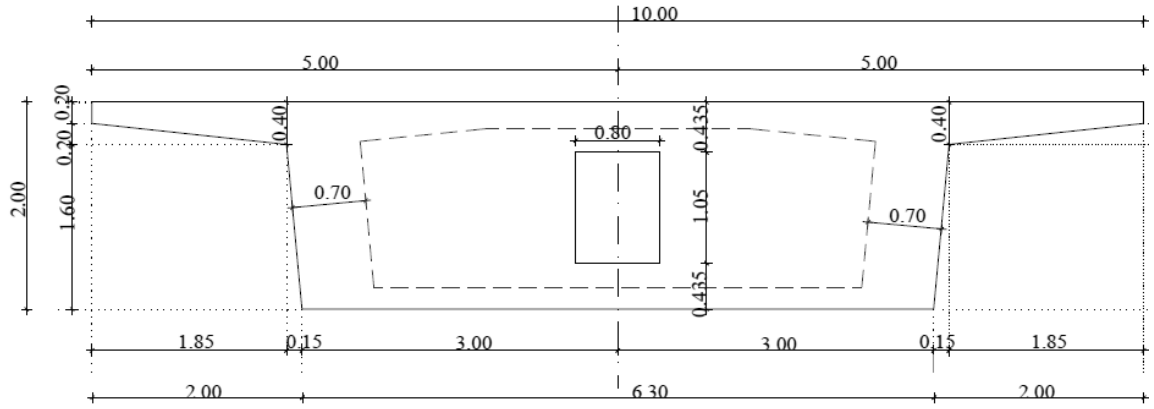

Section 1-1 in Fig. 3.6

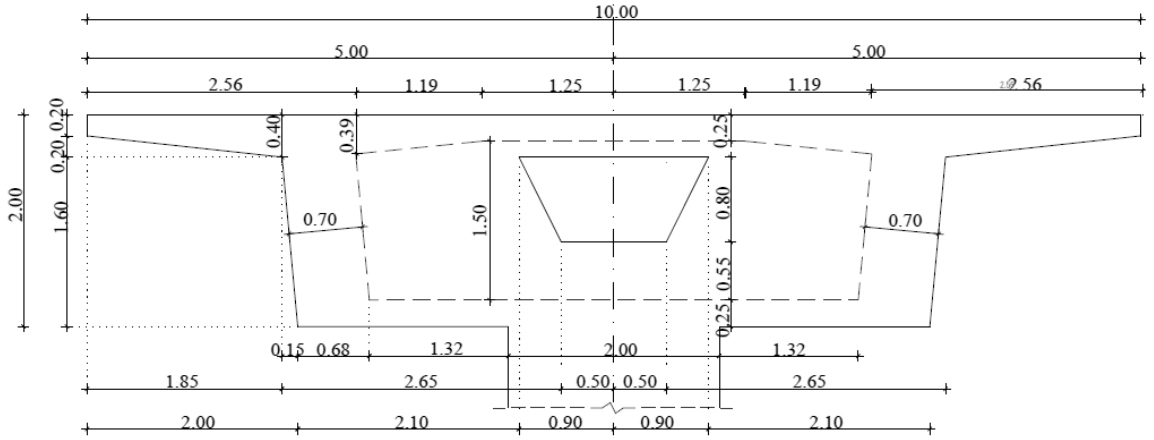

Section 3-3 in Fig. 3.6

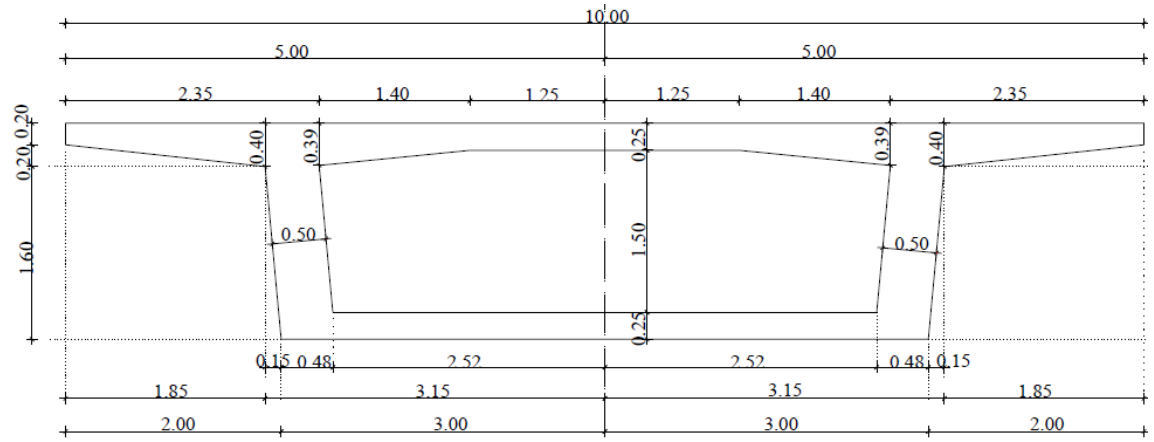

Section 4-4 in Fig. 3.6

Fig. A.2 Box girder deck sections of Overpass T7 (Egnatia Motorway 2002, Paraskeva 2013)

A.1.2 Application of the Def-BD procedure [§3.3.5], Assessment of design [§3.3.6]

Table A.1 Critical design and assessment quantities for ZII

No.	Steps 1, 2 (EQII)		Design	Design		Assessment		Design	Design		Assessment	
			RSA	SP2	NLRHA	SP2	NLRHA	RSA	SP2	NLRHA	SP2	NLRHA
	Member		Pier 1					Pier 2				
1	EI_y / EI_g (%)	Base	43	66		61		43	66		62	
2		Top	43	66		61		43	66		62	
3	μ_φ	Base	2.31	2.72	3.17	2.43	2.25	2.31	2.73	2.19	2.51	1.71
4		Top	-	2.76	0.71	2.46	0.65	-	2.77	0.71	2.55	0.71
5	μ_θ	Base	1.65	1.79	2.00	1.67	1.59	1.55	1.62	1.42	1.55	1.26
6		Top	-	2.08	0.71	1.89	0.65	-	1.81	0.71	1.71	0.71
7	μ_u		-	-	1.70	-	1.46	-	-	1.25	-	1.17
8	Col. Drift (%)		-	-	0.68	-	0.63	-	-	0.64	-	0.62
9	h_{eq} (m)	Base	3.69	-	3.94	-	3.87	4.66	-	5.11	-	4.95
10		Top	2.25	-	2.96	-	2.97	3.27	-	3.95	-	3.96
-	Member		Abutment 1					Abutment 2				
11	γ_q (%)		71	100	65	100	63	102	100	88	100	92

No.	Step 3 (EQIII)		Design	Design		Assessment		Design	Design		Assessment	
			$\rho_{w,min}$	SP3	NLRHA	SP3	NLRHA	$\rho_{w,min}$	SP3	NLRHA	SP3	NLRHA
	Member		Pier 1					Pier 2				
12	μ_φ	Base	9.48	14.85	9.00	14.28	5.55	9.48	14.86	7.24	14.47	6.12
13		Top	9.59	15.04	4.02	14.48	1.40	9.66	15.18	3.22	14.74	2.16
14	μ_θ	Base	4.78	7.26	4.62	7.10	3.09	3.98	5.87	3.19	5.83	2.84
15		Top	6.26	9.62	2.85	9.25	1.23	4.97	7.51	1.98	7.31	1.53
16	μ_u		-	-	3.51	-	2.44	-	-	2.54	-	2.22
17	Col. Drift (%)		-	-	1.43	-	1.09	-	-	1.30	-	1.23
18	h_{eq} (m)	Base	-	-	4.02	-	3.95	-	-	5.17	-	5.06
19		Top	-	-	2.96	-	2.97	-	-	3.95	-	3.96
-	Member		Abutment 1					Abutment 2				
20	γ_q (%)			200	116	200	100		200	158	200	168

No.	Step 4 (EQIV)		Design	Design		Assessment		Design	Design		Assessment	
			NLRHA	SP4	SF·Step3	SP4	NLRHA	NLRHA	SP4	SF·Step3	SP4	NLRHA
	Member		Pier 1					Pier 2				
21	μ_φ	Base	21.27		18.01	19.22	15.44	17.23		14.48	15.54	15.28
22		Top	16.45		8.03	19.50	10.90	12.43		6.44	15.79	10.71
23	μ_θ	Base	10.03		9.23	9.42	7.67	6.70		6.38	6.16	6.07
24		Top	10.46	-	5.70	12.34	7.06	6.24	-	3.97	7.80	5.46
25	μ_u		7.62		7.02	-	5.72	5.20		5.08	-	4.67
26	Col. Drift (%)		3.09		2.85	-	2.59	2.71		2.61	-	2.64
27	h_{eq} (m)	Base	4.07		-	-	3.93	5.17		-	-	5.11
28		Top	2.96		-	-	2.96	3.96		-	-	3.95
-	Member		Abutment 1					Abutment 2				
30	γ_q (%)		228	368	232	392	186	290	369	316	388	305

Table A.2 Critical design and assessment quantities for ZIII

No.	Steps 1, 2 (EQII)		Design	Design		Assessment		Design	Design		Assessment	
			RSA	SP2	NLRHA	SP2	NLRHA	RSA	SP2	NLRHA	SP2	NLRHA
	Member		Pier 1					Pier 2				
1	EI_y / EI_g (%)	Base	39	43		41		39	42		41	
2		Top	39	43		41		39	42		41	
3	μ_φ	Base	2.49	2.56	2.42	2.28	1.73	2.49	3.01	2.29	2.80	1.60
4		Top	-	2.61	0.32	2.32	0.34	-	3.11	0.47	2.88	0.48
5	μ_θ	Base	1.58	1.57	1.52	1.49	1.28	1.48	1.60	1.39	1.57	1.19
6		Top	-	2.03	0.32	1.83	0.34	-	2.01	0.47	1.89	0.48
7	μ_u		-	-	1.42	-	1.26	-	-	1.30	-	1.18
8	Col. Drift (%)		-	-	0.72	-	0.69	-	-	0.71	-	0.66
9	h_{eq} (m)	Base	4.65	-	4.98	-	4.70	5.67	-	6.12	-	5.71
10		Top	1.29	-	2.84	-	2.89	2.26	-	3.78	-	3.85
-	Member		Abutment 1					Abutment 2				
11	γ_q (%)		96	100	80	100	92	107	100	101	100	104

No.	Step 3 (EQIII)		Design	Design		Assessment		Design	Design		Assessment	
			$\rho_{w,min}$	SP3	NLRHA	SP3	NLRHA	$\rho_{w,min}$	SP3	NLRHA	SP3	NLRHA
	Member		Pier 1					Pier 2				
12	μ_φ	Base	9.14	14.11	7.17	13.20	4.89	10.84	16.77	8.38	13.44	6.28
13		Top	9.30	14.35	0.59	13.43	0.52	11.15	17.25	0.95	13.85	0.78
14	μ_θ	Base	3.99	5.89	3.33	5.58	2.46	3.88	5.76	3.24	4.81	2.63
15		Top	6.31	9.53	0.59	8.81	0.52	5.87	8.76	0.90	7.06	0.78
16	μ_u		-	-	2.89	-	2.13	-	-	2.77	-	2.24
17	Col. Drift (%)		-	-	1.43	-	1.21	-	-	1.51	-	1.30
18	h_{eq} (m)	Base	-	-	4.86	-	4.83	-	-	6.02	-	5.92
19		Top	-	-	2.84	-	2.89	-	-	3.80	-	3.85
-	Member		Abutment 1					Abutment 2				
20	γ_q (%)			200	125	200	129		200	197	200	186

No.	Step 4 (EQIV)		Design		Design	Assessment		Design		Design	Assessment	
			NLRHA	SP4	$SF \cdot$Step3	SP4	NLRHA	NLRHA	SP4	$SF \cdot$Step3	SP4	NLRHA
	Member		Pier 1					Pier 2				
21	μ_φ	Base	20.49		14.34	18.39	14.17	22.42		16.76	16.65	17.74
22		Top	7.29		1.18	18.74	2.70	7.83		1.89	17.09	7.09
23	μ_θ	Base	8.20		6.66	7.52	5.93	7.28		6.49	5.67	6.03
24		Top	5.01	-	1.18	12.13	2.07	5.73	-	1.81	8.58	3.87
25	μ_u		6.57		5.78	-	4.82	6.05		5.54	-	4.88
26	Col. Drift (%)		3.31		2.87	-	2.72	3.37		3.02	-	2.91
27	h_{eq} (m)	Base	4.94		-	-	4.84	6.20		-	-	6.08
28		Top	2.84		-	-	2.89	3.78		-	-	3.85
-	Member		Abutment 1					Abutment 2				
30	γ_q (%)		272	316	251	303	232	420	302	394	306	384

Annex B
Supplement to Chapter 4

B.1 Analysis Framework [§4.2]

B.1.1 Representation of seismic action [§4.2.2]

The correlation coefficient as expressed by Eq. (B.1) for two discrete acceleration histories (k, l) of n time intervals (dt) (i.e. *Pearson* coefficient) is defined by Eq. (B.1);

$$r\left(\ddot{u}_{g,k}, \ddot{u}_{g,l}\right) = \frac{1}{n-1}\sum_{i=1}^{n}\left(\frac{\ddot{u}_{g,k}(t_i) - \hat{\ddot{u}}_{g,k}}{s_{\ddot{u}_{g,k}}}\right)\left(\frac{\ddot{u}_{g,l}(t_i) - \hat{\ddot{u}}_{g,l}}{s_{\ddot{u}_{g,l}}}\right) \tag{B.1}$$

$\hat{\ddot{u}}_g$ and $s_{\ddot{u}g}$ in Eq. (B.1) represent the arithmetic mean (Eq. (B.2)) and the sample standard deviation (Eq. (B.3)) of $\ddot{u}_g$, respectively;

$$\hat{\ddot{u}}_{g,k(l)} = \frac{1}{n}\sum_{i=1}^{n}\left(\ddot{u}_{g,k(l)}(t_i)\right) \tag{B.2}$$

$$s_{\ddot{u}_{g,k(l)}} = \sqrt{\frac{1}{n-1}\sum_{i=1}^{n}\left(\ddot{u}_{g,k(l)}(t_i) - \hat{\ddot{u}}_{g,k(l)}\right)^2} \tag{B.3}$$

r coefficients for all possible combinations of the generated artificial accelerograms and those selected to form Art D suite, are provided for the pairs of horizontal components (H1, H2) in Table B.1.

In the case of natural records, the counter-clockwise rotation angle $\theta_{r=0}$ for which the correlation coefficient between k and l (unrotated) acceleration histories is zero is given by Eq. (B.4) (Rezaeian & Der Kiureghian 2012) where k is an integer introduced to constraint $\theta_{r=0}$ within the first quadrant.

$$\theta_{r=0} = \frac{1}{2}\tan^{-1}\left(\frac{2r\left(\ddot{u}_{g,k}, \ddot{u}_{g,l}\right)s_{\ddot{u}_{g,k}}s_{\ddot{u}_{g,l}}}{s^2_{\ddot{u}_{g,k}} - s^2_{\ddot{u}_{g,l}}}\right) + k\frac{\pi}{2}, \quad (\theta \text{ in rad}) \tag{B.4}$$

Rotated acceleration histories (k_θ, l_θ) are then calculated using the orthogonal transformation of Eq. (B.5);

$$\begin{bmatrix}\ddot{u}_{g,k_\theta}(t)\\ \ddot{u}_{g,l_\theta}(t)\end{bmatrix} = \begin{bmatrix}\cos(\theta_{r=0}) & \sin(\theta_{r=0})\\ -\sin(\theta_{r=0}) & \cos(\theta_{r=0})\end{bmatrix}\begin{bmatrix}\ddot{u}_{g,k}(t)\\ \ddot{u}_{g,l}(t)\end{bmatrix} \tag{B.5}$$

Table B.1 Correlation coefficient matrix of artificial records (in green: H1-H2 component coefficients for Art D)

No.	1	2	3	4	5	6	7	8	9	10	11	12	13	14	15	16	17	18	19	20
1	**1**																			
2	0.02	**1**																		
3	-0.01	0.07	**1**																	
4	0.02	0.02	0.11	**1**																
5	0.02	0.09	0.06	-0.02	**1**															
6	0.00	-0.11	0.02	0.06	-0.02	**1**														
7	-0.01	0.00	-0.01	0.02	-0.01	0.03	**1**													
8	0.01	0.02	-0.07	-0.08	-0.03	-0.03	-0.03	**1**												
9	-0.03	-0.01	-0.02	0.00	-0.03	-0.10	0.09	0.03	**1**											
10	0.00	-0.04	0.00	-0.08	-0.01	-0.01	-0.03	-0.06	0.03	**1**										
11	0.02	-0.15	-0.13	-0.23	-0.02	0.06	0.01	-0.03	0.03	0.05	**1**									
12	0.00	-0.04	-0.11	-0.02	-0.01	0.05	-0.08	0.01	-0.02	0.10	0.00	**1**								
13	-0.07	-0.02	-0.02	-0.03	-0.11	-0.01	0.04	0.03	0.07	-0.05	-0.06	-0.08	**1**							
14	0.13	0.00	0.07	0.03	-0.04	-0.04	0.03	-0.03	-0.05	0.05	-0.04	0.03	-0.06	**1**						
15	-0.05	-0.03	-0.06	-0.05	-0.03	0.02	-0.12	0.12	0.01	0.23	-0.02	0.03	0.04	0.00	**1**					
16	-0.02	-0.04	-0.13	0.03	-0.03	-0.03	0.04	0.00	0.02	0.01	0.06	0.01	-0.11	0.01	0.01	**1**				
17	0.06	0.15	0.09	-0.01	0.17	-0.08	0.00	-0.04	0.05	0.04	-0.03	0.02	-0.07	-0.01	0.00	0.00	**1**			
18	0.03	0.13	-0.06	-0.11	-0.09	-0.05	-0.03	-0.04	-0.04	-0.03	0.20	-0.06	-0.04	-0.05	-0.05	0.09	-0.04	**1**		
19	-0.02	-0.03	0.06	0.01	-0.06	-0.04	0.02	-0.02	0.03	0.01	-0.01	0.06	0.00	0.03	0.02	0.02	0.11	-0.08	**1**	
20	0.02	0.16	-0.09	0.11	-0.04	0.03	-0.02	0.01	0.04	0.00	-0.11	0.02	-0.01	-0.04	0.00	0.20	-0.02	0.06	0.01	**1**
Max| |	0.13	0.16	0.13	0.23	0.17	0.10	0.12	0.12	0.07	0.23	0.20	0.08	0.11	0.05	0.05	0.20	0.11	0.08	0.01	-

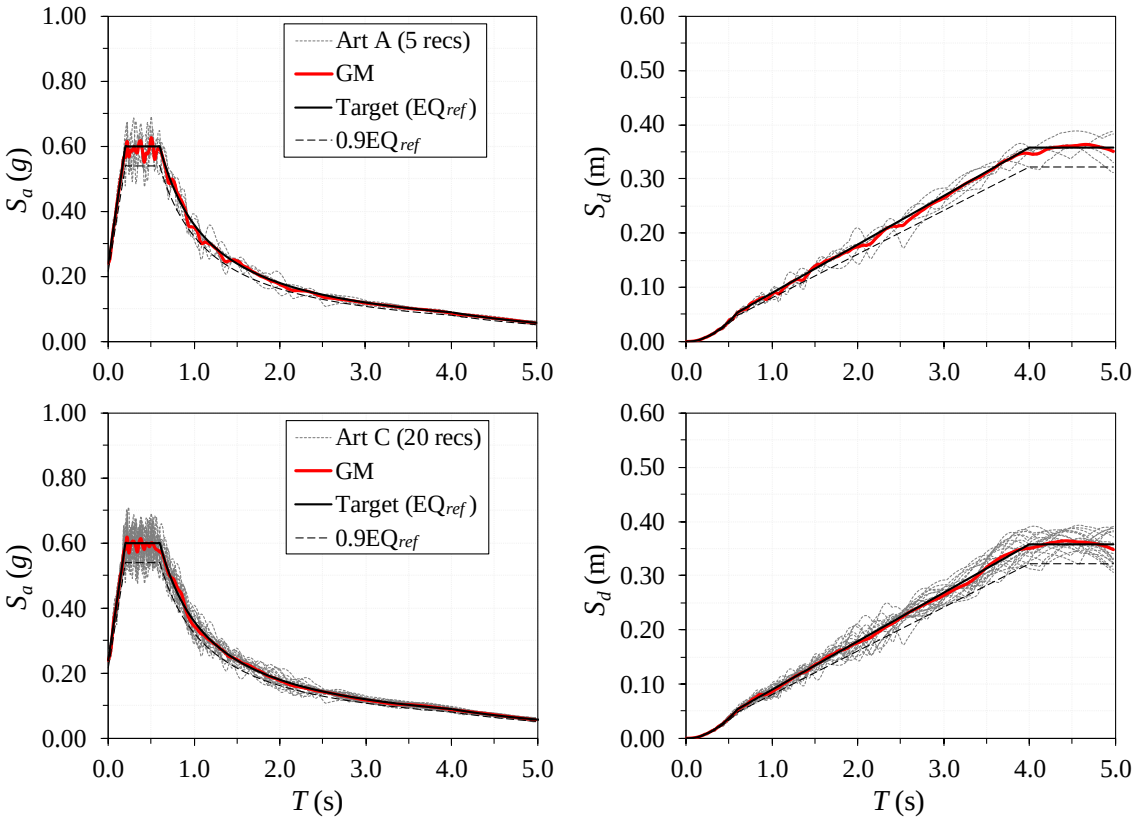

Fig. B.1 Spectral matching of response acceleration (left) and displacement (right) geometric mean (*GM*) spectra to the 1D target spectrum (*PGA* of 0.21*g*, site 'C', $T_{R,ref}$) for Art A, C) of artificial records

Values of design peak ground velocity (*PGV*) $\dot{u}_{g0}$ calculated from relationships proposed in recent research studies as a function of maximum spectral velocity (S_v) (i.e. Eq. (B.6)-(B.9)) of the target spectrum compared to the estimate provided by EN1998-2 (CEN 2005a) and the Italian Code (NTC 2008) (i.e. Eq. (B.10)) are provided in Table B.2.

$$\dot{u}_{g0} = \max S_v / 1.63 \text{ (Malhotra 2006)} \tag{B.6}$$

$$\dot{u}_{g0} = \max S_v / 1.59 \text{ (Bommer \& Alarcon 2006)} \tag{B.7}$$

$$\dot{u}_{g0} = \max S_v / 2.3 \text{ (Booth 2007)} \tag{B.8}$$

$$\dot{u}_{g0} = \max S_v / 1.7 \text{ (Palermo } et\ al. \text{ 2014)} \tag{B.9}$$

$$\dot{u}_{g0} = ST_C \ddot{u}_{g0} / 2\pi \text{ (CEN 2005a, NTC 2008)} \tag{B.10}$$

Table B.2 *PGV* estimation for T_R=475yrs (SF_{EQ}=1) and unidirectional excitation

Source	*PGV* (m/s)
Malhotra (2006)	0.345
Bommer & Alarcon (2006)	0.295
Booth (2007)	0.244
Palermo *et al.* (2014)	0.331
Geometric Mean (*GM*)	0.301
CEN (2005a), NTC (2008)	0.225

B.1.2 Statistical processing of key response quantities [§4.2.4]

For n recorded response quantities y_i sampled from lognormally distributed data, the sample geometric mean (*GM*) is determined according to Eq. (B.11);

$$GM(y) = \exp\left(\frac{\sum_{i=1}^{n} \ln y_i}{n}\right) = \sqrt[n]{\prod_{i=1}^{n} y_i} = \sqrt[n]{y_1 \cdot y_2 \cdot \ldots \cdot y_n} \tag{B.11}$$

The standard error of the sample geometric mean (*SEGM*) estimate is expressed as (Norris 1940);

$$SEGM(y) = GM(y)\frac{\delta(\ln y)}{\sqrt{n-1}} \tag{B.12}$$

The sample standard deviation of the natural logarithms (δ) of y_i in the previous equation is given by Eq. (B.13);

$$\delta\left(\ln y\right)=\sqrt{\frac{1}{n-1}\sum_{i=1}^{n}\left(\ln y_i-\ln GM\left(y\right)\right)^2} \tag{B.13}$$

Assuming that the sample size is small (i.e. n < 30) and the true (i.e. the population) standard deviation unknown, the random variable of Eq. (B.14) will follow a *Student*'s *t-distribution*;

$$\frac{\ln GM\left(y\right)-\ln GM_t}{SEGM\left(y\right)}=t \tag{B.14}$$

Exact confidence intervals can therefore be found as follows (Alf & Grossberg 1979); considering an (1-a) % confidence level (CL) and n-1 degrees of freedom df for the two-sided *Student*-t probability density function, the lower (L) and upper (U) GM intervals are first calculated by Eqs. (B.15) and (B.16) where the t-factor depends on CL assigned to predict the response estimate and a represents the significance level;

$$GM_L\left(y\right)=\exp\left(\ln GM\left(y\right)-\frac{\delta\left(\ln y\right)}{\sqrt{n-1}}t\left(\frac{a}{2},df\right)\right)=\frac{GM\left(y\right)}{\exp\left(\frac{\delta\left(\ln y\right)}{\sqrt{n-1}}t\left(\frac{a}{2},df\right)\right)} \tag{B.15}$$

$$\begin{aligned}GM_U\left(y\right)=\exp\left(\ln GM\left(y\right)+\frac{\delta\left(\ln y\right)}{\sqrt{n-1}}t\left(\frac{a}{2},df\right)\right)=\ldots\\ \ldots=GM\left(y\right)\exp\left(\frac{\delta\left(\ln y\right)}{\sqrt{n-1}}t\left(\frac{a}{2},df\right)\right)\end{aligned} \tag{B.16}$$

Associated $SEGM$ limits defined as percentages of the estimated geometric mean can be subsequently retrieved from Eqs. (B.17) and (B.18);

$$SEGM_L\left(\%\right)=\frac{GM\left(y\right)-GM_L\left(y\right)}{GM\left(y\right)}100 \tag{B.17}$$

$$SEGM_U\left(\%\right)=\frac{GM_U\left(y\right)-GM\left(y\right)}{GM\left(y\right)}100 \tag{B.18}$$

Annex C
Supplement to Chapter 5

C.1 Case Study [§5.3]

C.1.1 Unidirectional excitation [§5.3.5]

C.1.1.1 Application of the Def-BD procedure [§5.3.5.1]

See Table C.1. Displacement values included in Table C.1 and in the following tables represent relative displacements of passive devices (i.e. isolators, dampers).

C.1.1.2 Assessment of design [§5.3.5.2]

See Table C.2.

C.1.2 Bidirectional excitation [§5.3.6]

C.1.2.1 Application of the Def-BD procedure [§5.3.6.1]

See Table C.3. 'LRBs: 1D (H2 // *y*-*y*), D_p = 1.2 m' case included in the table represents results from the application of the method under unidirectional excitation (i.e. identical to those of Table C.1) to facilitate comparisons.

C.1.2.2 Assessment of design [§5.3.6.2]

See Table C.4. 'LRBs: 1D (Art B // *y*-*y*), D_p = 1.2 m' case included in the table, represents results from the application of the method under unidirectional excitation (i.e. identical to those of Table C.2) to facilitate comparisons.

Table C.1 Comparative evaluation of Def-BD for three different isolation schemes (Steps 1-3): Design stage

No.	Step		Property		LRBs				Prop.	LDRBs + LVDs (a=1.0)				LDRBs + NLVDs (a=0.2)				Design Criterion
	Step	EQ	Response	DP	Abt 1	Pier 1	Pier 2	Abt 2	DP	Abt 1	Pier 1	Pier 2	Abt 2	Abt 1	Pier 1	Pier 2	Abt 2	
1	1	IV	u_0 (m)	LB	0.256	0.256	0.256	0.256	LB	0.240	0.240	0.240	0.240	0.240	0.240	0.240	0.240	
2			V (kN)		948	1026	1026	948		1132	1132	1132	1132	1132	1132	1132	1132	
3			T_{eff} (s)		2.54					2.50				2.50				
4			u_0 (m)	UB	0.144	0.144	0.144	0.144	UB	0.183	0.183	0.183	0.183	0.178	0.178	0.178	0.178	
5			V (kN)		1174	1350	1350	1174		1289	1289	1289	1289	1261	1261	1261	1261	
6			T_{eff} (s)		1.73					2.10				2.10				
7			F_0 (kN)		-	-	-	-		558	558	558	558	413	413	413	413	$F_{0,NL}/F_{0,L} \geq 0.25$
8			ρ_l (‰)		-	6.05	11.09	-		-	4.71	10.08	-	-	4.37	9.41	-	$> \rho_{l,min}$=2.5
9			M_y (kNm)		-	4235	5104	-		-	4016	4922	-	-	3955	4813	-	$\varepsilon_{cu} \leq$ 3.5-4.0‰
10	2	II	u_{res} (m)	UB-E	0.004	0.003	0.002	0.005	-	-	-	-	-	-	-	-	-	< 0.015
11			γ_q (%)	LB-I	30	22	17	41	-	-	-	-	-	-	-	-	-	< 50
12				LB-E	21	19	18	23	LB-E	35	34	33	36	33	27	19	21	
13	3	III	u_0 (m)	UB-E	0.082	0.072	0.068	0.098	UB-E	0.094	0.093	0.088	0.099	0.076	0.069	0.062	0.076	
14			u_{res} (m)		0.005	0.005	0.005	0.005		-	-	-	-	-	-	-	-	0.015-0.030
15			u_{res}[5] (m)		0.006	0.006	0.006	0.006		-	-	-	-	-	-	-	-	
16			u_{res}/u_0 (m)		0.07	0.07	0.08	0.05		-	-	-	-	-	-	-	-	$\leq$ 0.10
17			γ_q (%)	LB-I	70	62	59	84	LB-I	75	73	70	78	62	57	51	63	100
18				LB-E	43	41	39	45	LB-E	69	68	65	71	56	52	47	53	
19			M (kNm)	UB-E	-	4194	5075	-	UB-E	-	2917	3250	-	-	3056	3453	-	$\leq M_y$

Contnd. Comparative evaluation of Def-BD for three different isolation schemes (Steps 4, 5): Design stage

No.	Step		Property		LRBs				Prop.	LDRBs + LVDs (a=1.0)				LDRBs + NLVDs (a=0.2)				Design Criterion
	Step	EQ	Response	DP	Abt 1	Pier 1	Pier 2	Abt 2	DP	Abt 1	Pier 1	Pier 2	Abt 2	Abt 1	Pier 1	Pier 2	Abt 2	
20	4	IV	u_0 (m)	UB-E	0.172	0.151	0.137	0.180	UB-E	0.190	0.177	0.166	0.198	0.182	0.163	0.146	0.182	
21				LB-I	0.306	0.269	0.243	0.321	LB-I	0.249	0.232	0.218	0.259	0.245	0.220	0.196	0.245	
22			u_0+u_{res}[5] (m)	LB-I	0.312	0.275	0.249	0.326	-	-	-	-	-	-	-	-	-	
23			γ_q (%)		139	122	111	145	LB-I	151	140	132	157	149	133	119	148	< 250
24			γ_c (%)		105	227	220	118		91	213	212	99	92	208	203	98	
25			γ_{tot} (%)		243	350	331	263		241	354	344	256	241	341	322	246	< 700
26			N_{cr}'/N_{max}		3.56	1.64	1.70	3.15		6.57	2.79	2.81	6.01	6.46	2.86	2.94	6.08	> 1.10
27			u_0 (m)	LB-E	0.255	0.246	0.238	0.266	LB-E	0.229	0.220	0.212	0.236	0.221	0.205	0.195	0.225	
28			σ_t (MPa)	UB-E	1.59	-	-	1.99	UB-E	1.29	-	-	1.55	1.66	-	-	2.00	$< 2G_R = 2.2$
29			F_0 (kN)		-	-	-	-		633	608	571	652	453	449	447	455	$F_{0,NL}/F_{0,L} \geq 0.25$
30			μ_φ		-	4.09	3.91	-		-	4.09	3.20	-	-	3.99	3.26	-	$\varepsilon_{cu} \leq$ 3.5-4.0‰
31			$\mu_\varphi(\varepsilon_{cu})$		-	≤4.2-4.8	≤3.5-4.0	-		-	≤4.4-5.1	≤3.6-4.1	-	-	≤4.5-5.1	≤3.7-4.2	-	
32	5	IV	V (kN)	UB-E	1263	1298	1284	1301	UB-E	1399	1230	1172	1449	1432	1232	1174	1447	
33			ρ_w (‰)		-	7.09	7.09	-		-	6.67	6.30	-	-	6.67	6.30	-	$> \rho_{w,min} = 5.2$

Table C.2 Comparative evaluation of Def-BD for three different isolation schemes (Steps 1-5): Assessment stage

No.	Step		Property		LRBs				Prop.	LDRBs + LVDs (a=1.0)				LDRBs + NLVDs (a=0.2)				Design Criterion
	Step	EQ	Response	DP	Abt 1	Pier 1	Pier 2	Abt 2	DP	Abt 1	Pier 1	Pier 2	Abt 2	Abt 1	Pier 1	Pier 2	Abt 2	
1	A	II	u_{res} (m)	UB-E	0.003	0.002	0.001	0.004	-	-	-	-	-	-	-	-	-	< 0.015
2			γ_q (%)	LB-E	16	14	13	19	LB-E	37	36	34	38	23	18	13	19	< 50
3		III	u_0 (m)	UB-E	0.057	0.046	0.041	0.072	UB-E	0.098	0.095	0.090	0.102	0.060	0.055	0.049	0.061	
4			u_{res} (m)		0.005	0.005	0.004	0.005		-	-	-	-	-	-	-	-	0.015-0.030
5			u_{res}^{5} (m)		0.006	0.006	0.005	0.006		-	-	-	-	-	-	-	-	
6			u_{res}/u_0 (m)		0.09	0.10	0.11	0.07		-	-	-	-	-	-	-	-	≤ 0.10
7			γ_q (%)	LB-E	40	38	36	43	LB-E	73	72	69	76	53	48	43	49	100
8			M (kNm)	UB-E	-	3944	4568	-	UB-E	-	2856	3197	-	-	2636	2904	-	≤ M_y
9		IV	u_0 (m)	LB-E	0.247	0.240	0.231	0.257	LB-E	0.242	0.232	0.224	0.250	0.221	0.210	0.200	0.225	
10			$u_0+u_{res}^{5}$ (m)		0.253	0.245	0.237	0.263		-	-	-	-	-	-	-	-	
11			γ_q (%)		113	109	105	117		147	141	136	151	134	128	121	136	< 250
12			γ_{tot} (%)		184	307	307	196		226	348	345	238	209	323	318	217	< 700
13			N_{cr}'/N_{max}		5.24	1.88	1.85	4.73		7.48	2.87	2.84	6.84	7.94	3.04	3.02	7.35	> 1.10
14			σ_t (MPa)	UB-E	0.51	-	-	0.81	UB-E	0.97	-	-	1.20	0.74	-	-	0.96	< $2G_R$=*2.2*
15			F_0 (kN)		-	-	-	-		570	561	532	591	437	436	434	440	$F_{0,NL}/F_{0,L}$ ≥0.25
16			μ_φ		-	3.07	2.15	-		-	4.20	3.20	-	-	3.84	2.95	-	ε_{cu} ≤ 3.5-4.0‰
17			$\mu_\varphi(\varepsilon_{cu})$		-	≤ 4.1-4.7	≤ 3.1-3.6	-		-	≤ 4.4-5.0	≤ 3.5-4.0	-	-	≤ 4.5-5.1	≤ 3.6-4.1	-	
18			V (kN)		1125	1202	1192	1192		1391	1230	1172	1447	1320	1175	1125	1401	

Table C.3 Comparative evaluation of Def-BD for the LRB scheme under unidirectional and bidirectional excitation (Steps 1-3): Design stage

No.	Step		Property		LRBs: 1D ($\ddot{U}_0$ // y-y), D_p=1.2m				Prop.	LRBs: 2D ($\ddot{U}_0$ // y-y), D_p=1.5m				LRBs: 2D ($\ddot{U}_0$ // x-x), D_p=1.5m				Design Criterion
	Step	EQ	Response	DP	Abt 1	Pier 1	Pier 2	Abt 2	DP	Abt 1	Pier 1	Pier 2	Abt 2	Abt 1	Pier 1	Pier 2	Abt 2	
1	1	IV	u_0 (m)	LB	0.256	0.256	0.256	0.256	LB	0.390	0.390	0.390	0.390	0.390	0.390	0.390	0.390	
2			V (kN)		948	1026	1026	948		1276	1354	1354	1276	1276	1354	1354	1276	
3			T_{eff} (s)		2.54					2.66				2.66				
4			u_0 (m)	UB	0.144	0.144	0.144	0.144	UB	0.218	0.218	0.218	0.218	0.218	0.218	0.218	0.218	
5			V (kN)		1174	1350	1350	1174		1546	1721	1721	1546	1546	1721	1721	1546	
6			T_{eff} (s)		1.73					1.90				1.90				
7			ρ_l (‰)		-	6.05	11.09	-		-	6.94	9.72	-	-	**8.33**	**15.00**	-	$> \rho_{l,min}$=2.5
8			M_y (kNm)		-	4235	5104	-		-	8546	11477	-	-	**8546**	**11477**	-	$\varepsilon_{cu} \leq$ 3.5-4.0‰

No.	Step		Property		LRBs: 1D (H2 // y-y), D_p=1.2m				Prop.	LRBs: 2D (θ_{EQ}=0°), D_p=1.5m				LRBs: 2D (θ_{EQ}=90°), D_p=1.5m				Design Criterion
	Step	EQ	Response	DP	Abt 1	Pier 1	Pier 2	Abt 2	DP	Abt 1	Pier 1	Pier 2	Abt 2	Abt 1	Pier 1	Pier 2	Abt 2	
9	2	II	u_{res} (m)	UB-E	0.004	0.003	0.002	0.005	UB-E	0.005	0.005	0.004	0.005	0.005	0.005	0.004	0.005	< 0.015
10			γ_q (%)	LB-E	21	19	18	23	LB-E	32	30	**28**	32	**33**	**30**	27	**33**	< 50
11	3	III	u_0 (m)	UB-E	0.082	0.072	0.068	0.098	UB-E	0.121	0.115	0.105	0.128	0.130	0.114	0.093	0.129	
12			u_{res} (m)		0.005	0.005	0.005	0.005		0.005	0.005	0.005	0.005	0.005	0.005	0.005	0.005	0.015-0.030
13			u_{res}^5 (m)		0.006	0.006	0.006	0.006		0.005	0.006	0.006	0.005	0.005	0.006	0.006	0.005	
14			u_{res}/u_0 (m)		0.07	0.07	0.08	0.05		0.04	0.05	0.05	0.04	0.04	0.05	**0.06**	0.04	$\leq$ 0.10
15			γ_q (%)	LB-E	43	41	39	45	LB-E	66	65	**62**	67	**71**	**67**	61	**70**	100
16			M (kNm)	UB-E	-	4194	5075	-	UB-E	-	6184	7266	-	-	**6718**	**8249**	-	$\leq M_y$

Contnd. Comparative evaluation of Def-BD for the LRB scheme under unidirectional and bidirectional excitation (Steps 4, 5): Design stage

No.	Step		Property		LRBs: 1D (H2 // *y*-*y*), D_p=1.2m				Prop.	LRBs: 2D (θ_{EQ}=0°), D_p=1.5m				LRBs: 2D (θ_{EQ}=90°), D_p=1.5m				Design Criterion
	Step	EQ	Response	DP	Abt 1	Pier 1	Pier 2	Abt 2	DP	Abt 1	Pier 1	Pier 2	Abt 2	Abt 1	Pier 1	Pier 2	Abt 2	
17	4	IV	u_0 (m)	LB-E	0.255	0.246	0.238	0.266	LB-E	0.402	0.389	**0.375**	0.407	**0.411**	**0.391**	0.368	**0.413**	
18			u_0+u_{res}[5] (m)		0.260	0.252	0.244	0.272		0.407	0.395	**0.381**	0.412	**0.416**	**0.397**	0.374	**0.418**	
19			γ_q (%)		116	112	109	121		181	176	**169**	183	**185**	176	166	**186**	< 250
20			γ_c (%)		75	203	207	83		**129**	328	**326**	**142**	121	328	315	134	
21			γ_{tot} (%)		190	315	316	204		**310**	504	**495**	**325**	306	504	481	320	< 700
22			N_{cr}'/N_{max}		5.00	1.83	1.80	4.50		**2.90**	1.14	**1.14**	**2.62**	3.07	1.14	1.19	2.77	> 1.10
23			σ_t (MPa)	UB-E	1.59	-	-	1.99	UB-E	1.52	-	-	1.77	**1.77**	-	-	**2.00**	< 2*G*=*2.2*
24			μ_φ		-	4.09	3.91	-		-	2.15	1.31	-	-	**2.97**	**2.34**	-	$\varepsilon_{cu} \leq$ 3.5-4.0‰
25			$\mu_\varphi(\varepsilon_{cu})$		-	≤4.2-4.8	≤3.5-4.0	-		-	≤3.7-4.3	≤2.5-2.9	-	-	≤3.7-4.3	≤2.5-2.9	-	
26	5	IV	V (kN)	UB-E	1263	1298	1284	1301	UB-E	1753	**1749**	**1812**	1764	**1802**	1735	1685	**1796**	
27			ρ_w (‰)		-	7.09	7.09	-		-	**5.92**	**6.35**	-	-	5.92	6.35	-	> $\rho_{w,min}$

Table C.4 Comparative evaluation of Def-BD for the LRB scheme under unidirectional and bidirectional excitation (Steps 1-5): Assessment stage

No.	Step		Property		LRBs: 1D (Art B // y-y), D_p=1.2				Prop.	LRBs: 2D (Art D), D_p=1.5m				θ_{EQ} (deg)				Design Criterion
	Step	EQ	Response	DP	Abt 1	Pier 1	Pier 2	Abt 2	DP	Abt 1	Pier 1	Pier 2	Abt 2	Abt 1	Pier 1	Pier 2	Abt 2	
1		II	u_{res} (m)	UB-E	0.003	0.002	0.001	0.004	UB-E	0.004	0.003	0.001	0.004	0, 22.5	45	90	90	< 0.015
2			γ_q (%)	LB-E	16	14	13	19	LB-E	22	20	18	24	45	45	135	45	< 50
3		III	u_0 (m)	UB-E	0.057	0.046	0.041	0.072	UB-E	0.077	0.068	0.053	0.083	157.5, 0	67.5	67.5	22.5	
4			u_{res} (m)		0.005	0.005	0.004	0.005		0.005	0.005	0.005	0.005	157.5, 0	67.5	67.5	22.5	0.015-0.030
5			u_{res}^5 (m)		0.006	0.006	0.005	0.006		0.006	0.006	0.006	0.006	-	-	-	-	
6			u_{res}/u_0 (m)		0.09	0.10	0.11	0.07		0.07	0.08	0.09	0.06	-	-	-	-	≤ 0.10
7			γ_q (%)	LB-E	40	38	36	43	LB-E	62	58	54	62	45	45	157.5	45	100
8			M (kNm)	UB-E	-	3944	4568	-	UB-E	-	5903	7179	-	-	90	90	-	≤ M_y
9	A	IV	u_0 (m)	LB-E	0.247	0.240	0.231	0.257	LB-E	0.404	0.387	0.374	0.404	45	45	135	45	
10			$u_0+u_{res}^5$ (m)		0.253	0.245	0.237	0.263		0.410	0.393	0.380	0.410	-	-	-	-	
11			γ_q (%)		113	109	105	117		182	174	169	182	45	45	135	45	< 250
12			γ_{tot} (%)		184	307	307	196		312	499	495	326	-	-	-	-	< 700
13			N_{cr}'/N_{max}		5.24	1.88	1.85	4.73		2.87	1.15	1.14	2.59	157.5, 180				> 1.10
14			σ_t (MPa)	UB-E	0.51	-	-	0.81	UB-E	0.28	-	-	0.76	22.5,135	-	-	22.5,135	< 2G=2.2
15			μ_φ		-	3.07	2.15	-		-	1.31	0.92	-	-	67.5	67.5	-	ε_{cu} ≤ 3.5-4.0‰
16			$\mu_\varphi(\varepsilon_{cu})$		-	≤ 4.1-4.7	≤ 3.1-3.6	-		-	≤3.5-4.1	≤2.3-2.7	-	-	-	-	-	
17			V (kN)		1125	1202	1192	1192		1500	1566	1524	1514	45	90	0	90	

Annex D
Supplement to Chapter 6

D.1 Bridge Designed for Ductile Behaviour of the Piers [§6.2]

D.1.1 Assessment of Code-BD and comparison with Def-BD [§6.2.5]

Table D.1 Critical assessment quantities for Code-BDn case

No.	Case		EQII (A/A_d=2.3)				EQIII (A/A_d=4.5)				EQIV (A/A_d=9.1)			
			SP2	NLRHA	SP2	NLRHA	SP3	NLRHA	SP3	NLRHA	SP4	NLRHA	SP4	NLRHA
	Member		Pier 1		Pier 2		Pier 1		Pier 2		Pier 1		Pier 2	
1	EI_y / EI_g (%)	Base	39.6		39.5		39.6		39.5		39.6		39.5	
2		Top	39.6		39.5		39.6		39.5		39.6		39.5	
3	μ_φ	Base	2.25	2.96	2.25	2.18	12.64	8.00	12.59	7.53	14.58	21.32	14.54	21.34
4		Top	2.30	0.22	2.30	0.28	12.88	0.39	12.90	0.49	14.85	1.30	14.90	2.65
5	μ_θ	Base	1.43	1.68	1.34	1.32	4.91	3.35	4.08	2.73	5.51	7.75	4.57	6.44
6		Top	1.86	0.22	1.64	0.28	8.87	0.39	6.87	0.49	10.16	1.15	7.85	1.80
7	μ_u		-	1.61	-	1.26	-	2.99	-	2.40	-	6.42	-	5.62
8	Col. Drift (%)		-	0.88	-	0.87	-	1.68	-	1.71	-	3.70	-	4.04
9	h_{eq} (m)	Base	-	5.26	-	6.68	-	5.40	-	6.82	-	5.47	-	6.88
10		Top	-	2.74	-	3.68	-	2.74	-	3.68	-	2.74	-	3.68
-	Member		Abutment 1		Abutment 2		Abutment 1		Abutment 2		Abutment 1		Abutment 2	
11	γ_q (%)		100	227	100	261	200	301	200	453	500	558	500	968

D.2 Seismically Isolated Bridge [§6.3]

D.2.1 Application of the EN1998-2 design procedure [§6.3.4], Assessment of EN1998-2 design and comparison with Def-BD [§6.3.5]

Table D.2 Critical EN1998-2 design and assessment quantities for the LRB scheme under bidirectional excitation

No.	EQ	Property		EN1998-2: Design, D_p=1.5m				Prop.	Assessment (Art D), D_p=1.5m				θ_{EQ} (deg)				Design Criterion
		Response	DP	Abt 1	Pier 1	Pier 2	Abt 2	DP	Abt 1	Pier 1	Pier 2	Abt 2	Abt 1	Pier 1	Pier 2	Abt 2	
1	II	u_{res} (m)	UB-E	-	-	-	-	UB-E	0.004	0.003	0.002	0.004	22.5	45	90	90	< 0.015
2		γ_q (%)	LB-E	-	-	-	-	LB-E	22	21	19	24	45	135	0, 180	135	< 50
3	III	u_0 (m)	UB-E	0.047	0.034	0.022	0.050	UB-E	0.076	0.068	0.052	0.083	0	67.5	67.5	22.5	
4		u_{res} (m)		0.005	0.004	0.003	0.005		0.005	0.005	0.005	0.005	0	67.5	67.5	22.5	0.015-0.030
5		u_{res}^{5} (m)		0.006	0.005	0.004	0.006		0.006	0.006	0.006	0.006	-	-	-	-	
6		u_{res}/u_0 (m)		0.10	0.12	0.13	0.10		0.07	0.08	0.09	0.06	-	-	-	-	≤ 0.10
7		u_0 (m)	LB-E	0.110	0.103	0.100	0.115	LB-E	0.138	0.131	0.123	0.139	45	45	157.5	45	
8		γ_q (%)		49	46	45	51		61	58	55	62	45	45	157.5	45	100
9		M (kNm)	UB-E	-	3373	3793	-	UB-E	-	5961	6821	-	-	90	90	-	≤ M_y
10	IV	u_0 (m)	LB-E	0.219	0.207	0.200	0.230	LB-E	0.401	0.381	0.359	0.401	45	135	135	45, 135	
11		$u_0+u_{res}^{5}$ (m)		0.225	0.212	0.205	0.236		0.406	0.387	0.365	0.407	-	-	-	-	
12		γ_q (%)		100	94	91	105		181	172	162	181	45	135	135	45, 135	< 250
13		γ_{tot} (%)		168	274	277	182		309	489	472	322	-	-	-	-	< 700
14		N_{cr}'/N_{max}		5.45	2.07	2.01	4.83		2.91	1.18	1.20	2.64	0, 135, 180				> 1.10
15		u_0 (m)	UB-E	0.096	0.085	0.080	0.126	UB-E	0.241	0.202	0.173	0.244	45	45, 135	157.5	45	
16		σ_t (MPa)		0.14	-	-	0.76		0.84	-	-	1.35	22.5,135	-	-	22.5,135	< 2G=2.2
17		μ_φ		-	-	-	-		-	7.41	12.25	-	-	67.5	67.5	-	ε_{cu} ≤ 3.5-4.0‰
18		$\mu_\varphi(\varepsilon_{cu})$		-	-	-	-		-	≤5.2-6.0	≤5.2-6.0	-	-	-	-	-	
19		V (kN)		750	889	903	849		1518	1517	1449	1533	45	112.5	157.5	45	

Annex E
References

AASHTO (American Association of State Highway and Transportation Officials) (1991) *Guide Specifications for Seismic Isolation Design*. AASHTO, WA, US

AASHTO (2009) *Guide Specifications for LRFD Seismic Bridge Design*. AASHTO, WA, USA

AASHTO (2010) *Guide Specifications for Seismic Isolation Design*. AASHTO, WA, USA

AASHTO (2011) *Guide Specifications for LRFD Seismic Bridge Design (2nd Ed)*. AASHTO, WA, USA

AASHTO (2012) *LRFD Bridge Design Specification*. AASHTO, WA, USA

ACI (American Concrete Institute) (2016) *Report on the Seismic Design of Bridge Columns Based on Drift*. ACI, MI, USA, Report 341.4R-16

Adhikari G, Petrini L, Calvi GM (2010) Application of direct displacement based design to long span bridges. *Bulletin of Earthquake Engineering* **8**(4):897–919

Alf EF, Grossberg JM (1979) The geometric mean: Confidence limits and significance tests. *Perception & Psychophysics* **26**(5): 419–421

Alvarez Botero JC (2004) *Displacement-Based Design of Continuous Concrete Bridges under Transverse Seismic Excitation*. MSc Dissertation, Rose School, IUSS, Pavia, IT

Ancheta DT, Darragh RB, Stewart JP, Seyhan E, Silva WJ, Chiou BSJ, Wooddell KE, Graves RW, Kottke AR, Boore DM, Kishida T, Donahue JL (2013) *PEER NGA-West 2 Database*. Pacific Earthquake Engineering Research Center (PEER), CA, USA, Report 2013/03

ASCE (American Society of Civil Engineers) (2016) *Minimum Design Loads and Associated Criteria for Buildings and Other Structures (ASCE/SEI 7-16)*. ASCE, VA, USA

ATC (Applied Technology Council) (1996) *Seismic Evaluation and Retrofit of Concrete Buildings (ATC-40)*. ATC, CA, USA

ATC (2012) *Seismic Performance Assessment of Buildings (ATC-58)*. ATC, CA, USA

ATC/MCEER (Multidisciplinary Center for Earthquake Engineering Research) (2004) *Recommended LRFD Guidelines for the Seismic Design of Highway Bridges. Part I: Specifications, Part II: Commentary and Appendices*. ATC, CA, USA, Report ATC-49

Attary N, Symans M, Nagarajaiah S, Reinhorn AM, Constantinou MC, Sarlis AA, Pasala DTR, Taylor D (2015) Numerical simulations of a highway bridge structure employing passive negative stiffness device for seismic protection. *Earthquake Engineering & Structural Dynamics* **44**(6): 973–995

Aviram A, Mackie K, Stojadinović B (2008) *Guidelines for Nonlinear Analysis of Bridge Structures in California*. PEER, CA, USA, Report 2008/03

Ayala G, Escamilla MA (2013) Modal irregularity in continuous reinforced concrete bridges. Detection, effect on the simplified seismic performance evaluation and ways of solution. In: Lavan O, De Stefano M (Eds) *Seismic Behaviour and Design of Irregular and Complex Civil Structures*. Springer

Aydınoğlu MN (2004) An improved pushover procedure for engineering practice: Incremental response spectrum analysis (IRSA). In: Fajfar P, Krawinkler H (Eds) *Performance-Based Seismic Design: Concepts and Implementation*. PEER, CA, USA, Report 2004/05

Aydınoğlu MN, Önem G (2009) Nonlinear performance assessment of bridges with incremental response spectrum analysis (IRSA) procedure. In: Papadrakakis M, Charmpis DC, Tsompanakis Y, Lagaros ND (Eds) *Computational structural dynamics and earthquake engineering*. CRC Press

Aydınoğlu MN, Önem G (2010) Evaluation of analysis procedures for seismic assessment and retrofit design. In: Garevski M, Ansal A (Eds) *Earthquake Engineering in Europe*. Springer

Baker JW, Cornell AC (2006) Spectral shape, epsilon and record selection. *Earthquake Engineering & Structural Dynamics* **35**(9): 1077–1095

Bardakis VG, Fardis MN (2011a) A displacement-based seismic design procedure for concrete bridges having deck integral with the piers. *Bulletin of Earthquake Engineering* **9**(2): 537–560

Bardakis VG, Fardis MN (2011b) Nonlinear dynamic v elastic analysis for seismic deformation demands in concrete bridges having deck integral with the piers. *Bulletin of Earthquake Engineering* **9**(2): 519–535

Basu B, Bursi OS, Casciati F, Casciati S, Del Grosso AE, Domaneschi M, Faravelli L, Holnicki-Szulc J, Irschik H, Krommer M, Lepidi M, Martelli A, Ozturk B, Pozo F, Pujol G, Rakicevic Z, Rodellar J (2014) A European association for the control of structures joint perspective. Recent studies in civil structural control across Europe. *Structural Control & Health Monitoring* **21**(12): 1414–1436

Biskinis DE, Fardis MN (2010a) Deformations at flexural yielding of members with continuous or lap-spliced bars. *Structural Concrete* **11**(3):127–138

Biskinis DE, Fardis MN (2010b) Flexure-controlled ultimate deformations of members with continuous or lap-spliced bars. *Structural Concrete* **11**(2):93–108

Biskinis DE, Fardis MN (2013) Stiffness and cyclic deformation capacity of circular RC columns with or without lap-splices and FRP-wrapping. *Bulletin of Earthquake Engineering* **11**(5): 1447–1466

Blume JA (1973) Elements of a dynamic-inelastic design code. *5th World Conference on Earthquake Engineering (WCEE)*, Rome, IT

Bocchini P, Frangopol DM (2012) Restoration of bridge networks after an earthquake: Multicriteria intervention optimization. *Earthquake Spectra* **28**(2): 426–455

Bommer JJ, Alarcon JE (2006) The prediction and use of peak ground velocity. *Journal of Earthquake Engineering* **10**(1): 1–31

Booth E (2007) The estimation of peak ground-motion parameters from spectral ordinates. *Journal of Earthquake Engineering* **11**(1): 13–32

Bracci JM, Kunnath SK, Reinhorn AM (1997) Seismic performance and retrofit evaluation for reinforced concrete structures. *Journal of Structural Engineering* **123**(1):3–10

Buckle IG, Liu H (1994) Critical loads of elastomeric isolators at high shear strain. In: Buckle IG, Friedland I (Eds) *Proceedings of the 3rd US-Japan Workshop on Earthquake Protective Systems for Bridges*. MCEER, NY, USA, Report 94-0009

Buckle IG, Constantinou MC, Dicleli M, Ghasemi H (2006) *Seismic Isolation of Highway Bridges*. MCEER, NY, USA, Report 06-SP07

Caltrans (California Department of Transportation) (2013) *Seismic Design Criteria (Ver 1.7)*. Caltrans, CA, USA

Calvi GM, Kingsley GR (1995) Displacement based seismic design of multi-degree-of-freedom bridge structures. *Earthquake Engineering & Structural Dynamics* **24**(9): 1247–1266

Calvi GM, Pavese A (1997) Conceptual design of isolation systems for bridge structures. *Journal of Earthquake Engineering* **1**(1):193–218

Calvi GM, Cecconi M, Paolucci R (2014) Seismic displacement based design of structures: Relevance of soil structure interaction. In: Maugeri M, Soccodato C (Eds) *Earthquake Geotechnical Engineering Design*. Springer

Calvi GM, Priestley MJN, Kowalsky MJ (2013) Displacement-based seismic design of bridges. *Structural Engineering International* **23**(2): 112–121

Calvi GM, Sullivan TJ, Villani A (2010) Conceptual seismic design of cable-stayed bridges. *Journal of Earthquake Engineering* **14**(8): 1139–1171

Calvi PM, Moratti M, & Calvi GM (2016) Seismic isolation devices based on sliding between surfaces with variable friction coefficient. *Earthquake Spectra* **32**(4): 2291–2315

Cardone D (2014) Displacement limits and performance displacement profiles in support of direct displacement-based seismic assessment of bridges. *Earthquake Engineering & Structural Dynamics* **43**(8): 1239–1263

Cardone D, Dolce M, Palermo G (2009) Direct displacement-based design of seismically isolated bridges. *Bulletin of Earthquake Engineering* **7**(2): 391–410

Cardone D, Gesualdi G, Brancato P (2015) Restoring capability of friction pendulum seismic isolation systems. *Bulletin of Earthquake Engineering* **13**(8): 2449–2480

Carr AJ (2004a) *RUAUMOKO: Theory and User Guide to Associated Programs*. University of Canterbury, NZ

Carr AJ (2004b) *RUAUMOKO 3D: Inelastic dynamic analysis program*. University of Canterbury, NZ

Carr AJ (2004c) *RUAUMOKO DYNAPLOT: Dynamic Analysis Results Post-Processor*. University of Canterbury, NZ

CEN (Comité Européen de Normalisation) (2002) *Eurocode: Basis of Structural Design (EN1990)*. CEN, Brussels, BE

CEN (2004a) *Eurocode 2: Design of Concrete Structures – Part 1-1: General Rules and Rules for Buildings (EN1992-1-1)*. CEN, Brussels, BE

CEN (2004b) *Eurocode 8: Design of Structures for Earthquake Resistance – Part 1: General Rules, Seismic Actions and Rules for Buildings (EN1998-1)*. CEN, Brussels, BE

CEN (2005a) *Eurocode 8: Design of Structures for Earthquake Resistance – Part 2: Bridges (EN1998-2)*. CEN, Brussels, BE

CEN (2005b) *Structural Bearings – Part 3: Elastomeric Bearings (EN1337-3)*. CEN, Brussels, BE

CEN (2006) *Eurocode 8: Design of Structures for Earthquake Resistance – Part 3: Assessment and Retrofitting of Buildings (EN1998-3)*. CEN, Brussels, BE

CEN (2009) *Antiseismic Devices (EN15129)*. CEN, Brussels, BE

Cha YJ, Agrawal AK, Phillips BM, Spencer BF (2014) Direct performance-based design with 200 kN MR dampers using multi-objective cost effective optimization for steel MRFs. *Engineering Structures* **71**: 60–72

Chen WF, Duan L (2003) *Bridge Engineering: Seismic Design*. CRC Press

Chiou B, Darragh R, Gregor N, Silva W (2008) NGA project strong-motion database. *Earthquake Spectra* **24**(1): 23–44

Choi E, DesRoches R, Nielson B (2004) Seismic fragility of typical bridges in moderate seismic zones. *Engineering Structures* **26**(2), 187–199

Chopra AK (2012) *Dynamics of Structures: Theory and Applications to Earthquake Engineering (4th Ed)*. Prentice Hall, New Jersey, USA

Chopra AK, Goel RK (1999) Capacity-demand-diagram methods based on inelastic design spectrum. *Earthquake Spectra* **15**(4): 637–656

Chopra AK, Goel RK (2000) Evaluation of NSP to Estimate Seismic Deformation: SDF Systems. *Journal of Structural Engineering* **126**(4): 482–490

Chopra AK, Goel RK (2001) Direct displacement-based design: Use of inelastic vs. elastic design spectra. *Earthquake Spectra* **17**(1): 47–64

Chopra AK, Goel RK (2002) A modal pushover analysis procedure for estimating seismic demands for buildings. *Earthquake Engineering & Structural Dynamics* **31**(3): 1439–1462

Chopra AK, McKenna F (2016) Modeling viscous damping in nonlinear response history analysis of buildings for earthquake excitation. *Earthquake Engineering & Structural Dynamics* **45**(2): 193–211

Christopoulos C, Filiatrault A (2006) *Principles of Passive Supplemental Damping and Seismic Isolation*. IUSS Press, Pavia, IT

Cimellaro GP (2016) *Urban Resilience for Emergency Response and Recovery: Fundamental Concepts and Applications*. Springer

Clough RW, Penzien J (2003) *Dynamics of Structures (3rd Ed)*. Computers and Structures Inc. (CSI), CA, USA

Constantinou MC, Quarshie JK (1998) *Response Modification Factors for Seismically Isolated Bridges*. MCEER, NY, USA, Report 98-0014

Constantinou MC, Kalpakidis I, Filiatrault A, Ecker Lay RA (2011) *LRFD-Based Analysis and Design Procedures for Bridge Bearings and Seismic Isolators*. MCEER, NY, USA, Report 11-0004

Constantinou MC, Whittaker AS, Fenz DM, Apostolakis G (2007a) *Seismic Isolation of Bridges*. University at Buffalo, NY, USA, Project Report 65A0174

Constantinou MC, Whittaker AS, Kalpakidis Y, Fenz DM, Warn GP (2007b) *Performance of Seismic Isolation Hardware Under Service and Seismic Loading*. MCEER, NY, USA, Report 07-0012

Cox DR, Hinkley DV (1974) *Theoretical Statistics*. Chapman & Hall / CRC Press

CSI (2009) *SAP2000: Three Dimensional Static and Dynamic Finite Element Analysis and Design of Structures*. CSI, CA, USA

CSI (2015) *SAP2000: Three Dimensional Static and Dynamic Finite Element Analysis and Design of Structures*. CSI, CA, USA

De Rue GM (1998) *Nonlinear Static Procedure Analysis of 3D Structures for Design Applications*. MSc Dissertation, University at Buffalo, NY, USA

Decò A, Bocchini P, Frangopol DM (2013) A probabilistic approach for the prediction of seismic resilience of bridges. *Earthquake Engineering & Structural Dynamics* **42**(10): 1469–1487

Deng L, Kutter BL, Kunnath SK (2014) Seismic design of rocking shallow foundations: Displacement-based methodology. *Journal of Bridge Engineering* **19**(11): 04014043

Di Paola M, Navarra G (2009) Stochastic seismic analysis of MDOF structures with nonlinear viscous dampers. *Structural Control & Health Monitoring* **16**(3): 303–319

Dicleli M, Buddaram S (2006) Effect of isolator and ground motion characteristics on the performance of seismic-isolated bridges. *Earthquake Engineering & Structural Dynamics* **35**(2): 233–250

Dicleli M, Buddaram S (2007a) Comprehensive evaluation of equivalent linear analysis method for seismic-isolated structures represented by sdof systems. *Engineering Structures* **29**(8): 2653–1663

Dicleli M, Buddaram S (2007b) Equivalent linear analysis of seismic-isolated bridges subjected to near-fault ground motions with forward rupture directivity effect. *Engineering Structures* **29**(1): 21–32

Domaneschi M, Martinelli L (2016) Earthquake-resilience-based control solutions for the extended benchmark cable-stayed bridge. *Journal of Structural Engineering* **142**(8): C4015009

Douglas J, Aochi H (2008) A survey of techniques for predicting earthquake ground motions for engineering purposes. *Surveys in Geophysics* **29**(3): 187–220

Dwairi H, Kowalsky M (2006) Implementation of inelastic displacement patterns in direct displacement-based design of continuous bridge structures. *Earthquake Spectra* **22**(3): 631–662

Dwairi HM, Kowalsky MJ, Nau JM (2007) Equivalent damping in support of direct displacement-based design. *Journal of Earthquake Engineering* **11**(4): 512–530

Egnatia Motorway (2002) *Overpass T7: Final Design Report*. Egnatia Motorway SA, Greece

EPPO (Earthquake Planning & Protection Organisation) (2000) *Guidelines for Earthquake Resistant Design of Bridges (E39-99)*. EPPO, Athens, GR (in Greek)

Fajfar P (1999) Capacity spectrum method based on inelastic demand spectra. *Earthquake Engineering & Structural Dynamics* **28**(9): 979–993

Fajfar P (2000) A nonlinear analysis method for performance-based seismic design. *Earthquake Spectra* **16**(3): 573–592

Fajfar P (2007) Seismic assessment of structures by a practice oriented method. In: Ibrahimbegovic A, Kozar I (Eds) *Extreme Man-Made and Natural Hazards in Dynamics of Structures*. Springer

Fajfar P, Fischinger M (1987) Non-linear seismic analysis of RC buildings: Implications of a case study. *European Earthquake Engineering* **1**(1) :31–43

Falamarz-Sheikhabadi MR, Zerva A (2017) Analytical seismic assessment of a tall long-span curved reinforced-concrete bridge. Part II: Structural response. *Journal of Earthquake Engineering* **21**(8): 1335–1364

Fardis MN (2007) *Lessloss Report: Guidelines for Displacement-based Design of Buildings and Bridges*. IUSS Press, Pavia, IT, Report 2007/05

Fardis MN (2013) Performance- and displacement-based seismic design and assessment of concrete structures in *fib* Model Code 2010. *Structural Concrete* **14**(3): 215–229

Fardis MN, Kolias B, Pecker A (2012) *Designer's Guide to Eurocode 8: Design of Bridges for Earthquake Resistance EN 1998-2*. ICE Publishing, London, UK

FEMA (Federal Emergency Management Agency) (1997) *NEHRP guidelines for the seismic rehabilitation of buildings (FEMA 273)*. FEMA, WA, USA

FEMA (2009) *NEHRP Recommended Seismic Provisions for New Buildings and Other Structures*. FEMA, WA, USA, Report P-750

Fenz DM, Constantinou MC (2008) Spherical sliding isolation bearings with adaptive behaviour: Theory. *Earthquake Engineering & Structural Dynamics* **37**(2): 163–183

FHWA (Federal Highway Administration) (2006) *Seismic Retrofitting Manual for Highway Structures: Part 1 – Bridges*. MCEER, NY, USA, Report 06-SP10

fib (féderation internationale du béton) (2003) *Displacement-Based Seismic Design of Reinforced Concrete Buildings*. *fib*, Lausanne, CH, Bulletin No. 25

fib (2007) *Seismic Bridge Design and Retrofit - Structural Solutions*. *fib*, Lausanne, CH, Bulletin No. 39

fib (2012a) *Model Code 2010 (Vol 1)*. *fib*, Lausanne, CH, Bulletin No. 65

fib (2012b) *Model Code 2010 (Vol 2*). *fib*, Lausanne, CH, Bulletin No. 66

fib (2012c) *Probabilistic Performance-Based Seismic Design*. *fib*, Lausanne, CH, Bulletin No. 68

Fragiadakis M, Vamvatsikos D, Karlaftis MG, Lagaros ND, Papadrakakis M (2015) Seismic assessment of structures and lifelines. *Journal of Sound & Vibration* **334**: 29–56

Franchin P, Monti G, Pinto PE (2001) On the accuracy of simplified methods for the analysis of isolated bridges. *Earthquake Engineering & Structural Dynamics* **30**(3): 363–382

Freeman SA, Nicoletti JP, Tyrell JV (1975) Evaluations of existing buildings for seismic risk - a case study of Puget Sound Naval Shipyard, Bremerton, Washington. In: *Proceedings of the 1st US National Conference on Earthquake Engineering*, CA, USA

Gasparini DA, Vanmarcke EH (1976) *Simulated Earthquake Motions Compatible with Prescribed Response Spectra*. Massachusetts Institute of Technology, MA, USA

Gkatzogias KI, Kappos AJ (2016a) Seismic design of concrete bridges: Some key issues to be addressed during the evolution of Eurocode 8 – Part 2. *17th Hellenic Conference on Concrete Structures*, Thessaloniki, GR

Gkatzogias KI, Kappos AJ (2016b) Semi-active control systems in bridge engineering: A review of the current state of practice. *Structural Engineering International* **26**(4): 290–300

Gkatzogias KI, Kappos AJ (2017) Deformation-based design of seismically isolated concrete bridges. *16th WCEE*, Santiago, CL

Goodnight JC, Kowalsky MJ, Nau JM (2016) Strain limit states for circular RC bridge columns. *Earthquake Spectra* **32**(3): 1627–1652

Google Earth 7.1.2.2041 (2011) *Greece 41°01'18.50" N, 24°41'20.66" E, elevation 268 ft, eye altitude 191 ft*. Street View, US Dept. of State Geographer 2014, [Accessed 3 November 2014]

Grant DN, Blandon CA, Priestley MJN (2005) *Modelling Inelastic Response in Direct Displacement-Based Design*. IUSS Press, Pavia, IT, Report 2005/03

Guo JWW, Christopoulos C (2013) Performance spectra based method for the seismic design of structures equipped with passive supplemental damping systems. *Earthquake Engineering & Structural Dynamics* **42**(6): 935–952

Hall JF (2016) Discussion of 'Modelling viscous damping in nonlinear response history analysis of buildings for earthquake excitation' by Anil K. Chopra and Frank McKenna. *Earthquake Engineering & Structural Dynamics* **45**(13): 2229–2233

Hancock J, Bommer JJ, Stafford PJ (2008) Numbers of scaled and matched accelerograms required for inelastic dynamic analyses. *Earthquake Engineering & Structural Dynamics* **37**(14): 1585–1607

Hancock J, Watson-Lamprey J, Abrahamson NA, Bommer JJ, Markatis A, McCoy E, Mendis E (2006) An improved method of matching response spectra of recorded earthquake ground motion using wavelets. *Journal of Earthquake Engineering* **10**(S1): 67–89

Housner GW, Bergman LA, Caughey TK, Chassiakos AG, Claus RO, Masri SF, Skelton RE, Soong TT, Spencer BF, Yao JTP (1997) Structural control: Past, present, and future. *Journal of Engineering Mechanics* **123**(9): 897–971

Huang WH (2002) *Bi-directional Testing, Modeling, and System Response of Seismically Isolated Bridges*. PhD Dissertation, University of California, Berkeley, CA, USA

Hwang JS, Chiou JM (1996) An equivalent linear model of lead-rubber seismic isolation bearings *Engineering Structures* **18**(7): 528–536

Hwang JS, Sheng LH (1993) Effective stiffness and equivalent damping of base-isolated bridges. *Journal of Structural Engineering* **119**(10): 3094–3101

Hwang JS, Sheng LH (1994) Equivalent elastic seismic analysis of base-isolated bridges with lead-rubber bearings. *Engineering Structures* **16**(3): 201–209

Hwang JS, Tseng, YS (2005) Design formulations for supplemental viscous dampers to highway bridges. *Earthquake Engineering & Structural Dynamics* **34**(13): 1627–1642

Iervolino I, De Luca F, Cosenza E (2010) Spectral shape-based assessment of SDOF nonlinear response to real, adjusted and artificial accelerograms. *Engineering Structures* **32**(9): 2776–2792

Iervolino I, Galasso C, Cosenza E (2009) REXEL: Computer aided record selection for code-based seismic structural analysis. *Bulletin of Earthquake Engineering* **8**(2): 339–362

Inaudi JA, Kelly JM (1993) Optimum damping in linear isolation systems. *Earthquake Engineering & Structural Dynamics* **22**(7) 583–598

Isaković T, Fischinger M (2006) Higher modes in simplified inelastic seismic analysis of single column bent viaducts. *Earthquake Engineering & Structural Dynamics* **35**(1): 95–114

Isaković T, Fischinger M (2011) Applicability of pushover methods to the seismic analyses of an RC bridge, experimentally tested on three shake tables. *Journal of Earthquake Engineering* **15**(2):303–320

Isaković T, Fischinger M (2014) Seismic analysis and design of bridges with an emphasis to Eurocode standards. In: Ansal A (Ed) *Perspectives on European Earthquake Engineering and Seismology (Vol 1)*. Springer

Isaković T, Bevc L, Fischinger M (2008a) Modeling the cyclic flexural and shear response of the R.C. hollow box columns of an existing viaduct. *Journal of Earthquake Engineering* **12**(7): 1120–1138

Isaković T, Lazaro Nino MP, Fischinger M (2008b) Applicability of pushover methods for the seismic analysis of single column bent viaducts. *Earthquake Engineering & Structural Dynamics* **37**(8): 1185–1202

Isaković T, Arêde A, Cardone D, Delgado P, Fischinger M, Kappos AJ, Pouca NV, Pinho R, Sextos A (2012) Case studies and comparative evaluation of methods. In: Kappos AJ, Saiidi M, Aydinoglu N, Isaković T (Eds) *Seismic Design and Assessment of Bridges: Inelastic Methods of Analysis and Case Studies*. Springer

Iwan W, Gates NC (1979) The effective period and damping of a class of hysteretic structures‖. *Earthquake Engineering & Structural Dynamics* **7**(3): 199–211

Jara M, Casas J (2006) A direct displacement-based method for the seismic design of bridges on bi-linear isolation devices. *Engineering Structures* **28**(6): 869–879

Jara M, Jara J, Olmos B, Casas J (2012) Improved procedure for equivalent linearization of bridges supported on hysteretic isolators. *Engineering Structures* **35**: 99–106

Jara J, Villanueva D, Jara M, Olmos B (2013) Isolation parameters for improving the seismic performance of irregular bridges. *Bulletin of Earthquake Engineering* **11**(2): 663–686

JCSS (Joint Committee on Structural Safety) (2001) *Probabilistic Model Code*. JCSS [http://www.jcss.byg.dtu.dk/Publications/Probabilistic_Model_Code]

Jennings PC (1968) Equivalent viscous damping for yielding structures. *Journal of Engineering Mechanics Division* **94**(1), 103–116

Kappos AJ (1991) Analytical prediction of the collapse earthquake for R/C buildings: Suggested methodology. *Earthquake Engineering & Structural Dynamics* **20**(2): 167–176

Kappos AJ (1997) Partial inelastic analysis procedure for optimum capacity design of buildings. In: Fajfar P, Krawinkler H (Eds) *Seismic Design Methodologies for the Next Generation of Codes*. Balkelma (CRC Press), Rotterdam, NL

Kappos AJ (2015a) Performance-based seismic design and assessment of bridges. In: Ansal A (Ed) *Perspectives on European Earthquake Engineering and Seismology (Vol 2)*. Springer

Kappos AJ (2015b) Seismic analysis of concrete bridges: Numerical modeling. In: Beer M, Kougioumtzoglou IA, Patelli E, Au S-K (Eds) *Encyclopedia of Earthquake Engineering*. Springer

Kappos AJ, Manafpour A (2001) Seismic design of R/C buildings with the aid of advanced analytical techniques. *Engineering Structures* **23**(4): 319–332

Kappos AJ, Panagopoulos G (2004) Performance-based seismic design of 3D R/C buildings using inelastic static and dynamic analysis procedures. *ISET Journal of Earthquake Technology* **41**(1): 141–158

Kappos AJ, Panagopoulos G (2011) *RCCOLA.NET - A Program for the Inelastic Analysis of Reinforced Concrete Cross Sections*. Aristotle University of Thessaloniki, GR

Kappos AJ, Stefanidou S (2010) A deformation-based seismic design method for 3D R/C irregular buildings using inelastic dynamic analysis. *Bulletin of Earthquake Engineering* **8**(4): 875–895

Kappos AJ, Gidaris IG, Gkatzogias KI (2012a) Problems associated with direct displacement-based design of concrete bridges with single-column piers, and some suggested improvements. *Bulletin of Earthquake Engineering* **10**(4): 1237–1266

Kappos AJ, Gkatzogias KI, Gidaris IG (2013) Extension of direct displacement-based design methodology for bridges to account for higher mode effects. *Earthquake Engineering & Structural Dynamics* **42**(4): 581–602

Kappos AJ, Goutzika E, Stefanidou S (2007) An improved performance-based design method for 3D R/C buildings using inelastic analysis. *1st International Conference on Computational Methods in Structural Dynamics and Earthquake Engineering (COMPDYN)*, Rethymno, GR

Kappos AJ, Saiidi M, Aydinoglu N, Isaković T (2012b) *Seismic Design and Assessment of Bridges: Inelastic Methods of Analysis and Case Studies*. Springer

Karamlou A, Bocchini P (2015) Computation of bridge seismic fragility by large-scale simulation for probabilistic resilience analysis. *Earthquake Engineering & Structural Dynamics* **44**(12): 1959–1978

Katsaras CP, Panagiotakos TB and Kolias B (2008) Restoring capability of bilinear hysteretic seismic isolation systems. *Earthquake Engineering & Structural Dynamics* **37**(4): 557–575

Katsaras CP, Panagiotakos TB, Kolias B (2009) Effect of torsional stiffness of prestressed concrete box girders and uplift of abutment bearings on seismic performance of bridges. *Bulletin of Earthquake Engineering* **7**(2): 363–375

Katsanos EI, Sextos AG (2013) ISSARS: An integrated software environment for structure-specific earthquake ground motion selection. *Advances in Engineering Software* **58**: 70–85

Katsanos EI, Sextos AG, Manolis GD (2010) Selection of earthquake ground motion records: A state-of-the-art review from a structural engineering perspective. *Soil Dynamics & Earthquake Engineering* **30**(4): 157–169

Kawashima K, Takahashi Y, Ge H, Wu Z, Zhang J (2009) Reconnaissance report on damage of bridges in 2008 Wenchuan, China, Earthquake. *Journal of Earthquake Engineering* **13**(7): 965–996

Kawashima K, Unjoh S, Hoshikuma JI, Kosa K (2011) Damage of bridges due to the 2010 Maule, Chile, earthquake. *Journal of Earthquake Engineering* **15**(7): 1036–1068

Khan E, Kowalsky MJ, Nau JM (2016) Equivalent viscous damping model for short-period reinforced concrete bridges. *Journal of Bridge Engineering* **21**(2): 04015047

Khan E, Sullivan TJ, Kowalsky MJ (2014) Direct displacement-based seismic design of reinforced concrete arch bridges. *Journal of Bridge Engineering* **19**(1): 44–58

Konstantinidis D, Kelly J, Makris N (2008) *Experimental Investigation on the Seismic Response of Bridge Bearings*. University of California Berkeley/Earthquake Engineering Research Center (EERC), CA, USA, Report 2008/02

Kowalsky MJ (2000) Deformation limit states for circular reinforced concrete bridge columns. *Journal of Structural Engineering* **126**(8): 869–878

Kowalsky MJ (2002) A displacement-based design approach for the seismic design of continuous concrete bridges. *Earthquake Engineering & Structural Dynamics* **31**(3): 719–747

Kowalsky MJ, Priestley MJN, MacRae GA (1995) Displacement-based design of RC bridge columns in seismic regions. *Earthquake Engineering & Structural Dynamics* **24**(12): 1623–1643

Krawinkler H, Deierlein GG (2014) Challenges towards achieving earthquake resilience through performance-based earthquake engineering. In: Fischinger M (Ed) *Performance-Based Seismic Engineering: Vision for an Earthquake Resilient Society*. Springer

Krawinkler H, Zareian F, Medina RA, Ibarra LF (2006) Decision support for conceptual performance-based design. *Earthquake Engineering & Structural Dynamics* **35**(1): 115–133

Kurata N, Kobori T, Koshika N (2002) Performance-based design with semi-active structural control technique. *Earthquake Engineering & Structural Dynamics* **31**(4): 445–458

Liang X, Mosalam KM, Günay S (2016) Direct integration algorithms for efficient nonlinear seismic response of reinforced concrete highway bridges. *Journal of Bridge Engineering* **21**(7): 04016041

Lin WH, Chopra AK (2002) Earthquake response of elastic SDF systems with non-linear fluid viscous dampers. *Earthquake Engineering & Structural Dynamics* **31**(9): 1623–1642

López OA, Hernández JJ, Bonilla R, Fernández A (2006) Response spectra for multicomponent structural analysis. *Earthquake Spectra* **22**(1): 85–113

Mackie K, Stojadinović B (2003) *Seismic Demands for Performance-Based Design of Bridges*. PEER, CA, USA, Report 2003/16

Mackie KR, Kucukvar M, Tatari O, Elgamal A (2016) Sustainability metrics for performance-based seismic bridge response. *Journal of Structural Engineering* **142**(8): C4015001

Makris N, Black CJ (2004) Dimensional analysis of bilinear oscillators under pulse-type excitations. *Journal of Engineering Mechanics* **130**(9):1019–1031

Makris N, Chang SP (2000) Effect of viscous, viscoplastic, and friction damping on the response of seismic isolated structures. *Earthquake Engineering & Structural Dynamics* **29**(1): 85–107

Makris N, Kampas G (2013a) Estimating the 'effective period' of bilinear systems with linearization methods, wavelet and time-domain analyses: From inelastic displacements to modal identification. *Soil Dynamics and Earthquake Engineering* **45**: 80–88

Makris N, Kampas G (2013b) The engineering merit of the "effective period" of bilinear isolation systems. *Earthquakes & Structures* **4**(4): 397–428

Makris N, Vassiliou MF (2011) The existence of 'complete similarities' in the response of seismic isolated structures subjected to pulse-like ground motions and their implications in analysis. *Earthquake Engineering & Structural Dynamics* **40**(10): 1103–1121

Malhotra PK (2006) Smooth spectra of horizontal and vertical ground motions. *Bulletin of the Seismological Society of America* **96**(2): 506–518

Mander JB, Priestley MJN, Park R (1988) Theoretical stress-strain model for confined concrete. *Journal of Structural Engineering* **114**(8): 1804–1825

Martelli A, Clemente P, De Stefano A, Forni M, Salvatori A (2014) Recent development and application of seismic isolation and energy dissipation and conditions for their correct use. In: Ansal A (Ed) *Perspectives on European Earthquake Engineering and Seismology (Vol 1)*. Springer

Mathworks (2016) *MATLAB and Statistics Toolbox Release 2016b*. The MathWorks, Inc., MA, USA

Miranda E, Ruiz-Garcia J (2002) Evaluation of approximate methods to estimate maximum inelastic displacement demands. *Earthquake Engineering & Structural Dynamics* **31**(3): 539–560

Mori A (1993) *Investigation of the Behaviour of Seismic Isolation Systems for Bridges*. PhD Dissertation, University of Canterbury, Christchurch, NZ

Mori A, Moss PJ, Carr AJ, Cooke N (1997) Behaviour of laminated elastomeric bearings. *Structural Engineering and Mechanics* **5**(4): 451–469

Moschonas IF, Kappos AJ (2013) Assessment of concrete bridges subjected to ground motion with an arbitrary angle of incidence: static and dynamic approach. *Bulletin of Earthquake Engineering* **11**(2): 581–605

Naeim F, Kelly JM (1999) *Design of Seismic Isolated Structures: From Theory to Practice*. Wiley, New York, USA

Nassar A, Krawinkler H (1991) *Seismic Demands for SDOF and MDOF Systems*. John A. Blume Earthquake Engineering Center, Stanford University, CA, USA, Report 95

NEHRP (National Earthquake Hazards Reduction Program) Consultants Joint Venture (2011) *Selection and Scaling Earthquake Ground Motions for Performing Response-History Analyses*. National Institute of Standards and Technology (NIST), USA, Report GCR 11-917-15

Nielson BG (2005) *Analytical Fragility Curves for Highway Bridges in Moderate Seismic Zones*. PhD Dissertation, Georgia Institute of Technology, GA, USA

Norris N (1940) The standard errors of the geometric and harmonic means and their application to index numbers. *The Annals of Mathematical Statistics* **11**(4): 445–448

NTC (Norme Tecniche per le Costruzioni) (2008) *New Technical Standards for Constructions*. Ministry of Infrastructure and Transportation, IT (in Italian)

NZTA (New Zealand Transport Agency) (2013) *Bridge Manual (SP/M/022)*. NZTA, Wellington, NZ

Ortiz Restrepo JC (2006) *Displacement-Based Design of Continuous Concrete Bridges under Transverse Seismic Excitation*. MSc Dissertation, ROSE School, IUSS, Pavia, IT

Padgett JE (2007) *Seismic Vulnerability Assessment of Retrofitted Bridges Using Probabilistic Methods*. PhD Dissertation, Georgia Institute of Technology, GA, USA

Palermo M, Silvestri S, Gasparini G, Trombetti T (2014) A statistical study on the peak ground parameters and amplification factors for an updated design displacement spectrum and a criterion for the selection of recorded ground motions. *Engineering Structures* **76**: 163–176

Palermo M, Silvestri S, Landi L, Gasparinin G, Trombetti M (2016) Peak velocities estimation for a direct five-step design procedure of inter-storey viscous dampers. *Bulletin of Earthquake Engineering* **14**(2): 599–619

Panagiotakos TB, Fardis MN (1999) Deformation-controlled earthquake resistant design of RC buildings. *Journal of Earthquake Engineering* **3**(4): 495–518

Panagiotakos TB, Fardis MN (2001) A displacement-based seismic design procedure for RC buildings and comparison with EC8. *Earthquake Engineering & Structural Dynamics* **30**(10): 1439–1462

Paolucci R, Figini R, Petrini L (2013) Introducing dynamic nonlinear soil-foundation-structure interaction effects in displacement-based seismic design. *Earthquake Spectra* **29**(2): 475–496

Papia M, Russo G (1989) Compressive concrete strain at buckling of longitudinal reinforcement. *Journal of Structural Engineering* **115**(2): 382–397

Paraskeva TS (2013) *Inelastic Analysis of the Dynamic Structural Response of Concrete Bridges*. PhD Dissertation, Aristotle University of Thessaloniki, GR, (in Greek)

Paraskeva TS, Kappos AJ (2010) Further development of a multimodal pushover analysis procedure for seismic assessment of bridges. *Earthquake Engineering & Structural Dynamics* **39**(2): 211–222

Paraskeva TS, Kappos AJ, Sextos AG (2006) Extension of modal pushover analysis to seismic assessment of bridges. *Earthquake Engineering & Structural Dynamics* **35**(11): 1269–1293

Park R, Paulay T (1975) *Reinforced Concrete Structures*. John Wiley & Sons, New York, USA

Park R, Sampson RA (1972) Ductility of reinforced concrete column sections in seismic design. *Journal of the ACI* **69**(9): 543–551

Paulay T (2002) An estimation of displacement limits for ductile systems. *Earthquake Engineering & Structural Dynamics* **31**(3): 583–599

Paulay T, Priestley MJN (1992) *Seismic Design of Reinforced Concrete and Masonry Buildings*. Wiley, New York, USA

Pekcan G, Mander JB, Chen S (1999) Fundamental considerations for the design of non-linear viscous dampers. *Earthquake Engineering & Structural Dynamics* **28**(11): 1405–1425

Penzien J, Watabe M (1974) Characteristics of 3-dimensional earthquake ground motions. *Earthquake Engineering & Structural Dynamics* **3**(4): 365–373

Porter KA (2004) *A Survey of Bridge Practitioners to Relate Damage to Closure*. California Institute of Technology, CA, USA, Report EERL 2004-07

Priestley MJN (1993) Myths and fallacies in earthquake engineering - Conflicts between design and reality. *Bulletin of the New Zealand National Society for Earthquake Engineering* **26**(3): 329–341

Priestley MJN (2003) *The Ninth Mallet-Milne Lecture: Myths and Fallacies in Earthquake Engineering, Revisited*. IUSS Press, Pavia, IT

Priestley MJN, Grant DN (2005) Viscous damping in seismic design and analysis. *Journal of Structural Engineering* **9**(SP2): 229–255

Priestley MJN, Calvi GM, Kowalsky MJ (2007) *Displacement-Based Seismic Design of Structures*. IUSS Press, Pavia, IT

Priestley MJN, Seible F, Calvi GM (1996) *Seismic Design and Retrofit of Bridges*. Wiley, NY, USA

Ramallo JC, Johnson EA, Spencer BF (2002) 'Smart' base isolation systems. *Journal of Engineering Mechanics* **128**(10): 1088–1100

Ramirez OM, Constantinou MC, Gomez JD, Whittaker AS, Chrysostomou CZ (2002) Evaluation of simplified methods of analysis of yielding structures with damping systems. *Earthquake Spectra* **18**(3): 501–530

Ray T, Reinhorn AM, Nagarajaiah S (2013) Nonlinear elastic and inelastic spectra with inherent and supplemental damping. *Earthquake Engineering & Structural Dynamics* **42**(14): 2151–2165

Rezaeian S, Der Kiureghian A (2012) Simulation of orthogonal horizontal ground motion components for specified earthquake and site characteristics. *Engineering & Structural Dynamics* **41**(2): 335–353

Rosenblueth E, Herrera I (1964) On a kind of hysteretic damping. *Journal of Engineering Mechanics* **90**(4): 37–48

Ryan KL, Chopra AK (2004a) Estimating the seismic displacement of friction pendulum isolators based on non-linear response history analysis. *Earthquake Engineering & Structural Dynamics* **33**(3): 359–373

Ryan KL, Chopra AK (2004b) Estimation of seismic demands on isolators based on nonlinear analysis. *Journal of Structural Engineering* **130**(3): 392–402

Ryan KL, Chopra AK (2006) Estimating bearing response in symmetric and asymmetric-plan isolated buildings with rocking and torsion. *Earthquake Engineering & Structural Dynamics* **35**(8): 1009–1036

Ryan K, Polanco J (2008) Problems with Rayleigh damping in base-isolated buildings. *Journal of Structural Engineering* **134**(11): 1780–1784

Ryan KL, Kelly JM, Chopra AK (2005) Nonlinear model for lead-rubber bearings including axial-load effects. *Journal of Engineering Mechanics* **131**(2): 1270–1278

Sanchez J, Masroor A, Mosqueda G, Ryan K (2013) Static and dynamic stability of elastomeric bearings for seismic protection of structures. *Journal of Structural Engineering* **139**(7): 1149–1159

Saragoni GR, Hart GC (1973) Simulation of artificial earthquakes. *Earthquake Engineering & Structural Dynamics* **2**(3): 249–267

Sarkis AI, Palermo A (2018) Low damage technologies and resilience-based design for concrete bridges: Beyond ductility concepts. In: Hordijk DA, Luković M (Eds) *High Tech Concrete: Where Technology and Engineering Meet*. Springer

Sayani PJ, Ryan KL (2009) Evaluation of approaches to characterize seismic isolation systems for design. *Journal of Earthquake Engineering* **13**(6): 835–851

SEAOC (*Seismology Committee of Structural Engineers Association of California*) (1995) Performance based seismic engineering of buildings: Vision 2000. SEAOC, Sacramento, CA, USA

SEAOC (1999) *Recommended Lateral Force Requirements and Commentary (Blue Book)*. SEAOC, Sacramento, CA, USA

Seismosoft (2016) *SeismoArtif: A Computer Program for Generation of Artificial Earthquake Accelerograms*. [www.seismosoft.com]

Sextos A (2013) Effect of soil-structure interaction and spatial variability of ground motion on seismic risk assessment of bridges. In: Tesfamariam S, Goda K (Eds) *Handbook of Seismic Risk Analysis and Management of Civil Infrastructure Systems*. Elsevier

Sextos AG, Katsanos EI, Manolis GD (2011) EC8-based earthquake record selection procedure evaluation: Validation study based on observed damage of an irregular R/C building. *Soil Dynamics & Earthquake Engineering* **31**(4): 583–597

Sextos AG, Pitilakis KD, Kappos AJ (2003) Inelastic dynamic analysis of RC bridges accounting for spatial variability of ground motion, site effects and soil-structure interaction phenomena. Part 1: Methodology and analytical tools. *Earthquake Engineering & Structural Dynamics* **32**(4): 607–627

Shibata A, Sozen MA (1976) Substitute structure method for seismic design in R/C. *Journal of the Structural Division* **102**(1): 1–18

Shome N, Cornell CA, Bazzurro P, Carballo JE (1998) Earthquakes, records, and nonlinear responses. *Earthquake Spectra* **14**(3): 469–500

Soong TT, Masri SF, Housner GW (1991) An overview of active structural control under seismic loads. *Earthquake Spectra* **7**(3): 483–505

Spencer BF, Nagarajaiah S (2003) State of the art of structural control. *Journal of. Structural Engineering* **129**(7): 845–856

Stone WC, Taylor AW (1994) ISDP: Integrated approach to seismic design of reinforced concrete structures. *Journal of Structural Engineering* **120**(12): 3548–3566

Suarez V, Kowalsky MJ (2007) Displacement-based seismic design of drilled shaft bents with soil-structure interaction. *Journal of Earthquake Engineering* **11**(6): 1010–1030

Suarez VA, Kowalsky MJ (2010) Direct displacement-based design as an alternative method for seismic design of bridges. In: Silva PF, Valluvan R (Eds) *Structural Concrete in Performance-Based Seismic Design of Bridges (SP-271)*. ACI, Special Publication

Suarez VA, Kowalsky MJ (2011) A stability-based target displacement for direct-displacement-based design of bridge piers. *Journal of Earthquake Engineering* **15**(5): 754–774

Sullivan TJ, Calvi GM, Priestley MJN, Kowalsky MJ (2003) The limitations and performances of different displacement based procedures. *Journal of Earthquake Engineering* **7**(S1): 201–241

Symans MD, Constantinou MC (1999) Semi-active control systems for seismic protection of structures: A state-of-the-art review. *Engineering Structures* **21**(6): 469–487

Tsiavos A, Mackie KR, Vassiliou MF, Stojadinović B (2017) Dynamics of inelastic base-isolated structures subjected to recorded ground motions. *Bulletin of Earthquake Engineering* **15**(4): 1807–1830

Vamvatsikos D, Cornell CA (2002) Incremental dynamic analysis. *Earthquake Engineering & Structural Dynamics* **31**(3): 491–514

Vamvatsikos D, Cornell CA (2004) Applied incremental dynamic analysis. *Earthquake Spectra* **20**(2): 523–553

Van Engelen NC, Kelly JM (2015) Correcting for the Influence of bulk compressibility on the design properties of elastomeric bearings. *Journal of Engineering Mechanics* **141**(6): 04014170 1–11

Vassiliou MF, Tsiavos A, Stojadinović B (2013) Dynamics of inelastic base-isolated structures subjected to analytical pulse ground motions. *Earthquake Engineering & Structural Dynamics* **42**(14): 2043–2060

Warn GP, Whittaker AS (2006) *A Study of the Coupled Horizontal-Vertical Behavior of Elastomeric and Lead-Rubber Seismic Isolation Bearings*. MCEER, NY, USA, Report 06-0011

Weatherill G, Crowley H, Danciu L (2010) *Report on Seismic Hazard Definitions Needed for Structural Design Applications*. SHARE Project, Deliverable 2.2

Weatherill G, Crowley H, Danciu L (2013) *Preliminary Reference Euro-Mediterranean Seismic Hazard Zonation*. SHARE Project, Deliverable 2.7

Weisman J, Warn GP (2012) Stability of elastomeric and lead-rubber seismic isolation bearings. *Journal of Structural Engineering* **138**(2): 215–223

Wen YK (1975) Approximate method for nonlinear random vibration. *Journal of the Engineering Mechanics Division* **101**(4): 389–401

Wen YK (1976) Method for random vibration of hysteretic systems. *Journal of the Engineering Mechanics Division* **102**(2): 249–263

Whittle JK, Williams MS, Karavasilis TL, Blakeborough A (2012) A comparison of viscous damper placement methods for improving seismic building design. *Journal of Earthquake Engineering* **16**(4): 540–560

Annex F
Relevant Publications

Gkatzogias KI, Kappos AJ (2015a) Deformation-based seismic design of concrete bridges. *Earthquakes & Structures* **9**(5): 1045–1067; doi: 10.12989/eas.2015.9.5.1045

Gkatzogias KI, Kappos AJ (2015b) Performance-based seismic design of concrete bridges. *SECED 2015 Conference: Earthquake Risk and Engineering towards a Resilient World*, Cambridge, UK (pdf)

Gkatzogias KI, Kappos AJ (2016a) Seismic design of concrete bridges: Some key issues to be addressed during the evolution of Eurocode 8 - Part 2. *17th Hellenic Conference on Concrete Structures*, Thessaloniki, GR (pdf)

Gkatzogias KI, Kappos AJ (2016b) Semi-active control systems in bridge engineering: A review of the current state of practice. *Structural Engineering International* **26**(4): 290–300; doi: 10.2749/101686616X145554 29844040

Gkatzogias KI, Kappos AJ (2017a) Deformation-based design of seismically isolated concrete bridges. *16th World Conference on Earthquake Engineering (WCEE)*, Santiago, CL; Paper No.997 (pdf)

Gkatzogias KI, Kappos AJ (2017b) Performance-based design and assessment of seismically isolated bridges with non-linear viscous dampers. *6th International Conference on Computational Methods in Structural Dynamics and Earthquake Engineering (COMPDYN)*, Rhodes Island, GR; **1**: 578–594; doi: 10.7712/120117.5442.17855

Gkatzogias KI, Kappos AJ (2018) Deformation-based design of seismically isolated bridges. *Earthquake Engineering & Structural Dynamics* (under preparation)

Kappos AJ, Gidaris IG, Gkatzogias KI (2012) Problems associated with direct displacement-based design of concrete bridges with single-column piers, and some suggested improvements. *Bulletin of Earthquake Engineering* **10**(4): 1237–1266; doi: 10.1007/s10518-012-9354-y

Kappos AJ, Gkatzogias KI (2017) Deformation-based design of concrete bridges (Invited paper). *International Workshop on Performance-Based Seismic Design of Structures (Resilience, Robustness) (PESDES)*, Shanghai, CN; (pdf)

Kappos AJ, Gkatzogias KI, Gidaris IG (2013) Extension of direct displacement-based design methodology for bridges to account for higher mode effects. *Earthquake Engineering & Structural Dynamics* **42**(4): 581–602; doi: 10.1002/eqe.2229